Radiolarians in the Geological Record

M. S. Afanasieva*, E. O. Amon,
Yu. V. Agarkov***, and D. S. Boltovskoy******

*Paleontological Institute, Russian Academy of Sciences, Profsoyuznaya ul. 123, Moscow, 117647 Russia

e-mail: marina.afanasieva@mtu-net.ru

**Institute of Geology and Geochemistry, Ural Branch, Russian Academy of Sciences, Pochtovyi per. 7, Yekaterinburg, 620151 Russia

e-mail: amon@igg.uran.ru

***Rostov State University, Geology Faculty, ul. Zorge 40, Rostov-on-Don, 344090 Russia

e-mail: agarkov@aaanet.ru

****Departamento Ecologia, Genetica y Evolucion, Facultad de Ciencias Exactas y Naturales, Universidad de Buenos Aires, C1428EHA Buenos Aires, Argentina

e-mail: demetrio@bg.fcen.uba.ar

Received September 1, 2004

Contents

Vol. 39, Suppl. 3, 2005

The supplement is published only in English by MAIK "Nauka/Interperiodica" (Russia).
Paleontological Journal ISSN 0031-0301.

Paleontological Journal, Vol. 39, Suppl. 3, 2005, pp. S135–S392.

Abstract—This study is dedicated to the comprehensive description of radiolarians, the discussion of their morphology, problems of classification, and their important role in the history of the Earth's biosphere. It contributes to the solution of the fundamental problems of the evolutionary morphology of radiolarians, related to the study of the morphogenesis of their skeletons at various structural levels through geological time, aiming at the creation of a morphological basis for the phylogeny and classification of the phylum Radiolaria. The book describes the 200-year history of radiolarian classification. The biology and morphology of radiolarians are discussed. The study deals with the successive stages of the ontogeny of radiolarians and the main patterns of skeletal morphogenesis: appearance and growth of skeletal elements, biomineralization, and secondary transformation of skeletons. A new classification of the phylum Radiolaria, uniting two superclasses Phaeodaria and Polycystina, is proposed. The superclass Polycystina is composed of six classes: Aculearia, Sphaerellaria, Spumellaria, Stauraxonaria, Nassellaria, and Collodaria. Patterns in the appearance/disappearance and distribution in time of higher taxa of Polycystina are discussed, and critical levels in the evolution of radiolarians at the major stages of the Phanerozoic are revealed. Four phases and nine stages in the evolution of radiolarians are recognized. Problems of the biology, ecology, and taphonomy of radiolarians are discussed. It is shown that the biomass of polycystine radiolarians is greatest at depths of 50–400 m. The conclusion is made that radiolarians cannot be regarded as indicators of exclusively oceanic deep-water conditions. In the geological past, the maximum density and diversity of the population of radiolarians was observed in the coastal regions or zones of aulacogens and active tectonic faults.

Statistical analysis of the biodiversity of radiolarians in the Phanerozoic is conducted based on the informational system RADBASE containing information on 1722 genera of radiolarians and their synonyms.

The study is expected to be of use to a broad range of readers in paleontology, biostratigraphy, paleoecology, and as a textbook for the university courses. It contains 67 figures, 11 tables, 33 plates, and an appendix. The list of references includes 461 names.

Key words: Radiolaria, morphology, classification, evolution, habitats, taphonomy, informational technologies.

INTRODUCTION

The 200-year history of radiolarian studies began from the first report of the Russian scientist Tilesius von Tilenau (1806–1809) on extant planktonic unicellular organisms with a siliceous skeleton from the modern oceans. In the history of studies and classification of radiolarians the following basic events are recognized: (1) the rise of the classification bases of Radiolaria in the 19th century (1806–1887); (2) establishment of classification schemes of Radiolaria in the middle of the 20th century (1953–1979); and (3) development of new trends in the classification of Radiolaria at the boundary of the 20th and 21st centuries (1980–recent).

Radiolarians represent one of the earliest groups of microorganisms, which has been inhabiting various regions of the ocean from the Early Cambrian to the present. Such a long duration and wide distribution are largely explained by the ecological plasticity of this group, which allows radiolarians to inhabit various marine and oceanic bionomic zones. During their evolution, radiolarians repeatedly changed the strategy of distribution and colonization of the new zones of the sea, but several main features apparently remained unchanged. These include a planktonic mode of life, heterotrophic feeding, and, hence, dependence on the food resource, reliance on the concentration of SiO_2 dissolved in the sea water, mutually beneficial symbiosis with microscopic unicellular algae defining the preferred habitats (mainly the upper layers of the water column, where zooplankton feeds on the intensely producing phytoplankton and bacteria).

In the modern oceans, living radiolarians inhabit all marine and oceanic bionomic zones. They live at all levels, from the surface to maximum depths; however, the Polycystina are particularly abundant in the interval 50–400 m of depth, while the Phaeodaria are at more than 100–200 m of depth (Petrushevskaya, 1986; Kling and Boltovskoy, 1995; Abelmann and Gowing, 1997; Boltovskoy, 1998, 1999; Zasko, 2004).

In addition, heterotrophic feeding on bacteria, silicoflagellates, diatoms, etc. provides radiolarians with proteins, fats, and carbohydrates, allowing them to live and reproduce in an environment of competition with other planktonic organisms.

Bottom thanatocenoses and taphocenoses of radiolarians may form in all zones, including the central oligotrophic regions of the oceans. However, the main "radiolarian rain" occurs in the zone which is not deeper than 500 m. It would have been a serious mistake to regard radiolarians as indicators of exclusively oceanic depths comparable with the depths of the modern bathyal and abyssal.

The geological past of radiolarians is much richer than their modern state. This is seen from the example of radiolarians inhabiting the Domanik (Late Devonian) basins under conditions of hydrosulphuric con-

tamination, or the example of the distribution of Carboniferous and Early Permian radiolarians in the regions of reefs, or the example of different environments of accumulation of radiolarian mud in the Paleozoic, Mesozoic, Cenozoic, and modern oceans.

The modern science acknowledges that the evolutionary morphology of radiolarians is a wide field for the comprehensive study of the appearance and development of taxa to reveal the morphological patterns of the evolutionary process. Each organism and its structural features "may and should be studied from at least four points of views: constructive-morphological, physiological, ecological, and historical. Each of these points of view is permissible, necessary, and unique" (Beklemishev, 1964, p. 78).

The present study is directed toward the solution of the fundamental problem of the evolutionary morphology of radiolarians, related to the complex study of the patterns of the radiolarian skeletal morphogenesis in time, at different structural levels with the purpose of creating a morphological basis for the phylogeny and classification of the phylum Radiolaria. The study of radiolarians was conducted from various aspects, considering their morphology and ecology, and with a obligatory reference to all evolutionary transformations in the geological past.

Advanced scientific research brings a new understanding of the relationships between morphology and phylogeny and classification, because the study of macrostructure is supplemented by research at ultrastructural level. Knowledge of the evolution of the internal and external skeletal elements of radiolarians requires a complex approach to the study of this faunal group. Hence, emphasis in this study is placed on the successive stages of individual development of radiolarians. The study revealed major patterns in the morphogenesis of the radiolarian skeletons: problems of the appearance and growth of skeletal elements. Biomineralization and secondary transformation of the skeletons is considered.

A new radiolarian classification is developed. The phylum Radiolaria consists of two superclasses Pheodaria and Polycystina. The superclass Polycystina includes six classes: Aculearia, Sphaerellaria, Spumellaria, Stauraxonaria, Nassellaria, and Collodaria. The diagnoses of 285 higher radiolarian taxa are given: 1 phylum, 2 superclasses, 6 classes, 26 orders, 14 superfamilies, 132 families, and 104 subfamilies, comprising 1131 genera of Phanerozoic Radiolaria.

The study of the morphogenesis of the skeletons of radiolarians at various structural levels in geological time revealed patterns of the appearance/disappearance and expansion of higher taxa of polycystine radiolarians through time which aimed to recognize critical moments (crises, catastrophes) in the evolution of radiolarians in the history of the Earth at the major boundaries within the Phanerozoic. Four phases and nine stages of the evolution of radiolarians are recognized. At each of the evolutionary stages of radiolarians, various taxa experienced considerable changes in composition and quantity, with a change in the leading group. The statistical analysis of the change in radiolarian biodiversity in the Phanerozoic was based on the informational system (IS) RADBASE, containing information of 1722 radiolarian genera and their synonyms (Agarkov, 1998, 1999, 2004).

The novelty of the study conducted is that it was based on a uniquely extensive material, which has no equivalents worldwide. This, in turn, provided a fundamental study of morphology, ecology, and historical development of radiolarians in the Phanerozoic, and allowed new information on the total biodiversity of radiolarians. The new classification of Phanerozoic radiolarians is based on a computer-based system of fixed combinations of morphological characters of the skeletons used for describing radiolarians of different taxonomic ranks.

The novelty in the approach to the creation of the uniform classification of radiolarians implies a complex study of various radiolarian groups with different durations and ecology to reconstruct a general pattern of the biodiversity of radiolarians and more complete characterization of the evolution of the phylum Radiolaria.

CHAPTER 1. THE HISTORY OF THE STUDY AND CLASSIFICATION OF RADIOLARIA

The study of Radiolaria has a history of about 200 years, during which the following basic events are recognized (Table 1): (1) the rise of classification bases of Radiolaria in the 19th century (1806–1887), (2) establishment of classification schemes of Radiolaria in the middle of the 20th century (1953–1979), and (3) the development of new trends in the classification of Radiolaria at the boundary of the 20th and 21st centuries (1980-recent) (Afanasieva *et al.*, 2004a, 2004b).

THE RISE OF THE CLASSIFICATION BASES OF RADIOLARIA IN THE 19th CENTURY (1806–1887)

Radiolarian studies began with the first report of Tilesius von Tilenau (1769–1857) about extant single-celled organisms with a siliceous skeleton found among the plankton of modern oceans. Tilesius von Tilenau was a German botanist, a member of the St. Petersburg Academy of Sciences, who was employed in Russia from 1803. In 1803–1806, he was the doctor and naturalist on the Russian circumnavigation of the world under I.F. Krusenschtern and Yu.F. Lisyanskii. Unfortunately, this first record of radiolarians (which were only named such half a century later), published in 1806–1809 in the reports of this Russian scientific expedition remained unnoticed within the bulk of biological material described.[1]

[1] The information on the first record of radiolarians by Tilesius von Tilenau is cited after Khabakov *et al.* (1959) and Petrushevskaya (1986).

Table 1. Main events in the history of radiolarian classification

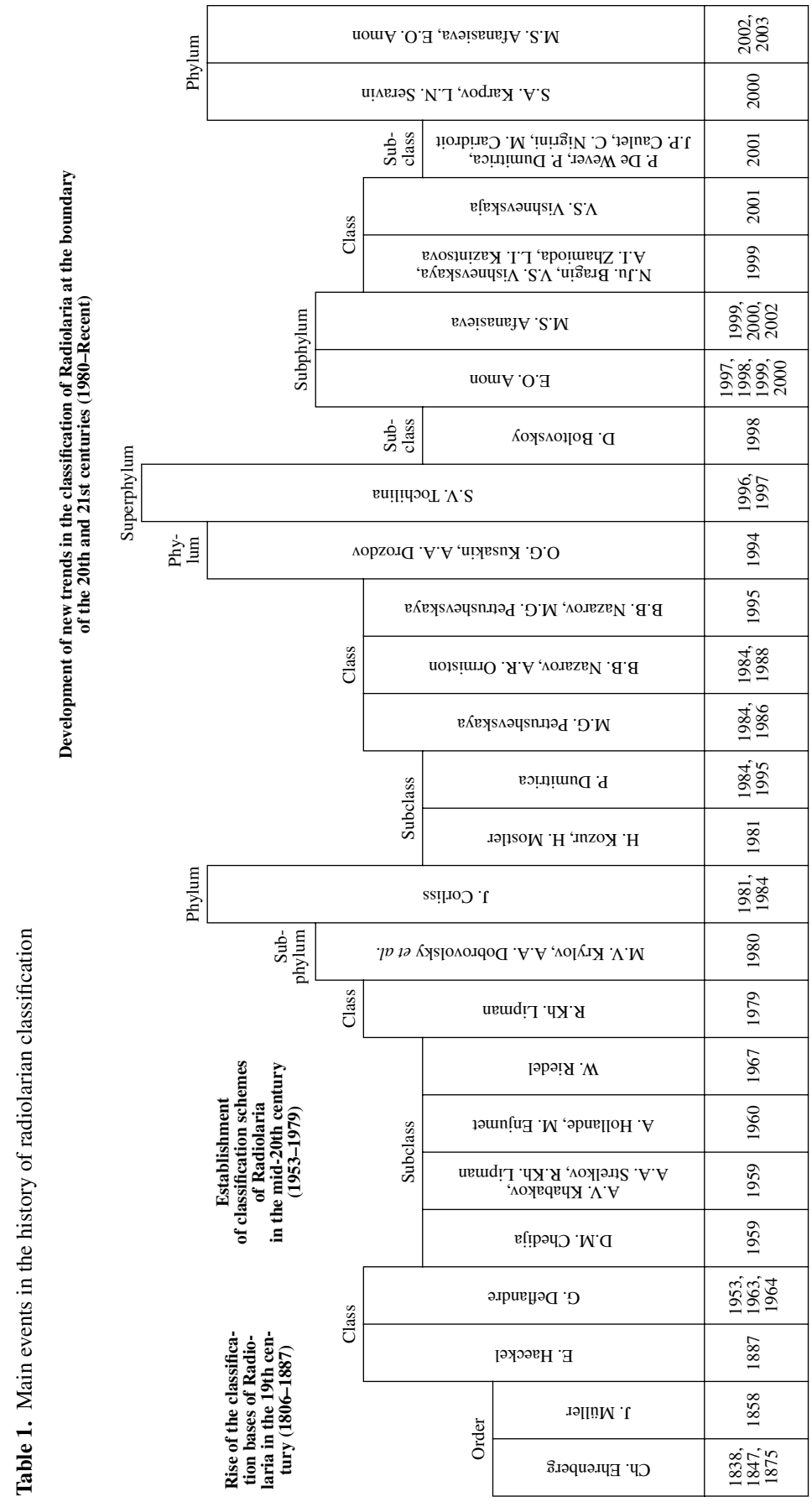

One of the first illustrations of fossil radiolarians was published by Meyer in 1834[2] in his fundamental study of the fossils of Germany. However, the data of Meyen (1834a, 1834b) on extant radiolarians (*Physematium*, *Sphaerozoum*) in the report of zoological studies from the circumnavigation caused a real sensation among scientists.

It is noteworthy that the first Recent radiolarians to be described were large colonial taxa (soft-bodied, or with a skeleton of isolated spines submerged in the calymma): Meyen described two genera of Collodaria.

The systematic study of Radiolaria was commenced by Ehrenberg (1838), who proposed the name Polycystina, and Müller (1858), who proposed the name Radiolaria, which quickly became popular. The excellently illustrated monograph by Haeckel (1887) made Radiolaria a widely known group.

The general system of Radiolaria was proposed by Haeckel (1887) based on the study of extant radiolarians from the *Challenger* expedition.

Over the following century, many workers noted the formal nature and incompleteness of Haeckel's system, although nothing equivalent except for the classification of Petrushevskaya (1971, 1981a, 1986) was proposed by the end of the 20th century. Tan Sin Hok (1926) suggested that Haeckel, who proposed the first systematics of radiolarians, fully understood that it was a hypothetical and provisional work. Later amendments and modifications of Haeckel's system were only small.

ESTABLISHMENT OF CLASSIFICATION SCHEMES OF RADIOLARIA IN THE MIDDLE OF THE 20th CENTURY (1953–1979)

The following papers were particularly important for the development of the radiolarian system after Haeckel's studies.

Brandt (1905) began the classification of colonial radiolarians, which was developed by Strelkov and Reshetnyak (1971). Jörgensen (1905) studied the inner spiny skeleton of Nassellaria and proposed to homologize the spines by assigning them letters. Haecker (1908) somewhat simplified and rationalized Haeckel's system based on studies of the skeletons of extant Radiolaria. Popofsky (1908, 1912, 1913) developed the principles of the classification of Nassellaria based on spines proposed by Jörgensen, and proposed a new taxonomy of Nassellaria, which was not widely accepted.

Schewiakoff (1926) wrote a fundamental monograph on the system and zoology of extant acantharians. Dogel (1950, 1951) published on phylogeny of Radiolaria. In her first monograph on Phaeodaria, Reshetnyak (1966) thoroughly analyzed the taxonomy of deepwater Phaeodaria and revealed patterns of their geographic distribution.

In the middle of the 20th century, two fundamental paleontological handbooks were published at almost the same time in France by Deflandre (1952, 1953b) and in Russia by Khabakov *et al.* (1959). These large paleontological handbooks contain sections on ancient Radiolaria. Each book is different from the others in its focus, coverage of material, and structure. In these monumental studies, Haeckel's system is on the one hand canonized and recommended as an essential work, and on the other hand amended and refined, without compromising the major ideas and principles of Haeckel. Revised versions of radiolarian taxonomy became extremely popular for a short time, but then, Haeckel's system, in both its classical interpretation and its modified versions, came in for renewed criticism.

Campbell (1954) wrote the section on Radiolaria in "Treatise on Invertebrate Paleontology" published in the United States. This book contained phylogeny and classification of the subclass Radiolaria with short diagnoses of all Acantharia, Spumellaria, Nassellaria, and Phaeodaria genera known at that time and their stratigraphic significance was emphasized. However, the Campbell's attempt to modify the radiolarian taxonomy to match the requirements of the "International Code of Zoological Nomenclature" made it very confused. Campbell changed names or endings in almost all of Haeckel's taxa (orders, suborders, superfamilies, and families) and he placed his name on all these taxa because of the changes he made. He also deleted many generic names, which have been widely used in the paleontological literature. The classification proposed by Campbell was severely criticized by Riedel (1958). It was not accepted in the Russian *Fundamentals* of *Paleontology* (Khabakov *et al.*, 1959). Deflandre (1960), the oldest specialist in Radiolaria, published a severe but justified criticism of Campbell's study. He was supported by Petrushevskaya (1971) and Lipman (1974).

Chedija (1959) published "A Review of Radiolarian Taxonomy: A Handbook for the Study of Fossil Radiolaria" containing short diagnoses of 649 genera of extinct and extant Nassellaria and Spumellaria based on Haeckel's and later studies.

Hollande and Enjumet (1960) published a taxonomically important monograph. They discovered a close connection between the structure and size of the central capsule shell and the morphology of the intranuclear complex and showed that the cytoplasmic structure of Sphaeroidea determines the skeletal morphology.

Riedel (1967) proposed a new classification of all radiolarians. He followed the principle of priority and resurrected the name Polycystina, which was the first to be proposed for this group by Ehrenberg. He assigned to true radiolarians only those taxa with a siliceous skeleton, and he considered Spumellaria and Nassellaria as suborders of the order Polycystina.

Lipman (1979), based on the studies of radiolarians from almost all stratigraphic intervals from the Lower

[2] The information on the first illustration of fossil radiolarians by Meyer (1834) is cited after Khabakov *et al.* (1959) and Petrushevskaya (1986).

Paleozoic to the Recent and the analysis of all known classifications beginning from one proposed by Ehrenberg, concluded that Haeckel's taxonomy should remain a firm foundation for higher taxa in this group (orders, suborders, and most families). However, she emphasized that Haeckel's taxonomy should be significantly refined based on ontogenetic studies and ontogenetic and individual variability.

DEVELOPMENT OF NEW TRENDS IN THE CLASSIFICATION OF RADIOLARIA AT THE BOUNDARY OF THE 20th AND 21st CENTURIES (1980–RECENT)

In the new classifications that appeared at the boundary of the 20th and 21st centuries, the principle of classification of radiolarian skeletons based on their symmetry did not lose its importance. However, this time it was not the symmetry in the sense of promorphology previously used by Haeckel for his taxonomy, but rather the general geometry of the skeleton, although referred to as symmetry. On the one hand, the significance and role of symmetry was essentially reduced in the classifications of De Wever and Origlia (1984), Dumitrica (1984), and Amon (1999a, 2000a, 2000b, 2000c), while on the other hand, the type of symmetry was often used as a basis for establishing new taxa of higher rank in classifications by Petrushevskaya (1971, 1979, 1981a, 1984, 1986), Nazarov (1974a, 1974b, 1975, 1981, 1988), Afanasieva (1997a, 1999, 2000a, 2000b, 2002), De Wever *et al.* (2001).

Kozur and Mostler (1972) were the first to publish data on rich and diverse assemblages of Triassic radiolarians. This paper began a period of intense studies of Triassic radiolarians; they described over 300 new species, 150 genera, and many new families. Kozur and Mostler (1984) proposed the first classification of Triassic radiolarians.

Dumitrica (1984) proposed a classification of Sphaerellaria, in which he selected groups of characters with the intention of using only those which provide the best basis for classification of radiolarians. In this paper, he indicated the principles of classification of Sphaerellaria, recognized basic classification characters (groups of characters), and gave a diagnosis of the order (suborder) Sphaerellaria. Ten years later, Dumitrica (1995) in the atlas of Mesozoic Radiolaria published in Switzerland, proposed a new system of the subclass for the suborders Spumellaria (five superfamilies with 19 families) and Nassellaria (16 families).

Petrushevskaya (1971, 1979, 1981a, 1984, 1986) published a significantly revised taxonomy of the higher taxa of Radiolaria. She proposed two of the most important principles of classification: (1) a natural system of animals should be a reflection of our knowledge of the origin and phylogeny of particular taxonomic groups; (2) a natural system should be prognostic. A logical and balanced radiolarian system of proposed by Petrushevskaya strictly followed the requirements of ICZN, embraced all groups of extinct and extant Radiolaria known at that time, took into account new cytological data, and determined the taxonomic status of all morphological characters of skeletons. Petrushevskaya's taxonomy reflects the diversity of morphotypes and phylogenetic relationships in higher taxa of Radiolaria better than Haeckel's taxonomy and is more developed than the taxonomy proposed by other workers. At the same time, Radiolaria are still considered as a class with two subclasses, Euradiolaria and Acantharia.

The taxonomy of Paleozoic Radiolaria proposed by Nazarov (1974a, 1974b, 1975, 1981, 1984, 1988) and, later, by Nazarov and Ormiston (1984, 1993) revolutionized the ancient radiolarian studies and destroyed the myth of their stratigraphic uselessness. Nazarov's (1984, 1988) radiolarian taxonomy is better in that all available characters are used in classification, rather than selected characters or groups of characters. Nazarov carefully valued the importance of morphological characters of skeletons and defined their taxonomic status. Studies by Nazarov and Ormiston (Nazarov, 1974a, 1974b, 1975, 1981, 1984, 1988; Nazarov and Ormiston, 1984, 1993) contained a revision, descriptions, and redescriptions of 16 families, seven subfamilies, 77 genera and about 400 species of Radiolaria from all Paleozoic series.

The only attempt to create a general systematics of Phanerozoic Radiolaria based on the unification of separate classifications of Cenozoic, Mesozoic, and Paleozoic Radiolaria proposed based on the studies in the 1960s–1980s, was undertaken by Nazarov and Petrushevskaya (1995). This classification was based on detailed skeletal morphology, stratigraphic distribution of taxa and evolutionary lineages, on the refinement of the term *cephalis*, and on the homology of skeletal structures. A system of morphological skeletal characters to recognize taxa of various hierarchic levels was proposed. The position within the cell and the structure of the nucleoaxopodial complex, which influence the morphology of the central capsule and skeletal morphology, are taken into account to distinguish taxa of higher taxonomic ranks. The taxonomy of species, genera, and sometimes families is based solely on skeletal morphology.

Tochilina (1996, 1997) established a new phylum, Nassellaria, which comprises radiolarians from the Paleozoic, Mesozoic, and Cenozoic and includes two new classes, the Trisymmetris (with the orders Plectaniida Haeckel, 1887; Spyridida Ehrenberg, 1847; and Lychnocaniida Haeckel, 1881) and Axisymmetris (with the orders Sethocapsida Haeckel, 1862; Eucyrtida Ehrenberg, 1847; Parvicingulida Pessagno, 1977; and Palinandromeda Pessagno, Blome et Hall, 1993). Tochilina suggested that Radiolaria include three types of organisms with the skeletons composed of silicon oxide: Nassellaria, Spumellaria, and Phaeodaria. The three taxa are characterized by different patterns of the

axopodial apparatus, general structural organization, symmetry, and spatial arrangement of skeletal elements. The key characteristics of the mineral skeleton of radiolarians are its chemical composition and crystal structure. These two properties are interrelated and determine entirely the symmetry of the skeleton.

Amon (1997, 1999a, 2000a, 2000b, 2000c) proposed a classification of Paleozoic and Mesozoic radiolarian higher taxa based on new classification principles. He discussed the problems related to the adequate use of theory of symmetry in the classification of Radiolaria. He concluded that the theory of symmetry (including the Curie principle) may be used as a tool only for an idealized (formal) description of radiolarians, whereas in the classification it may only be an auxiliary approach.

Boltovskoy (1998) presented a large monograph on classification and distribution of extant radiolarians in the South Atlantic on the website of the international internet journal "Palaeontologica Electronica". He paid much attention to the morphology and physiology of radiolarians and considered the morphological characters of the skeleton as a classification basis. Boltovskoy analyzed the phylogenetic lineages of Cenozoic Radiolaria and concluded that the most important skeletal characters used by Haeckel (1887) to build his system are of little or no importance at the suprageneric level. At the same time, characters that traditionally were treated as unimportant reflect evolutionary trends and, hence, are useful to recognize taxa of higher rank.

In their practical handbook in the Mesozoic Radiolaria, Bragin, Vishvevskaya, Zhamoida, and Kazintsova (1999) noted that unfortunately no generally accepted classification exists, despite the fact that several versions were proposed. All the diversity and varieties of radiolarian skeletons can be reduced to four major types: spherical, ellipsoid, discoid, and cyrtoid. The first three types are characteristic of the radiolarians from the order Spumellaria. Cyrtoid skeletons are typical of the Mesozoic Nassellaria. Hence, a somewhat "synthetic" classification based on genera is accepted in this paper. The study contains descriptions of 142 radiolarian taxa from the Mesozoic of northern Eurasia: three orders, one suborder, three superfamilies, 32 families, 5 subfamilies, and 98 genera. Thirty-seven Sphaerellaria genera are assigned to 13 families, of which only three were established by Haeckel (and all three superfamilies). Of Nassellaria, 55 genera are assigned to 19 families, of which only two were described by Haeckel.

The atlas by Afanasieva (2000a) was the first up-to-date comprehensive study of Paleozoic radiolarians, using new methods of radiolarian analysis and computer technologies. Afanasieva (1999, 2000a, 2000b, 2002) considered radiolarians as a subphylum with two classes, Phaeodaria and Polycystina. The class Polycystina contains seven orders: Sphaerellaria Haeckel, 1881; Pylomaria Afanasieva, 1999; Stauraxonaria Afanasieva, 2000; Aculearia Afanasieva, 1999; Albaillellaria Deflandre, 1953, emend. Afanasieva, 2000; Nassellaria Ehrenberg, 1847; and Collodaria Haeckel, 1881. A system of fixed association of morphological characters for the diagnostics and descriptions of Paleozoic radiolarians of various taxonomic levels is proposed by Afanasieva (1997a, 1997b, 2000a, 2000b, 2002). The atlas of Paleozoic radiolarians contains monographic descriptions of 308 radiolarian taxa, including five orders, 17 superfamilies, 28 families, 48 subfamilies, 50 genera, and 160 species. Of these, 120 taxa were established for the first time (Afanasieva, 2000a).

The monograph of Vishnevskaya (2001) dealt with Jurassic and Cretaceous radiolarians (from the Hettangian to Maastrichtian inclusive). In that study radiolarians were assigned to the class Radiolaria. The study contained monographic descriptions of 35 new and 474 characteristic species of Jurassic and Cretaceous radiolarians belonging to 136 genera and 52 families, which had not been previously recorded from Russia. The atlas of Jurassic and Cretaceous radiolarians of Russia includes 140 plates and their detailed explanations.

The book by De Wever, Dumitrica, Caulet, Nigrini, and Caridroit (2001) "Radiolarians in the Sedimentary Record" is a comprehensive analysis of fossil and extant radiolarians. A new classification of radiolarians follows the traditions of Haeckel, Ehrenberg, and Deflandre, which are developed and amended. According to this tradition, radiolarians are still considered within the class Actinopoda. On the other hand, the new classification contains a number of new approaches to the taxonomy of orders and superfamilies and to the distribution of families in the orders. The introduction of the new orders was one of the most significant innovations. These are the order Archaeospicularia, including Early–Middle Paleozoic radiolarians with a specific spiculate skeleton and the order Latentifistularia, which includes stauraxon radiolarians. In addition, Collodaria and Albaillellaria are regarded as orders. These innovations are among other progressive trends in radiolarian studies. The principles of shape and type of the skeleton and relationships of the basic skeletal elements are used for recognizing the orders. The study contained diagnoses of over 130 families of Phanerozoic radiolarians, most of which are excellently illustrated. The weak point of the classification proposed is the taxonomic level of orders and of radiolarians in total, which are considered as a subclass. The latter does not agree with modern view of biologists developing an integrated system of protists (Margulis, 1974; Levine *et al.*, 1980; Krylov *et al.*, 1980; Corliss, 1981, 1984, 1994; Cavalier-Smith, 1993; Kusakin and Drozdov, 1994; Protists, 2000).

Afanasieva and Amon (2002, 2003a, 2003b) proposed a new classification of higher taxa of radiolarians. The recognition of the phylum Radiolaria agrees with the advanced research of the protist macrosystem by biologists over the last three decades. The phylum

Radiolaria includes two superclasses, Phaeodaria and Polycystina. The superclass Polycystina contains five classes: Sphaerellaria Haeckel, 1881; Spumellaria Ehrenberg, 1875; Stauraxonaria Afanasieva, 2000; Aculearia Afanasieva, 1999, status nov., 2003; and Nassellaria Ehrenberg, 1847.

Thus, existing taxonomies of radiolarians from different time intervals are not connected and often contradict each other. Unfortunately none of the existing classifications are generally accepted and almost all of them are incompatible:

Phanerozoic: Haeckel (1887), Deflandre (1952a, 1953); Khabakov *et al.* (1959), Chedija (1959), Riedel (1967), Petrushevskaya (1986), Nazarov and Petrushevskaya (1995), De Wever *et al.* (2001); Afanasieva and Amon (2002, 2003a, 2003b);

Cenozoic: Dogel (1951), Hollande and Enjumet (1960), Petrushevskaya (1971, 1979, 1984, 1986), Tochilina (1996, 1997), Boltovskoy (1998);

Mesozoic: Zhamoida and Kozlova (1971), Lipman (1979), Pessagno (1973, 1976, 1977), Kozur and Mostler (1984), Dumitrica (1984, 1995); Bragin *et al.* (1999), Amon (1997, 2000c), Vishnevskaya (2001);

Paleozoic: Nazarov (1975, 1984, 1988), Nazarov and Ormiston (1984); Amon (1997, 1999a, 2000a, 2000b), Afanasieva (1999, 2000a, 2000b, 2002).

Just a few attempts were made to create a *uniform* classification of Phanerozoic radiolarians, including radiolarians from all geological periods and the Recent. The problem of the uniform classification for Radiolaria remains unresolved.

At the same time, Zhamoida (1967) wrote that the general system of the Phanerozoic Radiolaria should be based primarily on extant members. The symmetry of the skeleton is the most accurate basis for a general system of Radiolaria. Because the radial growth of spherical radiolarians from the center is supported by modern representatives, the appearance of adults depends on the main trends (vectors) of this growth. In addition, studies of modern species have shown that the structure of the skeleton and its elements are the most important characters of various taxonomic ranks.

This is very useful for paleontologists who have only skeletal remains to deal with. It is possible that the conservative nature of many radiolarian genera is only superficial and only reflects the extent of our knowledge of them (Zhamoida, 1967). The nature of fossil material restricts the possibility of its comprehensive study, although studying fossils is the only way to trace the evolution of taxa in time, or to verify phylogenetic reconstructions, which are the basis of all natural taxonomies.

CHAPTER 2. MORPHOLOGY OF RADIOLARIA

The shape of radiolarian skeletons is incredibly diverse and intricate. The morphologies exploited by radiolarians include spheres, icosahedrons, dodecahedrons, cylinders, cones, ellipsoids, discs, triangles, propellers, and many other peculiar shapes with varying numbers of different spines. This is even more surprising taking into account that they belong to the Protozoa, i.e., their body is made of a single cell, and they do not have specific anatomical tissues typical of the Metazoa.

CYTOPLASMIC STRUCTURES AND POSITION OF THE SKELETON IN THE CELL

The central capsule separating the endo- and ectoplasm of Polycystina and Phaeodaria is an important element of the radiolarian cell. Anderson (1983) attached great importance to this differentiation of the cytoplasm in radiolarians and considered it to be a specific stage in the specialization of the Protozoa.

Central Capsule

The membrane surrounding the central capsule is 60–80 nm thick and is composed of several glycoprotein layers with finely porous plates of irregular shape. A complex structure called the fusule is formed in the membrane of the central capsule to let out the axonemes of the axopodia (Hollande *et al.*, 1970; Petrushevskaya, 1986). The central capsule is destroyed immediately after the death of the organism.

Endoplasm

The endoplasm contains the nucleus, ribosomes, mitochondria, Golgi bodies, and endoplasmic reticulum. It usually has digestive vacuoles, concretions, and vacuoles storing lipid droplets. Remains of the food pigments responsible for specific coloring also float in endoplasm. The central capsules of many radiolarians are pink while the organism is alive (Anderson, 1983), or reddish brown, yellowish, or orange (Boltovskoy, 1998). This coloring allows live individuals to be distinguished from dead ones, which are not colored in this way (Boltovskoy, 1998).

Types of Cell Construction and Their Relationships with the Primary Radiolarian Skeleton

The primary skeleton of radiolarians is an integral construction composed of (1) an internal framework (hollow sphere, polyhedron, or spicule), with radiating rays and (2) a primary inner sphere that develops on the rays of the internal framework.

Two groups of the nucleoaxopodial apparatus of radiolarian cells are recognized based on the arrangement of organelles in the endoplasm in relation to the primary skeletal elements (Hollande and Enjumet, 1960; Cachon and Cachon, 1971, 1976a, 1976b; Petrushevskaya, 1986).

Exoaxoplastidy (Collodaria and Phaeodaria): the axonemes do not penetrate deep into the endoplasm. The axoplast, where the axonemes originate, is located near the central capsule (Fig. 1a).

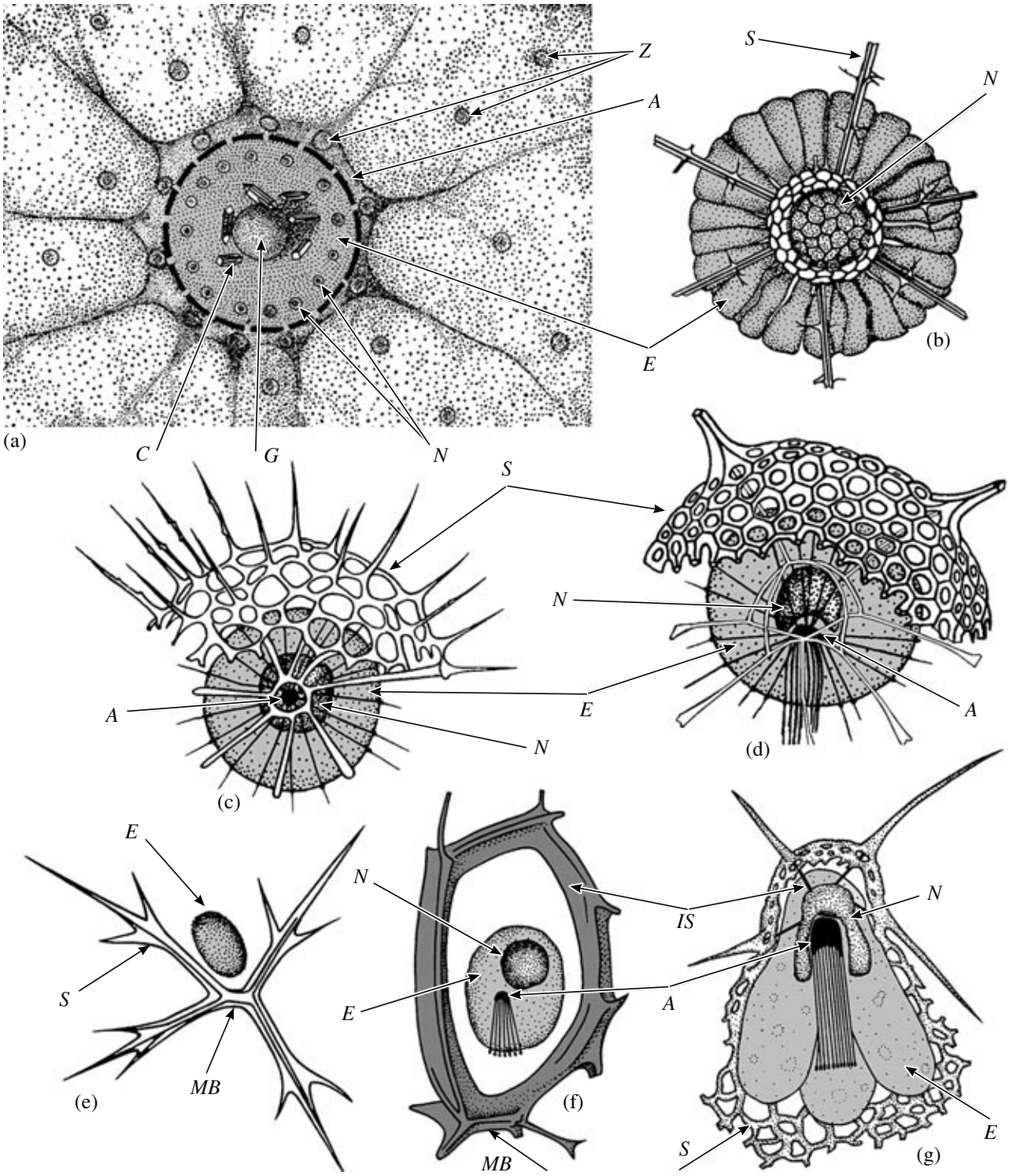

Fig. 1. Types of the nucleoaxopodial complexes of Polycystina: (a) exoaxoplastidy; (b–g) endoaxoplastidy: (b) cryptoaxoplastidy (anaxoplastidy), (c) centraxopastidy, (d) periaxoplastidy, (e, f) apoxoplastidy, and (g) proaxoplastidy. Designations: (*A*) axoplast and axopodia, (*C*) celestine crystals ($SrSO_4$), (*E*) endoplasm of the central capsule, (*G*) lipid droplet, (*IS*) spicule, (*MB*) median bar, (*S*) skeleton, (*N*) nucleus, and (*Z*) zooxanthellae.

Endoaxoplastidy (almost all Polycystina): the axonemes penetrate into the endoplasm, and often in the nucleus. Five types of nucleoaxopodial complexes are recognized (Figs. 1b–1g).

Cryptoaxoplastidy (anaxoplastidy). Instead of one axoplast, each axoneme is anchored outside the nucleus in numerous axoplasts. If the primary inner sphere is 60–100 μm in diameter (Fig. 1b), the spherical nucleus

does not contact it. In cases where the diameter of the primary sphere is small (less than 25 μm), it lies near the nucleus or cuts into the nucleus and divides it into lobes. Anaxoplastidy is observed in some Astrosphaeridae and many heliozoans.

Centraxoplastidy. A single axoplast is in the middle of the nucleus, while the axonemes penetrate the nucleus (Fig. 1c). The axopodial system, nucleus, central capsule, and the skeleton exhibit radial symmetry. The primary inner sphere of the skeleton, 15–40 μm in diameter, is located inside the nucleus. "As a radiolarian grows, the nucleus greatly increases in size. It embraces adjacent skeletal elements, which from now find themselves inside the nucleus" (Petrushevskaya, 1986, p. 56). Centraxoplastidy is characteristic of sphaerellarians and many heliozoans. Possibly, centraxoplastidy was typical of ancient Sphaerellaria, Spumellaria, and Stauraxonaria.

Periaxoplastidy. A single axoplast lies in the cup-like depression of the nucleus. The axonemes extend as a single bunch sideways, whereas singular threads radiate along the other radii (Fig. 1d). The axopodial system, nucleus, central capsule, and the skeleton are arranged heteropolarly. The diameter of the primary inner sphere is at least 30 μm. The extant sphaerellarians Hexastylinae are built in this way. Among the fossil radiolarians, a similar type of axoplastidy could have been developed in ancient nassellarians of the order Pylomariata (superfamilies Pylentonemoidea and Cessipyloroidea).

Apoaxoplastidy. A single axoplast lies either separately from, or near to the nucleus, sometimes even in the nucleus depression, but never contacting the nucleus (Figs. 1e, 1f). The axonemes, the mutual position of the nucleus and the axoplast, the entire central capsule, and the skeleton are arranged heteropolarly, even with some inclination to bilateral symmetry. The diameter of the primary inner sphere of the skeleton is 30–50 μm or even bigger. The apoaxoplastidy is observed in many spiny radiolarians of the order Fasciculata (family Plagiacanthidae) and nassellarians of the order Spyridinata.

Proaxoplastidy. The axoplast is in immediate contact with the nucleus and lies between its lobes next to the median bar of the inner spicule (Fig. 1g). The axopodial system, nucleus, central capsule, and the skeleton are distinctly heteropolar, sometimes with elements of triradiate and/or bilateral symmetry. The diameter of the first division of the skeleton (cephalis) does not usually exceed 30 μm. If the nucleus is not in the cephalis, but in the distal, wider region, the axoplast will still reside next to the median bar. This structure is typical of the majority of Mesozoic and Cenozoic nassellarians and apparently of ancient nassellarians from the order Pylomariata (superfamilies Proventocitoidea and Popofskyelloidea).

It is generally believed that the localization of the axoplast is a high-level taxonomic character (distinguishing orders or superfamilies) (Petrushevskaya, 1981a, 1986; Nazarov, 1988; etc.). Exoaxoplastidy is supposedly more primitive, while cryptoaxoplastidy, centraxoplastidy, periaxoplastidy, apoaxoplastidy, and proaxoplastidy are produced by the specialization of the endoaxoplastidian arrangement. On the other hand, details of the nucleoaxopodial system cannot be determined in fossils because they are not preserved. Hence, taxonomy based on the nucleoaxopodial system should be treated with great caution.

Radiolarian Skeleton

Radiolarians are very small, and most cannot be seen with the naked eye. The size of their living cell varies from several dozen μm to 1–3 mm, the average being 100–800 μm. The mineral skeleton lies inside the cytoplasm.

Chemical analysis of the opaline skeletons of Polycystina showed the presence of 98% of amorphous $SiO_2 \cdot nH_2O$ (Hurd and Takahashi, 1981; Petrushevskaya, 1981a; Takahashi and Honjo, 1981) with small amounts (1 to 4%) of Mg, Ca, Al, Na (Anderson, 1983).[3] Spectral analysis of the skeletons of Phaeodaria revealed the predominance of $SiO_2 \cdot nH_2O$, then, Al and up to 1% Mg and Ca (Reshetnyak, 1966).

"However, different the skeletons of radiolarians may be, the external structure that floats in the water is just a spherical, ellipsoid, or slightly depressed bubble of cytoplasm with many ciliary axopodia" (Petrushevskaya, 1986, p. 49). Only the ends of the longest spines may stick out of the cytoplasm, but even in this case, the ends are covered by an uninterrupted membrane. The radiolarian skeleton is always internal. It is not in contact with sea water and, therefore, it is not dissolved during the cell's life. Ultramicroscopic studies showed that even the parts of the skeleton that extend far outwards (mainly radial rays, or lobes) are covered by a continuous film of ectoplasm capable of regeneration of impaired parts of the skeleton (Anderson, 1983; Petrushevskaya, 1986).

The main physiological function of the skeleton is supporting the cytoplasmic body of a radiolarian and, hence, defining its entire shape. Parts of the skeletal structure support endo- and ectoplasm and axopodia. At the same time, skeletal constructions facilitate the segmentation of the polyploid nucleus and central capsule (Fig. 1), thus, intensifying the cell's metabolism (Anderson, 1983; Petrushevskaya, 1986). Anderson (1983) described the central capsule and mineral skeleton, comparing them to a stage on which physiological processes were performed.

For instance, the intensive development of small thorns and apophyses, which is characteristic of various skeletal elements (spines, bars, rods, etc.), apparently

[3] Hence, the statement of de Wever *et al*. (2001, p. 10) that "The skeleton of polycystine radiolarians is made of pure silica (SiO_2, nH_2O)" needs revision.

precludes the cytoplasm from displacement. The study of Recent Radiolaria revealed a pattern according to which, if the main skeleton is more than 150–300 μm in diameter, the radial spines are short (200–300 μm). If the skeleton's diameter is only several tens microns, the spine may reach 1200 μm. The space occupied by a single organism remains approximately the same, whereas the weight of the body varies (Anderson, 1980, 1981, 1983). Long spines and the complex lattice shells of the skeleton are natural bases for more supporting points, from where the cytoplasmic flows begin and where the biochemical base for the increased expandability and strength while catching food is provided (Anderson, 1984).

In addition, because the spines are used by the pseudopodia as axes, their number and position are fixed and defined by the fusules of the membranes of the central capsule. This position is characteristic of each taxon and indicates existing relationships between the cell and skeleton structure (De Wever *et al.*, 2001).

APPEARANCE OF SILICEOUS SKELETONS OF RADIOLARIA

The skeleton of Radiolaria is composed of opal ($SiO_2 \cdot nH_2O$), whereas the shell of their closest relatives Acantharia is built from celestine ($SrSO_4$). Interestingly, in all radiolarians, the skeleton begins its development ***outside*** the central capsule and surrounds it, whereas in Acantharia, the first incipient skeletal elements in a shape of centrally convergent short spines appear ***inside*** the central capsule.

As early as 1858, Müller (1858) described the presence of many crystals up to 50 μm in size (Fig. 1a) in the central capsule of the siliceous skeleton in the colonial radiolarians of the genus *Collosphaera* (Collodaria). These crystals were very similar to the crystals of celestine, which was supported by the size of the interplanar angles 103–105° in biocrystals and 104°50′ in celestine, and by chemical reactions. Haeckel (1862) also pointed out that from 5 to 30 crystals were present inside the central capsule of *Collosphaera*. He noted that they are strikingly similar in shape to celestite crystals, with characteristic interplanar angles of 103–105°. However, these facts were overlooked by subsequent workers, until Dogel (1950) suggested a joint ancestor for all radiolarians and acantharians that was supposedly close to collodarians. The further differentiation of protists took place in two directions: "Some groups lost the ability to synthesize $SrSO_4$ and became purely siliceous, others (Acantharia), in contrast, lost the ability to synthesize opal and became celestine-secreting organisms" (Dogel, 1950, p. 563).

The analysis of the evolution of the skeleton of Radiolaria and Acantharia and further development of Dogel's ideas suggests a different hypothesis of the origin and evolution of the siliceous skeleton of Radiolaria, which is of great phylogenetic importance (Afanasieva and Vishnevskaya, 1992; Afanasieva, 1993b, 1994, 2000a).

In the course of evolution, the early ancestors of radiolarians and acantharians began to build their shells from celestine. Perhaps, the sulfate-rich waters of ancient seas were more favorable for the synthesis of $SrSO_4$. This event was recorded genetically in Acantharia and led to the formation of the celestine skeleton, which was apparently retained throughout the Phanerozoic. Mikryukov (2000a, 2000b) suggested that the skeletons of early protists could be based on metabolic products such as crystals of some mineral salts, the ions of which were abundant in Paleozoic seas. Such crystals are deposited by many extant marine protists, and may also have been deposited by their sedentary ancestors. Celestite (strontium sulfate) could have been such a salt. Spores of extant radiolarians have a large crystal of strontium sulfate (Hollande and Martoja, 1974), which increases their similarity with Acantharia. Celestine crystals are also found in the cytoplasm of flagellate radiolarians (Mikryukov, 2000b).

In their further evolution, radiolarians apparently discontinued using strontium sulfate ($SrSO_4$) and began to synthesize opal ($SiO_2 \cdot nH_2O$), a hard gel of siliceous acid. Traces of this unusual transition to a completely new chemical basis of the skeleton (from a salt to a gel of an acid) can be observed today in the shells of the Collodaria radiolarians (genus *Collosphaera*). They are able to deposit both opal and celestite in their skeleton. In *Collosphaera*, crystals of the celestine type are formed inside the central capsule (Fig. 1a), i.e., in the zone where acantharians have a bunch of skeletal spines. It is possible that Radiolaria lost the ability to synthesize $SrSO_4$ and became strictly opaline.

The hypothetical common ancestors of all radiolarians could have been organisms with a celestine skeleton resembling that of Acantharia. The presence of celestine crystals in the cells of particular radiolarian taxa (Collodaria) suggests that the earliest members of Radiolaria had a celestine skeleton, which was subsequently replaced by an opaline skeleton (Mikryukov, 2000b).

BIOMINERALIZATION OF THE SKELETON

Living organisms and minerals are the most complex and structurally perfect hierarchic systems of the material world. They are the only independent objects whose morphology and function are determined mainly by internal rather than external factors. Therefore, the study of biomineral interrelations is of fundamental importance in a complex system of geological and paleontological sciences. Examination of biogenic mineral formation in extant and extinct organisms is presently one of the most important fields of biomineralogical studies (Yushkin, 1996).

Matrix biomineralization first appeared in ancient prokaryotes as early as the Cryptozoic. It became wide-

spread by the end of the Precambrian when unicellular and multicellular organisms (eukaryotes) acquired skeletons, and thus became a pinnacle in the evolution of the organic world (Sokolov, 1976, 1977; Rozanov, 1986, 1989).

The main principle of matrix biomineralization is that the development of any skeleton is controlled by previously formed organic matrix, which serves as a cast of the shell to be formed and which provides its development as a single, hard structure through the interactions of the organic and mineral skeletal components. It is also important that different organisms have different composition of organic matrices and different processes of their mineralization. In addition, the presence of a hierarchy of interrelated structural units in the skeletons of all organisms, including vertebrates, is now generally accepted (Barskov, 1975, 1982, 1984; Lowenstam, 1981, 1984; Golubev, 1981, 1984, 1987; Afanasieva, 1982, 1988, 1990a, 1990b, 1996, 1997b, 2000a; Mutvei, 1984; Barskov *et al.*, 1996). For instance, the mineralization of the calcareous skeletons of Coccolithophorales, Foraminifa, Radiolaria, and Mollusca begins from the appearance of small primary crystallites in the organic matrix of the future shell, which are progressively grouped in larger crystallite units.

Mineralization of the calcareous shells of Foraminifa begins from the appearance of small primary crystallites (isolated centers of crystallization) in the organic matrix of the future shell. These crystallites are observed with crossed nicols of the optical microscope as bright dots (Fig. 2a) (Bellemo, 1974; Angell, 1979). Gradually, primary crystallites are grouped into larger crystalline units *D*, *C*, *B*, *A* (Fig. 2; Pl. 1, figs. 1–9) (Afanasieva, 1982). The smallest rhombic units *D* are grouped together to form a column of the crystalline unites *C*. Units *C* constitute crystalline units *B*, which are in turn combined in units *A*. Units *A* and *B* are recognized within the previously proposed single element of the ultrastructure of the wall referred to as *crystalline unit* (Hansen, 1970; Bellemo, 1974).

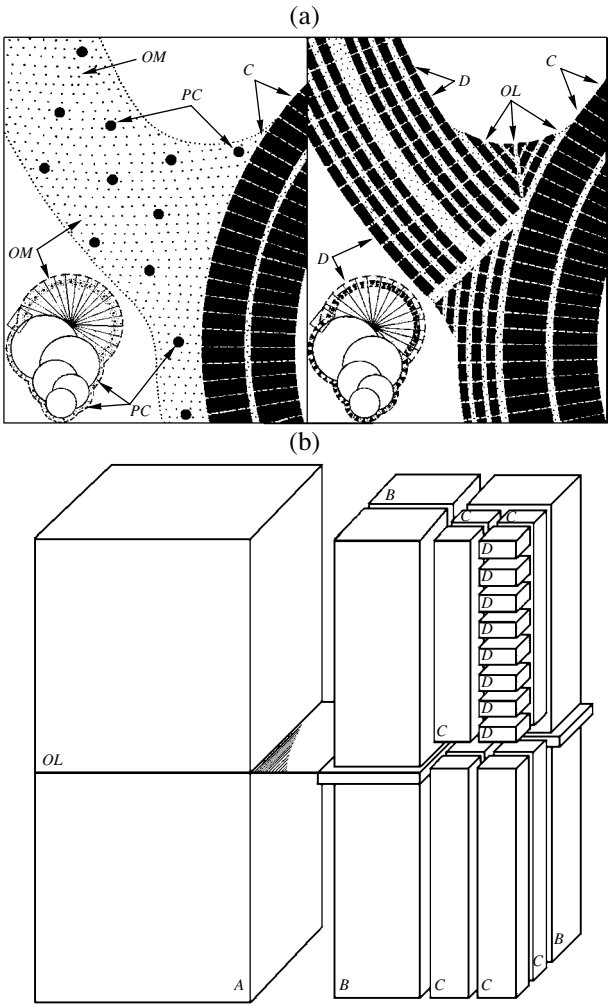

Fig. 2. Ultrastructural crystalline units in the foraminiferal test wall (after Afanasieva, 1982): (a) initial stages of formation shell wall, (b) scheme of ultrastructural calcareous units *A*, *B*, *C*, *D* of test wall in a hierarchic succession. Designations: (*OL*) organic lamella, (*OM*) organic matrix, and (*PC*) primary crystallites.

Each skeletal element, from an elementary crystal to the layers of the shell wall and entire skeleton, is surrounded by the residual nonmineralized organic matrix. The larger the structural skeletal element, the thicker and more complex are the organic lamellae embracing it, including very complex sheaths of prisms in mollusks (Barskov, 1975, 1982, 1984; Golubev, 1981, 1984, 1987). The resulting structure resembles cemented brick layers. The actual strength of the skeleton is largely determined by the energy of binding of organic and mineral components.

This combination of organic and mineral components of the skeleton is apparently the suggested "tool essential for survival, which prevents complete lithification" foreseen by recognized crystallographer Belov (1976, p. 287). Belov did not study biomineralization, but emphasized that organisms should have a mechanism to interrupt mineralization when necessary. The residual organic matrix, usually constituting 20–30% of the skeletons of living organisms, prevents the contact and fusion of neighboring mineral units (Golubev, 1981, 1987). This residual, nonmineralized matrix apparently represents a sort of conserving matter facilitating the retention of the latent primary structure of the skeleton throughout long geological time.

The crystallographic studies of Galiulin (1996a, 1996b) showed that, if the inner geometry of the incipient crystal coincides with the geometry of the space in which it is growing, the structure continues growing for some time. However, the space, in particular, the space of the organic matrix of skeletons is nonhomogeneous, and to attach the next atom, the crystal should prepare the space for it. Therefore, in the process of growth, the crystal changes the curvature of the space (Kuz'menkov, 1977; Galiulin, 1994). For a crystal to grow it is

Plate 1

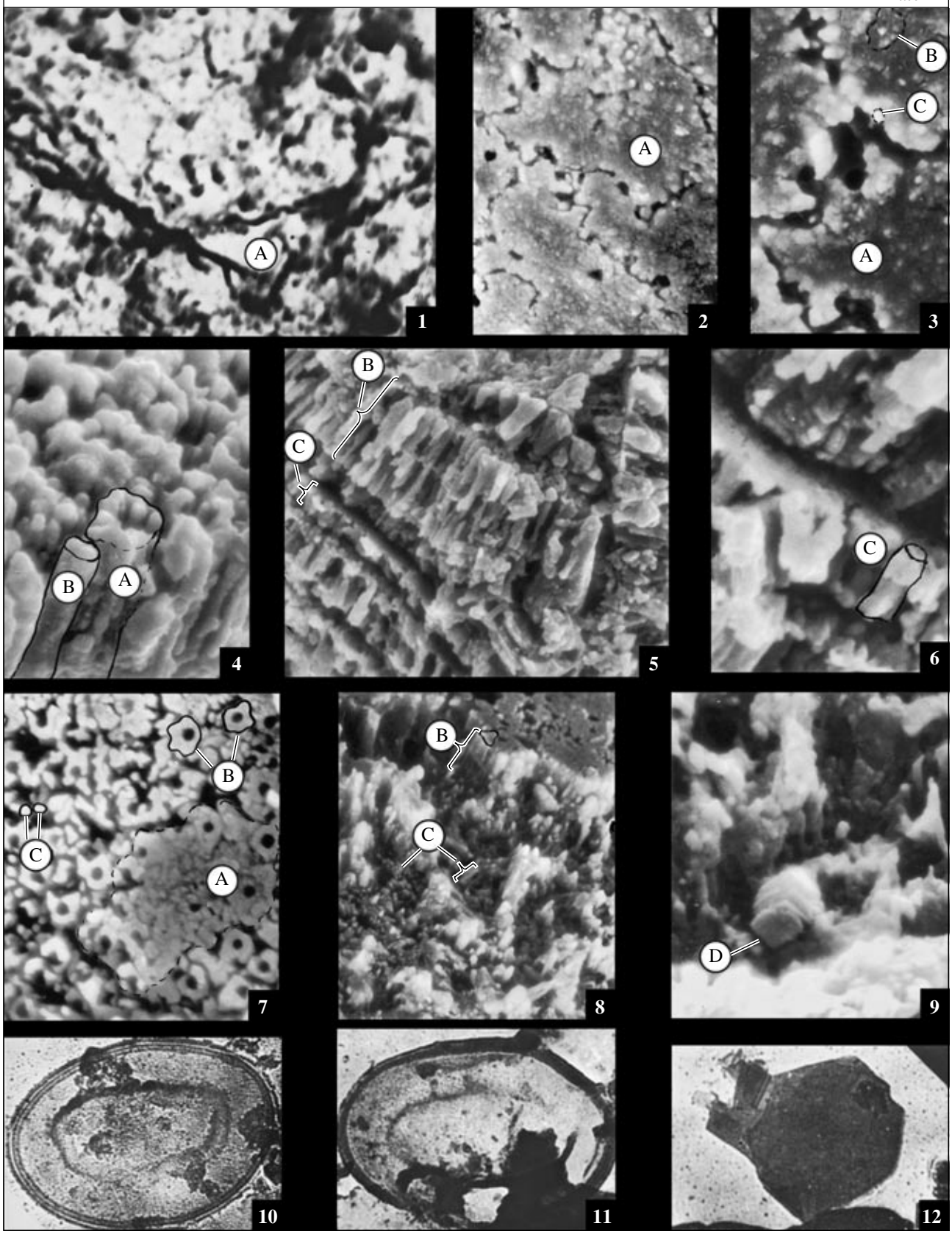

Crystalline units of the ultrastructure of the shell wall of foraminifers (1–9) and polysaccharide plates (10–12).

sufficient that its structure should be combinatorially regular. "If this combinatorial regularity could be maintained, nothing could prevent the combination of the entire macrocosm in a single crystal. However, the combinatorial regularity is unstable because it is always reduced to metric regularity, which is not compatible with the changing curvature of the space. In contrast to crystals, living organisms are not so strongly predetermined. The absence of determination is revealed by mutations, which eliminate the tensions between the growing structure and the space. However, the main difference between life and crystals is the unpredictability of the latter, and the unavoidable presence of irrational elements" (Galiulin, 1996b, pp. 103–104).

Structural Levels of Skeleton Organization

The final shape and structure of the skeleton result from the combination of two major factors, abiogenic and biogenic. Primary hydrated SiO_2 is received by the radiolarian cell from the sea water. Only a truly dissolved monomer of orthosilicic acid can enter the cell. This is a flexible building material abundant in the hydrosphere and lithosphere.

Globular silica of the organic matrix of radiolarian skeletons can be regarded as a generation of SiO_2, which was produced by the orthosilicic acid in its transition from a molecular-dispersed state to a colloid. The process of skeletal growth in the radiolarian cell is regulated by the cytobiogeochemical reactions managed by the Golgi bodies. The interaction of the living and mineral system does not allow SiO_2 to be fully crystallized as in minerals.

The interaction of the mineral and biogenic factors occurs at five levels: molecular, nano-, ultra-, micro-, and macrolevels (Afanasieva and Amon, 2004a, 2004c). This conventional succession represents a size increase in the particles and structures of a skeleton, and at the same time, the increase in the effect of the biogenic factor.

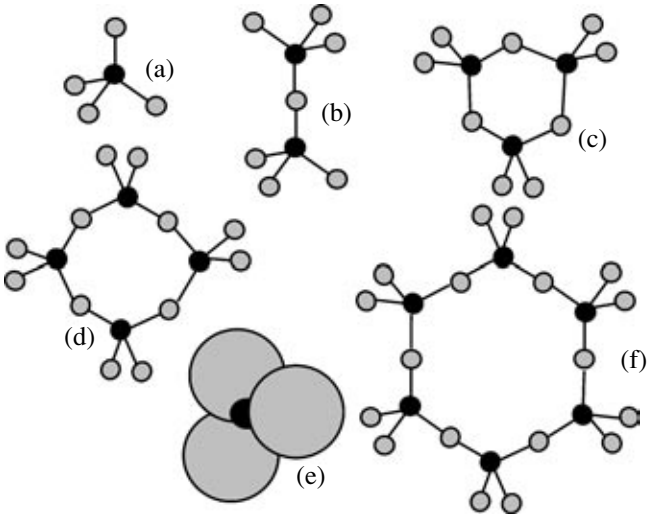

Fig. 3. The main silicaoxygeneous tetrahedron [SiO_4] and complex final groups of tetrahedrons (after Kukolev, 1966): (a) $(SiO_4)^{4-}$, orthogroup; (b) $(Si_2O_7)^{6-}$, diorthogroup; (c) $(Si_3O_9)^{6-}$; (d) $(Si_4O_{12})^{8-}$; (e) $(Si_6O_{12})^{12-}$; (f) densely packed tetrahedral groups O^{2-} around Si^{4+} in the most dense cubic packing. Black color marks the atom of silicon.

The molecular level is almost entirely determined by characteristics of the atoms of Si and O and the energy of the Si–O bond. Due to the crystallochemical properties of SiO_2, the mineral matter is always spatially structured as chains, bands, and layers at the molecular level (Fig. 3).

The nanolevel determines the appearance of primary particles (micelles) of the polymerized silica sol. It is important that micelles are capable of spontaneous growth and increase in molecular weight, and of development of reticulate structures. The ability of SiO_2 sol to grow flat and three-dimensional forms is retained at the nanolevel. The role of the biogenic factor at the nanolevel is small and is mainly related to the geneti-

Explanation of Plate 1

Fig. 1. *Bolivina dilitata* Reuss, Mediterranean Sea, Malta Channel, depth of 400 m, station 13 (depth 150–160 cm), Upper Würm, etched for 20 min. in 10% KOH, external surface of the middle part of the shell, crystalline units A (transmission electron microscopy, scale bar = 1 μm).

Figs. 2, 3, and 9. *Uvigerina mediterranea* Hofker, Tyrrhenian Sea, depth of 770 m, station 25: (2, 3) range 140–150 cm, Upper Würm, etched for 20 min. in 10% KOH, external surface of the middle part of the shell, crystalline units A, B, C: (2) bar = 10 μm; (3) fragment, bar = 5 μm; and (9) range 100–110 cm, Holocene, etched for 40 min. in 10% KOH, external surface of the middle part of the shell, crystalline units D (bar = 2 μm).

Figs. 4 and 8. *Bulimina marginata* d'Orbigny, Mediterranean Sea, Gulf of Sidra, depth of 1000 m, station 4, Upper Würm: (4) range 200–210 cm, etched for 20 min. in 10% KOH, external surface and split of a wall of the last eighth chambers, crystalline units A, B (bar = 5 μm); (8) range 160–170 cm, etched for 40 min. in 10% KOH, external surface of the distal part of the shell, crystalline units B, C (bar = 15 μm).

Figs. 5–7. *Bulimina gibba* Fornasini, Mediterranean Sea, Gulf of Lion, depth of 260 m, station 24, Upper Würm: (5, 6) range 53–55 cm, etched for 20 min. in 10% KOH, split of a wall at the joint between the initial and fourth chambers, crystalline units B, C: (5) bar = 15 μm, (6) fragment, crystalline units C (bar = 5 μm); and (7) range 60–62 cm, etched for 40 min. in 10% KOH, middle part of the shell, surface of an additional layer, crystalline units A, B, C (bar = 5 μm).

Figs. 10–12. Polysaccharide plates (photographs placed at our disposal by S.N. Golubev): (10) cyanobacterium *Mastigocladus* sp. (transmission electron microscopy, bar = 0.4 μm); (11) brachiopod *Pictothyris* sp. (transmission electron microscopy, bar = 0.4 μm); and (12) shield of a turtle (transmission electron microscopy, bar = 1.4 μm).

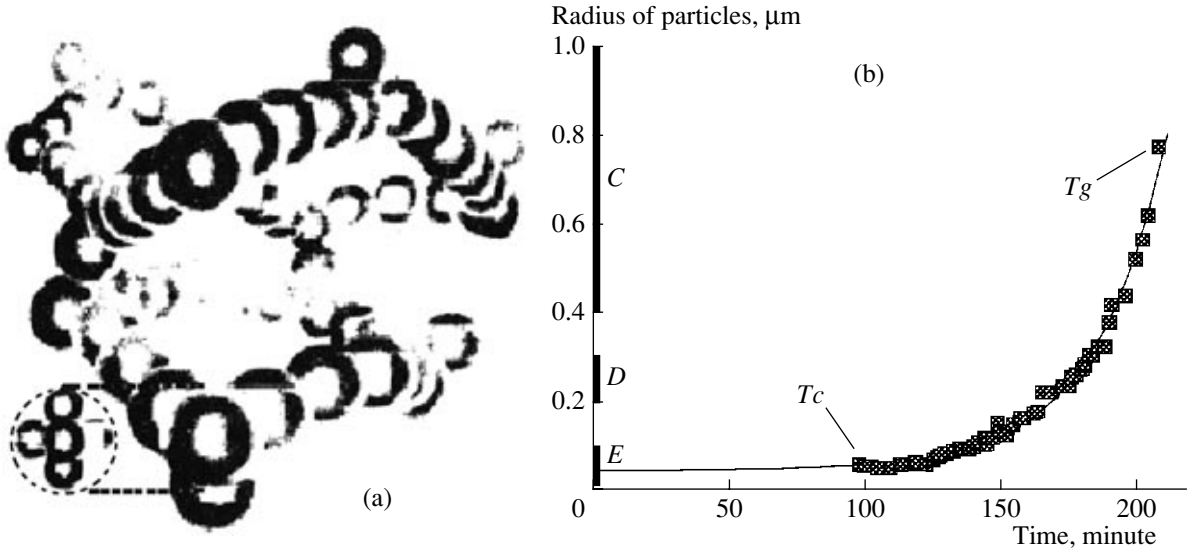

Fig. 4. Characteristic features of the gelation process: (a) an electronic photograph of chains forming gel structure (Fricke, 1988); (b) time dependence of average radius of sol particles (Popov and Tikhonov, 1996). Designations: (*Tg*) critical point of gelation, (*Tc*) critical point of reaction outcome; (*C*, *D*, *E*) ultrastructural silicic units of radiolarian test wall (Afanasieva, 2000a).

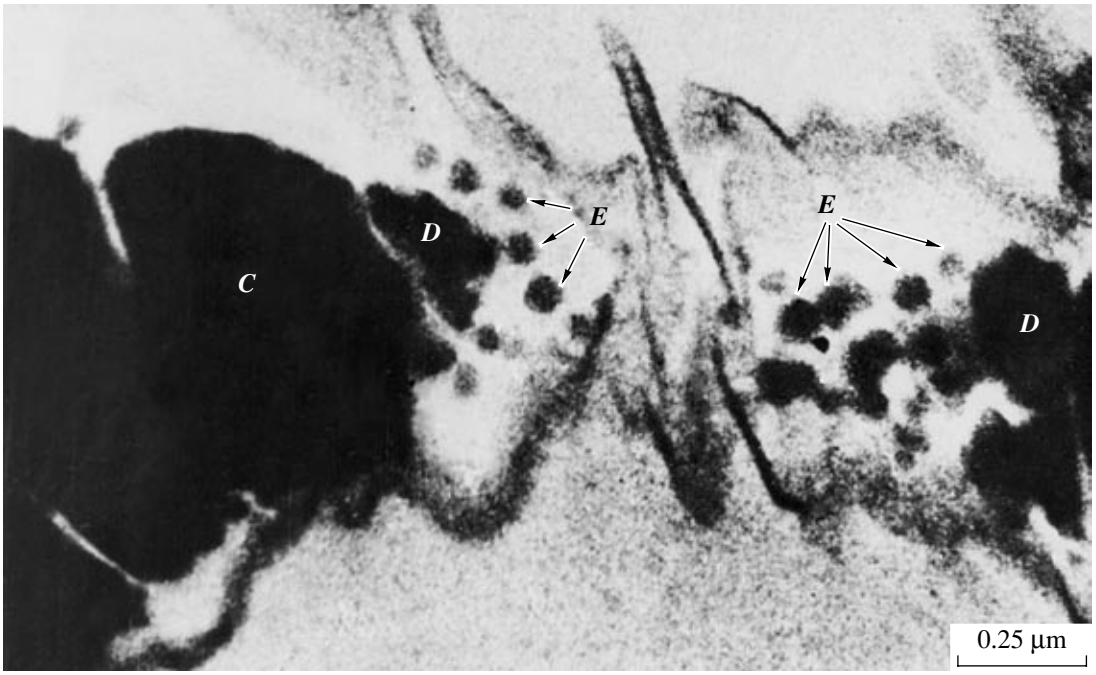

Fig. 5. Primary opal globules in the ultrathin section of living radiolarians in TEM (after Anderson, 1981, text-figs. 13-14); (*C*, *D*, *E*) crystalline elements of the skeletal ultrastructure.

cally predetermined choice of building material. This material potentially allows the production of complete skeletal constructions of any shape.

The ultralevel reflects the beginning of the production of the radiolarian skeleton according to the predetermined genetic program. It begins from a moment when primary globules of gel (Fig. 4) of polymerized silica 3–6 nm in size become able to form a sorption monolayer and become regulated by the cytobiochemical medium. At the first stage of the biomineralizaon of the radiolarian skeleton, primary globules of the amorphous opal *E* (Figs. 5, 6a) appear on the hexagonal sheaths of the organic matrix. Globules *E* are gradually grouped in the larger, hierarchically interrelated ultrastructural skeletal elements *D*, *C*, *B*, and *A*, each surrounded by organic lamellae (Fig. 6b). It is important

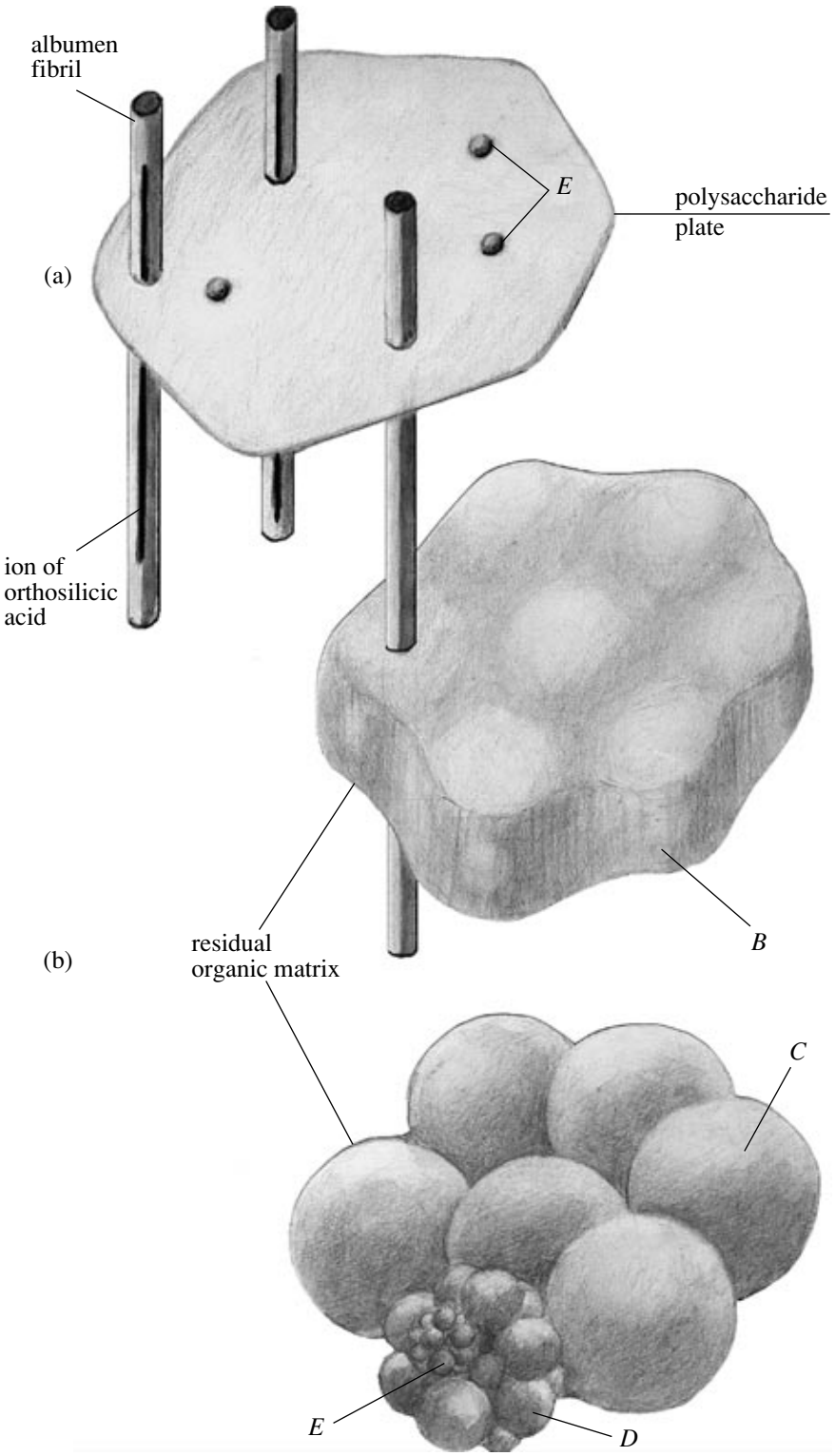

Fig. 6. Hypothetical model of radiolarian test biomineralization: (a) initial stage of skeleton biomineralization (after Golubev, 1987); (b) ultrastructural skeleton units in hierarchic succession (after Afanasieva, 1990a, 1990b); (*B*, *C*, *D*, *E*) ultrastructural silica units of the test wall.

that the skeletal growth is matrix-produced, because the process of biomineralization is controlled by the organic matrix, which is typical of all skeletal organisms (Afanasieva, 1990a, 1990b, 2000a).

The microlevel determines the development of the constituent morphological elements of the skeletal structure, which have taxonomic importance. The development of the primary four-rayed spicules of radi-

olarians is apparently defined by the structure of the primary opal, i.e., the nanolevel is revealed at the microlevel.

The macrolevel characterizes the entire radiolarian test. This level allows the classification of the high-rank taxa of Radiolaria.

The ultra-, micro-, and macrolevels are entirely under the cytobiochemical control of the organism. The crystallochemical nature of opal at these levels is inferior to its biological nature. Beginning from the ultralevel, opal, as an initial building material (now represented by biocrystals), becomes an element of a skeletal construction, which is formed by organisms according to their own targets and tasks.

A Model of the Biomineralization of the Radiolarian Skeleton

The physiology and morphology of radiolarian skeletons were for a long time partly hypothetical and speculative in the biological literature, although as early as 1887 Haeckel wrote that "It may indeed be assumed that these skeletons arise directly by a chemical metamorphosis (silicification, acanthinosis, etc.) of the pseudopodia and protoplasmic network; and this view seems especially justified in the case of the Astroid skeleton of the Acantharia, the Spongoid skeleton of the Spumellaria, the Plectoid skeleton of the Nassellaria, the Cannoid skeleton of the Phaeodaria, and several other types. On closer investigation, however, it appears yet more probable that the skeleton does not arise by direct chemical metamorphosis of the protoplasm, but by secretion from it: for when the dissolved skeletal material (silica, acanthin) passes from the fluid into the solid state, it does not appear imbedded in the plasma, but deposited from it. However, it must be borne in mind that a hard line of demarcation can scarcely, if at all, be drawn between these two processes" (Haeckel, 1887, p. 124).

However, this hypothesis did not receive further discussion, because no experimental studies were made. Only almost half a century later, Enriques (1931) again suggested that the silicification of the skeleton is biologically regulated.

The first convincing data on the biomineralization of the skeletons were received in 1971 when Jean and Monica Cachon (1971) found small vacuoles with layered membranes containing silica in the interlayers in the ectoplasm of living radiolarians. It was suggested that, at first, isolated globules 0.01–0.05 μm in size appear on the membranes. The globules were thought to merge later to form the radiolarian skeleton.

Ten years later, Anderson (1980, 1981, 1983) showed that the formation of skeletons of living Polycystina begins from the development of the organic matrix of the future skeleton (Fig. 5). It represents the organic model of the shell, defining its shape and ornamentation.

Afanasieva (1990a, 1990b) proposed a hypothetical model of biomineralization and fossilization of radiolarian skeletons based on experiments involving artificial annealing of skeletons.

Assumptions necessary to interpret biomineralization. The following three assumptions are required to gain an insight into the hypothetical model of radiolarian skeleton biomineralization and a better understanding of the process of transformation of their tests in lithogenesis:

(1) Gels have recently attracted much attention because they are widespread in organic nature in the form of biopolymers. Crystals appear and grow in gels (Demin, 1996; Rakin, 1996). Opal, a gel of orthosilicic acid ($SiO_2 \cdot nH_2O$), is a good example of such mineral growth.

Popov and Tikhonov (1996) showed that, if the development of gels is regarded as a process of appearance and evolution of a structure, the presence of critical points characterizing transitions between different structures and defining sharp changes in the macroscopic parameters of gel may be assumed (Fig. 4).

One of these is the *critical point of the reaction outcome*. The volume of sols in the first 100 minutes of the development of structural fragments of gel increased only slightly. However, when the particles of sol reached the size of a few tens of nanometers, the rate of their growth decreased, while the development of chains forming the gel structure became dominant. The electron micrograph of the silica aerogel published by Fricke (1988) clearly shows chains forming the gel structure with sol particles of about 3 nm (Fig. 4a). The point when the growth rate of particle size changes is a critical point of the reaction outcome (Popov and Tikhonov, 1996). At this point, structural fragments of the future gel, with the hydrodynamic radius described by the critical exponent, begin to grow (Fig. 4b).

Another point is referred to as the point of gelation (Fig. 4b). It defines the moment of the establishment of the macroscopic structure and indicates the qualitative modifications of the system during its quantitative changes.

If it is assumed that the SiO_2 sols are formed in the same way in the primary organic matrix of the radiolarian skeleton, the appearance of the globular opal (silica gel), which is formed in the radiolarian skeleton, may be explained to a certain extent.

(2) Laboratory experiments on the structure of the silica hydrosol by Melnik *et al.* (1973) have shown that different pH values affect the proportion of colloid to molecular soluble components of orthosilicic acid. In the alkaline medium, at pH 8.3–9.0, hydrosol SiO_2 with predominating colloid globular particles of several hundredth parts to 0.1 μm is formed.

The protoplasm of the majority of animal and plant cells contains an almost neutral mixture of acidic and alkaline substances (pH 7.0) (Villee, 1967). Therefore, it can be assumed that only a truly dissolved monomer

of the orthosilicic acid is received by the radiolarian cell from the sea water (pH 7.5–8.5). Later, ions of SiO_2 apparently proceed to the organic substance of the matrix, the pH of which should indicate a weakly alkaline medium and where the aggregation of opaline globules may take place. Therefore, the globular silica of the radiolarian skeletons can be considered as a generation of SiO_2 that was produced by the transition of the orthosilicic acid from the molecular dispersal to colloid state (Fig. 4). The presence of colloids is a typical feature of the biosphere. They are widespread in the structure of the living and mineral substances of the Earth's surface (Vernadsky, 1987).

(3) The detailed theoretical and experimental study of the organic matrix was conducted by Golubev (1987) using calcareous and siliceous skeletons of various organisms from the cyanobacteria *Mastigocladus* to Eukaryotes (tubes of the polychaete *Serpula s*p., the siliceous sponges *Hialospongia* sp. and *Euplectella aspergillum*, skeleton of the arthropod *Balanus* sp., shells of the cephalopods *Sepia* sp. and *Nautilus* sp., the bivalve *Mytilus edule*, the gastropod *Astrea rugosa*, the brachiopod *Pictothyris* sp., turtle carapace, and rib and cerebral sand of humans). He showed that the structure of any organic matrix is similar to a three-dimensional lattice composed of protein fibrils elongated vertically and of a system of polysaccharide elliptical or hexagonal plates about 1.5 μm long, which lies in a horizontal plane (Fig. 6a). These plates are formed in the Golgi bodies and become part of the organic matrix during the mineralization of the skeleton. Thereby, the law of epitaxis, for example, a directed mineralization of one matter at the surface of the other under the conditions of stereochemical interrelation of both substances (on the key–lock principle), is being realized between the organic matter of the polysaccharide plates and mineral particles. These plates control the initial orientation of the mineral particles and further formation of the skeleton. Thus, there exist obvious features of the biophysical community of appropriate mechanisms for biomineralization from prokaryotes to humans, which indicate a great similarity of biomineralization processes in the organic world. Thereby, biophysical uniformity is being realized in several chemical variants both on matrix composition and the composition of the mineral portion (Golubev, 1987).

It may be assumed, that radiolarian laminated membranes found by Cachon and Cachon (1971) in living organisms vacuoles are analogous to the hexagonal plates that have been established by Golubev (1987) in the calcareous and siliceous skeleton of various biological objects, including cyanobacteria, brachiopods, tortoise shells, etc. (Pl. 1, figs. 10–12).

Hypothetical model for the skeleton test biomineralization. Thus, based on the above assumptions and experimental and theoretical investigations of the skeletons of extant and fossil radiolarians, the following succession of the stages of biomineralization of the skeletons may be suggested (Fig. 6) (Afanasieva, 1990a, 1990b, 2000a).

(1) The process of the silicification of skeletons apparently begins from the appearance of the primary globules of silica *E* on the polysaccharide hexagonal plates of the organic matrix (Fig. 6a). The appearance of the smallest units of the skeletal ultrastructure *E* (0.01–0.15 μm) in the organic matrix corresponds to the critical point of the reaction outcome, i.e., exactly to the point where, according to Popov and Tikhonov (1996), the growth of structural elements of the future gel ($SiO_2 \cdot nH_2O$) begins (Fig. 4b).

Anderson (1981, text-fig. 13-14) discovered similar globules under transmission electron microscope in the ultrathin sections of living radiolarians in the form of rounded dark spots approximately 0.08 μm in size (Fig. 5). In addition, according to Bjørklund and Goll (1986), a smooth surface of the skeletons of living radiolarians is formed by the thin layer of epivitrium approximately 0.75 μm thick, which apparently also consists of primary opaline globules *E*.

SEM studies of the skeletons of the Early Permian (Artinskian) radiolarians *Bientactinosphaera strangulata* (Nazarov et Ormiston) and *Ruzhencevispongus plumatus* Nazarov et Ormiston showed the presence of the primary globules *E* in a shape of the smallest grains of silica 0.06–0.15 μm in size on the surface of the fossilized skeletons (Pl. 2, fig. 4; Pl. 3, figs. 2–4) (Afanasieva, 1990a, 1990b, 2000a).

(2) At the following stage, the primary globules *E* of silica are for the first time merged into larger ultrastructural units *D* (Figs. 5, 6b). The appearance of the units *D* corresponds to the interval between the two critical points (the point of the reaction outcome and the point of gelation) (Fig. 4b). In the ultrathin sections of extant radiolarians (Bjørklund and Goll, 1986) and on the surface of fossil skeletons (Afanasieva, 1990a, 1990b, 2000a), the size of globules *D* is 0.2–0.3 μm (Pl. 2, fig. 4; Pl. 3, figs. 2–4).

(3) Later, isolated globules *D* are combined in larger ultrastructural units, globules *C*, from 0.4 to 1 μm in size (Figs. 5, 6b). This modification of the skeleton is apparently connected with the point of gelation (Fig. 4b). When the silicification of the skeleton of extant radiolarians was relatively slow, primary globules *E* filled the spaces between globules *C* (Bjørklund and Goll, 1986, text-figs. 13–14).

In Early Permian radiolarians, fossilized globules *C* are readily observed on the skeleton's surface and on the costae (Pl. 2, figs. 2–4; Pl. 3, figs. 2–5). In these cases, it can be seen that globules *C* comprise *D*, which are in turn composed of primary globules *E*. In addition, the inner surface of the pores of *Bientactinosphaera strangulata* (Nazarov et Ormiston) and *Ruzhencevispongus plumatus* Nazarov et Ormiston has two or three layers 0.6 μm each, constituting the skeletal wall and comparable in size with globules *C* (Pl. 2, fig. 3; Pl. 3, figs. 2–5).

Plate 2

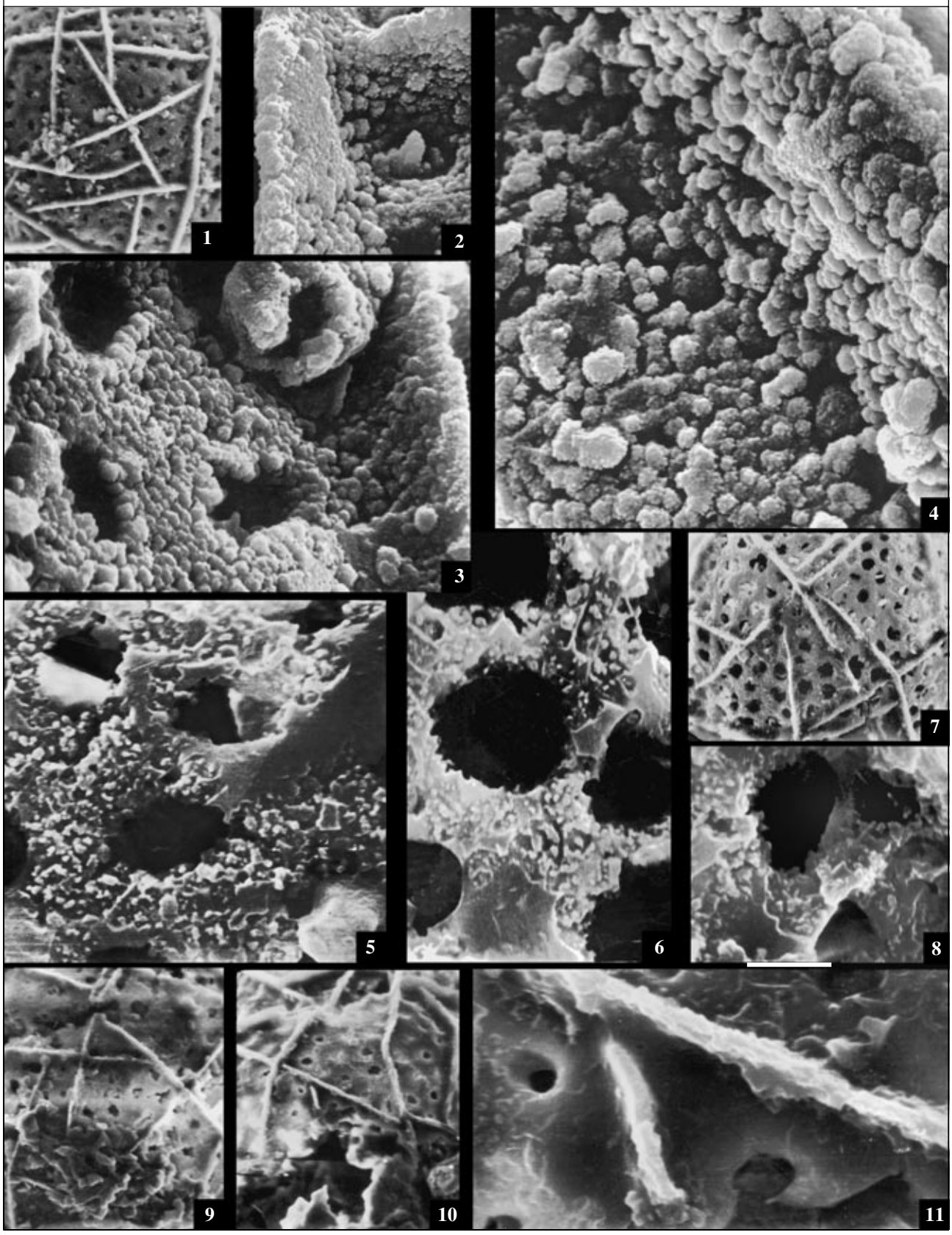

Simulation of the fossilization process in skeletons of Early Permian radiolarians by the example of *Bientactinosphaera strangulata.*

Table 2. Ultrastructural mineral units of coccolithophorid, foraminiferal, and radiolarian skeletons (in μm)

Mineral unit	Coccolithophorales	Foraminifa	Radiolaria		
	Golubev, 1981, 1987	Afanasieva, 1982	Cachon and Cachon, 1971	Anderson, 1981	Afanasieva, 1990, 2000a
A	–	2–9	–	–	3–8
B	~1.5	0.6–2	–	–	1–3
C	–	0.2–0.6	–	0.5–0.08	0.4–1
D	–	$0.6 \times 0.6 \times 0.05$	–	0.2–0.3	0.2–0.3
E	0.01–0.05	–	0.01–0.05	0.08	0.06–0.15

(4) Further mineralization proceeds through the aggregation of globules *C* into ultrastructural units *B*, which are isometric plates, often hexagonal in shape (Fig. 6b). The diameter of plates *B* ranges from 1 to 3 μm, while their thickness equals the size of globules *C*. Structural units *B* were observed on the surface of the skeletons of the Early Permian *Bientactinosphaera strangulata* (Nazarov et Ormiston) (Pl. 2, figs. 3, 4). They are comparable in size with the hexagonal polysaccharide plates (Figs. 6a, 6b), while their shape is probably derivative of "regulated" biomineralization of the skeleton.

(5) The largest ultrastructural skeletal elements *A* (3–10 μm in diameter) were discovered in the course of the thermal preparation of the skeletons of the Early Permian *Ruzhencevispongus plumatus* Nazarov et Ormiston (Pl. 3, figs. 6–8), which cracked along their boundaries. Theoretically, ultrastructural units *A* hierarchically comprise all the above units (*B*, *C*, *D*, *E*).

The size and function of the ultrastructural units *A*, *B*, *C*, *D*, *E* found in radiolarian skeletons closely correspond to those of the equivalent mineral units of foraminifers and coccolitophorids (Table 2). This supports the assumption that the major biomineralization patterns are the same for all organisms (Afanasieva, 1990a, 1990b, 2000a).

SECONDARY TRANSFORMATION OF RADIOLARIAN SKELETONS

The preservation and decay of radiolarian skeletons in the fossil state is related to the change in the nature of relationships of the organic and mineral components of the skeletons. The transformation of the skeletons of the living organisms in the fossil state is a continuous process determined by geological conditions. The selective preservation of the radiolarian skeletons is influenced by the transition of the skeletons from the water to the bottom sediment and further lithogenetic processes, which continue during the entire time when the fossils stayed, first within the bottom sediments at the stage of sedimentogenesis and, then, in the lithified deposits during the diagenetic period, and up to the physical-chemically modified rocks of the catagenetic stage (Kennett, 1982; Afanasieva, 1990a, 1990b, 2000a; Shilov, 2004). The reason for this phenomenon is the change in the character of relationships between the organic and mineral components in the process of fossilization of the skeleton.

A gradual transformation of the residual organic matrix is accompanied, on the one hand, by its complete destruction and, consequently, by the disintegration of the skeletons into isolated structural elements and, on the other hand, by the tanning and carbonization of the organic lamellae, which increases the strength of the shells. As a result of this process, the modified organic matrix is transformed from a complex system of conducting channels into a system of separating lamellae, the weight of which in the entire fossilized skeleton does not exceed 1% (Golubev, 1981).

The further almost complete destruction of the carbonized lamellae facilitates the merging of adjacent small mineral units into the larger ones, which apparently indicates the solid-phase diffusion process (Golubev, 1981), which occurred at increased temperatures and pressure over long periods of geological time. However, this is never taken into account in the paleontological investigations of organic remains.

Methods

Skeletal remains of organisms are constantly affected by temperature, pressure, and time during the process of fossilization. It is theoretically and experimentally shown (Senkovsky, 1977; Golubev, 1981, Logvinenko and Orlova, 1987; Afanasieva, 1990a, 1990b; Arkhipenko *et. al.*, 1996) that the intensity of

Explanation of Plate 2

Figs. 1–11. *Bientactinosphaera strangulata* (Nazarov et Ormiston), Lower Permian, Artinskian beds; southern Ural Mountains, Ural River, village of Donskoe, sample 5/41: (1–4) without annealing: (1) scale bar = 23 μm, (2, 3) bar = 6 μm, and (4) bar = 2 μm; (5–8) annealing for 48 hours on substrate of laboratory quartz glass at temperature 500°C: (5, 6, 8) bar = 4 μm and (7) bar = 21 μm; (9–11) annealing for 25 hours in the muffle oven in standard laboratory crucibles at temperature 1000°C: (9, 10) bar = 19 μm and (11) bar = 4 μm.

Plate 3

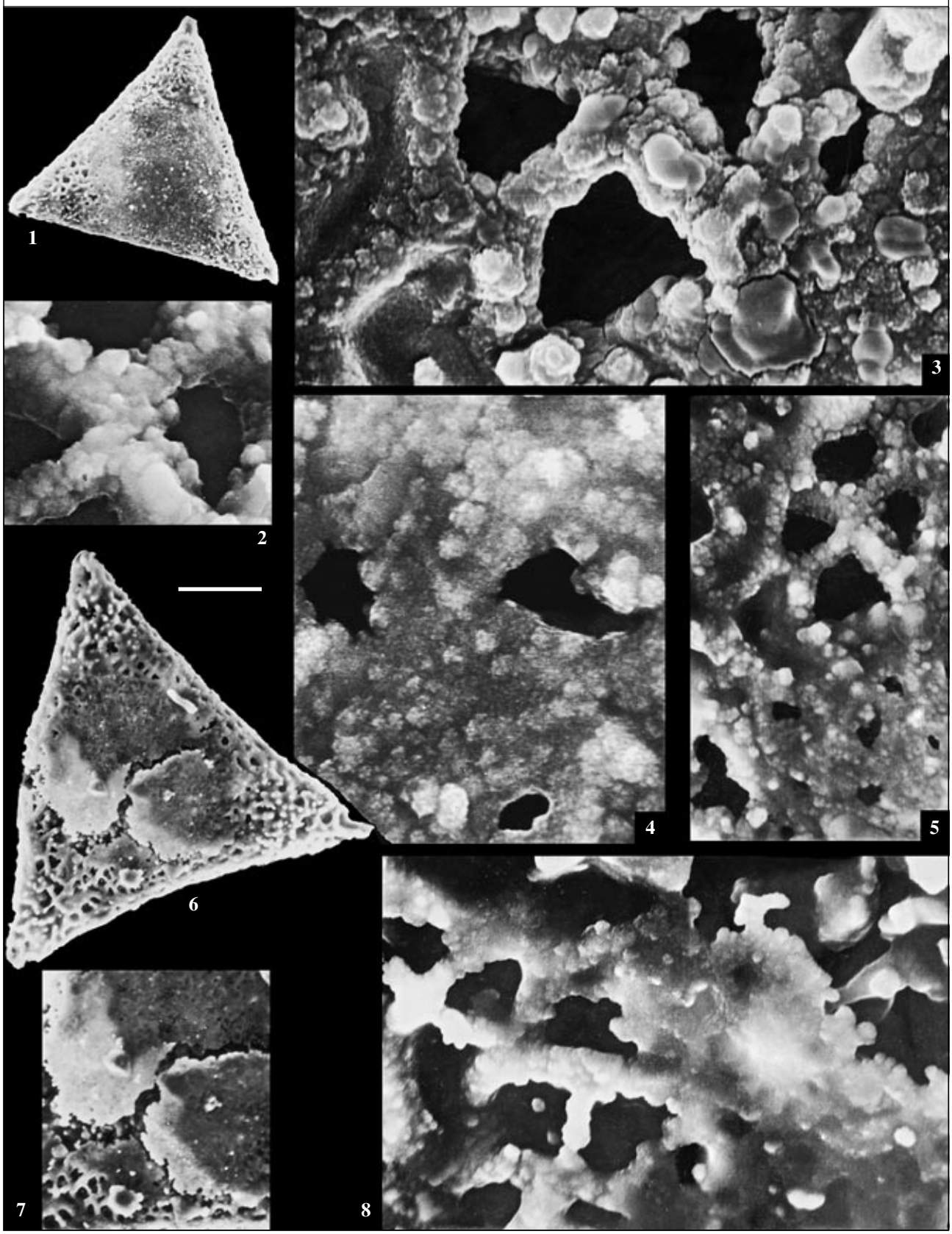

Simulation of the fossilization process in skeletons of Early Permian radiolarians by the example of *Ruzhencevispongus plumatus.*

alteration of minerals in sedimentary rocks and skeletal remains in the same conditions depends on the duration of the geological processes. Even slight changes in the mineral component of the skeletons occurring at the slowest rate can produce a significant effect if they continue over a longtime (on a geological scale). On the other hand, the same mineral changes may take place during short-term periods of high temperature, according to the van't Hoff empirical rule. An increase in temperature by 10°C increases the reaction rate two–four times (Kireev, 1951).

To compare the strength of the skeletons of the Recent and Late Paleozoic radiolarians and with the aim of simulating the initial stages of the secondary changes in the skeletons, the annealing process or heat treating of radiolarian skeletons was carried out. Annealing, to some extent, simulates the processes that may occur during fossilization of the skeletons over the geological time (Afanasieva, 1990a, 1990b). The high-temperature annealing of the radiolarian skeletons was conducted: (1) in air, at the temperature about 500°C for 48 hours, on the surface of a standard quartz laboratory glass; (2) in a muffle oven at the temperature about 1000°C for 25 hours, in standard laboratory crucibles.

Recent radiolaria

(1) As a result of the experiment, most skeletons of Recent Radiolaria were broken into isolated structural elements visible as fine debris under the optical microscope.

(2) A study of the largest tests which remained partly unbroken, namely, *Heliodiscus echiniscus* (Haeckel), *H. asteriscus* Haeckel, *Dictyocoryne profunda* (Ehrenberg), and *Spongaster tetras tetras* (Ehrenberg), revealed a change in skeleton color to a light brown.

(3) Morphological changes in the radiolarian skeletons were as follows:

• thinning of the skeleton's walls, increase in the size of pores, loss of some spines in *Heliodiscus asteriscus* (Pl. 4, figs. 1–5) and *Heliodiscus echiniscus* (Pl. 4, figs. 6–8);

• partial decay of the spongy structure in *Dictyocoryne profunda* (Pl. 5, figs. 1–5) and *Spongaster tetras tetras* (Pl. 5, figs. 6–11);

• secondary crystallization of the primary globular opal in the shells of *Heliodiscus echiniscus* into prismatic plates of the low-temperature tridymite, when the annealing in the air occurred at a temperature of 500°C (Pl. 4, figs. 9–11).

Paleozoic radiolaria

(1) Fossilized Early Permian Radiolaria were not totally destroyed by annealing, but underwent significant changes.

(2) The skeletons' color turns to gray.

(3) Morphological changes of skeletons:

(a) annealing in the air at a temperature 500°C showed that in *Bientactinosphaera strangulata* (Nazarov et Ormiston) (Pl. 2, figs. 1–4):

• pores increased (Pl. 2, figs. 5–8);

• prismatic plates of the low-temperature tridymite underwent secondary crystallization (Pl. 2, figs. 5, 6);

(b) annealing in the muffle oven at a temperature of 1000°C in *Bientactinosphaera strangulata* (Nazarov et Ormiston) (Pl. 2, figs. 9–11) led to:

• a decrease in pore diameter;

• guttering of the primarily globular skeletal surface;

(c) skeletons of *Ruzhencevispongus plumatus* Nazarov et Ormiston (Pl. 3, figs. 1–5) cracked along the boundaries of the largest elements of the shell ultrastructure after annealing in the muffle oven at a temperature of 1000°C (Pl. 3, figs. 6–8).

Model of Fossilization of Radiolarian Skeletons

The complete destruction of the primary organic matrix of the skeleton and different lithogenetic settings, on the one hand, cause the disintegration of the skeletons into fragments and, on the other hand, facilitate the merging of adjacent mineral units and realization of the tendency of silica towards the structural perfection in the successive row: opal-*A*—opal-*CT*—low-temperature tridymite—low-temperature quartz (Afanasieva, 1990a, 1990b, 2000a; Bohrmann *et al.*, 1994). The process of transformation of opal-*A* into opal-*CT* and quartz is regulated by temperature and time (Table 3). The full transformation of opal-*A* into quartz requires 30–40 m.y. in the zones of high sedimentation rates and 60–70 m.y. in the zones of medium rate (Afanasieva, 1990a, 1990b, 2000a; De Wever *et al.*, 1994). The transformation of the silica in radiolarian skeletons at the diagenetic and catagenetic stages allows the understanding of the postsedimentation settings of the modified sedimentary rocks (Table 3).

Sedimentogenesis. Secondary modifications of radiolarian skeletons in nature and, as a result, of the artificial annealing may be connected to the disruption of the relationships between the organic and mineral components of the skeleton. These modifications begin from

Explanation of Plate 3

Figs. 1–8. *Ruzhencevispongus plumatus* Nazarov et Ormiston, Lower Permian, Artinskian beds; southern Ural Mountains, Ural River, village of Donskoe, sample 5/41: (1–5) without annealing: (1) scale bar = 120 μm, (2–4) bar = 3 μm, and (5) bar = 15 μm; (6–8) annealing for 25 hours in a muffle oven in standard laboratory crucibles at temperature 1000°C: (6) bar = 90 μm, (7) bar = 66 μm, and (8) bar = 14 μm.

Plate 4

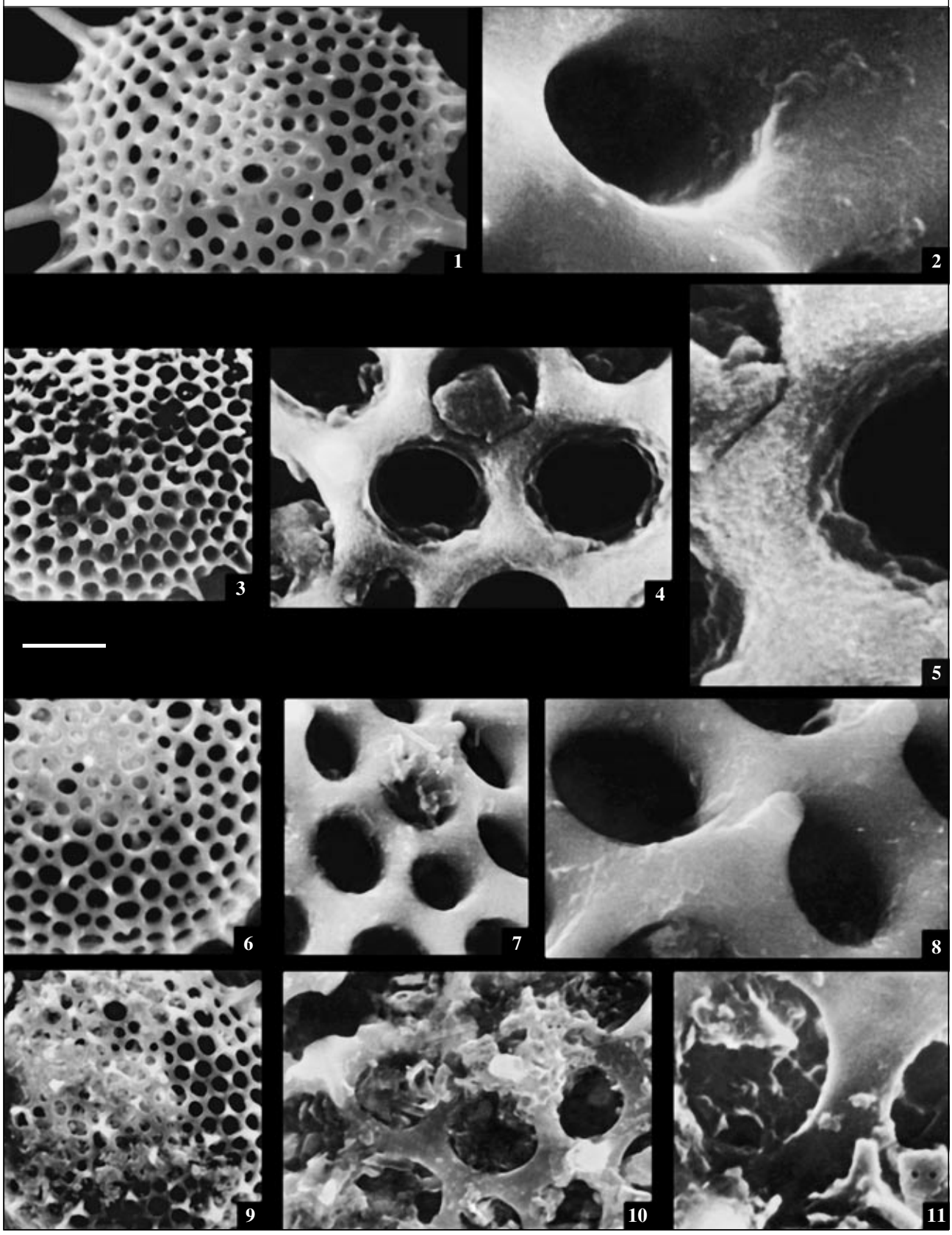

Simulation of the fossilization process in skeletons of Recent radiolarians by the example of (1–5) *Heliodiscus asteriscus* and (6–11) *Heliodiscus echiniiscus.*

destruction of the thinnest organic lamellae surrounding the smallest structural elements of the skeleton.

This residual nonmineralized organic matrix, apparently, represented a conservation matter contributing to the preservation in a latent state of the primary structure of the X-ray-amorphous opal during the stage of sedimentogenesis at the tempreatures not exceeding 20°C and at depth up to 1000 m (Melnik *et al.*, 1973; Senkovsky, 1977; Golubev, 1981, 1987; Vassoevich, 1986, 1990; Logvinenko and Orlova, 1987).

After the death of the organism and the decomposition of the cell cytoplasm, the nonfossilized shells of radiolarians retained their shape only due to the cementation of the silica globules by organic lamellae, which precluded contact and merging of neighboring mineral units (Fig. 6).

Diagenesis. The globular amorphous opal of radiolarian shells remaining in the latent state during the stage of sedimentogenesis was transformed into globular opal *CT* during diagenesis. The increase in temperatures at the depth of 1000–1500 m during diagenesis up to 20–40°C together with a long period of geological time apparently facilitated the beginning of the change in the residual organic matrix, which remained relatively inert at temperatures below 20°C.

The secondary changes in radiolarian skeletons in nature and during the artificial annealing may be related to the disruption of relationships between the organic and mineral components of the skeleton. These changes begin from the destruction of the thinnest organic lamellae surrounding the smallest structural elements of the skeleton. The thin surface later of the epivitrium is the first to be destroyed, leading to the exposure of the more coarsely grained surface of the skeletons (Bjørklund and Goll, 1986). An example of this process is provided by radiolarians from the natural Upper Paleozoic outcrops with a well-preserved globular structure of their skeletons (Afanasieva, 1990a, 1990b) (Pl. 2, figs. 1–4; Pl. 3, figs. 1–5).

The artificial annealing of the skeletons of the Recent radiolarians *Heliodiscus asteriscus* Haeckel, *Dictyocoryne profunda* (Ehrenberg) and *Spongaster tetras tetras* (Ehrenberg) resulted in the expanded pores of the skeletons and separation of the layers from the outer surface of the skeleton, which led to the thinning of its walls (Pl. 4, figs. 2–5; Pl. 5, figs. 3–5, 9–11). This process is apparently responsible for the disintegration of small thin-walled shells, while large skeletons affected in the same way only show changes in ornamentation.

Table 3. Transformation of silica in radiolarian skeletons and postsedimentary conditions of sedimentary rocks

<table>
<tr><th colspan="2">Modifications of silica in radiolarian skeletons and paleotemperatures</th><th colspan="2">Stage of lithogenesis</th></tr>
<tr><td>globular opal</td><td>+20°C</td><td colspan="2">sedimenogenesis</td></tr>
<tr><td>globular opal-CT</td><td>+40°C</td><td colspan="2">diagenesis +30°C</td></tr>
<tr><td rowspan="2">prismatic low-temperature trydimite</td><td rowspan="2">+120°C</td><td rowspan="3">catagenesis</td><td>+50°C
early
+100°C</td></tr>
<tr><td rowspan="2">late
+150°C</td></tr>
<tr><td>dipyramidal-prismatic low-temperature quartz</td><td>>+180°C</td></tr>
<tr><td colspan="4">>+200°C</td></tr>
</table>

Early Catagenesis. At the early stage of catagenesis, as the temperatures increase from 40 to 120°C at the depth of 1500–4000 m, the biogenic globular opal *CT* of the radiolarian skeletons can be transformed into prismatic tablets of the low-temperature tridymite (Senkovsky, 1977; Vassoevich, 1986, 1990; Logvinenko and Orlova, 1987). This phenomenon is apparently produced by the initial presence of polysaccharide plates in the complex structure of the organic matrix. The hexagonal outline of these plates and a system of their vertical arrangement is beneficial for forming subhexahedron skeletal units *B*, which in turn are converted to prismatic tablets of low-temperature tridymite under elevated temperature conditions of the early catagenetic stage (Pl. 2, figs. 5, 6).

There is no empirical data on the successive stages of fossilization of any skeletal remains. However, the long annealing at a temperature of 500°C on the surface of laboratory quartz glass, the secondary crystallization of some skeletons of Recent *Heliodiscus echiniscus* (Haeckel) (Pl. 4, figs. 9–11) and Early Permian *Bientactinosphaera strangulata* (Nazarov et Ormiston) (Pl. 2, figs. 5–8) was observed. Primary globular opal and opal–tridymite of the skeletons of these radiolarians was secondarily replaced by prismatic tablets of the low-temperature tridymite.

The presence of crystallized skeletons of radiolarians in natural deposits of Late Paleozoic age supported

Explanation of Plate 4

Recent bottom sediments of the Pacific Ocean (station 5139).

Figs. 1–5. *Heliodiscus asteriscus* Haeckel: (1–2) without annealing: (1) scale bar = 15 μm and (2) 3 μm; (3–5) annealing for 25 hours in a muffle oven in standard laboratory crucibles at temperature 1000°C: (3) bar = 26 μm, (4) bar = 4 μm, and (5) bar = 2 μm.

Figs. 6–11. *Heliodiscus echiniscus* (Haeckel): (6–8) without annealing: (6) bar = 16 μm, (7) bar = 4 μm, and (8) bar = 2 μm; (9–11) annealing for 48 hours on substrate of laboratory quartz glass at temperature 500°C: (9) bar = 13 μm, (10) bar = 4 μm, and (11) bar = 1 μm.

Plate 5

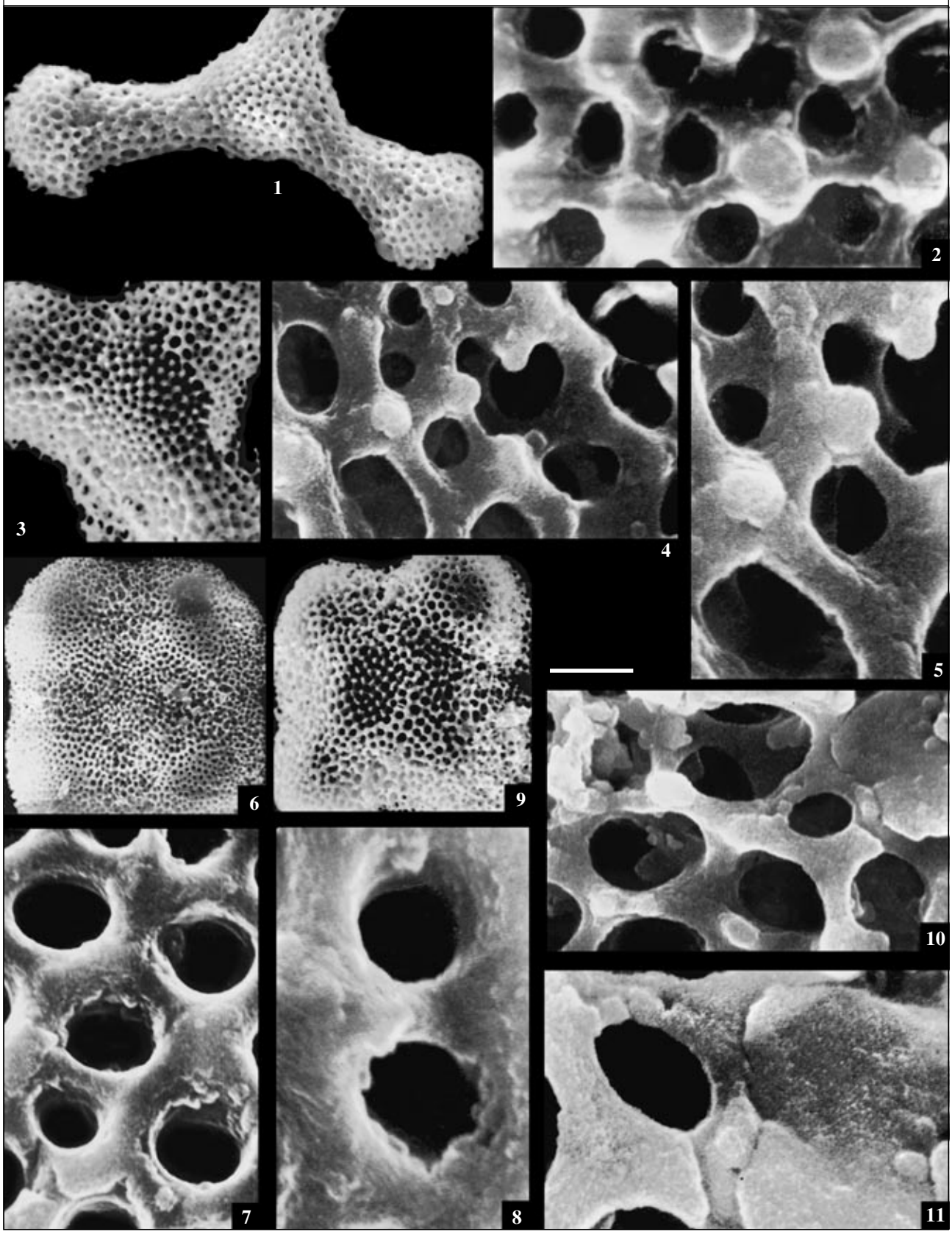

Simulation of the fossilization process in skeletons of Recent radiolarians by the example of (1–5) *Dictyocoryne profunda* and (6–11) *Spongaster tetras tetras.*

the experimental data. The comparative analysis of Early Permian *Bientactinosphaera strangulata* (Nazarov et Ormiston), *Ruzhencevispongus plumatus* Nazarov et Ormiston, *Copicyntra acilaxa* Nazarov and Early Carboniferous species of the genus *Caspiaza, C. aculeata* Afanasieva, *C. urceus* Afanasieva, from the under-salt deposits of the northern slope of the Caspian Depression and natural outcrops of the southern Ural and Tien Shan mountains showed significant differences in the character and degree of the preservation of their skeletons. Radiolarians from the natural outcrop usually have a shell with a well-preserved globular structure (Pl. 2, figs. 1–4; Pl. 3, figs. 1–5; Pl. 6, figs. 1–4). Poor preservation of radiolarian shells collected from the Upper Paleozoic under-salt beds north of the Caspian Region from the depth of 3000–4000 m is probably related to secondary changes in the structure of the skeletons under conditions of the early catagenetic stage (Pl. 6, figs. 5–8).

Late Catagenesis. Further transformation of prismatic low-temperature tridymite into more perfect structurally dipyramidal-prismatic crystals of the low-temperature quartz, probably occurred during the late catagenetic stage at the temperatures above 120°C, i.e., beyond the limit of stability of the low-temperature tridymite, a situation existing in nature only at the depth of deep drilling, that is, over 4000 m (Senkovsky, 1977; Vassoevich, 1986, 1990; Logvinenko and Orlova, 1987). Fossil radiolarians from the Upper Paleozoic beds north of the Caspian Region (depths of 4000–6000 m) have crystallized skeletons, which are mostly composed of elongated dipyramidal-prismatic crystals of the low-temperature quartz (Pl. 6, figs. 9–12). This structure is produced by the significant changes in the primary biostructure of the skeleton and apparently related to the almost complete destruction of the organic lamellae of the skeletons in the conditions of high temperatures of the late catagenetic stage.

The fusion of the crystalline unit resulting from the destruction of carbonized, tanned organic lamellae is apparently related to the solid-phase diffusion process, which is very important at the stage of catagenesis, but has never been taken into account or noted in paleontological studies of fossil remains. However, based on the study of crystallized skeletal remains of radiolarians from the deep bore core and taking into account results of the high-temperature annealing of the shells, only purely solid-phase changes in the skeletal structure may be suggested. A prolonged annealing of the Late Paleozoic radiolarian tests at the temperatures of 1000°C in the muffle oven cause melting of the globular surface of the skeletons of *Bientactinosphaera strangulata* (Nazarov et Ormiston) (Pl. 2, figs. 10. 11) and *Ruzhencevispongus plumatus* Nazarov et Ormiston (Pl. 3, fig. 7). The annealing caused diffusion exchange between the mineral units of the radiolarian skeletons, which led to the fusion and spontaneous cementing with silica of most pores in the skeletons of *Bientactinosphaera strangulata* (Nazarov et Ormiston) (Pl. 2, figs. 10, 11).

Pyritization of Skeletons

Apart from the natural transformation into quartz, the primary amorphous opal of radiolarian skeletons may be replaced by calcite, apatite, fluorite, and pyrite (Pl. 7). The study of the radiolarian skeletons from Domanik deposits (Upper Devonian, Middle Frasnian) of the Timan–Pechora Basin showed that secondary pyrite with a typical copper-yellow gleam completely replaces silica of the skeletons (Pl. 7) (Afanasieva, 2000a). The analysis of the structure of the radiolarian skeletons showed that secondary pyrite either replaces the entire skeleton (Pl. 7, figs. 1–3, 5–10), or only the central part of the radiolarian skeleton (Pl. 7, fig. 4). It is possible that pyritization of the skeletons could begin in organisms during life or immediately before death.

The hypothesis that secondary pyrite was formed in the skeletons of living radiolarians implies certain restrictions on the time and place of its formation. The environment of pyritization was unlikely to have included deep burial of the radiolarian skeletons in the sediment and long geological time. Moreover, the deposition of the Domanik oil source host beds (Middle Frasnian) containing radiolarian skeletal remains could occur only in an anoxic environment. According to Betekhtin (1950, p. 277), the formation of pyrite in sedimentary rocks "is related to the decomposition of organic remains without access of free oxygen into deeper parts of a basin." Pyrite often forms pseudomorphoses over various organism's remains. These pseudomorphoses are apparently formed when H_2S affects minerals. It is important that pyrite is formed through the reduction of sulfates and other sulfur-containing compounds by organic remains according to the scheme below:

$$2FeSO_4 + 2HSO_4–7O_2 = 2FeS_2 + 2H_2O.$$

Further in his study, Betekhtin discussed the results of a very interesting experiment: "a mouse submerged

Explanation of Plate 5

Recent bottom sediments of the Pacific Ocean (station 5139).

Figs. 1–5. *Dictyocoryne profunda* (Ehrenberg): (1–2) without annealing: (1) scale bar = 46 μm and (2) bar = 4 μm; (3–5) annealing for 25 hours in a muffle oven in standard laboratory crucibles at temperature 1000°C: (3) bar = 31 μm, (4) bar = 3 μm, and (5) bar = 2 μm.

Figs. 6–11. *Spongaster tetras tetras* (Ehrenberg): (6–8) without annealing: (6) bar = 27 μm, (7) bar = 4 μm, and (8) bar = 2 μm; (9–11) annealing for 25 hours in a muffle oven in standard laboratory crucibles at temperature 1000°C: (9) bar = 29 μm, (10) bar = 3 μm, and (11) bar = 2 μm.

Plate 6

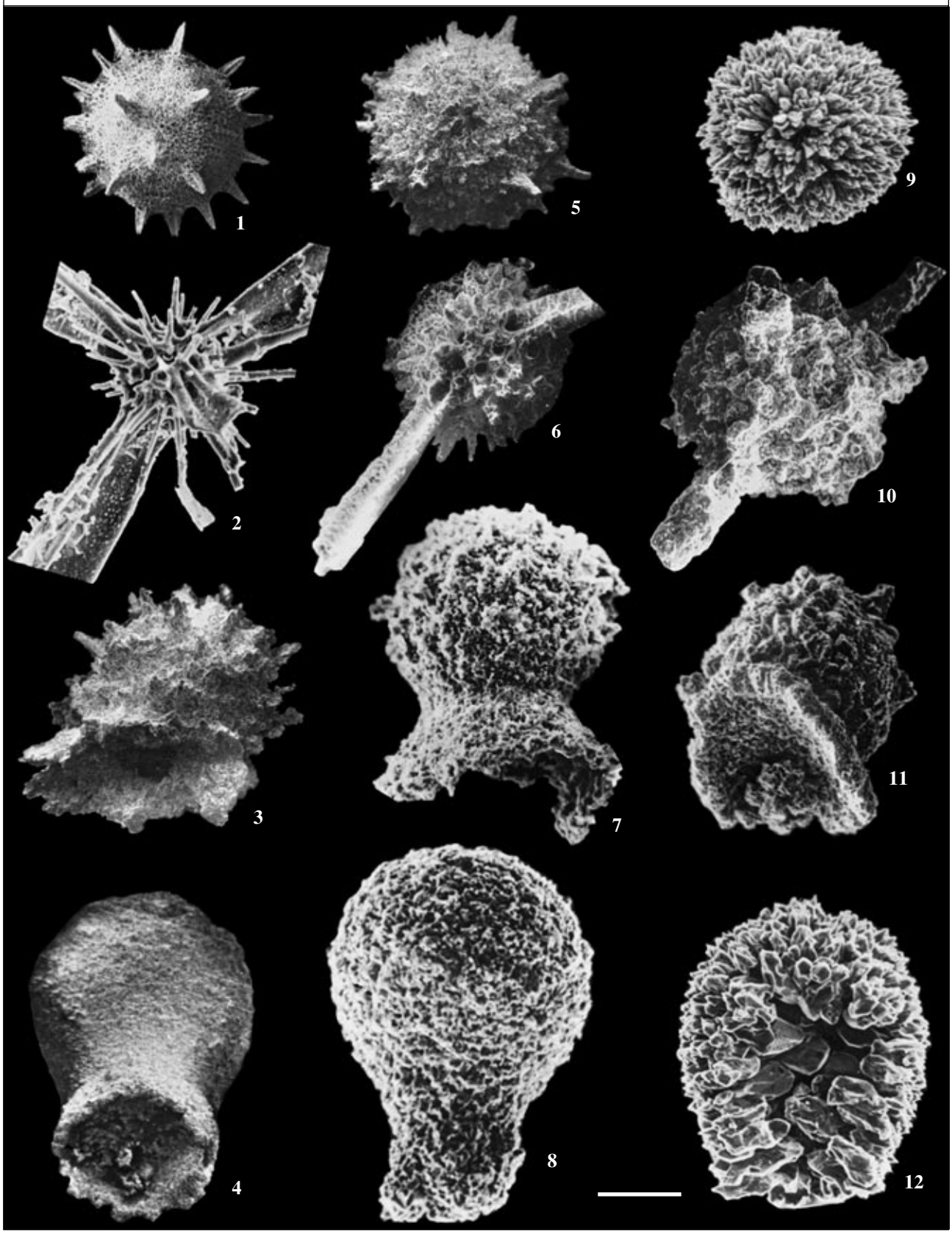

Consecutive stages of silica changes in radiolarian skeletons at the stages of (1–4) diagenesis, (5–8) early catagenesis, and (9–12) late catagenesis.

in a glass containing iron sulfate became totally pyritized after several years. Apparently, decomposition of proteins resulted in the release of hydrogen disulfide. Pyrite was produced by the reaction of ions of sulfur and iron" (Betekhtin, 1950, p. 278). In addition, Clark and Lutz (1980) reported pyritization of shells in living marine bivalves.

Our knowledge of pyritization involving the replacement of primary opal of the skeletons of living radiolarians by pyrite is rather incomplete. The best evidence of the nature of pyritization may be found in partly pyritized skeletons of radiolarians, including the secondarily pyritized spherical part of the skeletons (Pl. 7, fig. 4) and initially siliceous tips of spines. Possibly, pyritization occurred over the organic matrix of the primary skeletons of living radiolarians. Recrystallization began from the initial inner part of the skeleton and gradually spread toward the spine periphery. Secondary pyrite of the skeletons of radiolarians and other organisms is very much different from classical crystals or framboids of pyrite observed in nature. Here, pyrite is represented by tiny granules, which are combined into massive skeletons with the characteristic pyritic luster and color. Orientation of pyritic granules is probably similar to the arrangement of primary opaline granules in the radiolarian skeletons.

From the paleontological point of view, the hypothesis that pyrite begins replacement of opal in living radiolarians is the most essential. Although this process is still insufficiently studied, it is most likely that the pyritization occurred along the biomineralogical boundaries and in the growth direction of skeletons. This agrees with observations and illustrations of the partial and complete pyritization of the skeletons of radiolarians and other organisms (Pl. 7).

GROWTH OF RADIOLARIAN SKELETONS

A gradual succession of generations of Polycystina radiolarians has not been observed in laboratory. Difficulties of the laboratory cultivating of radiolarians is the main obstacle for the precise determination of the growth stages and life duration of these organisms. The biology of radiolarians is usually compiled based on subadult radiolarians captured in the sea and developed in the laboratory up to the stage of the gamete development (Cachon and Cachon, 1971; Swanberg and Harbison, 1980).

Although it is not possible at present to observe a successive change of radiolarian generations in laboratory cultures, successful cultivation of juveniles (<100 μm) of some large-sized radiolarian species enabled the determination of their life span and provided important information in relation to the growth stages and succession of the skeleton development.

The first data indicated that radiolarians live for about a month (Casey *et al.*, 1970). Takahashi (1983) established that radiolarians in plankton at the depths of 0–200 m live for about 16–42 days. The duration of the life in laboratory is established for some species of radiolarians and ranges from several days to several weeks (Anderson, 1980; Swanberg and Anderson, 1985; Matsuoka, 1992; Matsuoka and Anderson, 1992).

Ontogenetic Stages of Radiolaria

The development of the skeleton of radiolarians begins at early ontogenetic stages, while it grows and develops almost throughout life. The central parts of the skeleton are the first to appear, while the peripheral parts appear later.

In the ontogeny of nassellarians, the spicule appears first, followed by the adjacent arcs and walls of the cephalis. However, sometimes the cephalis is formed entirely at once, and sometimes even the cephalis and thorax together. In some species, the development of the skeleton is arrested at this stage, whereas the subsequent segments appear later gradually one by one. Other species show simultaneous appearance of three or four segments, while only the subsequent chambers grow gradually. The development of a skeleton may reach the stage of the formation of a developed aperture, or the skeletal growth may be interrupted earlier. The central capsule of Nassellaria gradually grows and fills not only the cephalis, but also the thorax, and even the succeeding parts (Petrushevskaya, 1986).

In spherical radiolarians, the spicule and inner skeletal shells are the first to appear. The outer skeletal shells appear later and become thicker as the organism grows. Depending on the position of the integrated axoplast in relation to the nucleus (crypto-, centro-, or peri-

Explanation of Plate 6

(Figs. 1 and 2) Lower Permian; southern Ural Mountains, Ural River, village of Donskoe, sample 5/41: (1) Asselian and (2) Artinskian stages; (Figs. 3 and 4) Lower Carboniferous, Serpukhovian Stage; Tien Shan, Ugam River, sample 803/24; (Figs. 5–12) Northern Caspian Region, Karachaganak Massif: (5, 6, and 10) Lower Permian, Artinskian Stage: (5, 6) borehole 13, sample 3061 (depth 4984–4990 m); and (10) borehole 20, sample 1 (depth 4602–4603 m); (7, 8, 11, and 12) Lower Carboniferous, Serpukhovian Stage: (7) borehole 33, sample 86913 (depth 4934-4941 m); (8) borehole 19, sample 113 (depth 4769–4778 m); (11) sample 112, borehole 19 (depth 4760–4769 m); and (12) sample 42, borehole 20 (depth 4748–4753 m); and (9) Middle Carboniferous, Bashkirian Stage, borehole 12, sample 633 (depth 4656–4663 m).

Figs. 1, 5, and 9. *Copicyntra acilaxa* Nazarov, scale bar = 115 μm.

Figs. 2, 6, and 10. *Entactinia pycnoclada* Nazarov et Ormiston, bar = 50 μm.

Figs. 3, 7, and 11. *Caspiaza aculeata* Afanasieva, bar = 100 μm.

Figs. 4, 8, and 12. *Caspiaza urceus* Afanasieva: (4) bar = 100 μm; (8) bar = 58 μm; and (12) bar = 40 μm.

Plate 7

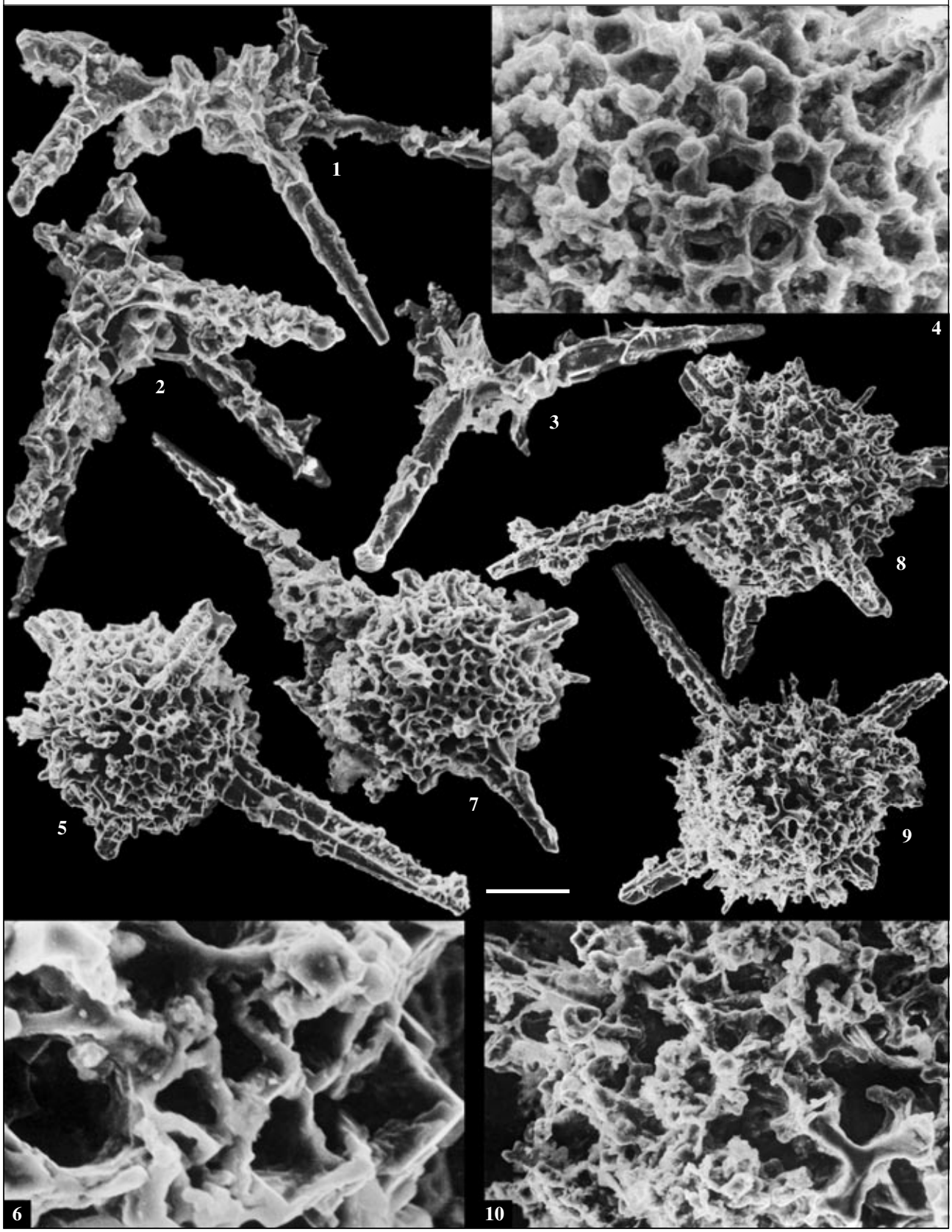

Pyritized radiolarian skeletons.

axoplastidy), the radiolarian skeleton is formed in the nucleus or outside it (Fig. 1).

The central capsule of juveniles is spherical. As the organism grows, the central capsule forms lobes and embraces more and more skeletal shells, beginning from the center. As the organism develops, they from originally extracapsular become intracapsular (Petrushevskaya, 1986; Nazarov and Petrushevskaya, 1995).

Growth of complex flattened, triangular skeletons of stauraxonic radiolarians also beings from the center (Fig. 7). Matsuoka (1992) and Matsuoka and Anderson (1992) observed the following in the cultivated radiolarians in the laboratory:

(1) biomineralization (involvement of silica and formation of the opaline skeleton) mainly depends on the cell physiology than on the environment;

(2) development of the skeleton invariably requires narrow temperature limits, but may allow considerable fluctuations in salinity;

(3) the skeletal growth in extant flattened, armed radiolarians occurs in several stages, during which the periods of intense growth and morphogenesis are interrupted and replaced by periods of stasis.

Four growth stages are distinguished in the ontogeny of the spongy armed radiolarian *Dictyocoryne truncatum* (Matsuoka, 1992; Matsuoka and Anderson, 1992). At the first stage, the skeleton is spongy, triangular, lacking arms or patagium (the skeleton is up to 120 μm high) (Fig. 7). At the second stage, three arms and lacelike patagium are developed (the skeleton is 120–200 μm high). The third stage is characterized by a considerable growth of a homogeneous spongy patagium (the skeleton is 200–280 μm high). In a completely mature individual (the fourth stage), the skeleton is biconvex, triangular, while the patagium grows outwardly (the skeleton is over 280 μm high).

The additional growth in adults occurs in the central part of the shell. The most intense growth was observed at the transition from the third to the fourth stage (skeleton increases on average by 5.4 μm per day). The ability of an organism to deposit silica inside the cytoplasm is extensively connected with the survivability of the organism. Weak, colorless individuals with poorly developed axopodia did not show skeletal growth. Matsuoka (1992) emphasized that the sporadic growth of the skeleton is very noticeable because periods of the rapid growth (increase by 15–20 μm per day) alternate with periods of either slowed growth, or no growth at all.

Studies of cultivated radiolarians showed that only few specimens in a group reach the adult, completely mature stage of development (Matsuoka, 1992). Similar results were reported by Petrushevskaya (1966) based on the observations of radiolarian distribution in the Indian and Pacific oceans and in the Antarctic waters. Strikingly many individuals with underdeveloped skeletons are contained in the plankton. An opposite picture was observed in the bottom sediment compared to the plankton, but this is because of the dissolution of tracery juveniles during their postmortem transport from the subsurface water to the bottom.

Hence, different developmental stages of an individual may be significantly different in the shape of the skeleton. This is the source of many mistakes in classification of extant radiolarians. Petrushevskaya (1986) and Paverd (1995) convincingly showed that Haeckel (1887) made a mistake with serious consequences when he proposed the classification of extant radiolarians, in which different growth stages of skeletons were assigned to different taxa. The early stages of multisegmented Nassellaria were described by Haeckel as independent species and are assigned to different families than the adults.

Development of the Skeleton

The development of the skeleton in the extant radiolarians Polycystina may occur in various ways and passes several stages (Enriques, 1932; Petrushevskaya, 1962, 1986; Anderson, 1980, 1981, 1983, 1986; De Wever, 1982; Afanasieva, 1990a, 1990b, 2000a; De Wever *et al.*, 1994, 2001).

Stage 1. Appearance of the skeleton. In all radiolarians, the beginning of the skeleton development, occurs simultaneous on the polysaccharide plates over the entire volume of the organic matrix of the future shell. Here, the primary silica globules are first appear to merge later into the larger elements of the skeletal ultrastructure (Figs. 5, 6).

Stage 2. Primary development of the skeleton. The further development of the skeleton occurs in two ways:

• *pellicular growth*: ultrastructural elements of the skeleton form a biomineral basis of the future shell with

Explanation of Plate 7

Upper Devonian, Middle Frasnian Substage, Domanik Formation, Timan–Pechora Province, borehole Ukhtinskaya-3B, sample 114 (depth 104.2–104.7 m).

Fig. 1. *Ceratoikiscum* cf. *ukhtensis* Afanasieva, scale bar = 42 μm.

Fig. 2. *Palaeoscenidium* cf. *cladophorum* Deflandre, bar = 33 μm.

Fig. 3. *Palacantholithus* cf. *stellatus*, bar = 42 μm.

Fig. 4. *Borisella maksimovae* Afanasieva, fragment, bar = 15 μm.

Figs. 5 and 6. *Bietntactinosphaera* cf. *variacantina* (Foreman): (5) bar = 63 μm and (6) fragment, bar = 8 μm.

Fig. 7. *Radiobisphaera* cf. *menneri* Afanasieva, bar = 42 μm.

Figs. 8–10. *Bietntactinosphaera* cf. *grandis* (Nazarov): (8) bar = 77 μm, (9) bar = 83 μm, and (10) fragment, bar = 30 μm.

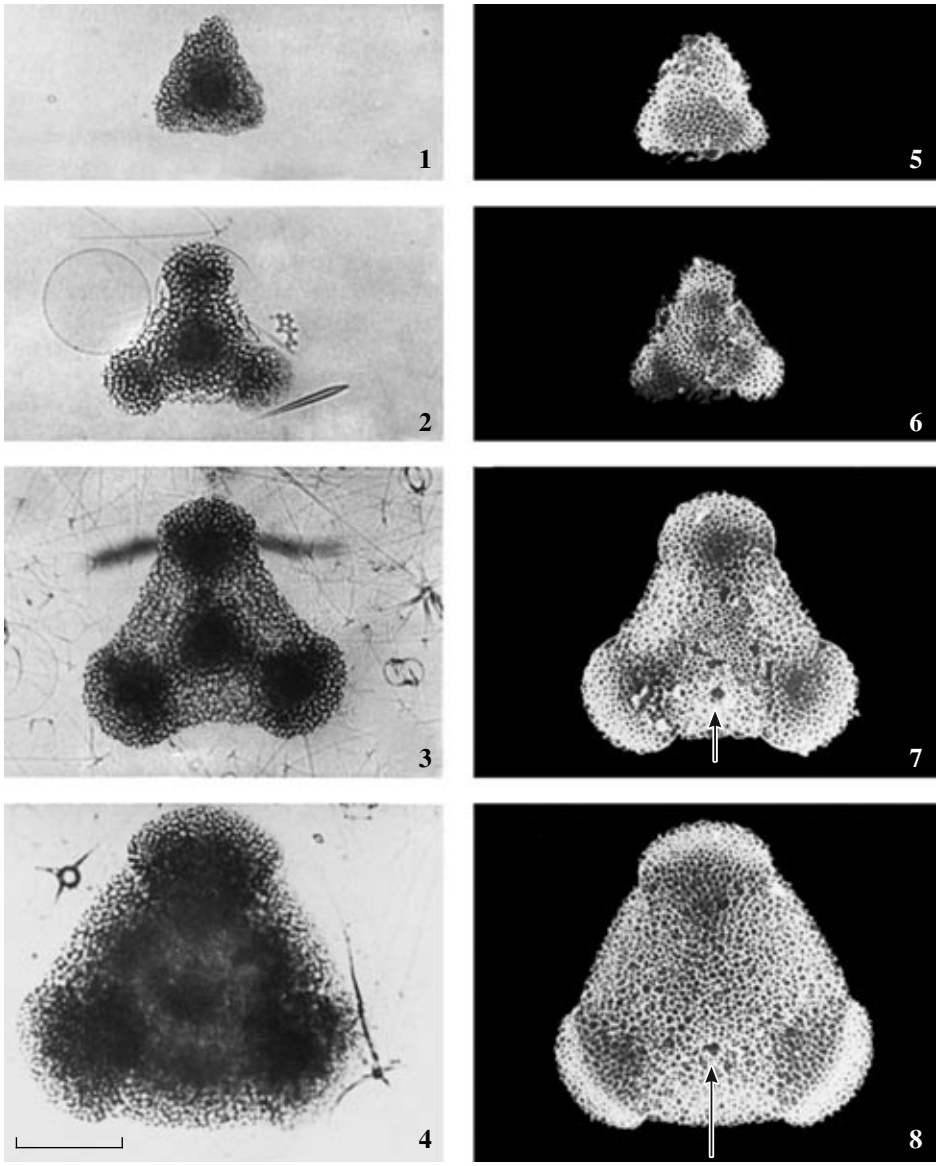

Fig. 7. Ontogenetic stages of *Dictyocoryne truncatum* (laboratory culture) (after Matsuoka, 1992, pl. 2, figs. 1–8): (1, 5) stage 1; (2, 6) stage 2; (3, 7) stage 3; (4, 8) stage 4. The arrow in (7 and 8) indicates the circular to subcircular pore, through which an axoflagellum emerged. (1–4) photomicrographs, (5–8) scanning electron micrographs. All figures are the same magnification. Scale bar, 100 μk.

thin walls and large hexahedral pores in the entire volume of the organic matrix;

• *bridge growth*: almost straight bars are formed in the organic matrix of the future skeleton, which elongate and connect with each other by bridges to form a shell with numerous polygonal pores.

Stage 3. Final stage of the skeletal development. The development of the skeleton is finalized in two ways:

• *bridge growth*: bars and bridges thicken to various extent to form delicate spongy and reticulate or a more coarsely lattice skeletal wall; bridge growth is the basis of the development of various skeletal structures (spicules, spines, apophyses, bars, beams, and so on);

• *rim growth*: edges of pores grow inwards, pores gradually narrow to form porous or lamellar shell structure.

All types of the skeletal growth may be observed in the same individual at different ontogenetic stages, or one of the patterns may be dominant (Petrushevskaya, 1962, 1986; Anderson, 1983; De Wever *et al.*, 1994, 2001; Anderson and Gupta, 1998).

For instance, in *Lithomelissa thoracites* Haeckel, the cephalis is formed by rim growth, while the thorax is developed by bridge growth (Petrushevskaya, 1962).

The porous skeleton at different stages of *Hexacontium* sp. and *Actinomma mediterranensis* Hollande et Enjumet is a delicate, very thin-walled shell, with large

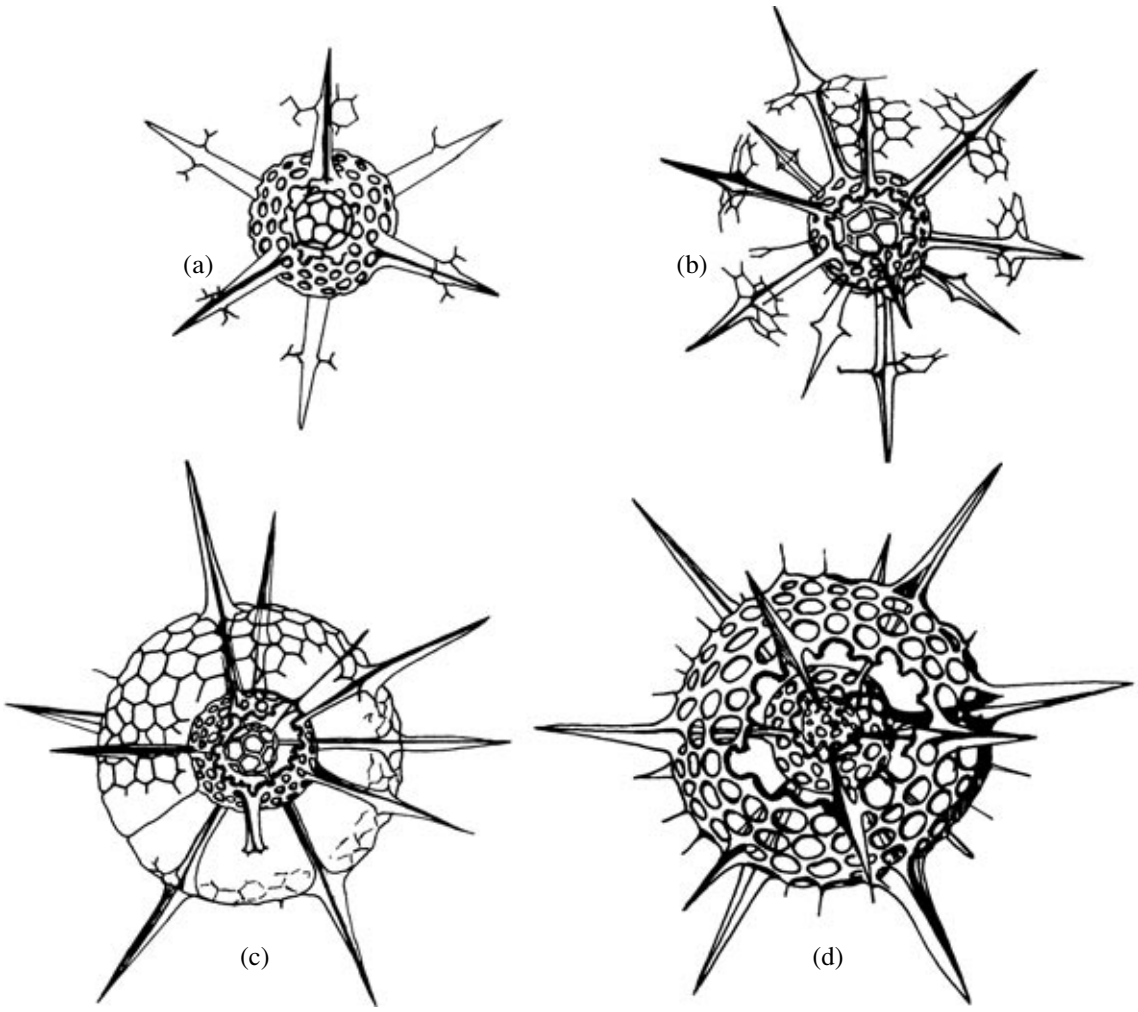

Fig. 8. Growth stages of a radiolarian porous skeleton (after Hollande and Enjumet, 1960): (a) young specimen of *Hexacontium* sp.; (b–d) different growth stages of *Actinomma mediterranensis* Hollande et Enjumet: (b) formation of the external shell as the spines branch, (c) formation of a slender shell with hexagonal pores and with a thin siliceous beam, (d) final shape of a porous shell.

hexagonal pores, which are formed by bridge growth (Figs. 8a–8c). The appearance and early growth of the outer shell of the skeleton begin with the main spines (Figs. 8a, 8b). Further, the shell wall thickens by rim growth, while the pore edges grow inwards, pores narrow, and a delicate skeleton is transformed into a thick-walled porous shell with rounded pores and a massive three-bladed spine (Fig. 8d) (De Wever, 1982; Anderson, 1986).

In Spumellaria, which have spongy, reticulate, or latticed skeletal tissue, the inner sphere may be porous.

All this apparently suggests that the primary skeleton of spines in the class Aculearia, spherical porous skeleton of the class Sphaerellaria, and spongy shells of the class Spumellaria, the first members of the nassellarian order Pylomariata, and the first discoidal members of the class Stauraxonaria appeared simultaneously in the phylogeny of Radiolaria.

SKELETAL MORPHOLOGY

Skeletons of Radiolaria are perfectly beautiful, proportional, well-designed, and elegant. However, while being complexly, but geometrically regularly designed, radiolarian skeletons are among the lightest of constructions. “Regular shapes in organisms are explained by the economy of material” (Mordukhai-Boltovskoy, 1936, p. 5).

Of all regular Platon’s bodies (tetrahedron, hexahedron, octahedron, dodecahedron, and icosahedron), the icosahedron with 20 faces has the smallest surface-to-volume ratio. The most economical skeletal shape, which has the smallest surface-to-volume ratio, is a sphere. Therefore, “if no special places for organs are designed, the shape of the organism should be spherical. However, as soon as this condition is imposed, the organism loses the spherical shape” (Mordukhai-Boltovskoy, 1936, p. 14).

Further differentiation is in the distinguishing differences between the oral and aboral parts of the shell. "In this case, one pole should be different from another. If we have descent and ascent, the former caused by gravity, the latter by hydrostatic apparatus, then, although the motion is performed in both directions, it is *different* in each of these directions. During ascent, the resistance of the liquid should be reduced, while it should be increased during descent to slow the fall. This explains the origin of the *unequipolar*, e.g., bell-shaped forms of radiolarian skeletons, which act like parachutes. The spherical shape is a solution of the task of *finding a shape uniform in all its points*" (Mordukhai-Boltovskoy, 1936, p. 39).

Even larger economy of building material is achieved by the development of pores in the skeleton. Pores on the surface of the skeleton and cells in the spongy, latticed, and reticulate forms are often hexagonal. "Why? Because of a simple calculation. The subdivision into regular multihedrons, as was noted by Pythagoras in the 6th century BC, is possible only into regular triangles, squares, or hexahedrons" (Mordukhai-Boltovskoy, 1936, p. 5). Mathematical calculations show that at the given surface area (S) triangle will have the largest perimeter ($4.559\sqrt{S}$) followed by a square ($4\sqrt{S}$). A hexahedron will have a smaller perimeter ($3.722\sqrt{S}$); therefore, the wall in this subdivision (although not perfect geometrically) will use the least material. In addition, "radiolarians have round pores in their skeleton, which are explained by the economy of material" (Mordukhai-Boltovskoy, 1936, p. 33).

However, square lattice also occurs in radiolarians. Mordukhai-Boltovskoy (1936) showed that different shapes of lattice serve different purpose. The hexagonal lattice is designed to resist even pressure (water pressure), whereas the square lattice is stronger and is designed to resist impact. Furthermore, some radiolarians, for instance, from the spumellarian family Astrosphaeridae, have various reticulate spheres one inside another: the outer, which resists impact, has square cells, while the inner sphere experiencing even water pressure has hexagonal cells (Mordukhai-Boltovskoy, 1936; Khabakov *et al.*, 1959).

When analyzing constructions of skeletons pierced by spines, Mordukhai-Boltovskoy (1936) showed that thin spines change the spherical shape of the skeleton only very little. At the same time, when the spines become thicker, the shape of the skeleton changes in that it becomes elongated along the spine to reach an elliptical, or even fusiform shape. This trend is observed in many taxa of extant and fossil stauraxonic radiolarians.

The mechanical and mathematical calculations and analysis of the knots formed at the places where skeletal elements are joined to make a single construction supports the importance of these bonds for the strength of the entire skeleton. Mechanical formulas show that the bonds of the skeletal construction in radiolarians provide that the strain is the same at each skeletal element, each bar, and each spine (Mordukhai-Boltovskoy, 1936).

According to Thompson (1942), skeletal geometry follows from the same physical laws that work for liquids. The hexagonal radiolarian frame is similar to the frame of the surface tension of artificial materials. The structure of the skeleton of *Callimitra agnesae* Haeckel is similar to the model of a tetrahedron received by the method of the surface tension during the submergence of a wire frame into a soap solution. In addition, in analyzing the geometry of the radiolarian skeleton, Thompson (1942) makes parallels with the spiny skeletons of sponges and coral polyps.

For the second time, the idea of the economy of silica in skeletons was proposed by Moore (1969) after the comparison of the Eocene–Quaternary radiolarians. The skeletons of Recent radiolarians were on average one-quarter of the weight of the most ancient taxa analyzed.

Schaaf (1981) used mathematical methods to substantiate the hypothesis that in the Cenozoic, the general trend in the evolution of the radiolarian skeletons (e.g., more regular arrangement and shape of pores) was towards the diminishing the amount of silica for the completion of the majority of skeletons.

To date, it is evident that the theoretically conceivable diversity of hollow polyhedrons, the limiting cases of which are the sphere and spheroid, is only partially realized in wild nature. This is associated with the program of "thrifty expenditure of substance and energy" after Voitekhovsky (2002). An important conclusion of Voitekhovsky (2002, 2004a, 2004b) is the biomineral homology between the polyhedrons of carbon fullerenes,[4] polyhedrons of viruses, radiolarian skeletons, and *Volvox colonies*. This homology is predetermined not only by their material content but mostly by the geometrical optimal shape requiring a minimum of energy and material expenditure. It is of interest that the fullerenes of the C60–C100 range (i.e., most symmetrical, with the least number of contacting faces) are potentially stable. These conditions correspond to the icosahedral and dodecahedral groups of polyhedrons, which are often used by spherical radiolarians (Afanasieva and Amon, 2004a).

The exclusive complexity of the skeleton structure and high diversity in shape are determined by the initial type of symmetry and an intricate combination of internal and external skeletal elements. The internal elements include the internal framework in the shape of a hollow sphere, or spicule, primary sphere, and spine-framed construction, whereas the outer elements include

[4] Fullerenes are a new class of hollow mineral polyhedrons, the experimental study of which was awarded the 1996 Nobel Prize for Chemistry. Carbon fullerenes have pentagonal and hexagonal faces, each three faces converging at each vertex. Fullerenes are closed, nontranslating in space, have a noncrystallographic symmetry, and are classified in mineralogy as mineraloids.

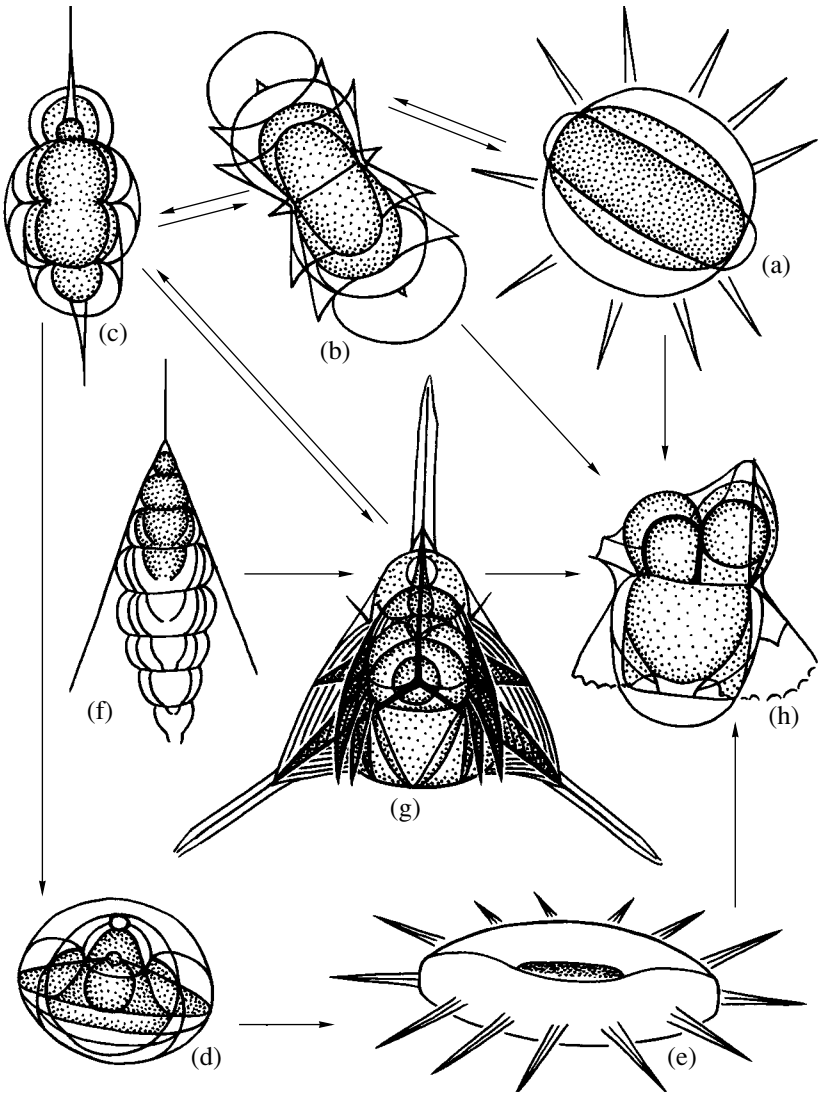

Fig. 9. Symmetry and possible transformations of the skeleton shape in the phylogeny of Polycystina (after Petrushevskaya, 1986, modified): (a) homaxonic: subspherical or ellipsoidal; (b–e) monaxonic: (b) dumbbell-shaped, (c) spindle-shaped, (d) flattened subspherical, (e) discoidal; (f, g) heteropolar: (f) subconical, (g) tripod; and (h) bilateral, variously shaped.

various skeletal covers and related structures (spines, spinules, apophyses, tunica, apertures, etc.). The outer elements embrace and cover the inner elements.

The morphological role and function of the inner elements is in the mechanical protection of the central capsule, which contains the entire endoplasm (nucleus, ribosomes, Golgi body, and endoplasmic reticulum), while the outer skeletal elements work as a mechanical support for the ectoplasm.

Symmetry and Shape of Skeletons

The geometry of radiolarian skeletons is very diverse (spheres, often enclosing one another, dumbbells, cylinders, towers, propellers, cones, helmets, crowns, etc.). The use of basic symmetrical shape is necessary to classify all these varieties and gain an insight into possible transformations of skeletons (Fig. 9; Table 4). Beklemishev (1964) recognized the following progressively more complex types of symmetry:

Homaxal type (Fig. 9a). Spherical skeletons and their derivatives, with endless number of similar axes. If the number of axes is reduced to 20, 6, or 4, the number of radii of symmetry is also reduced. Most often the radiolarian skeleton has a shape similar to a sphere. Probably, this is the best adaptation to the planktonic mode of life.

Monaxal type (Figs. 9b–9e). The number of axes is reduced to one. The skeleton is depressed in the direction of this very axis, or elongated along it.

Heteropolar type (Figs. 9f, 9g). The poles of the only axis are not equal. The number of radii of symmetry is uncertain, may be three or two. In the latter case,

Table 4. Main morphological characters of radiolarian skeletons

1. Symmetry of skeleton	1—homaxonic (axes are equal), 2—monoaxonic (one axis), 3—heteropolar (one axis, poles are unequal, 4—bilaterally symmetrical			
2. Skeleton	Geometrical shape		Construction	
	1—spherical, 2—conical, 3—square, 4—triangular, 5—pyramidal, 6—discoidal, 7—spindle-shaped, 8—oviform, 9—raylike, 10—intersecting spines, 11—other		1—skeleton proportions, 2—number of rays, 3—spines intersecting in one center, 4—three spines merged to form triangular frame	
3. Internal framework (Pls. 8–11; Pl. 12, figs. 1, 3, 5; Pl. 13, figs. 1–6; Pl. 14, figs. 1–3, 7)	Type		Construction	
	1—hollow sphere, 2—hemisphere, 3—polyhedron, 4—spicule, 5—subtriangular frame, 6—microsphere		4-rayed spicule, 6-rayed spicule, 8-rayed spicule, 12-rayed spicule, multi-rayed spicule; microsphere: spherical or multifaceted (4–6-faceted)	
4. Primary skeleton sphere (Pls. 12–14)	Structural type		Microstructure	
	1—porous, 2—latticed		1—finely porous, 2—microporous, 3—variously porous	
5. Internal skeletal spheres (Pls. 12–14, 18, figs. 7, 8)	Structural type	Microstructure		
	1—latticed, 2—cellular, 3—spongy, 4—porous	1—thick-walled, 2—thin-walled	1—macroporous, 2—finely porous, 3—microporous, 4—heteroporous	
6. External skeletal sphere (Pls. 15–19)	Structural type	Microstructure		
	1—latticed, 2—cellular, 3—spongy, 4—porous, 5—lamellar	1—thick-walled, 2—thin-walled	1—macroporous, 2—finely porous, 3—microporous, 4—heteroporous	
7. Number of skeleton spheres	1, 2, 3,… many			
8. Pores and structure of intervening bars (Pls. 16–18)	Pores		Intervening bars	
	Form	Dimensions	Shape of surface	Width
	1—circular, 2—oval, 3—rounded-polygonal, 4—angular-oval, 5—subtriangular, 6—angular-polygonal	1—large, 2—small, 3—smallest	1—flattened, 2—circular, 3—rounded-pointed	1—very wide, 2—wide, 3—narrow, 4—very narrow
9. Mouth and Pylome (Pl. 20)	Availability	Structure		
	1—absence, 2—presence	1—simple, 2—framed	1—ridge, 2—collar, 3—spines, 4—peristome	1—open, 2—partly open, 3—slitlike, 4—closed

Table 4. (Contd.)

10. Main spines (Pls. 21–27)	Numbers	Shape of spines	Section of spines	Shape of facet	Section of facet	Spine structure	Length	Thickness
	1, 2, 3, … many	1—tubular, 2—rodlike, 3—conical. 4—bladed	◀-shaped, Y-shaped, ●—circular, ■—subsquare	1—blade-shaped, 2—petaloid, 3—subtriangular	1—blade-shaped, 2—sub-rectangular	1—hollow, 2—solid, 3—depression in basal part, 4—straight, 5—curved, 6—double, 7—helical, 8—with apophyses	1—very long, 2—long, 3—short, 4—very short	1—massive, 2—thick, 3—thin, 4—slender

11. By-spines (Pl. 28)	Shape of by-spines	Section of spines	Length	Thickness
	1—conical, 2—rodlike, 3—bladed	▲—triangular, ●—circular	1—very long, 2—long, 3—short, 4—very short	1—very thick, 2—thick, 3—thin, 4—slender

12. Sculptural elements (Pl. 17, figs. 7–10; Pl. 29)	Type of sculpture	Shape of sculpture	Shape of apex	Shape of cells	Size	Thickness	Frequency
	1—thorns, 2—thorn-tubercles, 3—tubercles, 4—bars, 5—ridges	1—rodlike, 2—conical, 3—platelike	1—rounded, 2—rounded pointed, 3—tapering, 4—pointed	1—circular, 2—oval, 3—rounded-polygonal, 4—polygonal	1—very large, 2—large, 3—small, 4—very small	1—very thick, 2—thick, 3—thin, 4—very thin	1—very frequent, 2—frequent, 3—rare, 4—very rare

13. Ranked sizes of skeleton and its parts	Absolute			Relative
	D—diameter of external sphere, *tw*—wall thickness of external sphere, *dp*—pore diameter of external sphere, *wp*—width of intervening bars of external sphere, *D1*, *D2*, … *Dn*—diameter of internal spheres, *Ds*—diameter of primary skeleton sphere, *ts*—wall thickness of primary sphere, *ds*—pore diameter of primary sphere, *ws*—width of intervening bars of primary sphere, *L*—length of main spines, *wL*—width of main spines base, *dL*—width of main spines	*Lg*—length of main major spine, *wLg*—width of main major spine base, *l*—length of by-spines, *wl*—width of by-spine bases, *lh*—height of costa, *ld*—diameter of cell, formatted by costae, *lw*—width of costa, *ht*—height of thorns and tubercles, *A*—length of apophyses, *AL*—length of main spines from the base to apophyses, *dA*—width of apophyses, *zp*—thickness of rodlike bars	*a*—a-rod, *b*—b-rod, *i*—intersector, *at*, *bt*, *it*—triangular frame sides, *c*—cavea rib, *p*—patagium, *aL*, *bL*, *cL*—length of main spines, *al*, *bl*, *cl*—length of by-spines, *d*—pore diameter of spongy meshwork, *w*—width of intervening bars, *R*—arc radius	*L/D*, *cL/D*, *Lg/wLg*, *L/wL*, *L/dL*, *l/wl*, *AL/L*, *L/AL*, *dp/wp*, *ds/ws*

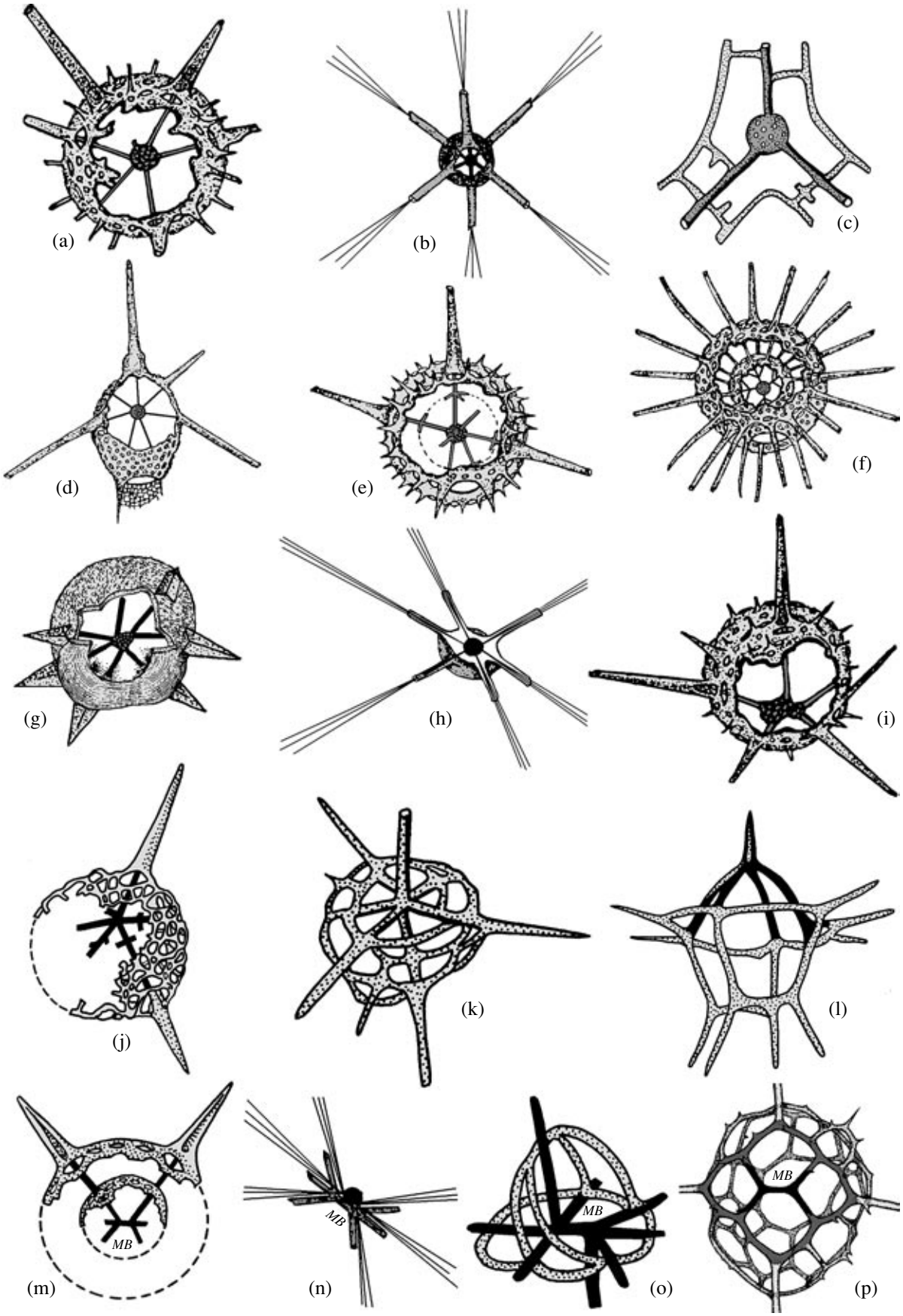
(a)
(b)
(c)
(d)
(e)
(f)
(g)
(h)
(i)
(j)
(k)
(l)
MB
(m)
MB
(n)
MB
(o)
MB
(p)

two halves of a skeleton can be theoretically matched by a rotation along the axis. Originally, heteropolar radiolarians (Pylomariata, Mesozoic–Cenozoic Nassellaria) have variably elongated skeletons, ranging in shape from a spindle, cylinder, or mushroom to a short cone, or umbrella. The number of radii of symmetry is 2–4, more rarely, 5–6, the most common number of external apophyses is three (so-called tripod).

Bilateral type (Fig. 9h). This shape is the completion stage of radiolarian specialization, involving both the interior of the skeleton and arrangement of chambers and segments, and suggests a plane of symmetry with an axis in it. This type of symmetry involves the differentiation of the skeleton in the direction of one morphological axis (conventionally up–down) and towards the anterior–posterior axis. The resulting halves of the skeleton are mirror images, e.g., Acanthodesmiidae, Cannobotryidae, and Albaillellata.

Symmetry is not only defined by the shape's geometry, but also by the biological properties of organisms. The center, axis, or plane of symmetry are recognized as such only under the condition that they are in a certain way produced by the organismic structure itself, i.e., they can always be found. The uncertainty of axes exists in the case of the indifferent balance, in the absence of active movements, and where the organism is adapted to passive floating. These are diverse spherical forms of the homaxal type of symmetry. The axis appears at the necessity of rotation, for maintaining stability and defining the direction of movement. In the case when the direction of motion is not important, the monaxal type exists. If there is some preference in the direction of motion, the heteropolar, or bilateral type of differentiation appear. This geometrical differentiation is caused by the scheme of biological differentiation (Mordukhai-Boltovskoy, 1936).

Internal Framework

The internal framework of radiolarians occupies the central place in the skeleton and has the shape of a hollow, nonporous sphere with radiating rays, an isometric polyhedron with cylindrical rays, four-, six, and eight-rayed spicule and a microsphere (Table 4, Fig. 10).

The function of the internal framework is still uncertain, because this structure is not present in the skeleton of extant Polycystina, except for Nassellaria. However, its correlation with other skeletal structures, primarily radial spines and shells should be noted. According to Hollande and Enjumet (1960), extant radiolarians show certain relationships between the skeletal structures and nucleoaxopodial complex influencing skeletal morphology and symmetry.

The internal framework is centrally or eccentrically positioned inside the primary inner sphere of the skeleton. It may be suggested that its position in relation to the axoplast is almost identical to the position of these structures in extant Nassellaria. In the cell of Nassellaria, the axoplast retains its position near the median bar of the skeleton (Fig. 1g).

The radial rays (spines) extending from the internal framework of Paleozoic radiolarians (Figs. 10b, 10h, 10m) could be orientated as the axopodial filaments (judging from extant Nassellaria). Similar to the axopodial system, the internal framework is connected with all other parts of the skeleton: the main spines of the skeleton are the direct continuations of the rays of the internal framework. Therefore, it is possible that, in the ancient radiolarians, the internal framework and axoplast with axopodia were connected into a single system.

Protozoologists believe that the axopodial system directly participates in the skeletal growth (Cachon and Cachon, 1972). In addition, the axopodia are involved in the most important functions (feeding and motion). Hence, the nucleoaxopodial complex was highly important in the metabolism. Because the axopodia are also organs of motion (Petrushevskaya, 1981a), their basal and proximal parts require support. Because of the above, three major types of the internal framework (hollow sphere, semisphere, isometric polyhedron) and spicule were developed almost simultaneously in the evolution of radiolarians (Nazarov, 1988) (Fig. 10).

Hollow sphere. Ancient radiolarians from the order Inaniguttata (Cambrian–Early Devonian) acquired support in the shape of a hollow nonperforated sphere with radiating hollow rays (Figs. 10a, 10b), which is well developed in the Ordovician and Silurian spherical Polycystina (Pl. 8, figs. 1, 2). The size of the spherical internal framework is 45–55 μm, while the diameter of the primary inner sphere in the extant centroperiaxoplastidian radiolarians is 15–40 μm (Figs. 1c, 1d). Therefore, it is possible that the axoplast of the Early Paleozoic radiolarians could occur inside the spherical internal framework, whereas the axopodia extended

Fig. 10. Type of the inner framework in Polycystina: (a–f) hollow sphere: (a) *Inanigutta*, Ordovician; (b) hypothetical model of the axoplast and spherical framework; (c) *Triactofenestrella*, Late Carboniferous; (d) *Proventocitum*, Early Ordovician; (e) *Cessipylorum*, Middle Ordovician; (f) *Aciferopylorum*, Silurian; (g) isometric polyhedron, *Caspiaza*, Late Devonian, Famennian; (h, i) semiclosed sphere: (h) hypothetical model of an axoplast and semispherical framework, (i) six spines, extending from the curved hemisphere, *Inanigutta*, Ordovician; (j–l) spicule with spines, extending from one center: (j) six branching spines, *Haplentactinia*, Ordovician, (k) six spines positioned oppositely to the free spine, *Secuicollacta*, Silurian, (l) four spines, positioned oppositely to one spine of the spicule on the microsphere, *Pentactinorbis*, Triassic; (m–o) spicule with a median bar (*MB*): (m) six-rayed spicule inside two porous shells, *Bientactinosphaera*, Devonian, (n) hypothetical model of an axoplast and six-rayed spicule, (o) six-rayed spicule and main arches in Nassellaria; (p) microsphere: tetrapetaloid spicule on the microsphere, apical view, *Hexalonche*, Early Jurassic; (a–f, h–k, m, n) after Nazarov, 1988; (g) after Afanasieva, 1986; (l, p) after Dumitrica (1978, 1985); and (o) after Petrushevskaya (1971).

Plate 8

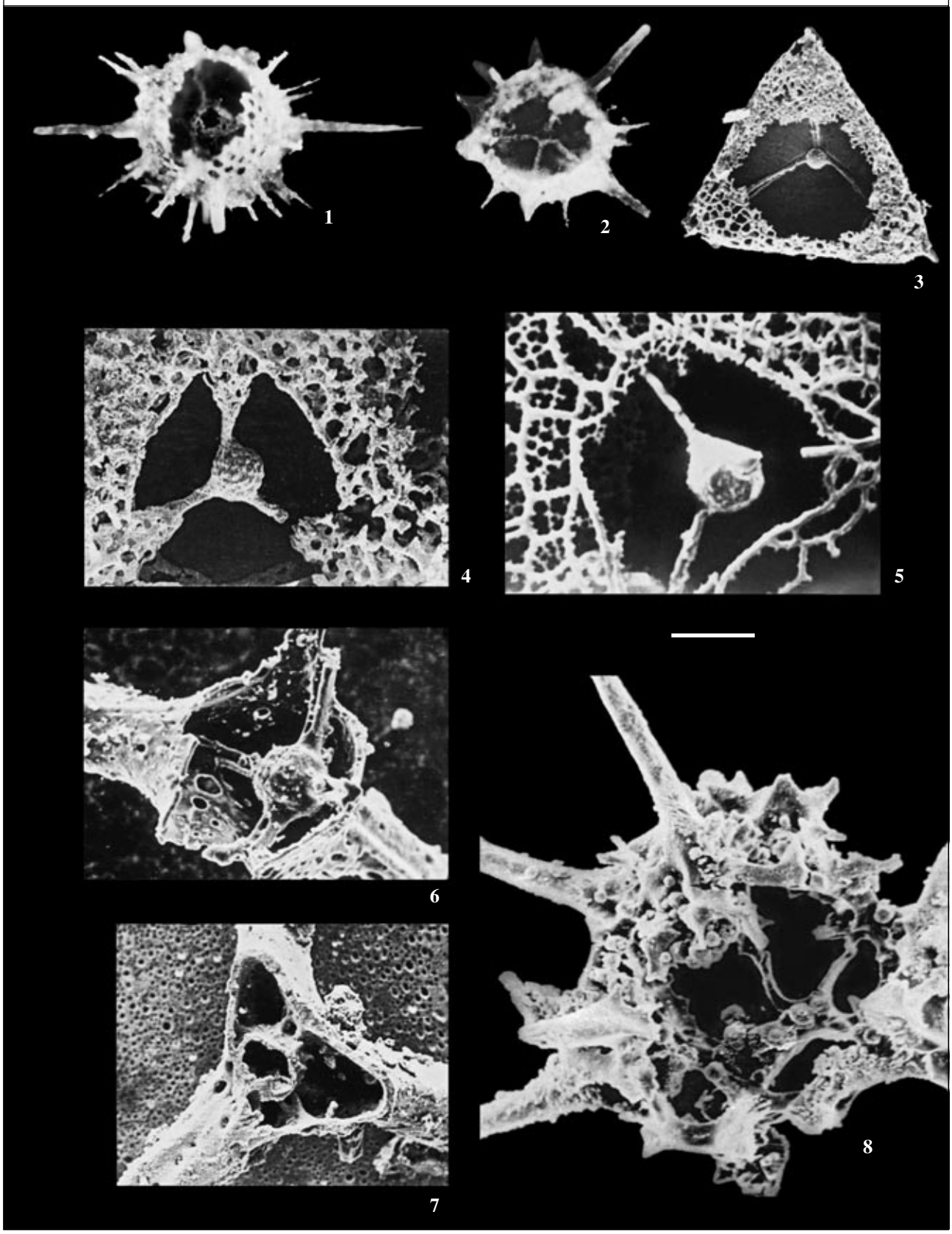

Inner framework in members of (1, 2, 8) the order Inaniguttata and (3–7) the class Stauraxonaria.

outwards through the hollow rays that were directly connected with the main spines (Fig. 10b).

However, the massive construction of the internal framework apparently influenced the segmentation of the nucleus and endoplasmic structures only slightly. In addition, the massive internal framework, apparently did not facilitate floating and precluded vertical migration. For these reasons, the structure of the internal framework did not become widespread in the evolution of spherical Polycystina (Nazarov, 1988).

At the same time, stauraxonic radiolarians, which appeared in the Late Cambrian, but flourished for the first time in the Carboniferous–Permian were characterized by the development of the inner sphere in the shape of a hollow sphere with extending hollow rays during the entire Paleozoic (Nazarov, 1988) (Fig. 10c; Pl. 8, figs. 3–7).

The internal framework of the radiolarians containing a pylome (order Pylomariata) occupies a central position in the subspherical skeleton. It has a shape of a hollow nonporous sphere with extending seven rays in the shells of the Cambrian–Ordovician Proventocitidae, Ordovician–Early Devonian Cessipylorinae, and Early Silurian Aciferopyloridae (Figs. 10d–10f) (Afanasieva, 1986, 2000a).

The Paleozoic stauraxonic Polycystina, except for the lenticular and discoid shells, do not show principal changes in the structure of the internal framework (Nazarov, 1988). The framework is not transformed into a spicule, but the number of rays extending from the sphere increases. In the Late Carboniferous, stauraxonic Polycystina with four or five rays appear, while in the Early Permian, they have seven or more rays (Nazarov and Ormiston, 1984). Only in the lenticular and discoid taxa from the order Pyramidata in the Early Permian the inner sphere become transforming into the three–four-rayed spicule (Nazarov, 1988).

There is a certain similarity between the inner spherical frame of the Early Paleozoic Radiolaria of the order Inaniguttata, stauraxonic taxa from the class Staurax-onaria, and Radiolaria with a pylome from the order Pylomariata. Two patterns are particularly persistent:

(a) the number of main (external) spines depends on the number of rays of the internal framework (spicule), or on the number of rays extending from the inner sphere;

(b) the number of inner and outer shells depends on the number of groups of apophyses developed on the rays of the internal framework.

Semisphere. It is possible that, in some ancient Polycystina, the axopodial complex was outside the sphere, which because of this became somewhat flattened (isometric semisphere or plate) (Figs. 10h, 10i) (Nazarov, 1988). However, this type of the internal framework is very rare and recorded in only some members of the Ordovician *Inanigutta* (Pl. 8, fig. 8). Apparently, this is an incidental malformation which was not fixed genetically and did not develop further.

Polyhedron. In the Late Devonian–Middle Carboniferous Caspiazinae, the internal framework is an isometric polyhedron with seven cylindrical rays (Fig. 10g, Pl. 9, figs. 8, 9). Perhaps, this is the first step of Radiolaria toward the lightening of the internal skeletal framework. However, this type of internal framework did not develop in other radiolarians.

Spicule. The spicule is an inner primary structure, the morphological center of the skeleton. It is a *n*-rayed body (where *n* is 4–6 to 24), formed by one primary four-rayed spicule (Figs. 10j, 10k, 10l) or by a combination of two primary four-rayed spicules (Figs. 10m–10p). The initial spicule is most often inside the sphere (in its center), but occasionally it is eccentric. The distal terminations of the rays of the spicule possess main spines of the skeleton.

The four-rayed spicule is a universal primary skeletal element of radiolarians, which is stable in space and time. The skeleton of Radiolaria is built of opal ($SiO_2 \cdot nH_2O$), the major structural unit of which is silicate tetrahedron $[SiO_4]^{4-}$, anion of orthosilicic acid (Afanasieva and Vishnevskaya, 1992; Afanasieva, 2000a). The vertices of the tetrahedron have atoms of

Explanation of Plate 8

(Figs. 1 and 2) Middle Ordovician, Llandeilo Series; eastern Kazakhstan, Chagan River; (Fig. 8) Upper Ordovician, Ashgillian Stage; Estonia, borehole Eikla; (Fig. 3) Upper Carboniferous, Gzelian Stage; southern Ural Mountains, Ural River, village of Nikol'skii; (Figs. 4–6) Lower Permian; southern Ural Mountains, Ural River, village of Donskoe: (4) Sakmarian and (5, 6) Artinskian stages; and (Fig. 7) Lower Permian, Sakmarian Stage; southern Ural Mountains, Sakmara River, village of Verkhnyaya Chernaya Rechka. (Figs. 1–8) after Nazarov (1988).

Fig. 1. *Inanigutta elongata* (Nazarov), scale bar = 150 μm.

Fig. 2. *Inanigutta unica* (Nazarov), bar = 150 μm.

Fig. 3. *Latentidiota semilamina* Nazarov, bar = 150 μm.

Fig. 4. *Tormentum circumfusum* Nazarov et Ormiston, bar = 60 μm.

Fig. 5. *Ruzhencevispongus cataphractus* Nazarov et Ormiston, bar = 65 μm.

Fig. 6. *Quinqueremis* sp., bar = 60 μm.

Fig. 7. *Latentifistula valdeinepta* Nazarov et Ormiston, bar = 60 μm.

Fig. 8. *Inanigutta eiklaensis* (Nazarov), bar = 50 μm.

Plate 9

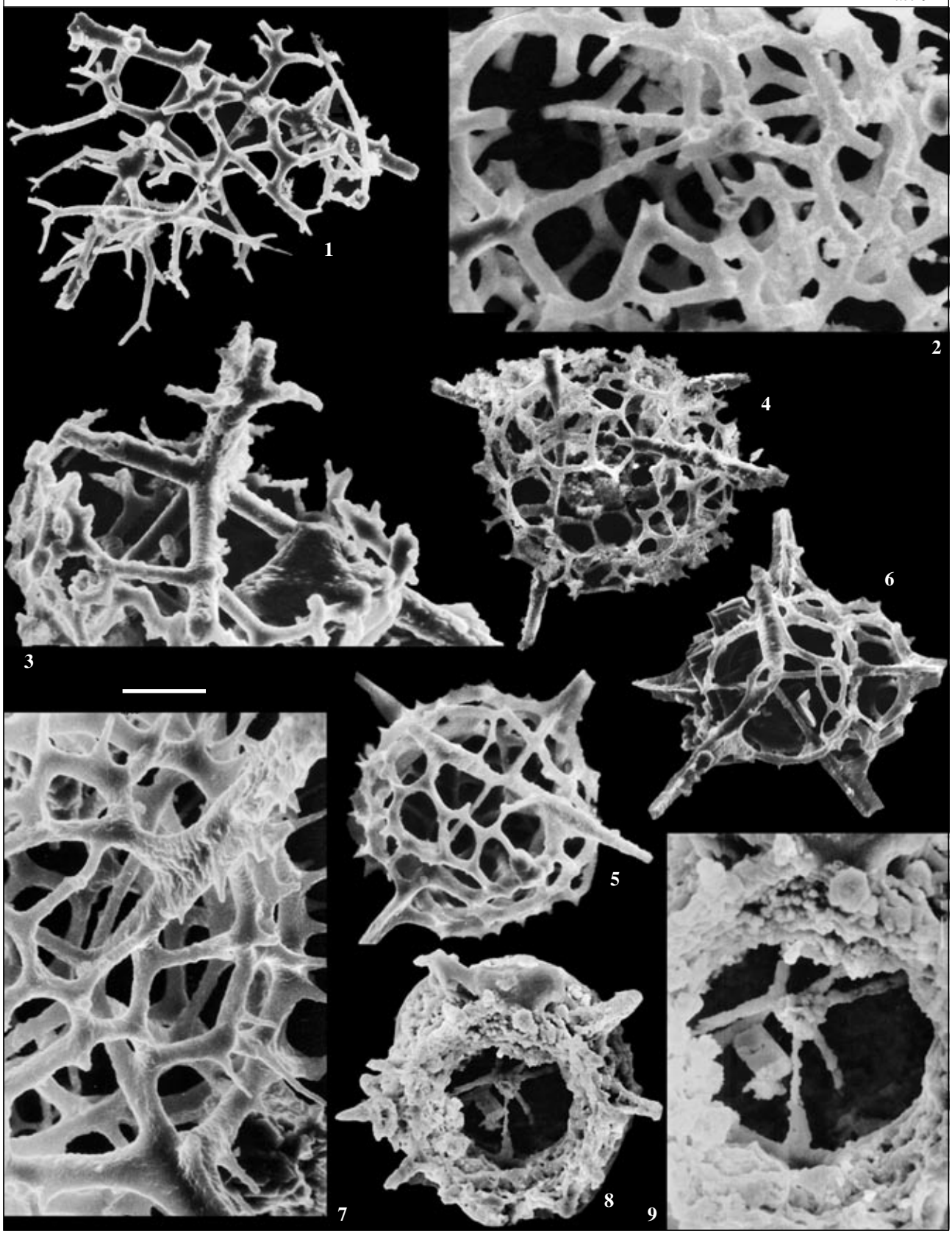

Inner framework in members of (1–7) the subfamily Haplentactiniinae and (8, 9) Pylomariata of the genus *Caspiaza.*

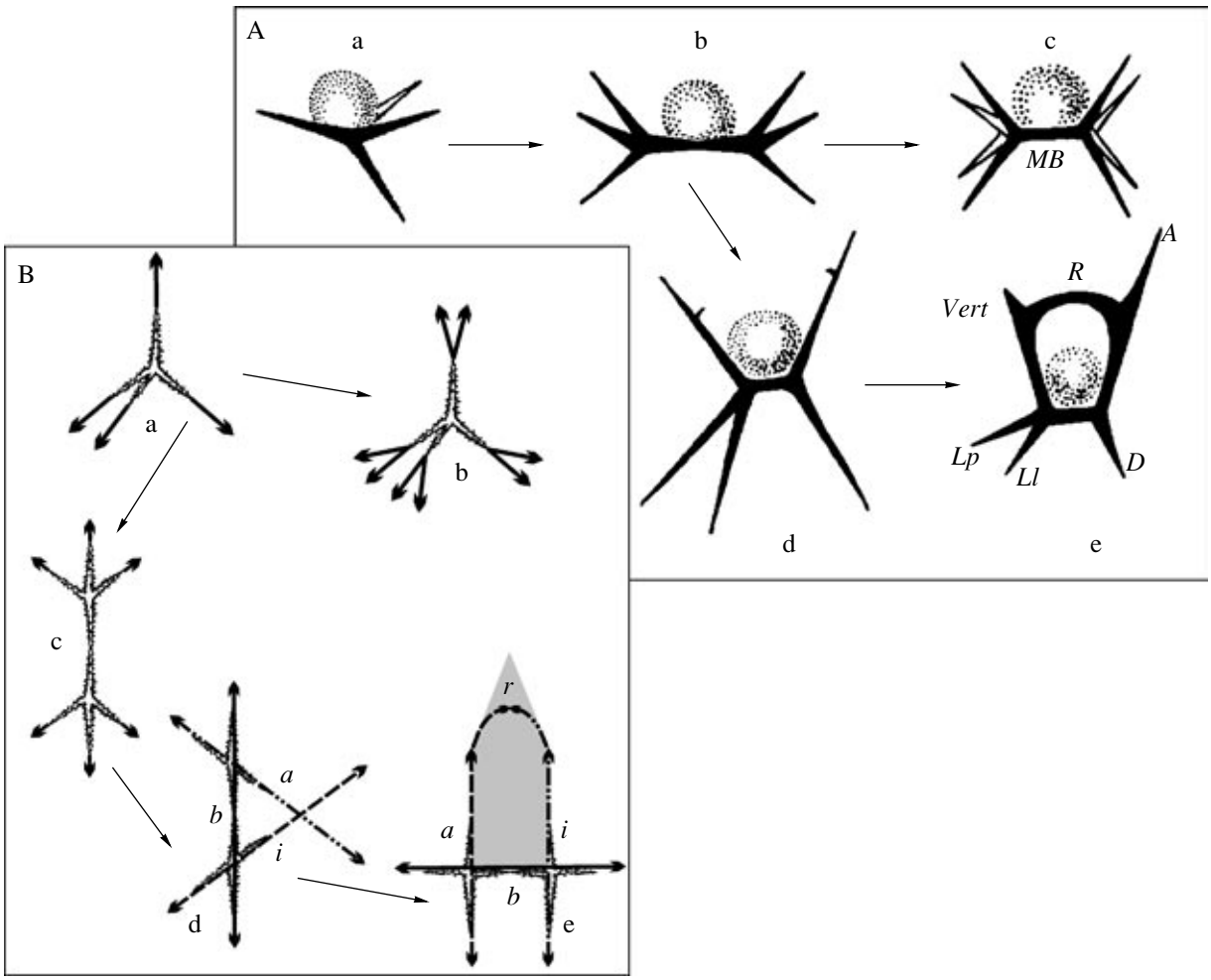

Fig. 11. Development of the spicule in Nassellaria and spiny skeleton of Aculearia: (A) a simplified way of the spicule development in some Nassellaria (after Popofsky, 1913 and Petrushevskaya, 1971): (a) *Plagoniscus*, (b) *Plagonium*, (c) *Polyplecta*, (d) *Plagiocarpa*, and (e) *Cortina*; (B) development of the spiny skeleton in Aculearia: (a) Palacantholithidae, (b) Palaeospiculinae, (c) Xiphocladiellidae, (d) Ceratoikiscidae, and (e) Albaillellata.

oxygen, whereas the atom of silicon is in the center. Biogenic amorphous silica (Francois, 1989) can make complex structures of short three-dimensional chains of tetrahedrons $[SiO_3]^{2-}$, which can form combinations of two or more anions through the shared atom of oxygen (Figs. 3a, 3b). The external shape of the skeleton reflects general patterns at the molecular level. This element of the ultrastructure of the primary opal is used as a basis in the development of the primary four-rayed spicule of radiolarians, i.e., the microlevel manifests itself at the macrolevel (Tochilina, 1997; Afanasieva and Amon, 2003c). Possibly, the four-rayed spicule was the prototype of the primary radiolarian skeleton.

Haeckel (1887) was the first to propose the four-rayed tripod as the incipient element of the Nassellaria

Explanation of Plate 9

Upper Devonian: (Figs. 1–7) Middle Frasnian Substage, Domanik Formation; Timan–Pechora Province: (1, 3, 6) Lyajol River, outcrop 1904, sample 6; (2, 4, 5, 7) borehole Shuda-Yag-1003: (2) sample 8 (depth 120.9–124 m), (4) sample 78 (depth 68.4–69.3 m), (5) sample 72 (depth 71.9–72.4 m), and (7) sample 68 (depth 73.3–73.5 m); (Figs. 8 and 9) Famennian Stage; Polar Ural, Lemvinskaya Area, sample 101/594k.

Fig. 1. *Tetragregnon quadrispinosa* (Foreman), scale bar = 50 μm.

Figs. 2–4. *Haplentactinia alekseevi* Afanasieva: (2) bar = 17 μm, (3) bar = 30 μm, and (4) bar = 37 μm.

Figs. 5 and 6. *Haplentactinia barskovi* Afanasieva: (5) bar = 33 μm and (6) bar = 37 μm.

Fig. 7. *Haplentactinia aperticuva* (Aitchison), bar = 15 μm.

Figs. 8 and 9. *Caspiaza spinifera* Afanasieva: (8) bar = 50 μm and (9) fragment, bar = 27 μm.

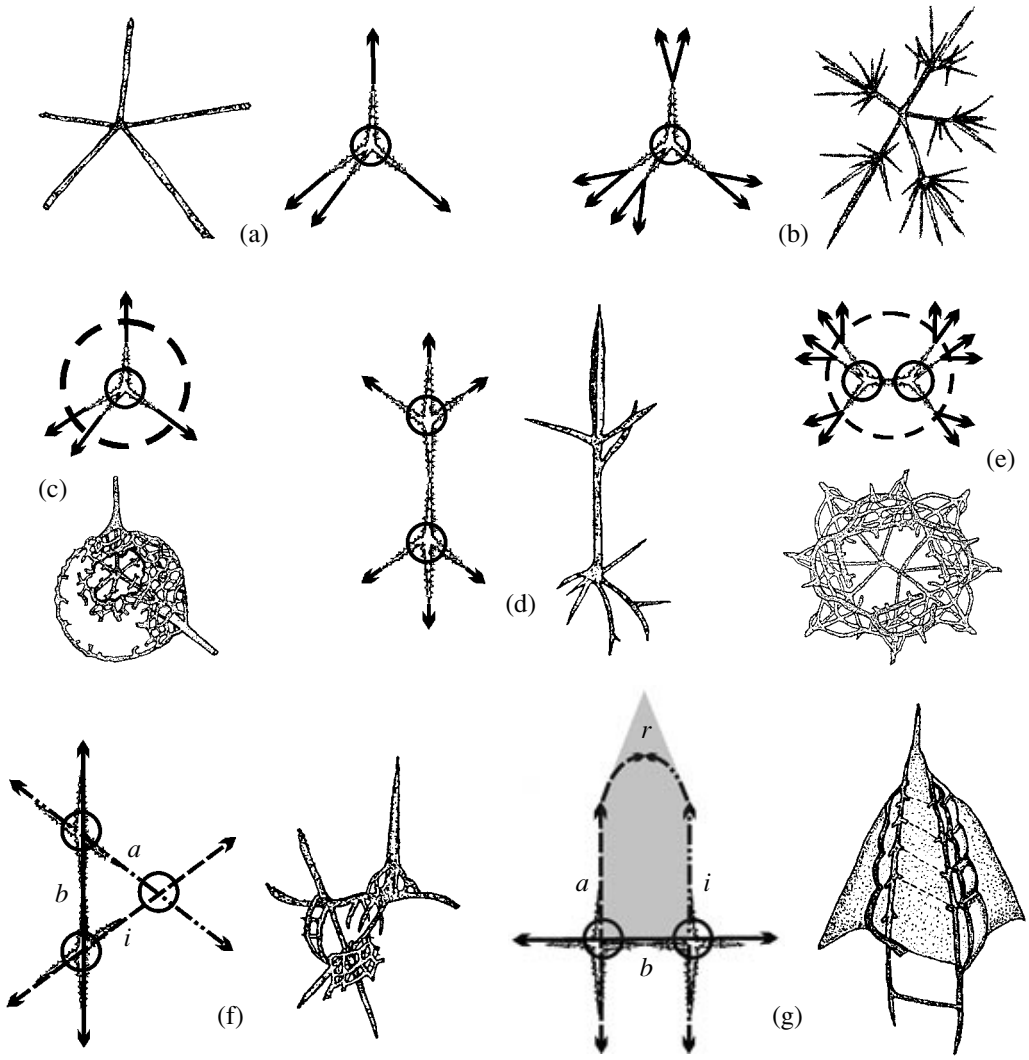

Fig. 12. Spiny skeletons of Aculearia and initial spicule of spherical radiolarians Spumellaria: (a) Palacantholithidae, (b) Palaeospiculinae, (c) Haplentactiniidae, (d) Xiphocladiellidae, (e) Polyentactiniidae, (f) Ceratoikiscidae, and (g) Albaillellata; (O) indicates morphological centers of the skeletal growth.

skeletons, the idea later developed in detail by Popofsky (1913). Popofsky believed that the skeleton of *Plagoniscus* (Fig. 11A, a) is similar to the skeletons in the family Thalassothamnidae (order Collodaria) and even suggested that Nassellaria evolved from these radiolarians. The four-rayed spicule in Popofsky's theory was treated not only as an initial skeletal element of all Nassellaria, but also as a bridge connecting it with spherical radiolarians. In the process of the further perfection of the Nassellaria skeleton, the primary tripod was changed. The median bar (*MB*) (Figs. 11A, b; 11A, c) and apophyses (Fig. 11A, d) appeared; spines *lr*, *ll*, and *Vert* (Fig. 11A, e) were added. The spines *A* and *Vert* were fused at the tips to form a sagittal ring (*R*) (Fig. 11A, e). Popofsky also suggested that various modifications of the spiny skeleton appeared at the earliest stage of evolution of Nassellaria and that they were repeated in derived taxa. The major stages of the skeletal development of the spiny radiolarians Aculearia (Fig. 11B) resemble the general scheme of the skeleton development in Nassellaria (Fig. 11A).

The spines of Aculearia cross in one or two points to form a skeleton similar to the initial spicule of spherical radiolarians (Fig. 12). These points (or knots) may be treated as morphological centers, from which the skeletons extended (Afanasieva and Amon, 2003c).

(1) The initial four-rayed spicule is the basic element of the earliest skeletons of Palacantholithidae (Fig. 12a).

(2) The initial four-rayed spicule with thorns and apophyses in Palaeospiculinae (Fig. 12b).

(3) The interlacing network of apophyses tends to form a bundle structure, which is a bridge to the spherical lattices of the order Cancelliata, in which the rays

of the spicule radiate from a single center (Figs. 10j, 10k; 12c; Pl. 9, figs. 1–7).

(4) The integration of two initial four-rayed spicules is the basis for the development of Xiphocladiellidae (Fig. 12d).

(5) The main triangular skeletal framework in the order Triangulata was formed as a result of the joining of two initial four-rayed spicules and development of its spines *a* and *b* and intersector *i* in one plane (Fig. 12f).

(6) The skeleton in the order Albaillellata is based on the united double initial four-rayed spicule, the spines of which *a* and *b* and intersector *i* develop in one plane, but with an initial **H**-shaped framework composed of subparallel spine *a* and intersector *i* joined by spine *b* at the base of the skeleton. In the apical part of the skeleton, the spine *a* and intersector *i* are closed to form *r*, a structure convergently similar to the sagittal ring of Nassellaria (Fig. 12g).

(7) In the Early Mesozoic (Triassic) Spumellaria, one apical spine of the spicule is opposite to four basal spines (Fig. 10l). The two latter are joined by the arcs in the proximal part to form four proximal pores. A similar spicule is developed in periaxoplastidian taxa of Pentactinocarpinae. The main spicule is inbuilt in the wall of the skeletal shell and is only slightly discernible.

Spicule with the median bar. The internal framework in the shape of a six-rayed spicule with a median bar (*MB*) apparently was more beneficial for the normal functions of the cell (Figs. 10m–10o). Both six-rayed and multi-rayed spicules with the median bar (*MB*) are formed by two initial four-rayed spicules (Fig. 12e). Such a spicule is present in the spherical spongy radiolarians of the order Spongiata (Pl. 10), porous members of the order Entactiniata (Pl. 11; Pl. 12, figs. 1, 3, 5; Pl. 13, figs. 1–6; Pl. 14, figs. 1–3, 7), and radiolarians with a pylome of the families Pylentonemidae and Popofskyellidae.

This constructions is retained in the spherical spongy radiolarians of the class Spumellaria (Pl. 10) and porous radiolarians of the order Entactiniata (class Sphaerellaria) (Pls. 11–14) during the entire Paleozoic, whereas in the Nassellaria, it has remained up to the present.

In the Nassellaria with a large cephalis (Fig. 10o), the spicule is readily visible, while in the cephalises less than 30 μm in diameter, it is not always noticeable, but the position of the rays of the spicule is rather uniform. It contains the median bar *MB*, spines *A*, *D*, *Lp*, *Ll*, and *Vert* forming a bilateral structure (Figs. 10o; 11A, e). The spicule may be included in the sagittal ring (Fig. 1f), forming a constriction in the central part of the nassellarian cell (Nazarov and Petrushevskaya, 1995).

Microsphere. The primary microsphere develops from the corners of the spicule. The microsphere is connected with the external shell of the skeleton by the spines, which are continuations of the spicule. One spine (antapical) extends from the antapical part of the primary microsphere.

The tetrapetaloid type of the initial spicule, which is quite widespread in the Mesozoic–Cenozoic Sphaerellaria and Spumellaria produced by the further development of the initial spicule. The initial spicule contains a short median bar (*MB*) and four main spines. The spines are joined by the arcs in the proximal part and form a characteristic tetrapetaloid structure with four wide pores and the median bar (*MB*) in the center (Fig. 10p).

The evolution of the internal framework shows the development of two major skeletal elements, which almost simultaneously appeared in the evolution of Radiolaria (the sphere that appeared in the Early Cambrian and the spicule indisputably found beginning from the Middle Cambrian).

It is noteworthy that, if the inner hollow sphere (Fig. 10b) was usually in the center, the inner spicule was located eccentrically, apparently close to the axoplast (Fig. 10m). In the course of the evolution of the skeletal elements of Radiolaria, massive rays of the inner spicule became thinner. The rays have acquired deepened bases that are clearly pronounced in the Late Ordovician–Late Silurian Polycystina.

Apparently, primitive skeletons of spiny Aculearia and the initial spicule of Sphaerellaria, Spumellaria, Nassellaria, and some Stauraxonaria are nothing more than crossed primary beams. Hence, all five types of radiolarians that are fundamentally different in their external appearance have a common ancestry and in fact represent a transformation of one simple basic skeletal type (Mordukhai-Boltovskoy, 1936).

It is possible that the internal framework in the shape of a hollow sphere and isometric polyhedron with extending rays, and four-, six-, and multi-rayed spicule, were the first skeletal elements to appear in the evolution of Radiolaria. Probably, in the case of the underdeveloped or absent inner spicule in the Mesozoic and Cenozoic radiolarians, the primary microsphere could have functioned to substitute it. Radial spines extending from the microsphere supported the basal and proximal parts of the axopodia. The microsphere is developed on the continuations of the rays of the spicule (Fig. 10p) and, therefore, is a secondary skeletal element with reference to the time of its appearance. On the other hand, the microsphere was produced by the evolutionary merging of two initial elements of the internal framework (sphere and spicule), but at the new evolutionary level.

Primary Inner Sphere

Rays extending from the spicule grow, while their distal ends branch and fuse to form a latticed sphere

Plate 10

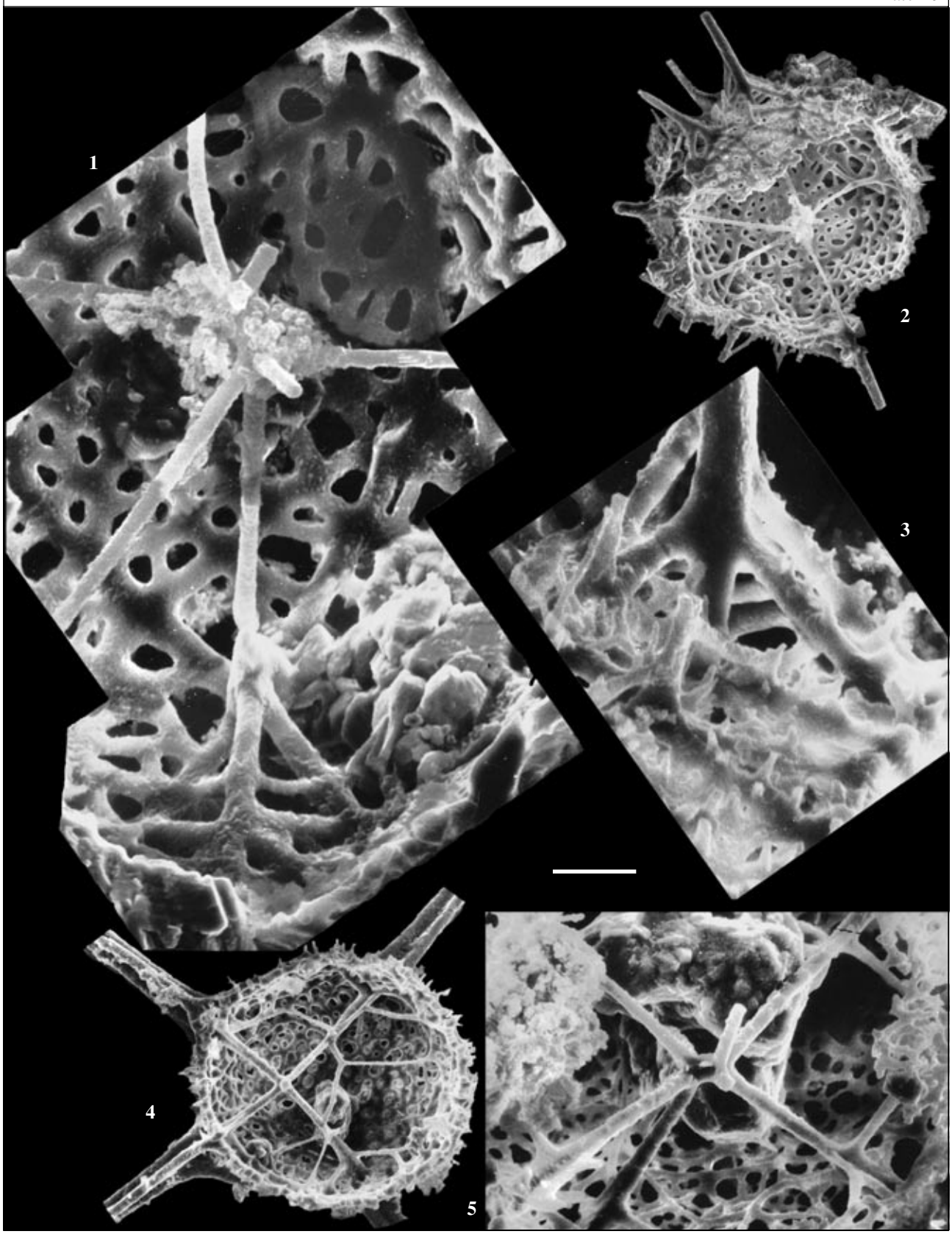

Inner framework in members of the subfamilies (1–3) Polyentactiniinae and (4, 5) Spongopolyentactiniinae.

(Table 4; Pl. 12–14) representing the primary shell of the skeleton.

The diameter of the primary sphere of extant radiolarians ranges from 15 to 50 μm and more (Petrushevskaya, 1986). The diameter of the primary sphere of Paleozoic radiolarians studied ranges from 35 to 85 μm (Table 5). It is noteworthy that Polycystina, in which the inner sphere is 15–25 μm and more so 10–15 μm are quite rare in the Paleozoic, probably because of the poor preservation of a very fine skeleton (Nazarov, 1988).

Based on the ratio of the diameters of the outer and primary inner shells (D/Ds), four types of the primary spheres can be recognized (Table 5): very large (D/Ds = 1.50–2.0), large (D/Ds = 2.01–2.3), small (D/Ds = 2.31–3.0), and very small (D/Ds = 3.1–4.5).

The wall of the primary sphere is thin, 1–3 μm (Table 5), which is comparable in size with the globules of crystalline units *C* and *B* of the skeletal ultrastructure (Table 2). Globules tightly contact each other to form the septa of the skeleton, with an equal height and width (Pl. 14, fig. 3).

The cephalis of nassellarians is the first chamber of their heteropolar skeleton, which is usually closed from the aboral pole and separated from the next chamber (thorax) by the median bar *MB* of the multi-rayed spicule, which is inside the skeleton (Figs. 1f, 1g).

The presence of homologous elements of the primary internal framework or their rudiments in most radiolarians suggests the monophyletic origin of this group. As early as 1936, Mordukhai-Boltovskoy concluded that "the rods with tetragonal pyramids superimposed on their cones are the main part of the skeleton. The pyramids contact by their faces to form a polyhedron… which we will name the inner polyhedron" (Mordukhai-Boltovskoy, 1936, pp. 39–40), which is transformed into the primary inner sphere. The rods of some radiolarians develop branching apophyses, which form a lattice of the outer polyhedron, which is transformed into the outer sphere. "In that case, we receive the outer polyhedron, representing the lattice, containing the soft body of a radiolarian, with the inner polyhedron inside it" (Mordukhai-Boltovskoy, 1936, p. 40).

Skeletal Shells

In studying polymerization in protists, Dogel (1951) concluded that, among the Foraminifera, multicameral taxa certainly represent the result of the further evolution of the unicameral taxa, similar to the latticed spheres of Spumellaria, up to four, one inside another. Similar modifications of the skeleton are caused by the periodical growing of cytoplasm of these taxa.

In the Phanerozoic evolution of Polycystina, changes in the skeleton show the polymerization of skeletal elements, which was apparently connected with the necessity to create finer subdivisions of the cytoplasm, i.e., an increase in the number of shells, chambers, radial spines, and pores. The trend toward polymerization began to manifest itself as early as the Paleozoic, but was strongest in Mesozoic radiolarians. Opposite trends are observed in Cenozoic taxa: the number of chambers decreases, their position and size become stable, whereas the skeleton becomes simpler and lighter, i.e., the process of oligomerization is noticeable (Petrushevskaya, 1986; Nazarov, 1988; Nazarov and Petrushevskaya, 1995).

The skeletal shells are to a varying extent characteristic of all classes of Radiolaria. Their main function is the support of the entity of the skeleton and of the entire cell. In addition, the skeleton promotes the subdivision of the external part of the cell and endoplasmic structures (nucleus, axoplast, and central capsule), thereby increasing the intensity of metabolism (Dogel, 1951; Petrushevskaya, 1981a, 1986). Compared to other parts of the skeleton, the shells show the highest degree of morphogenesis and complication (Nazarov, 1988).

Proportions of the shell sizes in polyspherical taxa is apparently very important for the normal functioning of the Polycystina cell. Usually radiolarians have external (cortical) shells and inner (medullar) shells. The cortical shells are usually closely spaced. The medullar shells are usually separated from each other at a distance equal to the half of the radius of the smallest medullar shell (Nazarov, 1988). The diameter of the outer shell in Paleozoic Radiolaria ranges from 55 to 360 μm, while the wall thickness ranges from 1 to 8 μm (Table 5). Based on the ratio of the diameter of the cortical shell and the wall thickness (D/tw), four types of the skeletal wall may be recognized (Table 5): very thick (D/tw = 10.0–20.0, thick (D/tw = 20.1–29.0), thin (D/tw = 29.1–100.0), and very thin (D/tw = 100.1–150.0).

In the Paleozoic, the number of medullar shells gradually increased (1–2–3–n) in all radiolarian lineages (see Chapter 4, Fig. 23): Inaniguttinae ⟶ Inanibiguttinae; Oriundoguttinae ⟶ Inanihellinae; Entactiniinae ⟶ Bientactinosphaerinae ⟶ Thecentactiniinae; Astroentactiniinae ⟶ Helioentactiniinae ⟶ Multisphaerinae; Haplentactiniinae ⟶ Pseudorotasphaerinae ⟶ Haplotaeniatinae; Polyentactiniinae ⟶ Magnisphaerinae; Retentactiniinae ⟶ Spongentactiniinae ⟶ Pluristratoentactiniinae; Spongopolyentactiniinae ⟶ Somphoentactiniinae ⟶ Plenoentactiniinae. This indicates the high taxonomic importance of the number of shells at the subfamily level.

Explanation of Plate 10

Upper Devonian, Middle Frasnian Substage, Domanik Formation; Timan–Pechora Province, borehole Shuda-Yag-1003.

Figs. 1–3. *Polyentactinia zhamoidai* Afanasieva, sample 68 (depth 73.3–73.5 m): (1) scale bar = 63 μm and (2, 3) fragment, bar = 15 μm.

Figs. 4 and 5. *Spongentactinella olafi* Afanasieva, sample 72 (depth 71.9–72.4 m): (4) bar = 67 μm and (5) bar = 32 μm.

Plate 11

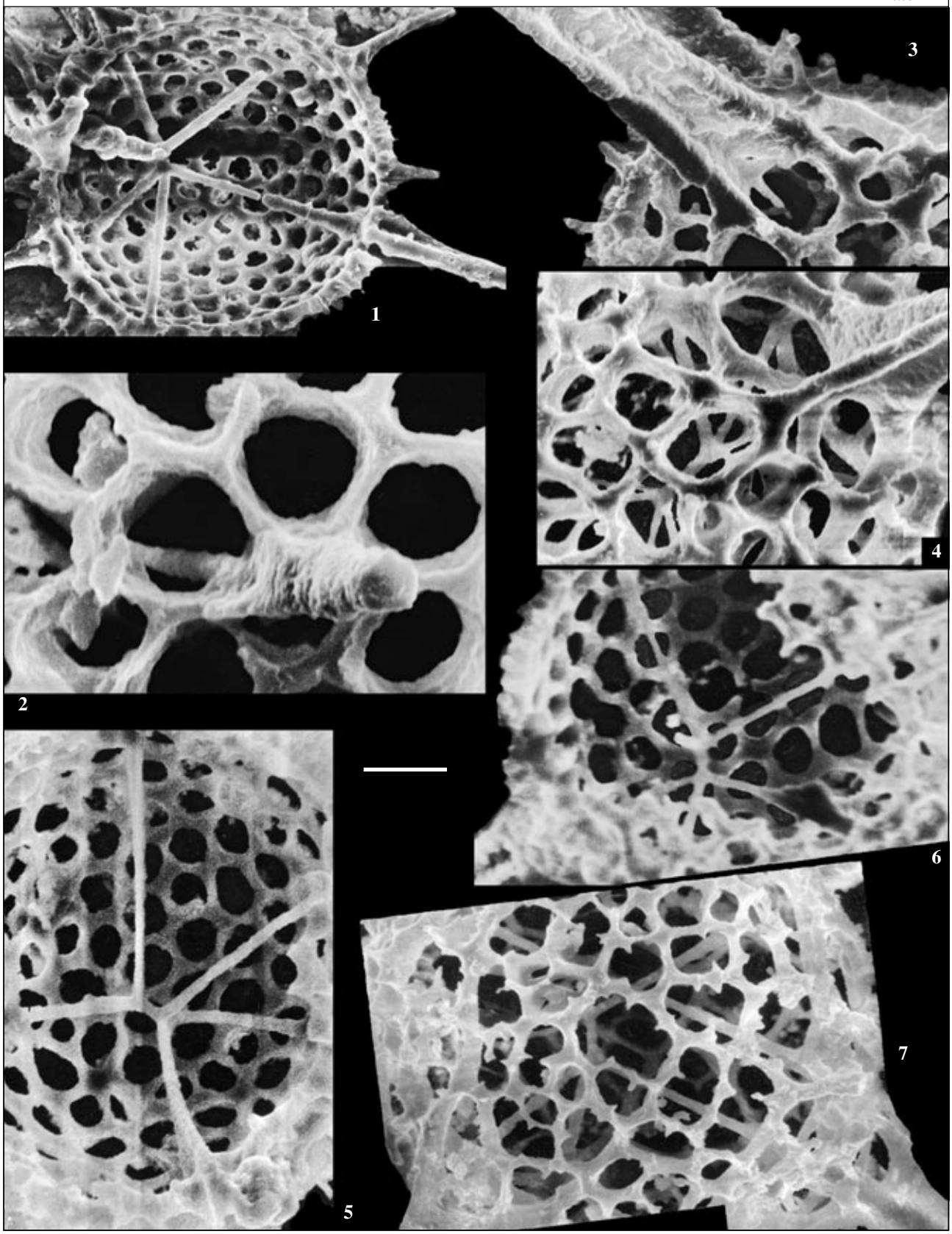

Inner framework in members of the subfamilies (1–4) Astroentactiniinae and (5–7) Entactiniinae.

The Cenozoic Litheliidae and some other subspherical spiral taxa have an intermediate position in this respect. The three-dimensional, partly reduced shells, appearing as narrow bands are typical of Pyloniidae. The chambers 3–30 μm are usual skeletal elements of many Polycystina. They are separated by radial and tangential bars and/or porous plates. The chambers are more often semispherical, similar in shape to the cytoplasmic vacuoles. The chambers may be arranged in one layer or in several layers: concentrically (Pseudoaulophacidae), spirally (Litheliidae), or irregularly (Spongodiscidae).

The heteropolar skeleton of Nassellaria consists of a cephalis separated from the following chamber (thorax) by a median bar of the multi-rayed spicule. These are followed by the abdomen and other skeletal segments. The last chambers are separated only by the external constrictions of the wall and/or inner ridges (or septa).

Five types of skeletal shells are recognized (Table 4). These are subjected to the two major types differing in the type of the skeletal growth: (1) latticed, reticulate, and spongy shells, in which the skeletal tissue is formed by the bridge growth pattern and (2) porous and lamellar shells, the skeletal tissue of which is formed by the rim growth pattern.

Latticed skeletal shells. Latticed skeletons are formed by a few thick and coarse rods (Pl. 15, figs. 1, 2). Auxiliary rods are arranged quite regularly to form large meshes. These rods outline and define the rounded, square, or isometric meshes of a latticed wall.

Reticulate skeletal shells. The rods forming reticulate spheres are thinner or not wider than the meshes between them and form an integrated net (Fig. 13; Pl. 15, figs. 3, 4). The net may be single-layered, or multi-layered. The net usually contains thick rods separating large meshes, which in turn contain thinner rods separating smaller meshes. The meshes may be rounded polygonal (Pl. 15, fig. 3) or subtriangular (Pl. 15, fig. 4), with the angles of the meshes always smoothed and rounded to increase the durability of the skeleton.

Spongy skeletal shells. The spongy shells are distinguished by the chaotic twirls of the thinnest skeletal threads that form a muddled fibrous structure (Pl. 15, figs. 5–9). The true spongy tissue is discernible even when radial and tangential rods have different length and thickness and are arranged irregularly to form meshes of various size (3–20 μm) and shape, and lying in different planes.

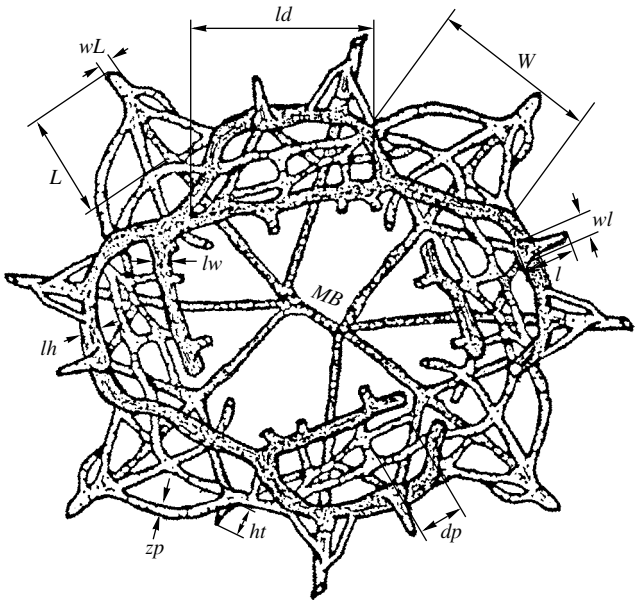

Fig. 13. Scheme of reticular skeleton structure of *Polyentactinia* (after Nazarov, 1988; Afanasieva, 2000a): (*L*) length of the main spines, (*wL*) width of the main spines, (*W*) distance between the supports of the main spines, (*l*) length of the by-spines, (*wl*) width of the by-spines, (*lh*) height of the ridge, (*ld*) diameter of the cell surrounded by the ridge, (*lw*) thickness of the ridge, (*ht*) height of thorns, (*dp*) diameter of pores, (*zp*) thickness of bars, and (*MB*) median bar of the spicule.

Spongy tissue is formed by the branching of lateral offshoots of well-developed main radial spines, while the skeleton is a complex tangled of bent fibers. Spongy tissue is known from the Cambrian. Multi-layered loose skeletons are very characteristic of many taxonomic groups of Mesozoic–Cenozoic and Recent Spumellaria. However, in the Cenozoic species, the rods of the spongy tissue are usually thinner than in Paleozoic species, while the meshes are larger (up to 50 μm in diameter), i.e., this skeletal tissue is more openwork than usually the spongy tissue may be.

Explanation of Plate 11

Upper Devonian, Middle Frasnian Substage, Domanik Formation; Timan–Pechora Province: (Figs. 1–4, 7) borehole Shuda-Yag-1003: (1) sample 73 (depth 71.4–71.9 m); (2, 4) sample 29 (depth 105–106 m); and (3, 7) sample 68 (depth 73.3–73.5 m); (Figs. 5 and 6) Lyajol River, outcrop 1904, sample 6.

Fig. 1. *Astroentactinia vishnevskayae* Afanasieva, scale bar = 33 μm.

Fig. 2. *Astroentactinia biaciculata* Nazarov, bar = 7 μm.

Fig. 3. *Moskovistella khaini* Afanasieva, bar = 15 μm).

Fig. 4. *Moskovistella victorialis* Afanasieva, bar = 15 μm.

Fig. 5. *Entactinia micula* Foreman, bar = 18 μm.

Fig. 6. *Borisella mariae* Afanasieva, bar = 21 μm.

Fig. 7. *Borisella pantosompha* (Foreman), bar = 17 μm.

Plate 12

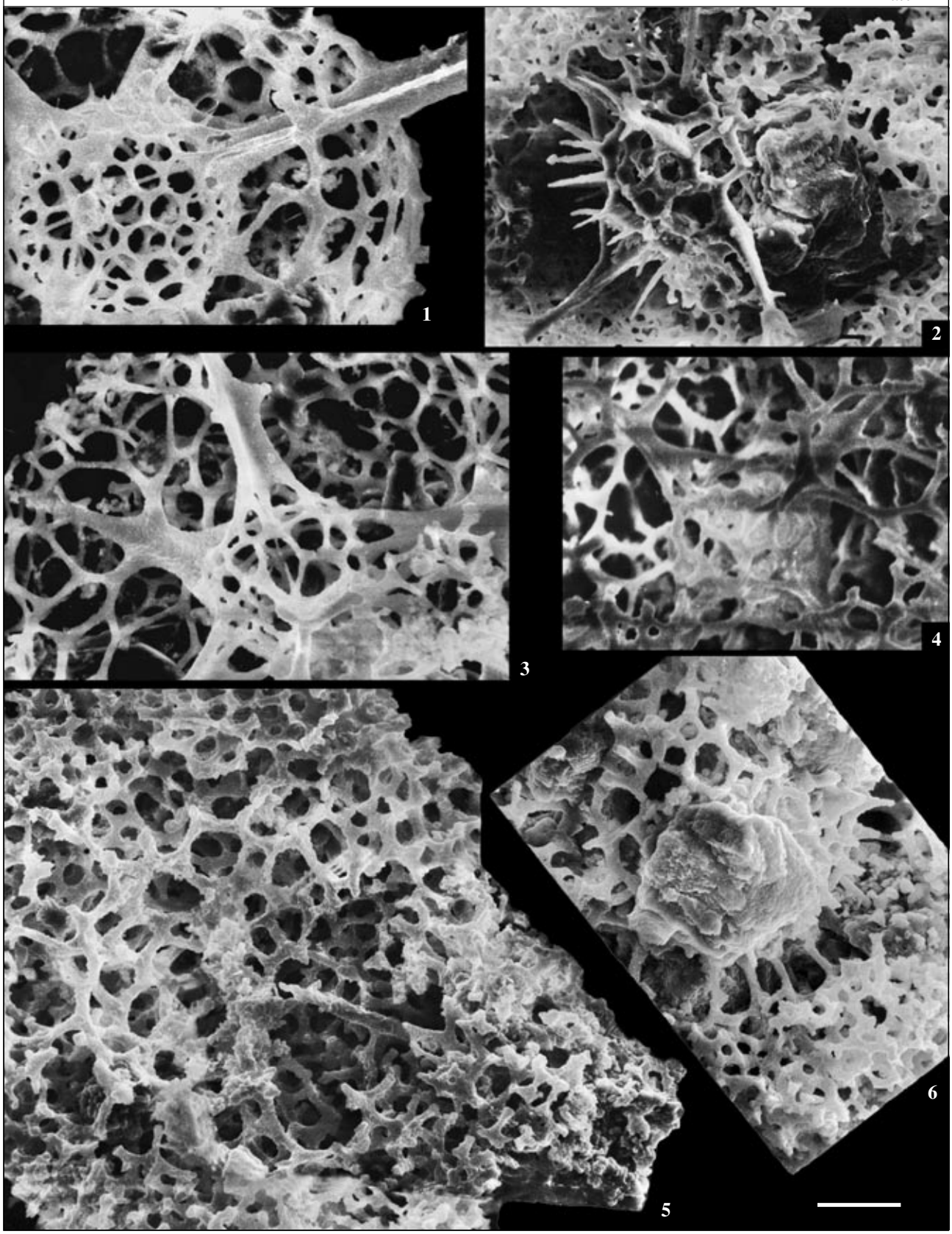

Inner framework and the first sphere in members of the subfamilies (1) Pseudorotasphaerinae, (2, 6) Spongentactiniinae, and (3–5) Somphoentactiniinae.

It is noteworthy that, in the polyspheric Polycystina, only the external test is spongy, whereas all inner shells are usually porous. Two varieties of Paleozoic spherical Polycystina are distinguished based on the way the spongy layer is formed. The spongy layer of varying thickness can rest on the porous base, or the skeleton may consist of the tangled fibers of various shapes only (Nazarov, 1988).

In the first case, the dense tangled skeletal fibers and numerous branching apophyses, spiny rims of the meshes and their connections lead to the development of quite thick outer spongy layer adjoining the porous shell (Pl. 15, fig. 9).

In the second case, the spongy skeletal shell is formed by the intense branching of the apophyses that are connected between each other by numerous bars, pillars, bridges, and short rods, which also branch and are connected to the neighboring structures. This lead to the development of a skeletal shell built from tangled fibers of various thicknesses (Pl. 15, figs. 5–8). In some cases, the bars are more regularly arranged to form regular meshes (Pl. 15, figs. 7, 8).

Such a structure is quite similar to the pseudospongy tissue of the Mesozoic–Cenozoic Spongodiscidae. In Cenozoic taxa, the pseudospongy tissue is distinguished in that it is never multi-layered, while the meshes in it are smaller (1–5 μm) than in the spongy tissue. The interlacing of straight weblike threads extending between the additional spines in a similar way to telegraph cables is called a weblike tissue. The meshes in the weblike tissue are 1–20 μm in cross section (Nazarov and Petrushevskaya, 1995).

The shell of the Stauraxonaria is mainly spongy. It is formed by the branching of offshoots extending from the proximal and distal zones of the rays of the internal framework (Nazarov, 1988). The shell of the discoidal–triangular and bladed taxa (Pl. 5, figs. 1, 3, 6, 9) is spongy. Only among the flat subtriangular stauraxonic Polycystina, there are taxa with a spongy–lamellar shell (Pl. 3, figs. 1, 6; Pl. 16, figs. 1, 2).

Lamellar skeletal shells. Nonperforated lamellar skeletal shells are widely known, but they occasionally have, although rare, polygonal pores (Fig. 14). The wall thickness ranges from 1 to 8 μm, or, rarely, more or less than this value.

The lamellar skeletal tissue is developed in some stauraxonic radiolarians. Flat, subtriangular taxa only have a spongy shell in the Late Carboniferous, but taxa with a lamellar central part and spongy periphery (Pl. 16, figs. 1, 2) appear as early as the Early Permian. In this case, the central parts of the skeleton are probably overgrown as a result of "the ageing" of the skeletal tissue.

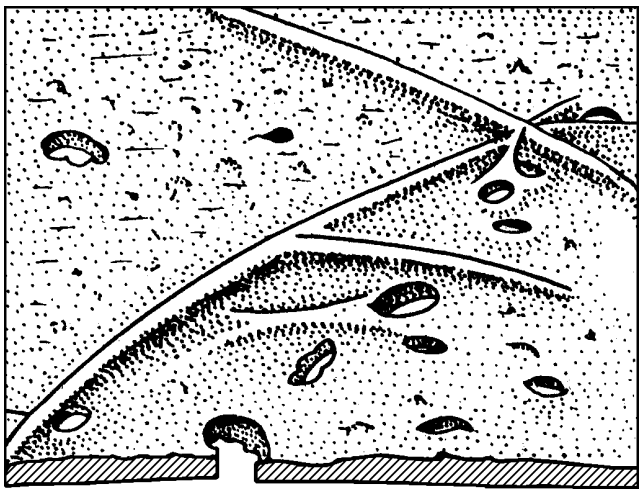

Fig. 14. Scheme of the lamellar skeleton structure (after Nazarov and Petrushevskaya, 1995).

The pylome opening in Pylomariata is rimmed by a wide nonporous plate appearing as a peristome of various shapes, which often developed on the main spines (Pl. 16, figs. 3, 4).

Many representatives of the class Aculearia have a tunic, a cover tissue made of lamellar, or lamellar-reticular skeletal tissue that forms a pseudoshell. It is developed on the main spines and caveal ribs of the triangular skeleton of Lapidopiscidae and covers the center of the spine intersection in Palaeoscenidiidae (Pl. 16, figs. 12–14).

The development of the lamellar skeletal tissue on the spines (columellae) and caveal ribs of the skeletons of Albaillellidae and Follicucullidae leads to the development of a subconical test with an opening aperture (pylome) in the basal part (Pl. 16, figs. 5–10).

The nonperforated test wall was preserved in evolution over a long time. Only from the Late Carboniferous, radiolarians with a few openings in the basal region appear (Pl. 16, fig. 10). In the Late Permian, the shells of such radiolarians became almost entirely

Explanation of Plate 12

Upper Devonian; Timan–Pechora Province: (Figs. 1–4) Middle Frasnian Substage, Domanik Formation, borehole Shuda-Yag-1003: (1, 3) sample 8 (depth 120.9–124 m); (2) sample 68 (depth 73.3–73.5 m); and (4) sample 72 (depth 71.9–72.4 m); (Figs. 5 and 6) Famennian Stage; borehole Zapadnaya Lekkeyaginskaya-65, sample 86g (depth 2460–2467 m).

Fig. 1. *Russirad kazintsovae* Afanasieva, scale bar = 20 μm.

Fig. 2. *Retisphaera exquisita* (Aitchison), bar = 33 μm.

Figs. 3 and 4. *Somphoentactinia gavrilovi* Afanasieva: (3, 4) scale bar = 20 μm.

Fig. 5. *Adamas cathedrarius* Afanasieva, bar = 23 μm.

Fig. 6. *Tetrentactinia barysphaera* Foreman, bar = 23 μm.

Plate 13

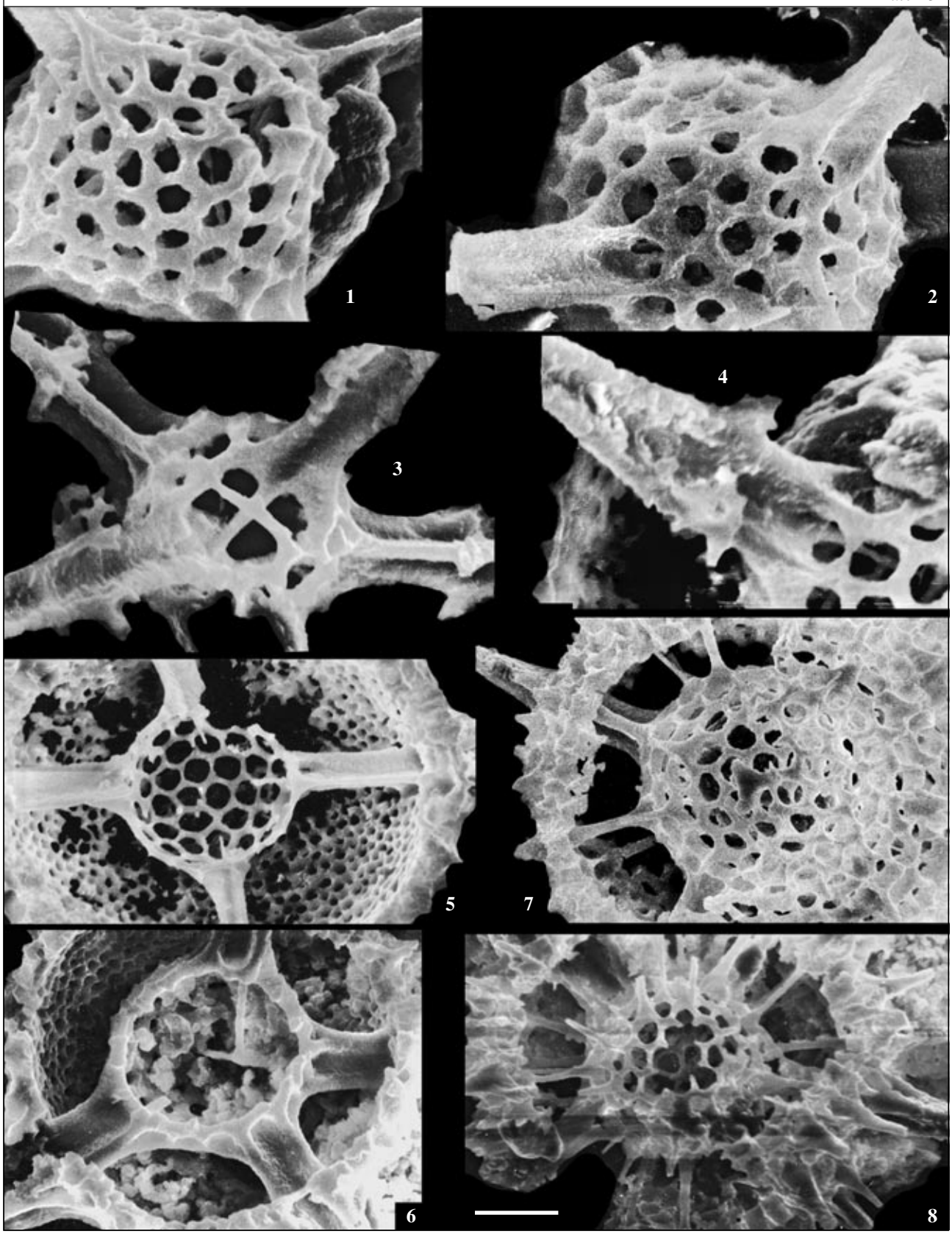

Inner framework and the first inner sphere in members of the subfamily Bientactinosphaerinae.

porous, except the apical part (Ishiga *et al.*, 1982; Takemura and Nakaseko, 1981; Nazarov, 1988).

Early bilaterally symmetrical radiolarians with a conical outline had a test undivided into segments. In the Carboniferous–Permian, some taxa developed segmentation, allowing the distinction of the apical, central, and basal parts (Pl. 16, figs. 5–9). The segmentation of tests of the bilaterally symmetrical radiolarians was apparently a manifestation of polymerization equivalent to the increase in number of shells in spherical and stauraxonic Polycystina (Ormiston and Babcock, 1979; Nazarov, 1988).

Porous skeletal shells. Porous shell, i.e., the test wall penetrated by variously shaped openings (Pls. 17–19) is the most common, especially in spherical Polycystina.

Paleozoic Radiolaria (Nazarov, 1988; Amon, 1999; Afanasieva, 2000a, 2000c), similar to Recent (Petrushevskaya, 1981a, 1984, 1986; Boltovskoy, 1981), and Meso-Cenozoic (Zhamoida, 1972; Lipman, 1974, 1979; Bragin *et al.*, 1999; Amon, 2000a; De Wever *et al.*, 2001), have similar and diverse pore outlines.

Pores may be (1) rounded and variously sized with rounded (Pl. 17, figs. 1–6) and flattened straight (Pl. 17, figs. 7, 8) bars; (2) rounded (Pl. 18, fig. 1) and angular-oval (Pl. 18, fig. 2) with intrapore denticles; (3) oval (Pl. 18, figs. 3, 4), and angular-oval (Pl. 18, figs. 5, 6), with false pore funnels; and (4) rounded-polygonal (Pl. 19, figs. 1–6).

The outer shell may possess a system of relatively high ridges that form a cellular structure of the shell surface, e.g., in the genus *Ornatoentactinia* (Table 4; Fig. 15; Pl. 18, figs. 7–10).

The distribution of pores may be irregular, if the pores are differently shaped and sized, or regular (mostly in diagonal rows). Sometimes, longitudinal or transverse rows of pores are more distinctly outlined because the walls between the rows are wider and/or thicker, than in the pores in the same row. In addition, large pores may be covered by fine latticed or porous plates (Nazarov and Petrushevskaya, 1995).

The pores are 1–35 μm in diameter (Table 5). They are separated by the interpore bars 1–5 μm wide, but sometimes the plates are very thin and have pores of 0.2–1 μm. Based on the ratio between the pore diameter and skeleton wall thickness (dp/tw), four types of pores are recognized (Table 5): (1) very narrow (*dp*/*tw* = 0.40–0.85); (2) narrow (*dp*/*tw* = 0.86–1.0); (3) wide (*dp*/*tw* = 1.01–3.41); and (4) very wide (*dp*/*tw* = 3.41–9.5). Based on the ratio of the diameter of the shell and pores penetrating it, the following varieties of pores are recognized (Table 5): (1) very large pores (*D*/*dp* = 4.0–10.0), (2) large pores (*D*/*dp* = 10.01–18.5), (3) small pores (*D*/*dp* = 18.51–63.0); and (4) very small pores (*D*/*dp* = 63.01–105.0).

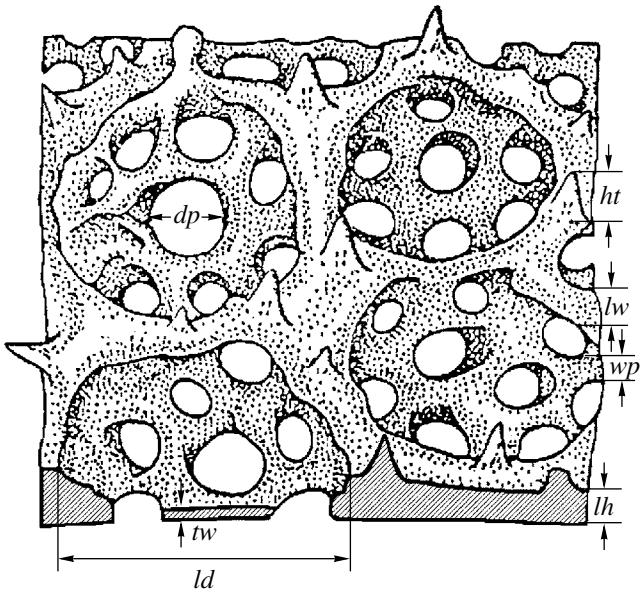

Fig. 15. Scheme of the cellular surface structure of the skeleton (after Nazarov and Petrushevskaya, 1995; Afanasieva, 2000a). Designations: (*lh*) height of the ridge, (*lw*) thickness of the ridge, (*ld*) diameter of the cell surrounded by the ridge, (*ht*) height of thorns, (*dp*) diameter of pores, (*wp*) width of the interpore bar, and (*tw*) wall thickness.

The interpore bars may be (Table 4): flat, rounded, or rounded subacute. In addition, based on the ratio between the pore diameter and the width of the interpore bars (Table 5), the following varieties are recognized: very narrow bars (*dp*/*wp* = 9.50–5.81), narrow bars (*dp*/*wp* = 5.80–4.11), wide bars (*dp*/*wp* = 4.10–2.01), and very wide bars (*dp*/*wp* = 2.00–0.50).

Explanation of Plate 13

Upper Devonian, Middle Frasnian Substage, Domanik Formation; Timan–Pechora Province: (Figs. 1–6) borehole Shuda-Yag-1003: (1, 2) sample 29 (depth 105–106 m); (3) sample 65 (depth 75–77.3 m); (4, 6) sample 72 (depth 71.9–72.4 m); and (5) sample 68 (depth 73.3–73.5 m); (Fig. 7) Ukhta River, sampling point no. 4, sample V-29; and (8) Lyajol River, outcrop 1904, sample 6.

Figs. 1 and 2. *Bientactinosphaera maslakovae* Afanasieva: (1) scale bar = 15 μm and (2) bar = 10 μm.

Fig. 3. *Bientactinosphaera morozovi* Afanasieva, bar = 7 μm.

Fig. 4. *Bientactinosphaera australis* (Aitchison), bar = 10 μm.

Fig. 5. *Bientactinosphaera miletenkoi* Afanasieva, bar = 20 μm.

Fig. 6. *Bientactinosphaera pinica* Afanasieva, bar = 20 μm.

Fig. 7. *Radiobisphaera domanicensis* (Bykova), bar = 20 μm.

Fig. 8. *Radiobisphaera assidera* (Nazarov), bar = 27 μm.

Table 5. Main skeleton parameters of the spherical Paleozoic radiolarians

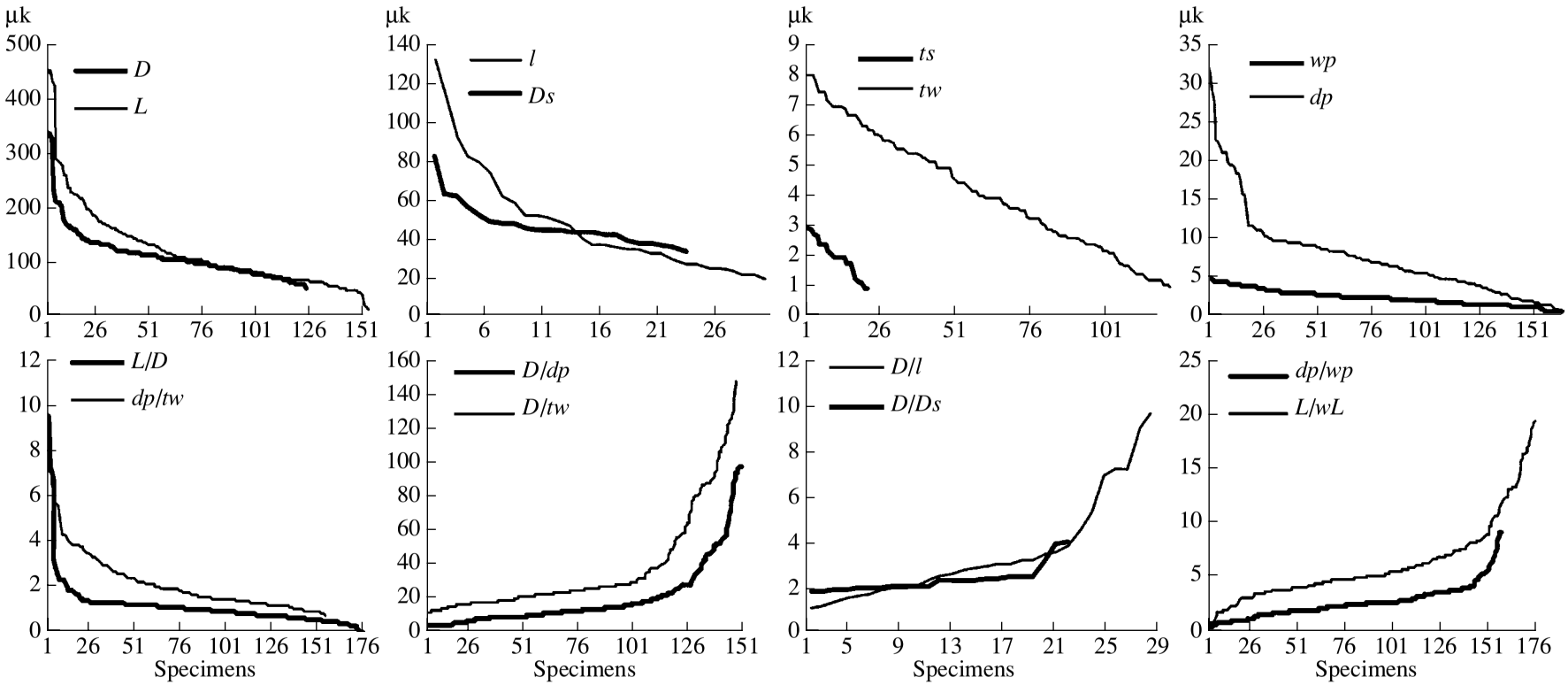

(a) Charts of hyperbolic function of the main parameters of radiolarian skeletons

Measurements, µm	Absolute									Relative												
	D	*Ds*	*L*	*l*	*dp*	*wp*	*tw*	*ts*	*ht*	*dp/tw*	*dp/wp*	*D/Ds*	*D/dp*	*D/tw*	*L/D*	*L/wL*	*D/l*	*l/wl*	*D/ht*	*D/ld*	*D/lh*	*lh/lw*
Very large, very long, etc.	360.0–180.1	85.0–60.1	470.0–350.1	135.0–90.1	35.0–25.1	5.0–4.1	8.0–7.1	–	15.1–20.0	9.5–3.41	0.5–2.0	1.50–2.00	4.0–10.0	10.0–20.0	10.00–2.21	0.50–4.00	1.00–2.00	3.00–4.50	8.00–20.00	4.00–7.00	18.00–28.00	1.00–1.50
Large, long, etc.	180.0–130.1	60.0–46.1	350.0–153.1	90.0–70.1	25.0–15.1	4.0–3.1	7.0–4.1	–	10.1–15.0	3.40–1.01	2.01–4.10	2.01–2.30	10.01–18.5	20.1–29.0	2.20–1.41	4.01–7.00	2.01–3.00	4.51–8.00	20.01–36.00	7.1–11.00	28.01–44.00	1.51–2.00
Small, short, etc.	130.0–88.1	46.0–40.1	153.0–52.1	70.0–29.1	15.0–6.1	3.0–2.1	4.0–2.1	3.0–2.1	5.1–10.0	1.00–0.86	4.11–5.80	2.31–3.00	18.51–63.0	29.1–100.0	1.40–0.41	7.01–13.00	3.01–8.00	8.01–10.99	36.01–60.00	11.01–14.00	44.01–57.00	2.01–2.50
Very small, very short, etc.	88.0–55.0	40.0–35.0	52.0–15.0	29.0–20.0	6.0–1.0	2.0–1.0	2.0–1.0	2.0–1.0	0.9–5.0	0.85–0.40	5.81–9.50	3.1–4.50	63.01–105.00	100.1–150.0	0.40–0.10	13.01–25.00	8.01–15.00	11.00–15.00	60.01–80.00	14.01–15.00	57.01–70.00	2.51–3.50

(b) Main absolute and relative measurements of radiolarian skeletons

(*D*) diameter of the external sphere, (*Ds*) diameter of the primary skeleton sphere, (*tw*) wall thickness of external sphere, (*ts*) wall thickness of the primary sphere, (*dp*) pore diameter of external sphere, (*wp*) width of intervening bars of external sphere, (*ld*) diameter of cell bordered by costae, (*lw*) width of costa, (*lh*) height of costa, (*L*) length of the main spines, (*wL*) width of the main spines base, (*l*) length of by-spines, (*wl*) width of by-spines base, and (*ht*) height of thorns and thorn-tubercles.

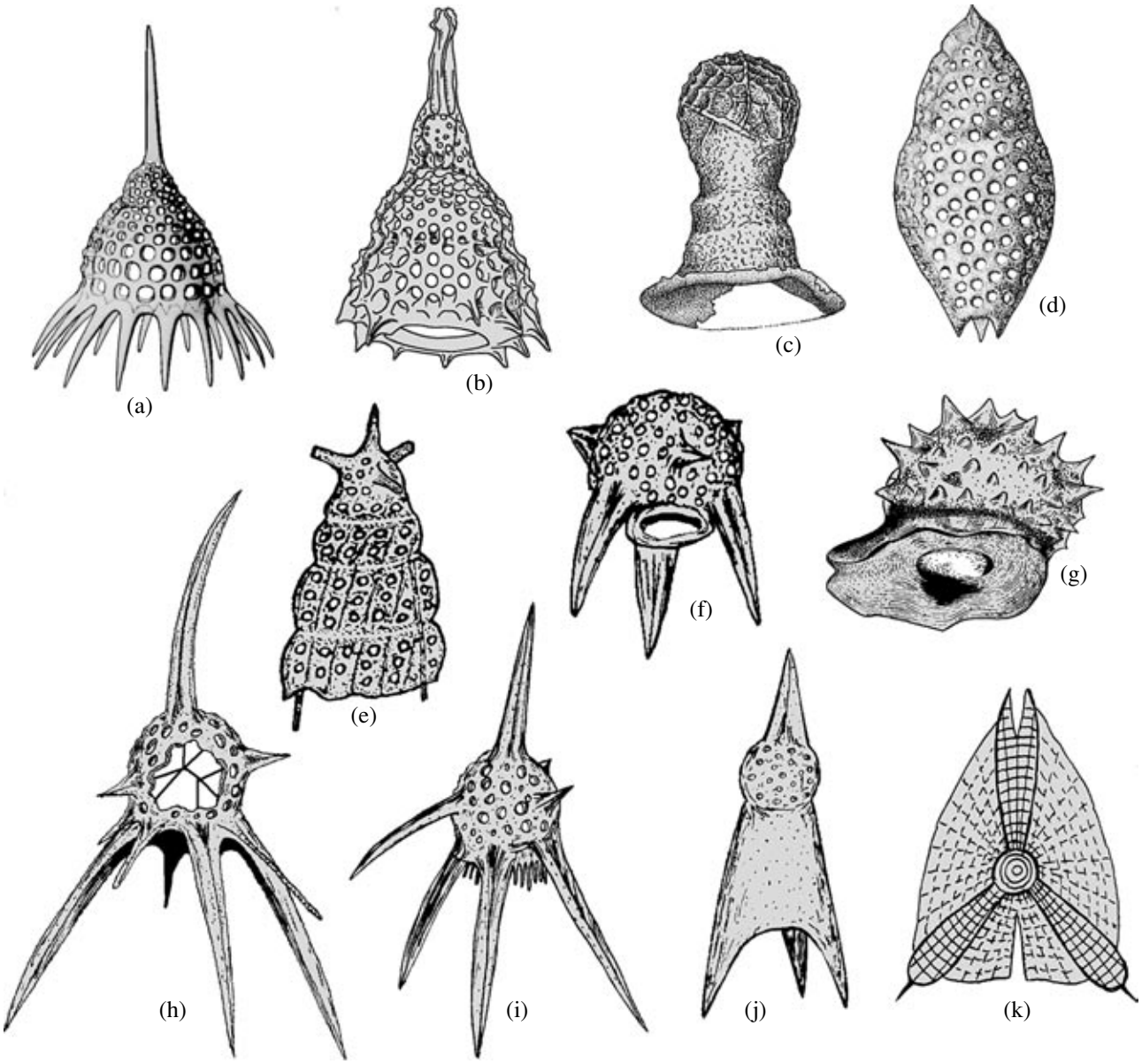

Fig. 16. Aperture and pylome in the skeletons of (a–j) Nassellaria and (k) Stauraxonaria: (a) *Clathrocyclas*, (b) *Lamprocyclas*, (c) *Bulbocyrtium*, (d) *Podocyrtis*, (e) *Popofskyellum*, (f) *Pylentonema*, (g) *Caspiaza*, (h) *Cyrtisphaeronemium*, (i) *Cyrtisphaeractenium*, (j) *Allocyrtium*, and (k) Hagiastridae after: (a) Haeckel, 1887, (b) Petrushevskaya, 1971, (c) Kozur and Mostler, 1982, (d) Kozlova and Gorbovets, 1966, (e) Nazarov, 1988, (f) Holdsworth *et al.*, 1978, (g) Afanasieva, 1993, (h, i) Deflandre, 1972, (j) Holdsworth, 1973, and (k) Bragin *et al.*, 1999.

Aperture and Pylome

The aperture and pylome, which are openings in the oral part of the shell, considerably larger than other pores, are a characteristic feature of Nassellaria, which distinguishes them from other Paleozoic Polycystina. Apparently, the development of the nucleoaxopodial complex facilitates the development of a special opening in the nassellarian skeleton to let out the axopodia.

• The periaxoplastidian type could be present in the early nassellarians Pylentonemidea and Cessipyloroidea from the order Pylomariata (Fig. 1d);

• The apoaxoplastidy is characteristic of spiny radiolarians of the order Fasciculata (Plagiacanthidae) and nassellarians of the order Spyridinata (Figs. 1e, 1f).

• The proaxoplastidian type of the nucleoaxopodial complex was present in most Mesozoic–Cenozoic nassellarians, and was possibly present in the early nassellarians Proventocitoidea and Popofskyelloidea from the order Pylomariata (Fig. 1g).

Aperture. The aperture in nassellarians is located at the distal end of the last chamber in the Mesozoic–Cenozoic Nassellaria and Paleozoic Proventocitoidea and Popofskyelloidea (Figs. 16a–16e). It can be open or

Plate 14

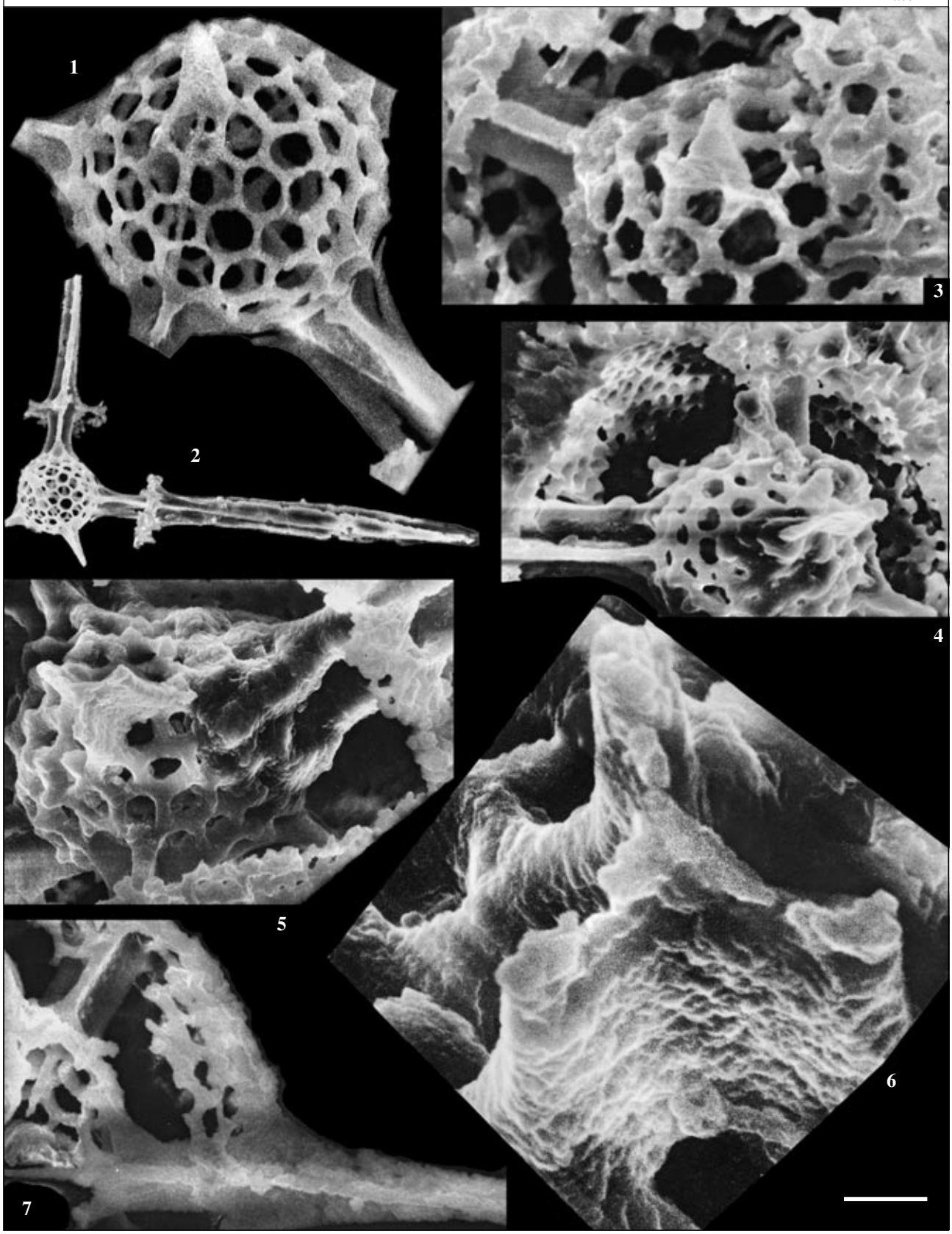

Inner framework, the first inner sphere, and initial stages of the formation of the main spines in members of the subfamily Bientactinosphaerinae.

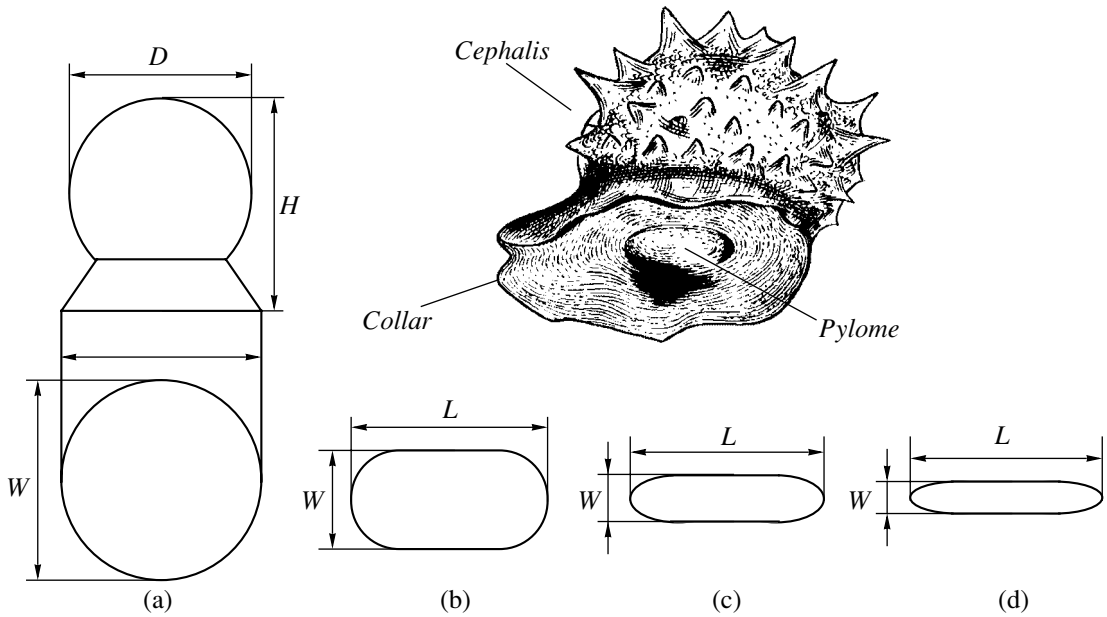

Fig. 17. Scheme of the skeleton of *Caspiaza* (after Afanasieva, 1986, 2000a). Designations: (*D*) diameter of the skeleton, (*H*) height, (*W*) width of the collar of the pylome, and (*L*) length; (a–d) shape of the opening of the pylome collar: (a) open collar (*W*/*L* = 1–0.9), (b) semiopen collar (*W*/*L* = 0.8–0.5), (c) slitlike collar (*W*/*L*=0.4–0.2), and (d) closed collar (*W*/*L* = 0.1–0).

closed. At the final stage of skeletal ontogeny, the aperture is either closed by a plate, or may possess a rim and/or denticles. Sometimes, the aperture is tube-shaped. The aperture in other species of Nassellaria remains open and simple during the entire life, or is sac-like closed at the end of growth (Petrushevskaya, 1986; Nazarov and Petrushevskaya, 1995).

Pylome. The pylome opening in the skeleton of Pylomariata is usually surrounded by well-developed skeletal structures (collar, peristome, rim, spines), the shape and combination of which vary in different genera (Table 4; Figs. 16f–16j). In many known representatives of Archocyrtiinae, the pylome is surrounded by three main spines. In the tests of *Cessipylorum* and *Pylentonema*, these are connected by a well-developed bridge (Fig. 16f), while in *Cytisphaeronemium* and *Cyrtisphaeractenium*, they alternate with the straight by-spines (Figs. 16h, 16i). In *Allocyrtium* (Fig. 16j), the pylome is quite differently rimmed in that in these skeletons the lamellar skeletal tissue is developed into the shape of a truncated conical peristome surrounding three main spines. The test, as a result, becomes elongated conical, which is different from the test shape of other Pylomariata.

The pylome in *Caspiaza* develops a peculiar morphological structure in the shape of a bent collar surrounding it (Fig. 16g). It can be extremely diverse (Fig. 17), which was most likely related to the benthic, sedentary mode of life of these organisms (Pl. 20, fig. 12): (1) completely open collar, W/L = 1–0.9 (Fig. 17a; Pl. 20, figs. 9–11); (2) semiopen collar, W/L = 0.8–0.5 (Fig. 17b; Pl. 20, figs. 5, 6, 8, 12); (3) slitlike collar, W/L = 0.4–0.2 (Fig. 17c; Pl. 20, figs. 3, 4, 7); and (4) closed collar, W/L = 0.1–0 (Fig. 17d; Pl. 20, figs. 1, 2) with secondarily fused margins (Afanasieva, 1986, 2000a).

The development of the pylome collar in *Caspiaza* (Fig. 16g) is repeated in the geologically younger (Middle–Late Triassic) and very peculiar *Bulbocyrtium* (Fig. 16c). This supports the hypothesis of the close relationships between Nassellaria and benthic sedentary taxa (Petrushevskaya, 1977, 1984; Afanasieva, 1986, 2000a).

Explanation of Plate 14

Upper Devonian, Middle Frasnian Substage, Domanik Formation; Timan–Pechora Province, borehole Shuda-Yag-1003: (Figs. 1, 2, 5, 6) sample 72 (depth 71.9–72.4 m); (Fig. 3) sample 56 (depth 81.6–83 m); (Fig. 4) sample 78 (depth 68.4–69.3 m); and (Fig. 7) sample 73 (depth 71.4–71.9 m).

Figs. 1 and 2. *Bientactinosphaera pinica* Afanasieva: (1) fragment, scale bar = 15 μm and (2) bar = 50 μm.

Fig. 3. *Bientactinosphaera symphypora* (Foreman), bar = 10 μm.

Fig. 4. *Ornatoentactinia solita* Afanasieva, bar = 18 μm.

Figs. 5 and 6. *Ornatoentactinia beljaevorum* Afanasieva: (5) bar = 17 μm and (6) bar = 4 μm.

Fig. 7. *Bientactinosphaera morozovi* Afanasieva, bar = 15 μm.

Plate 15

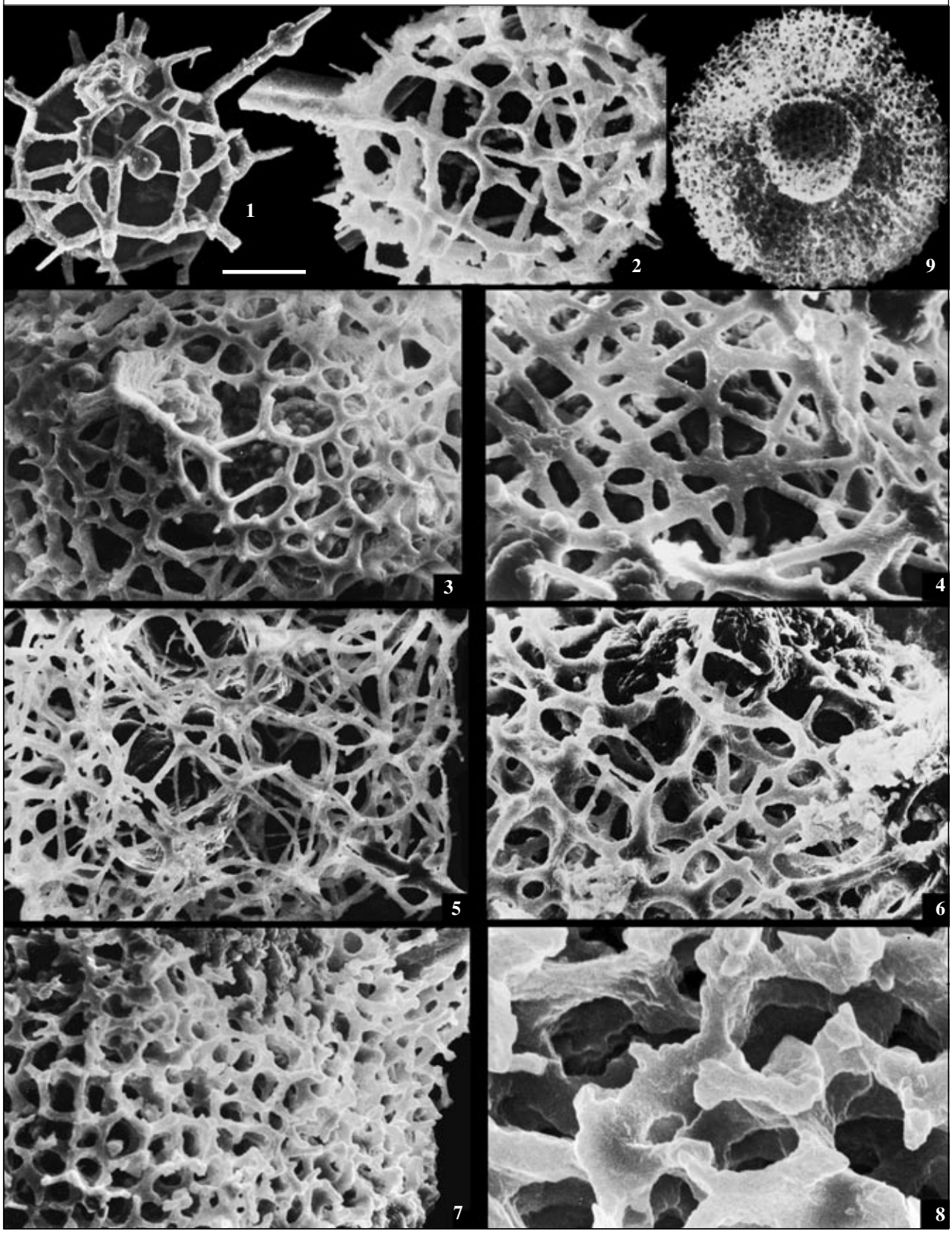

Latticed (1, 2), reticular (3, 4) and spongy (5–9) structures of the external skeletal sphere in members of the subfamilies (1, 2) Haplentactiniinae, (3) Pseudorotasphaerinae, (4) Polyentactiniinae, (5) Retentactiniinae, (6) Spongopolyentactiniinae, and (7–9) Somphoentactiniinae.

In multilayered skeletons of Stauraxonaria, the pylome can be funnel-shaped, or tubular, penetrating the skeletal tissue (Fig. 16k). Its margin may possess teeth, or spines. One of the skeletal processes of Hagiastridae may possess a pylome tube (brachiopile) (Fig. 16k) (Bragin *et al.*, 1999).

Spines

The external spines of various shape are very characteristic of Polycystina. They are functionally connected with the axopodia and serve as a support for their proximal parts. The axopodia extended along the rays of the inner sphere and extended outside the cortical shell through the large pores at the base of the radial spines. Their role as supports of euplasmatic structures is also very important.

The spines may be hollow, with an interior canal (Figs. 18a–18c), and solid (Figs. 18d–18l). The majority of Polycystina have solid spines lacking the interior canal. The shape of the main radial spines is very diverse (cylindrical, conical, or bladed), with varying cross sections of spines and their faces, and possessing additional skeletal structures (Table. 4; Figs. 18d–18l; Pls. 21–27).

The radial spines sometimes branch either irregularly, or retaining the axial spine, or dichotomously. The lateral processes (apophyses) of the spines may be similar to the spines in thickness and shape, or may be different (Fig. 18k; Pl. 26, figs. 4, 5).

In addition, radiolarians often have spines overgrown by skeletal tissue of the external shell (Fig. 18l; Pl. 27, figs. 1–4).

In Polycystina, spines are usually single and straight, although doubled (Pl. 27, figs. 5–7) and bent (Pl. 22, fig. 8; Pl. 27, figs. 8, 9) spines are also common as well as other various intricate shapes.

The main spines range in length (*L*) from 15 to 470 μm (Table. 5). A relative spine length is established based on the ratio of the spine length and the diameter of the skeleton (*L*/*D*): very long (*L*/*D* = 10.0–2.21), long (*L*/*D* = 2.2–1.41), short (*L*/*D* = 1.4–0.41), and very short (*L*/*D* = 0.4–0.1). The proportion of the spine length to the width at the base (*L*/*wL*) may indicate the relative thickness of spines: massive (*L*/*wL* = 0.5–4.0), thick (*L*/*wL* = 4.01–7.0), thin (*L*/*wL* = 7.01–13.0), and delicate (*L*/*wL* = 13.01–25.0) (Table 5).

Hollow spines. It is suggested that the subcylindrical or tubular hollow spines were the primary radial structures in Radiolaria (Figs. 18a–18c). An axopodium, or a bunch of axopodia may be located inside the tubes, or in the inner canal of spines. Spines of this kind are more often found in Collodaria (Collosphaeridae), more rarely in Nassellaria. The spine-tube structure is not very common in spherical Polycystina. However, some Paleozoic Sphaerellaria (*Anakrusa myriacantha, Inanigutta elongata*) and Spumellaria (*Polyentactinia circumretia, Tetragregnon quadrispinosa*) had similar primitive spines (Pl. 21, figs. 1–4) and rod-shaped bars of the skeleton (Pl. 21, figs. 5, 6), although this is probably simply a result of good preservation, while this type of spines and rods of the lattice-spongy skeletal tissue was more widespread in Paleozoic Radiolaria than is generally thought.

Peculiar hollow spines are present in Middle–Late Triassic representatives of the subfamily Capnuchosphaerinae (Fig. 18c). The spines are thick and hollow at the base. The middle part of spines is inflated, often screw-shaped. It is subdivided by inner vertical septa into three inner canals that open in three pores in the lower part of the spines. The ends of spines are thin and rod-shaped.

Rod-shaped spines. The rod-shaped spines are usually very thin and long, with a rounded cross section (Figs. 18d, 18e; Pl. 22, figs. 1, 2, 5–7). The skeletal rods may be included in the test wall (Pl. 22, figs. 6, 7), or be supported at the base by additional bars that appear like very wide wires or supports (Pl. 22, figs. 1, 2, 5).

Conical spines. The conical spines are stronger and more steady compared to the rod-shaped spines

Explanation of Plate 15

Upper Devonian: (Figs. 1–6) Middle Frasnian Substage, Domanik Formation; (Figs. 7–9) Famennian Stage. (Figs. 1–8) Timan–Pechora Province: (1) borehole Ukhtinskaya-3B, sample 116 (depth 100.6–101 m); (2–6) borehole Shuda-Yag-1003: (2) sample 28 (depth 106–107 m); (3) sample 29 (depth 105–106 m); (4) sample 68 (depth 73.3–73.5 m); (5) sample 73 (depth 71.4–71.9 m); and (6) sample 72 (depth 71.9–72.4 m); and (7, 8) borehole Zapadnaya Lekkeyaginskaya-65, sample 86g (depth 2460–2467 m); and (9) Belarus, Pripyat Depression (Fig. 9 after Nazarov, 1988).

Latticed

Fig. 1. *Haplentactinia labirinthica* Aitchison, scale bar = 56 μm.

Fig. 2. *Haplentactinia alekseevi* Afanasieva, bar = 23 μm.

Cellular

Fig. 3. *Russirad kazintsovae* Afanasieva, bar = 33 μm.

Fig. 4. *Polyentactinia zhamoidai* Afanasieva, bar = 15 μm.

Spongy

Fig. 5. *Retentactinia kelleri* Afanasieva, bar = 33 μm.

Fig. 6. *Spongentactinella olafi* Afanasieva, bar = 20 μm.

Figs. 7 and 8. *Adamas cathedrarius* Afanasieva: (7) bar = 27 μm and (8) bar = 7 μm.

Fig. 9. *Somphoentactinia* sp., bar = 85 μm.

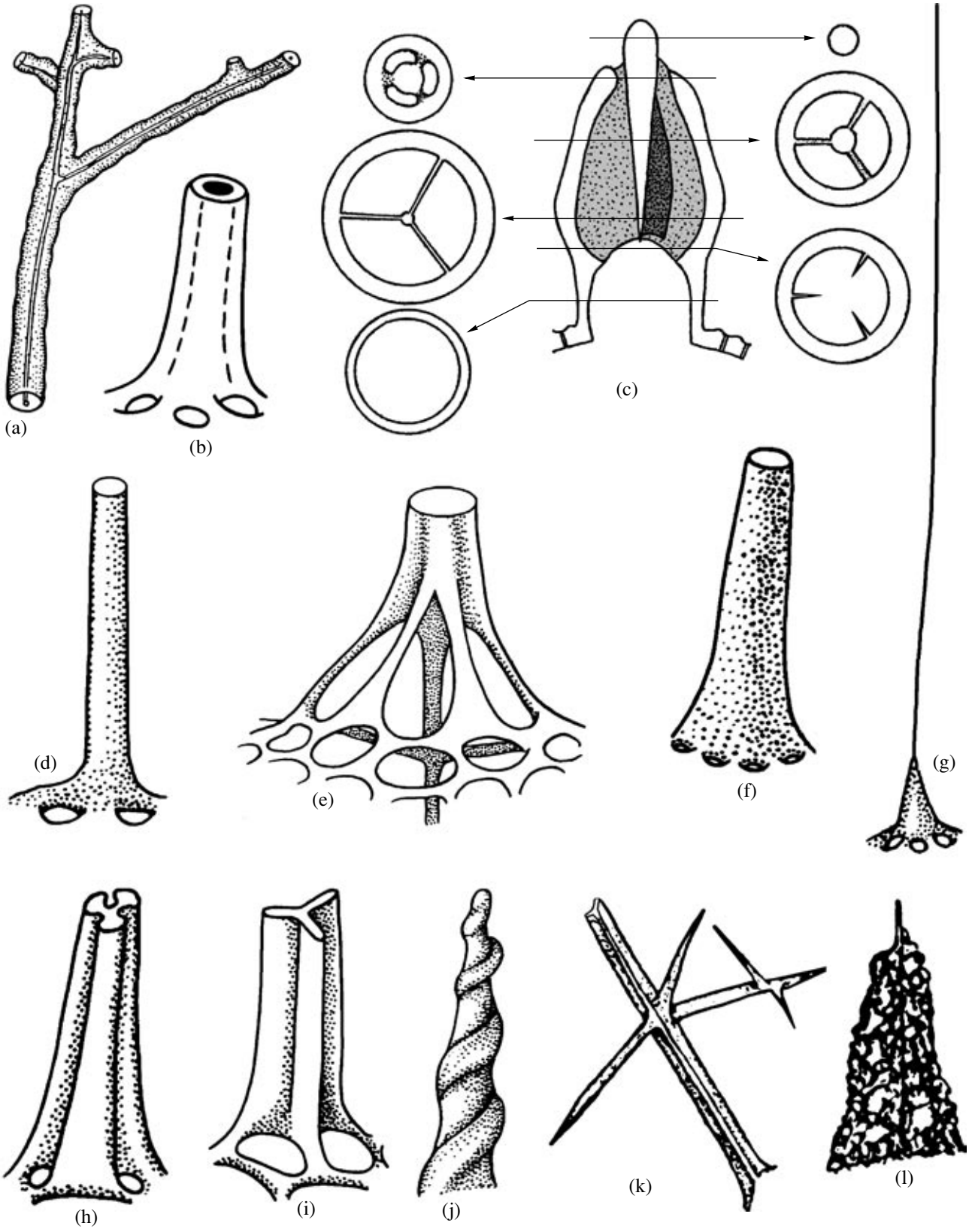
(a)
(b)
(c)
(d)
(e)
(f)
(g)
(h)
(i)
(j)
(k)
(l)

(Figs. 18f, 18g; Pl. 22, figs. 3, 4, 8, 9; Pl. 23, figs. 1, 2). They may be straight or bent and similar to the rod-shaped spines have a circular cross section. However, the spines at the base are sometimes three-bladed because of the false supports (Pl. 22, figs. 3, 4). Some Recent specimens from plankton show that the pointed tip of a spine has a very long hairlike continuation (Fig. 18g). Such spines cannot be preserved in fossils.

Bladed spines. Radiolarians apparently benefited from depressions developed in the basal region of the conical spines (Pl. 23, figs. 1, 2) and subsequently developed clear facets (Pl. 23, figs. 3–9). The strength provided by such spines is the same as that provided by conical spines, but with less material used. The spines consisting of three fused lamellae along one blade are most beneficial.

Some radiolarians have spines with a ✣-shaped cross section (Fig. 18h). These spines have a lobe-shaped section of the blades and may be thin and delicate (Pl. 23, figs. 5–9), or robust and very massive (Pl. 24).

The spines with **Y**-shaped sections and subrectangular sections of blades are apparently optimal. Blades of such spines may be subtriangular (Pl. 25), petaloid (Pl. 26, figs. 1–3), or narrow sword-shaped (Pl. 26, fig. 6).

The bladed spines are often spirallike (Fig. 18j). These spines are spiraled to the right (Pl. 26, figs. 7–11) or, more rarely, to the left (Pl. 26, figs. 12, 13).

By-spines. Apart from the main spines, connected to the internal framework, spherical Polycystina commonly have so-called additional or by-spines that are formed at the external shell surface and developing in the tangled joint of interpore bars (Pl. 28).

The length of the by-spines (l) ranges from 20 to 135 μm (Table. 5). Based on the proportion of the skeleton's diameter to the spine length (D/l), the relative length of the by-spines is calculated: very long (D/l = 1.0–2.0), long (D/l = 2.01–3.0), short (D/l = 3.01–8.0), and very short (D/l = 8.01–15.0). The ratio of the size of by-spines to the width of their bases is the relative thickness of the by-spines: very thick (l/wl = 3.0–4.5), thick (l/wl = 4.51–8.0), thin (l/wl = 8.01–10.99), and delicate (l/wl = 11.0–15.0) (Table 5).

The by-spines are less diverse in shape compared to the main spines and are mostly represented by (1) conical spines with ●-rounded section of the base (Pl. 28, figs. 1–6), (2) pyramidal spines with a ▲-triangular section of the base (Pl. 28, fig. 7).

It is noteworthy that those by-spines that have the same length as the main spines do not have depressions at the base (while the main spines have) and do not form blades.

Sculptural Elements

The shell surface often has auxiliary, quite diverse ornamentation (Table 4; Pl. 29) composed of thorns, thorn-tubercles, tubercles, rods, and ridges. These include rod-shaped thorns (Pl. 29, fig. 1), conical pointed thorns (Pl. 29, figs. 2–6), rounded thorns (Pl. 29, figs. 7, 8), and thorn-tubercles (Pl. 29, fig. 9). The ridges are usually lamellar and form either isometric (Pl. 2, figs. 1, 7, 9–11), or cellular structure of the shell surface (Fig. 14; Pl. 18, figs. 7–10).

The height (ht) of various thorns and thorn-tubercles ranges from 0.9 to 20 μm (Table 5). The ratio of the shell diameter to this height (D/ht) is the relative height of sculptural elements: very high (D/ht = 8.0–20.0), high (D/ht = 20.01–36.0), low (D/ht = 36.01–60.0), and very low (D/ht = 60.01–80.0) (Table 5).

Development of Radiolarian Spines

The main spines of radiolarian skeletons begin to develop at the very first stage of the skeleton's formation.

Haeckel (1887) was the first to show the early stage of the spine development. These stages were mathematically calculated by Mordukhai-Boltovskoy (1936). These researchers have shown that the initial rods (Fig. 19A, *c*) and the initial inner polyhedron (Fig. 19A, *a*) transforming into the primary inner sphere (Figs. 19B, *b*; 19C, *b*), are the main parts of the skeleton. The initial rods were apparently considered as a basis for the development of the main spines (Figs. 19B, *f*; 19C, *f*).

My SEM studies of spherical Paleozoic radiolarians supported the assumptions first pronounced over a hundred years ago and allows a new scheme of subsequent stages of development of the main spines in the radiolarian skeleton.

At the beginning, the internal framework in the shape of a spicule (Figs. 10; 19C, *d*) is developed. Later, the initial inner sphere (Figs. 19C, *b*; Pls. 12–13; Pl. 14, figs. 1–7) is formed.

The initial spines are developed on the surface of the initial inner sphere and on the continuation of the rays of the spicule (Fig. 19C, *e*; Pl. 14, figs. 1–3). The initial spines serve as a basis for the beginning of the develop-

Fig. 18. Shape and structure of the main spines in Polycystina: (a–c) hollow spines: (a) subcylindrical, irregularly branching spines or bars of the skeleton; (b) tubular; (c) scheme of spines of the subfamily Capnuchosphaerinae, based on a specimen of *Capnuchosphaera lea* De Wever, 1979, to show principal structural elements; each letter indicates a transverse section at the level indicated by a line; (d, e) rodlike spines: (d) rodlike spine; (e) rodlike spine enforced by the basal supports; (f, g) conical spines: (f) conical spine; (g) conical spine with a hairlike end; (h–l) bladed spines: (h) three-bladed spine with a ✣-like section; (i) three-bladed spine with a **Y**-like section; (j) spiral; (k) spine with apophyses; and (l) spine overgrown by the skeletal tissue of the external shell. (a, b, d–l) after Petrushevskaya, 1986, Nazarov and Petrushevskaya, 1995, modified; (c) after De Wever *et al.*, 1979.

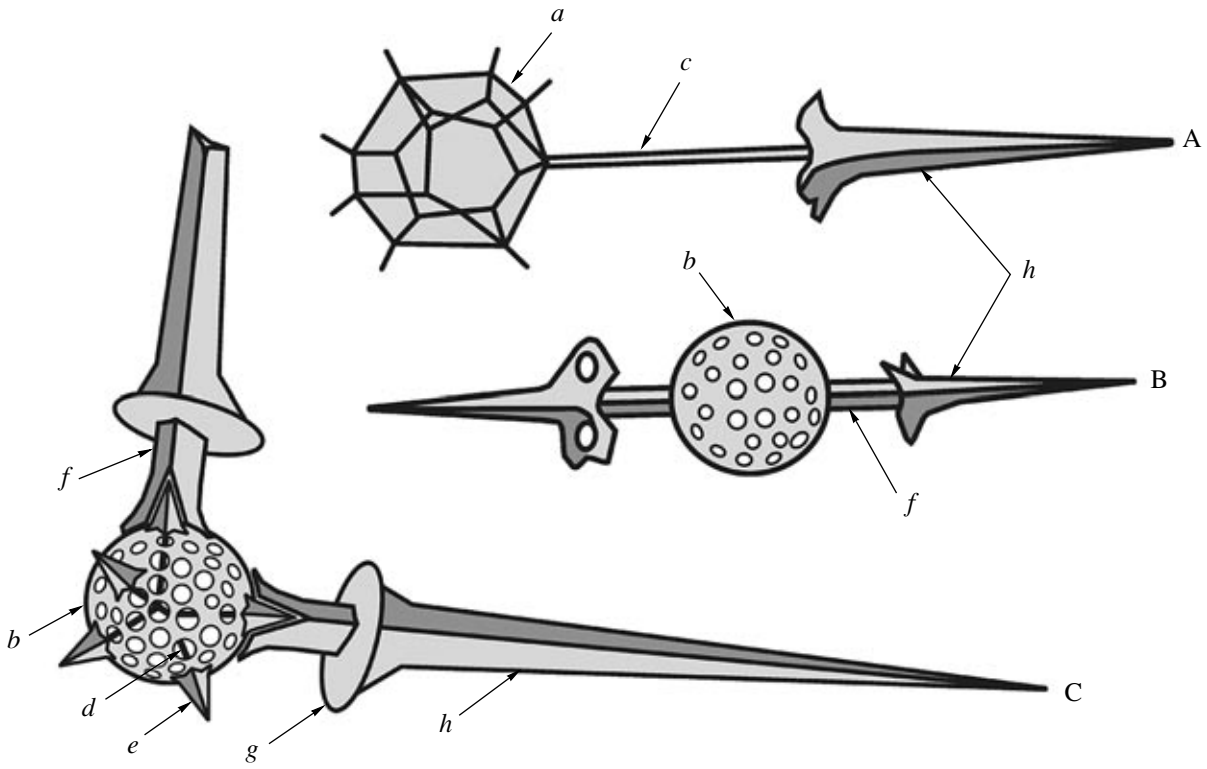

Fig. 19. Scheme of the initial stage of the development of the main spines (A, B) after Haeckel, 1887, (C) modern SEM study of a radiolarian skeleton (Pl. 14, fig. 2): (*a*) primary internal polyhedron, (*b*) primary internal sphere, (*c*) initial rod, (*d*) spicule, (*e*) primary spine, (*f*) initial stage of the development of the main spine, (*g*) part of the external sphere, and (*h*) main spine.

ment of the main spine. It is superimposed on the initial spine in a cone-in-cone way (Fig. 19C, *f*; Pl. 14, fig. 2).

This is followed by the ultimate development of the main spine (Fig. 19C, *h*; Pls. 30–32). It is somewhat different in details in different groups of radiolarians, although there is a general trend in a gradual growing of the skeleton of spines from the base in a distal direction, while the skeletal tissue is deposited spirally (Pl. 30, figs. 4–7; Pl. 32).

Differences in the growth of the skeletal tissue in different taxa are related to the development of different shape of spines.

Explanation of Plate 16

(Figs. 1, 2) Lower Permian, Sakmarian Stage; southern Ural Mountains, Ural River, village of Donskoe; (Figs. 3, 4) Lower Carboniferous, Germany, Rheinisches Schiefergebirge; (Figs. 6–8, 10) Upper Permian: (6, 10) southwestern Japan, Tamba District, Nabedzeriyama; (7, 8) North America, Western Texas, limestones Lamar; Guadalupian Stage; (Figs. 5, 9) Upper Carboniferous, Gzelian Stage; southern Ural Mountains, Ural River; (Fig. 11) Upper Devonian, Famennian Stage; polar Ural Mountains, Lemvinskaya Area, sample 101/594k; (Figs. 12–14) Upper Devonian, Middle Frasnian Substage, Domanik Formation, Timan–Pechora Province: (12) Lyajol River, outcrop 1904, sample 6; (13) borehole Shuda-Yag-1003, sample 29 (depth 105–106 m); and (14) Ukhta River, sampling point no. 4, sample B-22. (Figs. 1, 2, 5, 9) after Nazarov (1988); (Figs. 3, 4) after Won (1983); (Figs. 6, 10) after Ishiga *et al.* (1982); and (Figs. 7, 8) after Ormiston and Babcock (1979).

Figs. 1 and 2. *Ruzhencevispongus plumatus* Nazarov et Ormiston, scale bar = 150 μm.

Fig. 3. *Archocyrtium coronaesimile* Won, bar = 50 μm.

Fig. 4. *Cyrtisphaeractenium rurae* Won, bar = 37 μm.

Fig. 5. *Haplodiacanthus circinatus* Nazarov et Ormiston, bar = 130 μm.

Fig. 6. *Follicucullus scholasticus* Ormiston et Babcock, bar = 85 μm.

Figs. 7 and 8. *Follicucullus ventricosus* Ormiston et Babcock: (7) bar = 70 μm and (8) bar = 85 μm.

Fig. 9. *Albaillella amplificata* Nazarov et Ormiston, bar = 150 μm.

Fig. 10. *Neoalbaillella grypis* Ishiga, Kito et Imoto, bar = 85 μm.

Fig. 11. *Holoeciscus foremanae* Cheng, bar = 55 μm.

Fig. 12. *Palaeoscenidium robustum* Aitchison, bar = 21 μm.

Fig. 13. *Palaeoscenidium scaurum* Afanasieva, bar = 20 μm.

Fig. 14. *Palaeoscenidium tabernaculum* Aitchison, bar = 30 μm.

Plate 16

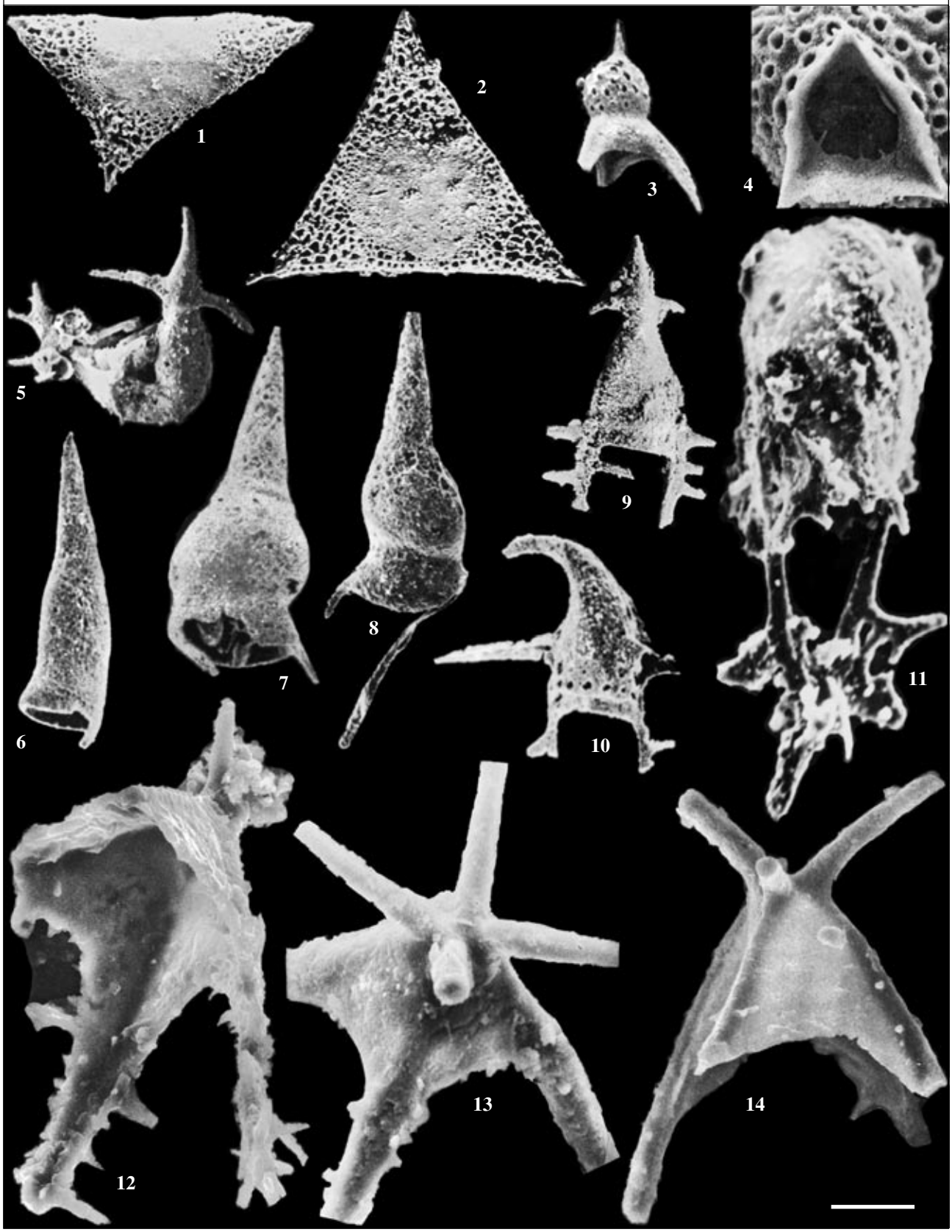

Lamellar structure of the external skeletal sphere in members of (1, 2) Stauraxonaria, (3, 4) Pylomariata, and (5–14) Aculearia.

Plate 17

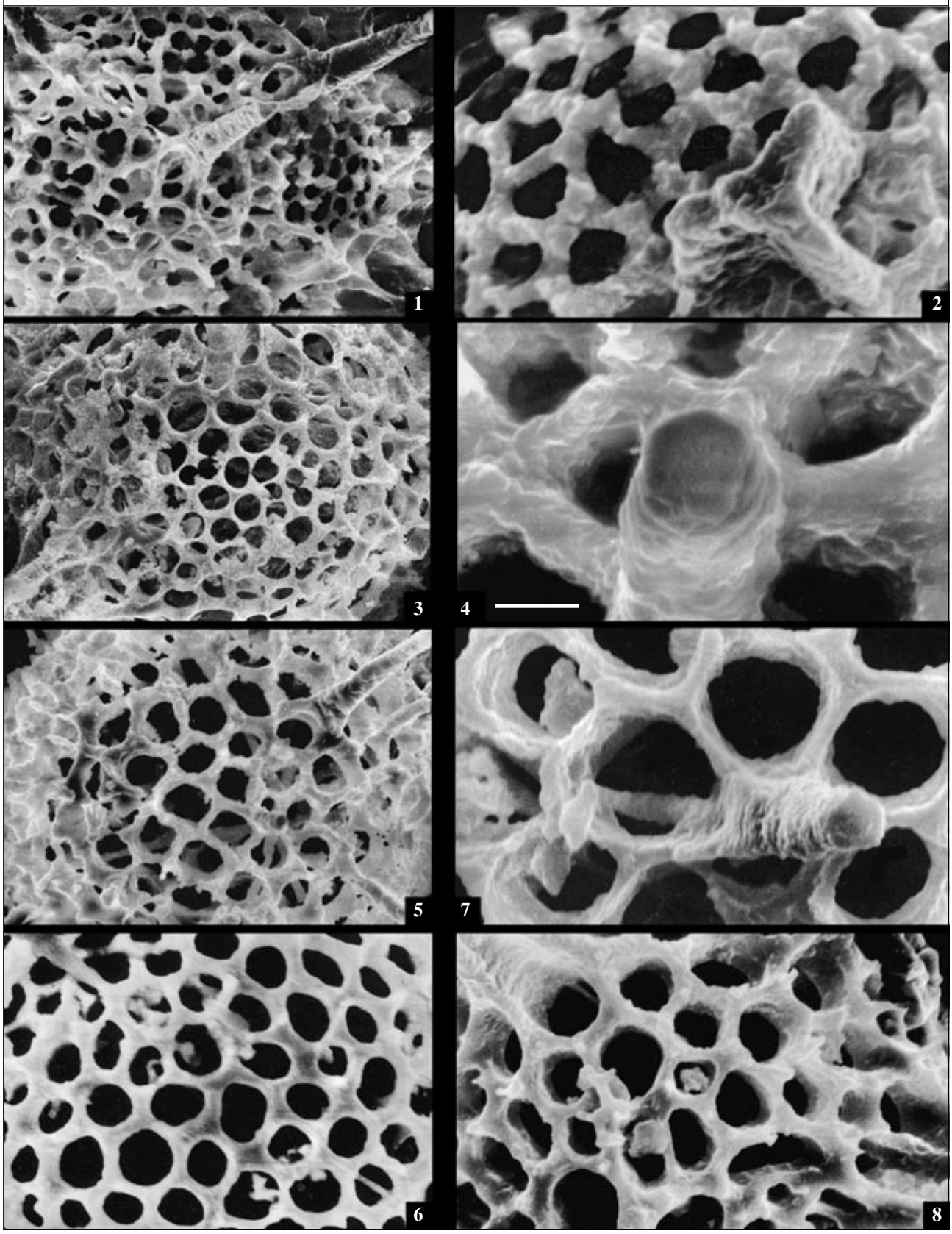

Porous structure of the external skeletal sphere in members of the subfamilies (1, 5, 7, 8) Astroentactiniinae, (2, 4) Bientactinosphaerinae, and (3, 6) Entactiniinae.

The three-edged spines of *Spongentactinella* with sword-shaped blades have a ⋖-shaped section at the base (Pl. 30, figs. 5–7) and **Y**-shaped section of the middle (Pl. 30, figs. 3, 4) and terminal (Pl. 30, figs. 1, 2) parts of the spines.

The three-bladed spines of *Bientactinosphaera* and *Helioentactinia* with a subtriangular shape of the blades have a ⋖-shaped section of the spine's base (Pl. 31, figs. 8, 9) and its middle part (Pl. 31, figs. 6, 7), ▲-triangular shaped terminal part of the spines (Pl. 31, figs. 3–5), and ●-rounded section of the tip of the spines (Pl. 31, figs. 1, 2).

Spiny radiolarians with rod-shaped spines display most clearly the process of the spiral growth of the skeletal tissue from the base of the spine towards its termination (Pl. 32).

Radiolarian Spines and Spicules of Sponges

The external morphology of spiny radiolarians and the initial spicule of spherical radiolarians resemble spicules of siliceous sponges. Because of this, there is no certainty whether the spiny taxa belong to radiolarians or to sponges (Won and Below, 1999; Won and Iams, 2002).

A wide hollow central canal is present in the rays of spicules of sponges (Pl. 33). The spiny radiolarians (Pl. 32) and even three-bladed spines of spherical radiolarians could also have a very narrow canal for the cytoplasmic cord or skeletal rod in the base or in the middle part of the spine (Pl. 30. figs. 3–7). A similar hollow canal was recorded by Won and Below (1999) and Won and Iams (2002) in the earliest known spiny radiolarians from the Middle and Upper Cambrian of Australia and Newfoundland.

A problem of genetic relationships or convergent similarity of the skeletons of sponges and spiny radiolarians is very interesting and requires further study. However, it should be remembered that the main difference of the radiolarian skeleton from the spicules of sponges is in the features of skeleton formation: spines of spiny radiolarians grow spirally (Pl. 30, figs. 4–7; Pl. 32), whereas spicules of sponges grow away from the center (Pl. 33).

PROBLEMS IN DIAGNOSING THE TAXA

A rapid introduction of computer methods into practical paleontology and creation of databases imposes reconsideration of the problem of diagnosing the taxa. At present, it is necessary to reassess the value of morphological characters of the skeleton for diagnostics of radiolarians, i.e., to review the tasks of the ongoing problem of comparison of paleontological objects: (1) classification, (2) diagnostics, (3) minimization of the number of characters defining a taxon (Vanchurov, 1973, 1975, 1979, 2000; Negadaev-Nikonov *et al.*, 1983; Petrushevskaya, 1986; Petrushevskaya and Menshutkin, 1990; Amon, 1995, 1996; Afanasieva, 1997a, 1997b, 2000a; Agarkov, 1998, 1999).

In paleontology the identification of objects is difficult. The problem is not the diagnostics itself but the fact that almost each new specimen brings the information that can change previously accepted views of the diagnostics of taxa and, hence, the classification. However, Petrushevskaya astutely observed that "if a radiolarian worker thinks that he can load his material into a computer in the hopes that it will resolve all taxonomic problems, he is making a mistake. These machines cannot be cleverer than people and cannot answer an incorrectly asked question" (Petrushevskaya, 1986, p. 178).

Classification (subdividing objects into taxa based on certain criteria) and diagnostics (assignment of the object to one of previously established taxa) may be resolved by various formal ways using the concept of the true and prohibited connections. In classification, the true connection describes that the objects belong to the same taxon. In diagnostics it defines the predominant connection between two objects, while one of these objects has contrasting relationships with all other objects. The alternative conclusion allows the fixation of a prohibited connection (Vanchurov, 1973, 1975, 1979, 2000; Negadaev-Nikonov *et al.*, 1983).

Explanation of Plate 17

Upper Devonian, Middle Frasnian Substage, Domanik Formation; Timan–Pechora Province: (Figs. 1, 2, 4, 5, 7) borehole Shuda-Yag-1003: (1) sample 73 (depth 71.4–71.9 m); (2, 5) sample 8 (depth 120.9–124 m); (4) sample 72 (depth 71.9–72.4 m); and (7) sample 29 (depth 105–106 m); (Fig. 3) Chut' River, outcrop 8, sample 7d; and (Fig. 6) Lyajol River, outcrop 1904, sample 6.

Circular, uniform-sized pores, with (1–6) rounded and (7) flattened straight bars

Fig. 1. *Moskovistella lucet* Afanasieva, scale bar = 18 μm.

Fig. 2. *Bientactinosphaera morozovi* Afanasieva, bar = 7 μm.

Fig. 3. *Entactinia parva* Won, bar = 33 μm.

Fig. 4. *Radiobisphaera assidera* (Nazarov), bar = 4 μm.

Fig. 5. *Astroentactinia vishnevskayae* Afanasieva, bar = 20 μm.

Fig. 6. *Borisella bykovae* Afanasieva, bar = 15 μm.

Fig. 7. *Astroentactinia biaciculata* Nazarov, bar = 7 μm.

Circular, variously sized pores, with flattened straight bars

Fig. 8. *Moskovistella octoradiata* Afanasieva, bar = 15 μm.

Plate 18

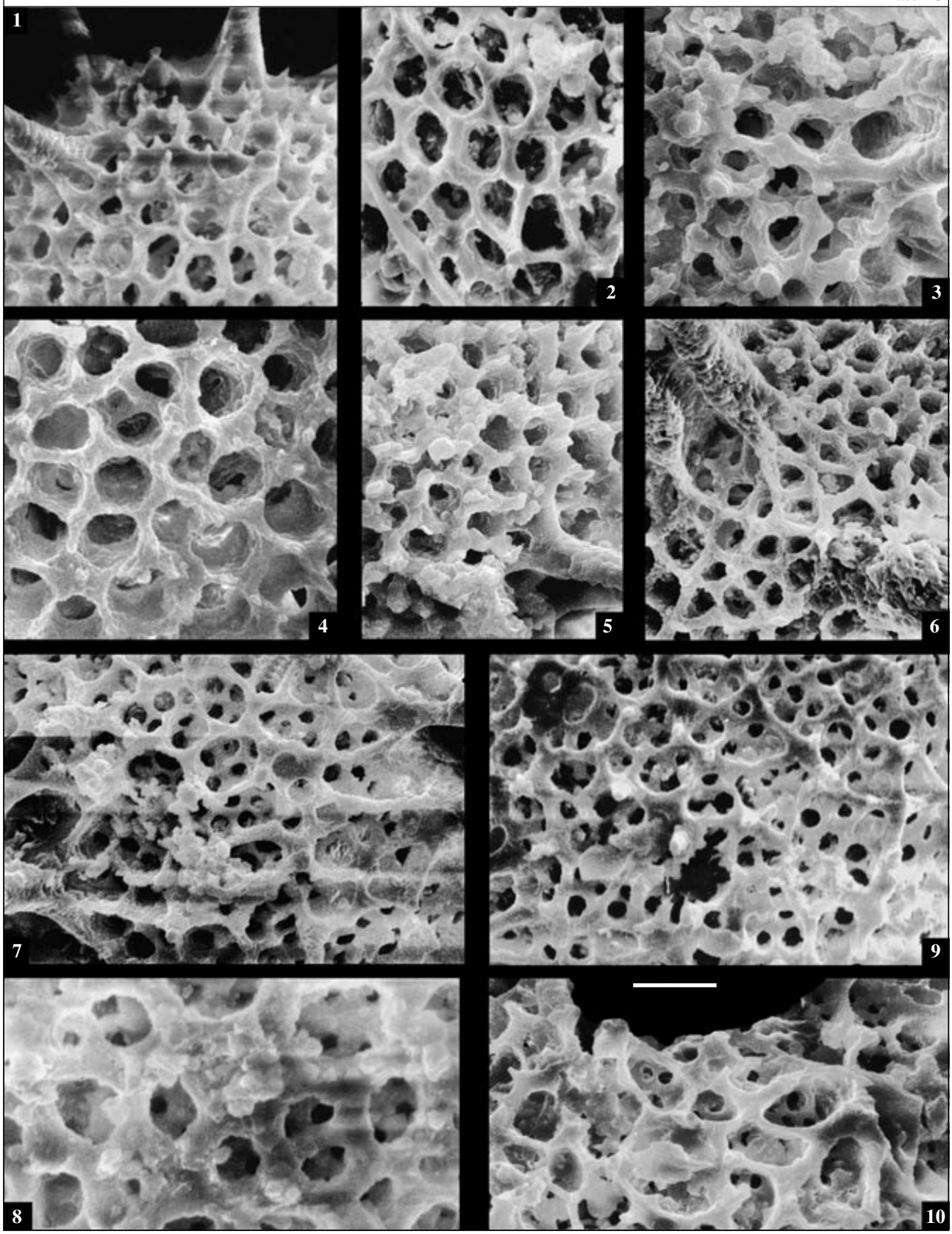

Porous (1–6) and cellular (7–10) structures of the external skeletal sphere in members of the subfamilies (1, 2) Astroentactiniinae, (3, 5, 6–10) Bientactinosphaerinae, and (4) Entactiniinae.

The uncertainty of the concept of the taxonomic significance of the characters and on taxonomic ranks leads to ambiguous, and even conflicting solutions of the same problems. Properties of various morphological characters need to be clearly and unambiguously interpreted to preclude equivocal understanding of the diagnosis (Vanchurov, 1973, 1975, 1979, 2000; Negadaev-Nikonov *et al.*, 1983; *Paleontology and Paleoecology*, 1995; Amon, 1996):

• *properties* are inherent in all objects and phenomena, anything that makes them similar or different;

• *character* is any fixed property of an object allowing its attribution, i.e., the demonstration of its similarity with some objects and its difference from the others;

• *diagnosis* is a minimal entirety of characters within a defined taxonomic unit, separating one taxon from all other taxa of a higher hierarchic level;

• *description* is a simplified model of an object made in a form of a verbal portrait with strictly unified terminology. The description consists of successively listed characters.

Descriptions are key elements of classification. The states of some characters change as the organism grows, while the state of others characterizes the variability of the group of individuals under study. Based on the morphological analysis of taxa it is possible to build a tree of a maximum similarity that would not conflict with the previously obtained data on phylogenetic relationships of taxa. To compare different taxonomic groups of organisms, it is necessary to determine the degree of stability of the values of each character, i.e., its variability and variability of the entirety of characters (Vanchurov, 1973, 1975, 1979, 2000; Negadaev-Nikonov *et al.*, 1983; Petrushevskaya, 1986; Petrushevskaya and Menshutkin, 1990; Amon, 1995, 1996).

Nevertheless, it is necessary to remember the famous statement of Linnaeus (1735), "It is the genus that gives the characters, and not the characters that make the genus" (see Petrushevskaya, 1986, p. 99). Qualities of any taxa exist objectively, i.e., they were, are, and will be irrespective of our will and desire. Moreover, there is no absolute identity, or absolute difference in nature. Hence, judgments and conclusions about the similarity or difference of paleontological taxa will always contain a certain degree of subjectivism. The negative side of any description is the absence of necessary information on the number of characters necessary to compare taxa of different levels.

SIGNIFICANCE OF MORPHOLOGICAL CHARACTERS OF RADIOLARIANS FOR THEIR CLASSIFICATION

Classification is the creation of a system of similarity and difference of objects, based on a minimal set of characters (sometimes as few as one). In reconstructing the system of fossil organisms, classification levels in its different parts are not equal. This enforces the search for the use of formal methods of computer technologies to resolve classification problems with large set of characters of objects classified. To diagnose a taxon of any rank it is necessary to know the minimal number of characters (or one character) that distinguish this taxon from other taxa. In addition, the diagnosis of a taxon of a higher rank should not contain characters of taxa of a lower rank, and vice versa taxa of a lower rank should not contain the description of characters of taxa of a higher rank.

A character may be either measured value, or simply data on the presence, absence, or state of a feature of the object. Adiagnostic character should (1) be relevant to one of three conditions: "and", "or", "no and should not be"; (2) agree with three principles: compulsory, desirable, sufficient; and (3) agree with a rule of feedback. Concepts "large", "small", etc., and any diagnostic quantitative value of the character (length, width, height, etc. and their ratios) should be constrained to the ranked size of skeletons (absolute and relative). In addition, the algorithm of the computer calculations of the

Explanation of Plate 18

Upper Devonian: (Figs. 1–5, 7–10) Middle Frasnian Substage, Domanik Formation; Timan–Pechora Province and (Fig. 6) Famennian Stage; (1, 2, 8, 9) borehole Shuda-Yag-1003: (1, 2) sample 8 (depth 120.9–124 m), (8) sample 29 (depth 105–106 m), and (9) sample 72 (depth 71.9–72.4 m); (3) Domanik River, outcrop 21, sample 38; (4, 5, 7) Ukhta River: (4, 7) sampling point no. 4, sample V-29, and (5) sampling point no. 2, sample 1m; (6) borehole Zapadnaya Lekkeyaginskaya-65, sample 86g (depth 2460–2467 m); and (10) borehole Ukhtinskaya-3B, sample 114 (depth 104.2–104.7 m).

Pores: (1) circular and (2) angular-oval, with intrapore denticles

Fig. 1. *Astroentactinia crassata* Nazarov, scale bar = 20 μm.

Fig. 2. *Astroentactinia paronae* (Hinde), bar = 20 μm.

Pores: (3, 4) oval and (5, 6) angular-oval with "false" pore-funnels

Fig. 3. *Bientactinosphaera obtusa* (Hinde), bar = 15 μm.

Fig. 4. *Entactinia herculea* Foreman, bar = 10 μm.

Fig. 5. *Bientactinosphaera miletenkoi* Afanasieva, bar = 15 μm.

Fig. 6. *Bientactinosphaera pinica* Afanasieva, bar = 20 μm.

Cellular surface of the skeleton of Ornatoentactinia

Fig. 7. *Ornatoentactinia solita* Afanasieva, bar = 15 μm.

Fig. 8. *Ornatoentactinia spinisica* Afanasieva, bar = 10 μm.

Figs. 9 and 10. *Ornatoentactinia spartaci* Afanasieva: (9, 10) bar = 15 μm.

Plate 19

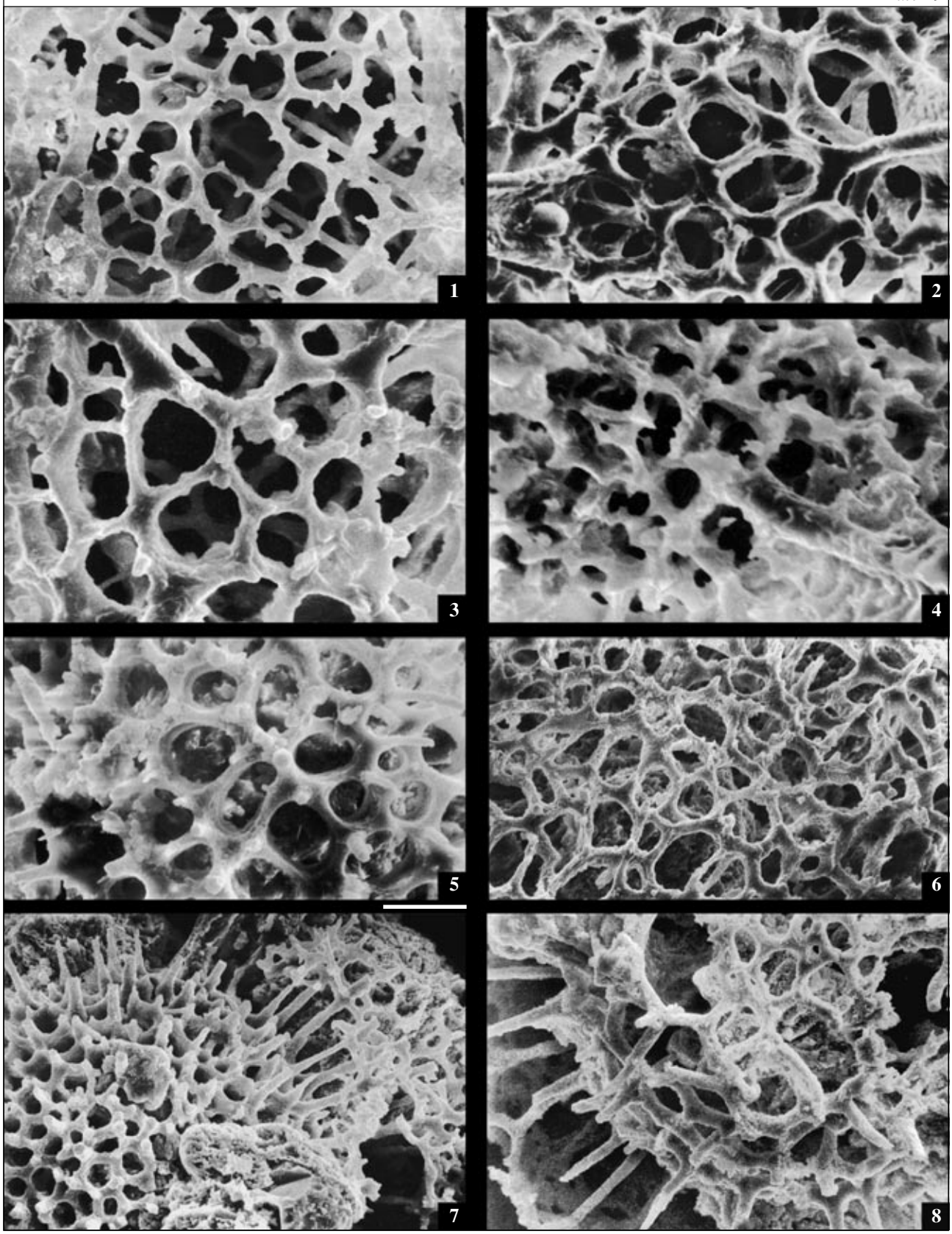

Porous structure of the external and internal shells in members of the subfamilies (1) Entactiniinae, (2–4) Astroentactiniinae, (5) Bientactinosphaerinae, and (6–8) Thecentactiniinae.

material; does not allow the use of pseudoquantitative values "more" or "less."

The analysis of morphological characters of Paleozoic radiolarians (Table 4) reveals a stable pattern of repetition and occurrence at certain hierarchic levels (Table 6). The statistical analysis of absolute and relative values of the parameters of skeletons of new species of radiolarians from the Middle Frasnian Domanik Formation of the Timan-Pechora Province showed a regular pattern of the change of quantitative values of the characters (Table 5) (Afanasieva, 2000a). The outline of the first two graphs largely correspond to the hyperbolic function, i.e., y = 1/x, whereas the two other graphs are their mirror images (Table 5a). This which allows the determination of probability coefficients of distributions (Rodionov, 1981; Aivazyan *et al.*, 1985).

The presence of such stable correlation allows the formalization of the process of data classification and use the terms "very large", "large", "small", and "very small", which correspond to certain quantitative values (Table 5b).

The statistical analysis of the values of absolute and relative parameters of the Paleozoic radiolarian skeletons was particularly useful for revealing fine differences in the structure of the skeletons of *Bientactinosphaera variacanthina* (Foreman)[5] and *B. grandis* (Nazarov)[6] (Fig. 20). The original diagnosis and description of these species do not give a clear idea of their differences. This is the source of much confusion in identifications of these species in paleontological papers. The analysis of absolute and relative (Figs. 20a, 20b) values of the length of the main spines (*L*), skeleton's diameter (*D*) and their ratio (*L*/*D*) in 26 skeletons of *B. grandis* and 28 skeletons of *B. variacanthina,* and the comparison of these values to those of holotypes of these species revealed very characteristic patterns in the ratio of the length of the main spines and the skeleton's diameter. Species clearly fall into two groups in relation to (*L*/*D*) = 1.2. This pattern is clearly seen in both the graph showing the transformation of each of the skeletal features considered and allows tracing of the change in the proportions (Fig. 20a) and in the scatter diagram, which allow comparison of the regions of determination of the parameters of the above two species (Fig. 20b).

Based on certain assumptions and the analysis of the taxonomic significance of morphological characters of the skeleton of Paleozoic radiolarians, taking into account the previous experience in studying extant and extinct radiolarians (Table 6), a system of fixed entirety of morphological characters is developed to diagnose and describe radiolarians of various taxonomic ranks.

class: (1) prevailing symmetry of the skeleton, (2) prevailing geometrical shape of the skeleton, (3) prevailing type of structure of outer shell, and (4) presence or absence of the pylome;

order: (1) geometrical shape of the skeleton, (2) type of the structure of the outer shell, and (3) prevailing type of the internal framework;

superfamily: (1) symmetry of the skeleton, (2) geometrical shape of the skeleton, and (3) type of internal framework;

family: (1) macrostructure of the skeleton, (2) structure of the outer shell; (3) number of (from/to) rays of the internal framework, and (4) type of additional skeletal tissue of the patagium;

subfamily: (1) number of skeletal shells; and (2) proportions of main spines;

genus: (1) macrostructure of the internal framework, (2) macrostructure of the pylome, (3) type of structure of internal frameworks and skeletal tissue of the patagium, (4) number of the main spines, (5) shape of the main spines, and (6) architecture of tangential structures on the skeleton's surface;

species: (1) microstructure of the outer skeletal shell and the skeletal tissue of the patagium, (2) microstructure of the internal shells of the skeleton, (3) macro-

[5] *Entactinosphaera variacanthina* Foreman, 1963, p. 278, pl. 3, fig. 8; pl. 4, figs. 3a, 3b: "One or two spherical lattice-shells with six three-bladed main spines of variable width and length, and long, needle-like by-spines…."

[6] *Entactinosphaera grandis* Nazarov, 1975, p. 65, pl. 5, figs. 11 and 12; pl. 7, figs. 1–4: "Shell with six large main spines that approximately equal in size…"

Explanation of Plate 19

Upper Devonian; Timan–Pechora Province: (Figs. 1–5) Middle Frasnian Substage, Domanik Formation; (Figs. 6–8) Famennian Stage. (1–5) borehole Shuda-Yag-1003: (1, 3) sample 68 (depth 73.3–73.5 m), (2) sample 29 (depth 105–106 m), (4) sample 56 (depth 81.6–83 m), and (5) sample 73 (depth 71.4–71.9 m); (6–8) borehole Zapadnaya Lekkeyaginskaya-65, sample 86g (depth 2460–2467 m).

Rounded polygonal pores of the external sphere

Fig. 1. *Borisella pantosompha* (Foreman), scale bar = 17 μm.

Fig. 2. *Moskovistella victorialis* Afanasieva, bar = 15 μm.

Fig. 3. *Moskovistella khaini* Afanasieva, bar = 12 μm.

Fig. 4. *Moskovistella sincera* Afanasieva, bar = 10 μm.

Fig. 5. *Bientactinosphaera variacanthina* (Foreman), bar = 20 μm.

Fig. 6. *Duplexia biexosphaera* (Nazarov), bar = 33 μm.

Circular (7) and rounded (8) polygonal pores of the second sphere

Fig. 7. *Duplexia spinocurva* Afanasieva, bar = 37 μm.

Fig. 8. *Duplexia biexosphaera* (Nazarov), bar = 42 μm.

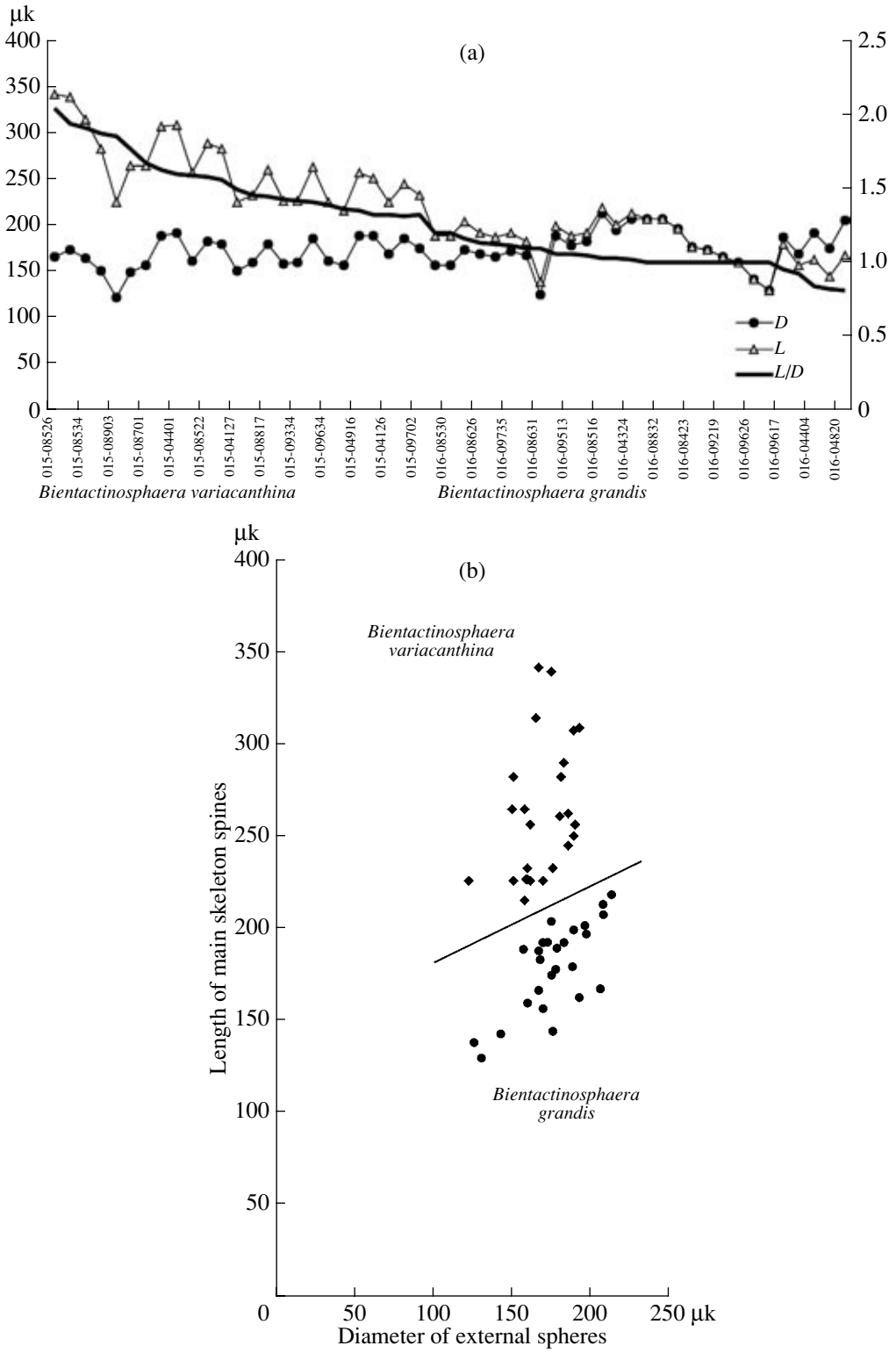

Fig. 20. Diagrams of the absolute (a) and relative (b) values of the length of the main spines (*L*), diameter of the external sphere (*D*) and their ratio (*L*/*D*) in *Bientactinosphaera grandis* (Nazarov) and *Bientactinosphaera variacanthina* (Foreman).

structure of the main spines; (4) shape and macrostructure of by-spines, (5) shape and macrostructure of tangential elements of the skeleton's surface, (6) sculptural elements, (7) shape and macrostructure of pores, pore canals and interpore bars, and (8) ranged dimensions of the skeleton and its parts (absolute and relative).

Table 6. Taxonomic significance of morphological characters of radiolarian skeletons

Author \ Taxa	Legion/Order	Suborder	Superfamily	Family	Subfamily	Genus
Ehrenberg, 1846, 1847, 1875	1. Axis of symmetry 2. Main shape of skeleton			Shape of skeleton		Number of chambers
Haeckel, 1887	1. Type of symmetry 2. Structure of central capsule 3. Position of nucleus in central capsule 4. Chemical composition of the skeleton	Morphotypes of skeletons, defined by the type of symmetry		1. Number of chambers 2. Shape of chambers 3. Open or closed last chamber 4. Structure of spherical shells 5. Spine shape 6. Number of chambers in Nassellaria, their shape and subdivision 7. Degree of closure of the last chamber of Nassellaria 8. Presence or absence of main spines 9. Number and arrangement of main spines		8. Number and arrangement of shells 9. Proportions of lengths of different spines 10. Presence or absence of main spines in Nassellaria
Hollande and Enjumet, 1960	1. External morphological characters of skeleton 2. Nucleus structure 3. Structure of the nucleoaxopodial apparatus		1. Arrangement of siliceous elements of skeleton 2. Structure of cytological body	–	–	–
Lipman, 1979	1. Type of skeleton			1. Number and shape of chambers 2. Open or closed last chambers 3. Presence or absence of spines 4. Number and arrangement of spines	5. Number of shells	6. Arrangement of shells 7. Structure of the rings (cameral rings) 8. Bars connecting cameral rings 9. Presence, shape, and arrangement of lobes and/or processes 10. Structure of lateral and wing-shaped spines 11. Structure of apertural spines 12. Structure of spines on the last chamber 13. Size of spines 14. Shape and arrangement of thorns and tubercles 15. Shape of the aperture 16. Structure of interchamber septa 17. Structure of facets and ridges separating them in pyramidal skeletons

Table 6. (Contd.)

Author \ Taxa	Order	Superfamily	Family	Subfamily	Genus
Nazarov, 1984, 1988	1. Prevailing geometrical shape of skeleton		1. Structure of internal framework 2. Symmetry of skeletal outline	1. Number of rays radiating from internal sphere or spicule 2. Number of external radial spines	1. Number of skeletal spheres: spherical or other shape 2. Structure of skeletal wall
Nazarov and Petrushevskaya, 1995	1. Arrangement of central capsule, nucleus, axoplast (or axoplasts), axonemes, and skeleton 2. Arrangement of microtubules in axoneme 3. Symmetry of the cell, prevailing geometrical shape of the skeleton 4. Structure of central capsule and its wall	1. Type of internal framework and approximate number of spines radiating from it 2. Approximate number of spherical shells or chambers (with spiral or linear arrangement) and ratio of their sizes and mode of their internal division 3. Types of skeletal structure of initial joints (spongy, lattice-like, porous, etc.) 4. Approximate number of external skeletal spheres			1. Number of spherical, spiral, or linear spheres, shells, chambers, joints, and ratios of their measurements 2. Number and measurements of internal septa between these parts of skeleton and characteristic features of wall structure 3. Arrangement, measurements, and number of pores, rods, costae, tubercles, etc. 4. Arrangement of main spine ramifications (verticils) 5. Number and shape of external shell apophyses
Afanasieva, 1997, 2000a, 2002	1. Dominant symmetry of skeleton 2. Dominant geometrical shape of skeleton 3. Dominant types of inner framework 4. Presence or absence of pylome	1. Symmetry of skeleton 2. Geometrical shape of skeleton 3. Structural type of outer shell 4. Type of inner framework	1. Structure of skeleton 2. Number (from/to) of rays of inner framework 3. Type of additional skeletal tissue of patagium	1. Number of skeletal shells 2. Ratios of main spines	1. Structure of inner framework 2. Structure of pylome 3. Structural type of inner shells and skeletal tissue of patagium 4. Number of main spines 5. Shape of main spines 6. Construction of tangential elements of skeletal surface
Amon, 1999, 2000	1. Predominant general skeletal geometry, its subdivision 2. Presence of radial and tangential structures, predominant shape of the latter 3. Type of inner framework 4. External structures 5. Structure of segments of skeleton	1. Type of inner framework 2. Number and shape of radial structures 3. Number, shape, and type of tangential structures 4. Predominant type of skeletal tissue structure 5. Topography of segments 6. Pylome 7. External apophyses	1. Characterization of inner framework 2. Characterization of skeletal tissue 3. Structure of segments and of walls between segments 4. Patagium	–	1. Outline of skeleton, total size 2. External surface, ornamentation 3. Patterns in arrangement of pores or external structures 4. Structure of pylome and patagium 5. Structure of external apophyses

Fig. 21. Position of radiolarians (Spumellarida) and acantharians (Symphyacanthida, Chaunacanthida) in the phylogenetic tree reconstructed based on the analysis of 16S ribosomal RNA (after Zettler *et al.,* 1997, text-fig. 2).

The number of the above characters for various taxa formally exceeds that of previously proposed classifications of the other authors (Table 6). In other words, the diagnostics have seemingly become more complicated. However, this is not true. The previously proposed systems of morphological characters (Table 6), firstly, do not take into account some morphological characters, and some skeletal characters involved do not correspond to the taxonomic rank considered, particularly so when undoubted species level characters (e.g., size) appear in the diagnoses of genera and even families; secondly, morphological characters of spiny radiolarians and radiolarians with a pylome are not taken into account; and thirdly, these systems of morphological characters do not meet the rigid requirements of computer technologies.

A new classification opens the opportunity to take into account almost any data on the fossils studied and allows the identification of the position of any new object of study in the phylogenetic reconstruction.

CHAPTER 3. CLASSIFICATION OF RADIOLARIA

In 19th century classifications, Radiolaria were initially regarded as an order (Ehrenberg, 1838; Müller, 1858) (Table 1). As a result of Haeckel's (1887) work, the taxonomic rank of Radiolaria was raised to that of a class.

Plate 20

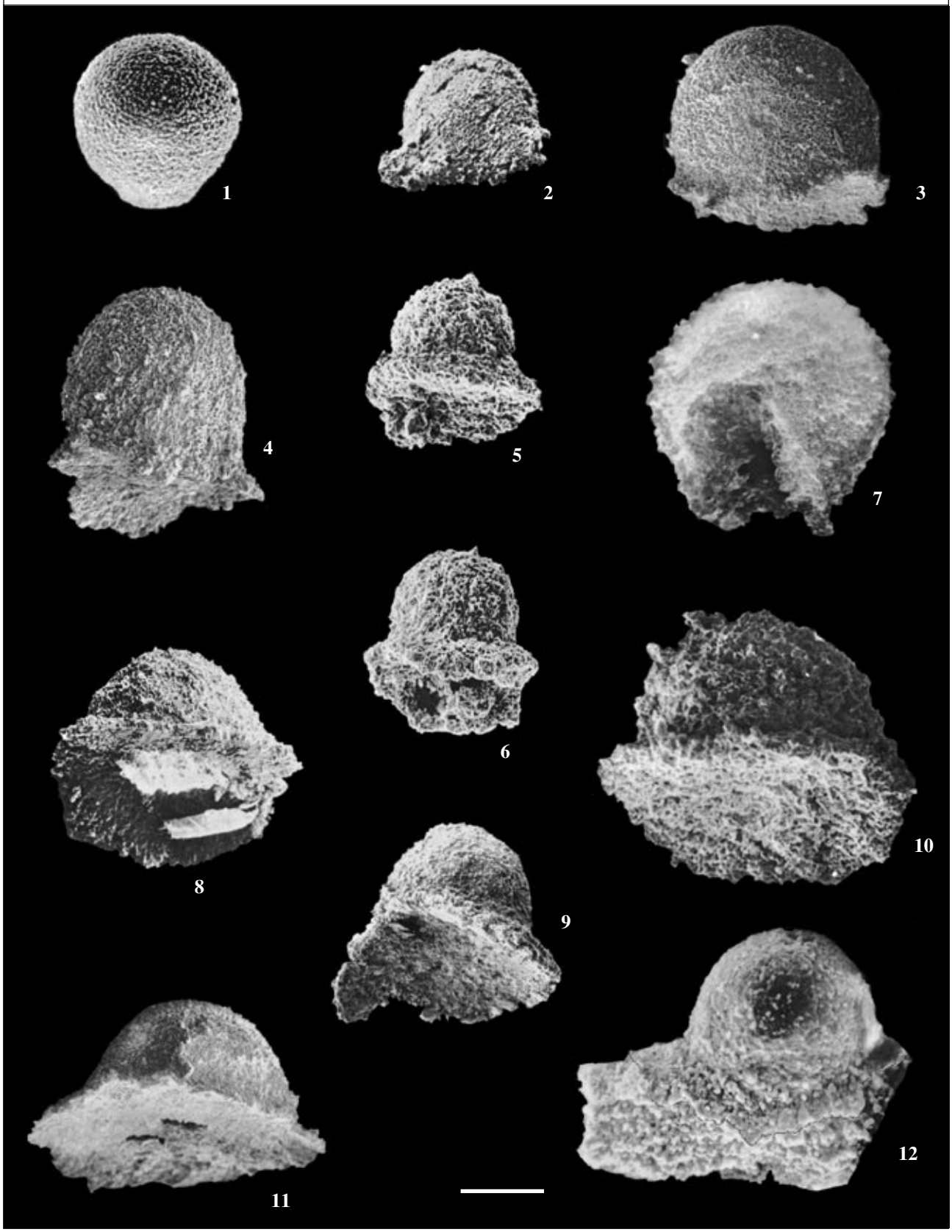

Pylome structure.

By the mid-20th century, the rank of Radiolaria remained no higher than a class (Deflandre, 1952a, 1952b, 1953a, 1953b, 1960, 1963, 1964a, 1964b; Deflandre and Deflandre-Rigaud, 1958; Lipman, 1979), and it was even treated as a subclass (Khabakov *et al.*, 1959; Chedija, 1959; Hollande and Enjumet, 1960; Riedel, 1967) (Table 1).

In the 1980s the general knowledge of organisms changed considerably. For instance, the concept that all organisms on Earth belong in two multikingdom systems, Prokaryota and Eukaryota, was proposed. The superkingdom Eukaryota includes the kingdom Animalia, which contains a subkingdom of lower Eukaryota (Protozoa). Many radiolarian paleontologists acknowledge that this kingdom is polyphyletic. In 1980 the committee on Systematics and Evolution of the International Society of Protozoologists proposed a new classification of Protozoa and recognized seven phyla within protists (Levine *et al.*, 1980). One of these, Sarcomastigophora, includes the superclass Actinopoda Calkins, 1909, composed of four classes, Acantharea Haeckel, 1881; Heliozoea Haeckel, 1866; Phaeodarea Haeckel, 1879; and Polycystinea Ehrenberg, 1838, the latter including two orders Spumellarida Haeckel, 1881 and Nassellarida Ehrenberg, 1848. Hence, the well-known name Radiolaria disappeared from the classification of Protozoa. This caused a justified objection by radiolarian workers, who continue to use the name Radiolaria, because the name Polycystina has virtually never been used in paleontology and geology (Zhamoida, 1981; Petrushevskaya, 1986; Nazarov, 1988; Vishnevskaya, 1993; Nazarov and Petrushevskaya, 1995; Amon, 1999a, 2000a, 2000b, 2000c; Afanasieva, 1999, 2000a, 2000b, 2002).

Simultaneously with the proposal of the International Committee, Russian protozoologists (Krylov *et al.*, 1980) proposed a better macrosystem of protists subdivided into nine phyla. In their system the phylum Actinopoda is not recognized, whereas unicellular organisms previously referred to it are assigned partly to the phylum Sarcodina and partly to the phylum Acantharea. According to this system, Radiolaria are a subphylum of the phylum Sarcodina, with two classes, Polycystina and Phaeodaria. A new concept of the position of the subphylum Radiolaria in the macrosystem of protists was published by Amon (1997, 1999a, 2000a, 2000b, 2000c) and Afanasieva (2000a, 2002).

Shul'man and Reshetnyak (1980) discussed the possibility of recognizing the orders Spumellaria Ehrenberg and Nassellaria Ehrenberg as separate classes. Later the phylum Radiolaria was proposed (Corliss, 1981, 1984, 1994; Kusakin and Drozdov, 1994), whereas Tochilina (1996, 1997) proposed the phylum Nassellaria.

Modern data from molecular biology suggest that Acantharia and Radiolaria are phylogenetically distant. These data are based on the comparison of the genes of ribosomal RNA and on the phylogenetic placement of Acantharia and Radiolaria on the general tree of protists (Zettler *et al.*, 1997; Mikryukov, 2000a, 2000b; Yuasa *et al.*, 2003) (Figs. 21, 22). They convincingly show that Radiolaria branched off the general stalk of protists at the very beginning of their radiation, and that Acantharia did this extremely late.

In addition, according to data from genome analysis and the topology of the phylogenetic tree of eukaryotes, the general separation of the radiolarian branch from other eukaryotes is clearly seen. The point of their branching (-/71) (Fig. 21) and the point of branching of Spumellaria into colonial and solitary (77/52) have lower values than the branching point of the major groups of eukaryotes (85/65). It is also clearly seen that solitary radiolarians branched off before colonial radiolarians (points 77/52 and 85/-, respectively) (Fig. 21) (Zettler *et al.*, 1997). Among the colonial forms Sphaerozoidae, Collosphaeridae, and *Siphonosphaera cyathina*, complete monophyly is shown only for Collosphaeridae and partly for Sphaerozoidae (Zettler *et al.*, 1998, 1999). In solitary radiolarians, complete monophyly is shown in Spongodiscidae (Yuasa *et al.*, 2003).

Zettler *et al.* (1997) concluded that the superclass Actinopoda, which consists of radiolarians, acantharians, and other microorganisms capable of forming axopodia, should not be used in the systematics of protists. The molecular studies of Acantharia and Spumellaria suggest that during evolution protist axopodia appeared and developed more than once and are very likely to be convergent structures that appeared as a response to similar ecological conditions during evolution.

Karpov and Seravin in their fundamental monograph *Protista: Handbook on Zoology* (2000) accepted the system of protists proposed by Corliss (1994), in which protists were arranged within five kingdoms of eukaryotes: Animalia, Fungi, Plantae, Chromista, and Protozoa. They wrote "Rhizopoda, Myxozoa, Foraminifera, Radiolaria, and other protists are macrotaxa comprising only amoeboid organisms" (*Protista*: …, 2000, p. 143). The acceptance of this system does not gener-

Explanation of Plate 20

(Figs. 1, 3, 8, 9, 11) Middle Carboniferous, Lower Bashkirian Substage; (Figs. 2, 4–7, 10, 12) Lower Carboniferous: (5) Upper Visean Substage and (2, 4, 6, 7, 10, 12) Serpukhovian Stage. (Figs. 1, 3, 5, 6, 8–11) Kazakhstan, Caspian Depression, northern slope, Karachaganak Massif: (1) borehole 12, sample 633 (depth 4656–4663 m); (3, 8, 9, 11) borehole 13, sample 3096 (depth 5109–5116.5 m); (5) borehole 29, sample 851827 (depth 5128–5135 m); (6, 10) borehole 19, sample 112 (depth 4760–4769 m); (Figs. 2, 4, 7, 12) Uzbekistans, Tien Shan, Ugam River, sample 803/24.

Figs. 1–12. *Caspiaza calva* Afanasieva, scale bar = 100 μm; (12) attachment of an individual by a semi-open collar of the pylome to a subcylindrical object (probably, a spine of a sea urchin).

Plate 21

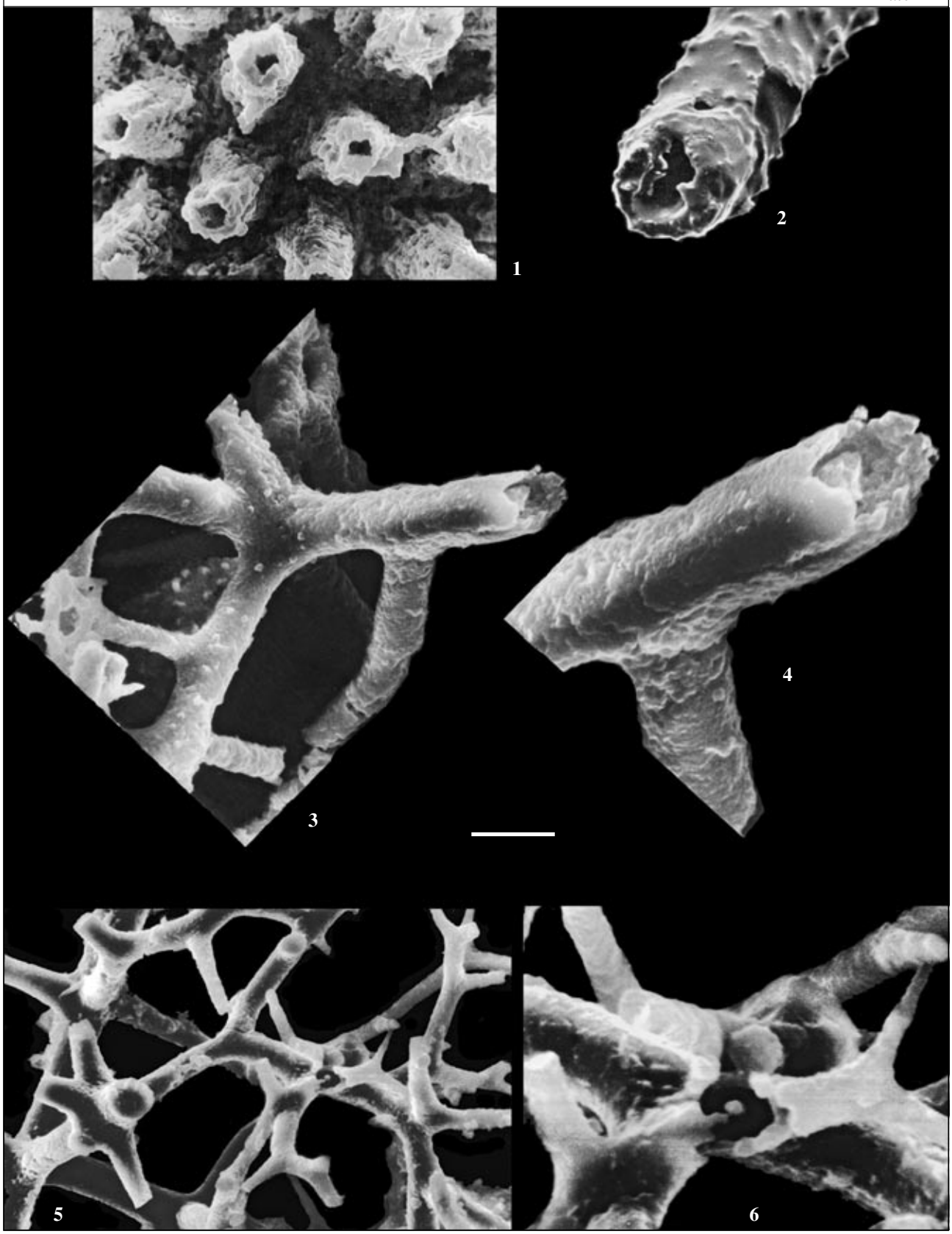

Structure of the main cylindrical spines (1–4) and crossbars of the skeleton (5, 6) with the internal canal.

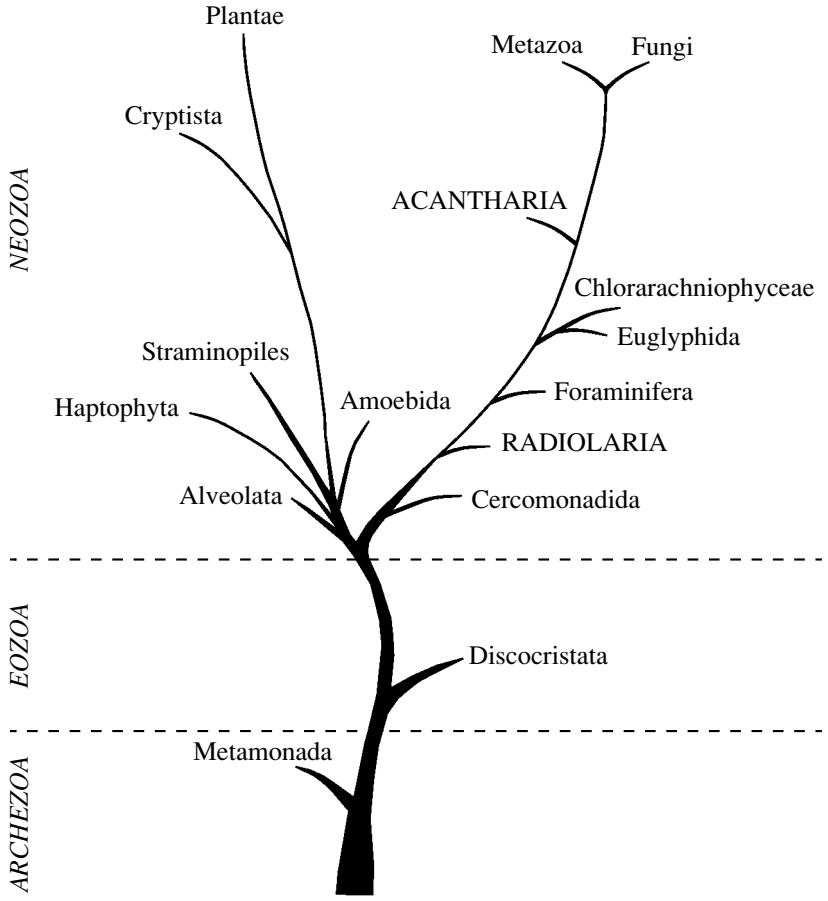

Fig. 22. Phylogenetic tree of Protista (after Mikryukov, 2000a, 2000b).

ally contradict the modern concept of the phylogenetic system of prokaryotes (*Protista*…, 2000).

Thus, our proposal (Afanasieva and Amon, 2003a, 2003b, 2003c) that Radiolaria should be recognized as a separate phylum is based on

(1) molecular studies by Zettler *et al.* (1997, 1998, 1999),

(2) advances in the study of the macrosystem of protists in the last three decades (Margulis, 1974; Levine *et al.*, 1980; Krylov *et al.*, 1980; Cavalier-Smith, 1993; Corliss, 1994; Kusakin and Drozdov, 1994; *Protista*…, 2000) (Table 1),

(3) evolutionary morphological studies of Radiolaria, and

(4) on the evidence of the almost simultaneous appearance of all five classes of Radiolaria in the Cambrian (Figs. 23, 24).

The origin of Radiolaria largely remains a mystery. It is clear from paleontological evidence that Radiolaria, one of the earliest groups of Protozoa, appeared in the Early Cambrian (Fig. 24). The hypothetical ancestor of radiolarians was not preserved in the fossil record, apparently because it did not have an articulated skeleton. It possibly had isolated spines or crystals composed of opal and/or celestine, although these morphological structures were likely to be very small. Data from genome analysis show that Radiolaria did not have a common ancestor with acantharians and foraminifers. The monophyly of radiolarians can be

Explanation of Plate 21

(Figs. 1, 2) Middle Ordovician, Llandellian Stage, eastern Kazakhstan, southwestern Predchingiz, Chagan River (after Nazarov, 1988); (Figs. 3–6) Upper Devonian, Middle Frasnian, Domanik Formation; Timan–Pechora Province: (3, 4) borehole Ukhtinskaya-3B, sample 143 (depth 83.4–84.0 m); and (5, 6) Lyajol River, outcrop 1904, sample 6.

Fig. 1. *Anakrusa myriacantha* Nazarov, scale bar = 30 μm.

Fig. 2. *Inanigutta elongata* (Nazarov), bar = 15 μm.

Figs. 3 and 4. *Polyentactinia circumretia* Nazarov et Ormiston: (3) bar = 15 μm and (4) bar = 7 μm.

Figs. 5 and 6. *Tetragregnon quadrispinosa* (Foreman): (5) bar = 20 μm and (4) bar = 7 μm.

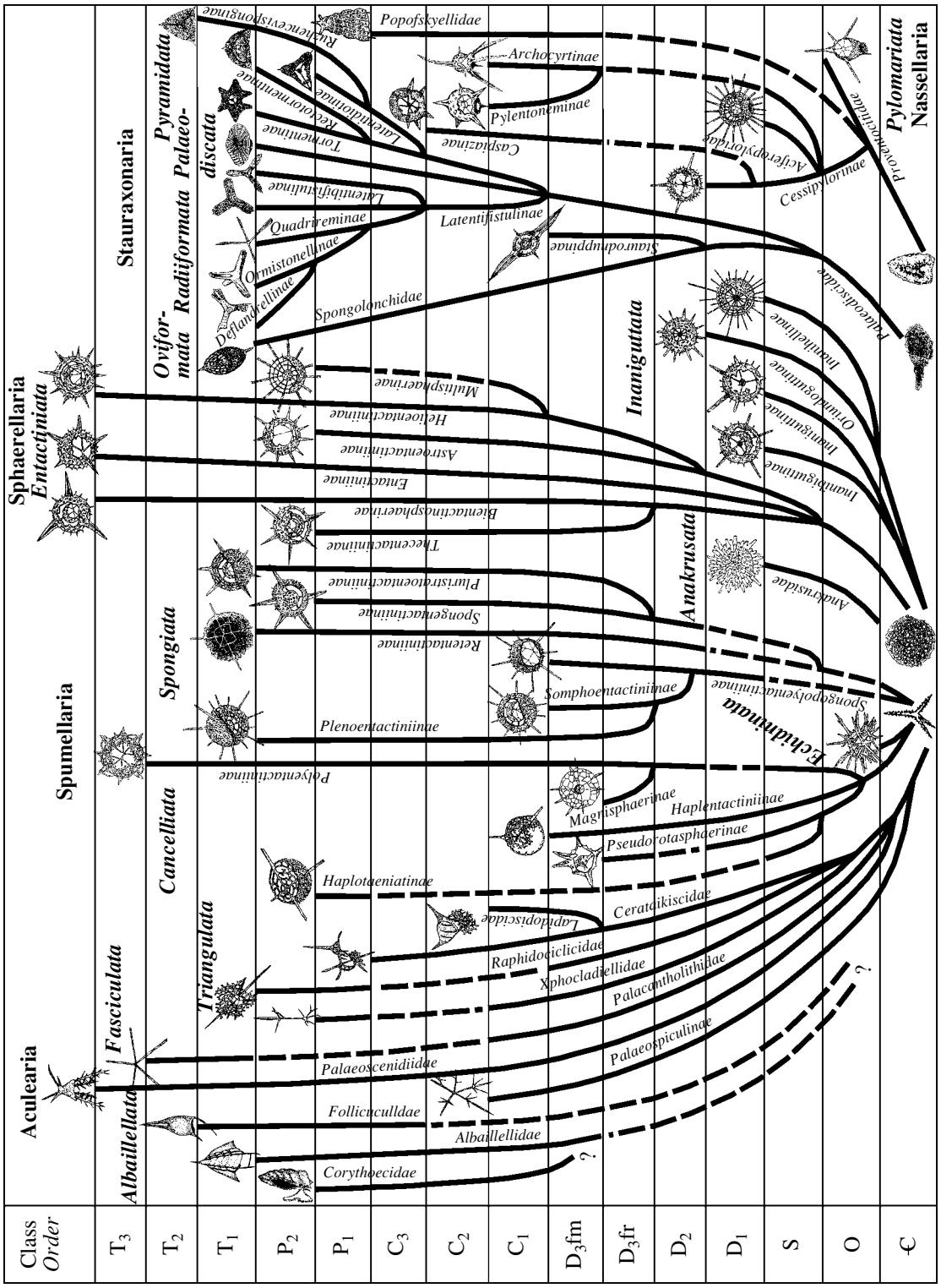

Fig. 23. Phylogenetic tree of the phylum Radiolaria in the Paleozoic.

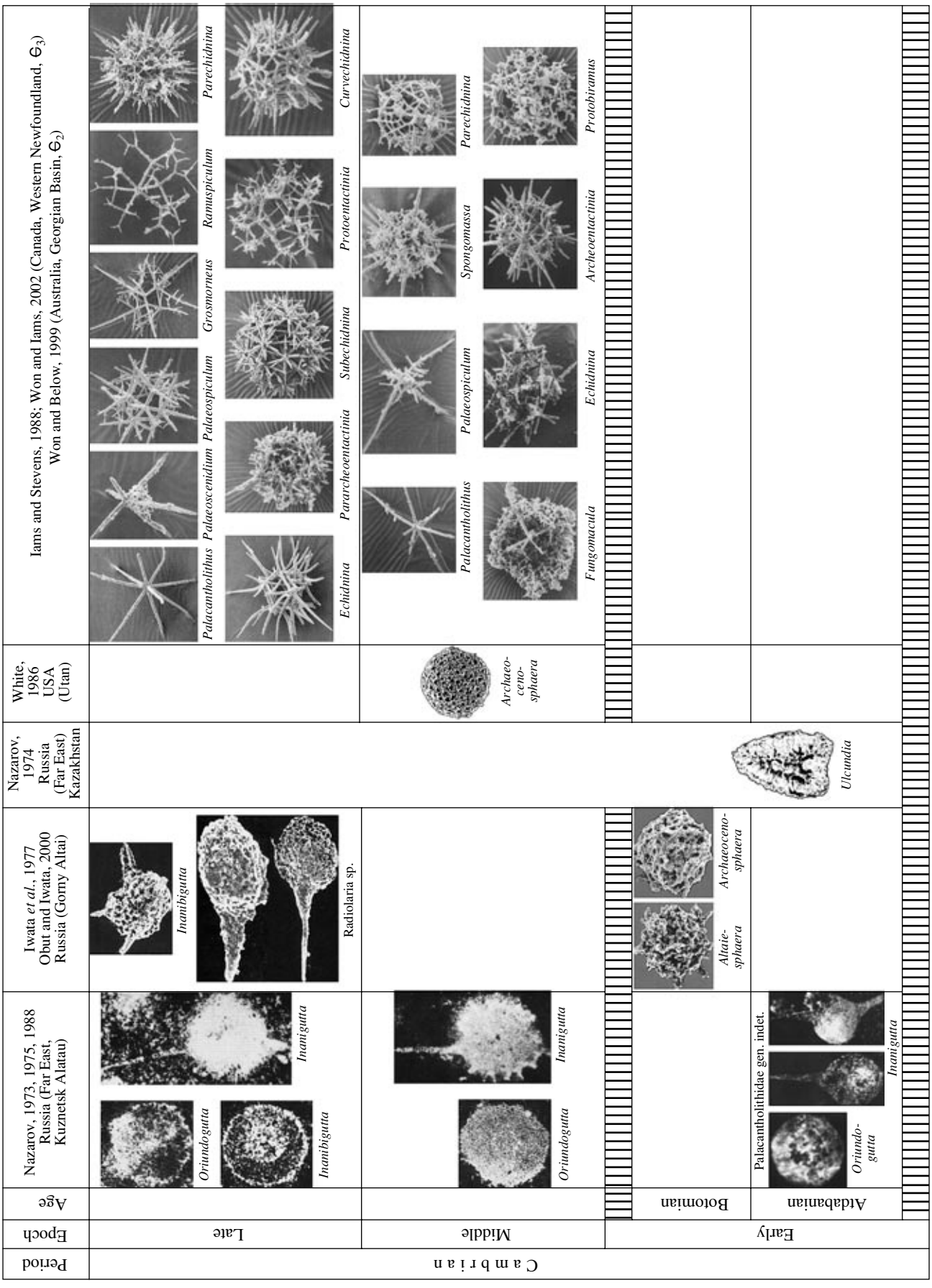

Fig. 24. Cambrian radiolarians.

Plate 22

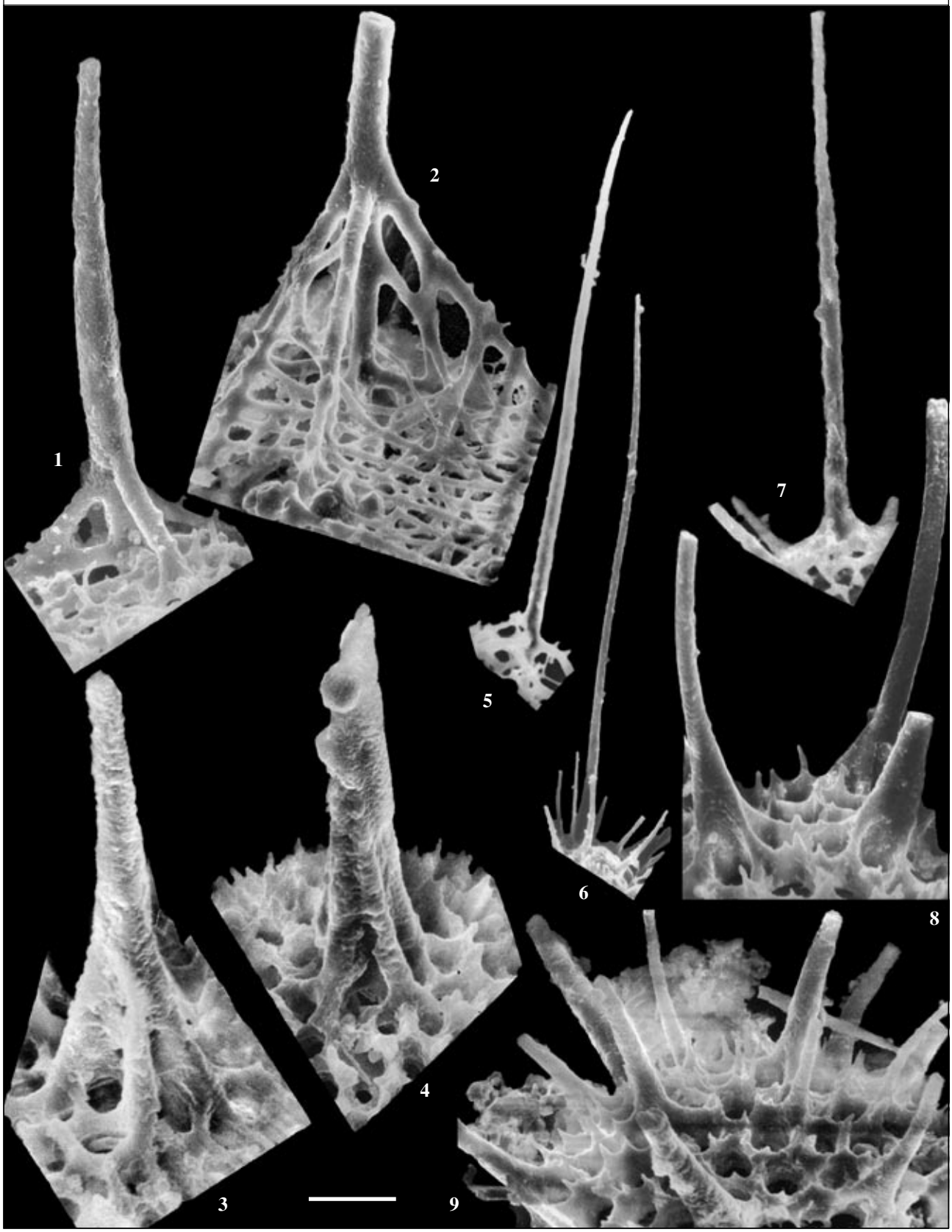

Cylindrical (1, 2, 5–7) and conical main spines (3, 4, 8, 9) in members of the subfamilies (1, 2) Polyentactiniinae, (4, 7–9) Astroentactiniinae, (3, 6) Entactiniinae, and (5) Haplentactiniinae.

accepted, and is supported by molecular-genetic evidence. The hypothetical ancestor of radiolarians may have been a sessile benthic organism that in the primordial ocean inhabited near-shore shallow zones, as was previously suggested (Petrushevskaya, 1977, 1986; Afanasieva, 1986, 2000a, 2000b; Afanasieva and Vishnevskaya, 1993a).

The evolution of the world's oceans in the Earth's history, increase in their sizes and depths and changes in their configuration, chemistry, hydrodynamics, and other parameters led to the appearance and diversification of more and more new ecological niches. This resulted in the appearance of the fused opaline skeleton, the transition from the sessile to the planktonic mode of life, and the rapid evolution of morphotypes of radiolarians.

It should be acknowledged, however, that the higher taxa of radiolarians that appeared in the Paleozoic were classes, judging from the general architecture of their skeletons. This may testify to a polyphyletic origin of the phylum Radiolaria. In addition, we can safely assume that the higher taxa of radiolarians were formed by combining high-rank characters that arose almost simultaneously in the Early Paleozoic. Firstly, it is reflected in their diversity, which is not observed in the appearance of the new higher taxa of radiolarians later, in the Mesozoic–Cenozoic, and secondly in the fact that the same taxon may have characters of spherical and spiny radiolarians. For instance, the initial spicule, which is present in the skeleton of almost all Paleozoic Spumellaria, Sphaerellaria, Stauraxonaria, and Pylomariata, is found in the cephalic and postcephalic skeletal chambersof Mesozoic and Cenozoic Nassellaria, but also forms separate skeletal elements of spiny Aculearia.

A new classification of the higher taxa of radiolarians may appear as follows (Table 7):

Phylum Radiolaria Müller, 1858

Superclass Phaeodaria Haeckel, 1879

Superclass Polycystina Ehrenberg, 1838

Class Aculearia Afanasieva, 1999, emend. Afanasieva et Amon, 2003

Order Fasciculata Afanasieva et Amon, 2003

Order Triangulata Afanasieva et Amon, 2003

Order Albaillellata Deflandre, 1953, emend. Afanasieva et Amon, 2003

Class Spumellaria Ehrenberg, 1875, emend. Afanasieva et Amon, nov.

Order Echidninata Kozur, Mostler, et Repetski, 1996

Order Cancelliata Afanasieva et Amon, 2003

Order Spongiata Afanasieva et Amon, 2003

Order Capsulata Afanasieva et Amon, ordo nov.

Order Prodigiata Afanasieva et Amon, ordo nov.

Order Saturnalata Afanasieva et Amon, ordo nov.

Class Sphaerellaria Haeckel, 1881, emend. Afanasieva et Amon, nov.

Order Inaniguttata Nazarov et Ormiston, 1984

Order Entactiniata Riedel, 1967

Order Anakrusata Nazarov, 1977

Order Hexalonchata Haeckel, 1881

Order Sphaerellata Haeckel, 1887

Order Actinommata Haeckel, 1862

Class Stauraxonaria Afanasieva et Amon, classis nov.

Order Palaeodiscata Afanasieva et Amon, ordo nov.

Explanation of Plate 22

Upper Devonian, Middle Frasnian Substage, Domanik Formation; Timan–Pechora Province: (Figs. 1–4, 6, 8, 9) borehole Shuda-Yag-1003: (1, 4) sample 72 (depth 71.9–72.4 m); (2, 6, 8) sample 68 (depth 73.3–73.5 m); (3) sample 73 (depth 71.4–71.9 m); and (9) sample 8 (depth 120.9–124 m); (Fig. 5) Lyajol River, outcrop 1904, sample 6; and (Fig. 7) borehole Ukhtinskaya-3B, sample 116 (depth 100.6–101 m).

Cylindrical spines reinforced at the base by additional spines forming very wide supports (tension bracings)

Fig. 1. *Polyentactinia kossistekensis* Nazarov, scale bar = 20 μm.

Fig. 2. *Polyentactinia zhamoidai* Afanasieva, bar = 20 μm.

Spines conical in the distal part and three-bladed at the base, because of development of false supports (tension bracings)

Fig. 3. *Entactinia diversita* Nazarov, bar = 15 μm.

Fig. 4. *Moskovistella rozanovi* Afanasieva, bar = 15 μm.

Very narrow cylindrical spines

Fig. 5. *Haplentactinia alekseevi* Afanasieva, bar = 42 μm.

Fig. 6. *Borisella mariae* Afanasieva, bar = 77 μm.

Fig. 7. *Astroentactinia vishnevskayae* Afanasieva, bar = 33 μm.

Conical spines: (8) curved and (9) straight

Fig. 8. *Astroentactinia rusaevi* Afanasieva, bar = 20 μm.

Fig. 9. *Astroentactinia tikhomirovi* Afanasieva, bar = 20 μm.

Table 7. Classification scheme of the radiolarian superclass Polycystina Ehrenberg, 1838

Class	Order	Family	Subfamily	Age
Aculearia Afanasieva, 1999, emend. Afanasieva et Amon, 2003	Fasciculata Afanasieva et Amon, 2003	Palacantholithidae Kozur et Mostler, 1981, emend. Afanasieva et Amon, nov.		Є–J
		Plagiacanthidae Hertwig, 1879, emend. Afanasieva et Amon, nov.	Palaeospiculinae Won in Won et Below, 1999	$Є_2$–C_1
			Plagiacanthinae Hertwig, 1879	T_2–Q
		Xiphocladiellidae Nazarov, 1984, emend. Afanasieva et Amon, nov.		$Є_3$–P_1
		Palaeoscenidiidae Riedel, 1967, emend. Nazarov et Rudenko, 1981		$Є_3$–T
	Triangulata Afanasieva et Amon, 2003	Ceratoikiscidae Holdsworth, 1969		O_2–C
		Raphidociclicidae Afanasieva, 1999, emend. Afanasieva et Amon, nov.		O_2–P
		Lapidopiscidae Deflandre, 1958, emend. Afanasieva, 1999		D_2–C_1
	Albaillellata Deflandre, 1953, emend. Afanasieva et Amon, 2003	Albaillellidae Deflandre, 1952		O_2–P
		Follicucullidae Ormiston et Babcock, 1979		O_2–T_1
		Corythoecidae Nazarov, 1981		D_3–P_1
Sphaerellaria Haeckel, 1881, emend. Afanasieva et Amon, nov.	Inaniguttata Nazarov et Ormiston, 1984	Inaniguttidae Nazarov et Ormiston, 1984, emend. Afanasieva, 1999	Inaniguttinae Nazarov et Ormiston, 1984, emend. Afanasieva, 1999	Є–S
			Inanibiguttinae Afanasieva, 1999	$Є_3$–S
		Oriundoguttidae Afanasieva, 1999	Oriundoguttinae Afanasieva, 1999	Є–D_1
			Inanihellinae Afanasieva, 1999	O–S
	Entactiniata Riedel, 1967	Entactiniidae Riedel, 1967, emend. Afanasieva, 1999	Entactiniinae Riedel, 1967, emend. Afanasieva, 1999	Є–T
			Bientactinosphaerinae Afanasieva, 1999	S–T
			Thecentactiniinae Afanasieva, 1999	D_3–P_1
		Astroentactiniidae Nazarov et Ormiston, 1985	Astroentactiniinae Nazarov et Ormiston, 1985, emend. Afanasieva, 1999	S–P_1
			Helioentactiniinae Afanasieva, 1999	D_2–T
			Multisphaerinae Nazarov et Afanasieva, 2000	C–P_1
		Hexastylidae Haeckel, 1881		T_2–Q
	Anakrusata Nazarov, 1977	Anakrusidae Nazarov, 1977		O–S
	Hexalonchata Haeckel, 1881	Kungalariidae Dumitrica et Carter, 1999		T_3–K
		Hexalonchidae Haeckel, 1881		J–Q
	Sphaerellata Haeckel, 1887	Xiphostylidae Haeckel, 1881, emend. De Wever et al., 2001	Xiphostylinae Haeckel, 1881, emend. De Wever et al., 2001	T–K
			Stylosphaerinae Haeckel, 1881	K_2–Q
			Entapiinae Dumitrica, 2001	$Pg_{1–2}$
		Pantanelliidae Pessagno, 1977	Capnuchosphaerinae De Wever, 1979, emend. Pessagno, 1979	$T_{2–3}$
			Capnodocinae Pessagno, 1979, emend. Blome, 1983	T_3
			Pantanelliinae Pessagno, 1977	T_3–K_1
		Parvivaccidae Pessagno et Yang, 1989, emend. De Wever et al., 2001	Parvivaccinae Pessagno et Yang, 1989, emend. De Wever et al., 2001	J_2–K_1
			Heleninae Hull, 1997	$J_{2–3}$
			Leugeoninae Yang et Wang, 1990	$J_{2–3}$
			Acaeniotylinae Yang, 1993	J_3–K
	Actinommata Haeckel, 1862	Actinommidae Haeckel, 1862, emend. De Wever et al., 2001		T–Q
		Astrosphaeridae Haeckel, 1881		T–Q
		Heliodiscidae Haeckel, 1881		Pg–Q

Table 7. (Contd.)

Class	Order	Family	Subfamily	Age
Spumellaria Ehrenberg, 1875, emend. Afanasieva et Amon, nov.	Echidninata Kozur, Mostler et Repetski, 1996	Echidninidae Kozur, Mostler et Repetski, 1996		$Є_{2–3}$
	Cancelliata Afanasieva et Amon, 2003	Haplentactiniidae Nazarov, 1980	Haplentactiniinae Nazarov, 1980	$Є_2–P_1$
			Pseudorotasphaerinae Noble, 1994	$O_2–D$
			Haplotaeniatinae Afanasieva et Amon, subfam. nov.	$S–P_1$
		Polyentactiniidae Nazarov, 1974	Polyentactiniinae Nazarov, 1975, emend. Afanasieva, 1999	$O_2–K$
			Magnisphaerinae Afanasieva, 1999	D_3
		Pentactinocarpidae Dumitrica, 1978		$T_{2–3}$
		Orosphaeridae Haeckel, 1887		K–Q
	Spongiata Afanasieva et Amon, 2003	Spongentactiniidae Nazarov, 1975	Retentactiniinae Won, 1997, emend. Afanasieva, 1999	$Є_2–P$
			Spongentactiniinae Nazarov, 1975, emend. Afanasieva, 1999	$S–P_1$
			Pluristratoentactiniinae Afanasieva, 1999	$D_3–P$
		Spongopolyentactiniidae Nazarov, 1975	Spongopolyentactiniinae Nazarov, 1975, emend. Afanasieva, 1999	$Є_2–D$
			Somphoentactiniinae Kozur et Mostler, 1981	$D_{2–3}$
			Plenoentactiniinae Afanasieva, 1999	$D_3–P$
		Conocaryommidae Lipman 1969, emend De Wever et al., 2001		$P_2–Pg_2$
	Capsulata Afanasieva et Amon, ordo nov.	Centrocubidae Hollande et Enjumet, 1960, emend. Dumitrica 1994		$T_2–Q$
		Quinquecapsulariidae Dumitrica, 1995		J–Q
		Rhizosphaeridae Haeckel, 1881, emend. Dumitrica, 1995		$J_3–Q$
	Prodigiata Afanasieva et Amon, ordo nov.	Eptingiidae Dumitrica, 1978		$T_2–J$
		Multiarcusellidae Kozur et Mostler, 1979	Multiarcusellinae Kozur et Mostler, 1979	$T_{2–3}$
			Austrisaturnalinae Kozur et Mostler, 1983	$T_{2–3}$
	Saturnalata Afanasieva et Amon, ordo nov.	Oertlispongidae Kozur et Mostler 1980		$T_{2–3}$
		Saturnalidae Deflandre, 1953	Heliosaturnalinae Kozur and Mostler, 1972	$T_3–J_1$
			Hexasaturnalinae Kozur et Mostler, 1983	$T_3–K_1$
			Saturnalinae Deflandre, 1953	$T_3–Q$
			Axopruninae Dumitrica, 1983	Pg–Q

Table 7. (Contd.)

Class	Order	Superfamily	Family	Subfamily	Age
Stauraxonaria Afanasieva et Amon, classis nov.	Palaeodiscata Afanasieva et Amon, ordo nov.		Palaeodiscidae Afanasieva, 2000		$\in_3$–P
	Oviformata Afanasieva et Amon, ordo nov.		Spongolonchidae Afanasieva et Amon, fam. nov.		S_1w–P
			Staurodruppidae Afanasieva, 2000		D
			Gomberellidae Kozur et Mostler 1981, emend. De Wever et al., 2001		T_2–K_1
			Archaeospongoprunidae Pessagno, 1973		T_2–Q
			Phaseliformidae Pessagno, 1972		K
	Radiiformata Afanasieva et Amon, ordo nov.		Latentifistulidae Nazarov et Ormiston, 1983	Latentifistulinae Nazarov et Ormiston, 1983	C–P
				Latentibifistulinae Afanasieva, 2000	C_3–P
			Quadriremidae Afanasieva, 2000		C_3–P
			Polyfistulidae Amon, 1999		P_1
			Ormistonellidae De Wever et Caridroit, 1984		P
			Deflandrellidae DeWever et Caridroit, 1984		P_2
	Pyramidata Afanasieva et Amon, ordo nov.		Tormentidae Nazarov et Ormiston, 1983	Tormentinae Nazarov et Ormiston, 1983	C–P
				Rectotormentinae Afanasieva, 2000	P
			Ruzhencevispongidae Nazarov et Ormiston, 1983	Latentidiotinae Afanasieva, 2000	C_3–P_1
				Ruzhencevisponginae Kozur, 1980, emend. Afanasieva, 2000	P–T_1
			Pyramispongiidae Kozur et Mostler, 1978, emend. De Wever et al., 2001		T_2–K
			Cavaspongiidae Pessagno, 1973		K
	Lobatiradiata Afanasieva et Amon, ordo nov.		Angulobracchiidae Baumgartner, 1980, emend. De Wever et al., 2001		T_2–K
			Patulibracchiidae Pessagno, 1971, emend. De Wever et al., 2001		T_3–N_2
			Hexaporobrachiidae Kozur et Mostler, 1979		T_3
			Hagiastridae Riedel, 1971		T_3–K
			Suttoniidae Schaaf, 1976, emend. Dumitrica, 1983		Pg_1–Q
			Myelastridae Riedel, 1971		Q
	Pyloniata Haeckel, 1881 emend. Dumitrica, 1989	Dactyliosphaeroidea Squinabol, 1904, emend De Wever et al., 2001	Patruliidae Dumitrica, 1989		T_2
			Veghicycliidae Kozur et Mostler, 1972		T_3–K_1
			Dactyliosphaeridae Squinabol, 1904, emend. De Wever et al., 2001		T_3–Pg
			Emiluviidae Dumitrica, 1995		J_2–K
			Catenopylidae Dumitrica, 1989		J_3–K
			Pseudoaulophacidae Riedel 1967, emend. Dumitrica, 1997	Pseudoaulophacinae Riedel, 1967, emend. De Wever et al., 2001	J_2–Pg_2
				Pentapyloniinae Dumitrica, 2001	K_2–Q
		Pylonioidea Haeckel, 1881	Miropylidae Dumitrica, 1988		K_2
			Pyloniidae Haeckel 1881, emend. Dumitrica, 1989	Palaeotetrapylinae Dumitrica, 1988	Pg_1
				Pyloniinae Haeckel, 1881, emend. Dumitrica, 1989	Pg_1–Q
				Pylodiscinae Haeckel, 1887	Pg_2–Q
				Dipylissinae Dumitrica, 1988	N_1–Q
		Larnacillioidea Haeckel, 1887	Larnacillidae Haeckel, 1887	Larnacillinae Haeckel, 1887	K_2–Q
				Histriastrinae Dumitrica, 1989	Pg_1–N_1
				Cryptolarnaciinae Dumitrica, 1989	Pg_1–Q
				Circodiscinae Dumitrica, 1989	Pg_1–Q
			Tholoniidae Haeckel, 1887		Pg_3–Q
	Spongurata Haeckel, 1862		Sponguridae Haeckel, 1862		T_2–Q
			Litheliidae Haeckel, 1862		T_3–Q
	Spongodiscata Haeckel, 1862		Relindellidae Kozur et Mostler, 1980		T_3
			Spongodiscidae Haeckel, 1862		K_2–Q
			Coccodiscidae Haeckel, 1862, emend. Sanfilippo et Riedel, 1980	Coccodiscinae Haeckel, 1862	Pg_2–Q
				Artiscinae Haeckel, 1881, emend. Riedel, 1967	Pg_3–Q

Table 7. (Contd.)

Class	Order	Superfamily	Family	Subfamily	Age
Nassellaria Ehrenberg, 1875, emend. Afanasieva et Amon, nov.	Pylomariata Afanasieva, 1999	Proventocitoidea Aitchison, 1998	Proventocitidae Aitchison, 1998		$\in$–O
		Cessipyloroidea Afanasieva, 1999	Cessipyloridae Afanasieva, 1999	Cessipylorinae Afanasieva, 1999	O_2–D_1
				Caspiazinae Afanasieva, 2000	D_3–T_2
			Aciferopyloridae Afanasieva, 1999		S
		Pylentonemoidea Deflandre, 1963	Pylentonemidae Deflandre, 1963	Archocyrtiinae Kozur et Mostler, 1981, emend. Afanasieva, 1999	S–T_2
				Pylentoneminae Deflandre, 1963, emend. Afanasieva, 1999	D_3–C_1
				Vallupinae Pessagno et MaxLeod, 1987	J_3
			Poulpidae De Wever 1981		T_2–K_1
			Tripedurnulidae Dumitrica 1991		T_2–K_1
		Popofskyelloidea Deflandre, 1964	Popofskyellidae Deflandre, 1964		D_3–P
			Hexapylocapsidae Dumitrica et Zugel, 1998		J_3
	Cyrtidinata Haeckel, 1862	Archipilioidea Haeckel, 1881	Archipiliidae Haeckel, 1881	Archipiliinae Haeckel, 1881	T–Q
				Clathromitrinae Petrushevskaya, 1971	T–Q
				Zamolxinae Dumitrica, 1982	T–Pg_2
				Nabolellinae Kozur et Mostler, 1979	$T_{2–3}$
				Lophophaeninae Haeckel, 1881	J–Q
				Sethopiliinae Haeckel, 1881	K–Q
				Dimelissinae Petrushevskaya, 1981	Pg–Q
				Plectaniinae Haeckel, 1881	Q
			Pseudosaturniformidae Kozur et Mostler, 1979		T_2–J
			Sethoperidae Haeckel, 1881	Sethoperinae Haeckel, 1881	J–Q
				Tetraplectinae Haeckel, 1881	Q
			Plagoniidae Haeckel, 1881		Q
			Cystidiidae Haeckel, 1883		Q
		Acropyramidoidea Haeckel, 1881	Sethophormididae Haeckel, 1881	Sethophormidinae Haeckel, 1881	T–Q
				Theopiliinae Haeckel, 1881	T–Q
				Rotaforminae Pessagno, 1970	K
				Neosciadiocapsinae Pessagno, 1969	K–Pg_2
				Enneaphormidinae Petrushevskaya, 1981	K–Q
			Bulbocyrtiidae Kozur et Mostler, 1981		$T_{2–3}$
			Acropyramididae Haeckel, 1881		K–Q
			Lampromitridae Haeckel, 1881	Lampromitrinae Haeckel, 1881	K–Q
				Lithocampaninae Petrushevskaya, 1981	K–Q
				Ceratocyrtinae Petrushevskaya, 1981	Pg–Q
		Lychnocanioidea Haeckel, 1881	Silicarmigeridae Kozur et Mostler, 1980		T–Q
			Lychnocaniidae Haeckel, 1881	Lychnocaniinae Haeckel, 1881	T–Q
				Lithochytridinae Petrushevskaya, 1981	K–Pg
				Ultranaporinae Pessagno, 1977	K–Q
				Bekominae Dumitrica, 2001	Pg–N
			Spongosilicarmigeridae Dumitrica, 2001		T_2
			Deflandrecyrtiidae Kozur et Mostler, 1979		$T_{2–3}$
			Spongolophophenidae Kozur et Mostler, 1994		T_2–J_1
			Foremanellidae Dumitrica, 1982		T_2–J_2
			Cuniculiformidae De Wever, 1982		T_2–J
			Livarellidae Kozur and Mostler 1981		T_3–J_1
			Theoperidae Haeckel, 1881		Pg–Q

Table 7. (Contd.)

Class	Order	Superfamily	Family	Subfamily	Age
Nassellaria Ehrenberg, 1875, emend. Afanasieva et Amon, nov.	Cyrtidinata Haeckel, 1862	Eucyrtidioidea Ehrenberg, 1847	Eucyrtidiidae Ehrenberg, 1847	Eucyrtidiinae Ehrenberg, 1847	T–Q
				Calocyclinae Haeckel, 1881	K–Q
				Theocotylinae Petrushevskaya, 1981	K–Q
			Planispinocyrtiidae Kozur et Mostler, 1981		$T_{2–3}$
			Ruesticyrtiidae Kozur et Mostler, 1979		$T_{2–3}$
			Pseudodictyomitridae Pessagno, 1977		T_3–K
			Eucyrtidiellidae Takemura, 1986		J_2–K_1
			Obeliscoitidae O'Dogherty, 1994		J_2–K
			Xitidae Pessagno, 1977		J_2–K
			Williriedellidae Dumitrica, 1970		J_2–K
			Carpocaniidae Haeckel, 1881		K–Q
			Artostrobiidae Riedel, 1967		K–Q
			Pterocoryidae Haeckel, 1881	Pterocoryinae Haeckel, 1881	K–Q
				Sethocoryinae Haeckel, 1881	K–Q
				Podocyrtiinae Haeckel, 1887	Pg–Q
			Lophocyrtiidae Sanfilippo, Caulet, 2001		Pg–Q
		Stichocapsoidea Haeckel, 1881	Stichocapsidae Haeckel, 1881	Stichocapsinae Haeckel, 1881	T–Q
				Sethocapsinae Haeckel, 1881	J–K
			Monicastericidae Kozur et Mostler, 1994		T_2
			Bagotidae Pessagno et Whalen, 1982		T_3–J_2
			Hsumidae Pessagno et Whalen, 1982		J–K_1
			Archaeodictyomitridae Pessagno, 1976		J–K
			Unumidae Kozur 1984		J_2–K_1
		Amphipyndacioidea Riedel, 1967, emend. De Wever et al., 2001	Canoptidae Pessagno, 1979		T_2–K_1
			Parvicingulidae Pessagno, 1977	Wrangelliinae Yeh, 1987	T_3–K_1
				Parvicingulinae Pessagno, 1977	J–K_1
			Syringocapsidae Foreman, 1973		J–N_1
			Spongocapsulidae Pessagno, 1977		J_2–K
			Amphipyndacidae Riedel, 1967		J_2–Q
		Cannobotryoidea Haeckel, 1881	Botryocyrtididae Petrushevskaya, 1981		K–Q
			Cannobotryidae Haeckel, 1881		K–Q
	Spyridinata Ehrenberg, 1847		Triospyrididae Haeckel, 1881	Dipodospyridinae Haeckel, 1881	Pg–N
				Archiphatninae Haeckel, 1881	Pg–Q
				Triospyridinae Haeckel, 1881	Pg–Q
				Tholospyridinae Haeckel, 1887	Pg_2–Q
				Androspyridinae Haeckel, 1887	N
				Nephrospyridinae Haeckel, 1887	N
			Stephaniidae Haeckel, 1887		Pg–Q
			Acanthodesmiidae Haeckel, 1862	Circospyridinae Haeckel, 1881	Pg_2–Q
				Perispyridinae Haeckel, 1881	N_1
				Acanthodesmiinae Haeckel, 1862	N–Q
				Paradictyinae Haeckel, 1881	N–Q
Collodaria Haeckel, 1881			Sphaerozoidae Haeckel, 1862		T–Q
			Collosphaeridae Müller, 1858		Pg_2–Q
			Thalassosphaeridae Haeckel, 1862		Q

Order Oviformata Afanasieva et Amon, ordo nov.

Order Radiiformata Afanasieva et Amon, ordo nov.

Order Pyramidata Afanasieva et Amon, ordo nov.

Order Lobatiradiata Afanasieva et Amon, ordo nov.

Order Pyloniata Haeckel, 1881, emend. Dumitrica, 1989

Order Spongurata Haeckel, 1862

Order Spongodiscata Haeckel, 1862

Class Nassellaria Ehrenberg, 1847, emend. Afanasieva et Amon, nov.

Order Pylomariata Afanasieva, 1999

Order Spyridinata Ehrenberg, 1847

Order Cyrtidinata Haeckel, 1862

Class Collodaria Haeckel, 1881

This classification is mainly based on the studies of Petrushevskaya (1971, 1984, 1986), Strelkov and Reshetnyak (1971), Nazarov (1988), Dumitrica (1988, 1989, 1995), Amon (1999), Afanasieva (1999, 2000a, 2000b, 2002), De Wever, Dumitrica, Caulet, Nigrini, and Caridroit (De Wever *et al.*, 2001), and Afanasieva and Amon (2003). The description of superfamilies, families, and subfamilies is based on the above contributions.

The system of Nassellaria sensu Petrushevskaya (1981a) has undergone the most considerable changes in accordance with the latest studies of Dumitrica (1995) and De Wever *et al.* (2001). These changes mostly concern Triassic, Jurassic, and Cretaceous nassellarians, which did not receive sufficient study in the papers of Petrushevskaya.

The generic composition of most families of Nassellaria is accepted based on the list of genera in the book by Petrushevskaya *Radiolarians of the Order Nassellaria from the World's Oceans* (Petrushevskaya, 1981a). At the same time, the generic content of the families of Nassellaria proposed by Petrushevskaya (1981a) was emended and updated according to the later studies of nassellarians (Bragin *et al.*, 1999; Kozlova, 1999; Amon, 2000).

SPINY RADIOLARIANS

Up to the present day, there is no agreement between specialists studying fossil and extant radiolarians on the composition, taxonomic rank, and position of heteropolar spiny radiolarians in the general system of Radiolaria.

Riedel (1967) acknowledged that Haeckel's classification is unsuitable to the systematics of the Late Eocene–Middle Pliocene spine-framed radiolarians of the family Orosphaeridae Haeckel, 1887 and tentatively assigned them to Phaeodaria.

Deflandre (1973, p. 290) emphasized the evident similarity between the spiny skeletons of *Palaeothalomnus* and those of modern representatives of *Thalassothamnus* (Figs. 25c, 25e). Petrushevskaya (1986, p. 130) wrote that the family Palaeoscenidiidae is closely related to Thalassothamnidae, differing in the distinct heteropolarity (Figs. 25f, 25g). At the same time, she combined the spiny radiolarians with Albaillellaria (Petrushevskaya 1979, 1984, 1986).

Nazarov initially identified spiny radiolarians as incertae sedis (Nazarov and Rudenko, 1981; Nazarov and Ormiston, 1983). Later Nazarov and Ormiston (1984, 1985, 1993) and Nazarov (1988) assigned the family Palaeoscenidiidae to the order Collodaria of the superorder Polycystina.

Kozur and Mostler (1982) subdivided the palaeoscenidians into several families and assigned them to the superfamilies Thalassothamnacea and Palaeoscenidiaceae of the suborder Entactinaria of the order Collodaria.

Dumitrica (1984) assigned the Triassic members of the families Palaeoscenidiidae and Pentactinocarpidae to the superfamily Hexastyloidea of the order Sphaerellaria.

Cheng (1986) and Tochilina (1966, 1997) assigned all spine-framed radiolarians to Nassellaria.

Amon (2000a, 2002a) placed the family Palaeoscenidiidae in the order Paleosphaerellida, incertae sedis.

Afanasieva (2000a, 2000b, 2002) assigned radiolarians with skeletons of spines and spiny frames to the order Aculearia.

However, the group of radiolarians with a simple skeleton made of crossed spines is one of the most primitive groups of early radiolarians and, possibly, the prototype of all more advanced bilaterally symmetrical and spongy spherical members, whereas the crossed spines could be a precursor of the spicule of Nassellaria and Paleozoic spherical radiolarians.

Won and Below (1999) discovered the earliest simple spiny skeletons, almost entirely lacking spinules and thorns, in the Middle Cambrian of Australia, and Won and Iams (2002) found them in the Upper Cambrian of Canada.

The youngest representatives of the most primitive spiny radiolarians were discovered by Yao and Kuwahara (1999a, 1999b, 2000) from the Lower and Middle Triassic of southern China (Guizhou and western Yunnan).

Morphology

A loose and broadly interpreted term "spiny radiolarians" is widely used by many researchers. More precisely, spiny radiolarians may be identified as taxa in

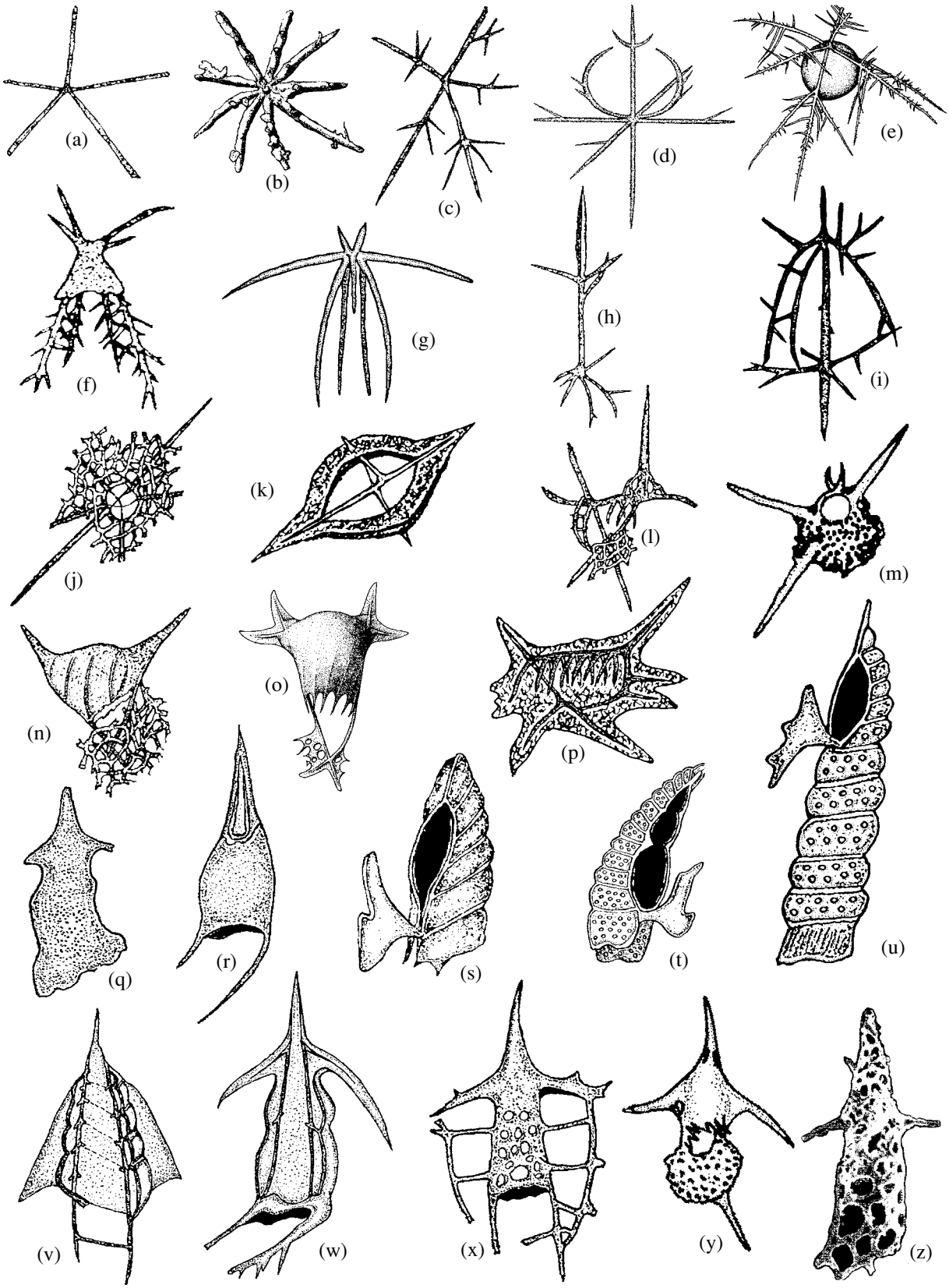
(a)
(b)
(c)
(d)
(e)
(f)
(g)
(h)
(i)
(j)
(k)
(l)
(m)
(n)
(o)
(p)
(q)
(r)
(s)
(t)
(u)
(v)
(w)
(x)
(y)
(z)

Fig. 25. Aculearia: (a–i) order Fasciculata, (j–p) order Triangulata, and (q–z) order Albaillellata: (a, b) Palacantholithidae (Cambrian–Jurassic): (a) *Palacantholithus stellatus* Deflandre, (b) *Palaeoumbraculum expandum* Amon et Braun; (c–e) Plagiacanthidae (Middle Cambrian–Recent): (c) *Palaeothalomnus antiquus* Deflandre, (d) *Nazarovites bioculus* Afanasieva, (e) *Thalassothamnus pinetum* Popofsky; (f, g) Palaeoscenidiidae (Late Cambrian–Late Triassic): (f) *Palaeoscenidium cladophorum* Deflandre, (g) *Palaeodecaradium umbelliforme* Goodbody; (h, i) Xiphocladiellidae (Ordovician–Early Permian): (h) *Xiphocladiella cuja* Deflandre, (i) *Campanulithus falcatus* Nazarov et Rudenko; (j, k) Raphidociclicidae (Middle Ordovician–Permian): (j) *Raphidociclicus hiulcus* Nazarov et Rudenko, (k) *Helenifore laticlavium* Nazarov et Ormiston; (l, m) Ceratoikiscidae (Middle Ordovician–Carboniferous): (l) *Ceratoikiscum bujugum* Foreman, (m) *Circulaforma delicata* Cheng; (n–p) Lapidopiscidae (Middle Devonian–Early Carboniferous): (n) *Lapidopiscum piveteaui* Deflandre, (o) *Holoeciscus auceps* Foreman, (p) *Neoholoeciscus cancermimus* Ormiston et Lane; (q, r) Follicucullidae (Middle Ordovician–Early Triassic): (q) *Parafollicucullus fusiformis* Holdsworth et Jones, (r) *Follicucullus ventricosus* Ormiston et Babcock; (s–u) Corythoecidae (Late Devonian–Early Permian): (s) *Corythoecia loxosegmentata* Nazarov, (t) *Camptoalatus benignus* Nazarov, (u) *Arrectoalatus cernuus* Nazarov et Ormiston; (v–z) Albaillellidae (Middle Ordovician–Permian): (v) *Albaillella pennata* Holdsworth, (w) *Haplodiacanthus anfractus* Nazarov et Rudenko, (x) *Neoalbaillella optima* Ishiga, Imoto et Kito, (y) *Protoalbaillella deflandrei* Cheng, 1986, and (z) *Etymalbaillella yennienii* Li.

the skeletons of which spines or bunches of spines intersect in one or more points (Figs. 12, 25, 26). These points or nodes are morphological centers from which the skeleton originated and grew.

If spines intersect in one node, the skeleton becomes cross-shaped or starlike. When there are three or more nodes, the skeleton is a complex spiny frame that is closed either partly or completely (Afanasieva, 2000a, 2000b, 2002c; Amon, 2002a, 2002b). In some cases two bunches of spines may be connected by a bar, which is suggestive of the fusion of two initial spicules (Figs. 11, 12, 26), and in this case two centers of spine intersections are evident. Among spiny skeletons, the heteropolar (axially symmetrical) and bilaterally symmetrical (disymetrical) skeletons prevail. Short and massive spines intersecting at one point form a skeleton resembling the initial spicule of Paleozoic spherical radiolarians and Mesozoic–Cenozoic nassellarians.

Thus, it can be assumed that the skeleton of spiny radiolarians is based on the initial four-rayed spicule, the transformation of which produces the entire range of spiny members of the class Aculearia (Figs. 12, 25–31).

(1) The earliest skeletons of Palacantholithidae Kozur et Mostler, 1981 are based on a simple initial four-rayed spicule.

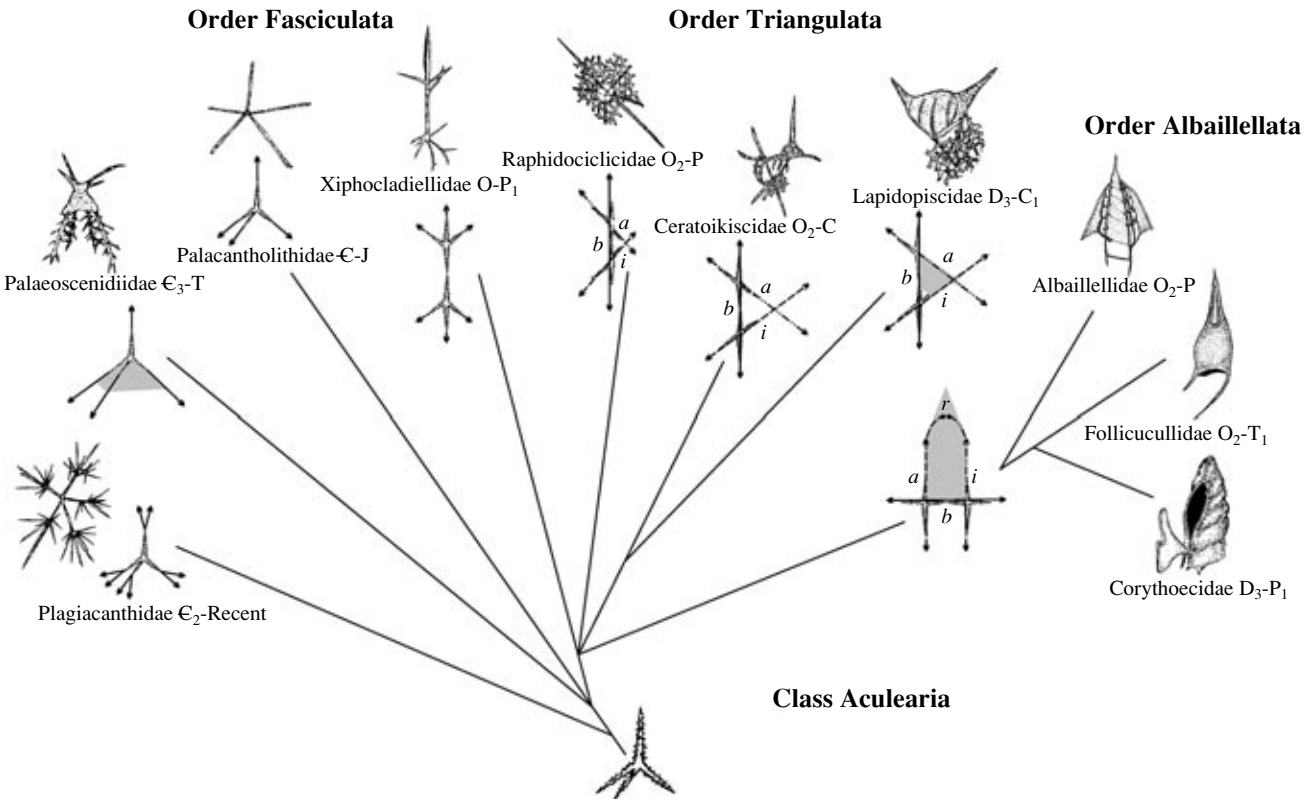

Fig. 26. Scheme of the skeleton development in spiny radiolarians of the class Aculearia. Designations: (*a*) A columella, (*b*) B columella, (*i*) intersector, and (*r*) subsagittal closure.

Plate 23

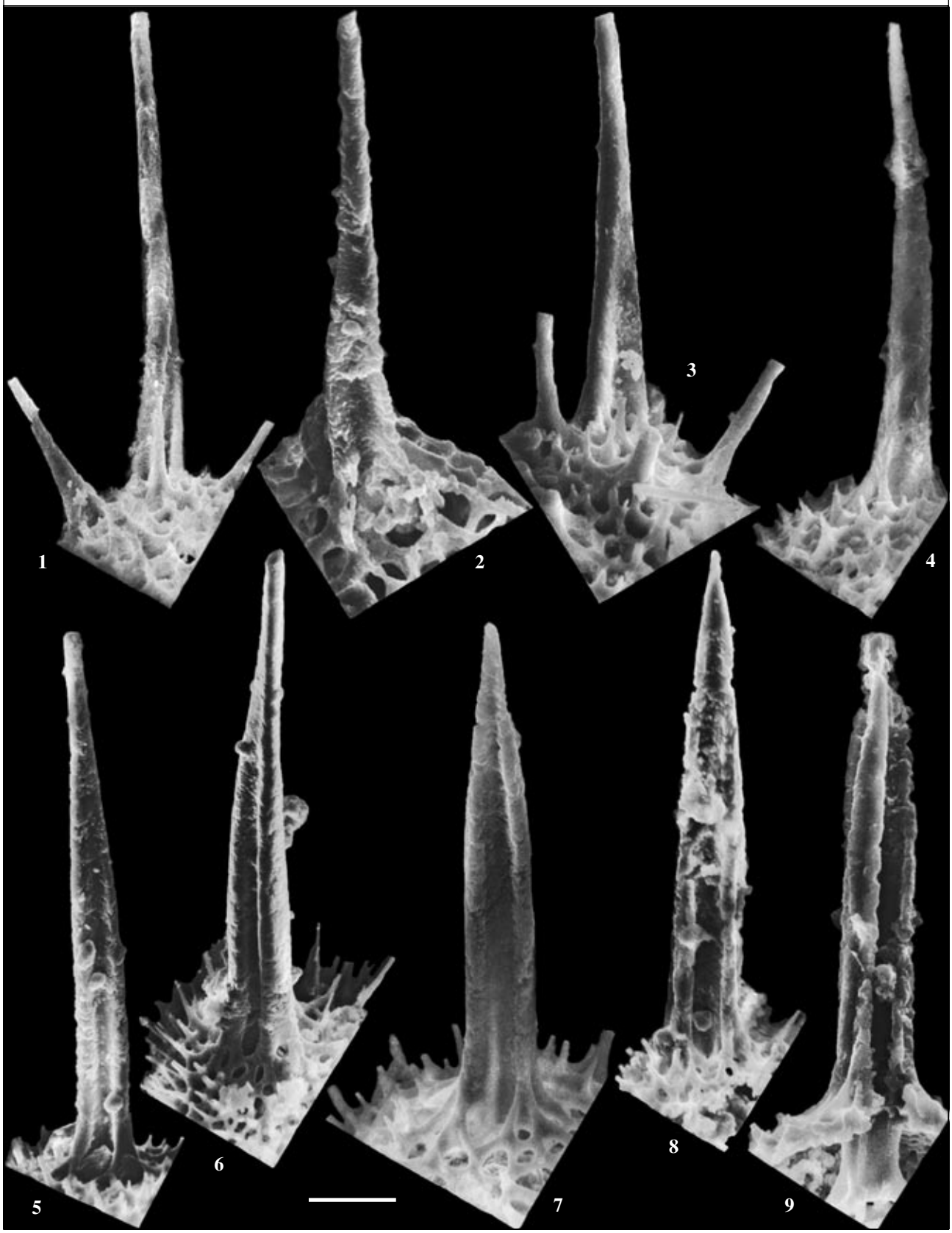

Conical (1, 2) and narrow three-bladed (3–8) main spines, with ✣-shaped, three-petalled cross section of the base in members of the subfamilies (1) Astroentactiniinae, (2) Entactiniinae, and (3–9) Bientactinosphaerinae.

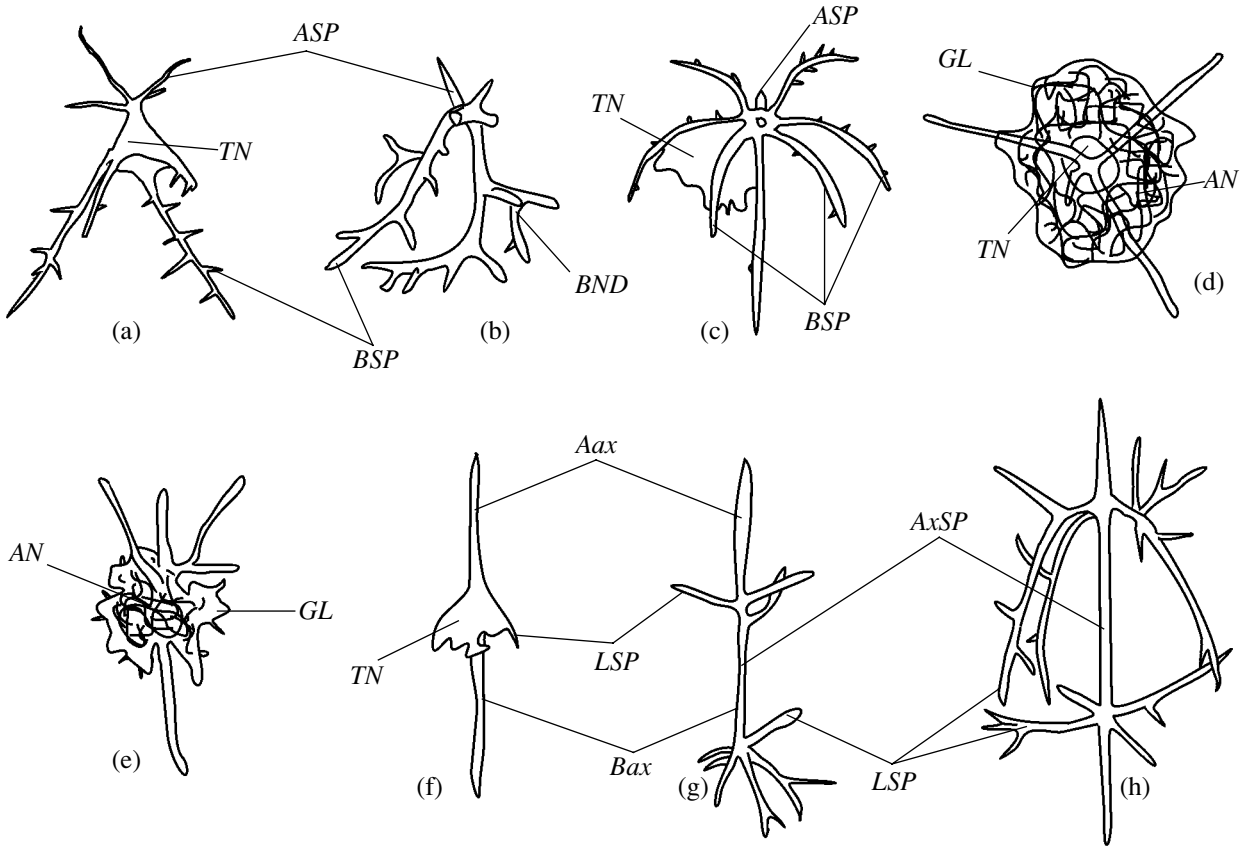

Fig. 27. Structural scheme of spiny radiolarians of the order Fasciculata: (a) *Palaeoscenidium*, (b) *Palaeoephippium*, (c) *Palaeoumbraculum*, (d) *Palaeothalomnus*, (e) *Nazarovites*, (f) *Xiphocabrium*, (g) *Xiphocladiella*, and (h) *Campanulithus* (partly after Nazarov, 1988). Designations: (*ASP*) apical spines, (*BSP*) basal spines, (*TN*) tunica, (*BND*) apophyses, (*AN*) anastomosis, (*GL*) glomerulus, (*AxSP*) axial spine, (*AAx*) apical part of the axial spine, (*Bax*) basal part of the axial spine, and (*LSP*) lateral spines.

(2) The initial four-rayed spicule, in association with spinules and apophyses, is present in Plagiacanthidae Hertwig, 1879. The tangled apophyses tend to form a globular structure, which is an intermediate link between this group and latticed and spongy forms.

(3) The initial four-rayed spicule in association with lamellar skeletal tissue that forms a pseudoshell covering the center of the intersection of the spicule's rays is characteristic of Palaeoscenidiidae Riedel, 1967, emend. Nazarov, 1981.

(4) The fusion of two initial four-rayed spicules is the basis for the development of the main axial spine in Xiphocladiellidae Nazarov, 1984, which is supplemented by the intersection of spines in two centers (apical and basal).

(5) The main triangular frame of the skeletons in the order Triangulata is produced by the fusion of two ini-

Explanation of Plate 23

Upper Devonian, Middle Frasnian Substage, Domanik Formation; Timan–Pechora Province, borehole Shuda-Yag-1003: (Figs. 1, 6–9) sample 72 (depth 71.9–72.4 m); (Figs. 2, 3) sample 68 (depth 73.3–73.5 m); (Fig. 4) sample 73 (depth 71.4–71.9 m); and (Fig. 5) sample 29 (depth 105–106 m).

Conical spines, with tripetalous cross section of the base

Fig. 1. *Astroentactinia paronae* (Hinde), scale bar = 33 μm.

Fig. 2. *Borisella pantosompha* (Foreman), bar = 17 μm.

Three-bladed spines, conical in the distal part

Fig. 3. *Radiobisphaera menneri* Afanasieva, bar = 21 μm.

Fig. 4. *Ornatoentactinia klevtsovae* Afanasieva, bar = 20 μm.

Figs. 5 and 6. *Bientactinosphaera variacanthina* (Foreman): (5) bar = 50 μm and (6) bar = 42 μm.

Narrow three-bladed spines

Fig. 7. *Bientactinosphaera grandis* (Nazarov), bar = 32 μm.

Figs. 8 and 9. *Bientactinosphaera pinica* Afanasieva: (8) bar = 33 μm and (9) bar = 23 μm.

Plate 24

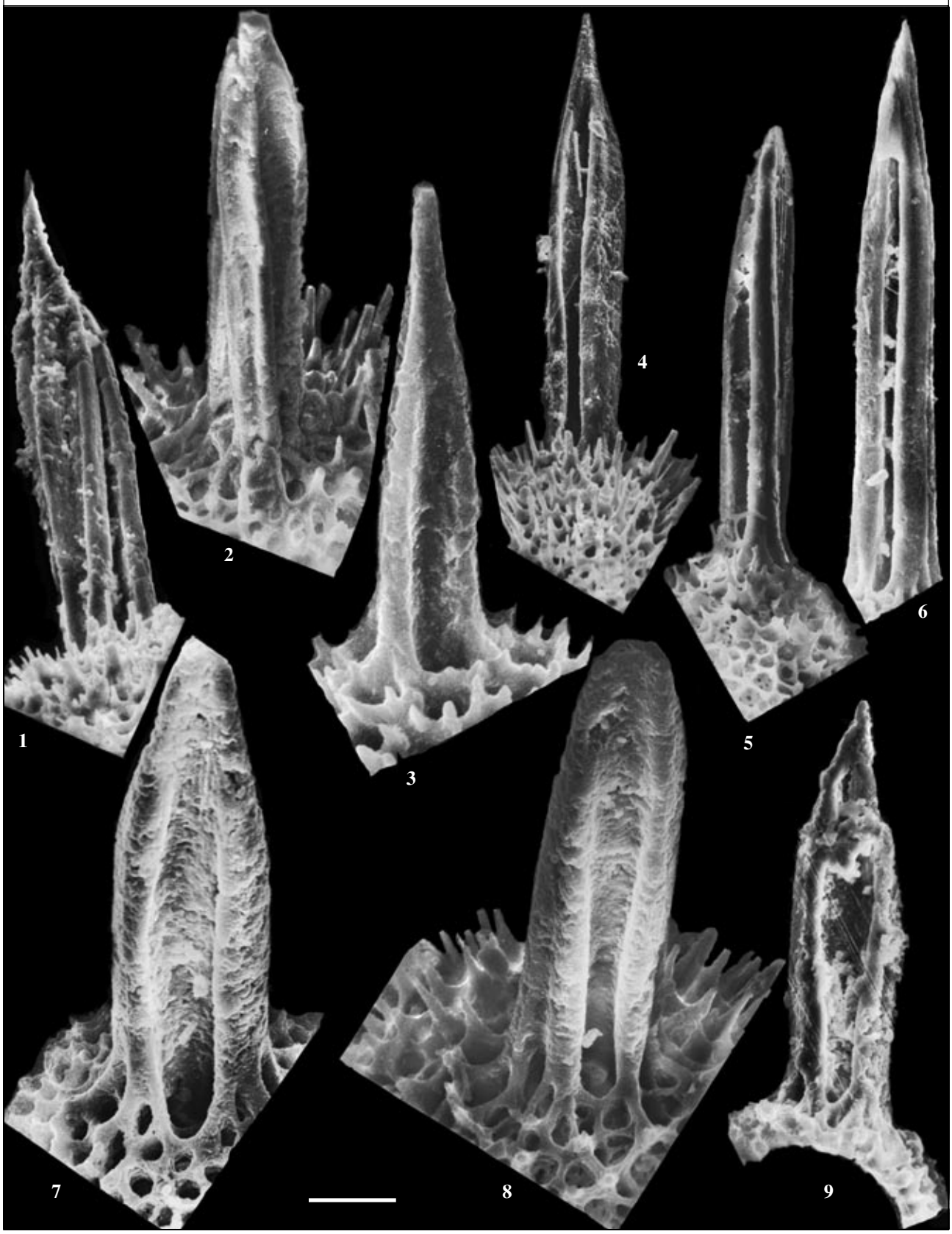

Thick (1–6) and massive (7–9) three-bladed main spines, with ✣-shaped, three-petalled cross section of the base in members of the subfamilies (1, 2, 4–6, 8, 9) Bientactinosphaerinae, (3) Astroentactiniinae, and (7) Entactiniinae.

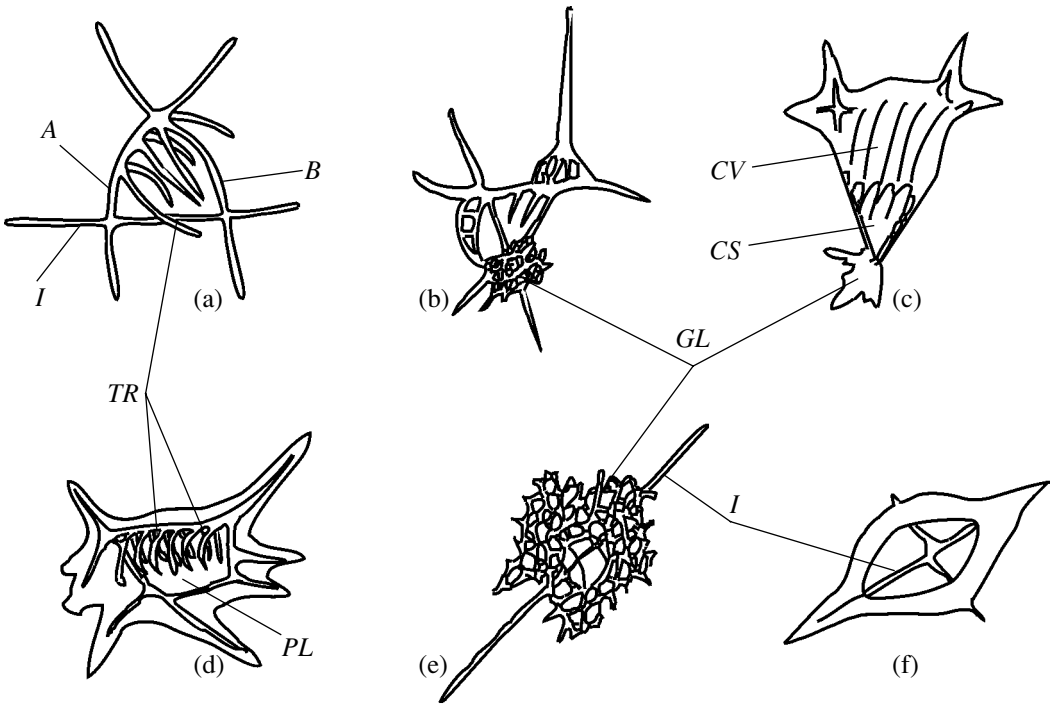

Fig. 28. Structural scheme of radiolarians of the order Triangulata: (a, b) *Ceratoikiscum*, (c) *Holoeciscus*, (d) *Neoholoeciscus*, (e) *Raphidociclicus*, and (f) *Helenifore* (partly after Nazarov, 1988). Designations: (*A*) A columella, (*B*) B columella, (*I*) intersector, (*TR*) trabecules, (*CV*) cavea, (*CS*) cusp, (*GL*) glomerulus, and (*PL*) pallium.

tial four-rayed spicules and the development of its spines *a*, *b*, and intersector (*i*) in the same plane.

(6) A fused double initial four-rayed spicule is the basic element of the skeleton in the order Albaillellata. The spines of the spicule *a*, *b*, and intersector (*i*) develop in the same plane, but with a primary **H**-shaped subparallel arrangement of spine *a* and intersector (*i*), connected by spine *b* at the base of the skeleton. In the apical part of the skeleton, spine *a* and intersector (*i*) are connected to form structure *r*, which is convergently similar to the sagittal ring of Nassellaria.

Based on the morphology of the spiny skeletons in the class Aculearia, three radiolarian groups may be recognized (Figs. 25, 26):

(1) some radiolarians have a heteropolar skeleton composed of spines intersecting in one or two centers (i.e., composed of one or two fascicles of spines connected by a median bar): the order Fasciculata Afanasieva et Amon, 2003 (the name of the order is derived from the Latin *fasciculus* (a bundle) (Figs. 25a–25i, 26, 27);

(2) in other radiolarians, connected spines form a triangular frame: the order Triangulata Afanasieva et Amon, 2003 (the name of the order is derived from the Latin *triangulum* (triangle) (Figs. 25j–25p, 26, 28);

(3) in other radiolarians, two long columellae connected below the aperture by a horizontal beam form an **H**-frame in the basal part of the skeleton and a subsagittal structure *r* in the apical region: the order Albaillellata Deflandre, 1953, emend. Afanasieva et Amon, 2003 (Figs. 25q–25z, 26, 29).

Explanation of Plate 24

Upper Devonian, Middle Frasnian Substage, Domanik Formation; Timan–Pechora Province: (Figs. 1–4, 6, 8, 9) borehole Shuda-Yag-1003: (1, 2) sample 29 (depth 105–106 m); (3, 4) sample 72 (depth 71.9–72.4 m); (6, 8) sample 68 (depth 73.3–73.5 m); and (9) sample 78 (depth 68.4–69.3 m); (Fig. 5) borehole Ukhtinskaya-3B, sample 114 (depth 104.2–104.7 m); and (Fig. 7) Ukhta River, sampling point no. 4, sample V-29.

Fig. 1. *Ornatoentactinia spinisica* Afanasieva, scale bar = 37 μm.

Fig. 2. *Bientactinosphaera grandis* (Nazarov), bar = 20 μm.

Fig. 3. *Moskovistella baccata* Afanasieva, bar = 15 μm.

Fig. 4. *Bientactinosphaera variacanthina* (Foreman), bar = 42 μm.

Fig. 5. *Ornatoentactinia spartaci* Afanasieva, bar = 37 μm.

Fig. 6. *Radiobisphaera menneri* Afanasieva, bar = 33 μm.

Fig. 7. *Entactinia herculea* Foreman, bar = 20 μm.

Fig. 8. *Ornatoentactinia agarkovi* Afanasieva, bar = 20 μm.

Fig. 9. *Bientactinosphaera guangxiensis* (Li et Wang), bar = 33 μm.

Plate 25

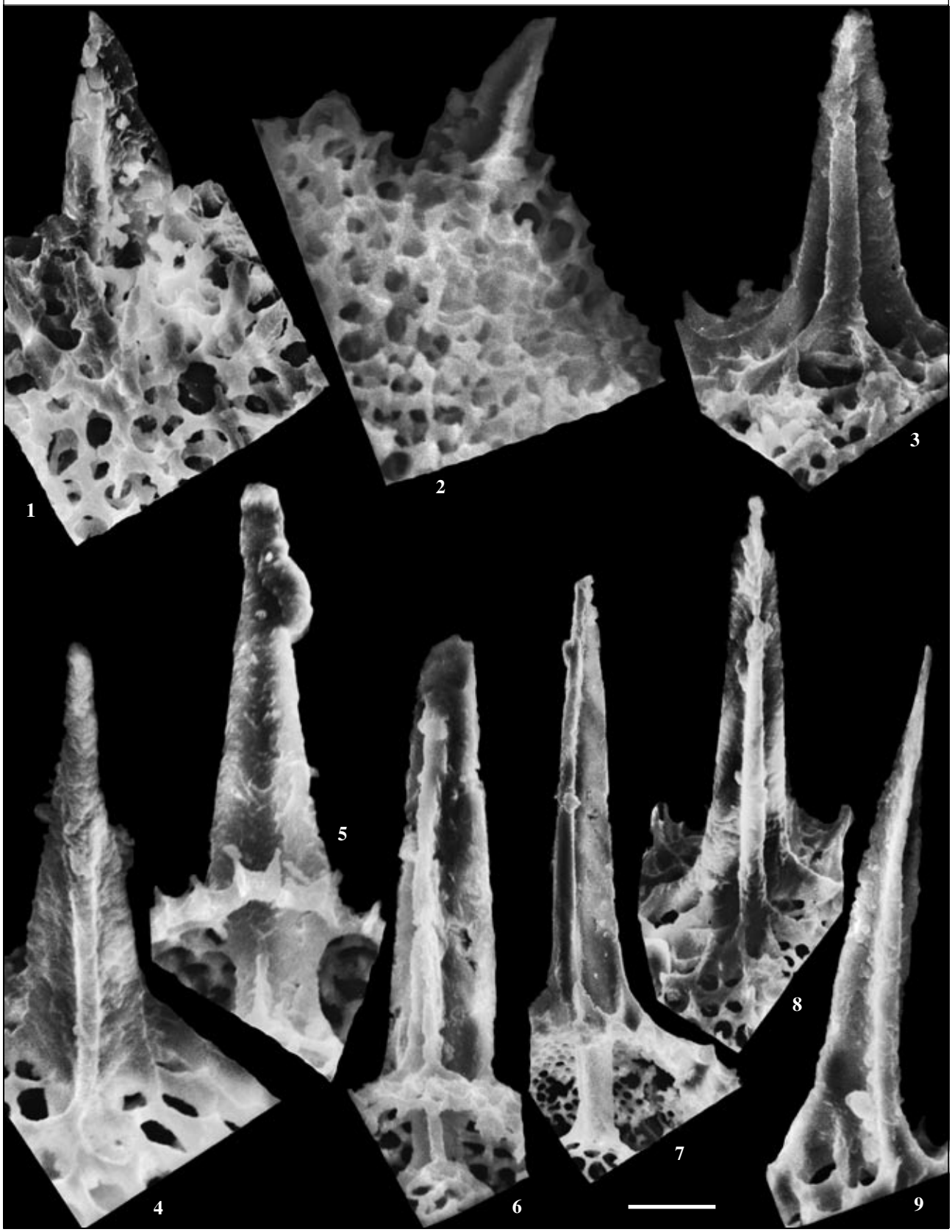

Three-bladed main spines, with **Y**-shaped cross section in members of the subfamilies (1) Pluristratoentactiniinae, (2) Spongopolyentactiniinae, (3–7) Bientactinosphaerinae, and (8, 9) Astroentactiniinae.

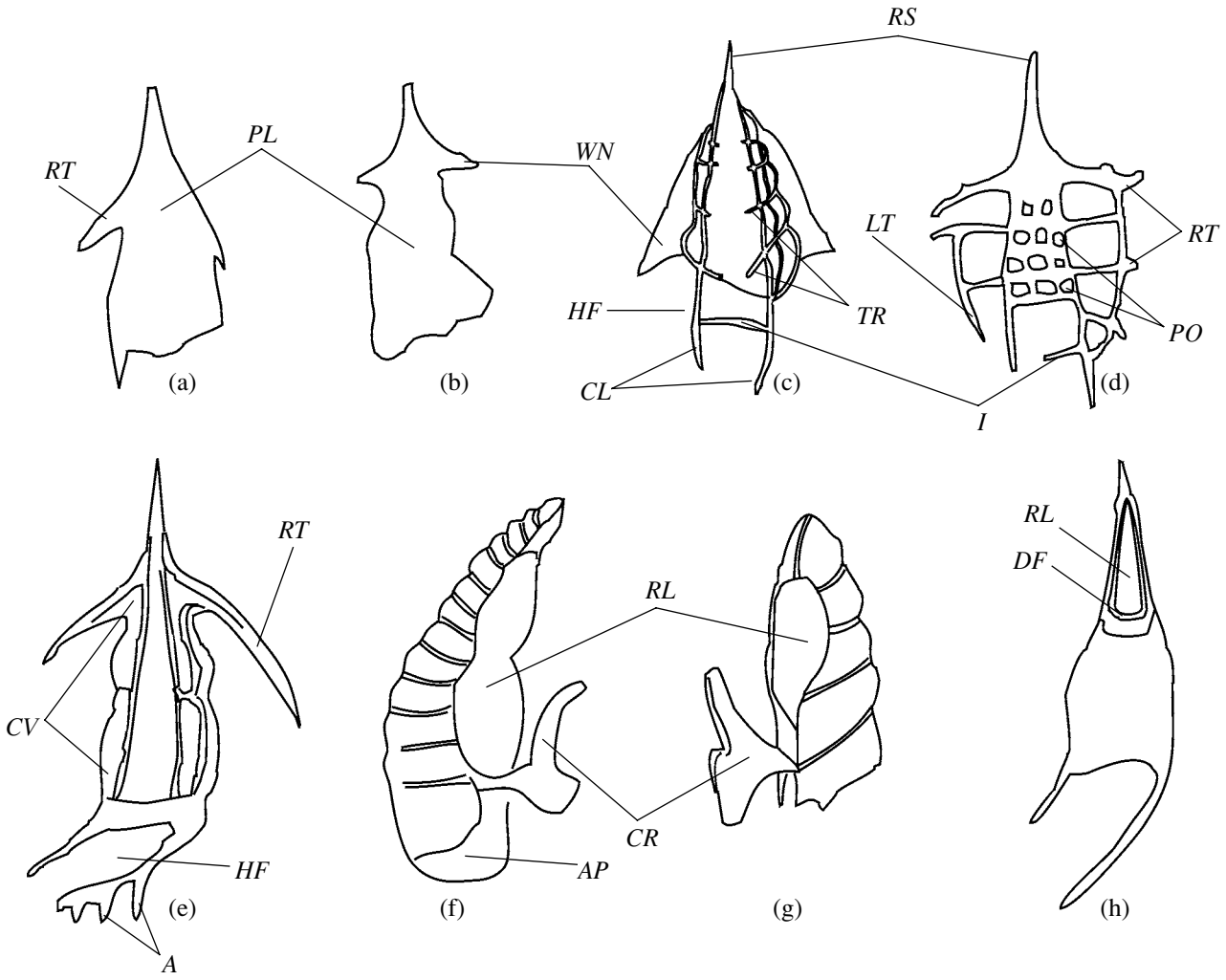

Fig. 29. Structural scheme of conical radiolarians of the order Albaillellata: (a) *Pseudoalbaillella*, (b) *Parafollicucullus*, (c) *Albaillella*, (d) *Neoalbaillella*, (e) *Haplodiacanthus*, (f) *Camptoalatus*, (g) *Corythoecia*, (h) *Follicucullus* (partly after Nazarov, 1988). Designations: (*CR*) crystule, (*CL*) columellae, (*TR*) trabecules, (*I*) intersector, (*PL*) pallium, (*WN*) wing, (*PO*) pores, (*RT*) rostrellumi, (*A*) apophyses, (*LT*) vertical bar, (*HF*) H framework, (*CV*) cavea, (*DF*) D framework, (*RL*) rimule, (*AP*) aperture, and (*RS*) rostrum.

Development and Spatial Orientation of the Skeleton during the Organism's Life

In the heteropolar skeletons of spiny radiolarians, the test is quite clearly subdivided into the apical and basal parts. In many groups of aculearians, the apex and base are determined conventionally, because their true position is not known.

Foreman (1963) and Holdsworth (1969) suggested that Albaillellaria are related to spiny Ceratoikiscidae,

Explanation of Plate 25

Upper Devonian, Middle Frasnian Substage, Domanik Formation; Timan–Pechora Province: (Figs. 1–3, 5–9) borehole Shuda-Yag-1003: (1, 8) sample 73 (depth 71.4–71.9 m); (2, 5) sample 8 (depth 120.9–124 m); (3) sample 69 (depth 73–73.3 m); (6) sample 56 (depth 81.6–83 m); (7) sample 68 (depth 73.3–73.5 m); and (9) sample 34 (depth 104.1–104.6 m); and (Fig. 4) borehole Ukhtinskaya-3B, sample 114 (depth 104.2–104.7 m).

Fig. 1. *Meschedea crassicortex* Won, scale bar = 15 μm.

Fig. 2. *Spongentactinella veles* (Foreman), bar = 15 μm.

Fig. 3. *Ornatoentactinia solita* Afanasieva, bar = 15 μm.

Figs. 4 and 5. *Bientactinosphaera morozovi* Afanasieva: (4) bar = 9 μm and (5) bar = 12 μm.

Fig. 6. *Bientactinosphaera symphypora* (Foreman), bar = 20 μm.

Fig. 7. *Bientactinosphaera miletenkoi* Afanasieva, bar = 27 μm.

Fig. 8. *Moskovistella lucet* Afanasieva, bar = 18 μm.

Fig. 9. *Moskovistella octoradiata* Afanasieva, bar = 18 μm.

Plate 26

Three-bladed main spines in members of the subfamilies (1) Entactiniinae, (2, 3, 10, 11) Bientactinosphaerinae, (4, 5, 7) Astroentactiniinae, (6) Pseudorotasphaerinae, (8) Helioentactiniinae, and (9, 12, 13) Spongopolyentactiniinae.

the triangular-framed skeleton of which is composed of three intersected spines, often surrounded by the spongy or reticular skeletal tissue (patagium, or pseudopatagium). They noted that the conical test of Albaillellidae was produced by the further development and reduction of some parts of spines of Ceratoikiscidae, i.e., the development of the skeletal tissue on the spines and caveal ribs leads to the bilateral subconical test with an open aperture in the basal region and two columellae that are connected by two beams below the aperture. They assumed that the columellae are spine *a* and intersector (*i*), whereas the transverse bar is spine *b*, and the trabeculae are caveal ribs. If this were the case, the resulting skeleton "would be tilted (lying on its side)" contradicting the original *Holoeciscus* and *Lapidopiscum*.

This change in the orientation of the skeleton supports the hypothesis that the bilateral or monoaxonic symmetry of many taxa was most likely produced in the situation when radiolarians with the test open on one end, as in classical Albaillellidae, "lay on the bottom and, thus, the top–bottom spatial direction was very important for their mode of life" (Petrushevskaya, 1984, p. 125).

Beklemishev (1964) discussed various types of symmetry in protozoans and other invertebrates and noted that the monoaxonic-heteropolar symmetry may arise any time in situations when different ends of the body experienced different impacts of the environment, resulting in these ends functioning differently in response to the environment. Most often such a shape appears when one end of the body is attached to the substrate, while the other is free. The same type of symmetry is found in organisms living in streams.

It is possible that the conical test resulted from an adaptation to life in a stream. It is known that the symmetry of a water medium in the state of rest is a symmetry of a regular sphere with $\infty L_\infty \infty PC$, while a gravity field at every point has the symmetry of a cone $L_\infty \infty P$. Vertical motion in the gravity field has a symmetry of one of the subgroups of the cones' symmetry of $L_n nP$ type. The motion of the water flow (stream) also has symmetry of one of subgroups of cone symmetry (Shafranovsky, 1968; Dmitriev and Potapova, 1971). If radiolarians existed in the water stream (in horizontal oceanic currents, vertical upwelling zones, horizontal and vertical daily and seasonal convectional flows or bottom currents, etc.), the moving water put pressure on the radiolarians, with the result that the skeleton gradually acquired a predominantly cone symmetry.

There is also a possibility of simply convergent similarity of highly specialized Albaillellata with members of the family Lapidopiscidae (*Holoeciscus* and *Lapidopiscum*) (Petrushevskaya, 1986). In addition, it can be assumed that in this case we observe the effect of the rule of Vavilov's homological rows in the hereditary variability, according to which, families have certain cycles of variability observed in all their genera (Nazarov and Petrushevskaya, 1995). In the lineage of the family Ceratoikiscidae, the primitive skeleton of three spines intersected as a triangle transformed into a pseudotest. In the Albaillellata lineage, the first members are not known, although the whole lineage shows similar trends of specialization toward the development of the most complex symmetry of the bilateral skeleton. Patterns of the evolution of higher taxa (considered as system groups) can also be traced, although not completely.

It is possible that the descendents of Albaillellidae exist among extant radiolarians. These may be extant species of the genus *Cornutella*. Therefore, it is possible that one of the lineages of Mesozoic–Cenozoic Nassellaria (Acropyramididae Haeckel, 1881) evolved from the Paleozoic Albaillellidae (Petrushevskaya,

Explanation of Plate 26

Upper Devonian; Timan–Pechora Province: (Figs. 1, 2, 4–13) Middle Frasnian Substage, Domanik Formation, borehole Shuda-Yag-1003: (1, 2, 8, 11) sample 73 (depth 71.4–71.9 m); (4, 6, 13) sample 29 (depth 105–106 m); (5, 9, 10, 12) sample 72 (depth 71.9–72.4 m); and (7) sample 8 (depth 120.9–124 m); and (Fig. 3) Famennian Stage, borehole Zapadnaya Lekkeyaginskaya-65, sample 86g (depth 2460–2467 m).

Spines with a Y-shaped cross section at the base and petaloid sides

Fig. 1. *Entactinia paula* Foreman, scale bar = 37 μm.

Fig. 2. *Bientactinosphaera variacanthina* (Foreman), bar = 42 μm.

Fig. 3. *Bientactinosphaera spinofoliacea* Nazarov et Afanasieva, bar = 67 μm.

Spines with apophyses

Figs. 4 and 5. *Moskovistella victorialis* Afanasieva, sp. nov.: (4) bar = 15 μm and (5) bar = 15 μm.

Spines with a Y-shaped cross section at the base and narrow, saber-shaped sides

Fig. 6. *Russirad kazintsovae* Afanasieva, bar = 15 μm.

Spines twisted (7–11) dextrally and (12, 13) sinisterly

Fig. 7. *Astroentactinia paronae* (Hinde), bar = 56 μm.

Fig. 8. *Helioentactinia unimana* (Nazarov), bar = 33 μm.

Fig. 9. *Spongentactinella corynacantha* Nazarov et Ormiston, bar = 27 μm.

Fig. 10. *Bientactinosphaera pinica* Afanasieva, bar = 33 μm.

Fig. 11. *Radiobisphaera menneri* Afanasieva, bar = 37 μm.

Figs. 12 and 13. *Spongentactinella olafi* Afanasieva, sp. nov.: (12) bar = 67 μm; and (13) bar = 32 μm.

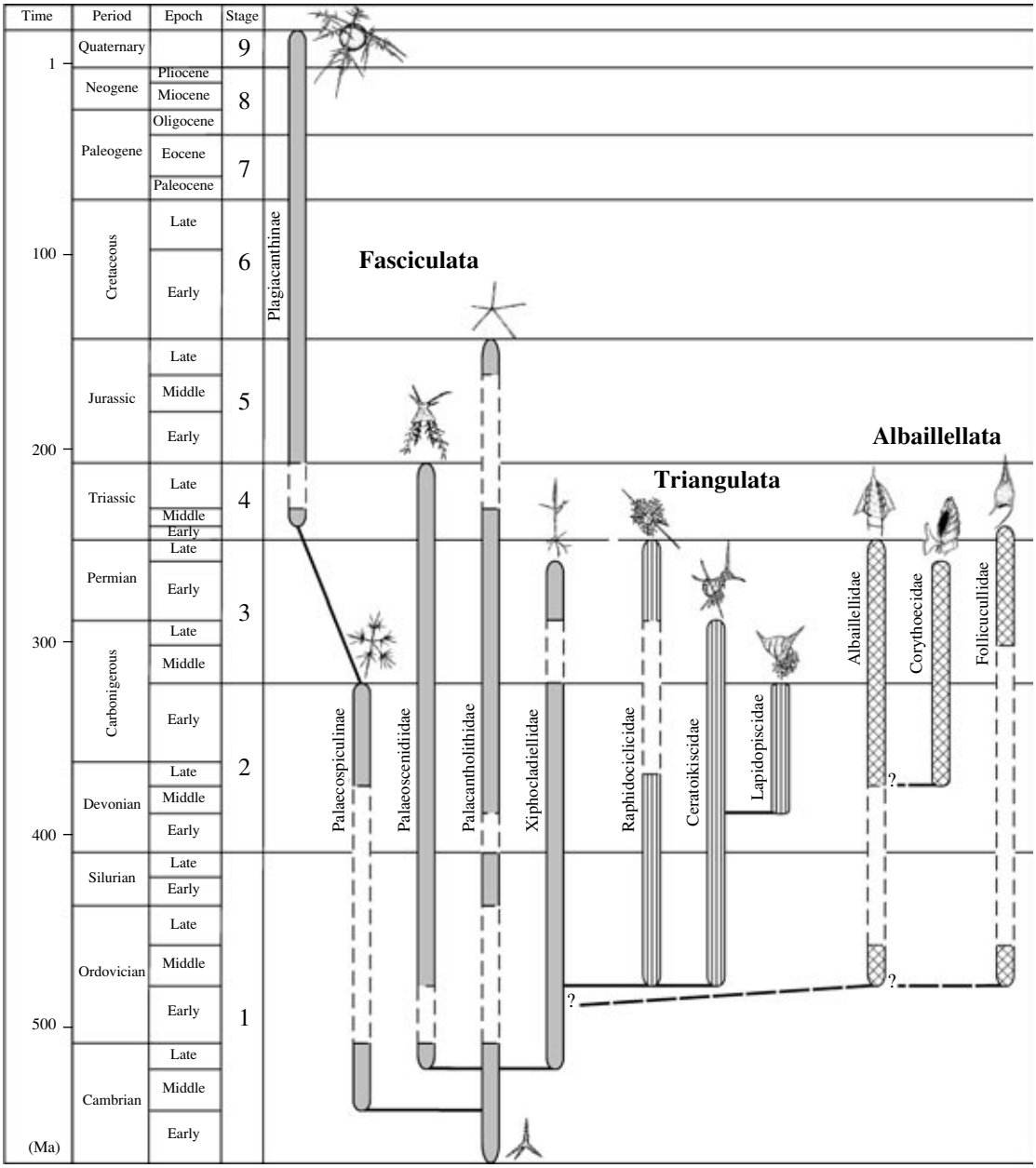

Fig. 30. Phylogenetic tree of the class Aculearia.

Fig. 31. Spumellaria: (a) order Echidninata, (b–j) order Spongiata, (k, l) order Saturnalata, (m–o) order Prodigiata, (p–w) order Cancelliata, and (x–z) order Capsulata: (a) Echidninidae (Middle–Late Cambrian): *Echidnina curvata* Won et Iams; (b–g) Spongopolyentactiniidae (Middle–Late Cambrian–Permian): (b) *Spongentactinella windyanensis* Nazarov, (c) *Multientactinia* sp., (d) *Somphoentactinia somphozona* (Foreman), (e) *Spongosphaera* sp., (f) *Provisocyntra amplissima* Nazarov et Ormiston, (g) Conocaryommidae (Late Permian–Eocene): *Conocaryomma aralensis* Lipman; (h–j) Spongentactiniidae (Middle–Late Cambrian–Permian): (h) *Retentactinia* sp., (i) *Pluristratoentactinia conspissata* Nazarov, 1981, (j) *Spongentactinia* sp.; (k) Oertlispongidae (Middle–Late Triassic): *Spongoserrula rarauana* Dumitrica; (l) Saturnalidae (Late Triassic–Recent): *Pseudoheliodiscus radiosus* De Wever; (m) Eptingiidae (Middle Triassic–Late Jurassic): *Eptingium manfredi* Dumitrica; (n, o) Multiarcusellidae (Middle–Late Triassic): (n) *Austrisaturnalis quadriradiatu*s Kozur et Mostler, (o) *Multiarcusella* sp.; (p) Polyentactiniidae (Middle Ordovician–Cretaceous): *Polyentactinia zhamoidai* Afanasieva; (q) Orosphaeridae (Cretaceous–Recent): *Oropelex pagoda* Friend et Riedel; (r–v) Haplentactiniidae (Middle Cambrian–Early Permian): (r) *Haplentactinia armillata* Nazarov, (s) *Secuicollacta cassa* Nazarov et Ormiston, (t) *Wonella* sp., (u) *Pseudorotasphaera* sp., (v) *Haplotaeniatum tegimentum* Nazarov et Ormiston; (w) Pentactinocarpidae (Middle–Late Triassic): *Pentactinocarpus tetracanthus* Dumitrica; (x) Centrocubidae (Middle Triassic–Recent): *Stauropylissa spongoidalis* Dumitrica; (y) Quinquecapsulariidae (Early Jurassic–Recent): *Quinquecapsularia spinosa* Pessagno; and (z) Rhizosphaeridae (Late Jurassic–Recent): *Haliomma* sp.

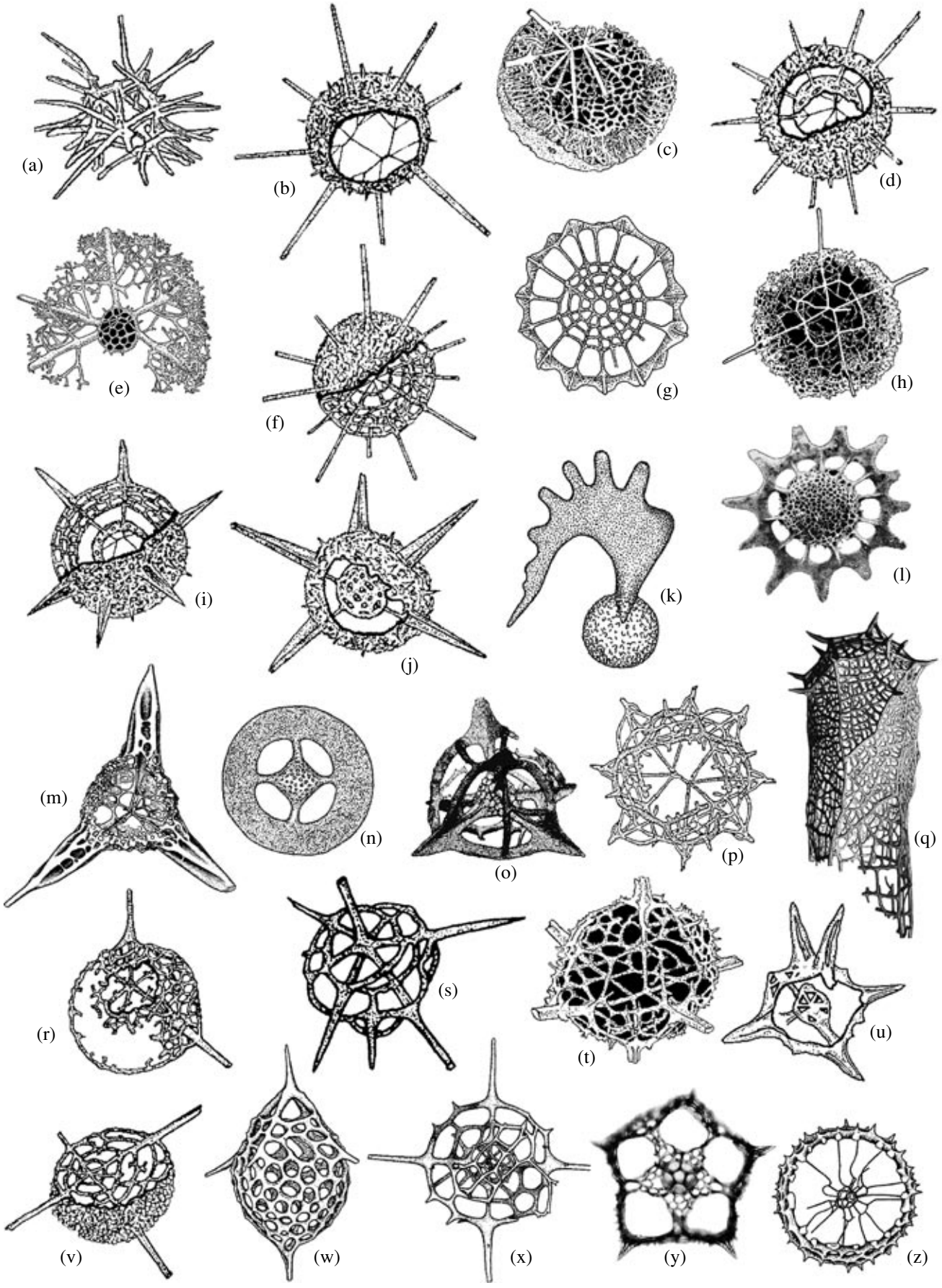
(a)
(b)
(c)
(d)
(e)
(f)
(g)
(h)
(i)
(j)
(k)
(l)
(m)
(n)
(o)
(p)
(q)
(r)
(s)
(t)
(u)
(v)
(w)
(x)
(y)
(z)

Plate 27

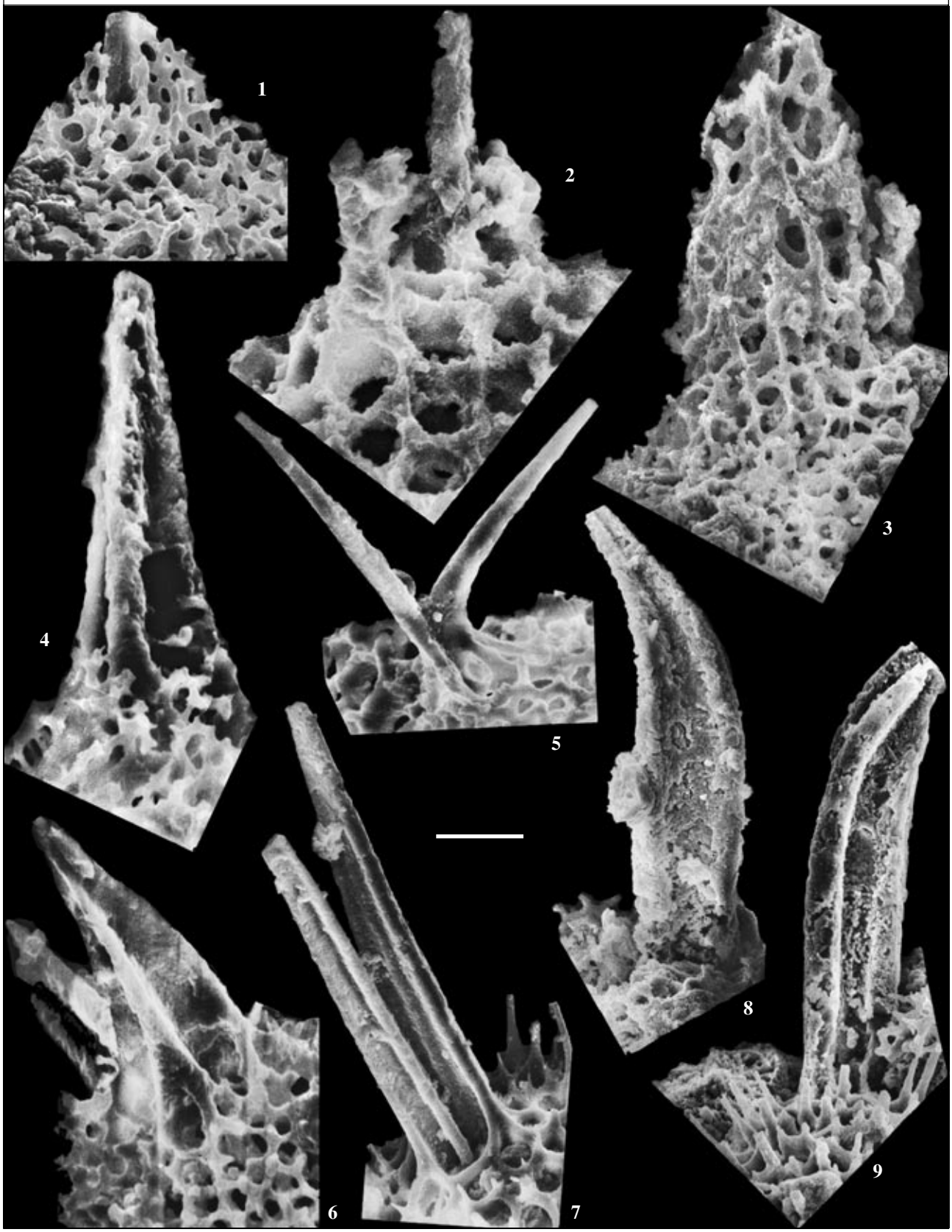

The main spines in members of the subfamilies (1) Somphoentactiniinae, (2, 7) Entactiniinae, (3) Spongentactiniinae, (4–6) Astroentactiniinae, and (8, 9) Thecentactiniinae.

1984, 1986; Afanasieva and Vishnevskaya, 1993; Afanasieva, 2000a, 2000b).

Major Features of Evolution

The history of the evolution of the class Aculearia embraces the whole of the Paleozoic, from the Early Cambrian, and the larger portion of the Mesozoic (Early–Middle Triassic and Late Jurassic), which is almost 400 mya (Fig. 30). All orders of spiny radiolarians appeared almost simultaneously in the Early Paleozoic at the first stage of the evolution of Radiolaria (Afanasieva *et al.*, 2004) (Fig. 23).

The analysis of the early evolution of the higher taxa of the class Aculearia suggests evolution in three separate lineages (Fig. 26). Three orders of Aculearia appeared very early, apparently in the Middle Cambrian, from the same ancestor with a four-rayed spicule (Figs. 24, 26, 30), and later evolved independently of each other.

Order Fasciculata. The earliest spiny radiolarians of the order Fasciculata from the Middle–Upper Cambrian already had well-developed skeletal structures (Figs. 24, 25a–25i, 26, 27). The most primitive Fasciculata with straight, non-branched spines-rays (Palacantholithidae) appeared in the Early Cambrian, whereas quite complex spiculate forms with branching and whorls (Palaeospiculinae) appeared in the Middle Cambrian. Skeletal constructions became more complex for the first time in the Late Cambrian. Pseudotests (Palaeoscenidiidae) appeared, as did skeletons consisting of a single massive main spine formed by the fusion of two primary four-rayed spicules (Xiphocladiellidae). Only Palaeoscenidiidae evolved without interruption, while the lineages of Plagiacanthidae, Palacantholithidae, and Xiphocladiellidae had long gaps in the record (Fig. 30).

At the same time Fasciculata are the longest surviving taxa of spiny radiolarians, whose evolution began in the Early Cambrian and continues up to now. Several representatives of the families Palaeoscenidiidae and Palacantholithidae crossed the crucial Permian–Triassic boundary and survived for some time, being found in the Lower Triassic of Japan (Sashida, 1983), in the uppermost Middle Triassic–beginning of the Upper Triassic of Italy and Romania (Dumitrica, 1978, 1982). Palacantholithidae completed their evolution in the Early Tithonian (Late Jurassic of southern Germany) (Dumitrica and Zugel, 2003). Plagiacanthinae are apparently direct descendants of Palaeospiculinae. They appeared in the Middle Triassic and survived until now (Fig. 30).

Order Triangulata. The oldest representatives of this order are known from the Middle Ordovician. They existed for about 230 mya and became extinct at the end of the Permian (Figs. 25j–25p, 30).

A long gap in the lineage of the family Raphidociclicidae is observed from the Famennian (Upper Devonian) to the end of the Carboniferous, i.e., ca. 80 mya. No interruptions are observed in the evolution of the family Ceratoikiscidae. More so, in the Middle Devonian, this family gave rise to a new, very unusual, although short-lived (Middle Devonian–Early Carboniferous) family, Lapidopiscidae. Similar to the Palaeoscenidiidae, the evolution of this group shows a trend toward the development of a pseudotest (Figs. 26, 28). Taking into account the data of Umeda (1998) on the simultaneous development of the lattice and lamellar tissue (the latter forms a lamellar patagium) in the species of the genus *Glanta*, it is possible to agree with Umeda's hypothesis that *Glanta* was an intermediate genus between Ceratoikiscidae and Lapidopiscidae. This transition took place at the Eifelian–Emsian boundary following the phylogenetic lineage *Ceratoikiscum—Glanta—Protoholoeciscus—Holoeciscus* (Umeda, 1998, p. 106). Previously Aitchison (1993) suggested that the evolutionary transition was shorter *Ceratoikiscum—Protoholoeciscus—Holoeciscus*.

Order Albaillellata. A peculiar group, the only one with bilateral symmetry (Figs. 25q–25z, 26; 29), which mysteriously appeared in the Middle Ordovician and completely disappeared in the Early Triassic (Fig. 30).

Explanation of Plate 27

Upper Devonian; Timan–Pechora Province: (Figs. 1, 3, 8, 9) Famennian Stage; borehole Zapadnaya Lekkeyaginskaya-65, sample 86g (depth 2460–2467 m); and (Figs. 2, 4–7) Middle Frasnian Substage, Domanik Formation; (2) borehole Ukhtinskaya-3B, sample 158 (depth 69.6–70.4 m); (4, 6, 7) borehole Shuda-Yag-1003: (4) sample 56 (depth 81.6–83 m), (6) sample 65 (depth 75–77.3 m), and (7) sample 34 (depth 104.1–104.6 m); and (5) Lyajol River, outcrop 1904, sample 6.

Spines overgrown by skeletal tissue of the external shell

Fig. 1. *Adamas cathedrarius* Afanasieva, scale bar = 27 μm.

Fig. 2. *Borisella invisitata* Afanasieva, bar = 15 μm.

Fig. 3. *Tetrentactinia barysphaera* Foreman, bar = 27 μm.

Fig. 4. *Moskovistella sincera* Afanasieva, bar = 15 μm.

Double spines

Fig. 5. *Moskovistella deorsiaca* (Nazarov et Ormiston), bar = 20 μm.

Fig. 6. *Moskovistella mira* Afanasieva, bar = 15 μm.

Fig. 7. *Entactinia bifida* Afanasieva, bar = 33 μm.

Curved spines

Figs. 8 and 9. *Duplexia spinocurva* Afanasieva: (8) bar = 37 μm and (9) bar = 37 μm.

Plate 28

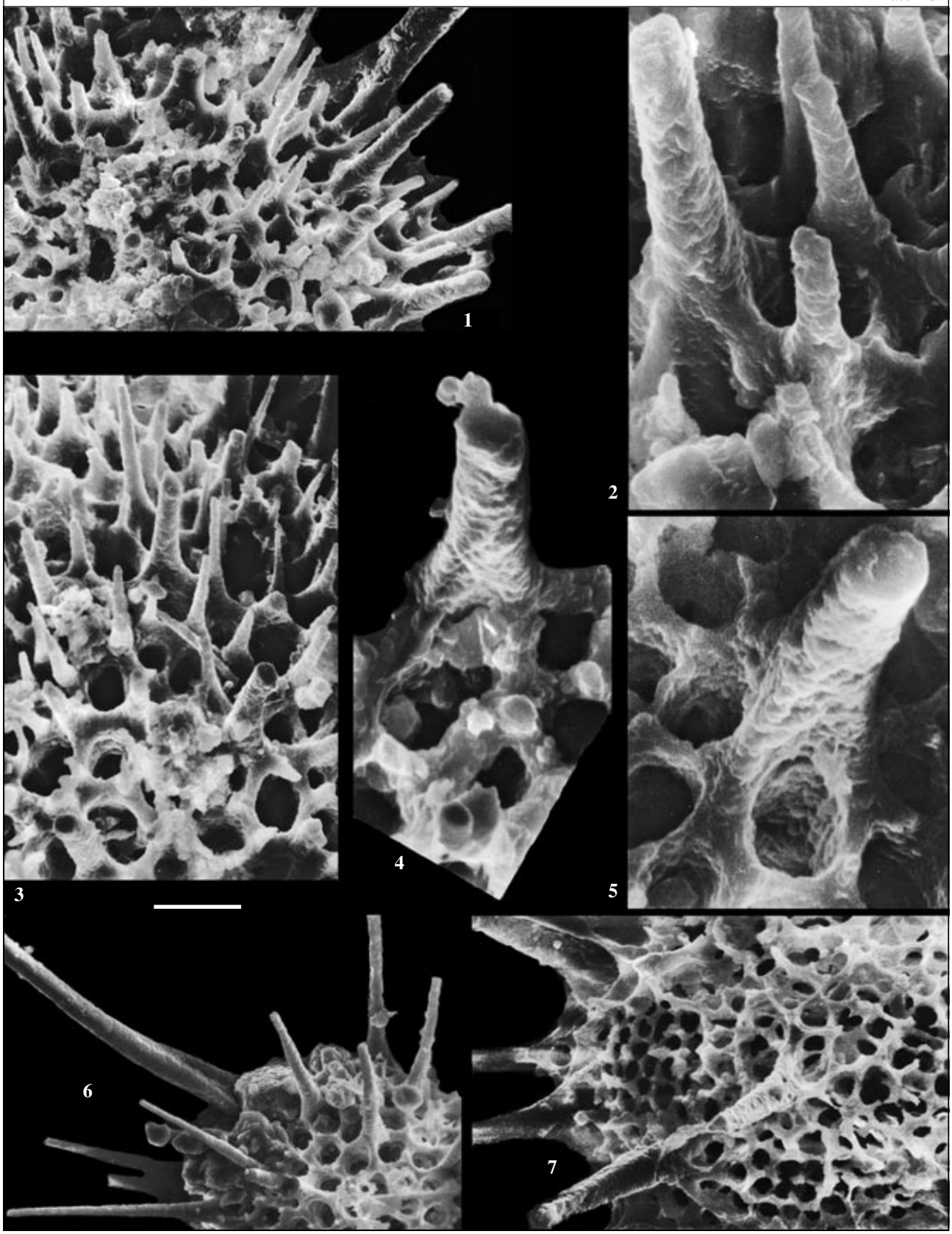

By-spines in members of the subfamilies (1–5) Bientactinosphaerinae, (6) Entactiniinae, and (7) Astroentactiniinae.

However, there is a large gap in the evolution of this radiolarian order, which embraces a long interval (Late Ordovician–Devonian) (95 mya), i.e. almost 40% of the total duration of the order Albaillellata. In addition, the new family Corythoecidae appeared in the Famennian (Late Devonian). The youngest members of the genus *Follicucullus* of the order Albaillellata are found in the Lower Triassic of Primorye (Russian Far East) (Bragin *et al.*, 1999; Bragin, 2002). Only one of 11 Albaillellata genera survived the great Permian–Triassic extinction, the geocratic epoch including almost all of the Late Permian and Triassic. This was the last representative of this order, after which Albaillellata disappeared forever from the fossil record (Fig. 30).

SPONGY SPHERICAL RADIOLARIA

Up to the present day, the position of spherical radiolarians with spongy, cellular, and lattice skeletons (Fig. 31) in the classification of Radiolaria is debatable. The Early Paleozoic radiolarians with lattice shells (families Secuicollactidae, Rotasphaeridae, Pseudorotasphaeridae, Haplentactiniidae, and Ehidninidae) are often included along with spongy and porous radiolarians in the order Spumellaria (Nazarov and Ormiston, 1984, 1993; Nazarov, 1988; Noble, 1994; Kozur *et al.*, 1996). Radiolarians with a reticular shell (Polyentactiniidae) were assigned to the order Collodaria (Nazarov and Ormiston, 1984, 1993; Nazarov, 1988).

Kozur and Mostler (1982) described the suborder Entactinaria Kozur et Mostler, 1982, which included all Polycystina and many Collodaria that have one well-developed spicule, irrespective of the degree of the development of tangential structures.

De Wever *et al.* (2001) include in the order Entactinaria distantly related radiolarian taxa: spherical spongy Spumellaria and porous varieties of Sphaerellaria, a few Stauraxonaria, some spiny Aculearia, and even some radiolarians with a pylome from the order Pylomariata.

As early as 1986 Petrushevskaya (1986) criticized the concept of Entactinaria. One of the main objections against the acceptance of Entactinaria concerned existing data on the considerable difference in the structure of the nucleus, nucleoaxopodial apparatus, and central capsule (Fig. 1) in completely different taxa that were supposed to be united in the Entactinaria. She wrote that "ignoring these pathophysiological data is a step backwards in the study of these Radiolaria" (Petrushevskaya, 1986, p. 122).

De Wever *et al.* (2001) somewhat oversimplified interpretation of the nucleoaxopodial apparatus and central capsule. These authors suggested that the periaxoplastic type of the nucleoaxopodial complex is typical only of the order Entactinaria (De Wever *et al.*, 2001, text-fig. 7A). However, it is not possible to reveal the details of the nucleoaxopodial complex in fossil radiolarians because it is simply not preserved in fossils.

Dumitrica *et al.* (2000) proposed a new approach to the classification of early radiolarians with a lattice skeleton from the Upper Cambrian–Silurian by assigning them and spiny radiolarians to a new order, Archaeospicularia.

Spongy radiolarians (Fig. 31) have one of the most complicated constructions of the skeleton, which is composed of three basic elements: (1) initial spicule or microsphere; (2) lattice polyhedron, (3) one, two, or more spongy, latticed, or reticular outer spherical or spheroid shells. It is easy to observe that the spongy radiolarians differ from the spiny radiolarians (aculearians) in the obligatory presence of the two latter elements.

A spicule is an inner initial structure (Fig. 10), morphological center of the skeleton, appearing as a *n*-rayed figure (*n* ranges from 4 to 24), formed by one initial four-rayed spicule or by a fusion of two initial four-rayed spicules (Figs. 12, 32). The initial spicule most often occurs inside the sphere in its center, but sometimes the spicule is eccentric. The microsphere develops on the continuations of the rays of the spicule (Fig. 10p) and is a skeletal element of secondary origin.

The rays extending from the spicule as a result of growing, branching, and fusion of distal ends form a lattice polyhedron, which is the initial shell.

The external shells are represented by one, two, or several spheres, which were initially formed by the tangled apophyses of the main skeletal spines and connected to each other by numerous bars, bridges, and poles. The surface of the spheres quite often possesses secondary ornamentation of apophyses, spinules, or thorns. The main spines are formed on the distal terminations of the rays of the spicule.

Explanation of Plate 28

Upper Devonian, Middle Frasnian Substage, Domanik Formation; Timan–Pechora Province, borehole Shuda-Yag-1003: (Figs. 1–4) sample 72 (depth 71.9–72.4 m); (Figs. 5, 6) sample 68 (depth 73.3–73.5 m); and (Fig. 7) sample 73 (depth 71.4–71.9 m).

Conical spines with ● circular cross section of the base

Figs. 1 and 2. *Bientactinosphaera conglobata* (Nazarov): (1) scale bar = 20 μm and (2) fragment, bar = 7 μm.

Fig. 3. *Bientactinosphaera variacanthina* (Foreman), bar = 15 μm.

Fig. 4. *Radiobisphaera assidera* (Nazarov), bar = 7 μm.

Fig. 5. *Radiobisphaera menneri* Afanasieva, bar = 7 μm.

Fig. 6. *Borisella mariae* Afanasieva, bar = 33 μm.

Pyramidal spines with ▲ triangular cross section of the base

Fig. 7. *Moskovistella lucet* Afanasieva, bar = 18 μm.

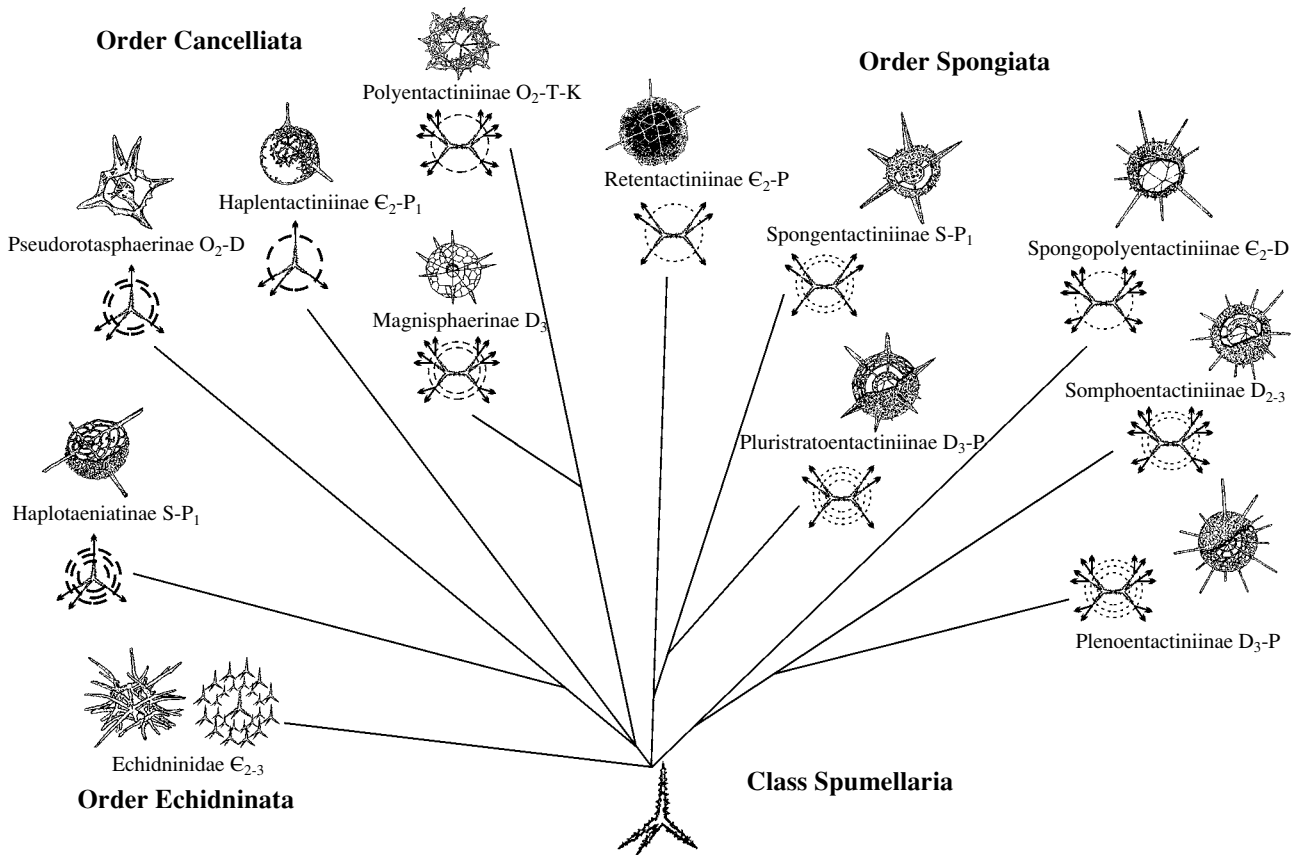

Fig. 32. Scheme of the development of spongy skeletons of Paleozoic spherical radiolarians (class Spumellaria).

Branching of the apophyses on the skeletal spines led to the appearance of spherical radiolarians with lattice, reticular, or spongy skeletons (Figs. 31, 32), which we assigned to the class Spumellaria Ehrenberg, 1875, in accordance with the etymology of the name of the class: from the Latin *spumeus* (covered by foam).

The skeletal rods that form lattice spheres are thicker and more robust (Pl. 15, figs. 1, 2), those forming the reticular spheres are thinner (Pl. 15, figs. 3, 4), whereas spongy forms show a chaotic interlacement of thin skeletal threads (Pl. 15, figs. 5–9).

The structure of the inner frame and outer shell allows the subdivision of the class of spongy radiolarians into six orders: Echidninata Kozur, Mostler, et Repetski, 1996; Cancelliata Afanasieva et Amon, 2003; Spongiata Afanasieva et Amon, 2003; Capsulata Afa-

Explanation of Plate 29

Upper Devonian, Middle Frasnian Substage, Domanik Formation; Timan–Pechora Province, borehole Shuda-Yag-1003: (Figs. 1, 2, 9) sample 72 (depth 71.9–72.4 m); (Figs. 3, 6, 8) sample 29 (depth 105–106 m); (Fig. 4) sample 68 (depth 73.3–73.5 m); (Fig. 5) sample 34 (depth 104.1–104.6 m); and (Fig. 7) sample 73 (depth 71.4–71.9 m).

Cylindrical thorns

Fig. 1. *Polyentactinia kossistekensis* Nazarov, scale bar = 20 μm.

Pointed conical thorns

Fig. 2. *Bientactinosphaera inusitata* (Foreman), bar = 10 μm.

Fig. 3. *Astroentactinia biaciculata* Nazarov, bar = 15 μm.

Fig. 4. *Astroentactinia rusaevi* Afanasieva, bar = 17 μm.

Fig. 5. *Entactinia bifida* Afanasieva, bar = 20 μm.

Fig. 6. *Bientactinosphaera variacanthina* (Foreman), bar = 15 μm.

Rounded conical thorns

Fig. 7. *Bientactinosphaera miletenkoi* Afanasieva, bar = 15 μm.

Fig. 8. *Radiobisphaera assidera* (Nazarov), bar = 15 μm.

Rounded thorns–tubercles

Fig. 9. *Moskovistella baccata* Afanasieva, bar = 10 μm.

Plate 29

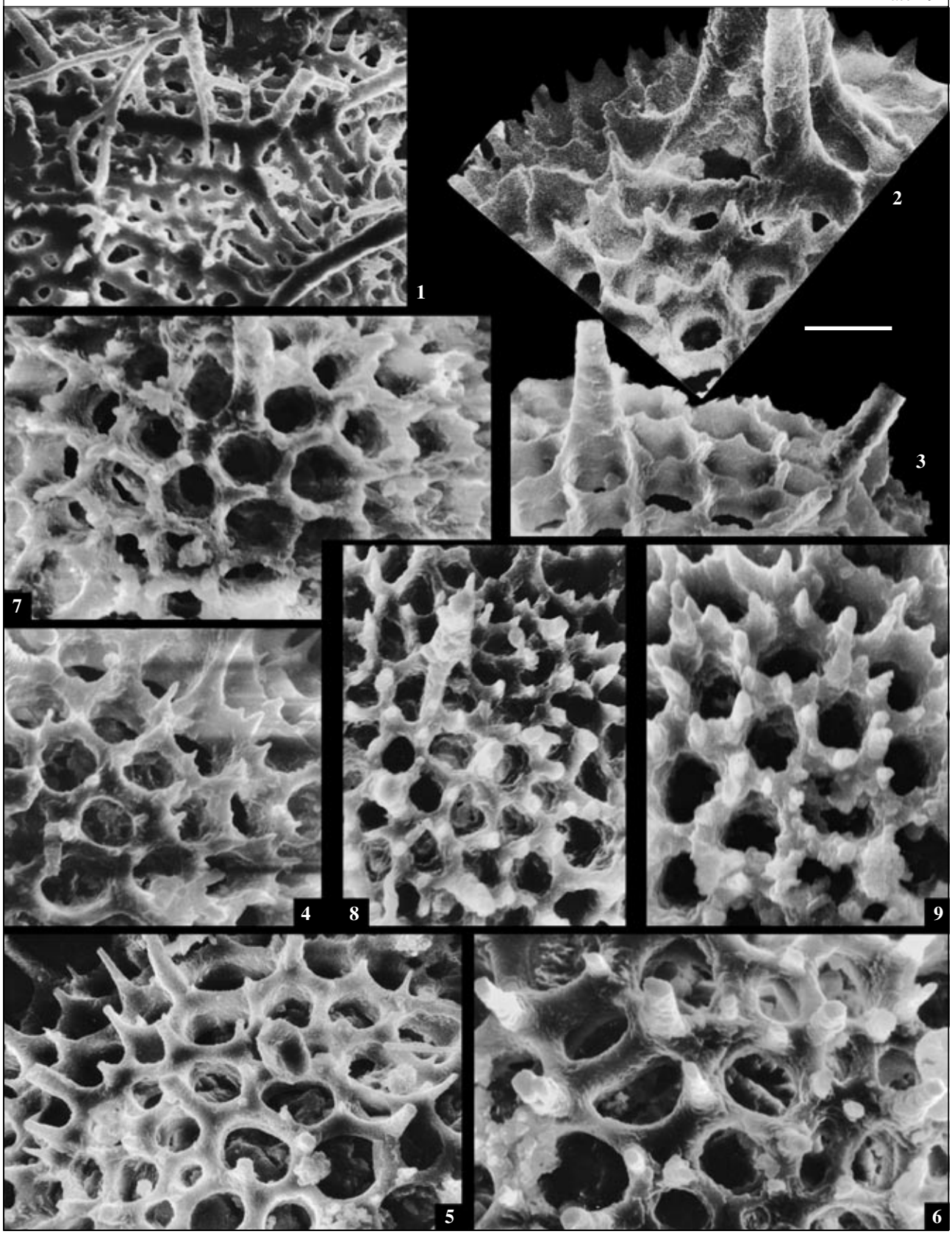

Thorns (1–8) and thorns–tubercles (9) in members of the subfamilies (1) Polyentactiniinae, (2, 6–8) Bientactinosphaerinae, (3, 4, 9) Astroentactiniinae, and (5) Entactiniinae.

Plate 30

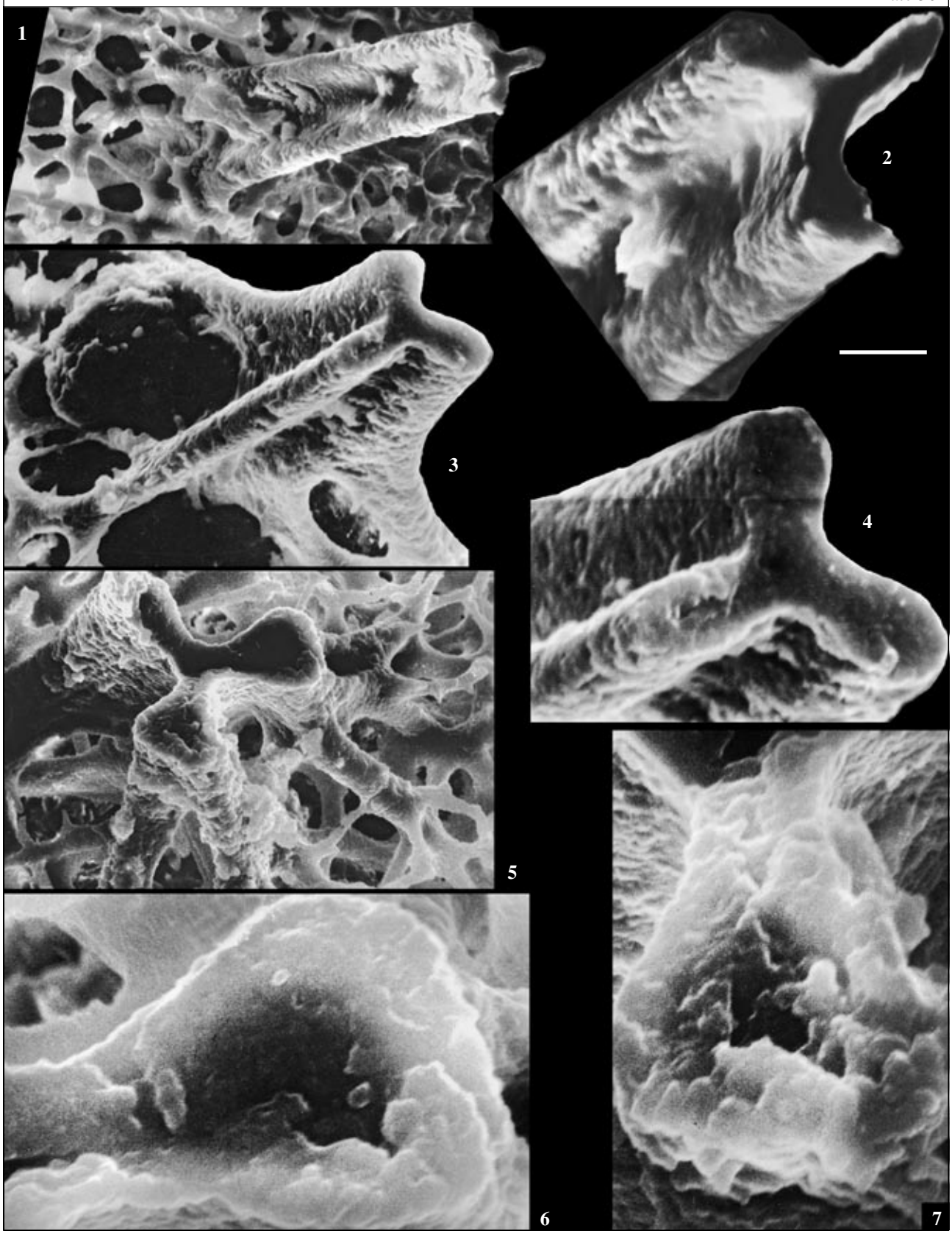

Structure and hypothetical stages of the formation of three-bladed spines in members of the subfamily Spongopolyentactiniinae by the example *Spongentactinella olafi* Afanasieva.

nasieva et Amon, order nov.; Prodigiata Afanasieva et Amon, order nov.; and Saturnalata Afanasieva et Amon, order nov. (Figs. 31, 33; Table 7).

The order Echidninata (Middle–Late Cambrian) includes the earliest spongy radiolarians the spherical skeleton of which is formed by a random interlacement of numerous spicules (Figs. 31a, 32, 33).

The order Cancelliata (from the Latin *cancelli*, "lattice") is characterized by a lattice sphere. The order is subdivided into four families (Figs. 31p–31w, 32, 33).

The family Haplentactiniidae Nazarov, 1980 (Middle Cambrian–Early Permian) is characterized by the presence of a simple initial spicule formed by the intersection of spines in a single center (Figs. 31r–31v, 32).

The family Polyentactiniidae Nazarov, 1975 (Middle Ordovician–Cretaceous) is characterized by a fused double initial spicule forming a median bar and a thinner reticular sphere (Figs. 31p, 32).

The family Pentactinocarpidae Dumitrica 1978 (Middle–Late Triassic) is typified by the presence of a single apical ray of the spicule opposite the four basal rays, which are united by arcs proximally to form four proximal pores (Fig. 31w).

The family Orosphaeridae Haeckel, 1887 (Cretaceous–Recent) has an initial spicule, which can sometimes be incorporated in the skeletal wall and is virtually indistinguishable from it, forming an **X**-shaped structure. In addition, skeletons acquire a pylome opening (Fig. 31q).

The order Spongiata (from the Latin *spongia* "sponge") comprises three families of radiolarians with a spongy, spherical shell (Figs. 31b–31j, 32, 33): Spongentactiniidae Nazarov, 1975 (Middle Cambrian–Permian); Spongopolyentactiniidae Nazarov, 1975 (Middle Cambrian–Permian); and Conocaryommidae Lipman, 1969 (Late Permian–Eocene).

The order Capsulata (from the Latin *capsulata* "capsule") has the inner frame in the shape of a microsphere and comprises three radiolarian families (Figs. 31x–31z, 33): Centrocubidae Hollande, Enjumet, 1960 (Middle Triassic–Recent); Quinquecapsulariidae Dumitrica, 1995 (Jurassic–Recent); and Rhizosphaeridae Haeckel, 1881 (Late Jurassic–Recent).

The order Prodigiata (from the Latin *prodigialis* "strange, unusual") has an inner frame of the nassellarian type and comprises two families (Figs. 31m–31o, 33): Eptingiidae Dumitrica, 1978 (Middle Triassic–Jurassic) and Multiarcusellidae Kozur et Mostler, 1979 (Middle-Late Triassic).

The order Saturnalata shows the development of the characteristic ring of varying shape with polar spines (Figs. 31k, 31l, 33). The order comprises two families: Oertlispongidae Kozur et Mostler, 1980 (Middle–Late Triassic) and Saturnalidae Deflandre, 1953 (Late Triassic–Recent).

The Saturnalata is a very characteristic Mesozoic radiolarian group. In the opinion of Kozur and Mostler (1982), the family Saturnalidae evolved from the family Oertlispongidae during the Carnian (Late Triassic). A few main tendencies are observed in the evolution of Saturnalidae: (a) disappearance of polar spines, (b) the replacement of a simple lobed ring by three-bladed rings, and (c) the loss of the ring when the skeleton is represented by the central spherical shell and two polar spines (Kozur, Mostler, 1982; De Wever *et al.*, 2001).

The subdivision of the family Saturnalidae into three subfamilies is based mainly on the presence or absence of the ring and on its structure. The ring is the most important element of the skeleton, the transformation of which is traced in the evolution of this family (Fig. 33). Besides, in most cases this is the only part of the skeleton preserved in fossils.

POROUS SPHERICAL RADIOLARIA

Radiolaria with porous skeletal tissue represent a distinct trend in the evolution of Polycystina. They evolved from a hypothetical Early Cambrian ancestor that had a spherical skeleton penetrated by pores.

For over the entire time when radiolarians have been studied, the spongy and porous taxa were assigned to the same taxon (Spumellaria). At the same time spongy and porous skeletons, apart from differences in the morphology of the shells, have a completely different origin and development of the skeletal tissue, especially at the end of the ontogeny.

The development of the lattice-spongy skeleton in its final stage is achieved by bridge growth (Anderson, 1980, 1981, 1983), when previously formed beams and bridges variously thicken to form an intricate spongy or lattice, or coarse latticed skeletal wall.

Explanation of Plate 30

Upper Devonian, Middle Frasnian Substage, Domanik Formation; Timan–Pechora Province: (Figs. 1, 2) Lyajol River, outcrop 1904, sample 6; (Figs. 3, 4–7) borehole Shuda-Yag-1003: (3, 4) sample 8 (depth 120.9–124 m); and (5–7) sample 72 (depth 71.9–72.4 m).

Y-shaped cross section at the middle of spines

Figs. 1–4. *Spongentactinella olafi* Afanasieva: (1) scale bar = 20 μm; (2) fragment, bar = 7 μm; (3) bar = 15 μm; and (4) fragment, bar = 7 μm.

-shaped cross section of the base of spines

Figs. 5–7. *Spongentactinella olafi* Afanasieva: (5) bar = 15 μm and (6, 7) fragment, bar = 4 μm.

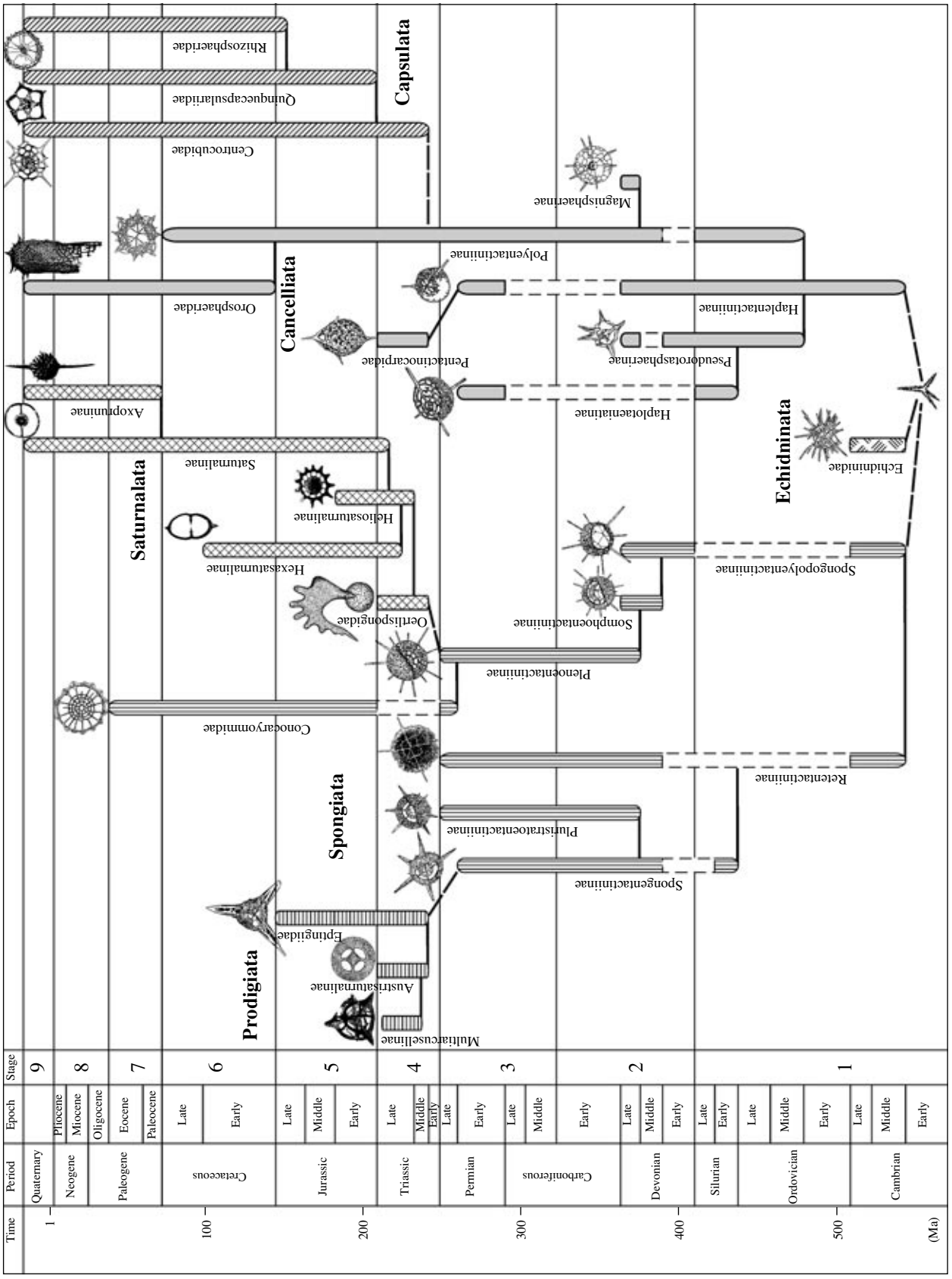

Fig. 33. Phylogenetic tree of the class Spumellaria.

The development of the porous skeleton (in contrast to the lattice-spongy skeleton) is completed by the rim growth, when the edges of the pores grow within, while pores narrow, the wall thickens to form a porous skeletal structure (Fig. 8d).

Radiolarians with a porous shell are assigned here to the class Sphaerellaria Haeckel, 1881. The structure of the inner frame, external and internal shells, and the structure and number of main spines allows the subdivision of the class of porous Radiolaria into six orders: Anakrusata Nazarov, 1977; Inaniguttata Nazarov et Ormiston, 1984; Entactiniata Riedel, 1967; Hexalonchata Haeckel, 1881; Actinommata Haeckel, 1862; and Sphaerellata Haeckel, 1887 (Figs. 34, 35; Table 7).

The order Anakrusata (Fig. 34a) shows the development of the main hollow spine of a cylindrical shape (the inner frame is not observed). It contains one family Anakrusidae (Ordovician–Silurian).

The order Inaniguttata (Figs. 34b–34e) comprises two families with the inner frame in a shape of a hollow sphere and conical main spines: Inaniguttidae Nazarov et Ormiston, 1984, emend. Afanasieva, 1999 (Cambrian–Silurian) and Oriundoguttidae Afanasieva, 1999 (Cambrian–Early Devonian).

The order Entactinata (Figs. 34f–34l) comprises three families with the inner initial skeleton in a shape of a spicule with a median bar (*MB*) and external main spines that are mostly three-bladed and, more rarely, rodlike: Entactiniidae Riedel, 1967, emend. Afanasieva, 1999 (Cambrian–Triassic); Astroentactiniidae Nazarov et Ormiston, 1985 (Silurian–Triassic); and Hexastylidae Haeckel, 1881 (Middle Triassic–Recent).

The order Hexalonchata (Fig. 34m) comprises two families with the inner frame in a shape of a tetrapetaloid spicule and initial microsphere, or spicule of the nassellarian type: Hexalonchidae Haeckel, 1881 (Early Jurassic–Recent) and Kungalariidae Dumitrica et Carter, 1999 (Late Triassic–Middle Jurassic).

The order Actinommata (Figs. 34n–34p) includes three families without the inner frame, with an initial microsphere, several internal and external shells, and numerous main spines: Astrosphaeridae Haeckel, 1881 (Triassic–Recent); Actinommidae Haeckel, 1862, emend. De Wever *et al.*, 2001 (Triassic–Recent); and Heliodiscidae Haeckel, 1881 (Paleocene–Recent).

The order Sphaerellata (Figs. 34q–34z) comprises three families with two to ten main spines (three-bladed and rodlike or cylindrical and hollow); the inner frame was not observed: Xiphostylidae Haeckel, 1881, emend. De Wever *et al.*, 2001 (Triassic–Recent); Parvivaccidae Pessagno et Yang, 1989 (Middle Jurassic–Late Cretaceous); and Pantanelliidae Pessagno, 1977 (Late Triassic–Early Cretaceous).

STAURAXONIC RADIOLARIA

The first unusual discoid and spindle-shaped radiolarians were described from the Devonian of England and Canada by Hinde and Fox (1895). The first record of "stauraxonia" with crossed axes lying in a plane perpendicular to the main axis belongs to Mordukhai-Boltovskoy (1936). Forty years after Ormiston and Lane (1976) described unusual discoid, pyramidal, and armed radiolarians from the Lower Carboniferous of the USA (Oklahoma).

Nazarov and Ormiston (1983) were the first to recognize the group of stauraxonic radiolarians in the order Polycystina. This group was the superfamily Latentifistulidea Nazarov et Ormiston, 1983, comprising three families: Latentifistulidae Nazarov et Ormiston, 1983; Tormentidae Nazarov et Ormiston, 1983; and Ruzhencevispongidae Kozur, 1980, emend. Nazarov et Ormiston, 1983.

Nazarov (1988) assigned this group of stauraxonic radiolarians, including all the above families, to the order Spumellaria.

Caridroit *et al.* (1999) assigned some stauraxonic radiolarians to the order Latentifistularia.

Afanasieva (2000a) and Amon (2000), independently of one another, redescribed all known stauraxonic radiolarians as new orders: Stauraxonaria Afanasieva, 2000 and Stauraxonarida Amon, 2000.

In this paper all presently known stauraxonic radiolarians are assigned to the class Stauraxonaria Afanasieva et Amon, classis nov., which comprises eight orders (Table 7): Palaeodiscata Afanasieva, 2000, emend. Afanasieva et Amon, nov. (Late Cambrian–Permian); Oviformata Afanasieva et Amon, order nov. (Silurian–Recent); Radiiformata Afanasieva et Amon, ordo nov. (Carboniferous–Permian); Pyramidata Afanasieva et Amon, order nov. (Carboniferous–Cretaceous); Lobatiradiata Afanasieva et Amon, ordo nov. (Middle Triassic–Recent); Pyloniata Haeckel, 1881 emend. Dumitrica, 1989 (Middle Triassic–Recent); Spongurata Haeckel, 1862 (Middle Triassic–Recent); and Spongodiscata Haeckel, 1862 (Late Triassic–Recent).

Morphology

The main feature of stauraxonic radiolarians that makes them fundamentally different from all other radiolarians is the peculiar shape of their skeleton, which varies from flattened discoidal and subtriangular to spindle-shaped and from pyramidal to those with three, five, or more lobes-arms (Fig. 36). This shape was apparently more advantageous for the planktonic lifestyle of these organisms and facilitated their wide geographic distribution.

From the very beginning of their evolution (Late Cambrian), stauraxonic Polycystina had a spongy skeletal shell, which is preserved in most representatives up to the Recent (Fig. 36).

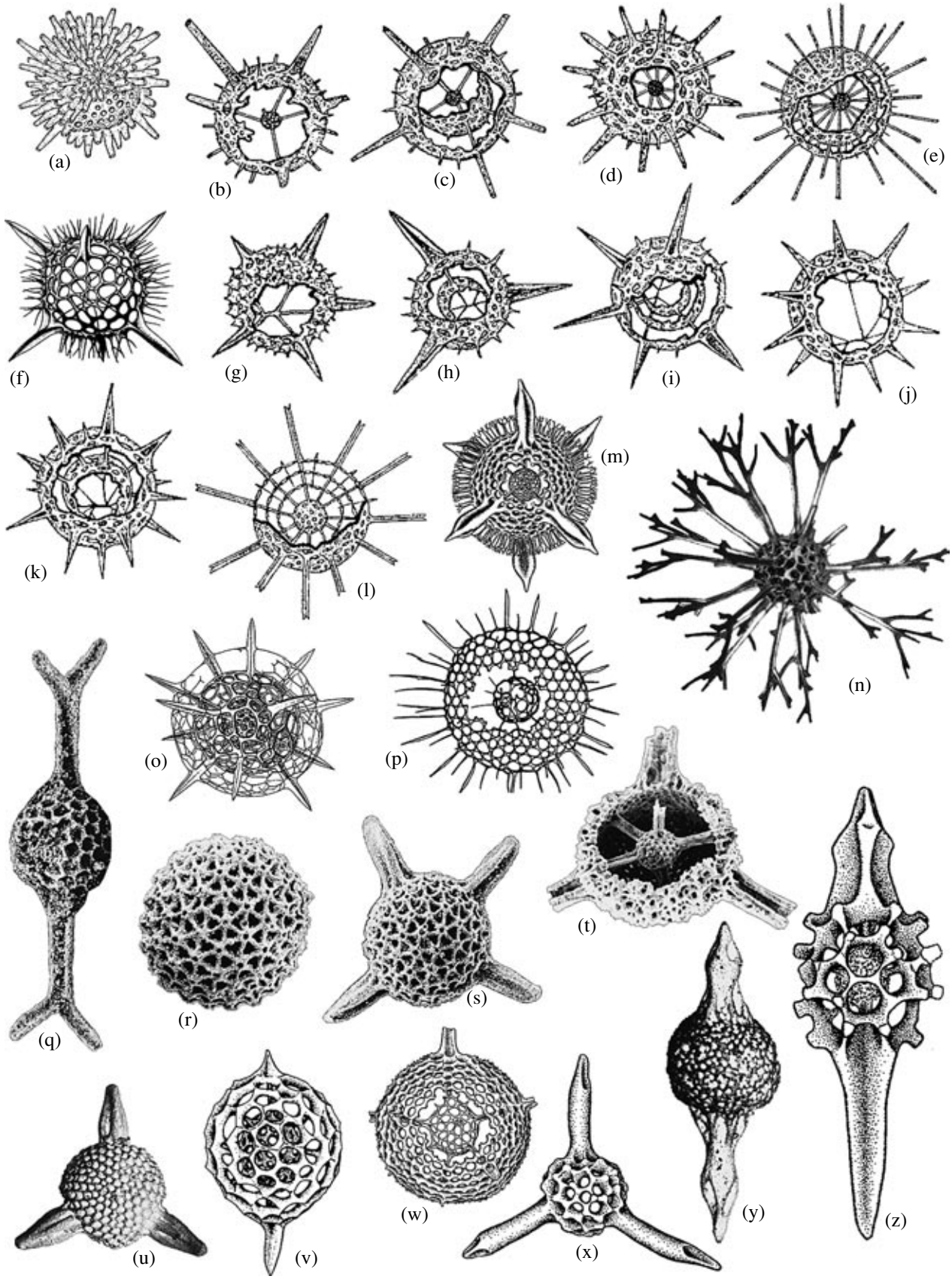
(a)
(b)
(c)
(d)
(e)
(f)
(g)
(h)
(i)
(j)
(k)
(l)
(m)
(n)
(o)
(p)
(q)
(r)
(s)
(t)
(u)
(v)
(w)
(x)
(y)
(z)

Stauraxonaria with a lenticular, subtriangular, or otherwise convex test (Fig. 37) had a chaotic, non-differentiated spongy tissue in the Early and Middle Paleozoic. However, by the Early Carboniferous, most of them had a differentiated spongy layer consisting of several envelopes.

Flat, subtriangular radiolarians in the Late Carboniferous had only a spongy shell, although already in the Early Permian there were radiolarians with a lamellar central part and spongy periphery (Fig. 38; Pl. 19, figs. 1, 2). Specimens with a flat, reticular, or finely cellular shell were less common.

Armed forms of Paleozoic Latentifistulidae and Mesozoic–Cenozoic Lobatiradiata had a spongy skeletal shell (Figs. 36f, 36g, 36k–36p). In the Late Carboniferous, however, Latentifistulidae gave rise to a group of radiolarians (Polyfistulidae, Quadriremidae, Ormistonellidae, and Deflandrellidae) in which spongy skeletal tissue became denser to form a lamellar skeleton and, frequently, small, surface meshes (Figs. 36h–36j; 39).

Stauraxonic radiolarians of the Early Paleozoic have an inner frame shaped like a hollow, unperforated sphere with three rays extending from the sphere at an angle of 120° (Figs. 10c, 38). In the Carboniferous and Permian, no fundamental changes were observed in the inner frame of stauraxonic polycystines; however, the number of rays extending from the sphere increased. Stauraxonic polycystines with four or five hollow rays appeared in the Late Carboniferous, whereas those with seven or more rays appeared in the Early Permian (Nazarov and Ormiston, 1984). Only in flattened Pyramidata in the Early Permian, the inner sphere becomes modified into a hemisphere and three- or four-rayed spicule (genus *Rectotormentum*, family Tormentidae) (Nazarov, 1988).

The inner frame of Mesozoic and Cenozoic stauraxonic radiolarians transformed into a heteropolar microsphere (De Wever, 1982; Dumitrica, 1988, 1889, 1995; De Wever *et al.*, 2001).

Major Evolutionary Trends

The first flattened discoidal stauraxonic radiolarians of the order Palaeodiscata probably appeared in the Late Cambrian (Fig. 24). Most likely, they evolved from the spherical spongy Spongentactiniidae as a result of favorable mutation. However, at the beginning of their evolution, they were simply misshapen relative to truly spherical radiolarians. During the first stage in the evolution of Radiolaria in the Cambrian–Silurian, the stauraxonic species were represented only by the first appearing spongy subdiscoidal Palaeodiscidae and spindle-shaped, ellipsoid Spongolonchidae (Fig. 40).

At the second stage of radiolarian evolution (Lower Devonian–Lower Carboniferous), 11 genera of 5 families are known among the stauraxonic radiolarians. These families are Palaeodiscidae, Spongolonchidae, Staurodruppidae, Tormentidae, and Latentifistulidae. The first radiation of the taxonomic diversity among the stauraxonic radiolarians and the appearance of the first members of the two families Tormentidae and Latentifistulidae occurred in the Early Carboniferous. On the whole, in the Devonian–Early Carboniferous, the orders Palaeodiscata and Oviformata dominate, constituting up to 70% of stauraxonic radiolarians (Fig. 40).

The third stage in the evolution (Middle Carboniferous–Permian) shows an outbreak of the taxonomic diversity of stauraxonic radiolarians (22 genera), which began in the Late Carboniferous (seven families and subfamilies) and reached its peak in the Late Permian (ten families and subfamilies). A wide distribution of diverse taxa of the four families of stauraxonic radiolarians—Tormentidae (31%), Latentifistulidae (19%), Ruzhencevispongidae (12%), and Palaeodiscidae (12%)—was the most characteristic feature of the Permian period of their evolution.

The evolution of Paleozoic stauraxonic radiolarians was not entirely a progressive, irreversible process. The history of their evolution shows a general degeneration as well. The lineage Quadriremidae—Ormistonellidae—Deflandrellidae shows the phenomenon of catamorphosis, i.e., a decrease in the number of skeletal rays over time from five to three (Fig. 40).

The exceptional variety of stauraxonic radiolarians present at the end of the Paleozoic, especially in the Artinskian, was probably related to the general warming of the climate. However, by the end of the Late Per-

Fig. 34. Sphaerellaria: (a) order Anakrusata, (b–e) order Inaniguttata, (f–l) order Entactinata, (m) order Hexalonchata, (n–p) order Actinommata, and (q–z) order Sphaerellata: (a) Anakrusidae (Ordovician–Silurian): *Anakrusa myriacantha* Nazarov; (b, c) Inaniguttidae (Cambrian–Silurian): (b) *Inanigutta unica* (Nazarov) and (c) *Inanibigutta aksakensis* (Nazarov); (d, e) Oriundoguttidae (Cambrian–Early Devonian): (d) *Oriundogutta ramificans* (Nazarov) and (e) *Inanihella bakanasensis* (Nazarov); (f) Hexastylidae (Middle Triassic–Recent): *Hexastylus horridus* Hollande et Enjumet; (g–i) Entactiniidae (Cambrian–Triassic): (g) *Entactinia diversita* Nazarov, (h) *Bientactinosphaera grandis* (Nazarov), and (i) *Thecentactinia* sp.; (j–l) Astroentactiniidae (Silurian–Triassic): (j) *Astroentactinia stellata* Nazarov, (k) *Helioentactinia perjuncta* Nazarov et Ormiston, and (l) *Multisphaera* sp.; (m) Hexalonchidae (Late Triassic–Recent): *Hexacontium drymodes* Haeckel; (n) Astrosphaeridae (Triassic–Recent): *Cladococcus megaceros* Hollande et Enjumet; (o) Actinommidae (Triassic–Recent): *Cromyomma circumtextum* Haeckel; (p) Heliodiscidae (Paleocene–Recent): *Heliodiscus viminalis* (Hollande et Enjumet); (q–t) Parvivaccidae (Middle Jurassic–Late Cretaceous): (q) *Dicroa periosa* Foreman, (r) *Levileugeo ordinarius* Yang et Wang, (s) *Leugeo* sp., and (t) *Acastea* sp.; (u–w) Xiphostylidae (Triassic–Recent): (u) *Triactoma blakei* (Pessagno), (v) *Druppatractus variabilis* Dumitrica, and (w) *Entapium chaenapium* Sanfilippo et Riedel; and (x–z) Pantanelliidae (Middle Triassic–Early Cretaceous): (x) *Capnodoce kochi* Blome, (y) *Spongopallium tubulispina* Kozur, Krainer et Mostler, and (z) *Pantanellium* sp.

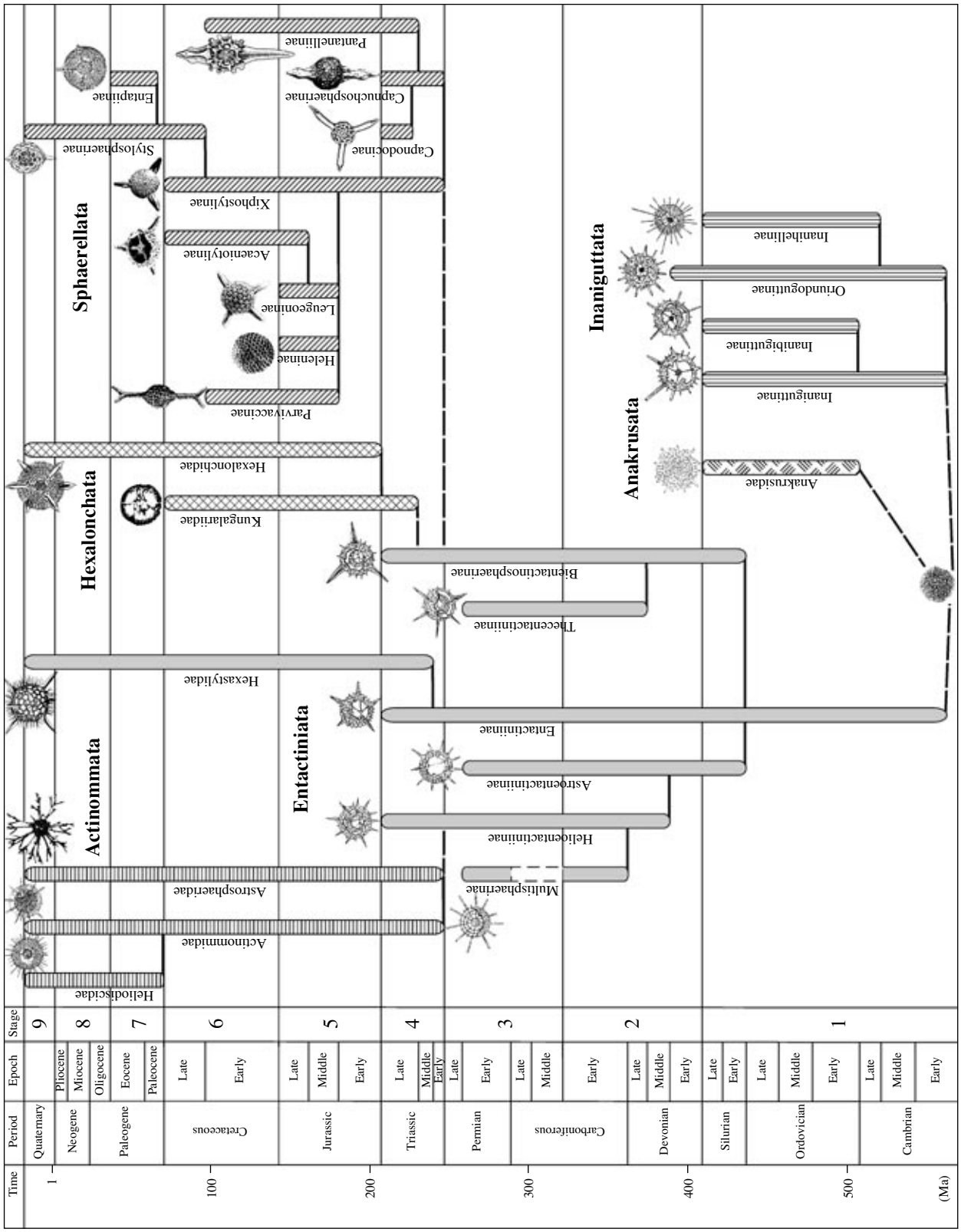

Fig. 35. Phylogenetic tree of the class Sphaerellaria.

mian, their diversity sharply decreased, and Paleozoic stauraxonic radiolarians eventually completely disappeared. On the other hand, among Mesozoic and Cenozoic radiolarians (Figs. 36k–36z), there were many genera strikingly similar to Paleozoic stauraxonic radiolarians (Figs. 36a–36j).

From the point of view of evolutionary paleontology, it is difficult to imagine that such complex taxa reappeared in the Mesozoic. Paleozoic stauraxonic radiolarians had had a very long history of evolution (almost 200 million years!) from comparatively simple species of the Late Cambrian–Early Devonian to intricate skeletons in the Carboniferous and Permian taxa. It is certain that in the Mesozoic their descendants should have given rise to new, advanced radiolarian groups. A striking morphological similarity of some Paleozoic, Mesozoic, and Cenozoic radiolarian taxa and the analysis of the skeletal structures allow the hypothesis of the uniform evolution of Phanerozoic stauraxonic radiolarians (Fig. 40).

The polygonal radiolarians of the family Tormentinae (Figs. 36b–36e), represented by six Paleozoic genera, were ancestors of Mesozoic taxa of the order Pyramidata: families Pyramispongiidae and Cavaspongiidae, (12 genera) (Figs. 36q, 36r).

The armlike taxa of the family Latentifistulinae (three genera *Ishigaum*, *Latentifistula*, and *Quadriremis*) (Figs. 36g, 36h) gave rise to numerous (44 genera) Mesozoic–Cenozoic descendants from the order Lobatiradiata (Figs. 36k–36p). This order contains six families, of which three (Angulobracchiidae, Hagiastridae, and Hexaporobrachiidae) are Mesozoic, two families (Suttoniidae, Myelastridae) are known only from the Cenozoic, and one family (Patulibracchiidae) existed from the Late Triassic to the end of the Neogene.

The spindle-shaped genera of the family Spongolonchidae (*Copiellintra* and *Spongocoela*) gave rise to the order Oviformata (Figs. 36s, 36t), containing ten genera of three families in the Mesozoic and Cenozoic (Fig. 40). Two families (Gomberellidae, Phaseliformidae) are known only from the Mesozoic, whereas members of the family Archaeospongoprunidae existed from the Late Triassic until now.

Discoidal Palaeodiscidae (Fig. 36a), which were represented by only 7 genera in the Paleozoic, produced numerous Mesozoic and Cenozoic descendants of 88 genera of three orders: Spongodiscata, Pyloniata, and Spongurata (Figs. 36u–36z).

Two families (Sponguridae and Litheliidae) of the order Spongurata (Fig. 36u) are known from the Mesozoic and Cenozoic and include only seven genera.

The order Spongodiscata (Fig. 36z) contains 36 genera of three families. The family Relindellidae (three genera) is known only from the Late Triassic. Other members of this order belong to the families Spongodiscidae (16 genera) and Coccodiscidae (17 genera) and are widely distributed from the Late Cretaceous–Eocene to the present.

The order Pyloniata (Figs. 36v–36y) show the greatest taxonomic diversity: 45 genera belonging to 10 families of three superfamilies. Dactyliosphaeroidea includes 19 genera of six families (Patruliidae, Catenopylidae, Emiluviidae, Veghicycliidae, Dactyliosphaeridae, and Pseudoaulophacidae), known mainly from the Mesozoic, and only members of the families Dactyliosphaeridae and Pseudoaulophacidae are known from the Cenozoic. The superfamilies Pylonioidea (11 genera of the families Pyloniidae and Miropylidae) and Larnacillioidea (15 genera of the families Larnacillidae and Tholoniidae) are known from the Late Cretaceous to the Recent.

Thus, to date we know only two genera of discoidal and spindle-shaped radiolarians that appeared in the Cambrian–Silurian: Radiolaria gen. indet., originally described by Iwata and Obut from the Late Cambrian (Iwata *et al.*, 1997), and *Spongolonche* Haeckel, 1881, which is known from the Early Silurian onward. In the Devonian–Early Carboniferous, the generic diversity of stauraxonic radiolarians increased up to 11 genera; in the Middle Carboniferous–Permian, up to 22 genera. The biotic crisis at the Permian–Triassic boundary resulted in the extinction of virtually all Paleozoic Radiolaria. As a response to these catastrophic events, the taxonomic diversity of stauraxonic radiolarians dramatically increased to reach 154 genera in the Mesozoic and Cenozoic.

NASSELLARIA

Nassellarians are the most diverse group of Polycystina and are found from the Early Cambrian to the present. The class Nassellaria contains three orders, 11 superfamilies, 88 families and subfamilies (Fig. 41; Table 7) and has the highest number of genera (594). While in the Paleozoic, at the first stages of the radiolarian evolution, the number of families and subfamilies of Nassellaria ranged from three to five; in the Triassic, the taxonomic diversity of Nassellaria sharply increased to 29 families and subfamilies. Beginning from the Jurassic stage of the evolution of radiolarians to the present, the taxonomic diversity of families and subfamilies of Nassellaria changed from 36 to 45. Thus, in the Mesozoic (except for Triassic) and in the Cenozoic, the class Nassellaria dominated over all other classes of Polycystina put together.

The evident (i.e., known from the fossil record) morphological evolution of Nassellaria began from the Early Cambrian, from the appearance of the first peculiar members of the family Proventocitidae *Ulcundia* (Cambrian–Ordovician) and *Proventocitum* (Early–Middle Ordovician) (Figs. 41, 42e, 42f, 43), which are similar to Sphaellaria and Aculearia (Albaillellata).

During the Cambrian–Silurian stage of the Paleozoic history of radiolarians, all superfamilies and most families of the order Pylomariata appeared: Proventocitoidea (Proventocitidae), Popofskyelloidea (Popof-

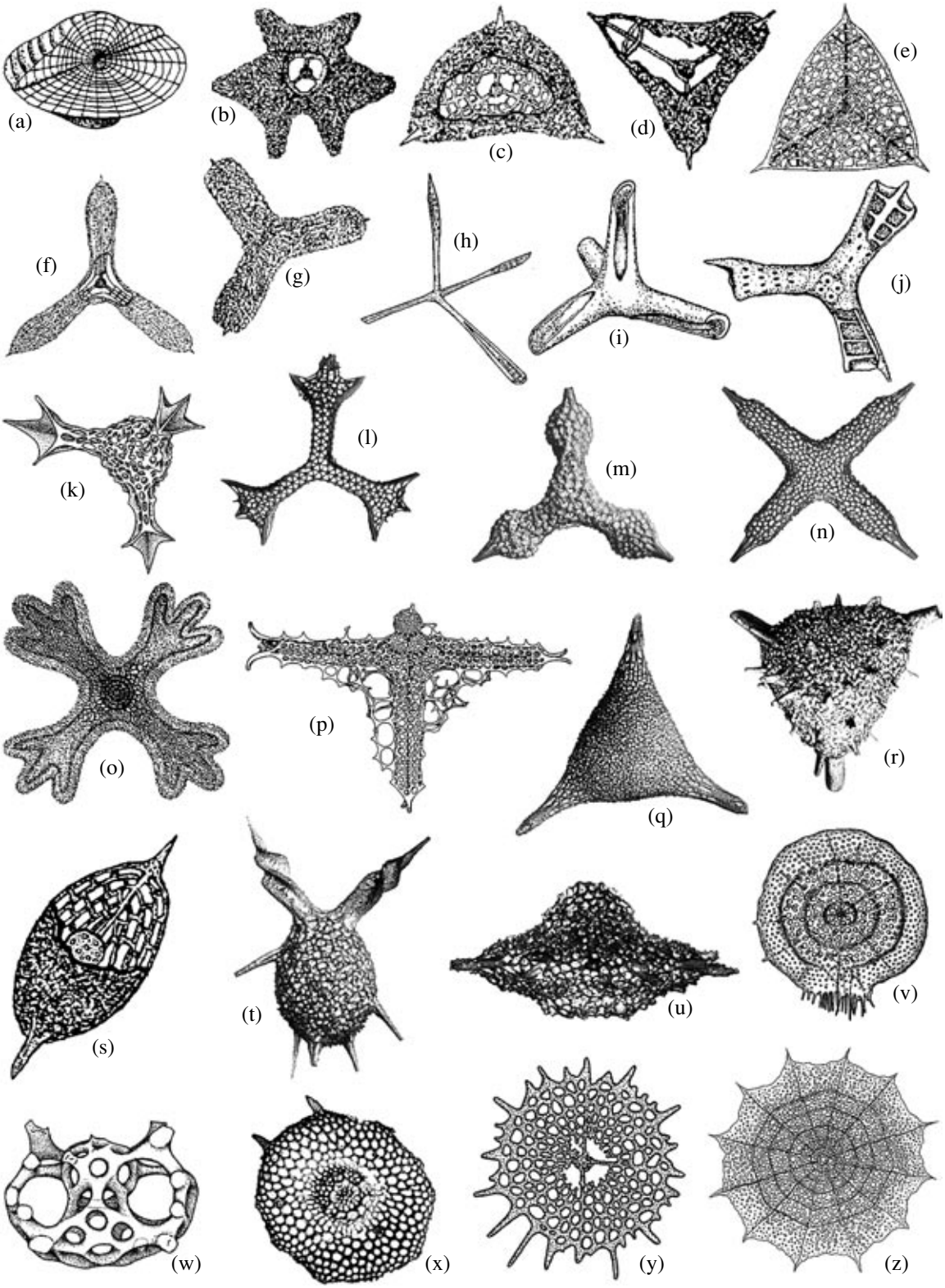
(a)
(b)
(c)
(d)
(e)
(f)
(g)
(h)
(i)
(j)
(k)
(l)
(m)
(n)
(o)
(p)
(q)
(r)
(s)
(t)
(u)
(v)
(w)
(x)
(y)
(z)

Fig. 36. Stauraxonaria: (a) order Palaeodiscata (Late Cambrian–Permian): *Eostylodictya eccentrica* Ormiston et Lane; (b–e, q, r) order Pyramidata (Carboniferous–Cretaceous): (b) *Tormentum* sp., (c) *Rectotormentum* sp., (d) *Latentidiota visenda* Nazarov et Ormiston, (e) *Ruzhencevispongus* sp., (q) *Dumitricaia sphaerica* (O'Dogherty), and (r) *Pyramispongia barmsteinensis* (Steider); (f–j) order Radiiformata (Carboniferous–Permian): (f) *Latentibifistula* sp., (g) *Latentifistula crux* Nazarov et Ormiston, (h) *Quadriremis gliptoacus* Nazarov et Ormiston, (i) *Ormistonella robusta* De Wever et Caridroit, and (j) *Deflandrella manica* De Wever et Caridroit; (k–p) order Lobatiradiata (Middle Triassic–Recent): (k) *Icrioma tetrancistrum* De Wever, (l) *Halesium sexangulum* Pessagno, (m) *Paronaella mulleri* Pessagno, (n) *Crucella euganea* (Squinabol), (o) *Dicranastrum wyvellei* Haeckel, and (p) *Suttonium praedicator* Schaaf; (s, t) order Oviformata (Silurian–Recent): (s) *Copiellintra diploacanta* Nazarov et Ormiston and (t) *Gomberellus hircicornus* Durnitrica, Kozur et Mostler; (u) order Spongurata (Middle Triassic–Recent): *Patellula helios* (Squinabol); (v–y) order Pyloniata (Middle Triassic–Recent): (v) *Circodiscus microporus* (Stöhr.), (w) *Palaeotetrapyle* sp., (x) *Dactyliosphaera silviae* Squinabol, and (y) *Veghicyclia reiflingensis* Kozur et Mostler; (z) order Spongodiscata (Late Triassic–Recent): *Stylochlamydium asteriscus* Haeckel.

skyellidae), Cessipyloroidea (Cessipyloridae, Aciferopyloridae), and Pylentonemoidea (Pylentonemidae) (Figs. 24, 41, 43).

The second stage in the evolution of Pylomariata was in the Devonian–Early Carboniferous, while the third stage was in the Middle Carboniferous–Permian, the fourth stage was in the Triassic, whereas the fifth was in the Jurassic, and the sixth was partly in the Cretaceous. At the end of the Early Cretaceous, Pylomariata finally disappeared from the fossil record (Figs. 41, 43).

Morphology of Paleozoic Nassellarians

The analysis of morphology of the skeletons of Paleozoic Nassellaria of the order Pylomariata (Fig. 42) showed that due to its morphological features this group of radiolarians is very important in answering some questions concerning the transition of radiolarians from the benthonic to the planktonic lifestyle.

Inner frame. The inner frame of Pylomariata is in a center of the subspherical skeleton with a pylome. It has a shape of a hollow, nonperforated sphere with seven rays extending from it in the tests of ancient Ordovician Proventocitidae (Fig. 10d) and Cessipylorinae (Figs. 10e, 44a) and Silurian Aciferopyloridae (Fig. 10f). In Late Devonian–Middle Carboniferous Caspiazinae, the inner frame is represented by an isometric polyhedron with seven cylindrical rays (Figs. 10g, 44b). The polyhedron is, in turn, transformed into seven- and four-rayed spicule in the skeletons of the Devonian and Early Carboniferous Pylentoneminae and Archocyrtiinae (Figs. 44c, 44d).

Shells. The external shell of Pylomariata is in most cases penetrated by variously shaped pores or has a tangled-fibrous (spongy) structure (Fig. 44b). In the Cambrian and Ordovician, Pylomariata had a robust, massive, and coarsely porous shell wall. However, at the end of their evolution in the Early Carboniferous, the forms with a lighter porous skeleton began to predominate. The members of Caspiazinae with a spongy skeleton are in a separate group. The test wall in these radiolarians represents a complex loose meshwork structure (Pl. 20).

Main spines. The number of main spines depends on the number of rays of the inner frame, while their shape apparently changes according to the shape of the inner frame (Figs. 42, 44). For instance, Cambrian and Ordovician Pylomariata with a massive inner frame have conical spines (Figs. 42f, 42g, 44a). The later, Silurian, taxa have a weak depression in the rodlike and conical spines (Figs. 42h, 42i). Devonian and Early Carboniferous Pylomariata, with a light inner spicule, have three-bladed spines (Figs. 42j, 42l–42w, 44b–44d), which apparently should be considered advanced because the development of three-bladed spines required less material than the conical spines, whereas

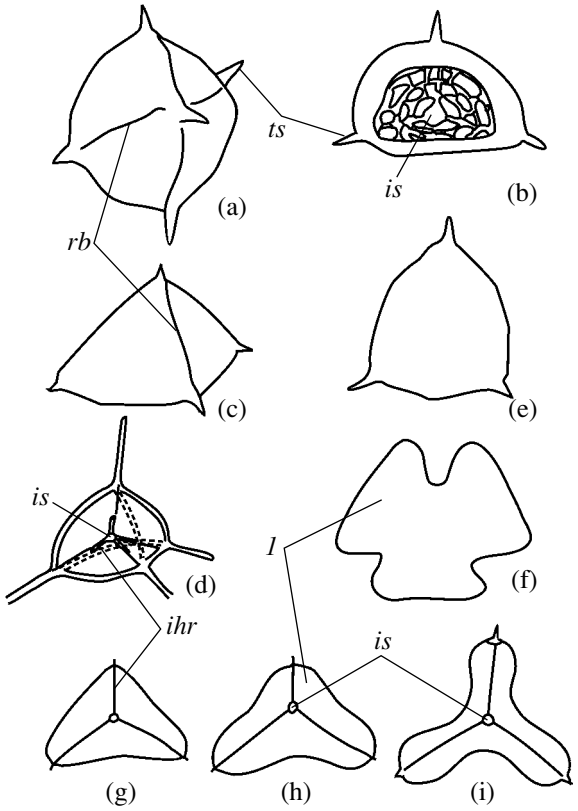

Fig. 37. Structural scheme of skeletons of discoidal and pyramidal stauraxonic radiolarians of the order Pyramidata (after Nazarov, 1988; Amon, 2000): (a) *Octatormentum*, (b) *Rectotormentum*, (c, d) *Tetratormentum*, (e, f) *Tormentum*, and (h–i) *Latentidiota*. Designations: (*is*) internal framework in the shape of a hollow sphere with radiating internal hollow rays (*ihr*), (*ts*) terminal spines, (*rb*) ribs, and (*l*) lobes.

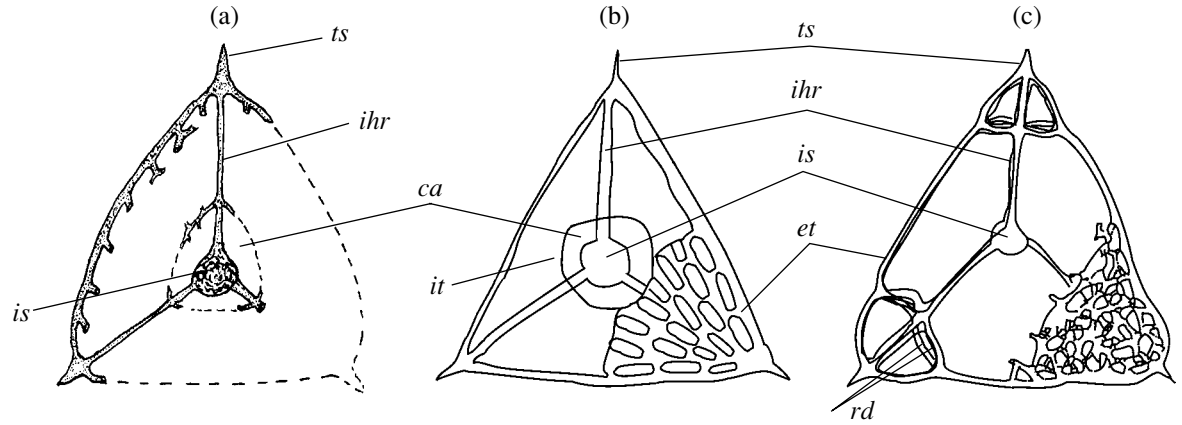

Fig. 38. Scheme of the inner structure of the skeletons of triangular and subtriangular stauraxonic radiolarians of the order Pyramidata (family Ruzhencevispongidae): (a, b) *Ruzhencevispongus*, (c) *Latentidiota*: (a) after Nazarov and Ormiston (1983); (b, c) after Amon (2000). Designations: (*ts*) terminal spines; (*is*) internal framework in the shape of a hollow sphere; (*ihr*) inner hollow rays radiating from the internal framework; (*rd*) rods of the inner rays; (*ca*) cavity; (*et*) external shell; and (*it*) internal shell.

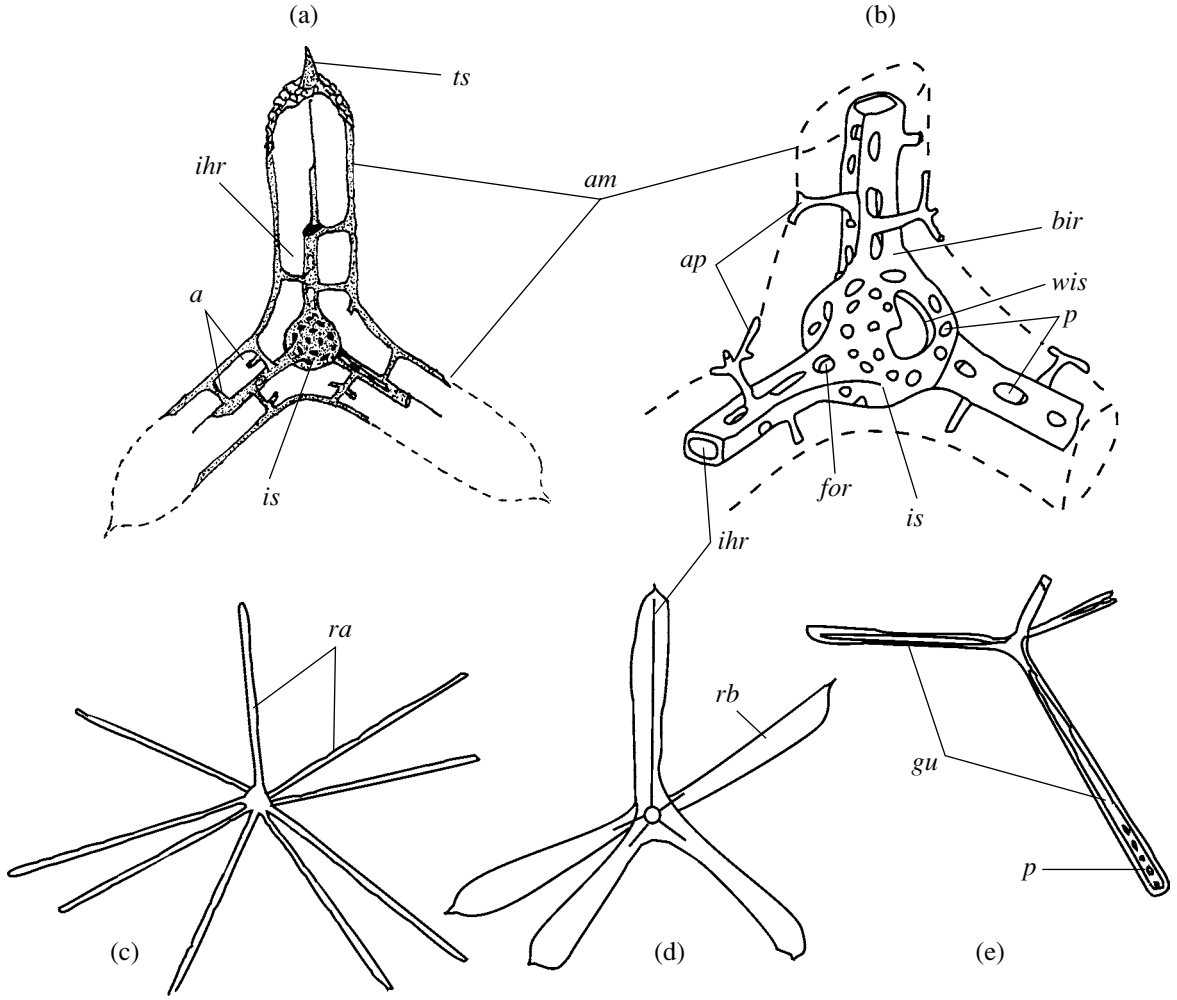

Fig. 39. Skeletons of rayed and armed stauraxonic radiolarians of the order Radiiformata (after Nazarov and Ormiston, 1983; Nazarov, 1988; Amon, 2000); (a, b) Latentifistulidae: (a) *Latentifistula*, (b) *Triactofenestrella*; (c) Polyfistulidae: *Polyfistula*; (d, e) Quadriremidae: (d) *Quinqueremis* and (e) *Quadriremis.* Designations: (*am*) arms, (*ap*) apophyses, (*bir*) basement of the inner hollow ray, (*gu*) gutter, (*for*) foramen at the base of the inner ray, (*is*) internal shaped like a hollow sphere with the radiating inner hollow rays *ihr*, (*p*) pores, (*ra*) (rays), (*rb*) ribs, (*ts*) terminal spines, and (*wis*) wall of the initial sphere.

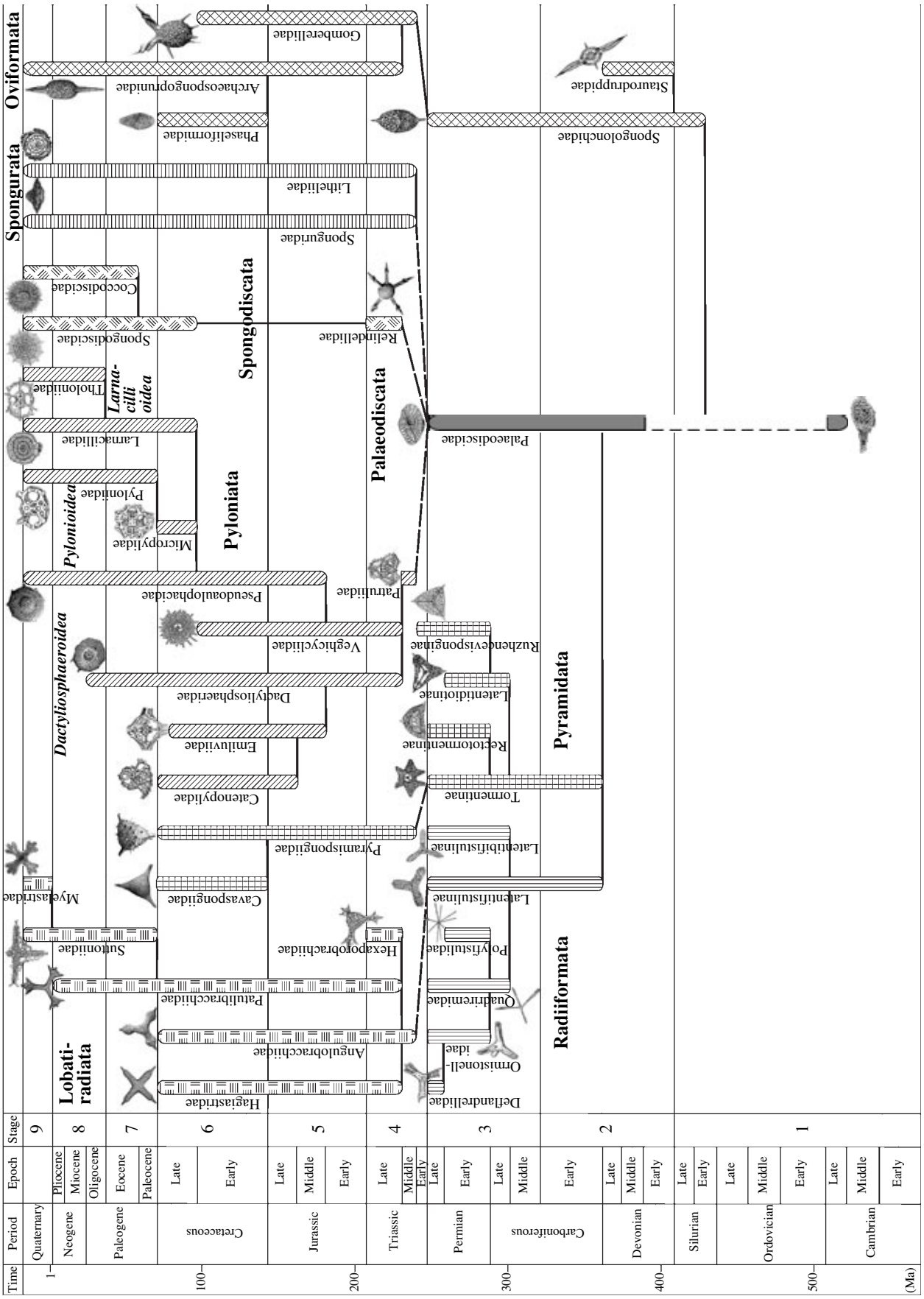

Fig. 40. Phylogenetic tree of the class Stauraxonaria.

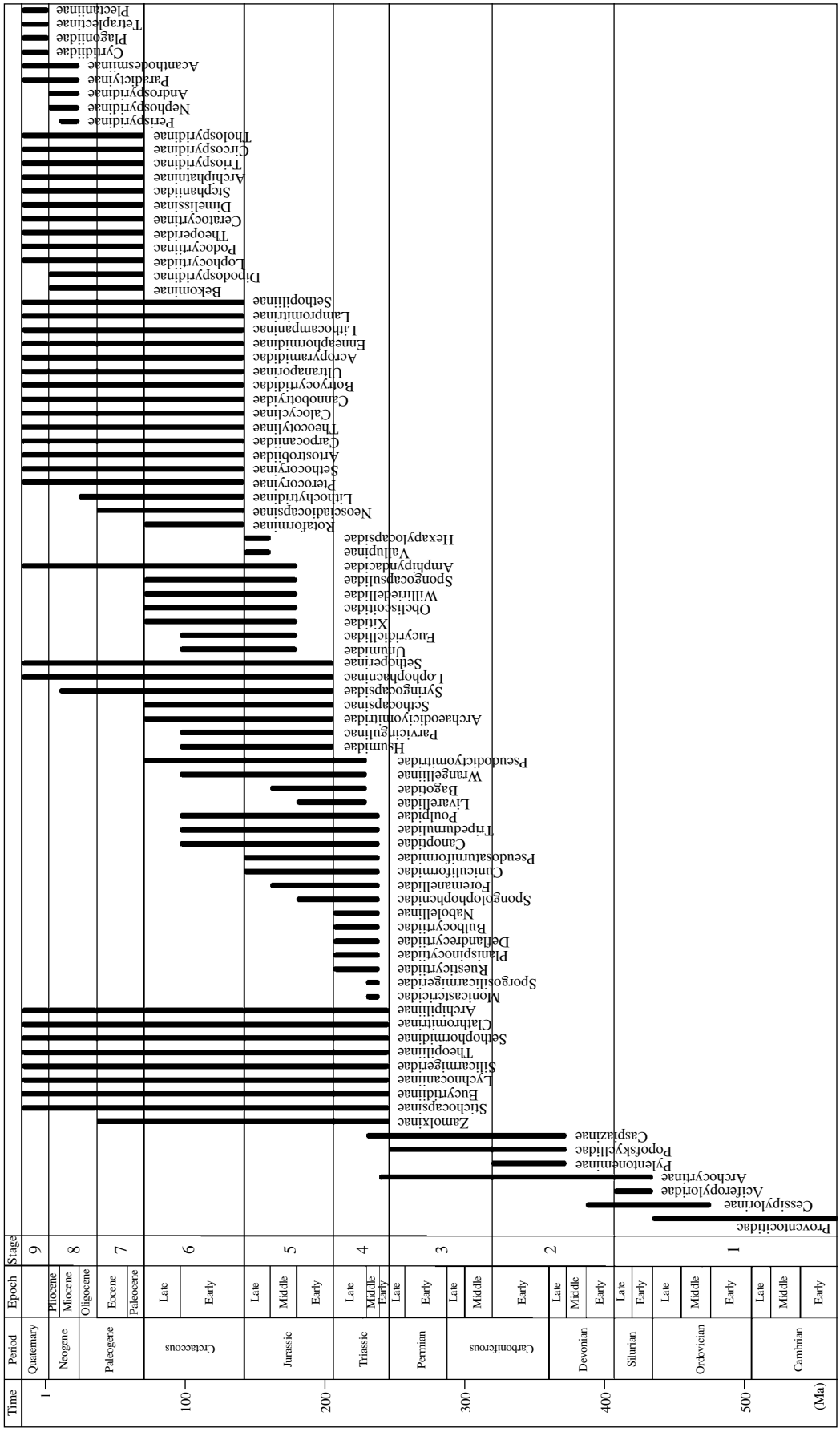

Fig. 41. Stratigraphic distribution of the class Nassellaria.

when such spines were present, the axopodia were better fixed (Mordukhai-Boltovskoy, 1937; Nazarov, 1984, 1988; Petrushevskaya, 1981a, 1986). However, the skeletons of some Early and Middle Carboniferous Caspiazinae show a reduction of main spines (Pl. 20), which was possibly related to the attached lifestyle of these organisms.

Conical by-spines are developed over the entire shell surface in the Ordovician and Silurian Cessipylorinae (Fig. 42g) and some Late Devonian–Early and Middle Carboniferous Caspiazinae (Fig. 42k). The rodlike by-spines form only the surrounding of the pylome opening in some Archocyrtinae (Figs. 42n, 44c).

Pylome. The pylome is an opening in the oral part of the test and is a characteristic feature of Pylomariata that distinguishes them from all other Paleozoic Polycystina. In benthic organisms such a structure is equivalent to the aperture in foraminifers and serves for the exit of pseudopodia, which contact the substrate. The pylome is usually surrounded by well-developed skeletal structures (collar, peristome, shelf, and spines), the shape and combination of which vary in different genera. The pylome in many known representatives of Pylomariata is surrounded by three main spines (Figs. 16f, 16h–16j). In the skeletons of *Cessipylorum* and *Pylentonema* (Fig. 16f), they are sort of connected by a well-developed shelf, whereas in the skeletons of *Cytisphaeronemium* and *Cyrtisphaeractenium*, they alternate with rodlike by-spines (Figs. 16h, 16i). The shells of *Allocyrtium* have an unusual surrounding of the pylome in which the lamellar skeletal tissue in a shape of truncated conical peristome surrounding three main spines, which are located around the test pylome of this genus (Fig. 16j). A peculiar skeletal structure in a shape of a wing collar is developed around the pylome in the shells of *Caspiaza* (Fig. 16g; Pl. 20).

Evolution of the Order Pylomariata

The pylome, an opening in the oral part of the shell surrounded by various structures (collar, peristome, shelf, and spines), the shape and combination of which vary in different genera is a characteristic feature of all Pylomariata. Assuming that the general construction of the organism defined by its ecological and morphological adaptations is an adequate reflection of a paleobiotope, the peculiar tests of Pylomariata allow the reconstruction of their habitats in the past (Afanasieva, 1986). The evolution of the order Pylomariata suggests that the radiolarians with a pylomes were apparently adapted to the benthic lifestyle and possibly attempted to change to the planktonic lifestyle.

The general evolution of Pylomariata in the Paleozoic shows four major trends (Fig. 43). The first begins with the appearance of the superfamily Proventocitoidea, the second was continued by the members of the superfamily Popofskyelloidea, the third was represented by the superfamily Cessipyloroidea, while the fourth is characterized by the superfamily Pylentonemoidea.

Superfamily Proventocitoidea

The superfamily Proventocitoidea contains the most primitively constructed Nassellaria. Their skeleton with a wide pylome is composed of one shell with a hypothetical inner frame in shape of a hollow sphere with four or more rays of the initial spicule.

Apparently, the development of the skeleton in the earliest Proventocitidae (or supposed ancestors) occurred in the Early Cambrian: the skeletons of the first *Ulcundia* could be elongated conical in shape (Figs. 24, 42e). The Ordovician *Proventocitum* has an unusual egg-shaped skeleton (Fig. 42f). It is conical in the upper part, almost spherical in the middle part, and reverse conical in the bottom part. The bilateral symmetry of *Proventocitum* is achieved by the development of two wing-shaped spines in the middle part, with distal ends directed downward, and two small spines surrounding the pylome. According to Nazarov (1988), these taxa may have inhabited the bottom water layers in ancient seas. These first radiolarians were described from the early Cambrian–Ordovician of Kazakhstan (Nazarov, 1973, 1974c, 1975).

In the Silurian–Devonian, Proventocitoidea could give rise to Popofskyelloidea (Fig. 43). In the Middle Ordovician, Proventocitoidea apparently gave rise to Cessipyloroidea, whereas at the beginning of the Silurian, a large and diverse superfamily Pylentonemoidea branched off the Cessipyloroidea (Fig. 43). These tests were already spherical, with a pylome through which the stalk attaching to the substrate or axopodia could pass.

Superfamily Popofskyelloidea

A general evolutionary trend that began Proventocitoidea was continued by another superfamily (Popofskyelloidea). This lineage apparently branched off in the Late Devonian (Fig. 43).

The beginning differentiation of the external shell of Popofskyelloidea into zones, which are the precursors of future segments of later Nassellaria; increasing complexity of the initial spicule; and appearance of columellae resulted in the appearance of a new type of skeletal construction. The skeleton of Popofskyelloidea consists of one conical or cylindrical cyrtodoid shell with an inner frame composed of three or more-rayed spicule and two columellae. The wall of the external skeleton becomes more complex, porous lamellar, or lattice. An incomplete simple segmentation of the nassellaroid type with differentiation of two or more "segments" takes place. The spicule becomes more complex. The prototypes of spines *MB*, *A*, *V*, *2L*, and *2l* appear, whereas arcs are absent. The cephalis possesses

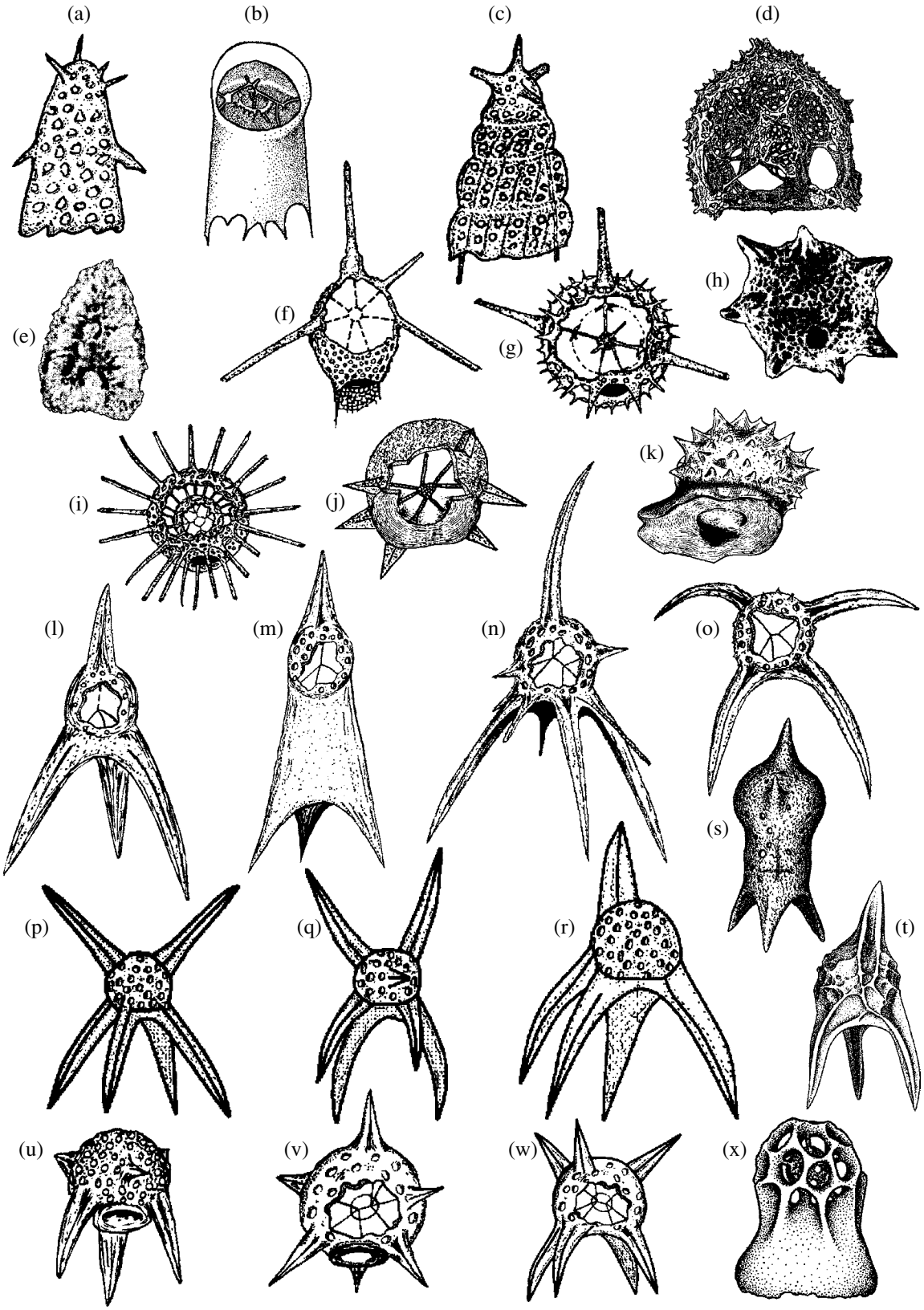
(a)
(b)
(c)
(d)
(e)
(f)
(g)
(h)
(i)
(j)
(k)
(l)
(m)
(n)
(o)
(p)
(q)
(r)
(s)
(t)
(u)
(v)
(w)
(x)

Fig. 42. Nassellaria: order Pylomariata: (a–d) Popofskyelloidea (Late Devonian–Late Jurassic): (a) *Tuscaritellum imitatum* Deflandre, (b) *Cyrtentactinia primotica* Foreman, (c) *Popofskyellum tardicarboniferum* Nazarov, and (d) *Hexapylocapsa anachoreta* Dumitrica et Zugel; (e, f) Proventocitoidea (Cambrian–Ordovician): (e) *Ulcundia incomperta* Nazarov, (f) *Proventocitum procerullum* (Nazarov); (g–k) Cessipyloroidea (Middle Ordovician–Middle Triassic): (g) *Cessipylorum apertum* (Nazarov), (h) *Fusalfanus konomoriensis* Aitchison, Hada, Ireland et Yoshikura, (i) *Aciferopylorum admirandum* Nazarov, (j) *Caspiaza calva* Afanasieva, and (k) *Caspiaza aculeata* Afanasieva; (l–x) Pylentonemoidea (Silurian–Early Cretaceous): (l) *Archocyrtium riedeli* Deflandre, (m) *Allocyrtlum costuligerum* (Deflandre), (n) *Cyrtisphaeronemium prudentigerum* Deflandre, (o) *Cyrtisphaeractenium mirabile* Deflandre, (p) *Robotium* sp., (q) *Mostlerium* sp., (r) *Deflandrellium* sp., (s) *Tripedocassis pessagnoi* Dumitrica, (t) *Hozmadia reticulata* Dumitrica, Kozur et Mostler, (u) *Pylentonema* sp., (v) *Pylentonema antiqua* Detlandre, (w) *Quadrapesus* sp., and (x) *Vallupus hopsoni* Pessagno et Blome.

an apical horn. The columellae are incorporated into the wall but sometimes continue outside it.

The family Popofskyellidae (Figs. 42a–42c) began its evolution from the Late Devonian and became extinct at the Permian–Triassic boundary. Later, after a considerable gap, possible descendants of these radiolarians again appeared for a short time in the Late Jurassic as members of the family Hexapylocapsidae (Fig. 42d). The latter have the features of degeneration, e.g., the reduced shell wall.

The evolution of Popofskyelloidea was not linear. Four pulses of evolution are recorded in the history of the development of this superfamily (Late Devonian–Early Carboniferous, Late Carboniferous, Late Per-

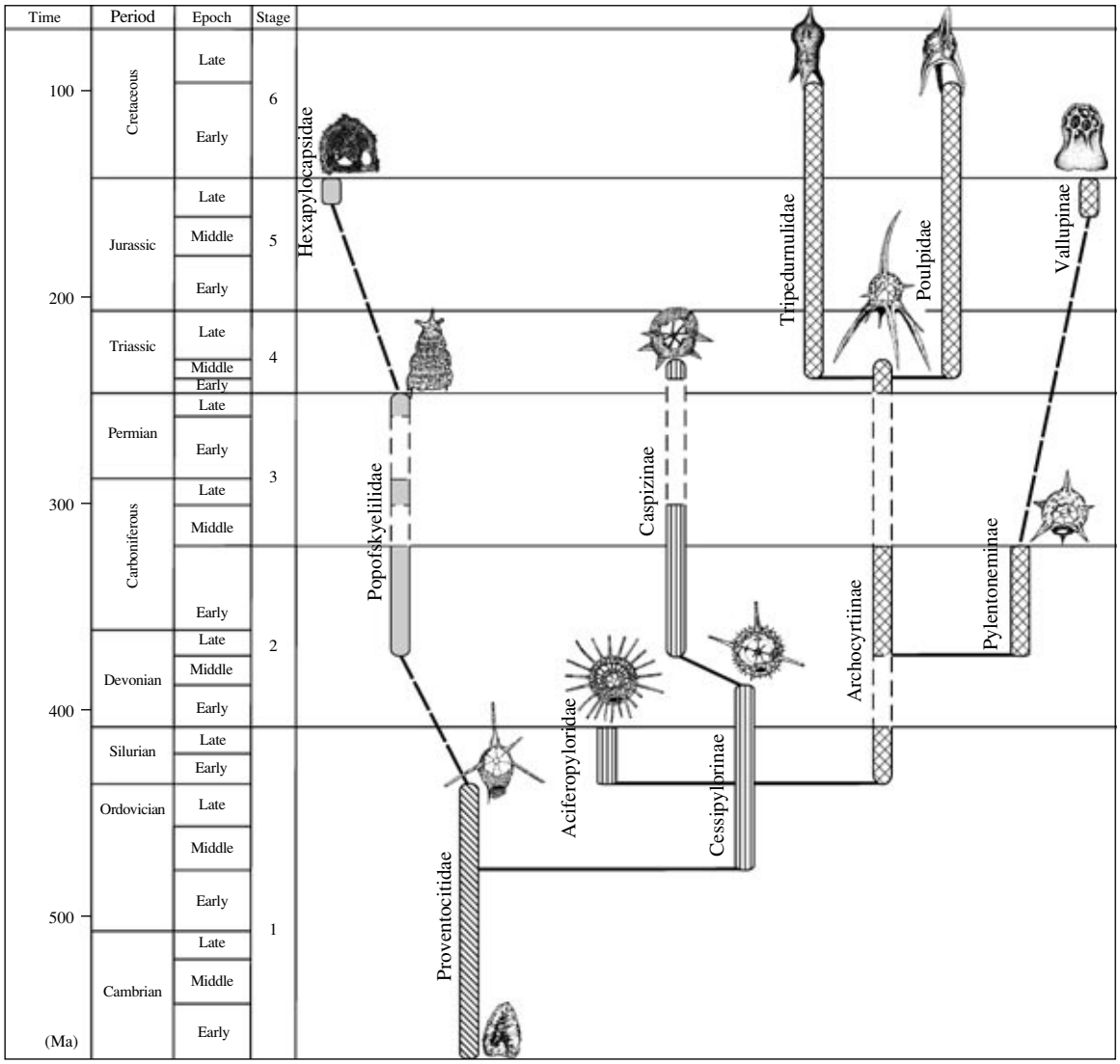

Fig. 43. Phylogenetic tree of the order Pylomariata.

Plate 31

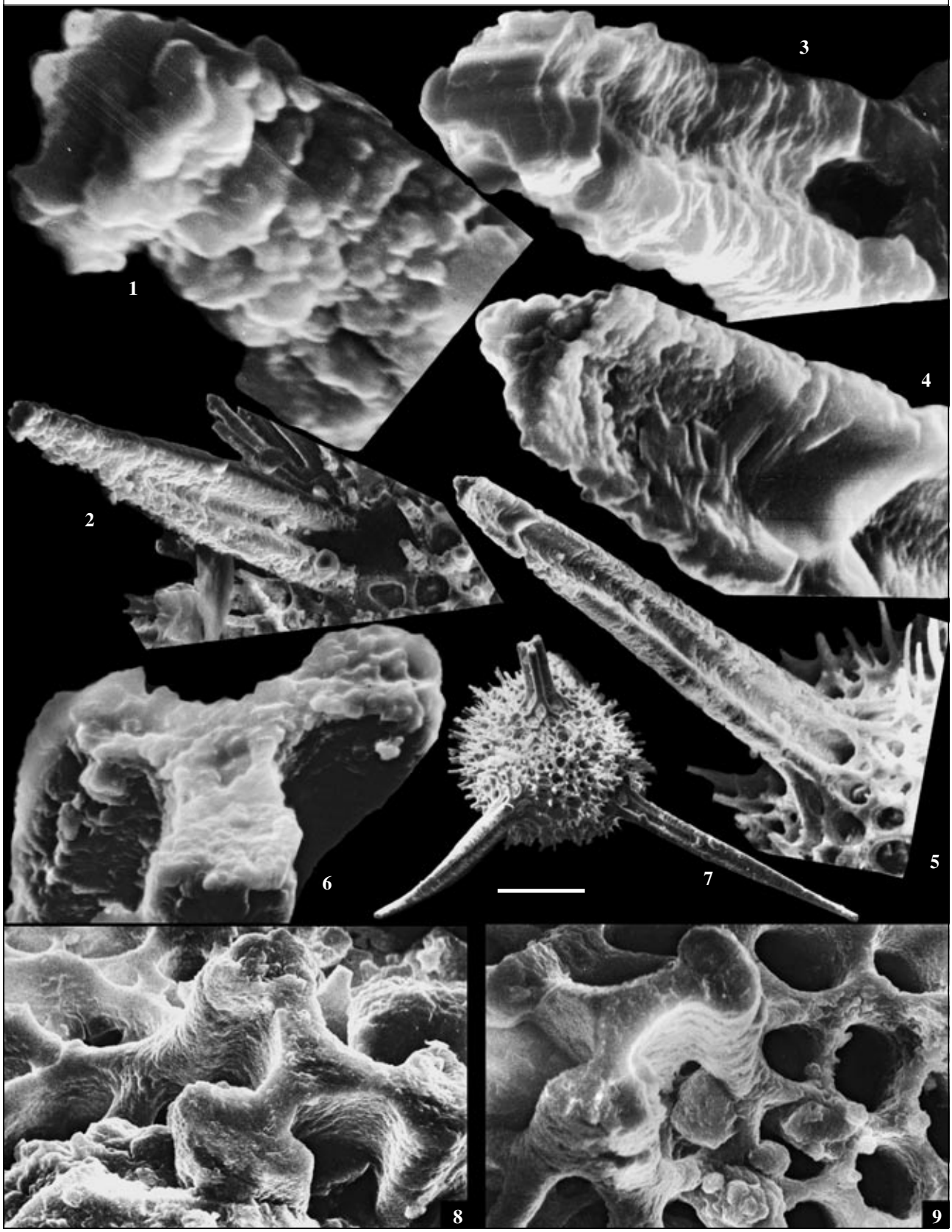

Structure and hypothetical stages of the formation of three-bladed spines in members of the subfamilies (1, 2, 4–9) Bientactinosphaerinae and (3) Helioentactiniinae.

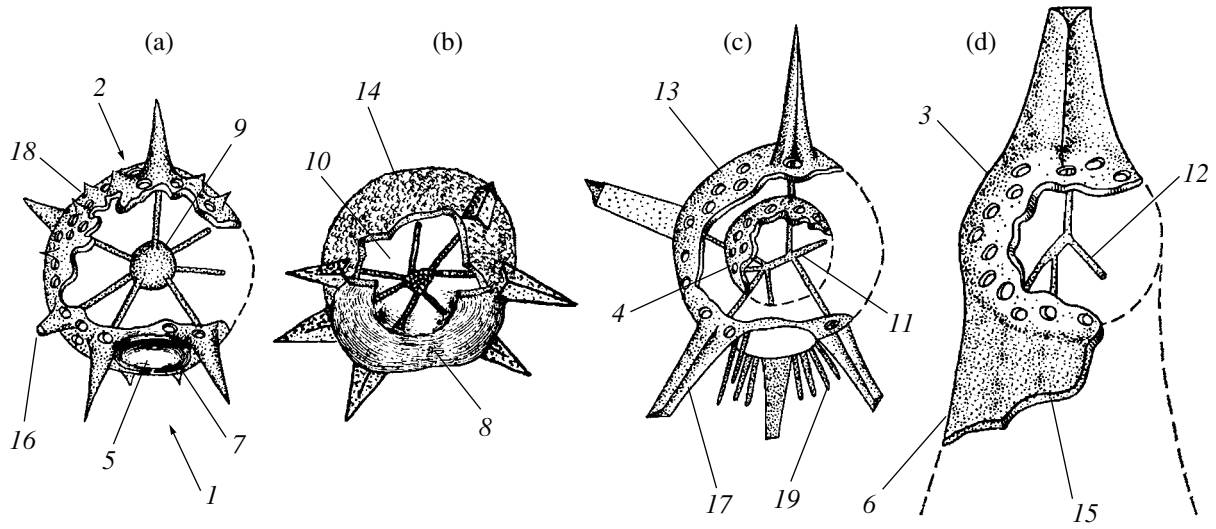

Fig. 44. Scheme of the skeleton structure of the order Pylomariata (after Afanasieva, 2000a): (a) nonperforated sphere with seven hollow cylindrical rays of the Ordovician Cessipylorinae, (b) isometric polyhedron with seven cylindrical rays of the Late Devonian–Middle Carboniferous Caspiazinae, (c) seven-rayed spicule of the Late Devonian–Early Carboniferous Pylentoneminae, and (d) four-rayed spicule of the Silurian–Early Carboniferous Archocyrtiinae. Designations: (*1–8*) parts of the shell: (*1*) oral, (*2*) aboral, (*3*) cephalis, (*4*) internal sphere, (*5*) pylome, (*6*) peristome, (*7*) shelf, and (*8*) collar; (*9–12*) types of the inner framework: (*9*) nonperforated sphere, (*10*) isometric polyhedron, (*11*) seven-rayed spicule, (*12*) four-rayed spicule; (*13–15*) types of the structure of the external shell: (*13*) porous, (*14*) spongy, (*15*) lamellar; (*16–17*) main spines: (*16*) conical spines, (*17*) three-bladed spines; (*18–19*) by-spines, and (*19*) rodlike spines.

mian, and Late Jurassic), which are separated by more or less long epochs of concealed evolution.

In their evolution, members of the superfamily Popofskyelloidea are an example of possible inhabitance of the bottom water ecological niches by the bilaterally symmetrical radiolarians. The early trends in the morphological evolution of Popofskyelloidea can be only guessed, although there is a possibility that they evolved from early *Proventocitum* (Fig. 42f) by the reduction of the lateral rodlike wing-shaped processes, decrease of the apical spine, and the formation of true segmentation of the test. This conclusion is based on the skeleton of the Early Carboniferous *Tuscaritellum* (Fig. 42a), and of the Late Devonian–Late Carboniferous *Popofskyellum* (Fig. 42c) (Deflandre, 1964b, 1972; Nazarov, 1988). The former have a porous nonsegmented test with small spine-shaped processes in the middle part of the skeleton and three or four short apical spines. The morphology of presently known members of Popofskyelloidea, which have a segmented test with a well delineated cephalis, suggests that the Mesozoic and Cenozoic Nassellaria could have evolved from the Late Paleozoic pylomate radiolarians Popofskyelloidea.

Superfamily Cessipyloroidea

Members of the superfamily Cessipyloroidea appeared in the Middle Ordovician, reached their acme in the Silurian, and became extinct in the Middle Triassic (Figs. 42g–42k, 43). In the spherical Cessipyloroidea with a porous or spongy wall of the external shell, the inner frame is transformed into the hollow sphere or isometric polyhedron.

Explanation of Plate 31

Upper Devonian, Middle Frasnian Substage, Domanik Formation; Timan–Pechora Province: (Figs. 1–7) borehole Shuda-Yag-1003: (1, 2, 6, 7) sample 29 (depth 105–106 m); (3) sample 72 (depth 71.9–72.4 m); (4, 5) sample 73 (depth 71.4–71.9 m); (Fig. 8) Ukhta River, sampling point no. 4, sample B-22; and (Fig. 9) borehole Shuda-Yag-1002, sample 14 (depth 66.6 m).

● circular cross section of the spine apex

Figs. 1 and 2. *Bientactinosphaera conglobata* (Nazarov): (1) scale bar = 6 μm and (2) bar = 33 μm.

▲ triangular cross section of the spine apex

Fig. 3. *Helioentactinia aster* Aitchison, bar = 4 μm.

Figs. 4 and 5. *Bientactinosphaera variacanthina* (Foreman): (4) bar = 33 μm and (5) bar = 7 μm.

⋈-shaped cross section of the middle (6, 7) and basal (8, 9) parts of spines

Figs. 6 and 7. *Bientactinosphaera variacanthina* (Foreman): (6) bar = 100 μm and (7) bar = 7 μm.

Figs. 8 and 9. *Bientactinosphaera pinica* Afanasieva: (8) bar = 10 μm and (9) bar = 15 μm.

Plate 32

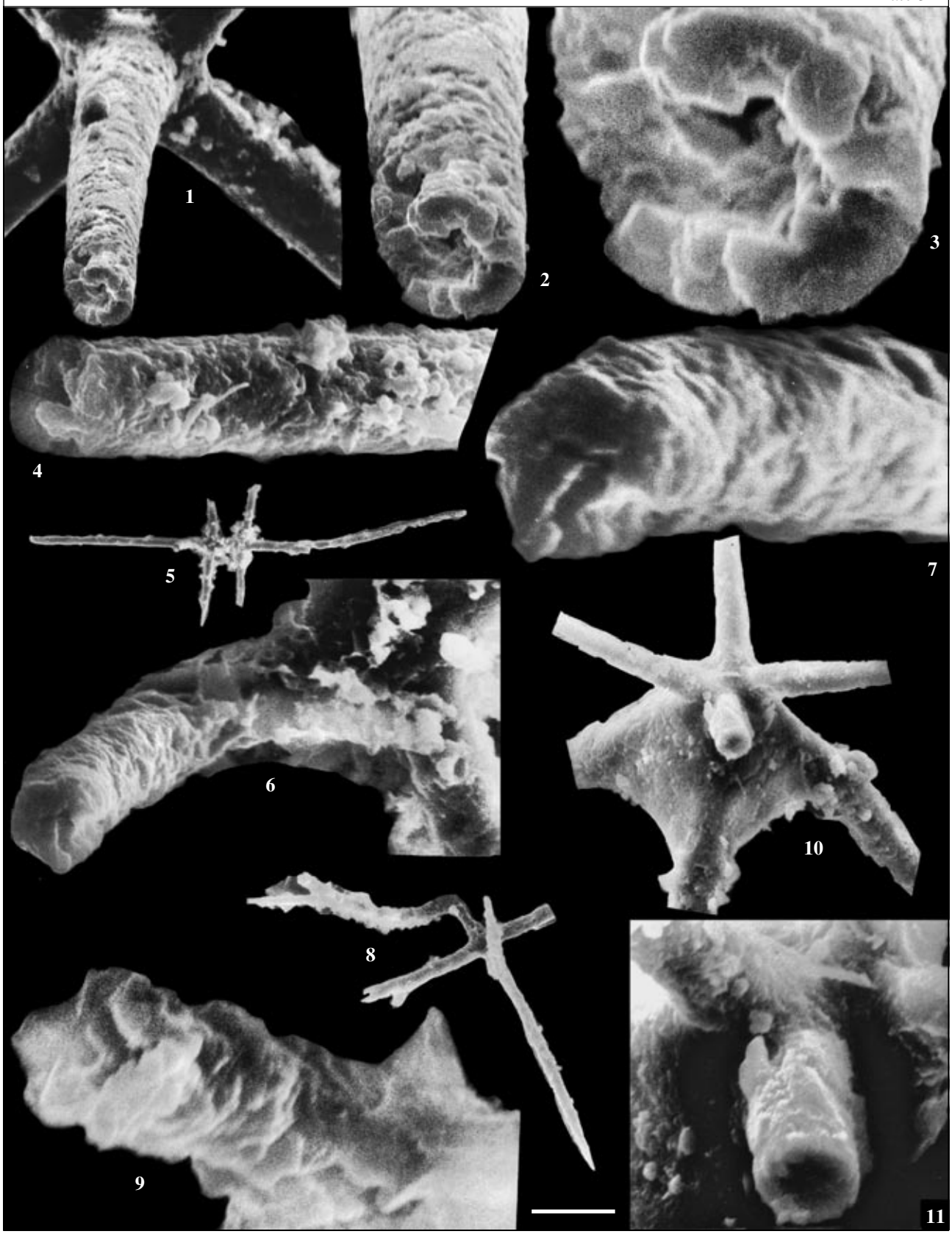

Spine structure in members of the order Aculearia.

Tests of Cessipylorinae (Figs. 42g, 42h) and Aciferopyloridae (Fig. 42i) from the Middle Ordovician–Silurian have a spherical skeleton with the inner frame in the shape of a hollow sphere and main conical spines distributed evenly over the entire test surface. This could make it difficult for organisms to acquire any fixed spatial orientation but allowed them to exist in a free lying state.

The peculiar subfamily Caspiazinae (Figs. 42j, 42k) apparently evolved from the Late Silurian spherical *Fusalfanus*, which were the last members of the subfamily Cessipylorinae (Fig. 42h). The evolution of the subfamily Caspiazinae in the Late Devonian–Middle Carboniferous could have been influenced by the occupation of a different ecological niche in the clearer water of reef-algal buildups, as happened on the reef massive Karachaganak in the Northern Caspian Sea region (Afanasieva, 1986, 1987). These taxa gradually adapted to life on the hard substrate by the prevailing development of the structures surrounding the pylome in a shape of a wide lamellar collar by which the shells were attached to the substrate. Besides, as in the convergently similar shells of the foraminifers *Tuberitina* (Poyarkov, 1979), the shape of the collar could be affected by the type of substrate. Individuals inhabiting even surfaces could develop a completely open collar (Fig. 17a; Pl. 20, figs. 9–11). In cases when the test was attached to subcylindrical objects such as the spines of sea urchins, a semi-open (Fig. 17b; Pl. 20, figs. 5, 6, 8, 12) or slitlike collar (Fig. 17c; Pl. 20, figs. 3, 4, 7) was likely to develop. A closed collar of the pylome (Fig. 17d; Pl. 20, figs. 1, 2), sometimes with secondarily fused edges, was apparently developed in radiolarians, which attached to threadlike objects or, possibly, the edges of algal thalli.

The last members of the subfamily Caspiazinae (genus *Glomeropyle*) was found in the Middle Triassic beds of eastern Siberia (Omolon Massif) and New Zealand (Waipapa Terrain) (Aita and Bragin, 1999) (Fig. 43).

Superfamily Pylentonemoidea

Spherical skeletons of Pylentonemoidea with their porous or, less commonly, spongy walls of the external sphere had an inner frame in a shape of a spicule (Figs. 42l–42x, 43). The general trend in the evolution of this superfamily followed the development of one or two long three-bladed main spines in the aboral part of the skeleton (Figs. 42l–42w, 43). The pylome of the shells is surrounded by three or four massive three-bladed main spines and, often, by many thin, rodlike by-spines. The development of such tests may be facilitated by the specific orientation of the bipolar skeleton, while the long spines probably precluded sinking of the organism into the semi-liquid sediment. Radiolarian with such a skeleton existed from the beginning of the Silurian to the end of the Early Cretaceous (Fig. 43).

The genus *Allocyrtium* (Figs. 16j, 42m) has a lamellar skeletal tissue developed on the three main spines surrounding the pylome, which makes the test elongated-conical in shape. The appearance of such shells in the Early Carboniferous was apparently one of the attempts of benthic organisms to proceed to a semiplanktonic mode of life in the bottom water layers. In the Late Jurassic, this attempt was repeated by the members of the family Vallupinae (Figs. 42x, 43).

More specialized members of Pylentonemoidea from the families Poulpidae and Tripedurnulidae appeared in the Middle Triassic and existed to the end of the Early Cretaceous (Figs. 42s, 42t, 43). The external skeletons in these taxa were segmented into the cephalis and thorax, while the first upper segment could be further subdivided into lobes in the late stages of the group's evolution. The rays of the spicule are directly connected to the main external spines. Strong feet are developed. The rays of the spicule contain spines *A*, *V*, *D*, *2L*, and *2l*, which extend from *MB*. However, the arcs connecting the rays on one level were yet to appear. The antapical part of the external skeleton has a large pylome surrounded by three or four spines.

In Tripedurnulidae the septum subdivides the cephalis into two chambers (lobes): the large chamber opening apically and a small chamber opening dorsally.

Morphological innovations of Pylentonemoidea allowed their longest existence among all Pylomariata, i.e., from the Silurian to the Early Cretaceous inclusive.

Similar to Popofskyelloidea, their evolution was pulsating: the impulses of their evolution were interrupted by hidden history. Direct descendants of this superfamily were not found in post-Cretaceous beds, thus suggesting that the excessive specialization of Pylentonemoidea in the Triassic–Early Cretaceous cut short the further evolution of this lineage.

Explanation of Plate 32

Upper Devonian, Middle Frasnian Substage, Domanik Formation; Timan–Pechora Province: (Figs. 1–3) Lyajol River, outcrop 1904, sample 6; (Fig. 4–11) borehole Shuda-Yag-1003: (4) sample 73 (depth 71.4–71.9 m), (5–9) sample 28 (depth 106-107 m), and (10, 11) sample 29 (depth 105-106 m).

Figs. 1–4. *Palacantholithus stellatus* Deflandre: (1) scale bar = 21 μm; (2) fragment, bar = 10 μm; (3) fragment, bar = 5 μm; and (4) bar = 7 μm.

Figs. 5–7. *Ceratoikiscum?* cf. *vimenum* Nazarov et Ormiston: (5) bar = 72 μm; (6) fragment, bar = 7 μm; and (7) fragment, bar = 4 μm.

Figs. 8 and 9. *Nazarovites pinnula* Afanasieva: (8) bar = 42 μm and (9) bar = 4 μm.

Figs. 10 and 11. *Palaeoscenidium scaurum* Afanasieva: (10) bar = 20 μm and (11) fragment, bar = 7 μm.

Plate 33

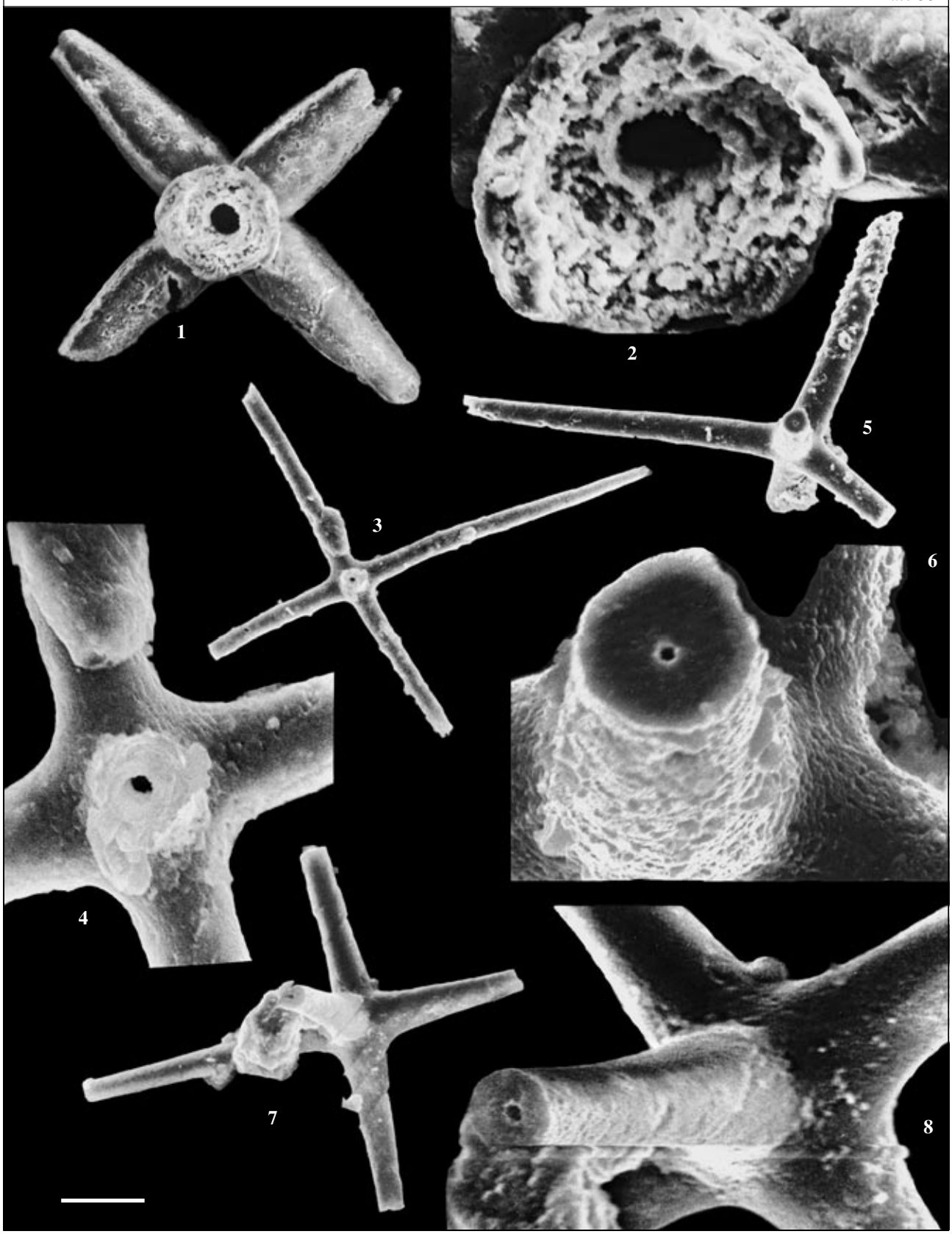

Spicules of sponges.

During their evolution the superfamilies Proventocitoidea, Popofskyelloidea, and Pylentonemoidea developed general features of the nassellarian type of the skeleton, characterized by the presence of the initial spicule with a stable number and morphology of spines and by the heteropolar external sphere with a pylome and aperture, which is subdivided into segments, or chambers. The further evolution of nassellarians occurring in the Mesozoic and Cenozoic and based on the morphology achieved by the superfamilies Proventocitoidea, Popofskyelloidea, and Pylentonemoidea led to the appearance of a vast number of various topologies of the spicule, of the ways how it was attached to the external shell, of different number and many various shapes of the segments of the shell, number and shape of the external spines, etc.

On the other hand, the analysis of the morphological characters of radiolarians with a pylome that are known at present and their comparison with the extant and fossils foraminifers supports the hypothesis by Petrushevskaya (1971, 1977, 1981a, 1984, 1986) who suggested that Nassellaria were related to the benthic sessile taxa. In addition, the structures surrounding the pylome of *Caspiaza* in a shape of a collar (Fig. 16g) are repeated in the younger (Middle–Late Triassic) and very peculiar nasselarians *Bulbocyrtium* (Figs. 16c, 45z).

"The connection of the modern planktonic groups with their benthic ancestors is so great that these groups cannot be discussed other than in the connection with the benthic Actinopoda. … Probably, the ancestors of all radiolarians had a mineral skeleton as an adaptation to the benthic way of life" (Petrushevskaya, 1981b, p. 16).

Morphology of Mesozoic and Cenozoic Nassellarians

The siliceous skeleton of nassellarians are extremely complex (Fig. 45). According to Petrushevskaya (1971, 1981a, 1984, 1986; Petrushevskaya and Menshutkin, 1990; Nazarov and Petrushevskaya, 1995) several groups of morphological elements almost equally participating in the skeletons can be recognized. Firstly, these are internal and external structures (initial spicule and inner polyhedron), secondly, external shell with its segmentation and ornamentation (Fig. 46).

The shape of the skeleton. Externally, the shell is most often heteropolar, conical, pyramidal, conical, spindle-shaped, bell-shaped, helmet-shaped, cup-shaped, etc. The apical and antapical parts (or ends) of the test are recognized. In illustrations, the apical end is shown at the top, whereas the antapical end is shown at the bottom. The number of segments in the shell does not make any difference.

The skeleton of Nassellaria usually consists of the cephalis (*cep*), thorax (*tor*), abdomen (*abd*), and the postabdominal segments (*pab*) (Fig. 46a). Sometimes, the segments are grouped into portions of the test that are designated by the terms: cephalic, thoracic, postthoracic, postabdominal parts, and cephalothorax.

One of the main features of Nassellaria is that the vast diversity of their skeletons is achieved by the additional structures on their cephalis that increase the heteropolarity of their body. These add-ons are connected to the main spines and represent chambers (segments) delineated from each other by more or less sharp constrictions, sometimes by inner rims (Fig. 46a).

The apical part of the test (cephalis) often possesses one or several apical horns. The antapical part of the shell possesses a pylome, an aperture, and apertural appendages. The last antapical segment possessing the aperture is often narrowed distally and is elongated to form a peristome tube (Fig. 46a).

The external surface of the thorax often possesses peculiar basal feet, or external appendages of the test of Nassellaria usually formed by spines *D*, L_l, and L_r, which are as long as the thorax, and sometimes continuing further down. Apart from the feet, the external appendages include wings, or porous lateral appendages of the test of Nassellaria, which are the external continuations of the spines *D*, L_l, and L_r, connected to the test wall.

Spines. The spines (rays) meet in the center of the skeleton somewhat eccentrically. The number and arrangement of spines of Nassellaria is stable (Figs. 46a, 46b). Jörgensen (1905) was first to introduce letters to designate these spines. Presently, it is agreed that spines *A*, *D*, and *2l* extend from one end of the median bar *MB*, while spines *V*, *2L*, and *Ax* extend from the other end (Figs. 46, 47).

The median bar (*MB*) is a skeletal bar of the spicule from which the main spines extend and which is located at the boundary between the cephalis and thorax. The apical spine (*A*) extends from the same end of the median bar (*MB*) and forms an apical horn outside the shell. The dorsal spine (*D*) is the main spine of the skeleton of Nassellaria, extending from the same end of the median bar *MB*. Spine *D*, like spine *A*, extends through the shell wall at the boundary of the cephalis and thorax

Explanation of Plate 33

Upper Devonian, Frasnian Stage; Timan–Pechora Province: (Figs. 1, 2, 5, 6) Middle Frasnian Substage, Domanik Formation: (1, 2) Domanik River, quarry 2, sample 5; and (5, 6) Lyajol River, outcrop 1904, sample 6; (Figs. 3, 4) Upper Frasnian Substage; Ukhta River, sampling point no. 1, sample 7001; and (Figs. 7, 8) Lower Frasnian Substage; Chut' River, outcrop 7, sample 1.2b.

Figs. 1 and 2. Triaxonida? sp. 403: (1) scale bar = 67 μm and (2) fragment, bar = 21 μm.

Figs. 3–8. Triaxonida? sp. 407: (3) bar = 40 μm; (4) fragment, bar = 10 μm; (5) bar = 67 μm; (6) fragment, bar = 10 μm; (7) bar = 32 μm; and (8) fragment, bar = 10 μm.

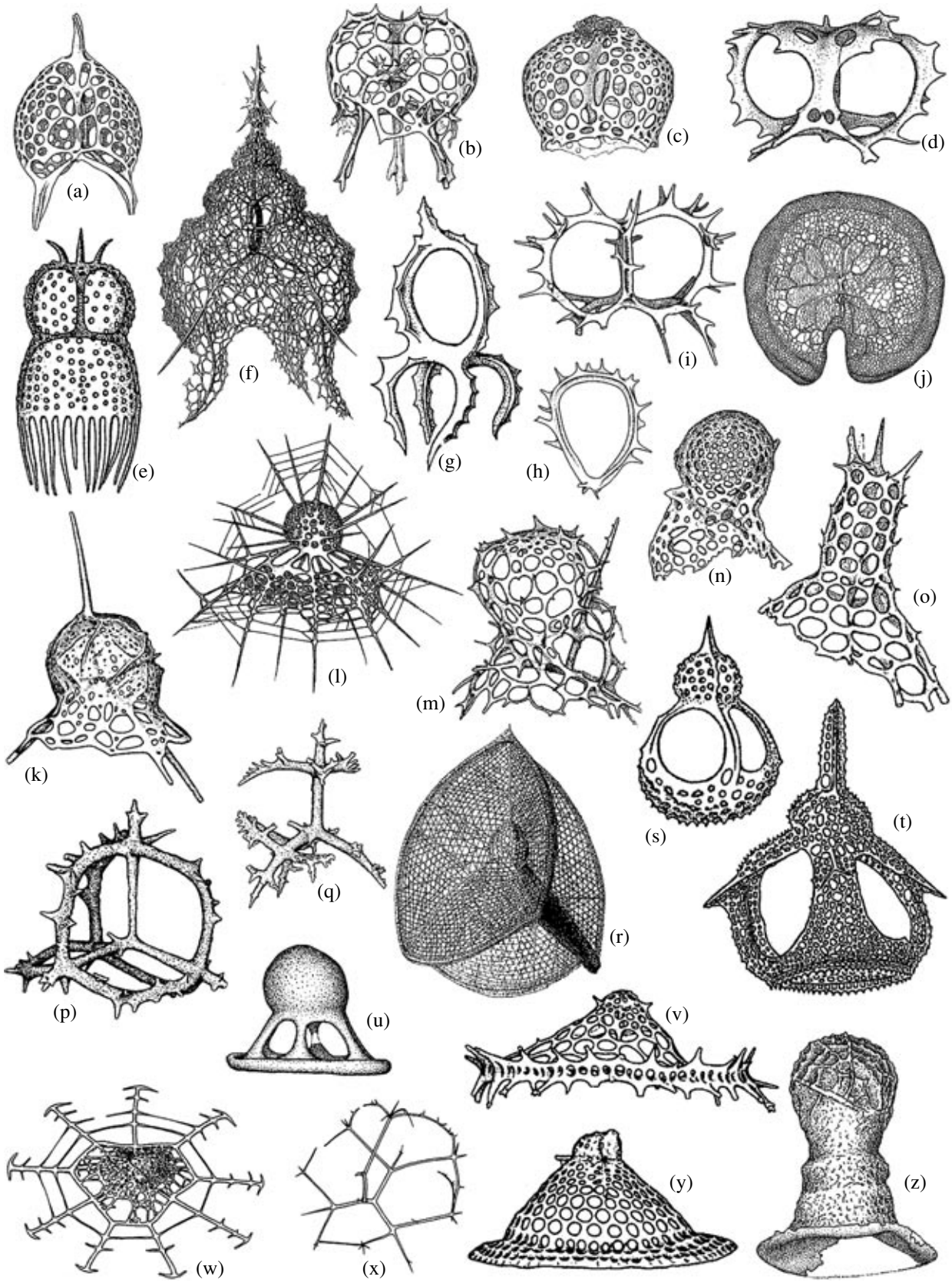
(a)
(b)
(c)
(d)
(e)
(f)
(g)
(h)
(i)
(j)
(k)
(l)
(m)
(n)
(o)
(p)
(q)
(r)
(s)
(t)
(u)
(v)
(w)
(x)
(y)
(z)

Fig. 45. Nassellaria: (a–j) order Spyridinata, and order (k–z) Cyrtidinata: (a–f) family Triospyrididae (Paleogene–Recent): (a) *Tholospyris acuminata* Hertwig, (b) *Triceraspyris* sp., (c) *Ceratospyris* sp., (d) *Corythospyris damaecornis* Haeckel, (e) *Rhodospyris tricornis* Haeckel, and (f) *Lamprospyris darwinii* Haeckel; (g, h) family Stephaniidae (Paleogene–Recent): (g) *Stephanium quadrupes* Haeckel and (h) *Zygocircus productus* (Hertwig); (i, j) family Acanthodesmiidae (Eocene–Recent): (i) *Acanthodesmia vinculata* (Müller) and (j) *Paradictyum paradoxum* Haeckel; (k–q) family Archipiliidae (Triassic–Recent): (k) *Nabolella* sp., (l) *Arachnocorys circumtexta* Haeckel, (m) *Phormacantha hystrix* (Jogensen), (n) *Lophophaena ehrenbergii* (Bütschli), (o) *Amphiplecta cylindrocephala* Dumitrica, (p) *Zamolxis corona* Dumitrica, and (q) *Tetrarchiplagia arborescens* Dumitrica; (r–t) family Sethoperidae (Jurassic–Recent): (r) *Callimitra agnesae* Haeckel, (s) *Sethopera tricostata* Haeckel, and (t) *Clathrocanium diadema* Haeckel; (u) family Pseudosaturniformidae (Middle Triassic–Jurassic): *Pseudosaturniforma minuta* Blome; (v) family Lampromitridae (Cretaceous–Recent): *Lampromitra petrushevskayae* Dumitrica; (w–y) family Sethophormididae (Triassic–Recent): (w) *Enneaphormis rotula* Haeckel, (x) *Protoscenium simplex* (Cleve), and (y) *Cecryphalium sestrodiscus* Haeckel; and (z) family Bulbocyrtiidae (Middle–Late Triassic): *Bulbocyrtium reticulatum* Kozur and Mostler.

and forms the external appendage on the wall of the thorax. Secondary lateral spines l_r and l_l are paired (right and left) spines, symmetrically diverging from the same end of *MB* as the spines *A* and *D*. They may sometimes form external appendages of the shell connected to the wall of the thorax (Fig. 46).

The vertical spine (*V*) is the main spine extending from the same end of the median bar (*MB*) as spines *L* and *Ax*. It can form an external horn or tube on the cephalis. The main lateral spines (L_r and L_l) are paired (right and left) spines extending in Nassellaria from the same end of the median bar *MB* as spine *V*. The axial spine or

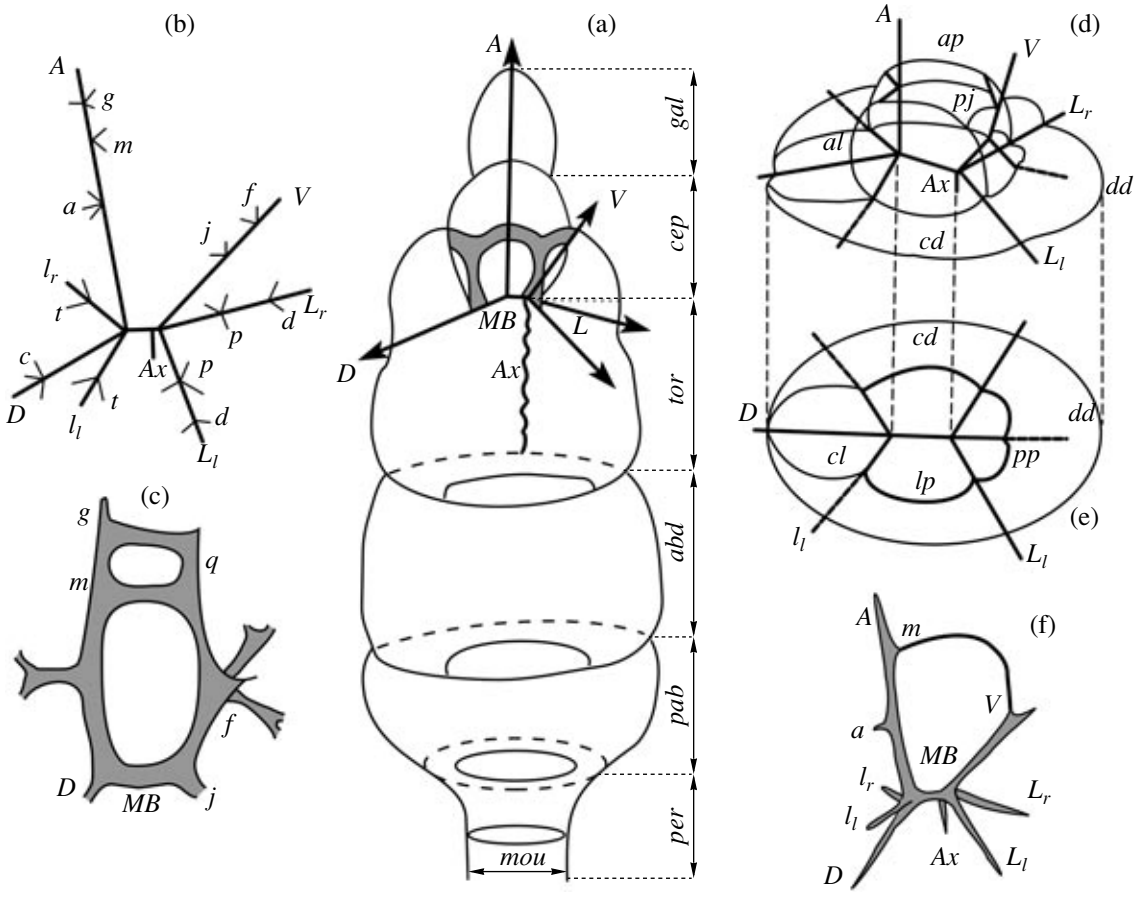

Fig. 46. Scheme of the skeleton structure of Nassellaria (after Petrushevskaya, 1981a). (a) external test; (b, f) initial spicule; (c) sagittal and galear rings; and (d, e) main archs, lateral view and from above. Designations: (*A*) apical spine; (*a*) anterior apophyses of the apical spine *A*; (*abd*) abdomen; (*al*, *ap*, *aa*, *pj*, *cd*, *cl*, *lp*, *pp*, *dd*) arches of the cephalis; (*Ante*) antecephalic lobe of the cephalis; (*Ax*) axobate; (*c*) cervical apophyses of the dorsal spine *D*; (*cep*) cephalis; (*D*) dorsal spine; (*d*) apophyses of spine *L*, following after the pectoral apophyses; (*Euc*) eucephalic lobe of the cephalis; (*f*) furcal apophyses of spine *V*; (*g*) galear apophyses of spine *A*; (*gal*) galea; (*j*) jugal apophyses of spine *V*; (L_r) and (L_l) right and left main lateral spines; (l_r) and (l_l) right and left additional lateral spines; (*MB*) median bar; (*m*) mitral apophyses of spine *A*; (*nec*) neck; (*p*) pectoral apophyses of spine *L*; (*pab*) postabdominal segment; (*per*) peristome; (*mou*) mouth; (*Pstc*) postcephslic segment of the cephalis, (*q*) apophyses of the sagittal ring, (*t*) tergal apophyses of spine *l*, (*tor*) thorax, and (*V*) vertical spine.

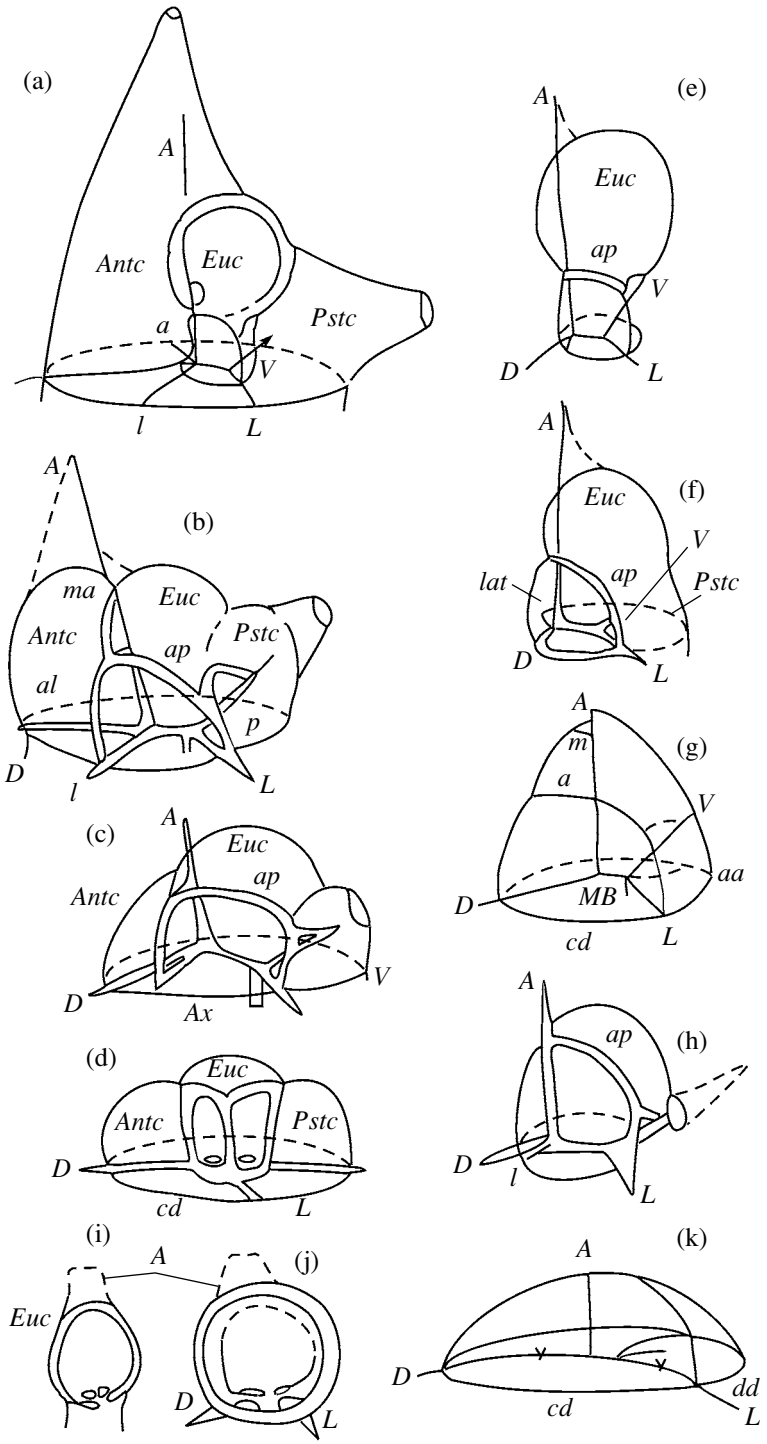

Fig. 47. Types of cephales of Nassellaria (after Petrushevskaya, 1981a): (a, b) botryd, (c) artostrobid, (d) carpocanid, (e) with a constricted neck, (f) pterocoryd, (g) with a columella, (h) acropyramid of the second type, (i) bulbous, (j) theoperid, and (k) acropyramid of the first type. Designations of arches of the cephalis: (*Antc*) antecephalic, (*Euc*) eucephalic, (*Pstc*) postcephalic, (*lat*) lateral. Indices for spines and arches as in Fig. 46.

axobate (*Ax*) is a spine extending from the median bar *MB* and directed toward the cavity of the thorax and subsequent segments. It can be split and composed of several parallel filaments.

Inner frame. Nassellaria often have the inner tangential structure of the first type within 5–15 μm of the meeting point of main spines in a shape of arched bars, or arcs, together with the main spines of the initial spi-

cule composing a so-called central inner frame, which Mordukhai-Boltovskoy (1936) called the inner polyhedron. The next layer of tangential structures of Nassellaria sometimes forms an inner polyhedron of the second type, about 50 μm in diameter. While the first inner polyhedron is located somewhat eccentrically, the walls of both polyhedrons may be connected in a point to represent the complex (Fig. 47) of the first segment of the cephalis of Nassellaria (Petrushevskaya, 1971, 1981a). The arcs of polyhedrons are also designated by letters (Fig. 46) (Petrushevskaya, 1971, 1981a; De Wever *et al.*, 2001).

The inner polyhedron of the first type sometimes, especially, in primitive groups (Carpocaniidae), is enclosed within the walls of the cephalis or is fused with them. The inner polyhedron of the third type is extremely rarely present in Nassellaria. It represents bars adjacent to the walls of the cephalis (*Nephrodictyum*) and is connected not to the main spines, extending from the central frame, but to the auxiliary spinules rising toward the surface of the cephalis.

Cephalis. From the works of Haeckel (1887) onward, the cephalis of Nassellaria has been identified as the first segment of the porous shell. According to Petrushevskaya (1971, 1981a), the cephalis is the most important part of the nassellarian skeleton, which is formed by the complex of (a) radial spines, (b) small arcs (5–15 μm), and (c) external porous walls and/or arcs 30–50 μm in radius (Fig. 47).

The following types of the cephalis of Nassellaria are recognized (Fig. 47): botryd; artostrobid; carpocanid, with constricted neck; pterocoryd, with a columella; acropyramid of the first, second, and third types; bulbous; and theoperid (Petrushevskaya, 1981a).

The cephalis may be subdivided into parts, or lobes (Fig. 47), which are separated from each other by the arcs of the inner polyhedrons of the first and second types and by the main spines of the initial spicules (Fig. 46). The following segments are recognized: eucephalic lobe, containing the main elements (*MB*, *A*); antecephalic lobe (containing spine *D* at its base); postcephalic lobe, connected to the spine *V*; and lateral lobes, delineated by the arcs *al* and *ap*.

Depending on the development and proportions of the lobes, different types of cephales in Nassellaria are recognized. This is the basis for their classification. The cephalis possesses cephalic horns, or external appendages in a shape of more or less massive spines, which are formed on the cephalis by main spines *A* and *V* and by secondary spines.

Sometimes, the appendages of the cephalis appear not on the side of *MB* or aperture, but on the opposite pole. These are the galea (*gal*), and the tubes of the antecephalic lobe of the cephalis connected to spine *A* and tubes connected to spine *V* (Fig. 46a) (Haeckel, 1887; Popofsky, 1913; Petrushevskaya, 1971, 1981a). The galea is the helmet-shaped segment of the Nassellaria test, connected to the apical horn. The upper wall of the cephalis is the basis of the galea. Usually, the mitral and galear apophyses of spine *A* and the sagittal ring are connected to the galea. In Spyridinata a galear ring is present, i.e., connected skeletal appendages *g* and *q* that form a galear structure occurring in the sagittal cavity (Fig. 46c). The galear apophyses (*g*) are the processes of the apical spine of Nassellaria extending further from its base than the mitral bars. The mitral rods or apophyses and bars (*m*) are the appendages of the apical spine of the skeleton of Nassellaria extending further from its base that appendages *a* but closer than galear apophyses *g* (Fig. 46a). The Spyridinata have a mitral horizontal ring lying in a plane perpendicular to the sagittal ring and parallel to the basal ring; usual formed by the arcs *mq*.

Shells. Nassellaria have a very complex construction of the shell wall. It may be (1) a relatively solid wall with rare and small pores (lamellar tissue); (2) a shell with large, densely spaced pores (porous tissue); (3) fine meshwork composed of polygonal meshes (lattice and reticular tissue); and (4) irregular loose, multilayered intersections of filaments and thin bars (spongy tissue).

Pores can be rounded, ellipsoid, or irregular in shape. The thin-walled shell is usually perforated by closely spaced pores. The width of the bars in these cases is often less than the diameter of the pores themselves. The wall usually has thickened zones creating a meshwork (irregular, hexagonal, or close to orthogonal) that forms polyhedrons 8–20 μm in diameter. The latter may not be filled by the skeletal matter and appear as large pores. Sometimes they are covered by a thin meshwork of thin bars retaining small pores (Acropyramididae, Theopiliinae). The pores may be arranged randomly or regularly. In the latter case, the pores are arranged in a linear pattern on the vertices of squares or rectangles (as much as the curved surfaces of spheres allow). Sometimes, the pores may be arranged in diagonal rows, resembling the optimal "hexagonal package," but the hexagonal shape of the pores is never perfect, because their angles are always slightly rounded.

The most regular pattern of pore arrangement (checkerboard or hexagonal pattern) combined with the situation when the bars are thinner and the total area of pores is larger results in a completely irregular, so-called spongy pattern of the arrangement of the skeletal elements. The irregular meshwork of very fine bars may be considered to be the highest level of the development of tangential skeletal structures of Polycystina. The spongy type of the skeletal tissue, including the spongy envelopes around the porous shell, has been known to exist in Nassellaria for a long time. Besides, sometimes they have an openwork modification when the entire skeleton is formed from the very fine threads (Petrushevskaya, 1971, 1981a).

COLLODARIA

Records of colonial Radiolaria accumulated from the mid-19th century onward. Meyen (1834a) was the first to mention them in the report about his circumnavigation of the world. He described three varieties of *Physematium* discovered by him in a gelatinous medium. Colonial radiolarians as a new group of colonial protists (Polyzoa) as opposed to the solitary radiolarians (Solitaria) were recognized by Müller (1858) when he studied the composition of plankton in the Mediterranean Sea.

Haeckel (1862) subdivided radiolarians into two groups, Polyzoa and Monozoa. In his fundamental monograph, Haeckel (1887) subdivided the legion Spumellaria into two suborders, Collodaria (lacking skeleton, or with a skeleton of separate spicules) and Sphaerellaria (with a skeleton represented by a complete latticed shell). The superorder Collodaria was subdivided into two orders: Colloidea and Beloidea (Table 8). For the system of colonial radiolarians, Haeckel (1887) used the presence or absence of the skeleton, main features of its structure (as isolated spicules or as variously constructed shells): the family Collozoidae (the colony is formed by individuals containing only central capsules), the family Sphaerozoidae (the central capsules of the colonies are surrounded by spinules), and the family Collosphaeridae (central capsules are surrounded by shells).

The further history of study of colonial radiolarians is connected with the research of Brandt (1882, 1902, 1905). Brandt studied the entire colony and revealed a large scope of individual variability within the colonies of different species. He recognized colonial radiolarians as a separate group Sphaerozoa (Polyzoa) and united two families of colonial radiolarians (Sphaerozoidae and Collosphaeridae) into the superfamily Sphaerozoida (Table 8).

Haecker (1908) proposed the following classification of colonial and large solitary radiolarians (Table 8). The suborder Polycyttaria includes all colonial radiolarians: both those with a skeleton formed by spicules (Sphaerozoidae) and those with a latticed test (Collosphaeridae). The suborder Collodaria includes solitary radiolarians that either lack a skeleton (Thalassicollidae and Thalassophysidae) or have the skeleton formed by isolated spicules (Physematidae, Thalassothamnidae) or the skeleton in a shape of a latticed sphere (Orosphaeridae).

The classification of colonial radiolarians proposed by Hollande and Enjumet (1953) was based on the cytoplasmic studies of the cell structure (Table 8).

Strelkov and Reshetnyak (1971) made a comprehensive study of the colonial radiolarians of the Pacific. Following Brandt (1902), they accepted the superfamily Sphaerozoida with two families, Sphaerozoidae and Collosphaeridae (Table 8).

In the monograph of Petrushevskaya (1986), Collodaria are considered as an order that comprises colonial and solitary taxa of eight families (Table 8): Thalassosphaeridae, Sphaerozoidae, Thalassicollidae, Thalassophysidae, Physematidae, Collosphaeridae, Orosphaeridae, and Thalassothamnidae (only three last taxa were described by her).

De Wever *et al.* (2001) considered Collodaria as an order that comprised large solitary or colonial taxa of three families (Table 8): Thalassosphaeridae, Sphaerozoidae, and Collosphaeridae.

In the present paper we suggest that the rank of colonial radiolarians be raised to a class, based on the exoaxoplastic type of shell construction (Fig. 1a). This type of cytological structure distinguishes colonial radiolarians Collodaria from all other radiolarians (excluding Phaeodaria) that have endoaxoplasty (Hollande and Enjumet, 1960; Cachon and Cachon, 1971, 1976a, 1976b; Petrushevskaya, 1986). The class Collodaria includes three families Thalassosphaeridae, Sphaerozoidae, and Collosphaeridae (Tables 7, 8).

The class Collodaria includes large solitary or colonial Polycystina. The colonies represent a variously shaped gelatinous substance up to 3 m long and containing numerous individuals up to 400–800 μm in size (Figs. 48a, 48d, 48f).

Each individual has a well-developed endo- and ectoplasm, which are separated by the wall of the central capsule, which is at least 100 μm in diameter. The wall may be porous but most often loose, almost spongy (Fig. 1a). Pseudopodia extending from the ectoplasm form anastomoses with the pseudopodia of neighboring individuals that penetrate the jelly layer of the colony (Figs. 1a, 48c). A system of pseudopodia provides a connection between all individuals and controls the distance between them.

The cell of Collodaria is multinuclear (Fig. 1a). Apart from the nuclei, the endoplasm contains a lipid droplet of and a few celestine crystals (Fig. 1a). The lipid droplet (less commonly two or three, but sometimes over 50 droplets) serves both as a hydrostatic apparatus and as nutrition (Müller, 1858; Hertwig, 1876, 1879; Haeckel, 1887; Strelkov and Reshetnyak, 1971).

Growth of celestine crystals begins with the appearance of elongated granules adjacent to the nucleus (Hertwig, 1876, 1879). Primary granules of celestine slowly grow into small crystals, which later move into gametes (Fig. 49a). After the exit of the gametes, large celestine crystals remain within the central capsule and the siliceous skeleton (Figs. 1a, 49b, 49c). Dogel (1950) placed a large importance to the presence of celestine crystals in the phylogeny of Radiolaria. He believed that the presence of large celestine crystals in the central capsule of colonial radiolarians was an important evidence of the primitiveness of the colonial taxa, the ancestors of which gave rise to all other taxa of Radiolaria.

Colonial Polycystina has (1) vegetative reproduction by the subdivision of the colony and (2) separation of the cytoplasmic body of individuals in the colony

Table 8. Comparison of the taxonomic schemes for the class Collodaria

Haeckel, 1887		Brandt, 1905		Haecker, 1908		Hollande and Enjumet, 1953	Strelkov and Reshetnyak, 1971	Petrushevskaya, 1986	De Wever *et al.*, 2001	Afanasieva and Amon, present paper
Beloidea	Thalassosphaeridae	Sphaerozodia		Polycyttaria		Thalassosphaeridae		Thalassosphaeridae	Thalassosphaeridae	Thalassosphaeridae
	Sphaerozoidae		Sphaerozoidae		Sphaerozoidae	Sphaerozoidae	Sphaerozoidae	Sphaerozoidae	Sphaerozoidae	Sphaerozoidae
Collozoidea	Collozoidae		Collosphaeridae		Collosphaeridae	Collosphaeridae	Collosphaeridae	Collosphaeridae	Collosphaeridae	Collosphaeridae
	Thalassicollidae			Collodaria						
					Thalassicollidae	Thalassicollidae		Thalassicollidae		
					Thalassophysidae	Thalassophysidae		Thalassophysidae		
					Physematidae	Physematidae		Physematidae		
					Orosphaeridae			Orosphaeridae		
					Thalassothamnidae			Thalassothamnidae		

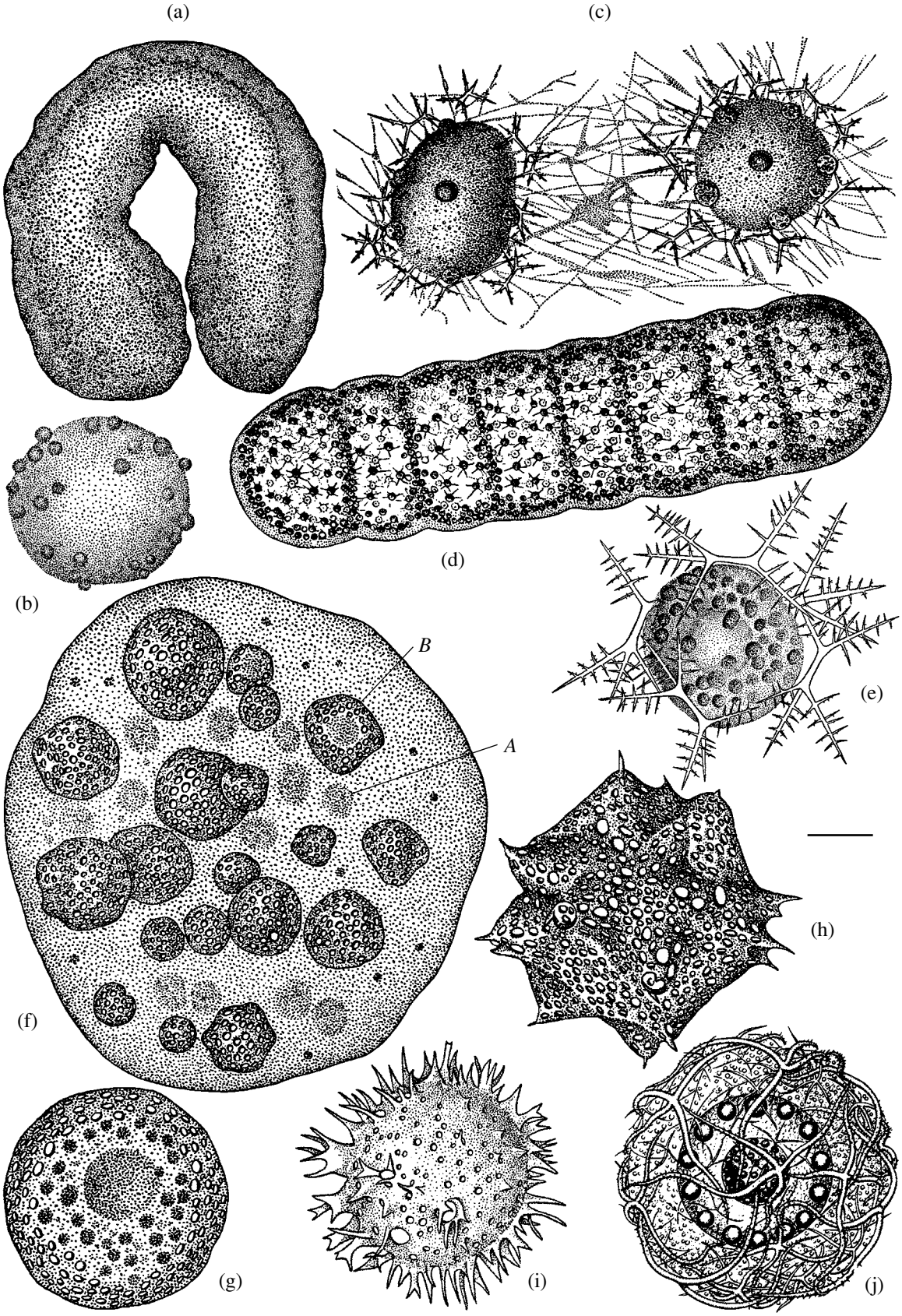
(a)
(c)
(b)
(d)
(e)
B
A
(f)
(h)
(g)
(i)
(j)

Fig. 48. Collodaria: (a, b) *Collozoum inerme* (Müller), 1855: (a) general view of the colony (hatch = 2.5 mm), (b) an individual (= 50 μm); (c–e) *Sphaerozoum punctatum* (Meyn, 1834): (c) tests of one colony connected to each other by pseudopodia (= 120 μm), (d) general view of a colony (= 1.5 mm), and (e) one individual (= 55 μm); (f, g) *Collosphaera huxleyi* (Müller), 1855: (f) general view of a colony (= 300 μm), (*A*) small dividing individual without skeletons, (*B*) large nondividing individuals surrounded by the skeleton, (g) one individual (= 95 μm); (h) *Solenosphaera collina* (Haeckel), 1887 (= 45 μm); (i) *Astrosphaera spinosa* (Haeckel), 1862 (= 50 μm); (j) *Thalassoxanthium medusinum* Haeckel, 1887 (= 60 μm); (a–i) after Strelkov and Reshetnyak (1971); (j) after Haeckel (1887).

into numerous gametes with crystals of celestine in each (Fig. 49a).

The ectoplasm contains a skeleton represented by tangentially arranged spines (Figs. 48e, 48j) or a porous shell (Figs. 48g–48i). The mineral skeleton is often absent (Fig. 48b).

SYSTEMATIC PALEONTOLOGY

Phylum Radiolaria Müller, 1858

Diagnosis. Marine, solitary or colonial, planktonic or benthic (fossil) Protozoa with internal secreted siliceous skeleton, extremely diverse, and strictly geometrical in shape. Cell cytoplasm composed of two parts: ecto- and endoplasm, separated by organic central capsule. Central capsule developed in all radiolarians. Thickened shell of the central capsule with pores (and fusules), through which intra- and extracapsular cytoplasm communicate with each other, and axopodia exit.

Proximal ends of the axonemes are fixed in axoplasts. Axoplasts are differently shaped and arranged in different groups (Fig. 1).

Ectoplasm is often vacuolated, and calymma is formed. At vegetative stage, radiolarians lack flagella, but have pseudopodia (axopodia or phylopodia) used to collect food. System of pseudopodia and calymma with vacuoles serve as hydrostatic apparatus for vertical migrations.

Vegetative stages usually mononuclear, except some Phaeodaria with two nuclei, and some Collodaria, which may be multinuclear. Encysting reproduction is unknown. Sporogenesis with flagellate isopores is observed. More rarely reproduction by subdivision into two is observed.

Radiolaria live in all oceans and seas with normal salinity (32–36‰ to 38‰) from surface waters to abyssal depths 5000–8000 m. Some radiolarians live in oceanic depressions at depths of 10000–11000 m.

Composition. Two superclasses: Polycystina Ehrenberg, 1838 and Phaeodaria Haeckel, 1879.

Occurrence. Cambrian–Recent.

Superclass Phaeodaria Haeckel, 1879

Diagnosis. Solitary Radiolaria, with pear-shaped central capsule possessing three large openings and wall composed of chitinous substance. Astropile (cytopharix) is main opening, which is responsible for transport of food and metabolic products between endo- and extracapsular plasm. Two smaller openings are parapiles (special) zones of wall of central capsules, in which the axoplasts are located. Axonemes extend from axoplasts but do not go deep inside central capsule, which is characteristic of exoaxoplasty (Fig. 1a). Microtubules in axonemes are hexavalent, bridges are poorly discernible. Siliceous skeleton from spine-shaped to globose (polyhedral), often heteropolar. Opaline skeletons of Phaeodaria mostly consist of amorphous $SiO_2 \cdot nH_2O$, Al, and up to 1% Mg and Ca. Wall of mineral skeleton often contains cavities and meshes. In Phaeodaria biomineral components of siliceous skeleton are loosely packed, and hence are virtually not preserved in fossils. Phaeodaria live in open seas and

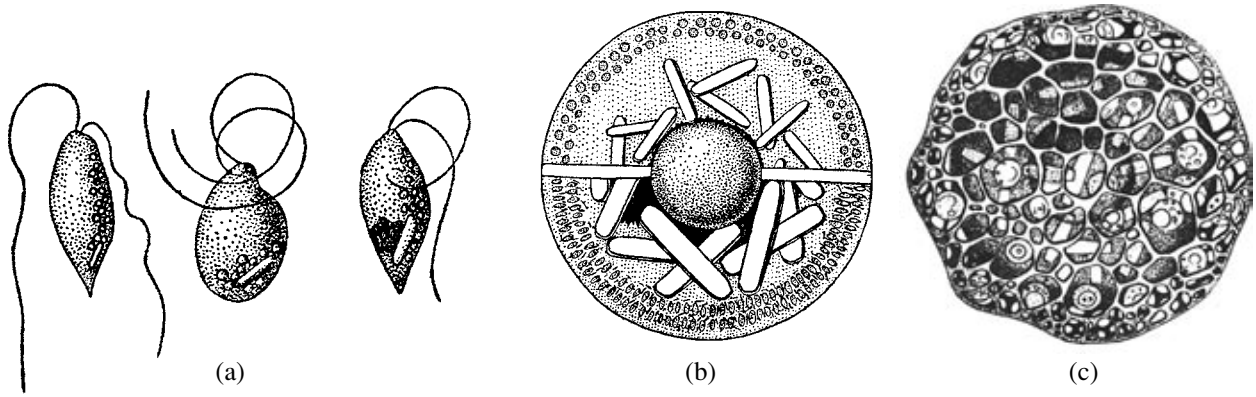

Fig. 49. Crystals of celestine in a cell of Collodaria: (a) gametes with celestine crystals (after Brandt, 1885); (b) arrangement of the celestine crystals in the central capsule (after Strelkov and Reshetnyak, 1971); and (c) *Collosphaera huxleyi* (Müller) with celestine crystals (after Dogel, 1950).

oceans with normal salinity ranging from 100 m to maximum depths, but are especially abundant at depths of 100–200 m.

Occurrence. Late Cretaceous–Recent.

Superclass Polycystina Ehrenberg, 1838

Diagnosis. Solitary and colonial Radiolaria, with variously shaped central capsule with wall, composed of glycoprotein plates. Nucleaxopodial complexes variable. In case of exopaxoplasty (Fig. 1a), axonemes have axoplast occurring outside, near central capsule (Class Collodaria). Endoaxoplastic polycystines (classes Nassellaria, Sphaerellaria, Spumellaria, Aculearia, and Stauraxonaria) have axonemes entering central capsule through fusules, where axoplast located (Figs. 1b–1g). Bivalent and trivalent microtubules alternate in axonemes.

Opaline skeletons of Polycystina very diverse in shape and for 98% consisting of amorphous $SiO_2 \cdot nH_2O$ with 1–4% admixture of Mg, Ca, Al, and Na. Ultrastructural elements in skeleton of Polycystines compactly packed, enabling their good preservation in fossils and their important biostratigraphic, paleoecological, and rock forming significance.

Polycystines live in seas and oceans with normal salinity from surface to maximum depth, but especially abundant at depth of 50–400 m.

Composition. Six classes: Aculearia Afanasieva, 1999, emend. Afanasieva et Amon, 2003; Sphaerellaria Haeckel, 1881; Spumellaria Ehrenberg, 1875, emend. Afanasieva et Amon, nov.; Stauraxonaria Afanasieva et Amon, classis nov.; Nassellaria Ehrenberg, 1847, emend. Afanasieva et Amon, nov.; and Collodaria Haeckel, 1881 (Table 7).

Occurrence. Cambrian–Recent.

Class Aculearia Afanasieva 1999, emend. Afanasieva et Amon, 2003

Diagnosis. Heteropolar and bilaterally symmetrical Polycystina with skeleton consisting of several intersecting spines: (1) spines intersecting in one or two centers; (2) three interconnecting spines form subtriangular frame; (3) two long columellae connected below aperture by horizontal bar, form **H**-frame in basal part of skeleton and subsagittal structure in apical region (Figs. 25, 26).

Composition. Three orders: Fasciculata Afanasieva et Amon, 2003; Triangulata Afanasieva et Amon, 2003; and Albaillellata Deflandre, 1953, emend. Afanasieva et Amon, 2003 (Figs. 26, 30; Table 7).

Remarks. Spiny radiolarians with spiny or spiny-framed skeletal constructions first described by Afanasieva (1999, 2000a, 2000b, 2002) as a separate order Aculearia. However, at present, based on skeletal morphology, spiny radiolarians are assigned to the class Aculearia, comprising three orders (Afanasieva and Amon, 2003, 2005) (Figs. 26, 30; Table 7).

Occurrence. Cambrian–Jurassic.

Order Fasciculata Afanasieva et Amon, 2003

Diagnosis. Aculearia wit ha heteropolar skeleton composed of several main spines intersecting in one or two centers (Figs. 25a–25i, 26, 27).

Composition. Four families: Palacantholithidae Kozur et Mostler, 1981, emend. Afanasieva et Amon, nov.; Plagiacanthidae Hertwig, 1879, emend. Afanasieva et Amon, nov.; Xiphocladiellidae Nazarov, 1984, emend. Afanasieva et Amon, nov.; and Palaeoscenidiidae Riedel, 1967, emend. Nazarov et Rudenko, 1981 (Figs. 26, 30; Table 7).

Occurrence. Cambrian–Recent.

Family Palacantholithidae Kozur et Mostler, 1981, emend. Afanasieva et Amon, nov.

Diagnosis. Fasciculata with skeleton, composed of spines intersected in one center. Main spines lacking auxiliary spines, or apophyses. (Figs. 25a, 25b, 26, 27c).

Composition. *Palacantholithus* Deflandre, 1973; *Palaeoumbraculum* Amon et Braun, 1995; and Palacantholithidae gen. et sp. indet. (Nazarov), 1988.

Remarks. This group of spiny radiolarians has the most simply constructed skeletons, and hence, separated in an independent family.

Occurrence. Cambrian–Late Jurassic.

Family Plagiacanthidae Hertwig, 1879, emend. Afanasieva et Amon, nov.

Diagnosis. Fasciculata with skeleton composed of main spines intersecting in one center and having spinules and apophyses (Figs. 25c–25e; 26).

Composition. Two subfamilies: Plagiacanthinae Hertwig, 1879 and Palaeospiculinae Won in Won et Below, 1999 (Fig. 30; Table 7).

Remarks. This group of spiny radiolarians also has a simple skeleton. Unlike the family Palacantholithidae, in Plagiacanthidae spines have spinules and apophyses, which can be tangled, or merged. The early Paleozoic Palaeospiculinae described by Won and Below (1999) and Won and Iams (2002) and Mesozoic–Cenozoic Hertwig, 1879 have a similar type of skeletal construction, but Plagiacanthinae has priority, hence the family name should be Plagiacanthidae.

Occurrence. Middle Cambrian–Recent.

Subfamily Palaeospiculinae Won in Won et Below, 1999

Diagnosis. Plagiacanthidae with skeleton consisting of main spines intersecting in one center and possessing spinules and apophyses. Tangled apophyses

tend to form ball representing link between lattice and spongy taxa (Figs. 25c, 25d; 27d, 27e).

Composition. *Archinella* Kozur et Mostler, 1981; *Nazarovites* Afanasieva 2000; *Palaeospiculum* Won in Won et Below, 1999; *Palaeothalomnus* Deflandre, 1973; and *Ramuspiculum* Won et Iams, 2002.

Occurrence. Middle Cambrian–Early Carboniferous.

Subfamily Plagiacanthinae Hertwig, 1879

Diagnosis. Plagiacanthidae with skeleton composed of three to five main spines exceeding from median bar of spicule (*MB*), sometimes almost indiscernible. Spines branch, and sometimes form anastomoses between each other (Figs. 25e).

Composition. *Archaeothamnulus* Dumitrica, 1982; *Conostylus* Popofsky, 1907; *Cytocladus* Schroder, 1906; *Deflandrella* Loeblich et Tappan, 1961; *Neosemantis* Popofsky, 1913; *Pseudocubus* Haeckel, 1887; *Pentaplagia* Cachon et Cachon, 1969; *Plagiacantha* Claparede, 1858; *Plagoniscus* Haeckel, 1887; *Plectophora* Haeckel, 1881; *Tetraplagia* Haeckel, 1881; *Tetrarchiplagia* Dumitrica, 1982; *Thalassothamnus* Haecker, 1906; *Triassothamnus* Kozur et Mostler, 1981; and *Triplagia* Haeckel, 1881.

Remarks. We placed the entire subfamily Plagiacanthinae Hertwig, 1879, sensu Petrushevskaya, 1981a from the Nassellaria in the order Fasciculata, with addition of some Triassic genera described by Kozur and Mostler (1981) and Dumitrica (1982). We made this change because apart from spines Plagiacanthinae do not have tangential structures typical of Nassellaria (wall, cephalis, cephalic structures, etc.).

Occurrence. Middle Triassic–Recent.

Family Xiphocladiellidae Nazarov, 1984, emend. Afanasieva et Amon, nov.

Diagnosis. Fasciculata with skeleton, represented by axial massive main spine, apical and basal parts of which possess main spines of varying length, but same thickness (Figs. 25h, 25i, 26, 27f–27h).

Composition. *Bissylentactinia* Nazarov, 1975; *Campanulithus* Nazarov et Rudenko, 1981; *Grosmorneus* Won et Iams, 2002; *Palhindeolithus* Deflandre, 1973; *Xiphocabrium* Deflandre, 1973; *Xiphocladiella* Deflandre, 1973; and *Xiphochistrella* Deflandre, 1973.

Remarks. Xiphocladiellidae, which were considered as a subfamily by Nazarov (1984, 1988) typically have a large axial spine, in which the apical and basal part are recognized. In our opinion, these features skeletal structure is a taxonomic character of a family rank. Hence, we raised this group to the family level and included some Late Cambrian taxa described Won and Iams (2002).

Occurrence. Late Cambrian–Early Permian.

Family Palaeoscenidiidae Riedel, 1967, emend. Nazarov et Rudenko, 1981

Diagnosis. Fasciculata, in which main spines intersect in apical part of skeleton and can be covered by auxiliary skeletal tissue. Apical part of skeleton is represented by one or two spines, although sometimes apical spines may be absent (Figs. 25f, 25g, 26, 27a, 27b).

Composition. *Apophysiactinia* Won, 1997; *Archaeosemantis* Dumitrica, 1978; *Deflantrica* Wakamatsu, Sugiyama, et Furutani, 1990; *Palaeoephippium* Goodbody, 1986; *Palaeodecaradium* Goodbody, 1986; *Palaeopyramidium* Goodbody, 1986; *Palaeorubus* Ishiga, 1987; *Palaeoscenidium* Deflandre, 1953; *Palaeotripus* Goodbody, 1986; and *Tandarnia* Dumitrica, 1982.

Occurrence. Late Cambrian–Late Triassic (Carnian).

Order Triangulata Afanasieva et Amon, 2003

Diagnosis. Aculearia, wit ha bilaterally symmetrical skeleton composed of three intersecting main spines forming an internal triangular frame. Main triangular frame of skeleton is formed by fusion of two initial four-rayed spicules and by development of spines that form it (*a*, *b*, *i*) in one plane (Figs. 25j–25p, 26, 28).

Composition. Three families: Ceratoikiscidae Holdsworth, 1969; Raphidociclicidae Afanasieva, 1999, emend. Afanasieva et Amon, nov.; and Lapidopiscidae Deflandre, 1958, emend. Afanasieva, 1999 (Figs. 25j–25p, 30; Table 7).

Occurrence. Middle Ordovician–Permian.

Family Ceratoikiscidae Holdsworth, 1969

Diagnosis. Triangulata, in which external parts of main spines may possess auxiliary spongy or latticed skeletal tissue. Intersection of main spines forms semiequilateral internal triangle (Figs. 25l, 25m, 26, 28a, 28b).

Composition. *Ceratoikiscum* Deflandre, 1953; *Circulaforma* Cheng, 1986; *Glanta* Wakamatsu, Sugiyama, et Furutani, 1990; and *Nazaromistonella* Furutani, 1990.

Occurrence. Middle Ordovician–Carboniferous.

Family Lapidopiscidae Deflandre, 1958, emend. Afanasieva, 1999

Diagnosis. Triangulata in which spines and hollow bars possess lamellar skeletal tissue forming pseudotest. Intersection of main spines of skeleton forms an isosceles triangle (Figs. 25n–25p; 26; 28c, 28d).

Composition. *Holoeciscus* Foreman, 1963; *Huasha* Cheng, 1986; *Lapidopiscum* Deflandre, 1958; *Protoholoeciscus* Aitchison, 1993; and *Neoholoeciscus* Ormiston et Lane, 1976.

Occurrence. Middle Devonian–Early Carboniferous.

Family Raphidociclicidae Afanasieva, 1999, emend. Afanasieva et Amon, nov.

D i a g n o s i s. Triangulata with skeleton where one of three main spines becomes dominant and robust, thick, while two other spines become thin and very short. External part of main spines may have auxiliary spongy or latticed skeletal tissue (Figs. 25j, 25k; 26; 28e, 28f). Intersection of main spines form very small semi-equilateral triangle.

C o m p o s i t i o n. *Helenifore* Nazarov et Ormiston, 1983; *Protoceratoikiscum* Goto, Umeda, et Ishiga, 1992; and *Raphidociclicus* Nazarov et Rudenko, 1981.

R e m a r k s. The dominance of one spine, which gives a peculiar shape to the entire test (e.g., in the nominal genus *Raphidociclicus*), is, from our point of view, a certain taxonomic characters of a family, which allows the separation of this group of triangulates in a family in its own right.

O c c u r r e n c e. Middle Ordovician–Permian.

O r d e r Albaillellata Deflandre, 1953, emend. Afanasieva et Amon, 2003

D i a g n o s i s. Bilaterally symmetrical Aculearia, with elongated, mainly conical skeleton with pylome. Internal frame formed by fusion of two initial four-rayed spicules and by development of spines *a*, *b*, and *i* in one plane, but either initial **H**-shaped subparallel development of spines *a* and *i*, connected by spine *b* at base of skeleton, and by development of subsagittal closure (*r*) of spines *a* and *i* in apical part of skeleton (Figs. 25q–25z; 26; 29).

C o m p o s i t i o n. Three families: Albaillellidae Deflandre, 1952; Follicucullidae Ormiston et Babcock, 1979; and Corythoecidae Nazarov, 1981 (Fig. 30; Table 7).

R e m a r k s. Based on the skeletal morphology the order Albaillellata presently includes three families: Albaillellidae, Follicucullidae, and Corythoecidae (Afanasieva and Amon, 2003), which is fewer than previously thought (Nazarov, 1988; De Wever *et al.*, 2001). In addition, the exclusion of the families Ceratoikiscidae, Lapidopiscidae, Palacantholithidae, and Popofskyellidae from the order composition (according to classification schemes of Nazarov, 1988 and De Wever *et al.*, 2001) is based on their skeletal morphology, which is different from the typical skeletal structure of Albaillellata.

O c c u r r e n c e. Middle Ordovician–Early Triassic.

Family Albaillellidae Deflandre, 1952

D i a g n o s i s. Albaillellata with test possessing two wings; with lamellar, less commonly basally porous wall of external shell. Family included tests with rostrellumi, **H**-frame, and without rimula (Figs. 25v–25z, 26; 29c–29e).

C o m p o s i t i o n. *Albaillella* Deflandre, 1952; *Haplodiacanthus* Nazarov et Rudenko, 1981; *Neoalbaillella* Takemura et Nakazeko, 1981; *Protoalbaillella* Cheng, 1986; *Etymalbaillella* Li, 1995; and *Spinodeflandrella* Kozur, 1981.

O c c u r r e n c e. Middle Ordovician–Permian.

Family Follicucullidae Ormiston et Babcock, 1979

D i a g n o s i s. Albaillellata with test lacking wings, with lamellar external shell wall. Simple forms lacking rostrellumi, or rimula (Figs. 25q, 25r, 26, 29a, 29b, 29h).

C o m p o s i t i o n. *Follicucullus* Ormiston et Babcock, 1979; *Parafollicucullus* Holdsworth et Jones, 1980; and *Pseudoalbaillella* Holdsworth et Jones, 1980.

O c c u r r e n c e. Middle Ordovician–Early Triassic.

Family Corythoecidae Nazarov, 1981

D i a g n o s i s. Albaillellata with pointed conical, segmented test with open aperture, auxiliary slitlike aperture and bilobed wing in apical part of skeleton. External shell is porous in the basal part of the skeleton. Inner frame is formed by two columellae connected in apical part of shell. Family includes tests with D-frame, rimula, and without rostrellumi (Figs. 25s–25u, 26; 29f, 29g).

C o m p o s i t i o n. *Arrectoalatus* Nazarov et Ormiston, 1985; *Camptoalatus* Nazarov et Rudenko, 1981; and *Corythoecia* Foreman, 1963.

O c c u r r e n c e. Late Devonian–Early Permian.

C l a s s Sphaerellaria Haeckel, 1881, emend. Afanasieva et Amon, nov.

D i a g n o s i s. Homoaxonic, radial-rayed Polycystina, with globular porous skeleton (Fig. 34), inner frame of which formed by sphere, spicule or microsphere (Figs. 10a, 10i, 10m, 10p).

C o m p o s i t i o n. Six Orders: Inaniguttata Nazarov et Ormiston, 1984; Entactiniata Riedel, 1967; Anakrusata Nazarov, 1977; Hexalonchata Haeckel, 1881; Sphaerellata Haeckel, 1887; and Actinommata Haeckel, 1862 (Fig. 35; Table 7).

R e m a r k s. Spherical polycystine radiolarians with a porous structure of the external shell represent a distinct trend in the evolution of Polycystina. Patterns in the development of the porous skeletal tissue allow the recognition of this radiolarian group as a separate class, which comprises six radiolarian orders distributed from the Cambrian to the Recent.

O c c u r r e n c e. Cambrian–Recent.

O r d e r Inaniguttata Nazarov et Ormiston, 1984

D i a g n o s i s. Sphaerellaria with inner frame in shape of hollow sphere (Figs. 10a, 10i, 34b–34e).

C o m p o s i t i o n. Two families: Inaniguttidae Nazarov et Ormiston, 1984, emend. Afanasieva, 1999 and Oriundoguttidae Afanasieva, 1999 (Fig. 35; Table 7).

O c c u r r e n c e. Cambrian–Early Devonian.

Family Inaniguttidae Nazarov et Ormiston, 1984, emend. Afanasieva, 1999

Diagnosis. Inaniguttata with an inner frame in shape of hollow sphere with six rays, which are connected to six external main conical spines (Figs. 10a, 10i, 34b, 34c).

Composition. Two subfamilies: Inaniguttinae Nazarov et Ormiston, 1984, emend. Afanasieva, 1999 and Inanibiguttinae Afanasieva, 1999 (Fig. 35; Table 7).

Remarks. In some Ordovician Inaniguttinae the inner frame is in a shape of isometric hemisphere or plate (Figs. 10h, 10i), which, however, did not develop further.

Occurrence. Cambrian–Silurian.

Subfamily Inaniguttinae Nazarov et Ormiston, 1984, emend. Afanasieva, 1999

Diagnosis. Inaniguttidae, with skeleton consisting of one shell (Figs. 10a, 10i, 34b).

Composition. *Inanigutta* Nazarov et Ormiston, 1984.

Occurrence. Cambrian–Silurian.

Subfamily Inanibiguttinae Afanasieva, 1999

Diagnosis. Inaniguttidae, with skeleton of two shells (Fig. 34c).

Composition. *Inanibigutta* Nazarov et Ormiston, 1990.

Occurrence. Late Cambrian–Silurian.

Family Oriundoguttidae Afanasieva, 1999

Diagnosis. Inaniguttata with inner frame in shape of hollow sphere with numerous rays, which are connected with many external rodlike main spines (Figs. 34d, 34e).

Composition. Two subfamilies: Oriundoguttinae Afanasieva, 1999 and Inanihellinae Afanasieva, 1999 (Fig. 35; Table 7).

Occurrence. Cambrian–Early Devonian.

Subfamily Oriundoguttinae Afanasieva, 1999

Diagnosis. Oriundoguttidae, with skeleton of one shell (Fig. 34d).

Composition. *Oriundogutta* Nazarov et Ormiston, 1990 and *Zadrappolus* Furutani, 1990.

Occurrence. Cambrian–Early Devonian.

Subfamily Inanihellinae Afanasieva, 1999

Diagnosis. Oriundoguttidae, with skeleton of two shells (Fig. 34e).

Composition. *Inanihella* Nazarov et Ormiston, 1984.

Occurrence. Ordovician–Silurian.

Order Entactiniata Riedel, 1967

Diagnosis. Sphaerellaria with porous wall of external shell and inner frame in shape of spicule with median bar (*MB*) (Figs. 10m; 34f–34l).

Composition. Three families: Entactiniidae Riedel, 1967, emend. Afanasieva, 1999; Astroentactiniidae Nazarov et Ormiston, 1985; and Hexastylidae Haeckel, 1881 (Fig. 35; Table 7).

Occurrence. Cambrian–Recent.

Family Entactiniidae Riedel, 1967, emend. Afanasieva, 1999

Diagnosis. Entactinata with inner frame in shape of six-rayed spicule. Rays are connected to six external three-bladed, less commonly rodlike main spines (Figs. 10m; 34g–34i).

Composition. Three subfamilies: Entactiniinae Riedel, 1967, emend. Afanasieva, 1999; Bientactinosphaerinae Afanasieva, 1999; and Thecentactiniinae Afanasieva, 1999 (Fig. 35; Table 7).

Occurrence. Cambrian–Triassic.

Subfamily Entactiniinae Riedel, 1967, emend. Afanasieva, 1999

Diagnosis. Entactiniidae, with skeleton of one shell (Fig. 34g).

Composition. *Altaiesphaera* Obut et Iwata, 2000; *Apophysisphaera* Won, 1997; *Archaeocenosphaera* Obut et Iwata, 2000; *Borisella* Afanasieva, 2000; *Entactinia* Foreman, 1963; and *Futobari* Furutani, 1990.

Occurrence. Cambrian–Triassic.

Subfamily Bientactinosphaerinae Afanasieva, 1999

Diagnosis. Entactiniidae, with skeleton of two shells (Figs. 10m; 34h).

Composition. *Bientactinosphaera* Afanasieva, 2000; *Hindeosphaera* Kozur et Mostler 1979; *Muelleritortis* Kozur 1988; *Mulderella* Kozur et Mostler 1981; *Ornatoentactinia* Afanasieva, 2000; *Palaeoactinosphaera* Noble, 1994; *Parasepsagon* Dumitrica, Kozur, et Mostler 1980; *Pseudostylosphaera* Kozur et Mostler 1981; *Radiobisphaera* Won, 1997; *Sepsagon* Dumitrica, Kozur, et Mostler 1980; and *Tritortis* Kozur 1988.

Occurrence. Silurian–Triassic.

Subfamily Thecentactiniinae Afanasieva, 1999

Diagnosis. Entactiniidae, with skeleton of three or more shells (Fig. 34i).

Composition. *Belowea* Won, 1983; *Cyclocarpus* Li et Wang, 1991; *Duplexia* Won, 1983; and *Thecentactinia* Nazarov, 1975.

Occurrence. Late Devonian–Early Permian.

Family Astroentactiniidae Nazarov et Ormiston, 1985

Diagnosis. Entactinata with an inner frame in shape of 8–12–24 or more rayed spicule, rays of which are connected to 8–12–24 and more external three-blades, or rodlike main spines (Figs. 34j–34l).

Composition. Three subfamilies: Astroentactiniinae Nazarov et Ormiston, 1985, emend. Afanasieva, 1999; Helioentactiniinae Afanasieva, 1999; and Multisphaerinae Nazarov et Afanasieva, 2000 (Fig. 35; Table 7).

Occurrence. Silurian–Triassic.

Subfamily Astroentactiniinae Nazarov et Ormiston, 1985, emend. Afanasieva, 1999

Diagnosis. Astroentactiniidae, with skeleton of one shell (Fig. 34j).

Composition. *Astroentactinia* Nazarov, 1975; *Cenosphaera* Ehrenberg, 1854 (*C. hexagonalis* Aberdeen, 1940); and *Moskovistella* Afanasieva, 2000.

Occurrence. Silurian–Early Permian.

Subfamily Helioentactiniinae Afanasieva, 1999

Diagnosis. Astroentactiniidae, with skeleton of two shells (Fig. 34k).

Composition. *Helioentactinia* Nazarov, 1975.

Occurrence. Middle Devonian–Triassic.

Subfamily Multisphaerinae Nazarov et Afanasieva, 2000

Diagnosis. Astroentactiniidae with skeleton of three or more shells (Fig. 34l).

Composition. *Calella* Won, 1983 and *Multisphaera* Nazarov et Afanasieva, 2000.

Occurrence. Carboniferous–Early Permian.

Family Hexastylidae Haeckel, 1881

Diagnosis. Entactinata with skeleton of one shell and very thin inner spicule (Figs. 34f; 35; Table 7).

Composition. *Centacontium* Popofsky, 1912; *Centrolonche* Popofsky, 1912; *Hexastylus* Haeckel, 1881; *Stigmosphaera* Haeckel, 1887; *Stigmosphaerusa* Hollande et Enjumet, 1960; and *Stigmostylus* Hollande et Enjumet, 1960.

Remarks. Members of this subfamily are similar to the subfamily Entactiniinae, although unfortunately poorly studied because the spicule is usually very thin and is easily destroyed, either straight after death, or during fossilization.

Occurrence. Middle Triassic–Recent.

Order Anakrusata Nazarov, 1977

Diagnosis. Sphaerellaria with porous, less commonly reticular wall of external shell and hollow main cylindrical spines. Inner frame not observed (Fig. 34a).

Composition. One family: Anakrusidae Nazarov, 1977 (Fig. 35; Table 7).

Remarks. These peculiar spherical Anakrusata with numerous hollow spines and unknown inner frame were first described by Nazarov (1977), and later by Amon (1999) in a rank of a family Anakrusidae as Radiolaria incertae sedis. However it was the spherical shape that allowed Afanasieva (2000a, 2002) to assign these polycystine radiolarians to the order Sphaerellaria in a rank of the superfamily Anakrusoidea. Now these polycystines are raised to an order by Afanasieva and Amon (2003a, 2003b).

Occurrence. Ordovician–Silurian.

Family Anakrusidae Nazarov, 1977

Diagnosis. Anakrusata, with skeleton of one shell with numerous external hollow cylindrical main spines (Fig. 34a).

Composition. *Anakrusa* Nazarov, 1977 and *Aulielina* Nazarov, 1977.

Occurrence. Ordovician–Silurian.

Order Hexalonchata Haeckel, 1881

Diagnosis. Sphaerellaria with inner frame in shape of tetrapetaloid spicule and initial microsphere or spicule of nassellarian type.

Composition. Two families: Kungalariidae Dumitrica et Carter, 1999 and Hexalonchidae Haeckel, 1881 (Fig. 35; Table 7).

Occurrence. Late Triassic–Recent.

Family Kungalariidae Dumitrica et Carter, 1999

Diagnosis. Hexalonchata, with skeleton consisting of two shells. Internal spicule of nassellarian type with median bar *MB* and rays *A*, *V*, *L*, and *l*, all same size. Main spines of external shell may or may not develop on continuations of rays of internal spicule. Internal sphere located eccentrically in relation to median bar *MB*, includes proximal parts of spines *A*, *V*, *L*, and *l* into its wall and resembles cephalis of Nassellaria (Fig. 35; Table 7).

Composition. *Cachecreekaria* Dumitrica et Carter, 1999; *Kungalaria* Dumitrica et Carter, 1999; and *Transylvanaria* Dumitrica et Carter, 1999.

Occurrence. Late Triassic (Rhaetian)–Late Cretaceous (Coniacian).

Family Hexalonchidae Haeckel, 1881

Diagnosis. Hexalonchata with inner frame in shape of tetrapetaloid spicule. Initial latticed shell developed in apical part of skeleton from angles of tetrapetaloid spicule. Initial shell connected to external shell by six spines, which are continuations of spicule: one spine apical, representing continuation of apical

ray of spicule; four spines develop from angles of petals of spicule, while one spine antapical, developing from antapical part of initial shell. All or only some spines develop on external shell and are three-bladed. External shell spherical or subspherical, porous, more rarely spongy (Figs. 10p, 34m, 35; Table 7).

Composition. *Heterosoma* Mast, 1910; *Hexacontium* Haeckel, 1881; *Hexalonche* Haeckel, 1881; *Hollandosphaera* Deflandre, 1973; *Nanina* Kozur et Mostler, 1982; and *Tetrapetalon* Hollande et Enjumet, 1960.

Remarks. Members of this family are morphologically similar to some representatives of the family Actinommidae with six spines, from which they differ by the presence of the tetrapetaloid spicule in the apical part of the initial shell (Fig. 10p).

Occurrence. Jurassic–Recent.

Order Sphaerellata Haeckel, 1887

Diagnosis. Sphaerellaria with porous external and internal shells and one to ten main spines (three-bladed, rodlike, cylindrical, hollow). Inner frame not known (Figs. 34q–34z).

Composition. Three families: Xiphostylidae Haeckel, 1881, emend. De Wever *et al.*, 2001; Pantanelliidae Pessagno, 1977; and Parvivaccidae Pessagno et Yang, 1989, emend. De Wever *et al.*, 2001 (Fig. 35; Table 7).

Occurrence. Triassic–Recent.

Family Xiphostylidae Haeckel, 1881, emend. De Wever *et al.*, 2001

Diagnosis. Sphaerellata with external and internal shells, mainly with two–three–six, main spines (Figs. 34u–34w).

Composition. Three subfamilies: Xiphostylinae Haeckel, 1881; Stylosphaerinae Haeckel, 1881; and Entapiinae Dumitrica, 2001 (Fig. 35; Table 7).

Occurrence. Triassic–Recent.

Subfamily Xiphostylinae Haeckel, 1881, emend. De Wever *et al.*, 2001

Diagnosis. Xiphostylidae with three main spines, secondary spines absent. Pores of external shell simple. Wall of external shell consists of thin inner layer and very thick outer layer with polygonal pore openings (Fig. 34u).

Composition. *Archaeocenosphaera* Pessagno et Yang in Pessagno *et al.*, 1989; *Suna* Wu, 1986; *Triactoma* Rüst, 1885, emend. Pessagno et Yang in Pessagno *et al.*, 1989; *Tripocyclia* Haeckel 1881, emend. Pessagno et Yang in Pessagno *et al.*, 1989; *Xiphostylus* Haeckel 1881, emend. Pessagno et Yang in Pessagno *et al.*, 1989; and *Zanola* Pessagno et Yang in Pessagno *et al.*, 1989.

Occurrence. Triassic–Cretaceous.

Subfamily Stylosphaerinae Haeckel, 1881

Diagnosis. Xiphostylidae with two main polar spines, which may or may not be surrounded by group of shorter polar by-spines. Main spines are usually three-bladed. They begin from surface of inner shell, connected with external shell by numerous radial bars, which did not become spines. Radial by-spines may sometimes be present on external shell. External shell has large pores (Fig. 34v).

Composition. *Druppatractus* Haeckel, 1887; *Lithomespilus* Haeckel, 1887; *Praestylosphaera* Empson-Morin, 1981; *Protoxiphotractus* Pessagno, 1973; *Spongatractus* Haeckel, 1887; *Stylatractus* Haeckel, 1887; *Stylosphaera* Ehrenberg, 1847; and *Xiphatractus* Haeckel, 1887.

Occurrence. Late Cretaceous (Cenomanian)–Recent.

Subfamily Entapiinae Dumitrica, 2001

Diagnosis. Xiphostylidae with pear-shaped inner shell, which can be open or closed distally. Inner skeleton tends to pull outside in evolution (Fig. 34w).

Composition. *Entapium* Sanfilippo et Riedel 1973 and *Zealithapium* O'Connor 1999.

Remarks. Two genera, included in this subfamily, represent two evolutionary stages. In these, the inner skeleton is withdrawn to outside and eventually disappears (De Wever *et al.*, 2001).

Occurrence. Late Paleocene–Eocene.

Family Pantanelliidae Pessagno, 1977

Diagnosis. Sphaerellata with two shells: delicate inner shell and rather robust outer shell, and two–three–six main spines. Primary radial rays continuing from inner sphere into main spines, which may be strong, three-bladed or cylindrical and with thin inner hollow channel (Figs. 34x–34z).

Composition. Three subfamilies: Capnuchosphaerinae De Wever, 1979; Capnodocinae Pessagno 1979, emend. Blome, 1983; and Pantanelliinae Pessagno, 1977 (Fig. 35; Table 7).

Occurrence. Middle Triassic–Early Cretaceous.

Subfamily Capnuchosphaerinae De Wever, 1979, emend. Pessagno, 1979

Diagnosis. Pantanelliidae with spherical or spheroid external shell with two to four main tubular spines, lying in one plane. Distal cavity of spines separated by vertical septa into three primary canals (Fig. 18). Inner spherical shell connected with external shell by radial spines. Main spines develop on continuations of these radial spines (Fig. 34y).

Composition. *Capnuchosphaera* De Wever, 1979; *Spongopallium* Dumitrica, Kozur, et Mostler, 1980; and *Weverella* Kozur et Mostler, 1979.

Occurrence. Middle Triassic (Early Ladinian)–Late Triassic (Norian).

Subfamily Capnodocinae Pessagno 1979, emend. Blome, 1983

Diagnosis. Pantanelliidae with two to four cylindrical, hollow main spines (Fig. 34x).

Composition. *Capnodoce* De Wever in De Wever *et al.*, 1979; *Justium* Blome, 1983; *Loffa* Pessagno, 1979; and *Renzium* Blome, 1983.

Occurrence. Late Triassic (Late Carnian–Middle Norian).

Subfamily Pantanelliinae Pessagno, 1977

Diagnosis. Pantanelliidae with two to four strong, three-bladed main spines (Fig. 34z).

Composition. *Betraccium* Pessagno, 1979; *Cantalum* Pessagno, 1979; *Cecrops* Pessagno, 1977; *Gorgansium* Pessagno et Blome, 1980; *Pachyonchus* Pessagno et Blome, 1980; *Pantanellium* Pessagno, 1977; *Pseudopantanellium* Yeh, 1987; *Trillus* Pessagno et Blome, 1980; and *Zartus* Pessagno et Blome, 1980.

Occurrence. Late Triassic (Carnian)–Early Cretaceous (Aptian).

Family Parvivaccidae Pessagno et Yang, 1989, emend. De Wever *et al.*, 2001

Diagnosis. Sphaerellata with one internal and one or two external shells. Inner shell not always preserved in fossils. Main spines (four to ten), beginning from inner shell and three-bladed. Pores round or polygonal. External shell and interpore bars possessing diverse ornamentation: thorns, rods, and ridges (Figs. 34q–34t).

Composition. Four subfamilies: Parvivaccinae Pessagno et Yang, 1989, emend. De Wever *et al.*, 2001; Heleninae Hull, 1997; Leugeoninae Yang et Wang, 1990; and Acaeniotylinae Yang, 1993 (Fig. 35; Table 7).

Occurrence. Middle Jurassic (Aalenian)–Late Cretaceous (Turonian).

Subfamily Parvivaccinae Pessagno et Yang 1989, emend. De Wever *et al.*, 2001

Diagnosis. Parvivaccidae with two to four main spines, often with two spines leveled along one axis. Pores simple, interpore bars sometimes in shape of ridges.

Composition. *Dicroa* Foreman, 1975; *Lanubus* Pessagno et Yang, 1989; and *Parvivacca* Pessagno et Yang, 1989.

Remarks. Parvivaccinae differ from members of other subfamilies in having simple pores, sometimes with a wider lumen in the middle part of the test wall (Fig. 34q).

Occurrence. Middle Jurassic (Aalenian)–Early Cretaceous (Barremian).

Subfamily Heleninae Hull, 1997

Diagnosis. Parvivaccidae with external shell possessing ornamentation in shape of system of ridges that form polygonal (usually hexagonal) rosettes. Main spines often absent.

Composition. *Helena* Hull, 1997 and *Tappanella* Hull, 1997.

Occurrence. Middle Jurassic (Bajocian)–Late Jurassic (Kimmeridgian).

Subfamily Leugeoninae Yang et Wang, 1990

Diagnosis. Parvivaccidae with monolayered or bilayered external shell. Monolayered shell consisting of rather regular system of pentagonal or hexagonal cells. Double-layered external layer of wall represent structure, composed of connected hexagons (Figs. 34r, 34s).

Composition. *Hexasphaera* Hull, 1997; *Levileugeo* Yang et Wang, 1990; and *Leugeo* Yang et Wang, 1990.

Occurrence. Middle Jurassic (Bajocian)–Late Jurassic (Tithonian).

Subfamily Acaeniotylinae Yang, 1993

Diagnosis. Parvivaccidae with tuberculate cortical shell (Fig. 34t).

Composition. *Acaeniotyle* Foreman, 1973; *Acaeniotylopsis* Kito et De Wever, 1994; *Acastea* Yang, 1993; *Acusten* Yang, 1993; *Nolita* Hull, 1997; *Novitripus* Hull, 1997; and *Praeconosphaera* Yang, 1993.

Occurrence. Late Jurassic (Oxfordian)–Late Cretaceous (Turonian).

Order Actinommata Haeckel, 1862

Diagnosis. Sphaerellata lacking internal frame, with initial microsphere, several internal and external shells and numerous main spines (Figs. 34n–34p).

Composition. Three families: Actinommidae Haeckel, 1862, emend. De Wever *et al.*, 2001; Astrosphaeridae Haeckel, 1881; and Heliodiscidae Haeckel, 1881 (Fig. 35; Table 7).

Occurrence. Triassic–Recent.

Family Actinommidae Haeckel, 1862, emend. De Wever *et al.*, 2001

Diagnosis. Actinommata with one or two internal and one or several external shells. Main spines numerous, but can be absent (Figs. 34o, 35; Table 7).

Composition. *Actinomma* Haeckel, 1860; *Bolena* Hull, 1997; *Carposphaera* Haeckel, 1881; *Cromyomma* Haeckel, 1862; *Cromyosphaera* Haeckel,

1881; *Mallanites* O'Dogherty, 1994; *Prunopyle* Dreyer, 1889; *Pseudacanthosphaera* O'Dogherty, 1994; *Sphaeropyle* Dreyer, 1889; *Staurosphaeretta* Squinabol, 1904; *Stuermeria* Deflandre, 1964; *Tetracanthellipsis* Squinabol, 1903; and *Thecosphaera* Haeckel, 1881.

Occurrence. Triassic–Recent.

Family Astrosphaeridae Haeckel, 1881

Diagnosis. Actinommata with one external shell and numerous main spines (Figs. 34n; 35; Table 7).

Composition. *Arachnosphaera* Haeckel, 1862; *Astrosphaera* Haeckel, 1887; *Astrospongus* Mast, 1910; *Cladococcus* Müller, 1856; *Diplosphaera* Haeckel, 1860; *Drymosphaera* Haeckel, 1881; *Elaphococcus* Haeckel, 1881; *Haeckeliella* Hollande et Enjumet, 1960; *Haplosphaera* Hollande et Enjumet, 1960; *Heliosphaera* Haeckel, 1860; *Heteracantha* Mast, 1910; *Hexancistra* Haeckel, 1881; *Hexapyramis* Squinabol, 1903; *Leptosphaera* Haeckel, 1887; *Lychnosphaera* Haeckel, 1881; *Porococcus* Hollande et Enjumet, 1960; *Rhizoplegma* Haeckel, 1881; *Rhizospongus*, Mast 1910; and *Thalassoplegma* Hollande et Enjumet, 1960.

Occurrence. Triassic–Recent.

Family Heliodiscidae Haeckel, 1881

Diagnosis. Actinommata with eccentrically positioned initial microsphere, and one or several external shells. External shells mostly spherical, but can be lenticular, discoidal, or oviform. Internal shell connected to external shell by numerous radial bars (Figs. 34p, 35; Table 7).

Composition. *Excentrococcus* Dumitrica, 1978; *Excentrodiscus* Hollande et Enjumet, 1960; *Excentrosphaerella* Dumitrica, 1978; and *Heliodiscus* Haeckel, 1862.

Remarks. The lenticular, discoidal, and oviform types of the skeleton resemble some members of the family Coccodiscidae (Class Stauraxonaria), from which they differ in the eccentric position of the initial microsphere.

Occurrence. Paleocene–Recent.

Class Spumellaria Ehrenberg, 1875, emend. Afanasieva et Amon, nov.

Diagnosis. Homoaxonic, radially-rayed Polycystina, with spherical latticed, reticular, or spongy skeleton (Fig. 31) and inner frame in shape of spicule or microsphere (Figs. 9j–9p).

Composition. Six orders: Echidninata Kozur, Mostler, et Repetski, 1996; Cancelliata Afanasieva et Amon, 2003; Spongiata Afanasieva et Amon, 2003; Capsulata Afanasieva et Amon, ordo nov.; Prodigiata Afanasieva et Amon, ordo nov.; and Saturnalata Afanasieva et Amon, ordo nov. (Figs. 32, 33; Table 7).

Remarks. Spumellaria have one of the most complex skeletons, which consists of three main components: (1) initial spicule or microsphere, (2) latticed polyhedrons, (3) one, two, or more spongy, latticed, or reticular external spherical or spheroid shells (Afanasieva and Amon, 2003). Spherical spongy radiolarians are noticeably different from spiny Aculearia in the presence of the two latter skeletal elements, while from the spherical porous Sphaerellaria they differ in the latticed, reticular, or spongy external shell. This allowed us to unify six orders of radiolarians with the above morphological features in a separate class Spumellaria, in accordance with the etymology of this name: from the Latin *spumeus* (covered in foam).

Occurrence. Middle Cambrian–Recent.

Order Echidninata Kozur, Mostler, et Repetski, 1996

Diagnosis. Spumellaria with spherical skeleton formed by randomly tangled numerous spicules (Fig. 31a).

Composition. One family: Echidninidae Kozur, Mostler, et Repetski, 1996 (Figs. 32, 33; Table 7).

Occurrence. Middle–Late Cambrian.

Family Echidninidae Kozur, Mostler, et Repetski, 1996

Diagnosis. Echidninata with one external shell and inner frame shaped like four to six rayed or multirayed spicule (Fig. 31a).

Composition. *Curvechidnina* Won et Iams, 2002; *Echidnina* Bengtson, 1986; *Protoentactinia* Kozur, Mostler, et Repetski, 1996; and *Subechidnina* Won et Iams, 2002.

Occurrence. Middle–Late Cambrian.

Order Cancelliata Afanasieva et Amon, 2003

Diagnosis. Spumellaria with reticular or latticed wall of external shell and inner frame in shape of simple or doubled initial spicule (Figs. 31p–31w).

Composition. Four families: Haplentactiniidae Nazarov, 1980; Polyentactiniidae Nazarov, 1974; Pentactinocarpidae Dumitrica 1978; and Orosphaeridae Haeckel 1887 (Figs. 32, 33; Table 7).

Occurrence. Middle Cambrian–Recent.

Family Haplentactiniidae Nazarov, 1980

Diagnosis. Cancelliata with latticed wall of external shell and inner frame in shape of six-rayed spicule, rays of which are connected to external three-bladed or rodlike main spines (Figs. 10j, 10k, 31r–31v, 32).

Composition. Three subfamilies: Haplentactiniinae Nazarov, 1980; Pseudorotasphaerinae Nazarov,

1980; and Haplotaeniatinae Afanasieva et Amon, subfam. nov. (Fig. 33; Table 7).

Occurrence. Middle Cambrian–Early Permian.

Subfamily Haplentactiniinae Nazarov, 1980

Diagnosis. Haplentactiniidae, with skeleton consisting of one shell (Figs. 10j, 10k, 31r–31t, 32).

Composition. *Archeoentactinia* Won in Won et Below, 1999; *Gracilentactinia* Kozur et Mostler, 1989; *Haplentactinia* Foreman, 1963; *Haplopolus* Li, 1995; *Magnentactinia* Won, 1997; *Protobiramus* Won in Won et Below, 1999; *Rotasphaera* Noble, 1994; *Secuicollacta* Nazarov et Ormiston, 1984; and *Wonella* Afanasieva, 2000.

Occurrence. Middle Cambrian–Early Permian.

Subfamily Pseudorotasphaerinae Noble, 1994

Diagnosis. Haplentactiniidae, with skeleton consisting of two shells (Figs. 31u, 32).

Composition. *Cancellosphaera* Afanasieva, 2000; *Diparvapila* MacDonald, 1998; *Intracorpus* Won, 1997; *Parvalanapila* MacDonald, 1998; *Pseudorotasphaera* Noble, 1994; *Russirad* Afanasieva, 2000; *Stylactinosphaera* Noble, 1994; and *Syntagentactinia* Nazarov, 1980.

Occurrence. Middle Ordovician–Devonian.

Subfamily Haplotaeniatinae Afanasieva et Amon, subfam. nov.

Type genus. *Haplotaeniatum* Nazarov et Ormiston, 1990.

Diagnosis. Haplentactiniidae, with skeleton of three or more shells, formed from apophyses of proximal parts of main spines (Figs. 31v; 32).

Composition. *Haplotaeniatum* Nazarov et Ormiston, 1990 and *Tetracircinata* Nazarov et Ormiston, 1984.

Remarks. The new subfamily is based on the presence of a characteristic feature, the formation of the skeleton from three or more spherical shells.

Occurrence. Early Silurian–Early Permian.

Family Polyentactiniidae Nazarov, 1975

Diagnosis. Cancelliata with reticular wall of external shell and inner frame in shape of eight or more rayed spicule with median bar, rays of which are connected to eight or more external main spines (three-bladed or rodlike) (Figs. 31p; 32).

Composition. Two subfamilies: Polyentactiniinae Nazarov, 1975, emend. Afanasieva, 1999 and Magnisphaerinae Afanasieva, 1999.

Occurrence. Middle Ordovician–Cretaceous.

Subfamily Polyentactiniinae Nazarov, 1975, emend. Afanasieva, 1999

Diagnosis. Polyentactiniidae with skeleton consisting of one shell (Figs. 31p; 32).

Composition. *Cuboctostylus* Bragina, 1999; *Polyentactinia* Foreman, 1963; and *Pyloctostylus* Dumitrica, 1994.

Occurrence. Middle Ordovician–Cretaceous.

Subfamily Magnisphaerinae Afanasieva, 1999

Diagnosis. Polyentactiniidae with skeleton composed of two shells (Fig. 32).

Composition. *Magnisphaera* Won, 1997.

Occurrence. Late Devonian (Early Frasnian).

Family Pentactinocarpidae Dumitrica 1978

Diagnosis. Cancelliata with latticed skeleton consisting of one, less commonly two, spherical or subspherical shells. One apical ray of spicule situated opposite four basal rays. Latter joined proximally by arcs to form four proximal pores. Thus, one latticed shell developed on continuations of rays of spicule (Figs. 10l, 31w). If skeleton has two shells, external reticular shell surrounds first latticed shell.

Composition. *Busuanga* Yeh, 1990; *Lobactinocapsa* Dumitrica, 1978; *Pentactinocapsa* Dumitrica, 1978; *Pentactinocarpus* Dumitrica, 1978; and *Pentactinorbis* Dumitrica, 1978.

Remarks. The initial spicule of this subfamily is very similar to that of Paleozoic members of subfamily Haplentactiniinae Nazarov, 1980. It differs in that the initial spicule is situated eccentrically in relation to the shell and is included in it (Figs. 10l; 31w).

Occurrence. Middle–Late Triassic.

Family Orosphaeridae Haeckel 1887

Diagnosis. Cancelliata, with reticular skeleton consisting of one, less commonly two shells, sometimes with pylome (Fig. 31q). Inner frame shaped like four- to eight-rayed spicule with median bar, rays of which are connected to rodlike external main spines.

Composition. *Orodapis* Friend et Riedel, 1967; *Oropelex* Friend et Riedel, 1967; *Orosphaera* Haeckel, 1887; and *Orostaurus* Friend et Riedel, 1967.

Remarks. The family Orosphaeridae, apparently, evolved from the Cretaceous members of the subfamily Polyentactiniinae. However, unlike those, some members of Orosphaeridae have a pylome opening (Fig. 31q), whereas the initial spicule may sometimes be included in the skeletal wall and forms an **X**-shaped structure being virtually indistinguishable from the wall.

Occurrence. Cretaceous–Recent.

Order Spongiata Afanasieva et Amon, 2003

Diagnosis. Spumellaria with spongy wall of external shell and inner frame in shape of doubled initial spicule (Figs. 31b–31j, 32).

Composition. Three families: Spongentactiniidae Nazarov, 1975; Spongopolyentactiniidae Nazarov, 1975; and Conocaryommidae Lipman 1969, emend. De Wever *et al.*, 2001 (Fig. 33; Table 7).

Occurrence. Middle Cambrian–Eocene.

Family Spongentactiniidae Nazarov, 1975

Diagnosis. Spongiata have inner frame in shape of four- to six-rayed spicule, rays of which are connected to four to six external main spines that are three-bladed, conical, or rodlike in shape (Figs. 31h–31j, 32).

Composition. Three subfamilies: Retentactiniinae Won, 1997, emend. Afanasieva, 1999; Spongentactiniinae Nazarov, 1975, emend. Afanasieva, 1999; and Pluristratoentactiniinae Afanasieva, 1999 (Figs. 32, 33; Table 7).

Occurrence. Middle Cambrian–Permian.

Subfamily Retentactiniinae Won, 1997, emend. Afanasieva, 1999

Diagnosis. Spongentactiniidae, skeleton of which consists of one shell (Figs. 31h; 32).

Composition. *Fungomacula* Won in Won et Below, 1999; *Pararcheoentactinia* Won et Iams, 2002; *Retentactinia* Won, 1997; and *Tetragregnon* Ormiston et Lane, 1976.

Occurrence. Middle Cambrian–Permian.

Subfamily Spongentactiniinae Nazarov, 1975, emend. Afanasieva, 1999

Diagnosis. Spongentactiniidae with skeleton consisting of two shells (Figs. 31j; 32).

Composition. *Retisphaera* Won, 1997; *Spongentactinia* Nazarov, 1975; and *Tetrentactinia* Foreman, 1963.

Occurrence. Silurian–Early Permian.

Subfamily Pluristratoentactiniinae Afanasieva, 1999

Diagnosis. Spongentactiniidae with skeleton consisting of three or more shells (Figs. 31i; 32).

Composition. *Meschedea* Won, 1983 and *Pluristratoentactinia* Nazarov, 1981.

Occurrence. Late Devonian–Permian.

Family Spongopolyentactiniidae Nazarov, 1975

Diagnosis. Spongiata with inner frame in shape of 8-, 12-, -24, or more-rayed spicule, rays of which are connected to 8, 12, 24, or more external main spines (three-bladed, conical, or rodlike in shape) (Figs. 31b–31g, 32).

Composition. Three subfamilies: Spongopolyentactiniinae Nazarov, 1975, emend. Afanasieva, 1999; Somphoentactiniinae Kozur et Mostler, 1981; and Plenoentactiniinae Afanasieva, 1999.

Occurrence. Middle Cambrian–Permian.

Subfamily Spongopolyentactiniinae Nazarov, 1975, emend. Afanasieva, 1999

Diagnosis. Spongopolyentactiniidae skeleton of which consists of one shell (Figs. 31b, 31c, 32).

Composition. *Duodecimentactinia* Won, 1997; *Multientactinia* Won, 1997; *Parechidnina* Kozur, Mostler, et Repetski, 1996; *Spongentactinella* Nazarov, 1975; and *Spongomassa* Won in Won et Below, 1999.

Occurrence. Middle Cambrian–Devonian.

Subfamily Somphoentactiniinae Kozur et Mostler, 1981

Diagnosis. Spongopolyentactiniidae, skeleton of which consists of two shells (Figs. 31d, 31e, 32).

Composition. *Adamas* Afanasieva, 2000; *Somphoentactinia* Nazarov, 1975; and *Spongosphaera* Won, 1997.

Occurrence. Middle–Late Devonian.

Subfamily Plenoentactiniinae Afanasieva, 1999

Diagnosis. Spongopolyentactiniidae, skeleton of which consists of three or more shells (Figs. 31f, 32).

Composition. *Copicyntra* Nazarov et Ormiston, 1985; *Plenoentactinia* Won, 1997; and *Provisocyntra* Nazarov et Ormiston, 1987.

Occurrence. Late Devonian–Permian.

Family Conocaryommidae Lipman, 1969, emend. De Wever *et al.*, 2001

Diagnosis. Spongiata with one external and three to five internal shells. Distance between external shell and inner shells is greater than distances between internal shells. External spherical shell possessing many tubercles connected to inner shell by three-bladed spines. External main spines connected to inner initial microsphere, while by-spines beginning from inner shells (Figs. 31g, 33).

Composition. *Conocaryomma* Lipman, 1969; *Hegleria* Nazarov et Ormiston, 1985; and *Praeconocaryomma* Pessagno, 1976.

Remarks. The monotypes of the family Conocaryommidae (*Conocaryomma* Lipman, 1969; Eocene) and the family Praeconocaryommidae Pessagno, 1976 (*Praeconocaryomma* Pessagno, 1976, Early Jurassic–Late Cretaceous) are structurally similar. The only difference is in the number of the inner shells. This was first recorded by De Wever *et al.*, 2001, who established

one family Conocaryommidae Lipman 1969, emend. De Wever *et al.*, 2001). We suggest expanding the size and range of this family by including the genus *Hegleria* Nazarov et Ormiston, 1985.

Occurrence. Late Permian–Eocene.

Order Capsulata Afanasieva et Amon, ordo nov.

Etymology. From the Latin *capsulata* (capsule).

Type family. Centrocubidae Hollande et Enjumet, 1960.

Diagnosis. Spumellaria with reticular or latticed external shell and one or two internal shells. Inner frame shaped like doubled initial spicule with median bar (*MB*), two apical and four basal rays. Multifaceted microsphere or latticed microsphere with subhexagonal holes formed on continuation of rays of spicule (Figs. 31x–31z).

Composition. Three families: Centrocubidae Hollande et Enjumet, 1960, emend. Dumitrica 1994; Quinquecapsulariidae Dumitrica, 1995; and Rhizosphaeridae Haeckel, 1881, emend. Dumitrica, 1995 (Fig. 33; Table 7).

Occurrence. Middle Triassic–Recent.

Family Centrocubidae Hollande et Enjumet, 1960, emend. Dumitrica 1994

Diagnosis. Capsulata with one external shell and four to ten external main spines. Apical rays of spicule are long or short, or completely absent. Basal rays of spicule always long, continuing into external main spines. Rays of spicule connected to each other by system of arched bars that form initial pseudocuboid microsphere (Figs. 31x, 33).

Composition. *Arachnostylus* Hollande et Enjumet, 1960; *Arcicubulus* Dumitrica, 1983; *Centrocubus* Haeckel, 1887; *Diplospongus* Mast, 1910; *Excentroconcha* Mast, 1910; *Gonosphaera* Jørgensen, 1905; *Heptacladus* Dumitrica, Kozur, et Mostler, 1980; *Lonchosphaera* Popofsky, 1908; *Octodendron* Haeckel, 1887; *Pessagnulus* Dumitrica, 1983; *Solicubulus* Dumitrica, 1983; *Stauropylissa* Dumitrica, 1989; *Welirella* Dumitrica, Kozur, et Mostler, 1980; and *Weverisphaera* Kozur et Mostler, 1981.

Occurrence. Middle Triassic (Middle Anisian)–Recent.

Family Quinquecapsulariidae Dumitrica, 1995

Diagnosis. Capsulata with external and internal shells and four to ten external main spines. Initial microsphere more or less perfect pentagonal prism. It formed on continuations of rays of initial spicule by development of two parallel pentagonal frames connected by bars. Ten primary main spines extending from vertices of pentagonal prism. Main spines connected at one or more levels by system of arched bars, which form internal shell repeating initial pentagonal prism of microsphere on larger scale (Figs. 31y, 33).

Composition. *Empirea* Whalen et Carter, 1998 and *Quinquecapsularia* Pessagno, 1972.

Occurrence. Early Jurassic (Hettangian)–Recent.

Family Rhizosphaeridae Haeckel, 1881, emend. Dumitrica, 1995

Diagnosis. Capsulata with external and one or two internal shells and six or more radial spines. Initial latticed microsphere with subhexagonal holes formed on continuations of spines of spicule (Figs. 31z, 33).

Composition. *Elatommura* Haeckel, 1887; *Haliomma* Haeckel, 1860; *Haliommilla* Haeckel, 1887; and *Rhizosphaera* Haeckel, 1860.

Occurrence. Late Jurassic (Tithonian)–Recent.

Order Prodigiata Afanasieva et Amon, ordo nov.

Etymology. From the Latin *prodigialis* (strange, unusual).

Type family. Eptingiidae Dumitrica, 1978.

Diagnosis. Spumellaria with spongy or latticed external and internal shells. Inner frame of nassellarian type or shaped like doubled initial spicule with median bar (*MB*), two apical and four basal spines (Figs. 31m–31o).

Composition. Two families: Eptingiidae Dumitrica, 1978 and Multiarcusellidae Kozur et Mostler, 1979 (Fig. 33; Table 7).

Occurrence. Middle Triassic–Jurassic.

Family Eptingiidae Dumitrica, 1978

Diagnosis. Prodigiata with one spongy or latticed external shell. Spicule of nassellarian type and asymmetric in relation to sagittal ring. Sometimes, spicule is included in shell wall (Figs. 31m, 33).

Composition. *Charlottea* Whalen et Carter, 1998; *Cryptostephanidium* Dumitrica, 1978; *Divatella* Kozur et Mostler, 1981; *Eptingium* Dumitrica, 1978; *Ferresium* Blome, 1984, emend. Carter 1993; *Perispyridium* Dumitrica, 1978; *Protoperispyridium* Yeh, 1987; *Pylostephanidium* Dumitrica, 1978; *Spongostephanidium* Dumitrica, 1978; *Tozerium* Whalen et Carter, 1998; *Triassistephanidium* Dumitrica, 1978; and *Xenorum* Blome, 1984.

Occurrence. Middle Triassic (Anisian)–Late Jurassic (Tithonian).

Family Multiarcusellidae Kozur et Mostler, 1979

Diagnosis. Prodigiata with external and internal shells. Inner frame is in shape of small initial spicule with median bar (*MB*), two apical and four basal rays. Internal shell has two layers: 1) more external latticed spherical shell, 2) internal shell is eccentrically formed

based on reduced lattice connecting four basal rays of spicule. Latticed external shell sometimes reduced to arched rods connecting main spines. Internal shell is connected to external shell by four to six primary spines, with main spines developed on their continuations on external side of shell (Figs. 31n, 31o).

Composition. Two subfamilies: Multiarcusellinae Kozur et Mostler, 1979 and Austrisaturnalinae Kozur et Mostler, 1983 (Fig. 33; Table 7).

Occurrence. Middle Triassic (Anisian)–Late Triassic (Norian).

Subfamily Multiarcusellinae Kozur et Mostler, 1979

Diagnosis. Multiarcusellidae, with skeleton possessing six main spines, representing continuations of rays of spicule and usually connected by arcs at level of external shell (Figs. 31o, 33).

Composition. *Baloghisphaera* Kozur et Mostler, 1979; *Beturiella* Dumitrica, Kozur, et Mostler, 1980; and *Multiarcusella* Kozur et Mostler, 1979.

Remarks. Three genera *Beturiella–Baloghisphaera–Multiarcusella* represent an evolution of skeletal elements and a trend toward reduction of external shell and development of string arcs.

Occurrence. Middle Triassic (Ladinian)–Late Triassic (Carnian).

Subfamily Austrisaturnalinae Kozur et Mostler, 1983

Diagnosis. Multiarcusellidae with or without latticed external shell. Four main spines, representing continuations of rays of spicule spine, joined by distal flat ring formed from arcs of external shell (Figs. 31n, 33).

Composition. *Austrisaturnalis* Kozur et Mostler, 1972; *Hungarosaturnalis* Kozur et Mostler, 1983; *Ornatisaturnalis* Mostler et Kreiner, 1994; *Praeheliostaurus* Kozur et Mostler, 1972; *Quadrisaturnalis* Yeh, 1989; *Solisaturnalis* Mostler et Kreiner, 1994; and *Tiborella* Dumitrica, Kozur, et Mostler, 1980.

Occurrence. Middle Triassic (Anisian)–Late Triassic (Norian).

Order Saturnalata Afanasieva et Amon, ordo nov.

Type family. Saturnalidae Deflandre, 1953.

Diagnosis. Spumellaria, with characteristic ring possessing polar spines around central spherical shell (Figs. 31k, 31l, 33).

Composition. Two families: Oertlispongidae Kozur et Mostler, 1980 and Saturnalidae Deflandre, 1953.

Remarks. The ring is the most important skeletal element, transformation of which is reflected in the evolution of this order (Fig. 33). The subdivision of the order into families and subfamilies is based on the presence or absence of the ring and its structure (Figs. 31k, 31l).

Occurrence. Middle Triassic–Recent.

Family Oertlispongidae Kozur et Mostler, 1980

Diagnosis. Saturnalata with spongy wall of external shell and numerous internal shells. Inner frame unknown. One main spine shaped like very large thin variously shaped plate. Secondary spine small, thin, straight, located directly opposite to main spine (Figs. 31k, 33).

Composition. *Baumgartneria* Dumitrica, 1982; *Bogdanella* Kolar–Jurkovsek, 1989; *Falcispongus* Dumitrica, 1982; *Gibberospongus* Kozur et Mostler, 1996; *Oertlispongus* Dumitrica, Kozur, et Mostler, 1980; *Paroertlispongus* Kozur et Mostler, 1981; *Pterospongus* Dumitrica, 1982; *Scutispongus* Kozur et Mostler, 1996; *Spongoserrula* Dumitrica, 1980; *Steigerispongus* Kozur et Mostler, 1996; and *Turospongus* Kozur et Mostler, 1994.

Occurrence. Middle Triassic (Late Anisian)–Late Triassic (Carnian).

Family Saturnalidae Deflandre, 1953

Diagnosis. Saturnalata with spherical or subspherical test surrounded by variously shaped ring (simple, complex, flat, or carinate, with or without spines). Sometimes ring not developed or underdeveloped. Skeleton spongy, porous, representing combination of both shell wall types (Fig. 31l).

Composition. Four subfamilies: Heliosaturnalinae Kozur and Mostler, 1972; Hexasaturnalinae Kozur et Mostler, 1983; Saturnalinae Deflandre, 1953; and Axopruninae Dumitrica, 1983 (Fig. 33; Table 7).

Occurrence. Late Triassic–Recent.

Subfamily Heliosaturnalinae Kozur et Mostler, 1972

Diagnosis. Saturnalidae with flat ring and polar spines (Figs. 31l, 33).

Composition. *Heliosaturnalis* Kozur and Mostler, 1972; *Palaeosaturnalis* Donofrio et Mostler, 1978; *Parasaturnalis* Kozur et Mostler, 1972; *Praehexasaturnalis* Kozur et Mostler, 1983; *Pseudoheliodiscus* Kozur et Mostler, 1972; *Spongosaturnaloides* Kozur et Mostler, 1972; and *Stauracanthocircus* Kozur et Mostler, 1983.

Occurrence. Late Triassic (Carnian)–Early Jurassic (Pliensbachian).

Subfamily Hexasaturnalinae Kozur et Mostler, 1983

Diagnosis. Saturnalidae with **Y**-shaped cross section of trifacial ring: one face lying on inner edge, and two faces on outer edge of ring. Polar spines present only in earliest members (Fig. 33).

Composition. *Dicerosaturnalis* Dumitrica et Dumitrica-Jud in O'Dogherty, 1994; *Eospongosaturninus* Kozur et Mostler, 1990; *Hexasaturnalis* Kozur et Mostler, 1983; and *Octosaturnalis* Kozur et Mostler, 1990.

Remarks. The only genus *Octosaturnalis* has polar spines. This genus appeared in the Norian and, in

the view of Kozur and Mostler (1990), was an ancestor of the genus *Hexasaturnalis*, in which polar spines gradually reduced.

Occurrence. Late Triassic (Norian)–Early Cretaceous (Albian).

Subfamily Saturnalinae Deflandre, 1953

Diagnosis. Saturnalidae with trifacial ring, having **Y**-shaped cross section, with one face lying on inner edge, and two faces on outer edge of ring. Less commonly ring tetrafacial or flat (in younger taxa). Polar spines absent (Fig. 33).

Composition. *Acanthocircus* Squinabol, 1903; *Aurisaturnalis* Dumitrica et Dumitrica-Jud, 1994; *Praeacanthocircus* Kozur et Mostler, 1983; *Pseudacanthocircus* Kozur et Mostler, 1990; *Saturnalis* Haeckel, 1887; *Spinoellipsella* Kozur et Mostler, 1990; *Spongosaturninus* Campbell et Clark, 1944; and *Vitorfus* Pessagno, 1977.

Occurrence. Late Triassic–Recent.

Subfamily Axopruninae Dumitrica, 1983

Diagnosis. Saturnalidae with latticed skeleton and two polar conical spines rounded in cross section. Ring not developed (Fig. 33).

Composition. *Amphisphaerella* Haeckel, 1887; *Axoprunum* Haeckel, 1887; *Stylacontarium* Popofsky, 1912; *Xiphosphaerella* Haeckel, 1887; and *Xiphostyletta* Haeckel, 1887.

Remarks. In opinion of Dumitrica (1985), external and internal skeletons of this group are quite similar to those of other Saturnalidae, only difference being in absence of ring.

Occurrence. Paleocene–Recent.

Class Stauraxonaria Afanasieva et Amon, classis nov.

Etymology. From the Greek σταυρος (cross) and the Latin *axis* (axis).

Diagnosis. Mono- or polyaxonic, or heteropolar stauraxonic Polycystina with variously flattened, convex, or armed skeletons (Figs. 36–41), with inner frame formed by hollow sphere, spicule, or microsphere (Fig. 10c).

Composition. Eight orders: Palaeodiscata Afanasieva et Amon, ordo nov.; Radiiformata Afanasieva et Amon, ordo nov.; Pyramidata Afanasieva et Amon, ordo nov.; Lobatiradiata Afanasieva et Amon, ordo nov.; Pyloniata Haeckel, 1881 emend. Dumitrica, 1989; Spongurata Haeckel, 1862; Oviformata Afanasieva et Amon, ordo nov.; and Spongodiscata Haeckel, 1862 (Fig. 40; Table 7).

Remarks. Stauraxonaria have been studied for over 100 years beginning from the first record of these unusual radiolarians from the Devonian of England and Canada (Hinde and Fox, 1895). However, until now no attempts have been made to unite all known Phanerozoic stauraxonic radiolarians into one taxon, although this group of peculiar radiolarians differs from all other Polycystina in having diverse skeletons and intersecting axes of symmetry that lie in a plane vertical to the main axis. All this allows the recognition of an independent class Stauraxonaria including eight orders of stauraxonic radiolarians ranging from Late Cambrian to present.

Occurrence. Late Cambrian–Recent.

Order Palaeodiscata Afanasieva et Amon, ordo nov.

Etymology. From the Greek παλαιος (ancient) and δισκος (disc).

Type family. Palaeodiscidae Afanasieva, 2000.

Diagnosis. Stauraxonaria with convex skeleton, subspherical or lenticular in shape, with spongy wall to external shells (Fig. 36a). Inner frame is in shape of hollow sphere or spicule with four to six or more rays, connected to external spines.

Composition. One family: Palaeodiscidae Afanasieva, 2000 (Fig. 40; Table 7).

Remarks. Originally discoidal, lenticular, flattened-ellipsoidal, spindle-shaped or lenticular radiolarians were recognized as a family Palaeodiscidae Afanasieva, 2000, which included two subfamilies Palaeodiscinae and Staurodruppinae from the Silurian to Permian (Afanasieva, 2000a). New discoveries of the Late Cambrian discoidal radiolarians (Iwata *et al.*, 1997) and comprehensive analysis of this group of stauraxonic radiolarians allowed us to raise the status of the subfamily Palaeodiscinae and to include all discoidal radiolarians in the separate order Palaeodiscata, ranging from Late Cambrian to Permian.

Occurrence. Late Cambrian–Permian.

Family Palaeodiscidae Afanasieva, 2000

Diagnosis. Palaeodiscata with a discoidal, or lenticular spongy skeleton consisting of numerous shells (Figs. 36a, 40; Table 7).

Composition. *Copicyntroides* Nazarov et Ormiston, 1985; *Eostylodictya* Ormiston et Lane, 1976; *Gedauia* Won, 1983; *Palaeodiscus* Afanasieva, 2000; *Primaritripus* Afanasieva, 2000; *Sphaerodiscus* Won, 1983; and *Radiolaria* gen. et sp. indet. Iwata *et al.*, 1997.

Occurrence. Late Cambrian–Permian.

Order Oviformata Afanasieva et Amon, ordo nov.

Etymology. From the Latin *oviformis* (oviform).

Type family. Spongolonchidae Afanasieva et Amon, fam. nov.

Diagnosis. Stauraxonaria with spindle-shaped or oviform, less commonly subspherical spongy skele-

ton (Figs. 36s, 36t). Inner frame in shape of hollow sphere or spicule with four to six or more rays, connected to external spines.

Composition. Five families: Spongolonchidae Afanasieva et Amon, fam. nov.; Staurodruppidae Afanasieva, 2000; Gomberellidae Kozur et Mostler, 1981; Archaeospongoprunidae Pessagno, 1973; and Phaseliformidae Pessagno, 1972 (Fig. 40; Table 7).

Remarks. A comprehensive analysis of this fusiform group of stauraxonic radiolarians allowed us to raise the status of the subfamily Staurodruppinae, to recognize a new family Spongolonchidae, and assign all spindle-shaped (fusiform) or oviform taxa to a new order Oviformata, ranging from the Silurian to the present

Occurrence. Silurian–Recent.

Family Spongolonchidae Afanasieva et Amon, fam. nov.

Type genus. *Spongolonche* Hinde, 1899.

Diagnosis. Oviform, fusiform, or flattened-ellipsoidal spongy skeleton consisting of numerous shells (Figs. 36s, 40; Table 7).

Composition. *Copiellintra* Nazarov et Ormiston, 1985 and *Spongolonche* Hinde, 1899.

Remarks. A skeleton consisting of numerous inner shells is a taxonomic character of a higher rank, which allowed us to recognize the new family Spongolonchidae.

Occurrence. Early Silurian (Wenlock)–Permian.

Family Staurodruppidae Afanasieva, 2000

Diagnosis. Oviformata with fusiform, porous skeleton consisting of two shells with two bipolar, three-bladed main spines (Fig. 40; Table 7).

Composition. *Spongocoela* Hinde, 1899 and *Staurodruppa* Hinde, 1899.

Occurrence. Devonian.

Family Gomberellidae Kozur et Mostler 1981, emend. De Wever *et al.*, 2001

Diagnosis. Oviformata with a spongy, heteropolar, oviform, more or less flattened skeleton. Two divergent spines occur at the narrow end of the skeleton; additional spongy tissue is developed at the wider end (Figs. 36t, 40; Table 7).

Composition. *Bernoullius* Baumgartner, 1984; *Gomberellus* Dumitrica, Kozur, et Mostler, 1980; *Karnospongella* Kozur et Mostler, 1981; and *Tamonella* Dumitrica, Kozur, et Mostler, 1980.

Occurrence. Middle Triassic–Early Cretaceous (Barremian).

Family Archaeospongoprunidae Pessagno, 1973

Diagnosis. Oviformata with a fusiform, cylindrical, or subspherical test, with two opposing polar spines (Fig. 40; Table 7).

Composition. *Archaeospongoprunum* Pessagno, 1973; *Pararchaeospongoprunum* Lahm, 1984; *Spongoprunum* Haeckel, 1887; and *Wilvemia* Pessagno, Blome, et Hull, 1993.

Occurrence. Middle Triassic–Recent.

Family Phaseliformidae Pessagno, 1972

Diagnosis. Oviform Oviformata, in which one of the ends of the skeleton is wider than the other. Spines are absent. The skeletal tissue is arranged into more or less concentric layers (Fig. 40; Table 7).

Composition. *Parvicuspis* Pessagno, 1972 and *Phaseliforma* Pessagno, 1972.

Occurrence. Cretaceous.

Order Radiiformata Afanasieva et Amon, ordo nov.

Etymology. From the Latin *radius* (ray) and *forma* (form).

Type family. Latentifistulidae Nazarov et Ormiston, 1983.

Diagnosis. Monaxonic or heteropolar Stauraxonaria, with skeleton with three or more divergent arms, with spongy, porous or lamellar wall of external shell (Figs. 36f–36j, 39).

Composition. Five families: Latentifistulidae Nazarov et Ormiston, 1983; Quadriremidae Afanasieva, 2000; Polyfistulidae Amon, 1999; Ormistonellidae De Wever et Caridroit, 1984; and Deflandrellidae De Wever et Caridroit, 1984 (Fig. 40; Table 7).

Remarks. The skeleton with three or more divergent arms is the main character based on which this group of radiolarians is recognized as the order Radiiformata.

Occurrence. Carboniferous–Permian.

Family Latentifistulidae Nazarov et Ormiston, 1983

Diagnosis. Radiiformata with three-armed spongy skeleton and inner frame hollow sphere shaped with three rays connected to external terminal spines (Figs. 36f, 36g, 39a, 39b).

Composition. Two subfamilies: Latentifistulinae Nazarov et Ormiston, 1983 and Latentibifistulinae Afanasieva, 2000 (Fig. 40; Table 7).

Occurrence. Carboniferous–Permian.

Subfamily Latentifistulinae Nazarov et Ormiston, 1983

Diagnosis. Latentifistulidae, with three-armed skeleton of one shell (Figs. 36g, 39a).

Composition. *Ishigaum* De Wever et Caridroit, 1984; *Latentifistula* Nazarov et Ormiston, 1983; and *Pseudotormentus* De Wever et Caridroit, 1984.

Occurrence. Carboniferous–Permian.

Subfamily Latentibifistulinae Afanasieva, 2000

Diagnosis. Latentifistulidae with a three-armed skeleton consisting of two shells (Figs. 10b; 36f; 39b).

Composition. *Latentibifistula* Nazarov et Ormiston, 1983 and *Triactofenestrella* Nazarov et Ormiston, 1984.

Occurrence. Late Carboniferous–Permian.

Family Quadriremidae Afanasieva, 2000

Diagnosis. Radiiformata with an inner frame in a shape of a hollow sphere with four or five rays, which are connected to external terminal spines of the four- or five-armed skeleton, consisting of one porous shell (Figs. 36h, 39d, 39e, 40; Table 7).

Composition. *Quadriremis* Nazarov et Ormiston, 1985 and *Quinqueremis* Nazarov et Ormiston, 1983.

Occurrence. Late Carboniferous–Permian.

Family Polyfistulidae Amon, 1999

Diagnosis. Radiiformata with an inner frame in a shape of a hollow sphere with four or more rays, which are connected to external terminal spines of four or more-armed skeleton, consisting of one lamellar shell (Figs. 39c, 40; Table 7).

Composition. *Polyfistula* Nazarov et Ormiston, 1984.

Occurrence. Early Permian.

Family Ormistonellidae De Wever et Caridroit, 1984

Diagnosis. Radiiformata with an inner frame in a shape of a hollow sphere with four or more rays, which are connected to external terminal spines of four or more-armed skeleton, consisting of one lamellar shell (Figs. 36i, 40; Table 7).

Composition. *Nazarovella* De Wever et Caridroit, 1984 and *Ormistonella* De Wever et Caridroit, 1984.

Occurrence. Permian.

Family Deflandrellidae De Wever et Caridroit, 1984

Diagnosis. Radiiformata with an inner frame in a shape of a hollow sphere with three rays, which are connected to external terminal spines of the three-armed skeleton, consisting of one lamellar shell (Figs. 36j, 40; Table 7).

Composition. *Deflandrella* De Wever et Caridroit, 1984.

Occurrence. Late Permian.

Order Pyramidata Afanasieva et Amon, ordo nov.

Etymology. From the Latin *pyramidis* (pyramid).

Type family. Tormentidae Nazarov et Ormiston, 1983.

Diagnosis. Stauraxonaria with external shells with spongy wall, with convex skeleton, pyramidal or flattened-pyramidal, less commonly subspherical in shape (approximate tetragon or cube) (Figs. 36b–36e, 36q, 36r, 37, 38). Inner frame in shape of hollow sphere with three-six rays, connected to external terminal spines.

Composition. Four families: Tormentidae Nazarov et Ormiston, 1983; Ruzhencevispongidae Kozur, 1980; Pyramispongiidae Kozur et Mostler, 1978, emend. De Wever *et al.*, 2001; and Cavaspongiidae Pessagno, 1973 (Fig. 40; Table 7).

Remarks. The pyramidal shape of the test of this group of radiolarians makes it distinct from all other stauraxonarians and is the basis for the recognition of the order Pyramidata.

Occurrence. Carboniferous–Cretaceous.

Family Tormentidae Nazarov et Ormiston, 1983

Diagnosis. Pyramidal and bipyramidal Pyramidata (Figs. 36b, 36c, 37a–37f).

Composition. Two subfamilies: Tormentinae Nazarov et Ormiston, 1983 and Rectotormentinae Afanasieva, 2000 (Fig. 40; Table 7).

Occurrence. Carboniferous–Permian.

Subfamily Tormentinae Nazarov et Ormiston, 1983

Diagnosis. Tormentidae, skeleton of which consists of one shell (Figs. 36b, 37c–37f).

Composition. *Grandetortura* Sashida et Tonishi, 1991; *Pseudolithelius* Kozur et Mostler, 1989; *Staurentactinia* Schwartzapfel et Holdsworth, 1996; *Tetraspongoactinia* Won, 1998; *Tetratormentum* Nazarov et Ormiston, 1985; and *Tormentum* Nazarov et Ormiston, 1983.

Occurrence. Carboniferous–Permian.

Subfamily Rectotormentinae Afanasieva, 2000

Diagnosis. Tormentidae, skeleton of which consists of numerous shells (Figs. 36c, 37a, 37b).

Composition. *Octatormentum* Nazarov et Ormiston, 1985 and *Rectotormentum* Nazarov et Ormiston, 1985.

Occurrence. Permian.

Family Ruzhencevispongidae Kozur, 1980, emend. Nazarov et Ormiston, 1983

Diagnosis. Monaxonic Pyramidata with flattened skeleton, triangular or subtriangular in shape,

with reticular, spongy, or partly lamellar wall of external shell. Inner frame in shape of hollow sphere with three rays, connected to external terminal spines (Figs. 36d, 36e, 37h, 37i, 38).

Composition. Two subfamilies: Latentidiotinae Afanasieva, 2000 and Ruzhencevisponginae Kozur, 1980, emend. Afanasieva, 2000 (Fig. 40; Table 7).

Occurrence. Late Carboniferous–Early Triassic.

Subfamily Latentidiotinae Afanasieva, 2000

Diagnosis. Ruzhencevispongidae, triangular or triangular-armed skeleton of which consists of one shell (Figs. 36d, 37h, 37i, 38c).

Composition. *Latentidiota* Nazarov et Ormiston, 1985.

Occurrence. Late Carboniferous–Early Permian.

Subfamily Ruzhencevisponginae Kozur, 1980, emend. Afanasieva, 2000

Diagnosis. Ruzhencevispongidae, triangular skeleton of which consist of two shells (Figs. 36e, 38a, 38b).

Composition. *Foremanhelena* De Wever et Caridroit, 1984 and *Ruzhencevispongus* Kozur, 1980.

Occurrence. Permian–Early Triassic.

Family Pyramispongiidae Kozur et Mostler, 1978, emend. De Wever *et al.*, 2001

Diagnosis. Pyramidata spongy, subspherical approximately tetragonal or cubical in shape, with a varying number of massive conical spines (Figs. 36r; 40; Table 7). The inner frame is not studied.

Composition. *Discokatorella* Kozur et Mostler, 1994; *Intermediella* Lahm, 1984; *Katorella* Kozur et Mostler, 1981; *Kulacella* Kozur et Mostler, 1981; *Neopaurinella* Kozur et Mostler, 1981; *Paurinella* Kozur et Mostler 1981; *Pyramispongia* Pessagno, 1973; *Rikivatella* Kozur et Mostler, 1981; and *Triassospongosphaera* Kozur et Mostler, 1981.

Occurrence. Middle Triassic–Cretaceous.

Family Cavaspongiidae Pessagno, 1973

Diagnosis. Pyramidata of tetrahedral, flattened–tetrahedral or lens-shape. Inner frame not studied. Internal shell spherical, reticular, surrounded by thick layer of spongy tissue. Spongy layer consists of many, very thin concentric layers connected by many spines, forming a radial structure of spongy tissue (Figs. 36q, 40; Table 7).

Composition. *Cavidiscus* Pessagno, 1976; *Cavaspongia* Pessagno, 1973; and *Dumitricaia* Pessagno, 1976.

Occurrence. Cretaceous.

Order Lobatiradiata Afanasieva et Amon, ordo nov.

Etymology. From the Latin *lobatus* (lobate) and *radius* (ray).

Type family. Angulobracchidae Baumgartner, 1980, emend. De Wever *et al.*, 2001.

Diagnosis. Stauraxonaria, with flattened spherical skeleton, with two to six lobes (arms), with or without pylome. Heteropolar microsphere consists of quadrangular primary ring, four-pillared apical cap with apical bar in vault, that forms an **H**-shaped structure, and antapical cap with one or two pores in vault. Apical bar has long primary apical bar in its proximal part, with two oppositely located branches lying in plane vertical to plane of apical bar. Four angles of primary quadrangular ring possess four primary bars, of which two are short and two are long, continuing toward exterior into spines or lobes (arms). These all usually have proximal verticils composed of two processes lying in plane vertical to that of primary ring. Upper part of first microspherical shell with more or less regular cross-shaped structure (Figs. 36k–36p).

Composition. Six families: Angulobracchidae Baumgartner, 1980, emend. De Wever *et al.*, 2001; Patulibracchiidae Pessagno, 1971, emend. De Wever *et al.*, 2001; Hexaporobrachiidae Kozur et Mostler, 1979; Hagiastridae Riedel, 1971; Suttoniidae Schaaf, 1976, emend. Dumitrica, 1983; and Myelastridae Riedel, 1971 (Fig. 40; Table 7).

Remarks. Morphology of the heteropolar microsphere, and the presence of very characteristic lobes (arms) allow the possibility of recognition of the order Lobatiradiata, which differs from the order Radiiformata in the development of an inner frame in the form of a microsphere.

Occurrence. Middle Triassic–Recent.

Family Angulobracchiidae Baumgartner, 1980, emend. De Wever *et al.*, 2001

Diagnosis. Lobatiradiata with spongy, less commonly reticular skeleton with two or three arms, one lying in same plane as apical bar, while two others lie in same plane as longitudinal bars of initial microsphere. Initial inner frame, which has shape of hollow microsphere, and system of girdles that are strictly heteropolar. Lower part of microsphere quite uneven. Apical bar of microsphere long, forming axis of apical arm of skeleton. Longitudinal bars usually long and always directed downwards forming axes of two other arms, similar to apical bar. Transverse bars of microsphere very short, not extending outside first system of girdles. All primary bars usually have pair of oppositely located processes lying vertically to plane of primary bars of microsphere. Sometimes apical arm or two others are strongly reduced. The pylome, if present, is open towards apical arm (Figs. 36m; 40; Table 7).

Composition. *Angulobracchia* Baumgartner, 1980; *Bistarkum* Yeh, 1987; *Cyclastrum* Ruest, 1898; *Danubea* Whalen et Carter, 1998; *Deviatus* Li, 1986; *Loupanus* Carter, 1993; *Paronaella* Pessagno, 1971; *Protopsium* Pessagno et Poisson, 1981; *Risella* Carter,

1993; *Sontonaella* Yeh, 1987; and *Thurstonia* Whalen et Carter, 1998.

Remarks: The structure of the initial microsphere and the system of girdles in the family Angulobracchiidae are very similar to those in the family Hagiastridae, from which it is different in the presence of the apical bar and the longitudinal bars of the microsphere directed downwards (these are the axes of the three arms). The plane, in which the arms of the Angulobracchiidae lie, is perpendicular to the plane containing the arms of the skeleton of Hagiastridae, which coincides to the equatorial plane of the microsphere and primary system of girdles.

Occurrence. Middle Triassic (Early Ladinian)–Late Cretaceous (Maastrichtian).

Family Patulibracchiidae Pessagno, 1971, emend. De Wever *et al.*, 2001

Diagnosis. Lobatiradiata with primary frame composed of three internal bars. Skeleton formed of three arms, each with three or four primary canals. Lobes are developed on continuation of apical and transverse bars of microsphere of primary frame. Lower part of microsphere strongly reduced. Pylome, if developed is open toward apical part (Figs. 36l, 40; Table 7).

Composition. *Archaeotritrabs* Steiger, 1992; *Ditrabs* Baumgartner, 1980; *Halesium* Pessagno, 1971; *Homoeoparonaella* Baumgartner, 1980; *Neoparonaella* Yang, 1993; *Patulibracchium* Pessagno, 1971; *Pessagnobracckia* Kozur et Mostler, 1978; *Trimanicula* Dumitrica 1991; and *Tritrabs* Baumgartner, 1980.

Remarks. Members of the family Patulibracchiidae are superficially similar to the family Angulobracchiidae in the presence of three arms, but differ in that two of these three rays are formed along the two transverse bars of the microsphere.

Occurrence. Late Triassic (Norian)–Neogene (Pliocene).

Family Hexaporobrachiidae Kozur et Mostler, 1979

Diagnosis. Lobatiradiata with four or six reticular tubular lobes (arms), occurring in one plane along three isometric axes or angles of tetrahedron. Initial inner frame not studied, although apparently consisting of inverted vaults (Figs. 36k, 40; Table 7).

Composition. *Hexaporobrachia* Kozur et Mostler, 1979 and *Icrioma* De Wever, 1979.

Occurrence. Late Triassic.

Family Hagiastridae Riedel, 1971

Diagnosis. Lobatiradiata with a microsphere and equatorial system of girdles. Test generally with narrow central and four, less commonly two lobes (arms) with two to four canals in continuations of four primary spines (Figs. 36n, 40; Table 7).

Composition. *Archaeohagiastrum* Baumgartner, 1984; *Crucella* Pessagno, 1971; *Hagiastrum* Haeckel, 1881; *Higumastra* Baumgartner, 1980; *Orbiculiforma* Pessagno, 1973; *Paratriassoastrum* Kozur et Mostler, 1981; *Pentaporobrachia* Kozur et Mostler, 1981; *Pseudocrucella* Baumgartner, 1980; *Pseudohagiastrum* Pessagno, 1979; *Pseudohigumastra* Yang, 1993; *Saldorfus* Pessagno, Blome, et Hull, 1993; *Savaryella* Jud, 1994; *Sophia* Whalen et Carter 1998; *Tetraditryma* Baumgartner, 1980; *Tetraporobrachia* Kozur et Mostler, 1979; *Tetratrabs* Baumgartner, 1980; and *Udalia* Whalen et Carter, 1998.

Occurrence. Late Triassic–Late Cretaceous (Maastrichtian).

Family Suttoniidae Schaaf, 1976, emend. Dumitrica, 1983

Diagnosis. Lobatiradiata with three-armed skeleton, built from coarsely reticular tissue with large pores. Three arms lie in one plane perpendicular to a small shell. The primary frame is not studied (Figs. 36p, 40; Table 7).

Composition. *Suttonium* Schaaf, 1976.

Occurrence. Early Paleogene (Late Paleocene)–Recent.

Family Myelastridae Riedel, 1971

Diagnosis. Lobatiradiata with a very small sturdy central part of the test formed by a few rings. The central part is surrounded by very thin tissue, which continues into simple or branching lobes (arms) (Figs. 36o, 40; Table 7).

Composition. *Dicranastrum* Haeckel, 1881; *Myelastrum* Haeckel, 1887; *Pentaphiastrum* Haeckel, 1887; *Tetracranastrum* Haeckel, 1887; and *Triastrum* Cleve, 1901.

Occurrence. Quaternary.

Order Pyloniata Haeckel, 1881, emend. Dumitrica, 1989

Diagnosis. Stauroxonaria, with skeleton built following pylonoid pattern, either completely or only at the early ontogenetic stage (initial frame is in a shape of a hollow sphere), i.e., represents a system of girdles twisted along their long axis for a complete turn, or along planes perpendicular to each other and fused at ends. This pattern of skeleton structure typically characterized by very large pores or gates (pylae) representing free spaces (openings) between ridges of variously curved and twisted girdles on surface of sphere. Initial frame is in shape of sphere and may be solid, hollow, nonperforated, rarely with few pores (Figs. 36v–36y).

Composition. Three superfamilies: Dactyliosphaeroidea Squinabol, 1904, emend. De Wever *et al.*,

2001; Pylonioidea Haeckel, 1881; and Larnacillioidea Haeckel, 1887 (Figs. 40; Table 7).

Occurrence. Middle Triassic–Recent.

Superfamily Dactyliosphaeroidea Squinabol, 1904, emend. De Wever *et al.*, 2001

Diagnosis. Pyloniata with microsphere, composed of one primary square ring, with two or four pairs of pylae opened to sides. Primary ring consists of four primary spines or bars, which may be coplanar, i.e., lie in one plane, or noncoplanar. Both sides of skeleton built above and below primary ring symmetrically to each other at 90° angle (Figs. 36x, 36y).

Composition. Six families: Patruliidae Dumitrica, 1989; Veghicycliidae Kozur et Mostler, 1972; Dactyliosphaeridae Squinabol, 1904, emend. De Wever *et al.*, 2001; Emiluviidae Dumitrica, 1995; Catenopylidae Dumitrica, 1989; and Pseudoaulophacidae Riedel 1967, emend. Dumitrica, 1997 (Fig. 40; Table 7).

Occurrence. Middle Triassic–Recent.

Family Patruliidae Dumitrica 1989

Diagnosis. Dactyliosphaeroidea with microsphere, two pairs of opposite pylae turned at 90° to each other, with four primary spines, which may be reduced, and two axial spines, as long or longer than the primary spines. The geometrical shape of the test resembles a tetrahedron with compressed angles and curved faces. The skeleton is formed by systems of three girdles. Sometimes skeleton reduced up to first system of girdles (Fig. 40; Table 7).

Composition. *Patrulius* Dumitrica, 1989 and *Tetratholura* Dumitrica, 1989.

Occurrence. Middle Triassic (Early Ladinian).

Family Veghicycliidae Kozur et Mostler, 1972

Diagnosis. Dactyliosphaeroidea with poorly studied very small microsphere. Four primary spines extend from microsphere crosslike in equatorial plane. Same plane contains monolayered reticular plate with large pores, which may be elongated on top near microsphere, surrounded by series of spines, and covered on both sides by spongy skeletal tissue. General shape of skeleton varies from spongy discoid to lens-shaped (Figs. 36y, 40; Table 7).

Composition. *Carinacyclia* Kozur et Mostler, 1972; *Praeorbiculiformella* Kozur et Mostler, 1978; and *Veghicyclia* Kozur et Mostler, 1972.

Occurrence. Late Triassic (Carnian)–Early Cretaceous (Hauterivian).

Family Dactyliosphaeridae Squinabol, 1904, emend. De Wever *et al.*, 2001

Diagnosis. Dactyliosphaeroidea with primary quadrangular ring, lying in equatorial plane, and two opposite four-pillared caps. Primary ring formed by four primary spines, growing from its corners. Caps have pair of large oppositely positioned gates and are symmetrical to each other after turn of 90°. Laterally, microsphere shaped like narrowing dome from one side and widening dome from another. General shape of skeleton is discoid or lenticular, with barrellike central part of test composed of one or two three-girdled systems, which form a characteristic crosslike structure with four wide, readily discernible gates. In stratigraphically young taxa, this structure is simplified, or may be reduced up to primary ring and four pairs of pillars. The peripheral skeleton is spongy or reticular with primary lobes (arms), with or without primary and secondary spines (Figs. 36x; 40; Table 7).

Composition. *Dactyliosphaera* Squinabol, 1904.

Occurrence. Late Triassic–Paleogene.

Family Emiluviidae Dumitrica, 1995

Diagnosis. Dactyliosphaeroidea with lenticular or flattened four-spined test with a double medullar shell and with a mono- or bilayered cortical shell separated from each other by a relatively wide space. The primary frame has a quadrangular primary ring and two oppositely positioned domes, symmetrical to one another after a turn of 90°. Each dome has six pillars (four pillars begin from the mid-sides of the primary ring, while two pillars begin from its angles), six gates, and four apical pores arranged in vertices of a rhomb. Two oppositely positioned wide gates are open in direction of short axis of this rhomb, while two pairs of smaller gates are open in direction of long axis. Second medullar shell reticular, quadrangular-lenticular, connected with microsphere by primary spines and by six bars on each side. Two groups of six bars structurally represent rows of girdles forming this shell and are also symmetrical to each other after a turn of 90°. Medullar shell is connected with cortical shell by four primary spines, lying in equatorial plane with varying numbers of radial bars. Spines are three-bladed. Each pair of oppositely positioned spines is turned in relation to each other for 90°. The spines lie in approximately one plane (Fig. 40; Table 7).

Composition. *Emiluvia* Foreman, 1973; *Kreutzstella* Empson–Morin, 1981; and *Tympaneides* Carter, 1988.

Occurrence. Middle Jurassic–Late Cretaceous (Campanian).

Family Catenopylidae Dumitrica, 1989

Diagnosis. Dactyliosphaeroidea with microsphere with two two-pillared caps and two pairs of oppositely positioned gates. Caps are symmetrical to each other in relation to equatorial plane after turn of 90°. Each dome of caps with two pores positioned perpendicular to gates. Outside microsphere, skeleton formed by systems of singular girdles. Each girdle of

two two-pillared caps turned for 90° in relation to each other around polar axis. Spherical or subspherical external cortical shell may be present (Fig. 40; Table 7).

Composition. *Catenopyle* Dumitrica, 1989 and *Praecatenopyle* Dumitrica, 1989.

Occurrence. Late Jurassic (Oxfordian)–Late Cretaceous (Maastrichtian).

Family Pseudoaulophacidae Riedel 1967, emend. Dumitrica, 1997

Diagnosis. Dactyliosphaeroidea with primary lobes (arms), if present, extending along primary spines. Pylome absent. Initial frame in shape of triangular prism. Primary spines lying in equatorial plane extend from each side of prism. Test is discoid, lenticular with tholi, spherical; or armed. Skeleton with 3–12 spines, three of which are primary. The external shell is spongy or reticular. The external ornamentation is present. Spongy skeletal tissue is built of concentric layers and, partly or completely, consists of isosceles triangular frames merged in massive nodes.

Composition. Two subfamilies: Pseudoaulophacinae Riedel, 1967, emend. De Wever *et al.*, 2001 and Pentapyloniinae Dumitrica, 2001 (Fig. 40; Table 7).

Occurrence. Middle Jurassic–Recent.

Subfamily Pseudoaulophacinae Riedel, 1967, emend. De Wever *et al.*, 2001

Diagnosis. Pseudoaulophacidae developing first extramicrospherical girdle. Skeleton lenticular, spongy, with typical pseudoaulofacoid ornamentation.

Composition. *Alievium* Pessagno, 1972; *Becus* Wu, 1986; *Dactyliodiscus* Squinabol, 1903; *Dispongotripus* Squinabol, 1903; *Godia* Wu, 1986; *Pessagnoella* Kozur et Mostler, 1978; and *Pseudoaulophacus* Pessagno, 1963.

Occurrence. Middle Jurassic–Paleogene (Eocene).

Subfamily Pentapyloniinae Dumitrica, 2001

Diagnosis. Pseudoaulophacidae not developing first extramicrospherical girdle. Test reticular, flattened, lenticular, or spherical.

Composition. *Pentapylonium* Dumitrica, 1991.

Occurrence. Late Cretaceous (Cenomanian)–Recent.

Superfamily Pylonioidea Haeckel, 1881

Diagnosis. Pyloniata, with a skeleton or only early stages of a skeleton fenestrated and built by systems of girdles in successively turned or perpendicular planes (Fig. 36w).

Composition. Two families: Micropylidae Dumitrica, 1988 and Pyloniidae Haeckel, 1881 (Fig. 40; Table 7).

Remarks. Pylonioidea is distinguished by the complete skeleton or only its early ontogenetic stages following a so-called pyloniacean mode of growth (Dumitrica, 1989; De Wever *et al.*, 2001). This growth pattern is completed by the development of the fenestrated skeleton, consisting of gates or pylae between the girdles of different levels.

Occurrence. Late Cretaceous (Cenomanian)–Recent.

Family Miropylidae Dumitrica, 1988

Diagnosis. Pylonioidea with eccentrically heteropolar microsphere, with four gates positioned in cross on antapical pole. First system four-girdled with four-pillared caps. Cortical test spherical or flattened, discoid, spongy or latticed, with annular chambers or arms in equatorial plane (Fig. 40; Table 7).

Composition. *Miropyle* Dumitrica, 1988.

Occurrence. Late Cretaceous (Cenomanian–Maastrichtian).

Family Pyloniidae Haeckel 1881, emend. Dumitrica, 1989

Diagnosis. Pylonioidea with eccentric heteropolar microsphere with single pair of gates on antapical end (Fig. 36w).

Composition. Four subfamilies: Palaeotetrapylinae Dumitrica, 1988; Pyloniinae Haeckel, 1881, emend. Dumitrica, 1989; Pylodiscinae Haeckel, 1887; and Dipylissinae Dumitrica, 1988 (Fig. 40; Table 7).

Occurrence. Paleogene (Paleocene)–Recent.

Subfamily Palaeotetrapylinae Dumitrica, 1988

Diagnosis. Pyloniidae with microsphere lacking antapical bar. First extramicrospherical girdle single capped, while succeeding are bi-capped (Fig. 36w).

Composition. Palaeotetrapyle Dumitrica, 1988.

Occurrence. Paleogene (Paleocene).

Subfamily Pyloniinae Haeckel, 1881, emend. Dumitrica, 1989

Diagnosis. Pyloniidae with a microsphere with antapical bar, four apical pores and six lateral pores. First and succeeding systems of extramicrospherical part of skeleton girdled, with caps. Girdles are elliptical, perpendicular to each other. Test is latticed spiral or spongy, maybe prunoid shell, with or without pylome (Fig. 36w).

Composition. *Larcospira* Haeckel, 1887; *Octopyle* Haeckel, 1881; *Pylonium* Haeckel, 1881; and *Tetrapyle* Mueller, 1858.

Occurrence. Paleogene (Paleocene)–Recent.

Subfamily Pylodiscinae Haeckel, 1887

Diagnosis. Pyloniidae with a microsphere with an antapical bar and bifurcating antapical cap. Test is three-armed in equatorial plane.

Composition. *Hexapyle* Haeckel, 1881; *Larcopyle* Dreyer, 1889; *Pylodiscus* Haeckel, 1887; and *Pylolena* Haeckel, 1887.

Occurrence. Paleogene (Middle Eocene)–Recent.

Subfamily Dipylissinae Dumitrica, 1988

Diagnosis. Pyloniidae with systems of two single-capped latticed girdles.

Composition. *Dipylissa* Dumitrica, 1988.

Occurrence. Neogene (Miocene)–Recent.

Superfamily Larnacillioidea Haeckel, 1887

Diagnosis. Pyloniata with two oppositely positioned gates, opened laterally in opposite directions. Initial frame heteropolar (Fig. 36v).

Composition. Two families: Larnacillidae Haeckel, 1887 and Tholoniidae Haeckel, 1887 (Fig. 40; Table 7).

Occurrence. Late Cretaceous (Cenomanian)–Recent.

Family Larnacillidae Haeckel, 1887

Diagnosis. Larnacillioidea, with skeleton formed completely or only at early ontogenetic stages is by systems of three large elliptical girdles lying in three perpendicular planes. All girdles, or only inner girdles have two pairs of gates (Fig. 36v).

Composition. Four subfamilies: Larnacillinae Haeckel, 1887; Histriastrinae Dumitrica, 1989; Cryptolarnaciinae Dumitrica, 1989; and Circodiscinae Dumitrica, 1989 (Fig. 40; Table 7).

Occurrence. Late Cretaceous (Cenomanian)–Recent.

Subfamily Larnacillinae Haeckel, 1887

Diagnosis. Larnacillidae with a skeleton, formed exclusively by systems of girdles, the last of which is with closed gates.

Composition. *Larnacilla* Haeckel, 1887; *Larnacopylomma* Dumitrica, 1989; and *Phorticium* Haeckel, 1881.

Occurrence. Late Cretaceous (Cenomanian)–Recent.

Subfamily Histriastrinae Dumitrica, 1989

Diagnosis. Larnacillidae, with a cortical shell having two four-chambered tubular lobes (arms). One of the latter possesses a pylome.

Composition. *Amphimenium* Haeckel, 1881; *Histiastrum* Ehrenberg, 1847; *Stauralastrum* Haeckel, 1887; and *Stephanastrum* Ehrenberg, 1847.

Occurrence. Paleogene (Late Paleocene)–Neogene (Early–Middle Miocene).

Subfamily Cryptolarnaciinae Dumitrica, 1989

Diagnosis. Larnacillidae, in which the primary inner frame is in a shape of a hollow sphere and surrounded by a spherical, lenticular or ellipsoidal cortical shell, while the latter is separated by an empty space. A pylome may be present.

Composition. *Coccolarnacium* Dumitrica, 1989; *Cryptolarnacium* Dumitrica, 1989; and *Spongopyle* Dreyer, 1889.

Occurrence. Paleogene (Late Paleocene)–Recent.

Subfamily Circodiscinae Dumitrica, 1989

Diagnosis. Larnacillidae with a discoid or lenticular skeleton, the central part of which is composed in a way common in all Larnacillidae and is surrounded by spongy or latticed tissue, lying in one plane (Fig. 36v).

Composition. *Circodiscus* Kozlova, 1972; *Plectodiscus* Kozlova, 1972; and *Spongodiscus* (part.) Ehrenberg, 1854.

Occurrence. Paleogene (Late Paleocene)–Recent.

Family Tholoniidae Haeckel, 1887

Diagnosis. Larnacillioidea, with closed gates (Fig. 40; Table 7).

Composition. *Tholocubus* Haeckel, 1887 and *Tholonium* Haeckel, 1887.

Occurrence. Paleogene (Oligocene)–Recent.

Order Spongurata Haeckel, 1862

Diagnosis. Spherical, ellipsoidal, discoidal, or subcylindrical Stauraxonaria (Fig. 36u). The inner frame is in shape of hollow sphere surrounded by spongy layer, which is arranged concentrically, spirally, radially, or irregularly.

Composition. Two families: Sponguridae Haeckel, 1862 and Litheliidae Haeckel, 1862 (Fig. 40; Table 7).

Occurrence. Middle Triassic–Recent.

Family Sponguridae Haeckel, 1862

Diagnosis. Discoidal or flatly convex, subcylindrical, less commonly ellipsoidal Spongurata with or without polar spines, with a pylome at one of the poles.

Spongy tissue is arranged in concentric layers (Figs. 36u, 40; Table 7).

Composition. *Amphibrachium* Haeckel, 1881; *Patellula* Kozlova, 1972; *Spongocore* Haeckel, 1887; *Prunobrachium* Kozlova, 1966; and *Spongurus* Haeckel, 1860.

Occurrence. Middle Triassic–Recent.

Family Litheliidae Haeckel, 1862

Diagnosis. Spherical or ellipsoidal Spongurata lacking polar spines. Spongy tissue is arranged in concentric layers or spirally (Fig. 40; Table 7).

Composition. *Cromyodruppa* Haeckel, 1887 and *Lithelius* Haeckel, 1860.

Occurrence. Late Triassic–Recent.

Order Spongodiscata Haeckel, 1862

Diagnosis. Discoidal, lenticular or spheroidal Stauraxonaria (Fig. 36z). Spongy skeleton with irregular or dense, concentrically or spirally arranged layers. The primary frame, which is in shape of hollow sphere, may sometimes be indiscernible. Radial arms may or may not be present.

Composition. Three families: Relindellidae Kozur et Mostler, 1980; Spongodiscidae Haeckel, 1862; and Coccodiscidae Haeckel, 1862, emend. Sanfilippo et Riedel, 1980 (Fig. 40; Table 7).

Occurrence. Late Triassic–Recent.

Family Relindellidae Kozur et Mostler, 1980

Diagnosis. Discoidal Spongodiscata with four or six equatorial spines (Fig. 40; Table 7).

Composition. *Pentaspongodiscus* Kozur et Mostler, 1979; *Relindella* Kozur et Mostler, 1980; and *Tetraspongodiscus* Kozur et Mostler, 1979.

Occurrence. Late Triassic (Carnian).

Family Spongodiscidae Haeckel, 1862

Diagnosis. Spongodiscata with flattened or lenticular skeleton and inner frame in shape of hollow concentric sphere. The shell is reticular, with concentric rings, or spongy, with irregularly built tissue or with densely spaced concentric or spiral rings. Spongy or chambered lobes may be developed (Figs. 36z, 40; Table 7).

Composition. *Amphirhopalum* Haeckel, 1881; *Chitonastrum* Haeckel, 1881; *Dictyocoryne* Ehrenberg, 1860; *Euchitonia* Ehrenberg, 1860; *Ommatodiscus* Stöhr, 1880; *Perichlamydium* Ehrenberg, 1847; *Porodiscus* Haeckel, 1881; *Rhopalastrum* Ehrenberg, 1847; *Spongaster* Ehrenberg, 1860; *Spongodiscus* Ehrenberg, 1854; *Spongotrochus* Haeckel, 1860; *Stylochlamydium* Haeckel, 1881; *Stylodictya* Ehrenberg, 1847; *Stylospongia* Haeckel, 1862; *Tessarastrum* Haeckel, 1887; *Tholodiscus* Kozlova, 1972; and *Trigonastrum* Haeckel, 1887.

Occurrence. Late Cretaceous–Recent.

Family Coccodiscidae Haeckel, 1862, emend. Sanfilippo et Riedel, 1980

Diagnosis. Lenticular, discoidal or ellipsoidal Spongodiscata with two internal shells. The inner frame is in shape of very small hollow sphere.

Composition. Two subfamilies: Coccodiscinae Haeckel, 1862 and Artiscinae Haeckel, 1881 (Fig. 40; Table 7).

Occurrence. Paleogene (Early Eocene)–Recent.

Subfamily Coccodiscinae Haeckel, 1862

Diagnosis. Coccodiscidae with discoidal or lenticular skeleton. Internal shell connected with external by bars positioned at poles. Skeleton may or may not have chambered lobes (arms).

Composition. *Astrophacus* Haeckel, 1881; *Coccocyclia* Haeckel, 1881; *Coccodiscus* Haeckel, 1862; *Heliosestrum* Haeckel, 1881; *Heliostylus* Haeckel, 1881; *Lithocyclia* Ehrenberg, 1847; *Periphaena* Ehrenberg, 1873; *Phacodiscus* Haeckel, 1881; *Phacostaurus* Haeckel, 1881; *Phacostylus* Haeckel, 1881; *Trigonactum* Haeckel, 1881; and *Sethostylus* Haeckel 1881.

Occurrence. Paleogene (Early Eocene)–Recent.

Subfamily Artiscinae Haeckel, 1881 emend. Riedel, 1967

Diagnosis. Coccodiscidae with ellipsoidal skeleton. Internal shell is connected with external by bars lying in equatorial or subequatorial plane.

Composition. *Cypassis* Haeckel, 1887; *Diartus* Sanfilippo et Riedel, 1980; *Didymocyrtis* Haeckel, 1862; *Ommatartus* Haeckel, 1881; and *Spongoliva* Haeckel 1887.

Occurrence. Paleogene (Late Oligocene)–Recent.

Class Nassellaria Ehrenberg, 1847, emend. Afanasieva et Amon, nov.

Diagnosis. Heteropolar or bilaterally-symmetrical Polycystina. Skeleton based on inner frame in shape of hollow sphere, polyhedron or spicule (Figs. 10d–10g, 10o), and external shell (conical, pyramidal, spindle-shaped, bell-shaped, helmet-shaped, cap-shape, or differently shaped test or external skeleton), often segmented (Figs. 42, 44–49). External skeleton subdivided into four main portions: (I) cephalis, (II) thorax, (III) abdomen, and (IV) postabdomen. The last portion may be further segmented (2–15 or more segments) (Fig. 46). Inner skeletal polyhedron (5–30 μm in diameter) and spicule included in cephalis, median bar of spicule separates cephalis from thorax. Number and position of rays (spines) of spicule stable: spines *A*, *D*, and *2l* arising from one end of median bar (*MB*), spines *V, 2L,* and *Ax* extending from another end.

Composition. Three orders: Pylomariata Afanasieva, 1999; Cyrtidinata Haeckel, 1862; and Spyridinata Ehrenberg, 1847 (Figs. 41, 43; Table 7).

Remarks. Nassellarians are the most taxonomically diverse in Polycystina. Their skeletons extremely complex, but all of them include several groups of morphological elements, almost equally participating in skeletons. First of all, there are internal and external constructions, i.e., initial spicule and internal polyhedron, and also the external skeleton with its segmentation and ornamentation. One of the features of nassellarians is that the diversity of their skeletons is achieved by the additions of superimpositions on the cephalis, which increase the heteropolarity of their body. Nassellarians have traditionally been studied only from the Mesozoic and Cenozoic, although Paleozoic ancestors of nassellarians (Pylomariata) suggest the appearance of primitive nassellarians as early as in the Middle Cambrian.

Paleozoic Pylomariata grouped together with Mesozoic and Cenozoic Cyrtidinata and Spyridinata extend the range of Nassellaria from the Middle Cambrian to the present, taking into account their distinct morphology enabling recognition of Nassellaria as a separate class.

Occurrence. Cambrian–Recent.

Order Pylomariata Afanasieva, 1999

Diagnosis. Heteropolar or bilaterally symmetrical Nassellaria (Figs. 17, 42, 43). External skeleton mainly spherical, less commonly oviform, segmented or not segmented, and with pylome. Inner frame formed by hollow sphere with extending rays, spicule, or spicule and two columellae.

Composition. Four superfamilies: Proventocitoidea Aitchison, 1998; Cessipyloroidea Afanasieva, 1999; Pylentonemoidea Deflandre, 1963; and Popofskyelloidea Deflandre, 1964 (Figs. 41, 43; Table 7).

Occurrence. Cambrian–Early Cretaceous.

Superfamily Proventocitoidea Aitchison, 1998

Diagnosis. Pylomariata with bilaterally-symmetrical, ovoid test, with porous wall of external sphere and hypothetical inner frame in shape of hollow sphere (Figs. 10d; 42e, 42f).

Composition. One family Proventocitidae Aitchison, 1998 (Figs. 41, 43; Table 7).

Occurrence. Cambrian–Ordovician.

Family Proventocitidae Aitchison, 1998

Diagnosis. Proventocitoidea with skeleton composed of one shell with hypothetical inner frame in shape of hollow sphere with four or more rays (Figs. 10d, 42e, 42f, 41, 43).

Composition. *Procyrtis* Li, 1995; *Proventocitum* Nazarov et Ormiston, 1990; and *Ulcundia* Nazarov, 1974.

Occurrence. Cambrian–Ordovician.

Superfamily Cessipyloroidea Afanasieva, 1999

Diagnosis. Spherical Pylomariata with porous or spongy wall of external shell and inner frame in shape of hollow sphere or isometric polyhedron (Figs. 10e–10f; 42g–42j, 44a, 44b).

Composition. Two families: Cessipyloridae Afanasieva, 1999 and Aciferopyloridae Afanasieva, 1999 (Figs. 41, 43; Table 7).

Occurrence. Middle Ordovician–Middle Triassic.

Family Cessipyloridae Afanasieva, 1999

Diagnosis. Cessipyloroidea with inner frame in shape of hollow sphere or isometric central polyhedron with six or seven rays connected with six or seven external main spines (Figs. 10e, 10g, 17, 42g, 42h, 42j, 44a, 44b).

Composition. Three subfamilies: Cessipylorinae Afanasieva, 1999; Caspiazinae Afanasieva, 2000 (Figs. 41, 43; Table 7).

Occurrence. Middle Ordovician–Middle Triassic.

Subfamily Cessipylorinae Afanasieva, 1999

Diagnosis. Cessipyloridae with skeleton composed of one or two spheres, inner frame in shape of hollow sphere, and rodlike external main spines (Figs. 10e, 42g, 42h, 44a, 41, 43).

Composition. *Cessipylorum* Nazarov et Ormiston, 1986 and *Fusalfanus* Furutani, 1990.

Occurrence. Middle Ordovician–Early Devonian.

Subfamily Caspiazinae Afanasieva, 2000

Diagnosis. Cessipyloridae with skeleton composed of one sphere, with inner frame in shape of isometric central polyhedron, and three-bladed external main spines (Figs. 10g, 17, 42j, 44b, 41, 43).

Composition. *Caspiaza* Afanasieva, 1986 and *Glomeropyle* Aita et Bragin, 1999.

Occurrence. Late Devonian–Middle Triassic.

Family Aciferopyloridae Afanasieva, 1999

Diagnosis. Cessipyloroidea with skeleton composed of two spheres, with inner frame in shape of hollow sphere with numerous rays connected to numerous rodlike external main spines (Figs. 10f, 42i, 41, 43; Table 7).

Composition. *Aciferopylorum* Nazarov et Ormiston, 1990.

Occurrence. Silurian.

Superfamily Pylentonemoidea Deflandre, 1963

Diagnosis. Spheroid or cylindroid Pylomariata with porous, less commonly spongy wall of external shell and inner initial frame represented by spicule. External skeleton sometimes segmented into portions ("cephalis," "thorax"); former portion may be further subdivided. Strong feet may be present (Figs. 42l–42x, 44c, 44d).

Composition. Three families: Pylentonemidae Deflandre, 1963; Poulpidae De Wever 1981; and Tripedurnulidae Dumitrica 1991 (Figs. 41, 43; Table 7).

Occurrence. Silurian–Cretaceous.

Family Pylentonemidae Deflandre, 1963

Diagnosis. Pylentonemoidea with inner frame in shape of four- to seven-rayed spicule, rays of which connected to four to seven three-bladed external main spines (Figs. 42l–42r, 42u–42w, 42x, 44c, 44d, 41, 43).

Composition. Three subfamilies: Archocyrtiinae Kozur et Mostler, 1981; Pylentoneminae Deflandre, 1963; and Vallupinae Pessagno et McLeod, 1987 (Figs. 41, 43; Table 7).

Occurrence. Silurian–Jurassic.

Subfamily Archocyrtiinae Kozur et Mostler, 1981, emend. Afanasieva, 1999

Diagnosis. Pylentonemidae with skeleton composed of one sphere (Figs. 42l–42r; 44d; 41; 43). Test monocyrtid, with initial spicule, formed by seven rays (*A*, *V*, *D*, *2L*, *2l*), extending from centrally or subcentrally positioned *MB*. All or some rays of spicule continue outside test as three-bladed main spines. Arcs connecting rays at one level absent. Basal part of external skeleton has large pylome, surrounded by three or four spines.

Composition. *Allocyrtium* Afanasieva, 1986; *Archocyrtium* Deflandre, 1972; *Cerarchocyrtium* Deflandre 1973; *Cyrtisphaeractenium* Deflandre, 1972; *Cyrtisphaeronemium* Deflandre, 1972; *Deflandrellium* Cheng, 1986; *Mostlerium* Cheng, 1986; *Robotium* Cheng, 1986; and *Pararchocyrtium* Deflandre 1972.

Occurrence. Silurian–Middle Triassic.

Subfamily Pylentoneminae Deflandre, 1963, emend. Afanasieva, 1999

Diagnosis. Pylentonemidae with skeleton composed of two spheres (Figs. 42u–42w, 44c, 41, 43).

Composition. *Pylentonema* Deflandre, 1963 and *Quadrapesus* Cheng, 1986.

Occurrence. Late Devonian–Early Carboniferous.

Subfamily Vallupinae Pessagno et McLeod, 1987

Diagnosis. Pylentonemidae with skeleton composed of two spheres with (or without) strong, three-bladed main spines (Figs. 42x, 41, 43). External shell with one or several tubular, nonperforated pylomes.

Composition. *Bivallupus* Pessagno et McLeod, 1987; *Mesovallupus* Pessagno et McLeod, 1987; *Neovallupus* Yang et Pessagno, 1989; *Protovallupus* Pessagno et McLeod, 1987; *Supervallupus* Yang et Pessagno, 1989; and *Vallupus* Pessagno et Blome 1984.

Occurrence. Late Jurassic (Oxfordian–Tithonian).

Family Poulpidae De Wever, 1981

Diagnosis. Pylentonemoidea with large spherical "cephalis," with three robust feet (Figs. 42t, 41, 43; Table 7). Feet representing continuations of spines *D* and *L* of initial spicule. Spicule located in center of base of "cephalis" or inside its cavity. It includes rays (spines) *A*, *D*, *V*, *L*, *l* connected by arcs *AV*, *Al*, *Dl*, *Ll*, *LV*. Inside "cephalis," apical spine *A* in subaxial position, not included in wall of "cephalis," and usually connecting with outside into apical horn. Ventral and secondary lateral rays may also continue into external spines.

Composition. *Eonapora* Kozur et Mostler, 1979; *Hozmadia* Dumitrica, Kozur, et Mostler, 1980; *Neopylentonema* Kozur, 1984; *Poulpus* De Wever, 1979; *Saitoum* Pessagno, 1977; and *Triassobipedis* Kozur, 1984.

Occurrence. Middle Triassic (Anisian)–Early Cretaceous (Albian).

Family Tripedurnulidae Dumitrica, 1991

Diagnosis. Pylentonemoidea (Figs. 42s, 41, 43; Table 7) with initial spicule, composed of *MB*, spines *A*, *V*, *D*, *L*, and *l* connected by arcs *Al, Dl*, *Ll*, and *LV*, while arc *AV* absent. Axial spine *V* very short. Test composed of relatively large "cephalis," with eccentrically positioned apical horn and three, rarely one, feet, representing external continuations of *D* and *L*. "Cephalis" with two chambers: one chamber large, opening apically and another chamber small dorsal, delineated by arcs *Al*.

Composition. *Baratuna* Kozur et Mostler, 1981; *Pseudopoulpus* Takemura, 1986; *Takoum* Takemura, 1986; *Tridentocyrtis* Steiger et Steiger, 1994; *Tripedocassis* Dumitrica, 1991; *Tripedocorbis* Dumitrica, 1991; *Tripedurnula* Dumitrica, 1991; and *Turanta* Pessagno et Blome, 1982.

Occurrence. Middle Triassic (Anisian)–Early Cretaceous (Albian).

Superfamily Popofskyelloidea Deflandre, 1964

Diagnosis. Pylomariata with bilaterally-symmetrical conical segmented external skeleton (Figs. 42a–42d). Subspherical apical segment present. Porous, lamellar external shell and inner frame in shape of spicule and two columellae.

Composition. Two families: Popofskyellidae Deflandre, 1964 and Hexapylocapsidae Dumitrica et Zugel, 1998 (Figs. 41, 43; Table 7).

Occurrence. Late Devonian–Jurassic.

Family Popofskyellidae Deflandre, 1964

Diagnosis. Popofskyelloidea with skeleton composed of one conical or cylindrical cyrtoid shell with inner frame in shape of three- and more-rayed spicule and two columellae (Figs. 42a–42c, 41, 43; Table 7). Segmentation of nassellariod type, with two or more "segments." When spicule preserved in "cephalis," it has discernible rays (spines) *MB*, *A*, *V*, *2L*, and *2l*. Arcs absent. "Cephalis" sometimes with two or more horns; columellae, located opposite to each other in the postcephalic region, and included in wall, sometimes continuing beyond it. Pores on porous wall arranged in transverse rows or irregularly.

Composition. *Cyrtentactinia* Foreman, 1963; *Popofskyellum* Deflandre, 1964; *Totollum* Schwartzapfel et Holdsworth, 1996; and *Tuscaritellum* Deflandre, 1972.

Occurrence. Late Devonian–Permian.

Family Hexapylocapsidae Dumitrica et Zugel, 1998

Diagnosis. Popofskyelloidea with "monocyrtid" bispherical test with isometric central polyhedron, which can be regarded as "cephalis" (Figs. 42d, 41, 43; Table 7). Spicule with *MB*, spines *A*, *V*, *D*, *L*, *l*, and arcs *Dl*, *lL*, *LV*, and apparently *Al*. "Cephalis" small, located inside wide open external skeleton and connected to it by rays of spicule.

Composition. *Hexapylocapsa* Dumitrica et Zugel, 1998.

Occurrence. Late Jurassic (Early Tithonian).

Order Cyrtidinata Haeckel, 1862

Diagnosis. Nassellaria with skeleton differentiated in direction of main heteropolar axis (Figs. 46k–46z). Multirayed initial spicule well developed. Spines *D*, *L*, *Ll* equally developed. Spine *A* is usually developed, and sometimes *V*, l_r, l_l, and *Ax*. Among arcs, *ap* and *aj* best developed. Spines and arcs not forming sagittal ring.

Composition. Seven superfamilies: Archipilioidea Haeckel, 1881; Acropyramidoidea Haeckel, 1881; Lychnocanioidea Haeckel, 1881; Eucyrtidioidea Ehrenberg, 1847; Stichocapsoidea Haeckel, 1881; Amphipyndacioidea Riedel, 1967, emend. De Wever *et al.*, 2001; and Cannobotryoidea Haeckel, 1881 (Fig. 41; Table 7).

Occurrence. Triassic–Recent.

Superfamily Archipilioidea Haeckel, 1881

Diagnosis. Cyrtidinata with one or two segments. Cephalis large. Spines *A*, *D*, *L*, *V*, *Ax* and bars of spicule large (Figs. 46k–46u). Spine *A* sometimes running free as columella; in this case, cephalis not subdivided into chambers and portions. Spine *A* developing in apical horn. Spines *D* and *L* often forming large feet, directed below and sideways. Walls may be of all types known in nassellarians. Often wall of thorax or all test not developed, only with tangled spicular bars and spicular cyst.

Composition. Five families: Archipiliidae Haeckel, 1881; Sethoperidae Haeckel, 1881; Plagoniidae Haeckel, 1887; Cystidiidae Haeckel, 1883; and Pseudosaturniformidae Kozur et Mostler, 1979 (Fig. 41; Table 7).

Occurrence. Triassic–Recent.

Family Archipiliidae Haeckel, 1881

Diagnosis. Archipilioidea with one or two segments (Figs. 46k–46q). Cephalis often lacking apical horn, small; internal bars *MB*, and *L* often almost reduced. Thorax wider cephalis, cylindrical or conical. Wall spongy or porous, with rounded or oval pores, which can be arranged irregularly in transverse rows. Spines *D* and *2L* extending in upper part of thorax as ridges, then forming terminal or lateral feet. Aperture either open, slightly narrowed, or blind. Thorax wall or entire test wall often not developed. Only tangled spicular bars forming spicular cyst present.

Composition. Eight subfamilies: Archipiliinae Haeckel, 1881; Clathromitrinae Petrushevskaya, 1971; Zamolxinae Dumitrica, 1982; Nabolellinae Kozur et Mostler, 1979; Lophophaeninae Haeckel, 1881; Sethopiliinae Haeckel, 1881; Dimelissinae Petrushevskaya, 1981; and Plectaniinae Haeckel, 1881 (Fig. 41; Table 7).

Occurrence. Triassic–Recent.

Subfamily Archipiliinae Haeckel, 1881

Diagnosis. The same as for family. Cephalis lacking horn.

Composition. *Archipilium* Haeckel, 1881; *Nothotripodiscinus* Deflandre, 1972; and *Parapoulpus* Kozur et Mostler, 1979.

Occurrence. Triassic–Recent.

Subfamily Clathromitrinae Petrushevskaya, 1971

Diagnosis. Dicyrtid Archipiliidae with well developed arcs of basal ring *cd* and *dd*, while collar constriction not noticeable. Eucephalic region of cephalis not delineated, cephalis large; thorax the same size as cephalis. Aperture open. Spine *A* running free in cavity of cephalis and represents columella, giving rise to processes *a*. Outside spines *A, D*, and *L* developing quite large horn and feet. Spines *D* and *L* directed obliquely down. In case of porous wall, pores having various shapes, arranged irregularly or forming longitudinal rows. Surface usually possessing spines, crests, in places spongy tissue.

Composition. *Archiscenium* Haeckel, 1881; *Clathromitra* Haeckel, 1881; *Corythomelissa* Campbell, 1951; *Euscenarium* Haeckel, 1887; *Euscenium* Haeckel, 1887; *Halicalyptra* Haeckel, 1881; *Phaenocalpis* Haeckel, 1887; *Phaenoscenium* Haeckel, 1887; *Spongomelissa* Haeckel, 1887; *Tripocalpis* Haeckel, 1881; *Tripodiscinus* Haeckel, 1887; *Tripodisculus* Haeckel, 1887; *Tripophaenoscenium* Campbell et Clark, 1944; and *Vicillata* Popofsky, 1913.

Occurrence. Triassic–Recent.

Subfamily Zamolxinae Dumitrica, 1982

Diagnosis. Archipiliidae with complex heteropolar spicular skeleton. Spicule apical basal (dorsal), vertical, and primarily-lateral, extending from short median bars (Figs. 46p, 46q). Axial and secondarily-lateral spines also occasionally present, although being short. Spines free or connected by arcs in frame (cyst). Spinules and thorns present, making characteristic teethed appearance on spines. External skeleton absent.

Composition. *Zaldacria* Dumitrica, 1982; *Zamolxis* Dumitrica, 1982; and *Tetrarchiplagia* Dumitrica, 1982.

Occurrence. Triassic (Anisian)–Eocene.

Subfamily Nabolellinae Kozur et Mostler, 1979

Diagnosis. Bicyrtid Archipiliidae (Fig. 46k) with initial spicule composed of *MB*, spines *A*, *D*, *V*, *L*, *l*, and arcs *AV*, *Al*, *Dl*, *Ll*, and *LV*. Spine *A* usually extending outside test wall into apical horn; *D* and *L* continuing along thorax in three feet. Cephalis large with pores uneven in size, shape, and arrangement; cephalis wall usually with intersected ridges. Thorax wide, conical, cylindrical or subcylindrical.

Composition. *Fueloepicyrtis* Kozur et Mostler, 1981 and *Nabolella* Petrushevskaya, 1981.

Occurrence. Middle Triassic–Late Triassic.

Subfamily Lophophaeninae Haeckel, 1881

Diagnosis. Archipiliidae with two segments (Figs. 46n, 46o). Porous eucephalic chamber egg-shaped, narrowing basally. Subsidiary lobes fused with thorax. Arcs *ap* extending obliquely, separating eucephalic chamber from remaining skeleton. Collar strictum not sharp. Processes *p* and spines *A* and *V* extending as ridges and appear as thorns on sides of cephalis. Spine *V* not stabilized. Axobate developed weakly. When thorax developed, it is being wide, conical, longer and wider than cephalis. Wall porous or cellular. Aperture widely open.

Composition. *Acanthocoronium* Haeckel, 1887; *Cephaluspinus* Alvira Martin, 1971; *Amphiplecta* Haeckel, 1881; *Arachnocorallium* Haeckel, 1887; *Dictyocryphalus* Haeckel, 1887; *Lophophaena* Ehrenberg, 1847 *Marimoum* Funakawa, 1994; *Ovum* De Wever, 1982; *Syscioscenium* Sugiyama, 1992; *Thetis* De Wever, 1982; and *Tripodocyrtis* Funakawa, 1994.

Occurrence. Jurassic–Recent.

Subfamily Sethopiliinae Haeckel, 1881

Diagnosis. Archipiliidae with cephalis, with oviform eucephalic chamber, strongly narrowing basally; subsidiary lobes small. Collar strictum sharp. Processes *p* of spine *L* and spine *V* directed upwards and extending into cephalic wall, forming ridges similar to those of spine *A*. Sometimes spine *V* not developed, while only three bars *MB* and *2L* developed in base of cephalis. Axobate developed weakly. Thorax sometimes present. If porous wall present, pores on cephalis round. Wall may be spongy and pseudoaulophacoid. Subsidiary spinules usually present on test surface. Aperture open or closed saclike.

Composition. *Arachocorallium* Haeckel, 1881; *Arachnocalpis* Haeckel, 1881; *Archibursa* Haeckel, 1881; *Peromelissa* Haeckel, 1881; *Plectacantha* Jorgensen, 1905; *Sethopilium* Haeckel, 1887; and *Tripodocorys* Haeckel, 1881.

Occurrence. Cretaceous–Recent.

Subfamily Dimelissinae Petrushevskaya, 1981

Diagnosis. Archipiliidae with ellipsoidal eucephalic chamber with porous or cellular walls, not narrowing basally (Figs. 46l, 46m). Arcs *ap* are raised and not lying at the base of cephalis. Collar strictum not sharp. Spine *V* may be fused with one of spines *L*. Axobate developed weakly. When thorax present, it somewhat wider than cephalis, but not longer. Aperture open or closed saclike.

Composition. *Acromelissa* Haeckel, 1881; *Arachnocorys* Haeckel, 1860; *Archiperidium* Haeckel, 1887; *Dicorys* Popofsky, 1913; *Dimelissa* Campbell, 1951; *Lithomelissa* Ehrenberg, 1847; *Lophophaenoma* Haeckel, 1887; *Phormacantha* Jorgensen, 1905; and *Psilomelissa* Haeckel, 1881.

Occurrence. Paleogene?–Recent.

Subfamily Plectaniinae Haeckel, 1881

Diagnosis. Archipiliidae with test or its rudiments absent, while entire skeleton represented by cephalis. Main spines well developed from initial spicule being straight and composed of three plates. Spines give rise to processes, sometimes with anastomoses producing fine web.

Composition. *Dumetum* Popofsky, 1908 and *Plectanium* Haeckel, 1881.

Occurrence. Quaternary.

Family Pseudosaturniformidae Kozur et Mostler, 1979

Diagnosis. Archipilioidea with spherical cephalis and conical or spindle-shaped thorax (Figs. 41, 46u;

Table 7). Initial spicule with spines *A*, *V*, *D*, *L*, and *l*. Spines *D* and *L* lie at the base of cephalis.

Composition. *Pseudosaturniforma* Kozur et Mostler, 1979.

Occurrence. Middle Triassic–Jurassic.

Family Sethoperidae Haeckel, 1881

Diagnosis. Archipilioidea with one to three segments (47r–47t). Cephalis spherical, neck not developed; basal arcs distinct, cephalis narrowed basally. If wall porous, pores rounded, arranged either irregularly or in transverse rows; pores rimmed or framed. Sometimes subsidiary spongy shell developed around test. Sometimes wall made of tangled finest threadlike bars or spiny frame present. Spine *A* extends free in cavity of cephalis as columella; apophyses *a* extending approximately from middle of columella. Spine *A* developed into large apical horn. Spine *V* weakly developed. Spines *D* and *2L* running in the walls of thorax as costae and producing lateral feet or wings. Apical horn and feet faced, composed of three plates with lateral apophyses. Thorax wider and longer than cephalis. Thorax may terminate as shelf and have three large windows in upper part. Often walls of thorax stretched between three costae, which produced by extensions of spines *D* and *2L*. Sometimes only one thin-walled cephalis with extending from it branching spines present. Abdomen rarely developed. Aperture either open, or closed saclike.

Composition. Two subfamilies: Sethoperinae Haeckel, 1881 and Tetraplectinae Haeckel, 1881 (Fig. 41; Table 7).

Occurrence. Early Jurassic (Pliensbachian)–Recent.

Subfamily Sethoperinae Haeckel, 1881

Diagnosis. Sethoperidae with a porous or cellular test containing one to three segments (Figs. 46r–46t).

Composition. *Arachnopilium* Haeckel, 1881; *Artopera* Haeckel, 1881; *Callimitra* Haeckel, 1881; *Cladoscenium* Haeckel, 1881; *Clathrocorona* Haeckel, 1881; *Clathrocorys* Haeckel, 1881; *Clathrolychnus* Haeckel, 1881; *Dictyocodoma* Haeckel, 1887; *Dictyocodon* Haeckel, 1881; *Periplecta* Haeckel, 1881; *Plectagonidium* Cachon et Cachon, 1969; *Pteropilium* Haeckel, 1881; *Sethopera* Haeckel, 1881; and *Tripocyrtis* Haeckel, 1887.

Occurrence. Early Jurassic (Pliensbachian)–Recent.

Subfamily Tetraplectinae Haeckel, 1881

Diagnosis. Sethoperidae with skeleton composed of main spines and their apophyses, connected by tangled finest bars. Cephalis wall absent.

Composition. *Enneaplegma* Haeckel, 1881; *Polyplecta* Haeckel, 1887; *Tetraplecta* Haeckel, 1881; and *Plectaniscus* Haeckel, 1887.

Occurrence. Quaternary.

Family Plagoniidae Haeckel, 1881

Diagnosis. Archipilioidea with cylindrical spines. Porous test not developed (Fig. 41; Table 7).

Composition. *Pentaplegma* Haeckel, 1881 and *Plagonium* Haeckel, 1881.

Occurrence. Quaternary.

Family Cystidiidae Haeckel, 1883

Diagnosis. Archipilioidea without mineral skeleton. Only central capsule present (Fig. 41; Table 7).

Composition. *Cystidium* Hertwig, 1879; *Nassella* Haeckel, 1897; and *Paracystidium* Cachon et Cachon, 1969.

Occurrence. Quaternary.

Superfamily Acropyramidoidea Haeckel, 1881

Diagnosis. Cyrtidinata with two, less commonly one to four or more segments (Figs. 46v–46z). Cephalis of various sizes. Three types of cephalis present.

(1) Spine *A* runs free as columella; cephalis not divided into lobes, being separating from thorax by basal arcs (Figs. 47l, 47g).

(2) Spine *A* near anterior wall (Fig. 47h). Eucephalic and lateral lobes present. Lateral lobes separated from thorax. Arcs of basal ring not developed.

(3) Lobes and main spines of cephalis poorly developed. Test mainly conical. External apophyses of spines *D* and *L* thin and poorly developed.

Thorax forming largest part of external skeleton. In cases of cephalis of types 2 or 3 thorax occasionally having constrictions or transverse thickenings of wall, separating it into two or three, rarely more portions. Walls most often porous. Pores arranged in longitudinal or transverse rows. Finest meshwork with irregular arrangement of bars relatively rarely developed.

Composition. Four families: Sethophormididae Haeckel, 1881; Bulbocyrtiidae Kozur et Mostler, 1981; Acropyramididae Haeckel, 1881; and Lampromitridae Haeckel, 1881 (Fig. 41; Table 7).

Occurrence. Triassic–Recent.

Family Sethophormididae Haeckel, 1881

Diagnosis. Acropyramidoidea with two or three segments, rarely more or less (Figs. 46w–46y). Second segment may be subdivided into pedestal and widened part or other portions. Cephalis of two types. Test walls are porous or cellular. Pores arranged in regular longitudinal or transverse rows. Often arrangement orthogo-

nal. Cephalis sometimes reduced to arcs and bars. Spines *V* and *l* absent.

Composition. Five subfamilies: Sethophormidinae Haeckel, 1881; Theopiliinae Haeckel, 1881; Rotaforminae Pessagno, 1970; Neosciadiocapsinae Pessagno, 1969; and Enneaphormidinae Petrushevskaya, 1981 (Fig. 41; Table 7).

Occurrence. Triassic–Recent.

Subfamily Sethophormidinae Haeckel, 1881

Diagnosis. Sethophormididae with two or three segments. Third segment not always well developed. Collar constriction distinct, basal ring developed. Cephalis of type 1, thorax large, umbrella-shaped, wider and longer cephalis. Aperture terminal, widely open or closed by plate of velum with skirt. Wall porous. Pores rounded or polygonal, arranged irregularly or in longitudinal rows. No significant apical horn or feet present.

Composition. *Astrophormis* Haeckel, 1887; *Sethophormis* Haeckel, 1881; *Theophormis* Haeckel, 1881; and *Velicuculus* Riedel et Campbell, 1952.

Occurrence. Triassic–Recent.

Subfamily Theopiliinae Haeckel, 1881

Diagnosis. Sethophormididae with two or three (or more, up to eight) segments, conical, flattened (Fig. 46y). Collar strictum indistinct. Arcs of basal ring developed. Cephalis of type 2 (Fig. 47h). In walls of thorax shelves and constrictions, its upper part may be separated by constriction with pedestal. Skirt extending sideways with one to six concentric rows of pores present or cylindrical orally narrowed terminal segment may be present. Aperture terminal, closed by velum, stretched on shelf, or open. Velum flat or bowl-shaped; penetrated or not penetrated by pores. Wall porous. Pores arranged in transverse concentric rows. Third segment (or skirt) sometimes have longitudinal and transverse rows of pores. Sometimes subsidiary spongy layer developed externally. Spine *A* externally develop significant apical horn. Short tube-cephalopyle or horn (almost similar to that as apical) connected to spine *V*. Spines *D* and *L* extending as costae in second part of second segment. Their ends sticking free in shape of faceted lateral apophyses of test, but they not forming significant feet.

Composition. *Anthocyrtella* Haeckel, 1881; *Cecryphalium* Haeckel, 1881; *Clathrocyclas* Haeckel, 1881; *Clathrocycloma* Haeckel, 1887; *Diplocyclas* Haeckel, 1881; *Eucecryphalus* Haeckel, 1860; *Haeckelicyrtium* Kozur et Mostler, 1979; *Phrenocodon* Haeckel, 1887; *Pterocorythium* Haeckel, 1887; *Salpingocapsa* Ruest, 1885; *Squinabolella* Pessagno, 1969; *Stichopilium* Haeckel, 1881; *Theocalyptra* Haeckel, 1881; and *Theopilium* Haeckel, 1881.

Occurrence. Triassic–Recent.

Subfamily Rotaforminae Pessagno, 1970

Diagnosis. Sethophormididae with two segments. Cephalis large, of type 1. Thorax short. Aperture open or closed, not terminal, but shifted on the side. Thorax wall closely joined with wall of cephalis. Wall thick, with rounded pores. Pores arranged irregularly. Wheel similar to that in Enneaphormidinae present. Spines *D* and *L* running in test wall and not forming significant feet. Apical horn weakly developed.

Composition. *Rotaforma* Pessagno, 1970 and *Saturniforma* Pessagno, 1970.

Occurrence. Cretaceous (Albian–Late Campanian).

Subfamily Neosciadiocapsinae Pessagno, 1969

Diagnosis. Sethophormididae, with initial spicule with spines *A*, *V*, *D*, *2L*, and *2l*. Cephalis of type 2. It usually with ventral tube and with horizontal or subhorizontal arc, subdivided its cavity into two parts. Test helmet-shaped with two or more segments. Last segment completely closed by velum.

Composition. *Coniforma* Pessagno, 1969; *Ewingella* Pessagno, 1969; *Ewingium* Pessagno, 1976; *Lipmanium* Pessagno, 1969; *Microsciadiocapsa* Pessagno, 1969; *Neosciadiocapsa* Pessagno, 1969; *Petasiforma* Pessagno, 1969; *Sciadiocapsa* Squinabol, 1904; and *Scyphiforma* Pessagno, 1969.

Occurrence. Cretaceous–Paleogene (Eocene).

Subfamily Enneaphormidinae Petrushevskaya, 1981

Diagnosis. Sethophormididae with one or two segments (Figs. 46w, 46x). Collar strictum distinct, basal ring developed. Cephalis of type 1. Thorax short, flattened, wider than cephalis. Aperture open terminally. Wall porous or cellular, or absent, (sometimes only irregular tangled finest bars) present. Pores on cephalis arranged irregularly, on thorax regularly in longitudinal and transverse rows. In case porous wall of thorax reduced, only radial bars, diverging as spokes of the wheel present. Cephalic wall often with thickened costae, extending in different directions. Some of these costae representing main cephalic arcs.

Composition. *Enneaphormis* Haeckel, 1881 and *Protoscenium* Jorgensen, 1905.

Occurrence. Cretaceous–Recent.

Family Bulbocyrtiidae Kozur et Mostler, 1981

Diagnosis. Acropyramidoidea with two or three segments with large cephalis (Figs. 41, 46z; Table 7). Initial spicule with *MB* in center of cephalic cavity and with spines *A*, *D*, *V*, *L*, and *l*, all or some of which continuing outside cephalic wall into horn of varying length. Spines connected by arcs *AV*, *VL*, *Ll*, and *LD*. External horns usually four-bladed, less commonly

rounded. Thorax and postthoracic segments narrower than cephalis, and separated by constriction.

Composition. *Bulbocyrtium* Kozur et Mostler, 1981; *Quasipetasus* Blome, 1984; and *Pessagnocyrtium* Kozur et Mostler, 1981.

Occurrence. Middle Triassic (Anisian)–Late Triassic (Tubular).

Family Acropyramididae Haeckel, 1881

Diagnosis. Acropyramidoidea with indistinct segmentation into two segments and conical (Fig. 41; Table 7). Cephalis of type 3, small. Apical horn developed to various extent. Spines of inner skeleton may be almost completely reduced. Spines *D* and *L* may produce lateral continuations, not forming feet. Walls cellular, less commonly porous. Longitudinal costae and internal transverse shelves present. Main portion of test 5–25 times larger, wider and longer than cephalis.

Composition. *Acropyramis* Haeckel, 1881; *Bathropyramis* Haeckel, 1881; *Cephalopyramis* Haeckel, 1881; *Cinclopyramis* Haeckel, 1881; *Cladachnidium* Haeckel, 1881; *Enneapleuris* Haeckel, 1887; *Haliphormatidium* Campbell, 1951; *Litharachnidium* Haeckel, 1887; *Litharachnium* Haeckel, 1860; *Peripyramis* Haeckel, 1881; *Plectopyramis* Haeckel, 1881; *Polypleuris* Haeckel, 1887; *Sethopyramis* Haeckel, 1881; and *Spongopyramis* Haeckel, 1887.

Occurrence. Cretaceous–Recent.

Family Lampromitridae Haeckel, 1881

Diagnosis. Acropyramidoidea with two, rarely one to three segments (Fig. 46v). Thorax not subdivided into segments. Cephales of all three types. Walls porous, less commonly cellular, sometimes hyaline. Pores arranged in longitudinal rows or spaced irregularly.

Composition. Three subfamilies: Lampromitrinae Haeckel, 1881; Ceratocyrtinae Petrushevskaya, 1981; and Lithocampaninae Petrushevskaya, 1981 (Fig. 41; Table 7).

Occurrence. Cretaceous–Recent.

Subfamily Lampromitrinae Haeckel, 1881

Diagnosis. Lampromitridae with two segments, cap-shaped (Fig. 46v). From outside cephalis separated from thorax. Arcs of basal ring may be weakly developed. Lateral lobes of cephalis often fused with thorax. Cephalis of types 1 or 2. Pores rounded or polygonal and arranged in longitudinal rows, less commonly spaced irregularly. No significant apical horn present. Spines *D* and *L* extend to thoracic wall forming costae, sometimes forming thin terminal feet. Axobate weakly developed. Aperture widely open, sometimes possessing narrow shelf or its derivatives. Occasionally aperture closed by plate of velum, supported by shelf.

Composition. *Anthocyrtoma* Haeckel, 1881; *Calyptocoryphe* Foreman, 1968; *Gongylothorax* Foreman, 1968; *Halicapsa* Haeckel, 1881; *Heliocryptocapsa* Dumitrica, 1970; *Hexaphormis* Haeckel, 1881; *Lamprodiscus* Ehrenberg, 1860; *Lampromitra* Haeckel, 1881; *Lamprotripus* Haeckel, 1881; *Micromelissa* Haeckel, 1881; *Platycryphalus* Haeckel, 1881; and *Theocorys* Haeckel, 1881.

Occurrence. Cretaceous–Recent.

Subfamily Lithocampaninae Petrushevskaya, 1981

Diagnosis. Lampromitridae with two segments, subcylindrical, droplike or spindle-shaped, porous. Cephalis variously constructed (although type 1 not present), of various sizes, sometimes with pedestal. Axobate weakly developed. Spines *A*, *D*, and *L* outside developed to varying extent, not forming costae in wall of seconds segment and not developing feet. Wall porous, sometimes spongy, often hyaline. Thoracic pores irregularly shaped or rounded, arranged in longitudinal or transverse rows or spaced irregularly. Aperture open, lacking subsidiary structures or closed saclike.

Composition. *Acidnomelos* Foreman, 1968; *Botryopera* Haeckel, 1887; *Ceratarachnium* Haeckel, 1881; *Cornutanna* Haeckel, 1881; *Cornutella* Ehrenberg, 1838; *Cornutosa* Haeckel, 1881; *Cornutura* Haeckel, 1881; *Lithocampana* Clark et Campbell, 1942; and *Trisulcus* Popofsky, 1913.

Occurrence. Cretaceous–Recent.

Subfamily Ceratocyrtinae Petrushevskaya, 1981

Diagnosis. Lampromitridae with two segments, conical, porous. Eucephalic lobe present, subsidiary lobes fused with thorax. Cephalis of type 3 not separated from thorax. Basal arcs absent. Pores irregularly shaped, arranged irregularly or in longitudinal rows. Apical and vertical horn present. Spines *D* and *L* not developing costae in wall of segment 2, sometimes developing feet. Aperture simple, widely open, saclike.

Composition. *Antarctissa* Petrushevskaya, 1967; *Bathrocalpis* Clark et Campbell, 1942; *Ceratocyrtis* Buetschli, 1882; *Gondwanaria* Petrushevskaya, 1975; *Helotholus* Jorgensen, 1905; *Periarachnium* Haeckel, 1881; *Phlebarachnium* Haeckel, 1881; and *Pseudodictyophimus* Petrushevskaya, 1971.

Occurrence. Paleogene–Recent.

Superfamily Lychnocanioidea Haeckel, 1881

Diagnosis. Cyrtidinata with two the to five (more often three) segments. Cephalis medium sized, theoperid (Fig. 47k) or archipilid. Cephalis always not more than one third of entire test. Strong external tripod formed by spines *D* and *2L*, or sometimes tetrapod being characteristic feature of superfamily.

Composition. Nine families: Silicarmigeridae Kozur et Mostler, 1980; Lychnocaniidae Haeckel, 1881; Spongosilicarmigeridae Dumitrica, 2001; Deflandrecyrtiidae Kozur et Mostler, 1979; Spongolophophenidae Kozur et Mostler, 1994; Foremanellidae Dumitrica, 1982; Cuniculiformidae De Wever, 1982; Livarellidae Kozur et Mostler, 1981; and Theoperidae Haeckel, 1881 (Fig. 41; Table 7).

Occurrence. Triassic–Recent.

Family Silicarmigeridae Kozur et Mostler, 1980

Diagnosis. Lychnocanioidea with test in shape of wide pyramid widening toward the aperture, from which basally wide feet extending sideways and somewhat downwards (Fig. 41; Table 7). Cephalis usually with two similar horns.

Composition. *Silicarmiger* Kozur et Mostler, 1980 and *Trictenartus* Haeckel, 1881.

Occurrence. Triassic–Recent.

Family Lychnocaniidae Haeckel, 1881

Diagnosis. Lychnocanioidea with two or three, rarely more segments, in shape of tripod with outlines of pyramid. Cephalis theoperid, clearly delineated from thorax. Thorax may terminate in inner shelf. Sometimes thorax and abdomen indistinctly separated. Abdomen, if present, variously constructed. Aperture of various types. Large apical horn of spine *A* extending from cephalis. Spine *V* not developing significant external horn. Spines *D* and *2L* extending into thoracic wall as costae or grooves to form three free feet. Wall porous, pores arranged hexagonally or irregularly. Sometimes pores arranged in longitudinal or transverse rows.

Composition. Four subfamilies: Lychnocaninae Haeckel, 1881; Ultranaporinae Pessagno, 1977; Lithochytridinae Petrushevskaya, 1981; and Bekominae Dumitrica, 2001 (Fig. 41; Table 7).

Occurrence. Triassic–Recent.

Subfamily Lychnocaniinae Haeckel, 1881

Diagnosis. Lychnocaniidae with two or three segments. Cephalis theoperid lacking pores. Apical horn significant. Thorax inflated, semispherical, terminating in shelf. Abdomen, if present, subcylindrical. Thoracic walls thick, with regularly positioned and rounded pores. Pores framed. Wall spinulate. Abdomen with thin walls and irregular pores, sometimes its surface covered by spongy layer. Spines *D* and *2L* extending into thoracic walls as grooves, producing subterminal or lateral feet, which not included in abdominal wall. Bisegmented tests always, and trisegmented tests usually, with open aperture.

Composition. *Acerahedrina* Vinassa, 1900; *Acerocanium* Vinassa, 1900; *Lithornithium* Ehrenberg, 1847; *Lychnocanium* Ehrenberg, 1847; *Lychnocanoma* Haeckel, 1887; *Sanfilippoella* Kozur et Mostler, 1979; and *Stichopilidium* Haeckel, 1887.

Occurrence. Triassic–Recent.

Subfamily Lithochytridinae Petrushevskaya, 1981

Diagnosis. Lychnocaniidae with two to four segments. Cephalis theoperid, thick-walled, lacking pores. Separation into thorax and abdomen indistinct. Thoracic walls and abdomen of similar thickness, with rounded pores. Spines *D* and *L* extending in upper part of test as costae, while they extending from lower part to form subterminal feet. Aperture closed or narrowed with shelf.

Composition. *Lithochytris* Ehrenberg, 1847; *Lithochytrodes* Haeckel, 1887; *Lychnocanella* Haeckel, 1887; *Sethochytris* Haeckel, 1881; and *Theopodium* Haeckel, 1887.

Occurrence. Cretaceous–Paleogene(?).

Subfamily Ultranaporinae Pessagno, 1977

Diagnosis. Lychnocaniidae with three segments. Cephalis theoperid, clearly delineated from thorax. Significant apical horn present. Thorax terminating in internal shelf and external constriction. Abdomen often developed very weakly. Thoracic and abdominal walls different. Thorax thick-walled, with rounded framed pores of similar size; interpore thickenings of walls merging in polygonal meshwork. Abdomen thin-walled, with pores of various size and shape, which positioned irregularly. Spines *D* and *2L* extending into thoracic walls, forming three grooves, and three costae in abdominal walls. Free ends of these costae forming terminal feet, directed downwards, sometimes somewhat laterally. Aperture widely open.

Composition. *Napora* Pessagno, 1977; *Pleuropodium* Haeckel, 1881; *Pterocanidium* Haeckel, 1887; *Pterocanium* Ehrenberg, 1847; *Stichopterium* Haeckel, 1881; *Triprionium* Haeckel, 1881; and *Ultranapora* Pessagno, 1977.

Occurrence. Cretaceous–Recent.

Subfamily Bekominae Dumitrica, 2001

Diagnosis. Lychnocaniidae with two segments. Initial spicule with *MB* and spines *A*, *V*, *D*, *L*, and *l*. Spines *L* and *D* continuing outside into three feet, of different length, which can be connected distally. Collar structure with six pores, indistinctly separated by constriction. Abdomen, when present, indistinct.

Composition. *Bekoma* Riedel et Sanfilippo, 1971; *Bekomiforma* Sanfilippo et Riedel, 1974; and *Orbula* Foreman, 1973.

Occurrence. Paleogene (Paleocene)–Neogene (Pliocene).

Family Spongosilicarmigeridae Dumitrica, 2001

Diagnosis. Lychnocanioidea with two segments (Fig. 41; Table 7). Initial spicule with spines *A*, *D*, *V*, *L*,

and *l* and arcs *Al*, *Dl*, *Ll*, and *LV*. Cephalic cavity apically continuing in conical or cylindrical perforated tube surrounding apical spine. This tube may be replaced by spongy tissue. Cephalis large, perforated. Thorax indistinctly separated from cephalis, both forming conical or cylindrical apophyses, continuing with spines *D* and *L* as wings or longitudinal ridges.

Composition. *Nofrema* Dumitrica, Kozur, et Mostler, 1980 and *Spongosilicarmiger* Kozur, 1984.

Occurrence. Middle Triassic.

Family Deflandrecyrtiidae Kozur et Mostler, 1979

Diagnosis. Lychnocanioidea with two segments (Fig. 41; Table 7). Thorax widely open; with distinct dorsoventral asymmetry, i.e., ventral part of test much longer and more inflated than dorsal part. Initial spicule with *MB* and spines *A*, *V*, *D*, *L*, and *l*. Arcs *Al, lL*, *LV*, and *AV* present. Apical horn well developed, three-bladed, massive. Thorax distally widening or with terminal feet.

Composition. *Deflandrecyrtium* Kozur et Mostler, 1979 and *Dreyericyrtium* Kozur et Mostler, 1979.

Occurrence. Middle Triassic (Anisian)–Late Triassic (Tubular).

Family Spongolophophenidae Kozur et Mostler, 1994

Diagnosis. Lychnocanioidea with two segments, spongy (Fig. 41; Table 7). Cephalis large, spherical or conical. Initial spicule with *MB*, spines *A*, *V*, *D*, *2L*, *2l*, and arcs *Al*, *lD*, *lL*, and *LV*. Thorax long, cylindrical or conical, distally widely open.

Composition. *Conospongocyrtis* Kozur et Mostler, 1994; *Maudia* Carter, 1988; *Spongolophophaena* Kozur et Mostler, 1994; and *Triassospongocyrtis* Kozur et Mostler, 1994.

Occurrence. Middle Triassic (Anisian)–Early Jurassic.

Family Foremanellidae Dumitrica, 1982

Diagnosis. Lychnocanioidea with two segments (Fig. 41; Table 7). Third segment, when present, appearing as velumlike continuation of thorax. Cephalis large with spines *MB*, *A*, *V*, *L*, and *l*. Spine *D* absent; *L* and *l* continuing outside four feet, and in shape of two horns, extending laterally or along thorax.

Composition. *Diceratigalea* Takemura et Nakaseko, 1982; *Farcus* Pessagno, Whalen, et Yeh, 1986; *Foremanellina* Dumitrica, 1982; *Hiliarisirex* Takemura et Nakaseko, 1982; *Recoarcoella* Dumitrica, 1982; *Riedelius* De Wever, 1982; and *Rolumbus* Pessagno, Whalen, et Yeh, 1986.

Occurrence. Middle Triassic–Middle Jurassic.

Family Cuniculiformidae De Wever, 1982

Diagnosis. Lychnocanioidea with two segments (Fig. 41; Table 7). Initial spicule lacking spine *D*. Primary and secondary lateral spines unequal. Secondary lateral spines may continue outside from walls as horns. Apical horn conical or faceted, at end of tubular continuation of cephalic cavity. Spine *V* continuing outside short horn. Cephalis small, perforated or nonperforated. Thorax widely open, conical, bell-shaped, with one or several constrictions.

Composition. *Cassideus* Pessagno, 1969; *Cuniculiformis* De Wever, 1982; and *Goestlingella* Kozur et Mostler, 1979.

Occurrence. Middle Triassic–Jurassic (Tithonian).

Family Livarellidae Kozur et Mostler, 1981

Diagnosis. Lychnocanioidea with two segments (Fig. 41; Table 7). Initial spicule with *MB* and spines *A*, *D*, *V*, *l*, and *L*. Thorax large, wide, flat, with laterally directed tubular widening spines or without those.

Composition. *Citriduma* De Wever, 1982; *Kozuria* Zhang, 1990; *Livarella* Kozur et Mostler, 1981; and *Praecitriduma* Kozur, 1984.

Occurrence. Late Triassic (Late Norian)–Early Jurassic (Toarcian).

Family Theoperidae Haeckel, 1881

Diagnosis. Lychnocaniidae with three-four, rarely more, segments (Fig. 41; Table 7). Cephalis theoperid, delineated from thorax (Fig. 47k), with significant apical horn. Thorax bell-shaped with internal shelf and external constriction. Abdomen in shape of funnel. Thoracic and abdominal walls perforated by rounded, regularly positioned pores. Spines *D* and *L* extending into thoracic and abdominal walls as relatively high costae. Their free ends forming feet, directed downwards and slightly laterally. Aperture narrowed or closed, sometimes with spine or long tubule.

Composition. *Artoperina* Campbell, 1951; *Dictyophimus* Ehrenberg, 1847; *Eusyringium* Haeckel, 1881; *Pterocyrtidium* Buetschli, 1882; *Rhopalatractus* Haeckel, 1881; *Rhopalocanium* Ehrenberg, 1847; *Theopera* Haeckel, 1881; and *Theophaena* Haeckel, 1881.

Occurrence. Paleogene–Recent.

Superfamily Eucyrtidioidea Ehrenberg, 1847

Diagnosis. Cyrtidinata with multi-segmented spindle-shaped skeleton, composed of two to six, rarely more segments (up to 20). Cephalis small, variously constructed, clearly delineated from thorax. Segmentation of postcephalic test clear. Cephalis and thorax sometimes forming stable cephalothorax. Second to fourth or fifth to eighth segments largest in volume, in many genera one segment hyperbolized. External apophyses corresponding to spines *A*, *D*, and *L* developed rarely and present only in oligosegmented taxa. Walls thin, with longitudinal arrangement of pore. Rows of pores may be separated by longitudinal costae. Pores

may also be arranged in transverse rows or ortho-hexagonally.

Composition. Twelve families: Eucyrtidiidae Ehrenberg, 1847; Planispinocyrtiidae Kozur et Mostler, 1981; Ruesticyrtiidae Kozur et Mostler, 1979; Pseudodictyomitridae Pessagno, 1977; Eucyrtidiellidae Takemura, 1986; Obeliscoitidae O'Dogherty, 1994; Xitidae Pessagno, 1977; Williriedellidae Dumitrica, 1970; Carpocaniidae Haeckel, 1881; Artostrobiidae Riedel, 1967; Pterocoryidae Haeckel, 1881; and Lophocyrtiidae Sanfilippo et Caulet, 2001 (Fig. 41; Table 7).

Occurrence. Triassic–Recent.

Family Eucyrtidiidae Ehrenberg, 1847

Diagnosis. Eucyrtidioidea with two to six, rarely more, segments. Cephalis theoperid not segmented into chambers or lobes. Segmentation distinct, but septa between segments absent. Only shelves present. External apophyses, corresponding to spines *D* and *L* developed rarely. Aperture variously constructed, can be closed blindly, or elongated in tube, or possessing terminal spine. Pores on thorax and successive segments rounded, in longitudinal rows.

Composition. Three subfamilies: Eucyrtidiinae Ehrenberg, 1847; Calocyclinae Haeckel, 1881; and Theocotylinae Petrushevskaya, 1981 (Fig. 41; Table 7).

Occurrence. Triassic–Recent.

Subfamily Eucyrtidiinae Ehrenberg, 1847

Diagnosis. Eucyrtidiidae with three to ten segments. No specific cephalothorax present.

Composition. *Acanthocyrtis* Haeckel, 1881; *Artocapsa* Haeckel, 1881; *Artocyrtis* Haeckel, 1997; *Artophormis* Haeckel, 1881; *Clathropyrgus* Haeckel, 1881; *Cyrtocapsella* Haeckel, 1887; *Cyrtocapsoma* Haeckel, 1887; *Cyrtophormis* Haeckel, 1887; *Cyrtophormiscus* Haeckel, 1887; *Eucyrtidium* Ehrenberg, 1847; *Eusyringoma* Haeckel, 1887; *Glomaria* Sanfilippo et Riedel, 1970; *Immersothorax* Dumitrica, 1970; *Lithocampe* Ehrenberg, 1838; *Lithomitrissa* Haeckel, 1887; *Lithopera* Ehrenberg, 1847; *Spirocyrtoma* Haeckel, 1887; *Stychocorys* Haeckel, 1881; *Stichopodium* Haeckel, 1881; *Stichopterygium* Haeckel, 1881; *Syringium* Principi, 1909; *Theocampe* Haeckel, 1887; and *Trocolocamptra* Haeckel, 1887.

Occurrence. Triassic–Recent.

Subfamily Calocyclinae Haeckel, 1881

Diagnosis. Eucyrtidiidae with three segments. No specific cephalothorax present. Thorax hyperbolized. Abdomen the same size as thorax, or larger, sometimes absent. Internal shelf and external constriction present between second and third segments. Aperture closed, sometimes festooned. Apical horn, when present, large.

Composition. *Calocyclas* Ehrenberg, 1847; *Theocapsomma* Haeckel, 1887; and *Theocoronoium* Haeckel, 1887.

Occurrence. Cretaceous–Recent.

Subfamily Theocotylinae Petrushevskaya, 1981

Diagnosis. Eucyrtidiidae with two or three segments. Abdomen hyperbolized. Abdominal pores larger than on thorax. Thorax and abdomen separated by deep internal shelf and clear external constriction. Apical horn significant. Aperture elongated in tube or with three festoons.

Composition. *Axocorys* Haeckel, 1887; *Calocycloma* Haeckel, 1887; *Calocyclura* Haeckel, 1887; *Cycladophora* Ehrenberg, 1847; *Dictyopodium* Ehrenberg, 1847; *Lampterium* Haeckel, 1881; *Lamptidium* Haeckel, 1887; *Lamptonium* Haeckel, 1887; *Lophoconus* Haeckel, 1887; *Podocyrtecium* Haeckel, 1887; *Podocyrtonium* Haeckel, 1887; *Pterocodon* Ehrenberg, 1847; *Pterosyringium* Haeckel, 1887; *Tetralocorys* Haeckel, 1881; *Theocotyle* Riedel et Sanfilippo, 1970; and *Thyrsocyrtis* Ehrenberg, 1847.

Occurrence. Cretaceous–Recent.

Family Planispinocyrtiidae Kozur et Mostler, 1981

Diagnosis. Eucyrtidioidea with multisegmented test (Fig. 41; Table 7). Initial spicule without spine *D*, cephalis nonperforated, small. Spine *A* continuing into significant, usually faceted apical horn. Spine *V* short, directed downwards, forming ridge along test. Thorax perforated, larger than abdomen and postabdominal segments, last segment widened.

Composition. *Ladinocampe* Kozur, 1984; *Planispinocyrtis* Kozur et Mostler, 1981; and *Spinotriassocampe* Kozur, 1984.

Occurrence. Middle Triassic (Anisian)–Late Triassic (Carnian).

Family Ruesticyrtiidae Kozur et Mostler, 1979

Diagnosis. Eucyrtidioidea with long multisegmented test with distal skirt. *MB* of initial spicule occurring in center of lower region of cephalic cavity. Spines *A*, *V*, *D*, *2L*, and *21* and arcs *LV*, *Ll*, and *lD* present. Spine *A* and sometimes *V* may continue outside as external horn. Segments of distal end widened (Fig. 41; Table 7).

Composition. *Annulotriassocampe* Kozur, 1994; *Nevanellus* Kozur et Mostler, 1981; *Paratriassocampe* Kozur et Mostler, 1994; *Pseudotriassocampe* Kozur et Mostler, 1994; *Ruesticyrtium* Kozur et Mostler, 1979; *Striatotriassocampe* Kozur et Mostler, 1994; *Triassocampe* Dumitrica, Kozur, et Mostler, 1980;

Xiphotheca De Wever, 1979; and *Yehamia* Nakaseko et Nishimura, 1979.

Occurrence. Middle Triassic (Anisian)–Late Triassic (Norian).

Family Pseudodictyomitridae Pessagno, 1977

Diagnosis. Multisegmented Eucyrtidioidea with elongated conical test (Fig. 41; Table 7). Cephalis conical, simple, not subdivided into lobes, lacking horn and collar pores. Cephalis and thorax nonperforated, smooth or with weakly developed costae. Thorax trapezoid. Successive segments subcylindrical, relatively rapidly increasing is width and less rapidly in height distally. Abdomen separated from thorax by one or two rows of pores. Abdomen and successive segments separated by double rows of pores. These segments possessing costae.

Composition. *Corum* Blome, 1984; *Latium* Blome, 1984; *Loopus* Yang, 1993; *Pachus* Blome, 1984; *Pseudodictyomitra* Pessagno, 1977; and *Shana* Wu et Pessagno, 1993.

Occurrence. Late Triassic (Norian–Late Cretaceous (Maastrichtian).

Family Eucyrtidiellidae Takemura, 1986

Diagnosis. Eucyrtidioidea with four or five segments, conical (Fig. 41; Table 7). Initial spicule lacking lateral rays. Spine *A* included in cephalic wall, forming internal costa. Spine *V* associated with ventral tube. Last segment thin-walled, rarely preserved.

Composition. *Eucyrtidiellum* Baumgartner, 1984.

Occurrence. Middle Jurassic (Aalenian)–Early Cretaceous (Berriasian).

Family Obeliscoitidae O'Dogherty, 1994

Diagnosis. Multisegmented Eucyrtidioidea with proximal part of test acutely conical, composed of many segments, and inflated distal part. Apical horn. Terminal aperture may be present (Fig. 41; Table 7).

Composition. *Birkenmajeria* Widz et De Wever, 1993; *Obeliscoites* O'Dogherty, 1994; and *Olanda* Hull, 1997.

Occurrence. Middle Jurassic (Bajocian)–Late Cretaceous (Cenomanian).

Family Xitidae Pessagno, 1977

Diagnosis. Eucyrtidioidea with multisegmented elongated conical or ovoid test (Fig. 41; Table 7). Cephalis simple, not subdivided into lobes, nonperforated, with four collar pores. Thorax trapezoid, monolayered. Abdomen and postabdominal segments trapezoid or cylindrical, with bilayered wall. Internal layer of walls with rounded pores. External layer formed by numerous tubercles and nodes, connected by bars in polygonal meshwork.

Composition. *Clavaxitus* Dumitrica, 1997; *Crolanium* Pessagno, 1977; *Foremanina* Empson–Morin, 1981; *Neorelumbra* Kiessling, 1995; *Novixitus* Pessagno, 1977; *Praexitus* Dumitrica, 1997; *Pseudoxitus* Wu et Pessagno, 1993; *Tugurium* O'Dogherty, 1994; and *Xitus* Pessagno, 1977.

Occurrence. Middle Jurassic (Bajocian)–Late Cretaceous (Maastrichtian).

Family Williriedellidae Dumitrica, 1970

Diagnosis. Eucyrtidioidea with three-four segments, spherical or droplike (Fig. 41; Table 7). Cephalis theoperid, apical horn not present. External apophyses, corresponding to spines *D* and *L*, weakly developed. Feet absent. Cephalothorax stabilized. Thorax spherical. Thorax for one-third, one-half, or (often) completely placed inside abdomen, retaining its own walls and rounded aperture with shelf. Abdomen blindly closed, or possessing large pore (aperture). Abdominal pores rounded, arranged hexagonally or in longitudinal rows. Sometimes wall with thickenings, nodes, and tubercles.

Composition. *Complexapora* Kiessling, 1992; *Cryptamphorella* Dumitrica, 1970; *Cryptocephalus* Haeckel, 1881; *Excentropylomma* Dumitrica, 1970; *Hemicryptocapsa* Tan Sin Hok, 1927; *Holocryptocanium* Dumitrica 1970; *Holocryptocapsa* Tan Sin Hok 1927; *Kozurium* Pessagno, 1977; *Williriedellum* Dumitrica, 1970; and *Zhamoidellum* Dumitrica, 1970.

Occurrence. Middle Jurassic–Cretaceous.

Family Carpocaniidae Haeckel, 1881

Diagnosis. Eucyrtidioidea with two or three segments (Fig. 41; Table 7). Cephalis carpocanid or theoperid (Figs. 47d, 47k). Spines *D* and *2L* extending outside as grooves or costae, but nor forming feet. Apical horn small (spinule). First and second segments fused in cephalothorax. Thorax and abdomen separated by internal shelf lacking external constrictions. Third segment may represent peristome, i.e., short tube lacking pores. Pores on second segment arranged in longitudinal rows, separated by ridges. These ridges and rows may continue in walls of third segments, if it present. Pores on third segment arranged irregularly near aperture.

Composition. *Asecta* Popofsky, 1913; *Carpocanarium* Haeckel, 1887; *Carpocanistrum* Haeckel, 1887; *Carpocanium* Ehrenberg, 1847; *Carpocanobium* Haeckel, 1887; *Carpocanopsis* Riedel et Sanfilippo, 1971; *Carpocryptocapsa* Petrushevskaya, 1981; *Cyrtocalpis* Haeckel, 1860; *Cystophormis* Haeckel, 1887; *Diacanthocapsa* Squinabol, 1903; *Myllocercion* Foreman, 1968; *Sethamphorus* Burma, 1959; and *Trocolocapsa* Haeckel, 1881.

Occurrence. Cretaceous–Recent.

Family Artostrobiidae Riedel, 1967

Diagnosis. Eucyrtidioidea with three to ten segments, ellipsoidal, cigar-shaped, cylindrical, highly conical (Fig. 41; Table 7). Cephalis complex (Fig. 47c). Antecephalic and eucephalic parts present, postcephalic portion transformed into tube connected with spines *V*. Boundary between cephalis and thorax indistinct, cephalis widened basally. Spines *D* and *L* extending into thoracic walls as costae, not producing free feet. Apical horn significant. Cephalothorax specialized. Thorax terminating in internal shelf. Postthoracic portion larger than cephalothorax and subdivided into segments. Aperture compressed, simple, but sometimes with shelf or tube of peristome, terminating aperture present.

Composition. *Artostrobium* Haeckel, 1887; *Botryostrobus* Haeckel, 1887; *Buryella* Foreman, 1973; *Dictyoprora* Haeckel, 1881; *Lithomitra* Buetschli, 1882; *Lithomitrella* Haeckel, 1887; *Lithamphora* Popofsky, 1908; *Lophocorys* Haeckel, 1881; *Phormosctichoartus* Campbell, 1951; *Poroamphora* Popofsky, 1908; *Siphocampe* Haeckel, 1887; *Siphocampula* Haeckel, 1887; *Siphostichartus* Nigrini, 1977; *Spirocyrtis* Haeckel, 1881; *Theocamptra* Haeckel, 1887; and *Tricolocampium* Haeckel, 1887.

Occurrence. Cretaceous–Recent.

Family Pterocoryidae Haeckel, 1881

Diagnosis. Eucyrtidioidea with one to three segments, conical, spindle-shaped. Cephalis pterocorid with collar, lateral lobes, apical horn (Fig. 47f); cephalis and thorax forming characteristic stabilized cephalothorax. Thorax terminating in internal shelf. Abdomen, when present, appearing in shape more or less high "barrel." Aperture possessing shelf peristome, sometimes with teeth. Sometimes aperture blindly closed or remaining open and simple. Spine *V* not forming either tube, or horn. Spines *D* and *2L* extending into walls of upper part of thorax. Their free ends may form lateral thin apophyses. Pores rounded, densely spaced, forming hexagonal pattern, with almost always discernible longitudinal rows. Pores in widened zone larger than pores located near ends. Test surface, especially near aperture, may possess many thickenings, nodes, and tubercles. Surface of thorax may have longitudinal ridges, which may continue downwards, to form costal projections surrounding aperture.

Composition. Three subfamilies: Podocyrtiinae Haeckel, 1887; Sethocoryinae Haeckel, 1881; and Pterocoryinae Haeckel, 1881 (Fig. 41; Table 7).

Occurrence. Cretaceous–Recent.

Subfamily Pterocoryinae Haeckel, 1881

Diagnosis. Pterocoryidae with highly conical test. Cephalis variously constructed. Abdomen of same size as cephalis. Abdomen terminating saclike or aperture possessing shelf or short tube of peristome.

Composition. *Androcyclas* Jorgensen, 1905; *Craterocyclas* Haecker, 1908; *Ectonocorys* Foreman, 1968; *Hexalodus* Haecker, 1908; *Lamprocycloma* Haeckel, 1887; *Lamrocyclas* Haeckel, 1881; *Lipmanella* Loeblich et Tappan, 1961; *Lithopilium* Popofsky, 1913; *Tetracorethra* Haeckel, 1887; *Theocapsilla* Haeckel, 1887; *Theocapsura* Haeckel, 1887; *Theoconus* Haeckel, 1887; *Theocorbis* Haeckel, 1887; and *Theocorythium* Haeckel, 1887.

Occurrence. Cretaceous–Recent.

Subfamily Sethocoryinae Haeckel, 1881

Diagnosis. Pterocoryidae with two segments, helmet-shaped. Abdomen not present. Largest segment being thorax. Its upper, narrower part may be separated and may appear as pedestal of cephalis. Cephalis specialized, high, narrow basally, with distinct low lateral lobes. Apical horn present. Aperture possessing shelf, smooth or toothed. In test wall apertural oral teeth, conical or beak-shaped usually present. Pores densely spaced.

Composition. *Antocyrtissa* Haeckel, 1887; *Antocyrtura* Haeckel, 1887; *Conarachnium* Haeckel, 1881; *Phormocampe* Haeckel, 1887; *Sethocorys* Haeckel, 1881; and *Sethocyrtis* Haeckel, 1887.

Occurrence. Cretaceous–Recent.

Subfamily Podocyrtiinae Haeckel, 1887

Diagnosis. Pterocoryidae with three segments, spindle-shaped, less commonly test in upper part conical, and in lower subcylindrical. Abdomen as wide as thorax. Abdominal walls on aperture end lacking pores and terminally elongated into 3–15 plates, forming coastal projections of flat ribbon-shaped festoons surrounding aperture. Shelf terminating abdomen and beak-shaped teeth in abdominal walls not developed. Pores on thorax and abdomen similar. Longitudinal rows of pores on thorax and abdomen may be separated by longitudinal ridges.

Composition. *Anthocyrtonium* Haeckel, 1887; *Calocycletta* Haeckel, 1887; *Phormocyrtis* Haeckel, 1887; *Podocyrtis* Ehrenberg, 1847; and *Theocyrtis* Haeckel, 1887.

Occurrence. Paleogene–Recent.

Family Lophocyrtiidae Sanfilippo et Caulet, 2001

Diagnosis. Three-segmented Eucyrtidioidea with perforated or nonperforated cephalis (Fig. 41; Table 7). Cephalis with apical horn or without it. Thorax small, thick-walled, porous. Abdomen widely open or closed, without feet.

Composition. *Aphetocyrtis* Sanfilippo et Caulet, 1998; *Apoplanius* Sanfilippo et Caulet, 1998; *Clinorhabdus* Sanfilippo et Caulet, 1998; *Cyclampterium* Haeckel, 1887; *Lophocyrtis* Haeckel, 1887; *Paralamp-*

terium Sanfilippo, 1990; and *Sciadiopeplus* Sanfilippo, 1990.

Occurrence. Paleogene (Paleocene)–Recent.

Superfamily Stichocapsoidea Haeckel, 1881

Diagnosis. Cyrtidinata with 4–15 or more segments. Segmentation indistinct, especially in apical part of test. Cephalis variously constructed. Test lacking apertural skirt and compressed aperturally. External apophyses, corresponding to spines *D* and *L*, if developed, representing costae in test walls. Pores arranged in transverse rows or irregularly, thickened. Walls may be spongy.

Composition. Six families: Stichocapsidae Haeckel, 1881; Archaeodictyomitridae Pessagno, 1976; Monicastericidae Kozur et Mostler, 1994; Bagotidae Pessagno et Whalen, 1982; Hsumidae Pessagno et Whalen, 1982; and Unumidae Kozur 1984 (Fig. 41; Table 7).

Occurrence. Triassic–Recent, mainly Mesozoic.

Family Stichocapsidae Haeckel, 1881

Diagnosis. Stichocapsoidea with five to ten segments, less commonly more, conical, pyramidal, spindle-shaped, droplike. Cephalis variously constructed, with apical horn. Inner structure of cephalis and internal bars of cephalis weakly developed. External apophyses, corresponding to spines *D* and *L* when present, representing costae in walls of portions II–IV. Thorax same size as cephalis. Cephalothorax not stabilized. Portions separated by deep internal septa. Portions III or IV may very sharp differ in size from cephalis, thorax, and cephalothorax. Aperture compressed with internal shelf or elongated as tube and possessing terminal spine. Sometimes apertural apophyses (lobes, spines) present. From portion II onward, pores rounded, arranged in transverse rows or hexagonally, or irregularly. Wall may possess ridges, costae, thickenings, forming ornamentation. Often wall spongy. Sometimes walls of first segments thickened and lacking penetrating pores.

Composition. Two subfamilies: Stichocapsinae Haeckel, 1881 and Sethocapsinae Haeckel, 1881 (Fig. 41; Table 7).

Occurrence. Triassic–Recent.

Subfamily Stichocapsinae Haeckel, 1881

Diagnosis. Stichocapsidae with 3–15, more often 6–12 segments, spindle-shaped, conical. Segmentation distinct. Fourth to sixth segments enlarged. Apical horn weakly developed. Aperture widely open. Wall of the third and successive segments may possess ridges, costae, thickenings, forming ornamentation.

Composition. *Amphipterius* Foreman, 1973; *Anthocorys* Haeckel, 1881; *Conostrobus* Haeckel, 1881; *Cornustrobus* Haeckel, 1881; *Dictyomitrella* Haeckel, 1887; *Dictyomitrissa* Haeckel, 1887; *Eucyrtis* Haeckel, 1881; *Kassinia* Chabakov, 1937; *Lithocampium* Haeckel, 1887; *Lithostrobu*s Buetschli, 1882; *Pseudocyrtis* Pessagno, 1977; *Siphocampium* Haeckel, 1881; *Spirocampe* Haeckel, 1881; *Spirocapsa* Ruest, 1892; *Stichocapsa* Haeckel, 1881; *Stichophatna* Haeckel, 1881; *Triassocyrtium* Kozur et Mostler, 1979; and *Tricolocampe* Haeckel, 1881.

Occurrence. Triassic–Recent.

Subfamily Sethocapsinae Haeckel, 1881

Diagnosis. Stichocapsidae with three to ten segments, spindle-shaped, strongly inflated in middle or apertural part. One of distal segments being distinct (usually third or fourth to seventh segments). Segmentation indistinct in proximal part of test. This part of test terminates in large apical tube, or horn. In this case test generally conical. Apertural distal segments generally similar (indistinct segmentation, conical shape, thin walls, tubular, or sharp termination). When these segments absent, aperture closed blindly. Terminal tube may be present. Lateral spines or perforated porous wings may be present. These are sometimes relatively long, not connected with internal main skeleton.

Composition. *Acotripus* Haeckel, 1881; *Cryptocapsa* Haeckel, 1881; *Sethocapsa* Haeckel, 1881; *Tetracapsa* Haeckel, 1881; *Tripodiscus* Haeckel, 1881; *Trisyringium* Vinassa, 1900; and *Urocyrtis* Pantanelli, 1880.

Occurrence. Jurassic–Cretaceous.

Family Monicastericidae Kozur et Mostler, 1994

Diagnosis. Multisegmented Stichocapsoidea, spindle-shaped, cylindrical, with large apical horn and tube and weak segmentation (Fig. 41; Table 7). Spines of initial skeleton *A*, *V*, *2L*, and *2l* continue outside the test wall. Cephalis large, weakly delineated from postcephalic portion. Spine *D* absent. Arcs of cephalis indistinct. Postcephalic portion narrower than cephalis, external segmentation indistinct. Pores arranged irregularly, usually absent in last tubular segment.

Composition. *Monicasterix* Kozur et Mostler, 1994 and *Tubotriassocyrtis* Kozur et Mostler, 1994.

Occurrence. Middle Triassic.

Family Bagotidae Pessagno et Whalen, 1982

Diagnosis. Stichocapsoidea with conical or ellipsoidal test (Fig. 41; Table 7). Test wall two-layered.

Composition. *Bagotum* Pessagno et Whalen, 1982; *Broctus* Pessagno et Whalen, 1982; *Canutus* Pessagno et Whalen, 1982; *Droltus* Pessagno et Whalen, 1982; and *Noritus* Pessagno et Whalen, 1982.

Occurrence. Late Triassic (Rhaetian)–Middle Jurassic.

Family Hsumidae Pessagno et Whalen, 1982

Diagnosis. Stichocapsoidea (Fig. 41; Table 7) with wall of abdomen and of postabdominal segments possessing square or rectangular frames of pores. Pores separated by costae, continuing from segments to segment. One or two rows of pores present between costae.

Composition. *Combusta* Yeh, 1987; *Fantus* Yeh, 1987; *Hsuum* Pessagno, 1977; *Linaresia* El Kadiri, 1992; *Parahsuum* Yao, 1982; *Pseudohsuum* Zhang, 1990; *Semihsuum* Pessagno, Blome, et Hull, 1993; and *Transhsuum* Takemura, 1986.

Occurrence. Early Jurassic (Pliensbachian)–Early Cretaceous (Barremian).

Family Archaeodictyomitridae Pessagno, 1976

Diagnosis. Stichocapsoidea with three or more segments (Fig. 41; Table 7). Test conical in upper part, then cylindrical, sometimes narrowing toward aperture. Position of widest segment not stabilized. Fourth to seventh segments usually twice as large as cephalis. Wall of segments porous. Pores rounded, arranged in transverse rows. Longitudinal rows often present. These rows separated by ridges, continuing, like costae from segments to segment. Some rows of pores and, hence, ridges may begin not from the apex, or from first or second segments, but intercalating closer to aperture. Sometimes ridges transformed into large thin plates. Apical horn not present or present rarely. Aperture possessing continuing costae, resembling frills or festoons.

Composition. *Archaeodictyomitra* Pessagno, 1976; *Cyrtocapsa* Haeckel, 1881; *Dictyomitra* Zittel, 1876; *Diplosrobus* Squinabol, 1903; *Mita* Pessagno, 1977; *Polystichia* Pantanelli, 1880; *Solenotryma* Foreman, 1868; *Stichomitra* Cayeux, 1897; *Thanarla* Pessagno, 1977; and *Zifonidium* Pessagno, 1977.

Occurrence. Jurassic–Cretaceous.

Family Unumidae Kozur, 1984

Diagnosis. Multisegmented spindle-shaped. Stichocapsoidea with large longitudinal costae. Two or more longitudinal rows pores in each intercostal space.

Composition. *Protunuma* Ichikawa et Yao 1976; *Turbocapsula* O'Dogherty, 1994; and *Unuma* Ichikawa et Yao, 1976.

Occurrence. Middle Jurassic (Aalenian)–Early Cretaceous (Aptian).

Superfamily Amphipyndacioidea Riedel, 1967, emend. De Wever *et al.*, 2001

Diagnosis. Multisegmented Cyrtidinata with cephalis, subdivided into two opposite lobes by transverse septum. Septum formed by pair of horizontal and subhorizontal branches of spine *A*, which may be fused with spine *V*. Initial spicule with spines *A*, *D*, *V, L*, and *l*.

Composition. Five families: Amphipyndacidae Riedel, 1967; Canoptidae Pessagno, 1979; Parvicingulidae Pessagno, 1977; Syringocapsidae Foreman, 1973; and Spongocapsulidae Pessagno, 1977 (Fig. 41; Table 7).

Occurrence. Early Triassic–Recent.

Family Canoptidae Pessagno, 1979

Diagnosis. Multisegmented Amphipyndacioidea, spindle-shaped (when test complete) or conical (when test broken), with six or more postabdominal segments (Fig. 41; Table 7). Cephalis with apical horn or without it, subdivided into two opposite lobes by transverse arc, connecting spines *V* and *A*. Test wall composed of two layers: inner layer with a meshwork of frames of polygonal pores, and outer layer with separated pore frames. Primary pores often arranged on outer layer along ridges in places where segments connected.

Composition. *Canoptum* Pessagno, 1979; *Cinguloturris* Dumitrica, 1982; *Globolaxtorum* Carter, 1993; *Laxtorum* Blome, 1984; *Neocanoptum* Zhang 1990; and *Relanus* Pessagno et Whalen, 1982.

Occurrence. Late Triassic–Early Cretaceous.

Family Parvicingulidae Pessagno, 1977

Diagnosis. Multisegmented Amphipyndacioidea, conical, cylindrical or spindle-shaped. Cephalis nonperforated, with apical horn or without it, subdivided into two opposite lobes transverse by septum. Abdomen and postabdominal segments outside separated by closely spaced concentric ridges, which continue within as flat nonperforated plates. Plates rounded in outline, possessing central aperture. External ridges running around test with (or without) rows of nodes, hence appearing tuberculate. Nodes sometimes connected by bars. Test wall with one or more latticed layers.

Composition. Two subfamilies: Wrangelliinae Yeh 1987 and Parvicingulinae Pessagno, 1977 (Fig. 41; Table 7).

Occurrence. Late Triassic (Rhaetian)–Early Cretaceous (Aptian).

Subfamily Wrangelliinae Yeh, 1987

Diagnosis. Parvicingulidae lacking middle row of pores on postabdominal segments. It can be replaced by girdle (smooth or with longitudinal costae or rows of polygonal depressions).

Composition. *Neowrangellium* Yeh, 1987; *Paracanoptum* Yeh, 1987; *Proparvicingula* Carter, 1993; *Pseudocrolanium* Jud, 1994; *Svinitzium* Dumitrica, 1997; and *Wrangellium* Pessagno et Whalen, 1982.

Occurrence. Late Triassic (Rhaetian)–Early Cretaceous (Barremian).

Subfamily Parvicingulinae Pessagno, 1977

Diagnosis. Parvicingulidae with postabdominal segments generally possessing three rows of transverse pores. Number of rows varied (two to four).

Composition. *Caneta* Pessagno, Blome, et Hull, 1993; *Darvelus* Hull, 1995; *Eoxitus* Kozur, 1985; *Mirifusus* Pessagno, 1977; *Parvicingula* Pessagno 1977; *Praecaneta* Pessagno, Blome, et Hull, 1993; *Praeparvicingula* Pessagno, Blome, et Hull, 1993; *Pseudoristola* Yeh, 1987; *Ristola* Pessagno et Whalen, 1982; and *Tethysetta* Dumitrica, 1997.

Occurrence. Early Jurassic (Toarcian)–Early Cretaceous (Aptian).

Family Syringocapsidae Foreman, 1973

Diagnosis. Amphipyndacioidea with two- or multisegmented test, with small and narrow proximal part (Fig. 41; Table 7). One segment in distal part very large and inflated. Basal tube may be present. None of proximal segments concealed.

Composition. *Dibolachras* Foreman, 1973; *Dicolocapsa* Haeckel, 1881; *Parapodocapsa* Steiger, 1992; *Podobursa* Wisniowski, 1889; *Podocapsa* Rust, 1885; *Quarticella* Takemura, 1986; *Squinabollum* Dumitrica, 1970; *Syringocapsa* Neviani, 1900; and *Yamatoum* Takemura, 1986.

Occurrence. Jurassic–Neogene (Miocene).

Family Spongocapsulidae Pessagno, 1977

Diagnosis. Amphipyndacioidea with multisegmented test, with last segments inflated. Walls of cephalis and thorax solid, nonperforated. Walls of abdominal and postabdominal segments thick, porous, and spongy. Septal platforms solid, nonperforated, with central rounded aperture.

Composition. *Anachoreta* O'Dogherty, 1994; *Obesacapsula* Pessagno, 1977; *Spongocapsula* Pessagno, 1977; *Torculum* O'Dogherty, 1995; and *Tubilustrium* O'Dogherty, 1994.

Occurrence. Middle Jurassic–Late Cretaceous (Campanian).

Family Amphipyndacidae Riedel, 1967

Diagnosis. Multisegmented Amphipyndacioidea with cephalis, subdivided into two opposite lobes by septum (Fig. 41; Table 7).

Composition. *Amphipternis* Foreman, 1973; *Amphipyndax* Foreman, 1966; *Cyrtolagena* Haeckel, 1887; *Palinandromeda* Pessagno, Blome, et Hull, 1993; *Parvifavus* Takemura, 1986; *Protostichocapsa* Empson–Morin, 1982; *Sticholagena* Haeckel, 1887; *Stichophaena* Haeckel, 1881; *Stichophormis* Haeckel, 1887; *Stichophormium* Haeckel, 1887; and *Triversus* Takemura, 1986.

Occurrence. Middle Jurassic–Recent.

Superfamily Cannobotryoidea Haeckel, 1881

Diagnosis. Cyrtidinata with two or three segments. Cephalis specialized, multilobed (Figs. 47a, 47b), subdivided into lobes. Spines *A*, *L*, *l*, and *V* belonging to eucephalic portion with *MB* at the base of it. Lower collar portion delineated by arcs *ap* extending from spine *A*, collar region lacking walls. Anteriorly collar and upper zones of eucephalic lobe adjacent to antecephalic lobe. Spine *D* positioned at base of antecephalic lobe. Antecephalic lobe subdivided into upper (apical-dorsal) part and lower part, if unpaired apophysis *a* directed forward present. Posteriorly, postcephalic lobe adjacent to eucephalic lobe. Spine *V* occurring within postcephalic lobe. Antecephalic lobe larger than eucephalic. Cephalis elongated anteroposteriorly and laterally compressed. Thorax often joined with cephalis to produce specialized cephalothorax (almost entire test). Feet absent. Tubes connected with spines *A*, *V*, *D*, and *L* usual. Thorax and abdomen (when present) barrel-shaped, laterally compressed. Successive segments developed rarely. Segments separated by internal shelves. Aperture open, simple, or compressed and elongated into tube, sometimes closed saclike. Walls porous hyaline or multilayered, spongy. Pores arranged irregularly or in transverse rows.

Composition. Two families: Botryocyrtididae Petrushevskaya, 1981 and Cannobotryidae Haeckel, 1881 (Fig. 41; Table 7).

Occurrence. Cretaceous–Recent.

Family Botryocyrtididae Petrushevskaya, 1981

Diagnosis. Cannobotryoidea with three segments. Subdivision of eucephalic lobe into collar and upper parts not always clear. Long thin tubes not connected with antecephalic and postcephalic lobes, and with spines *A*, *D*, *L*, and *V*. Cephalis clearly separated from thorax. Wall multilayered and spongy.

Composition. *Acanthobotrys* Popofsky, 1913; *Amphimelissa* Jorgensen, 1905; *Bisphaerocephalus* Popofsky, 1908; *Botryocampe* Ehrenberg, 1860; *Botryocyrtis* Ehrenberg, 1860; *Botryometra* Petrushevskaya, 1975; and *Monotubus* Popofsky, 1913.

Occurrence. Cretaceous–Recent.

Family Cannobotryidae Haeckel, 1881

Diagnosis. Cannobotryoidea with two or three segments, rarely with many segments. Subdivision of eucephalic lobes into collar and upper parts distinct. More or less long thin tubes connected with antecephalic lobe, and with spines *D*, *L*, *l*, and *V*. Cephalis often indistinctly separated from thorax. Wall usually thick hyaline.

Composition. *Acrobotrissa* Haeckel, 1887; *Acrobotrys* Haeckel, 1881; *Artobotrys* Petrushevskaya, 1971; *Bisphaerocephalia* Petrushevskaya, 1965; *Botryocella* Haeckel, 1881; *Botryocylinder* Petrushevskaya, 1975; *Botryopyle* Haeckel, 1881; *Cannobotrys* Haeckel, 1881; *Centrobotrys* Petrushevskaya, 1965; *Cornutovum* Foreman, 1968; *Eribotris* Foreman, 1968;

Lithobotrys Ehrenberg, 1844; *Lithocoryphium* Ehrenberg, 1847; *Neobotrys* Popofsky, 1913; *Phormobotrys* Haeckel, 1881; *Pylobotrys* Haeckel, 1881; *Rhopalosyringium* Campbell et Clark, 1944; and *Saccospyris* Haecker, 1908.

Occurrence. Cretaceous (Aptian)–Recent.

Order Spyridinata Ehrenberg, 1847

Diagnosis. Nassellaria with skeleton, in which differentiation in direction of main heteropolar axis not always present (Figs. 46a–46j). Among spines of initial spicule, *A* and *V* developed better than others. They connected by arc *AV* into distinct **D**-shaped sagittal ring. Spines *D*, *2L*, and *2l* developed almost equally, *Ax* almost absent. Skeleton sometimes reduced to sagittal ring.

Composition. Three families: Triospyrididae Haeckel, 1881; Acanthodesmiidae Haeckel, 1862; Stephaniidae Haeckel, 1887 (Fig. 41; Table 7).

Occurrence. Paleogene (Paleocene)–Recent.

Family Triospyrididae Haeckel, 1881

Diagnosis. Spyridinata with developed differentiation in direction of main heteropolar axis, approximately coinciding with directions of spine *A* and apical horn (Figs. 46a–46f). Spines *L* and *D* similarly developed and more pronounced than spine *l*. The extending outside as external feet. Ante- and postcephalic lobes of cephalis developed when sagittal ring enclosed in cephalis and not projecting to outside. Galear structures may be present.

Composition. Six subfamilies: Triospyridinae Haeckel, 1881; Dipodospyridinae Haeckel, 1881; Archiphatninae Haeckel, 1881; Tholospyridinae Haeckel, 1887; Androspyridinae Haeckel, 1887; and Nephrospyridinae Haeckel, 1887 (Fig. 41; Table 7).

Occurrence. Paleogene (Paleocene)–Recent.

Subfamily Dipodospyridinae Haeckel, 1881

Diagnosis. Triospyrididae with test, flattened in frontal plane in direction of axis, perpendicular to heteropolar axis. Two feet *L*, well developed, occurring in one plane with spine *A*, continuing outside in shape of feet. No mitral-galear structures present. Sagittal ring not projecting to outside, from inside included in cephalic wall. Pore arrangement not affected. Wall porous, thick, Pores rounded.

Composition. *Dipodospyris* Haeckel, 1881; *Dorcadospyris* Haeckel, 1881; *Gamospyris* Haeckel, 1881; and *Stephanospyris* Haeckel, 1881.

Occurrence. Paleogene (Eocene)–Neogene (Miocene).

Subfamily Archiphatninae Haeckel, 1881

Diagnosis. Triospyrididae with cephalis and thorax, latter often longer than cephalis (Fig. 46e). Wall porous and thick. Sagittal ring not projecting outside, although it may be included in cephalic wall from inside. This affects arrangement and size of pores occurring close to sagittal ring. Porous girdles absent. Sometimes small galear structure present. Feet almost absent. Aperture possessing flat oral teeth directed downwards.

Composition. *Archiphatna* Haeckel, 1881; *Desmospyris* Haeckel, 1881; *Patagospyris* Haeckel, 1881; *Rhodospyris* Haeckel, 1881; and *Thamnospyris* Haeckel, 1881.

Occurrence. Paleogene (Paleocene)–Recent.

Subfamily Triospyridinae Haeckel, 1881

Diagnosis. Triospyrididae with bilateral symmetry in relation to sagittal ring (Figs. 46b–46d). Sagittal ring may be included cephalic wall and projecting outside, but occasionally remaining inside cephalis influencing arrangement of pores. If ring enclosed in test, pores placed asymmetrically in relation to sagittal plane. When ring projecting outside, pores placed symmetrically in relation to ring and in sagittal plane. Enlargement of pores near ring may lead to significant reduction of walls to isolated porous girdles. Number, degree of development, shape of feet and other oral apophyses vary. Mitral-galear structures absent.

Composition. *Acrospyris* Haeckel, 1881; *Aegospyris* Haeckel, 1881; *Anthospyris* Haeckel, 1881; *Brachiospyris* Haeckel, 1881; *Ceratospyris* Ehrenberg, 1847; *Cladospyris* Ehrenberg, 1847; *Corythospyris* Haeckel, 1881; *Dendrospyris* Haeckel, 1881; *Dictyocircus* Jorgensen, 1905; *Giraffospyris* Haeckel, 1881; *Gorgospyris* Haeckel, 1881; *Hexaspyridium* Haeckel, 1887; *Liriospyris* Haeckel, 1881; *Lophospyris* Haeckel, 1881; *Pentaspyris* Haeckel, 1881; *Petalospyrella* Haeckel, 1887; *Petalospyris* Ehrenberg, 1847; *Semantidium* Haeckel, 1887; *Semantiscus* Haeckel, 1887; *Semantrum* Haeckel, 1887; *Taurospyris* Haeckel, 1881; *Therospyris* Haeckel, 1881; *Triceraspyris* Haeckel, 1887; and *Triospyrium* Haeckel, 1887.

Occurrence. Paleogene (Paleocene)–Recent.

Subfamily Tholospyridinae Haeckel, 1887

Diagnosis. Triospyrididae with cephalis and galear structures. Skeleton compressed in anteroposterior direction (Fig. 46a). Sagittal ring included cephalis and projected onto external surface. Wall thin. Pores near sagittal ring larger than others. Porous girdles absent. Finely porous, cellular, and spongy walls. Sagittal ring thin, weakly developed, often open; sometimes rudimentary. Feet weakly developed; sometimes with lateral apophyses.

Composition. *Clathrobursa* Haeckel, 1881; *Cyrtostephanus* Popofsky, 1913; *Platybursa* Haeckel, 1881; *Tholospyris* Haeckel, 1881; *Tridictyopus* Haeckel, 1881; and *Tristylospyris* Haeckel, 1887.

Occurrence. Paleogene (Oligocene)–Recent.

Subfamily Androspyridinae Haeckel, 1887

Diagnosis. Triospyrididae with well developed thorax, feet and galear (Fig. 46f). Skeleton composed of branching apophyses of main spines, often forming loose spongy tissue. Sagittal ring not projecting outside, enclosed inside test or spongy tissue. Three feet and apical horn well developed and may branch.

Composition. *Androspyris* Haeckel, 1887 and *Lamprospyris* Haeckel, 1881.

Occurrence. Neogene.

Subfamily Nephrospyridinae Haeckel, 1887

Diagnosis. Triospyrididae with test compressed in anteroposterior direction and flattened in frontal. In disc of skeleton, parts, corresponding to cephalis, thorax and galea discernible. Skeleton may be represented by two thin parallel plates occasionally remaining unconnected on the sides. Sagittal ring projected outside and included in porous plates. Pores very large, occurring near ring. Separated feet and horn not developed.

Composition. *Nephrodictyum* Haeckel, 1881 and *Psychospyris* Riedel et Sanfilippo, 1971.

Occurrence. Neogene.

Family Stephaniidae Haeckel, 1887

Diagnosis. Spyridinata with cephalis and its parts absent, no galear, or other structures (Figs. 46g, 46h, 41; Table 7). Only sagittal rings and its apophyses developed. Spines *L* developed approximately as spines *D* and *l*.

Composition. *Cortina* Haeckel, 1881; *Plagiocarpa* Haeckel, 1881; *Stephanium* Haeckel, 1887; and *Zygocircus* Buetschli, 1882.

Occurrence. Paleogene (Paleocene)–Recent.

Family Acanthodesmiidae Haeckel, 1862

Diagnosis. Spyridinata with cephalis or its derivatives (Figs. 46i, 46j). Differentiation in direction of main heteropolar axis indistinct even in inner skeletons. Spines *L* developed more weakly than spine *D* and *l*. External apophyses, compared with feet formed by spines *L* absent. Ante- and postcephalic lobes of cephalis developed very strongly. May be developed mitral–galear structures.

Composition. Four subfamilies: Circospyridinae Haeckel, 1881; Perispyridinae Haeckel, 1881; Acanthodesmiinae Haeckel, 1862; and Paradictyinae Haeckel, 1881 (Fig. 41; Table 7).

Occurrence. Paleogene (Eocene)–Recent.

Subfamily Circospyridinae Haeckel, 1881

Diagnosis. Acanthodesmiidae, in which porous test weakly developed or absent. in latter case latticed frame of isolated bars with distinct girdles. Sagittal ring not always completely projected on surface of skeleton due to developed ante- and postcephalic zones. Galea and thorax not present. Bars *l* and *j* form the base of the basal girdle. Bars *m* and *q* at the top forming the base of the mitral girdle. Bars *a* and *f* not immediately diverging laterally from sagittal ring. Apophyses *a*, projected anteriorly of the general base, diverge laterally to form the base of antecephalic region of skeleton. *V* packed in between apophyses *f* and forming fork together with those being main postcephalic structure. Skeleton enlarged in anteroposterior direction and flattened in dorsoventral direction. Frontal gird not developed. Basal plate present with four to six basal pores. Well developed equatorial girdle with porous Walls. Eucephalic zone not separated by its own walls from subsidiary parts of cephalis.

Composition. *Amphispyris* Haeckel, 1881; *Archicircus* Haeckel, 1887; *Circospyris* Haeckel, 1881; *Lithocircus* Müller, 1856; *Sphaerospyris* Haeckel, 1887; *Spyridobotrys* Haeckel, 1862; *Toxarium* Haeckel, 1887; and *Toxidium* Haeckel, 1887.

Occurrence. Paleogene (Eocene)–Recent.

Subfamily Perispyridinae Haeckel, 1881

Diagnosis. Acanthodesmiidae with porous test, with eucephalic parts, galea, and thorax. Thorax with closed aperture, externally identical to galea. Sagittal ring included in wall of eucephalic part. Frontal girdle (or ring) and other girdles not developed. Bars *a*, *l*, *m*, and other extending from sagittal ring immediately laterally, not developing forks, not branching, not producing feet or horns.

Composition. *Lithotympanum* Haeckel, 1881; *Microcubus* Haeckel, 1881; *Perispyris* Haeckel, 1881; and *Tricolospyris* Haeckel, 1881.

Occurrence. Neogene (Miocene).

Subfamily Acanthodesmiinae Haeckel, 1862

Diagnosis. Acanthodesmiidae with latticed frame, corresponding to eucephalic part of cephalis. Sagittal ring completely projected outside, forming basis of this frame. Apophyses symmetrically extending from it to form frontal and basal rings or girdles. In basal ring, only one pair of arcs visible. Sometimes mitral girdle present and sometimes not developed better than basal ring. Equatorial girdle connected to apophyses *a* very rarely present. All bars extending from sagittal ring immediately laterally, not developing forks, but can branch and form feet and horn.

Composition. *Acanthodesmia* Müller, 1856; *Acrocubus* Haeckel, 1881; *Dipocoronis* Haeckel, 1881; *Eucoronis* Haeckel, 1881; *Semantis* Haeckel, 1887; *Tetracubus* Haeckel, 1887; *Tricyclidium* Haeckel, 1881; *Tripocubus* Haeckel, 1887; *Trissocyclus* Haeckel, 1881; *Trissocyrcus* Haeckel, 1881; *Tympanidium* Haeckel, 1881; *Tympaniscus* Haeckel, 1887; *Tympa-*

nomma Haeckel, 1887; and *Zygostephanus* Haeckel, 1862.

Occurrence. Neogene–Recent.

Subfamily Paradictyinae Haeckel, 1881

Diagnosis. Acanthodesmiidae without porous test. Ante- and postcephalic parts of cephalis fused with eucephalic part. No galear or thoracic structures present. Strongly branching bars forming woodlike tissue (Fig. 46j). Sagittal ring enclosed inside skeletal latticework and projecting outside only when this latticework is not developed. All bars, extending from sagittal ring present. Bars *a* and *f* producing forks. Basal and mitral plates or girdles almost indiscernible. Skeleton compressed dorsoventrally. Feet or horns absent.

Composition. *Paradictyum* Haeckel, 1881.

Occurrence. Neogene (Miocene)–Recent.

Class Collodaria Haeckel, 1881

Diagnosis. Large solitary and colonial Polycystina: some individuals up to 400–800 μm, colonies up to three meters long. Ectoplasm may have skeleton represented by of tangentially arranged spines (Figs. 48e, 48j) or porous shell (Figs. 48g–48i), although mineral skeleton often absent (Fig. 48b).

Composition. Three families: Sphaerozoidae Müller, 1858; Collosphaeridae Müller, 1858; and Thalassosphaeridae Haeckel, 1862 (Table 7).

Occurrence. Triassic–Recent.

Family Sphaerozoidae Haeckel, 1862

Diagnosis. Colonial Collodaria with spiny skeleton, represented by simple or paired spines arranged tangentially around each individual of colony (Figs. 48c–48e). Mineral skeleton may be absent (Figs. 48a, 48b).

Composition. *Belonozoum* Haeckel, 1887; *Collozoum* Haeckel, 1862; *Raphidozoum* Haeckel, 1862; and *Sphaerozoum* Meyen, 1834.

Occurrence. Triassic–Recent.

Family Collosphaeridae Müller, 1858

Diagnosis. Colonial Collodaria, with spherical porous skeleton in each individual of colony (Figs. 48f–48i).

Composition. *Acrosphaera* Haeckel, 1881; *Buccinosphaera* Haeckel, 1887; *Collosphaera* Müller, 1855; *Polysolenia* Ehrenberg, 1872; *Siphonosphaera* Müller, 1858; *Solenosphaera* Haeckel, 1887; *Tribonosphaera* Haeckel, 1881; and *Trisolenia* Ehrenberg, 1860.

Occurrence. Eocene–Recent.

Family Thalassosphaeridae Haeckel, 1862

Diagnosis. Large solitary Collodaria, with simple or paired spines arranged tangentially around central capsule or scattered in jellylike shell (Fig. 48j).

Composition. *Thalassoraphis* Campbell, 1953; *Thalassosphaera* Haeckel, 1862; and *Thalassoxanthium* Haeckel, 1881.

Occurrence. Quaternary.

CHAPTER 4. STAGES IN THE EVOLUTION OF POLYCYSTINE RADIOLARIANS IN THE PHANEROZOIC

The origin, major patterns, and large biotic crises in the evolution of radiolarians in the Phanerozoic were closely connected with the geological history of the Earth. As in all organisms, the evolution of radiolarians was driven by several main factors. Among these were the evolution of the Earth, expressed in irreversible changes in the composition of the atmosphere and hydrosphere (Dobretsov, 2003), and general trends in the evolution of the Earth from the Precambrian to the Recent in the direction of the increasing contrast of the relief of the planet and development of the basins from shallow-water marine basins to epicontinental seas and further to epicontinental marginal seas and oceans (Timofeev and Kholodov, 1984; Khvorova, 1984).

The geological history of the silica in the biosphere is very interesting. In the Precambrian the waters were so strongly saturated with silica that siliceous gel could precipitate directly from the water to form siliceous beds. When organisms began to extract SiO_2 to build their skeletons, the total amount of silica in the seawater had to decrease progressively below the level of dispersion. Gradually the ocean was transformed into a siliceous vacuum because of the appearance of sponges, radiolarians, diatoms, and silicoflagellates (Kaleda, 1987; Fedonkin, 2003). At the same time, volcanism and the rise of highly siliceous water through faults in the zones of rifts created favorable conditions for intensive chemogenic and biogenic accumulation of silica (*Geochemistry*…, 1966; Egorkin, 2000; Klevtsova, 2000).

Climatic cooling and glaciation played a particularly important role in the evolution of the biota. The cool time of the Paleozoic was associated with glaciations at the beginning of the Early Cambrian (the completion of the glaciation, which began in the Late Vendian), in the Late Ordovician–Early Silurian, at the end of the Late Devonian–beginning of the Early Carboniferous, and in the Middle Carboniferous–beginning of the Late Permian. From the middle of the Eocene, periodically recurring glaciations of the Cenozoic began (Chumakov, 2001, 2004; Dobretsov and Chumakov, 2001; Dobretsov, 2003) (Fig. 50).

The Vendian–Cambrian boundary is marked by a fundamental change in the entire biota related to the fact that many organisms acquired the ability to build a skeleton. This resulted in a true biological explosion at

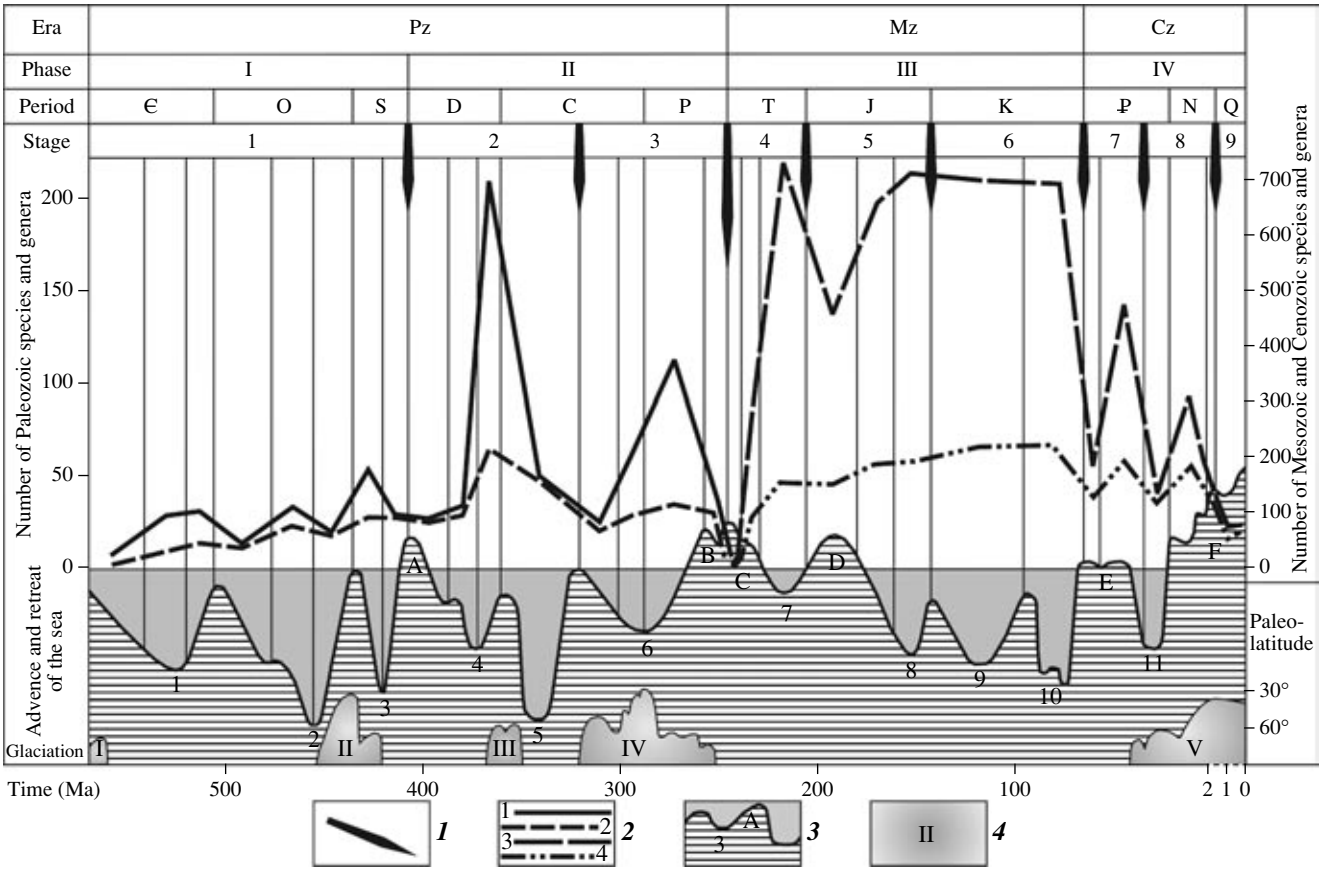

Fig. 50. Changes in the taxonomic diversity of radiolarians (Polycystina) and main cycles of the geological history of Earth in the Phanerozoic: (***1***) mass extinctions of radiolarians (Polycystina); (***2***) changes in the taxonomic diversity of radiolarians: (1) Paleozoic species, (2) Paleozoic genera, (3) Mesozoic and Cenozoic species, and (4) Mesozoic and Cenozoic genera; (***3***) transgressions: (1) Cambrian, (2) Ordovician, (3) Silurian, (4) Middle–Late Devonian, (5) Early Carboniferous, (6) Late Carboniferous–Early Permian, (7) Late Triassic, (8) Middle–Late Jurassic, (9) Early Cretaceous, (10) Late Cretaceous, and (11) Oligocene, geocratonic epochs: (A) Late Silurian–Early Devonian, (B) Permian, (C) Triassic, (D) Early Jurassic, (E) Paleocene–Eocene, and (F) Neogene–Quaternary (after Monin, 1977; Podobina and Rodygin, 2000); and (***4***) glaciations: (I) beginning of the Early Cambrian, (II) Late Ordovician–Early Silurian, (III) end of the Late Devonian–beginning of the Early Carboniferous, (IV) Middle Carboniferous–beginning of the Late Permian, and (V) Middle Eocene–Quarter (after Chumakov, 2001).

the very beginning of the Paleozoic, i.e., the mass appearance of almost all type of animals known in the Phanerozoic (Rozanov, 1989). In the Atdabanian (Early Cambrian), unicellular organisms with an internal siliceous skeleton, radiolarians of the superclass Polycystina, appeared and became widespread (Fig. 24) (Afanasieva and Amon, 2003). It is possible to assume that the eukaryotic sarcodinian ancestors of Polycystina appeared and became widespread as early as the Vendian.

Radiolarians probably appeared in shelf epicontinental basins. These were huge shallow-water basins with a specific trophic links that often occupied large areas of cratons, with depths equal to or above the photic zone, and saturated by microorganisms (Rozanov, 2003).

Presently, the monophyly of many eukaryotes is debated. For instance, according to Zavarzin (2003) it is impossible to build a stable biological system on a monophyletic base. The universal ancestor "cannot exist because it would have been a perpetual motion machine." The original group of organisms should have been diverse and functionally complementary (Zavarzin, 2003, p. 22). Zavarzin's hypothesis comes very close to allowing the idea of a polyphyletic origin of radiolarians because in the Cambrian all major constructions of radiolarians appeared almost simultaneously (spiny, spherical, stauraxonic, and pylomate). They gave rise to all the five classes of radiolarians of the superclass Polycystina: Aculearia, Spumellaria, Sphaerellaria, Stauraxonaria, and Nassellaria (Afanasieva and Amon, 2003).

Radiolarians of the superclass Phaeodaria are poorly preserved even in the bottom sediments because of the specific structure of the siliceous skeleton; thus, their geological history is not traced (Petrushevskaya, 1986). The earliest Phaeodaria of Late Cretaceous age were recently found in Sakhalin (Bragina, 2003).

The problem of stage in the evolution of radiolarians, changes in their biodiversity in time, and aspects of their extinctions is very rarely discussed in the literature.

Lipman (1979) was the first to recognize four cycles in the evolution of radiolarians: Paleozoic, Mesozoic, Paleogene, and Recent. The cycles are subdivided into stages and substages (Table 9). For the Paleozoic and Mesozoic cycles, three stages are recognized, corresponding to the periods; two substages corresponding to the epochs are recognized in the Cretaceous. Five stages corresponding to the ages or their parts are recognized in the Paleogene cycle. For substages corresponding to radiolarian zones are recognized in the Late Eocene. Each of the stages and substages (except Recent) is characterized to show the taxonomic composition and number of radiolarians in the assemblages, and the predominance of some taxa over the others.

Based on the materials of B.B. Nazarov for the Paleozoic, data of L.I. Kazintzova and his own studies of the Mesozoic, and using a the results of G.E. Kozlova, R.Kh. Lipman, N.P. Runeva, W. Riedel, A. Sanfilippo, and H. Foreman for the Cenozoic, Zhamoida (1981) offered a new scheme of classification of radiolarians during the entire Phanerozoic and recognized nine stages (Table 9).

Based on analysis of the evolution of radiolarians, Nazarov (1984; 1988) and Nazarov and Ormiston (1985, 1986, 1993) recognized three stages of that evolution in the Paleozoic (Table 9). The evolution of radiolarians in the Paleozoic shows a distinct trend towards increased complexity and differentiation of the skeleton. Three stages with different rates of evolutionary change in different orders, families, and genera are recognized. The first stage, Cambrian–Early Devonian, was a time of a relatively slow development of spherical radiolarians with a massive internal frame and (from the Wenlock) of spiny radiolarians. The second stage (Middle Devonian–Middle Carboniferous) shows a more intensive evolution of spherical Entactinaria and spiny radiolarians. The third stage in the Late Carboniferous–Permian shows a rapid evolution of stauraxonic radiolarians and albailellarians with a conical skeleton and a somewhat slow evolution of spherical spumellarians.

Bragin *et al.* (1999) analyzed the evolution and changes in the taxonomic composition of radiolarians in the Mesozoic at the level of families, subfamilies, and genera and the morphological transformations of the skeletons at the main stages of the evolution in the Triassic, Jurassic, and Cretaceous. Major critical levels in the evolution of the Mesozoic radiolarians were substantiated (Table 9).

De Wever *et al.* (2001) represents a comprehensive review of fossil and modern radiolarians and showed an important role of these protists in thehistory of the Earth and development of the biosphere. At the same time, only the boundaries corresponding to the main crises in the evolution of radiolarians are discussed in a relatively detailed analysis of the evolutionary changes in Phanerozoic radiolarians at the levels of families (Table 9).

The above studies did not discuss the relationships between the evolution of radiolarians and the general evolution of the Earth, including directed changes in its lithosphere and hydrosphere. In addition, these studies virtually did not cite any exact figures on the biodiversity of radiolarians in different geological epochs. The monograph of De Wever *et al.* (2001) is an exception in this respect, because it contains graphs showing quantitative and qualitative changes in the composition of radiolarians at the family level during the Phanerozoic.

The present paper is a continuation of the studies of its authors (Table 9) of the stages in the evolution of radiolarians in the Paleozoic (Afanasieva, 2000a; Afanasieva and Amon, 2003; Afanasieva and Amon, 2003) and Mesozoic (Agarkov, 2000). The study is based on the precise statistical analysis of the biodiversity of radiolarians in the Phanerozoic (see Chapter 6) and discussion of the changes in the skeletons of radiolarians through geological time. This allows the tracing of the nature and patterns of the appearance/disappearance of orders, families, and genera at the main boundaries in the history of their evolution.

Evolution of radiolarians of the superclass Polycystina showed periodical cyclical changes, when the phase of the appearance of new taxa was replaced by the phase of their acme and then by that of their extinction. In the general dynamic model of the cyclic evolution of radiolarians, simple cycles are combined into cycles of a higher order (***stages***) characterizing the four major ***phases*** in the evolution of radiolarians in the Phanerozoic.

Each stage of evolution was characterized by considerable changes in the composition and number of radiolarians and a change in the dominant groups. Different taxa evolved, to some extent, in parallel, from the creation of a general archetype to the perfection of parts of the skeleton. The best combination of the morphological characters at certain stages determined the appearance of new higher taxa and the acquirement of clear evolutionary advantages.

We recognized four phases and nine stages in the Phanerozoic evolution of radiolarians (Fig. 50; Table 9):

Phase I. Early Paleozoic: Stage 1 (Cambrian–Silurian).

Phase II. Late Paleozoic: Stage 2 (Devonian–Early Carboniferous); Stage 3 (Middle Carboniferous–Permian).

Phase III. Mesozoic: Stage 4 (Triassic); Stage 5 (Jurassic); Stage 6 (Cretaceous).

Phase IV. Cenozoic: Stage 7 (Paleocene–Eocene); Stage 8 (Oligocene–Pliocene); Stage 9 (Quaternary).

Spherical and spiny skeleton were the first morphotypes in the history of radiolarians. A skeleton shaped like a simple sphere (classes Spumellaria and Sphaerellaria) or a spicule (class Aculearia) is optimal from the

Table 9. History of the recognition of cycles, phases, stages, and substages in the evolution of radiolarians

Period	Epoch	Lipman, 1979			Zhamoida, 1981		Nazarov, 1984, 1988; Nazarov and Ormiston, 1985, 1986, 1993	Bragin *et al.*, 1999	Afanasieva, 2000a; Agarkov, 2000; Afanasieva and Amon, 2003	De Wever *et al.*, 2001	Afanasieva *et al.*, 2004	
		Cycle	Stage	Substage	Stage	Substage	Stage	Stage	Stage	Major boundaries of evolutionary crises	Phase	Stage
Quarternary	Holocene	Recent			IX	Late Miocene – Quarternary					IV. Cenozoic	9. Quarternary
	Pleistocene											
Neogene	Pliocene											8. Oligocene – Pliocene
	Miocene											
Paleogene	Oligocene	Paleogene	5. Oligocene		VIII	(Middle?) Late Eocene – Early (Late?) Miocene				Oligocene		
	Eocene		4. Late Eocene	Liosphaeridae						Eocene		7. Paleocene – Eocene
				Heliodiscus lentis								
				Ellipsoxiphus chabakovi								
				Conocaryomma aralensis								
			3. Middle Eocene									
			2. Early Eocene		VII	Maastrichtian – Early Eocene				Paleocene		
	Paleocene		1. Paleocene									
Cretaceous	Late	Mesozoic	3. Cretaceous	Late	VI	2. Coniacian – Campanian		3. Cretaceous	3. Early Cretaceous (Aptian) – Late Cretaceous	Cretaceous	III. Mesozoic	6. Cretaceous
						1. Albian – Turonian						
	Early			Early	V	2. Hauterivian – Aptian			2. Jurassic – Early Cretaceous (Barremian)			
						1. Middle Jurassic – Valanginian						
Jurassic	Late		2. Jurassic					2. Jurassic		Jurassic		5. Jurassic
	Middle											
	Early				IV	2. Early Jurassic						
Triassic	Late		1. Triassic			1. Late Triassic		1. Triassic	1. Triassic	Triassic		4. Triassic
	Middle				III	Late Permian – Middle Triassic				Triassic		
	Early											
Permian	Late	Paleozoic	3. Carboniferous – Permian				3. Late Carboniferous – Late Permian		3. Middle Carboniferous – Permian	Permian	II. Late Paleozoic	3. Middle Carboniferous – Permian
	Early				II	2. Late Carboniferous – Early Permian						
Carboniferous	Late					1. Middle Devonian – Middle Carboniferous	2. Middle Devonian – Middle Carboniferous		2. Devonian – Early Carboniferous			2. Devonian – Early Carboniferous
	Middle											
	Early											
Devonian	Late		2. Devonian									
	Middle											
	Early				I	2. Silurian – Early Devonian						
Silurian	Late		1. Cambrian – Silurian				1. Cambrian – Early Devonian		1. Cambrian – Silurian		I. Early Paleozoic	1. Cambrian – Silurian
	Early					1. Cambrian – Ordovician						
Ordovician	Late											
	Middle											
	Early											
Cambrian	Late											
	Middle											
	Early											

point of view of energy, construction resources, and physiology (support of internal cell organelles).

It is possible that the first radiolarians with a pylome (order Pylomariata) were attached benthic organisms, with a biotope at the bottom water layer above the surface of the bottom sediment. A radiolarian cell was attached to the filaments of algae and sponge spicules by a cytoplasmic tendon protruding through a pylome. A sedentary way of life was present in some radiolarian groups almost through the entire Paleozoic (Petrushevskaya, 1986; Afanasieva, 2000a). At the same time, truly spherical radiolarians Spumellaria and Sphaerellaria and some Aculearia acquired an ability to float and became free floating in the plankton.

PHASE I. EARLY PALEOZOIC

During the Caledonian tectonic-magmatic cycle, five platforms of the southern hemisphere (African-Arabian, South American, Australian, Antarctic, and Indian) formed a single high-standing southern supercontinent, Gondwana (Monin, 1977; Khain, 2003). The Early Paleozoic basins were mostly marine. Most Paleozoic sediments were deposited in the shallow water marine basins (Strakhov, 1948; Timofeev and Kholodov, 1984; Rozanov, 2003).

It is possible that at the beginning of the Early Paleozoic phase in the evolution of radiolarians, in the Cambrian, there were three regional centers of origin and distribution of radiolarians. These centers (Altai–Kazakhstan, Australia, and Newfoundland) (Nazarov, 1973, 1974c, 1975; White, 1986; Iwata *et al.*, 1997; Won and Below, 1999; Obut and Iwata, 2000; Won and Iams, 2002).

Stage 1. Cambrian–Silurian

During the Early Paleozoic phase of their evolution, radiolarians, according to the presently existing data, did not play a significant role in either the ecology of the shallow-water epicontinental marine basins or in sedimentation. At the same time, at the beginning of the Early Paleozoic, all presently known morphotypes of radiolarians emerged and became widespread (Afanasieva and Amon, 2003a, 2003b). At the first stage of their evolution, radiolarians exhibited various skeletal structures (Fig. 23):

(1) various spiny forms of the class Aculearia appeared;

(2) spongy layer formed in the skeletons of radiolarians of the class Spumellaria;

(3) the first bilaterally symmetrical stauraxonic radiolarians of class Stauraxonaria appeared;

(4) specific morphotypes of radiolarians of the class Sphaerellaria with numerous spines (order Anakrusata) appeared;

(5) spherical porous Sphaerellaria with a massive internal frame shaped like a hollow sphere and rodlike spines of the order Inaniguttata were widely distributed;

(6) there was a relatively slow evolution of porous Sphaerellaria with internal frame shaped like a light spicule and three-bladed spines in the order Entactiniata;

(7) radiolarians with a pylome (order Pylomariata, class Nassellaria) became widespread; and

(8) the internal spheres in the skeletons of all spherical, pylomate, and stauraxonic radiolarians began to develop.

At the first stage of the evolution of radiolarians, most (59) higher taxa began to develop: all 5 classes, 11 orders (of 12 orders, known in the Paleozoic), 3 superfamilies, 23 families, and 17 subfamilies. In the Cambrian–Silurian 58 genera of radiolarians are known; of these 22 genera appeared in the Cambrian (Figs. 50, 51a).

The earliest, Early Cambrian Polycystina (Fig. 24) are restricted to four genera of two orders of the class Sphaerellaria (Nazarov, 1973; Obut and Iwata, 2000) and the first problematic remains of spiny radiolarians (Nazarov, 1988). The diversity of radiolarians from the Middle Cambrian increases to 12 genera (Nazarov, 1974c, 1975, 1988; White, 1986; Won and Below, 1999). They belong to seven orders of four classes: Nassellaria (Paleozoic order Pylomariata), Spumellaria, Sphaerellaria, and Aculearia, existing up to the present. In the Late Cambrian the diversity of radiolarians increases to 16 genera from eight orders (Nazarov, 1974c, 1975; Iwata *et al.*, 1997; Won and Iams, 2002). At this time a new class, Stauraxonaria, descendants of which survived until now, appeared.

In the Cambrian–Silurian 180 species of radiolarians are presently known to have existed. The species diversity of radiolarians changed from 7 species in the Early Cambrian to 53 species in the Early Silurian (Figs. 50; 51b). The rate of speciation of radiolarians at the first stage of evolution ranged from 0.3 to 3.0 species/Myr (on average 1.1 species/Myr) (Fig. 51b).

Global transgressions in the Ordovician and Silurian led to a sharp increase in the shelf zones of the basins (Monin, 1977; Khain, 2003). Consequently, an outburst of taxonomic diversity of radiolarians is registered for the Ordovician–Silurian: 42 genera and 119 species (Fig. 50; 51a, 51b).

The first critical level in the evolution of radiolarians is recorded at the Silurian–Devonian boundary (Fig. 50). A marine regression and long geocratic epoch at the end of the Silurian and beginning of the Devonian resulted in the almost complete disappearance of all typically Early Paleozoic taxa: members of the orders Echidninata and Anakrusata and radiolarians with an internal frame shaped like a hollow sphere from the orders Pylomariata and Inaniguttata became extinct. At the Silurian–Devonian boundary a complete renewal of the taxonomic composition of radiolarians at the level of species, genera, and some families and orders took place.

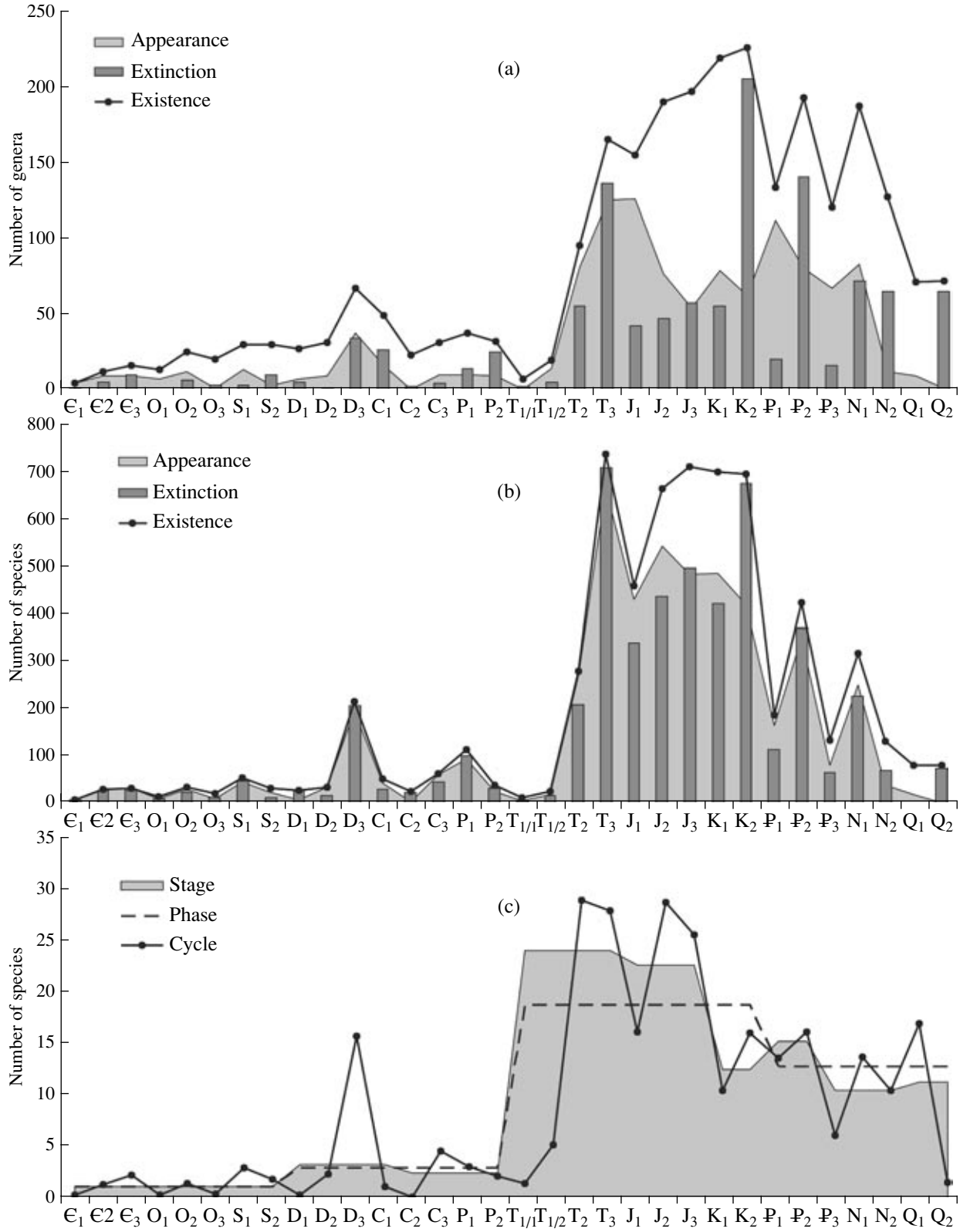

Fig. 51. Changes in the taxonomic diversity of polycystine radiolarians in the Phanerozoic; (a) changes in the generic diversity; (b) changes in the species diversity; and (c) changes in the rate of speciation.

PHASE II. LATE PALEOZOIC

At the beginning of the Hercynian tectonic-magmatic cycle (Devonian–Early Carboniferous), Eurasia and North America with Greenland rose to form a single supercontinent, Proto-Laurasia. Simultaneously the Paleo-Tethys and, possibly, Paleo-Atlantic opened between North America and Africa. In the Late Carboniferous and Early Permian, Laurasia and Gondwana almost complete merged into a single supercontinent, which, however, did not include China, which was situated between the two branches of the Paleo-Tethys. At the end of the Paleozoic Laurasia and Gondwana were completely united into a single continent, Pangea. In the Middle–Late Devonian, in the Early Carboniferous, and in the Late Carboniferous–Early Permian, three waves of transgressions took place, after which a long geocratic epoch continued through almost the entire Late Permian and Early–Middle Triassic (Fig. 50) (Monin, 1977; Khain, 2003). Marine transgressions facilitated the distribution and expansion of planktonic organisms. Regional faunas of radiolarians were formed in the basins adjacent to the zones of active Hercynian tectonics.

The phase of the Late Paleozoic was the time of the most favorable conditions of the life and evolution of radiolarians in the Paleozoic. A fantastic diversity of skeletons of Paleozoic radiolarians appeared precisely during the Devonian–Permian.

The role of radiolarians in the ecology of the primordial ocean and in the sedimentogenesis greatly increased in comparison with the Early Paleozoic phase of evolution. The density of the populations of radiolarians and the size of their biomass in some geological epochs was so great that the organic matter of the dead cell of radiolarians was one of the contributors to the organic material of oil (Afanasieva, 2000a), while the skeletons could form radiolarite beds on the bottom of the sedimentary basins (*Geochemistry …*, 1966; Kaleda, 1987). The Upper Devonian radiolarite jasper in the southern Urals and Middle Frasnian Domanik oil-bearing rock in the Timan-Pechora Oil- and Gas-Bearing Province are classic examples.

The majority of radiolarians of the Late Paleozoic phase in the evolution were, apparently, planktonic, but some Pylomariata (*Caspiaza*) were sessile or benthic-planktonic (*Albaillella*) when, during some early stages of its ontogeny, the organism was floating, but later in the ontogeny the adult organism was bottom-dwelling.

Stage 2. Devonian–Early Carboniferous

A large biotic crisis at the beginning of the Devonian was marked by a significant extinction of 65.5% genera and 88.9% species of the Early Paleozoic radiolarians, and of 58 genera known from the Cambrian–Silurian only 20 survived at the beginning of the Early Devonian (Figs. 50; 51a, 51b).

The second stage of evolution is marked by the maximum taxonomic diversity of radiolarians (67 higher taxa): 5 classes, 10 orders, three superfamilies, 23 families, and 26 subfamilies (Fig. 23). In the Devonian–Early Carboniferous, 19 new higher taxa appeared: order Radiiformata, superfamily Popofskyelloidea, five families (Spongopolyentactiniidae, Popofskyellidae, Corythoecidae, Tormentidae, and Latentifistulidae), and 12 subfamilies. In the Devonian–Early Carboniferous, 89 genera are presently known. In the Late Devonian an explosive radiation of radiolarians occurred. The taxonomic composition of them increased to 67 genera, and 37 genera appeared for the first time.

The second stage of the evolution includes 299 species of radiolarians, the species diversity of radiolarians changed from 27 species in the Early Devonian to 214 species in the Late Devonian (Figs. 50; 51b). The rate of speciation varied from 0.3 to 15.8 species/Myr, with an average rate of speciation of 3.3 species/Myr (Fig. 51c).

In the Devonian and Early Carboniferous, radiolarians had various types of skeletons, including spherical, spiny, and many bilaterally symmetrical forms. Spiny Aculearia were widespread at this time. The orders Fasciculata and Triangulata were very diverse. Bilaterally symmetrical Albaillellata began their evolution.

The evolution of the class Stauraxonaria was relatively slow. Diverse discoidal forms of the families Palaeodiscidae were dominant. In the Early Carboniferous first radiolarians of the subfamilies Tormentinae and Latentifistulinae appeared.

Numerous spongy Spumellaria were widespread. These included radiolarians with latticed skeletons belonging to the order Cancelliata and diverse light spongy skeletons of the order Spongiata.

A rapid evolutionary transformations of the spherical porous Sphaerellaria enabled the separation of six subfamilies of the order Entactiniata: Entactiniinae (Cambrian–Late Triassic), Bientactinosphaerinae (Silurian–Late Triassic), Thecentactiniinae (Late Devonian–Early Permian), Astroentactiniinae (Silurian–Early Permian), Helioentactiniinae (Middle Devonian–Late Triassic), and Multisphaerinae (Carboniferous–Early Permian).

The Devonian and, especially, the Early Carboniferous were the times of the acme of Pylentonemoidea. Their total diversity is 76% of all genera of the order Pylomariata. The proportions of Popofskyelloidea and Cessipyloroidea are only 14 and 10%, respectively.

The second stage of the evolution of radiolarians shows one general archetype of the main skeletal elements in porous Sphaerellaria, spongy Spumellaria, and radiolarians with a pylome of the order Pylomariata (Fig. 23):

(1) the last radiolarians with an internal frame shaped like a hollow nonporous sphere with extending rays (Oriundoguttidae and Cessipylorinae) disappeared;

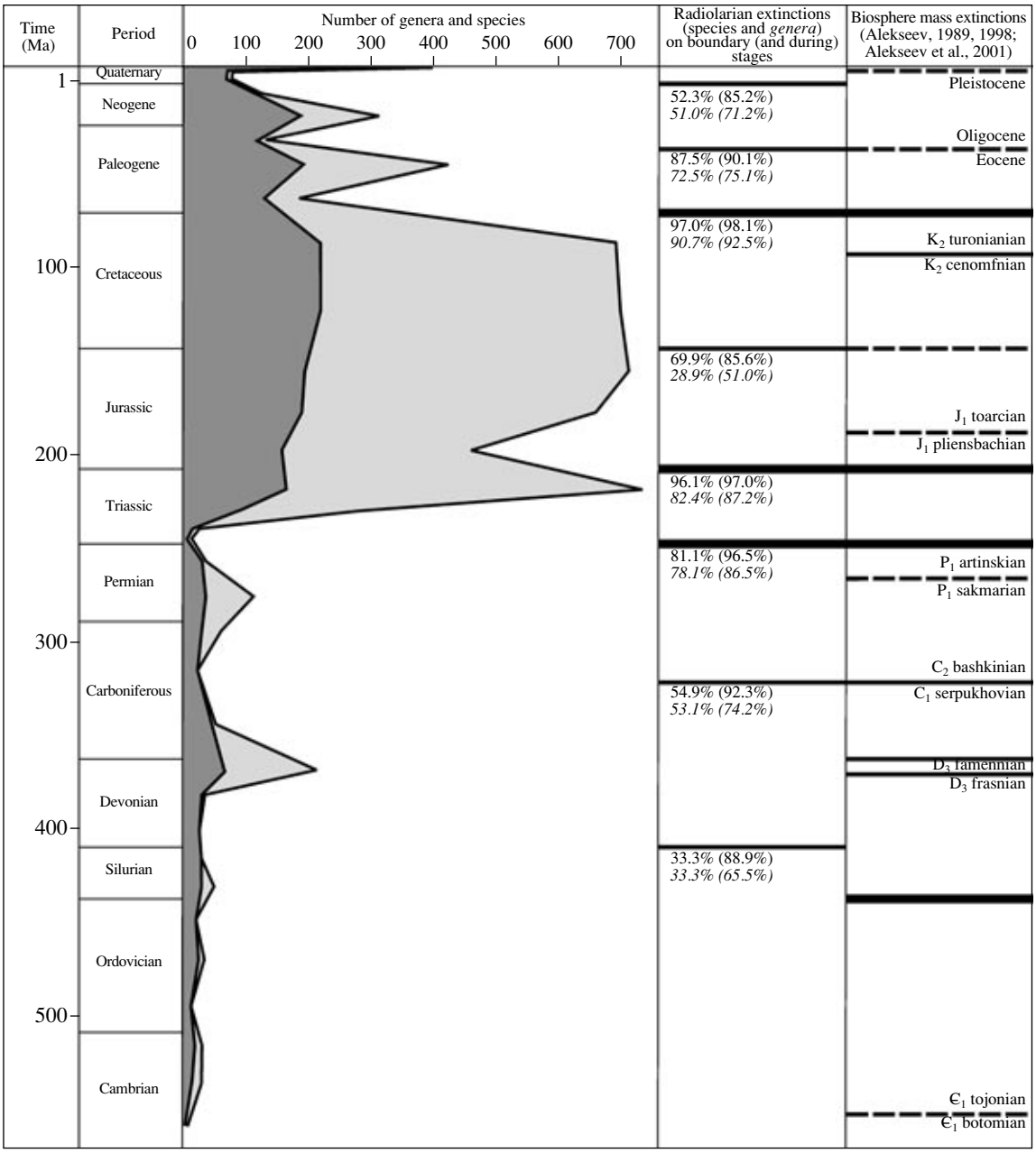

Fig. 52. Mass extinction of the Phanerozoic.

(2) the inner frame becomes less massive (shaped like a six- and multi-rayed spicule);

(3) there is a progressive increase in the number of internal shells of the skeleton;

(4) there is a transformation of the shape of the main spines of the skeleton: originally cylindrical and conical spines were gradually transformed into three-bladed.

The second turning point in the evolution of radiolarians was at the Early–Middle Carboniferous boundary: by the end of the second stage of the evolution, 66 (74.2%) genera and 276 (92.3%) species of the Devonian–Early Carboniferous radiolarians became extinct (Figs. 50; 51a, 51b).

By the end of the second stage, four families (Oriundoguttidae, Palaeoscenidiidae, Pylentonemidae, and Lapidopiscidae) and 11 subfamilies of the Devonian–Early Carboniferous radiolarians became extinct. At the mid-Carboniferous boundary, 53% of the genera and 54.9% of the species of radiolarians became extinct, and only 23 genera of the Early Carboniferous radiolarians continued to the Middle Carboniferous (Figs. 50; 51a).

Unfortunately, the Serpukhovian–Bashkirian mass extinction of the biota (Fig. 52), referred to as such by

Alekseev (1998) and Alekseev *et al.* (2001), is not a great extinction, although, apart from the above radiolarians, gigantoproductid brachiopods, most ammonoid genera, up to 80% of the coral genera, and a complete change in the generic composition of conodonts took place at this level.

Stage 3. Middle Carboniferous–Permian

A rapid evolution and distribution of the Devonian–Early Carboniferous radiolarians in the world's oceans was interrupted for a short time by a global cooling and glaciation in the Middle Carboniferous–Permian, which showed features of a total crisis (Horng-sheng *et al.*, 1999, 2001; Chumakov, 2001; Grossman *et al.*, 2002; Khain, 2003). This cooling resulted in a general reduction in the total number of radiolarians and in the decrease in their taxonomic diversity (Fig. 50).

In the Middle Carboniferous–Permian, 52 genera of radiolarians are known. Most of them (37 genera) existed in the Early Permian (Figs. 50; 51a). At the third stage of the evolution of radiolarians, two new families (Ruzhencevispongidae, Deflandrellidae) and seven subfamilies of stauraxonic radiolarians appeared (Fig. 23).

The third stage shows the decrease in the species diversity of radiolarians to 202 species, changing from 25 species in the Middle Carboniferous to 112 species in the Early Permian (Figs. 50; 51b). The rate of speciation of radiolarians in the Middle Carboniferous–Permian gradually decreased from 4.6 to 2.1 species/Myr at the average rate of 2.4 species/Myr (Fig. 51c).

At the same time, the third stage of the evolution of radiolarians shows an intensive development of stauraxonic and bilaterally symmetrical radiolarians and complete disappearance of radiolarians with a pylome of the order Pylomariata.

The main characteristic feature of the skeleton of stauraxonic radiolarians that makes them fundamentally different from all other radiolarians is a shape of their skeleton, which can be discoidal, polymorphic, subtriangular, pyramidal, spindle-shaped, and armed, with three to five or more arms (Fig. 23). The inner frame is a hollow sphere with extending hollow rays.

From the Late Carboniferous onward, an intensive process of segmentation of the skeleton in some bilaterally symmetrical radiolarians of the order Albaillellata began. In addition, the skeleton became distinctly segmented into the apical, central, and basal parts.

The last reliably established radiolarians with a pylome (genus *Caspiaza* of the order Pylomariata) were found in the Middle Carboniferous bioclastic limestones on the slope of the reef massif Karachaganak in the northern Caspian Sea region (Afanasieva, 1987, 2000a). The last Popofskyellidae, which were apparently the ancestors of the Mesozoic–Cenozoic Nassellaria, are known from the Late Carboniferous.

Generally in the Middle Carboniferous–Permian the following trends are observed:

- stabilization in the evolution of porous Sphaerellaria,
- somewhat slower evolution of the spongy Spumellaria,
- gradual extinction of spiny radiolarians of the orders Fasciculata and Triangulata from the class Aculearia.

The end of the Permian period was marked by the catastrophic extinction of radiolarians (Fig. 23). At the end of the Paleozoic, 37 of a total of 59 higher taxa of Paleozoic radiolarians became extinct (4 orders, 2 superfamilies, 14 families, and 17 subfamilies). Of the lower taxa existing at various times during the third stage of the Paleozoic history of radiolarians, 45 (86.5%) genera and 195 (96.5%) species died out. In total, during the Paleozoic, 149 genera (95.5%) and 640 species (98.9%) of radiolarians became extinct (Figs. 50; 51a, 51b).

The striking morphological similarity of some Paleozoic and Mesozoic–Cenozoic groups of radiolarians suggests the possibility of a general evolution of Phanerozoic radiolarians.

At the end of the Late Permian, the diversity of stauraxonic radiolarians sharply decreased. However, many genera among Mesozoic and Cenozoic radiolarians are strikingly similar to the Stauraxonaria, which disappeared at the end of the Paleozoic.

Early Pylomariata could be ancestral to Mesozoic–Cenozoic Nassellaria. For instance, Pylentoneminae, the unique skeletal morphology of which is very similar to the tripods of true Nassellaria, or Late Devonian–Carboniferous Popofskyellidae, the tests of which featured a distinct segmentation, delineated cephalis, and a well-developed pylome.

The conservative nature of spherical radiolarians is a well-known fact (this includes porous Sphaerellaria and spongy Spumellaria). However, more advanced taxa of these classes exist even now.

PHASE III. MESOZOIC

In the Mesozoic Pangea became split. In the Late Triassic and Early Jurassic, North America was separated from Africa and South America by a wide Caribbean–Sargasso Sea, whereas Greenland was isolated from Scandinavia by the North Atlantic Gulf of the future Arctic Ocean. The Mesozoic Tethys Ocean separated Eurasia from Gondwana. In the Late Jurassic and Early Cretaceous, Laurasia became split (the North Atlantic became completely open) and Gondwana began splitting (South America, Africa, India, and Antarctic-Australian blocks) were separated from each other by wide straits, from which South Atlantic and Indian Ocean were subsequently formed. In the Jurassic, and later, especially intensively in the Late Cretaceous, two waves of transgressions took place (Fig. 50) (Monin, 1977; Khain, 2003). In addition, the cool climate of the Paleozoic was replaced by the warm Meso-

zoic era. In the Late Jurassic the temperature in the middle latitudes was 25°C above the temperature now (Dobretsov and Chumakov, 2001; Zharkov and Chumakov, 2001; Dobretsov, 2003). "The presence of the warm period over 200 Myr against the background of the general cooling of the Earth is a noticeable anomaly" (Dobretsov, 2003, p. 9) and affected the evolution of radiolarians in the Mesozoic.

The change in the radiolarian associations at the Permian–Triassic boundary and predominance of the planktonic lifestyle in the Mesozoic radiolarian communities agrees well with the time of the development of modern oceans (Afanasieva and Vishnevskaya, 1993b). Simultaneously with the deepening of the primordial oceans, which began in the Mesozoic, the apparent reduction of the basins of the ancient epicontinental seas took place (Timofeev and Kholodov, 1984).

At present, a certain connection between the Mesozoic–Cenozoic and Paleozoic groups of radiolarians (Bragin, 2000, 2002) is established. Despite the fact that the Paleozoic–Mesozoic boundary radiolarians experienced a catastrophic extinction (only few Paleozoic taxa survived), they gave rise to a new wave of the evolution of radiolarians in the Mesozoic. The Early Mesozoic is marked by a rapid development of new taxa. This and the appearance of new orders of the class Nassellaria, which, perhaps, replaced Paleozoic Pylomariata, and many new morphotypes, which were the intermediate forms between Paleozoic and Mesozoic spherical and stauraxonic radiolarians (Bragin *et al.*, 1999).

The evolutionary selection resulted in that only planktonic forms remained and became diverse among radiolarians. However, very importantly, many Mesozoic ancestors of the future oceanic nassellarians inherited the adaptation to the benthic mode of life. For instance, the first true nassellarians *Hozmadia* appeared in the Early Triassic, and typical nassellarians (*Triassocampe*) emerged in the Middle Triassic. *Hozmadia* and *Napora* apparently originate from the Paleozoic bottom dwelling Pylentonemoidea, *Triassocampe* and *Canoptum* apparently evolved from the Paleozoic bilaterally symmetrical planktonic Popofskyelloidea. This kind of parachute-like radiolarian, which is well adapted to floating in the water, has remained until the present (Afanasieva and Vishnevskaya, 1993a; Afanasieva, 2000a).

Stage 4. Triassic

The Mesozoic phase in the evolution of radiolarians began in the Induan with seven genera of Paleozoic ancestors (Bragin, 2000, 2002) (Fig. 50). Only a small part of Paleozoic taxa continued into the Mesozoic and Cenozoic. Some morphotypes disappeared completely. At the same time, in the Triassic for the first time typical Mesozoic and Cenozoic taxa of radiolarians appeared. Therefore, this stage can be considered a beginning of the evolution of the fauna of Mesozoic radiolarians (Bragin *et al.*, 1999). Radiolarians of the Triassic include 69 families and subfamilies, of which 59 appeared for the first time.

Among the spiny Aculearia of the Triassic, the evolution of the Paleozoic Palacantholithidae and Palaeoscenidiidae continued; and first Plagiacanthinae appeared (Fig. 30). Spongy Spumellaria are represented by 11 families and subfamilies, among which Multiarcusellidae, Austrisaturnalinae, Oertlispongidae, and Pentactinocarpidae occur only in the Triassic. In the Middle Triassic the first Eptingiidae and Centrocubidae appeared. The Saturnalidae became widespread (Fig. 33). Porous Sphaerellaria, including 11 families and subfamilies, were widespread in the Triassic: typical Triassic Capnodocinae and Capnuchosphaerinae; the first Pantanelliinae, Xiphostylinae, Kungalariidae, Hexalonchata, and Actinommata; and the last Entactiniata (Fig. 35). The Triassic stauraxonic radiolarians include members of 14 families and subfamilies, of which Hexaporobrachiidae, Patruliidae, and Relindellidae are found only in the Triassic (Fig. 40). Nassellaria in the Triassic include members of 29 families and subfamilies (Fig. 41). Among radiolarians with a pylome from the order Pylomariata, the last Archocyrtiinae and the first Poulpidae and Tripedurnulidae are present (Fig. 43).

The total number of the Triassic radiolarian genera rapidly increased to 227. In the Olenek age of the Early Triassic, a low total diversity (19 genera) existed, but in the Middle Triassic it quickly increased to 95 genera. The maximum of generic diversity was in the Late Triassic (165 genera) (Figs. 50; 51a).

The total number of radiolarian species in the Triassic sharply increased to 967. The species diversity changed from 12 species in the Induan (Early Triassic) to 738 species in the Late Triassic (Figs. 50; 51b). The rate of speciation in the Triassic increased from 1.4 to 29.0 species/Myr, on average 24.1 species/Myr (Fig. 51c).

The Triassic–Jurassic boundary is characterized by the extinction of 22 families and subfamilies of radiolarians, including the last Paleozoic spiny Palacantholithidae and Follicucullidae; porous Helioentactiniinae, Entactiniinae, and Bientactinosphaerinae; and seven families and subfamilies of Nassellaria. At the end of the Triassic, 709 (96.1%) species and 136 (82.4%) genera disappeared. In total, during the Triassic, 938 (97.0%) species and 198 (87.2%) genera of radiolarians became extinct (Figs. 50; 51a, 51b).

Stage 5. Jurassic

Jurassic radiolarians included 71 families and subfamilies, of which 25 appeared for the first time.

Among spiny Aculearia, in the Jurassic, Palacantholithidae and Plagiacanthinae continued to exist (Fig. 30). Spongy Spumellaria are represented by nine families and subfamilies. In the Early and Late Jurassic,

the first Quinquecapsulariidae and Rhizosphaeridae appeared. Of spumellarians with an internal frame, in the Jurassic, rare Polyentactiniinae continued their existence (Fig. 33). Porous Sphaerellaria, including 11 families and subfamilies, were widespread in the Jurassic. Among these, spherical skeletons with two, three, and four spines; typical Jurassic Heleninae and Leugeoninae; and the first Parvivaccinae and Hexalonchidae were present. At the end of the Jurassic, radiolarians with a tuberculate surface (Acaeniotylinae) appeared (Fig. 35). Jurassic stauraxonic radiolarians included members of 13 families and subfamilies, among which Catenopylidae, Emiluviidae, and Pseudoaulophacinae appeared for the first time (Fig. 40).

At the Jurassic stage of the evolution radiolarians, nassellarians flourished. Beginning from the Jurassic and to the present, the taxonomic diversity of nassellarians was predominant compared with all other classes of polycystine radiolarians. Nassellaria in the Jurassic include representatives of 36 families and subfamilies, among which 15 appeared in the Jurassic, while Hexapylocapsidae and Vallupinae are restricted to the Jurassic (Fig. 41).

The Jurassic stage shows the highest in the Phanerozoic total number of known species of radiolarians (1486). The species diversity of the Jurassic radiolarians changes from 459 species in the Early Jurassic to 711 species in the Late Jurassic (Figs. 50; 51b). The rate of speciation in the Jurassic ranges from 16.2 to 28.8 species/Myr, on average 22.7 species/Myr (Fig. 51c). The total number of radiolarian genera in the Jurassic was 286, which is similar to the number of genera in the Triassic. The maximum total diversity was in the Late Jurassic (197 genera) (Figs. 50; 51a).

The Jurassic–Cretaceous boundary is known to be a moment of one of the mass extinctions of radiolarians. However, the reality of this event was, according to Alekseev (1989, 1998) and Alekseev *et al.* (2001), very doubtful, because there was no change in the marine faunas at this level. The level of extinction of genera of marine organisms does not exceed 30%, and only 5% of families (Sepkoski, 1996).

At the same time, this turning point in evolution of radiolarians is characterized by a significant change in the taxonomic composition of radiolarians: at the end of the Jurassic 13 (18.3%) families and subfamilies (Figs. 30, 33, 35, 40, 41), 57 (28.9%) genera, and 497 (69.9%) species became extinct. In total, stage 5 of the evolution of radiolarians is marked by the disappearance of 1272 (85.6%) species and 146 (51.0%) genera of Jurassic radiolarians (Figs. 50; 51a, 51b).

Stage 6. Cretaceous

The Early Cretaceous radiolarians were still very similar to their Jurassic ancestors. They included multichambered Cyrtidinata, skeletons of which with an apical spine were ornamented by longitudinal ribbing and transverse girdles, and tuberculate skeletons of Acaeniotylinae. Stauraxonic radiolarians were very numerous and diverse. Most of the Early Cretaceous families of radiolarians continued to the Late Cretaceous. Many of these reached their maximum only in the Late Cretaceous, but generally for the Cretaceous predominance of nassellarians is typical (Lipman, 1979; Bragin *et al.*, 1999).

The Cretaceous stage showed the highest total number of families and subfamilies in the Phanerozoic (82), of which 25 appeared for the first time.

Among spiny Aculearia, only Plagiacanthinae continued to the Cretaceous (Fig. 30). Spongy Spumellaria are represented by eight families and subfamilies. In the Early Cretaceous the first Orosphaeridae appeared. Of spumellarians with an internal frame in the Cretaceous, Polyentactiniinae completed their evolution (Fig. 33). Porous Sphaerellaria, including 10 families and subfamilies, were relatively widely distributed in the Cretaceous. Of these, Stylosphaerinae appeared for the first time (Fig. 35).

Cretaceous stauraxonic radiolarians are very diverse and unite members of 18 families and subfamilies, among which in the Late Cretaceous Larnacillinae, Pentapyloniinae, and Spongodiscidae appeared for the first time. Cavaspongiidae, Miropylidae, and Phaseliformidae are restricted to the Cretaceous (Fig. 40).

Cretaceous Nassellaria are the most diverse and include members of 45 families and subfamilies, of which 17 appeared at this level, while Rotaforminae were restricted to the Cretaceous (Fig. 41).

The species diversity of radiolarians decreased from 700 species in the Early Cretaceous to 696 species in the Late Cretaceous. However, the total number of radiolarian species reached 1118 (Figs. 50; 51b). The rate of speciation ranged from 10.5 to 16.1 species/Myr. The average rate of speciation decreased to 12.5 species/Myr, i.e., almost halved compared to the Jurassic stage (Fig. 51c). A total number of the genera of the Cretaceous radiolarians were 281, i.e., figure, comparable with those in the Triassic and Jurassic. The maximum generic diversity was in the Late Cretaceous (226 genera) (Figs. 50; 51a).

At the end of the Cretaceous 675 (97.0%) species and 205 (90.7%) genera of the Late Cretaceous radiolarians became extinct. In total, during the Cretaceous, 32 (39%) families and subfamilies, 1097 (98.1%) species, and 260 (92.5%) genera of radiolarians became extinct (Figs. 50; 51a, 51b).

The extinction of radiolarians at the Cretaceous–Paleogene boundary coincides with a total mass extinction almost in all groups of marine and land biota occurring at this level (Fig. 52) (Alekseev, 1984, 1989, 1998; Alekseev *et al.*, 2001). Radiolarian evolution was not at a stage of decline as was the case in ammonoids, belemnoids, or dinosaurs. The rank of the higher taxa that were lost during the mass extinction of radiolarians at the critical boundary did not exceed family level. Hence, the extinction of species, genera, and some families of radi-

olarians at the end of the Maastrichtian was most likely selective and concerned certain ecological types.

According to Alekseev (1984, 1989, 1998), the intensity of extinction in different groups of phyto- and zooplankton was different for organisms with calcareous and siliceous skeletons. In radiolarians and silicoflagellates, the intensity of extinction at the generic level was three to five times lower than in planktonic foraminifers and nannoplankton, although the background extinction level is approximately similar in these groups.

PHASE IV. CENOZOIC

In the Cenozoic, cold climate was dominant. From the middle Eocene a systematic cooling began, which was accompanied by sharp fluctuations of the temperature and glaciations (Zharkov and Chumakov, 2001; Dobretsov, 2003) (Fig. 50).

In the Cenozoic Laurasia split, and the North Atlantic Ocean opened between Europe and North America. The tectonics at the Cretaceous–Tertiary boundary and the glaciation that began in the Eocene facilitated the beginning of the geocratic epoch of the Cenozoic. The first geocratic phase began from the Paleogene. In the Oligocene the last wave of transgressions took place. From the Neogene a new geocratic epoch with a modern distribution of the land and sea began (Monin, 1977; Podobina and Rodygin, 2000; Khain, 2003). As the basins deepened, radiolarians occupied the open abyssal of the ocean (Afanasieva and Vishnevskaya, 1993b). However, unlike the epicontinental seas of the previous geological eras, modern oceanic basins have a diverse bacterial content, which is an excellent food source for microorganisms, only in the subsurface and bottom water layers, thus determining trophic specificity (Rozanov, 2003). This is one of the factors controlling the distribution of radiolarians mainly in the upper 500 m of the ocean.

Stage 7. Paleocene–Eocene

The Cenozoic evolution of radiolarians began with 29 species of Mesozoic ancestors. Many genera of Cretaceous spumellarians continued their existence and reached their maximum in the Paleogene, while the species of multicamerate nassellarians that appeared in the Late Cretaceous became extinct in the Paleogene. However, despite the evident continuance of the taxa, a sharp change in the faunas of radiolarians took place at the Cretaceous–Tertiary boundary. Multichambered nassellarians characteristic of the Jurassic and Cretaceous were replaced by one-, two-, and three-chambered skeletons. Moreover, spumellarians gradually became a dominant group in the Paleogene (Bragin *et al.*, 1999).

Radiolarians of stage 7 include 74 families and subfamilies, of which 28 appeared for the first time.

Spiny Aculearia in the Paleocene and Eocene are represented only by Plagiacanthinae (Fig. 30). The diversity of spongy Spumellaria is reduced to seven families and subfamilies, of which Axopruninae appeared for the first time (Fig. 33). The diversity of porous Sphaerellaria is also decreased to seven families and subfamilies. Among those were typical Paleocene–Eocene Entapiinae and the first Heliodiscidae (Fig. 35).

Stauraxonic radiolarians experienced a mass extinction of 10 (55.6%) families and subfamilies at the end of the Cretaceous. Stauraxonaria of the Paleocene–Eocene included members of 15 families and subfamilies, of which Suttoniidae, Pyloniidae (Pyloniinae, Pylodiscinae), Larnacillidae (Circodiscinae, Cryptolarnaciinae, Histriastrinae), and Coccodiscidae appeared for the first time. Members of Palaeotetrapylinae are known only from the Paleocene (Fig. 40; Table 7).

Nassellaria of the Paleocene–Eocene include 41 families and subfamilies, of which 12 appeared at this time (Fig. 41).

In the Paleocene and Eocene the number of radiolarians decreased to 537 species. The species diversity of radiolarians changed from 186 species in the Paleocene to 423 species in the Eocene (Figs. 50; 51b). The rate of speciation changed from 13.6 to 16.2 species/Myr (on average 15.3 species/Myr) (Fig. 51b). The total number of radiolarian genera at stage 7 was 213, i.e., figure, comparable with that in the stage of the Mesozoic phase of the evolution. The maximum generic diversity was in the Eocene (193 genera) (Figs. 50; 51a).

At the boundary between stages 7 and 8, only four subfamilies became extinct: Neosciadiocapsinae, Zamolxinae, Entapiinae, and Conocaryommidae (Figs. 33, 35, 41). However, among genera and species of radiolarians a mass change in the taxonomic composition took place: 370 (87.5%) species and 140 (72.5%) radiolarian genera became extinct. In total, in the Paleocene and Eocene 484 (90.1%) species and 160 (75.1%) genera of radiolarians disappeared.

Stage 8. Oligocene–Pliocene

This stage of the evolution is characterized by a new decrease in the total number of radiolarians. Radiolarians of stage 8 include 71 families and subfamilies, of which only three appeared for the first time.

Spiny radiolarians Plagiacanthinae (Fig. 30) continued their evolution. The diversity of spongy Spumellaria and porous Sphaerellaria decreased to six families and subfamilies, respectively (Figs. 33, 35). Stauraxonic radiolarians included members of 14 families and subfamilies, of which Tholoniidae, Coccodiscidae (Artiscinae), and Pyloniidae (Dipylissinae) appeared for the first time (Fig. 40; Table 7). Nassellaria of stage 8 included 44 families and subfamilies, of which Acanthodesmiinae and Paradictynae appeared for the first time and Androspyridinae, Nephrospyridinae, and Perispyridinae were restricted to the Neogene (Fig. 41).

The species diversity of radiolarians included 420 species and changed from 132–130 species in the Oligocene–Pliocene to 318 species in the Miocene (Figs. 50; 51b). The rate of speciation changed from 6.1 to 13.7 species/Myr, whereas the average rate of speciation decreased to 10.5 species/Myr compared to the preceding stages (Fig. 51b). Two hundred and fifteen genera of radiolarians existed in the Oligocene–Pliocene, which is comparable with that for stages 4 to 7. The maximum generic diversity was in the Miocene (187 genera) (Figs. 50; 51a).

The Neogene–Quaternary boundary is marked by the extinction of two families of stauraxonic radiolarians (Fig. 40), seven families and subfamilies of nassellarians (Fig. 41), and 68 (52.3%) species and 65 (51.0%) genera of radiolarians. In total, 358 (85.2%) species and 153 (71.2%) genera of radiolarians became extinct during stage 8. Generally, this stage shows a decrease in the evolution of radiolarians.

Stage 9. Quaternary

The Quaternary is a specific stage in the evolution of radiolarians, embracing too short a period of time (from the geological point of view). The taxonomic diversity of radiolarians of the Quaternary includes 65 families and subfamilies, of which five appeared for the first time.

Spiny radiolarians Plagiacanthinae continued their evolution (Fig. 30). Spongy Spumellaria and porous Sphaerellaria are represented by the same families and subfamilies as at the similar stage of the Oligocene–Pliocene (Figs. 33, 35). The diversity of stauraxonic radiolarians is reduced to 11 families and subfamilies, of which Myelastridae appeared for the first time (Fig. 40; Table 7). Quaternary nassellarians dominated among radiolarians but were less diverse. They included 41 families and subfamilies, of which Plectaniinae, Tetraplectinae, Plagoniidae, and Cystidiidae appeared for the first time (Fig. 41).

The beginning of the Quaternary stage of the evolution shows a sharp decrease in diversity of radiolarians to 79–80 species in the Eopleistocene and Pleistocene.

The Holocene, as widely believed, showed an explosive biodiversity and reached its maximum of 2114 species of Recent radiolarians. Haeckel (1887) described about 3500 species of Acantharia, Phaeodaria, and Polycystina, talking into account all juvenile stages and ecological varieties.

The diagnostics of species of modern Polycystina, is "a time-consuming and frustrating task" (Boltovskoy, 1998, p. 18), excluding a few widely distributed species, about which an agreement has been reached between zoologists and paleontologists. A precise determination of some species is often impossible because the identical morphotypes appear under different species and generic names and vice versa one name corresponds to different species (Boltovskoy and Jankilevich, 1985; Kruglikova, 1995, 2000).

Based on a careful study of the skeletal morphology and the analysis of characters on which the recognition of species and genera is based, Boltovskoy (1998) concluded that the actual number of Cenozoic species of radiolarians for which the diagnoses can be compiled using carefully selected morphological characters is considerably less than is usually believed, being limited only to 300–600 species, but certainly not to thousands (!). Kruglikova (1995, 2003) showed that the number of the radiolarian species in the modern bottom sediments varies from 60 species in the Arctic to 200 species in the North Pacific and is about 400 species in the equatorial zone.

In addition, Petrushevskaya (1986) noticed the pattern in the transition of radiolarians first into sediment and later into rock: (1) in the sediment, empty skeletons constitute 10–30% of the total number of live radiolarians; and (2) the number of radiolarian skeletons retained in the rock is tens of times less than in the loose sediments. Zasko (2004) studied modern Polycystina and also showed a decrease in the dominant taxa in the sediment by 15–55%.

Hence, only about 50% of the 2114 known modern species of radiolarians may transit into the loose sediment (taking into account species from the sediment and water). This makes 1057 species. This number agrees with the data of the separate counts of radiolarians in the bottom sediments (1037 species) and in the waters of seas and oceans (1077 species).

It may be assumed that in the distant future less than 100 species of Holocene radiolarians will remain in the rocks during the processes of diagenesis, i.e., a number comparable with those from the Eopleistocene (79 species) and Pleistocene (80 species). Thus, we came to a conclusion that no explosive biodiversity of radiolarians occurred in the Holocene. The Recent is not a unique period in the existence of the biota. The paleontological past of radiolarians, as in many other groups, was much richer and more diverse than the present.

MASS EXTINCTIONS

In the Phanerozoic, there were periods of relatively quiet evolution of the biota, separated by a few short moments of mass extinctions when the rate and level of extinctions increased many times compared to the background extinction (Alekseev, 1984, 1989, 1998). Radical changes in the environment and climate are reflected at the initial stages of the development of new aromorphoses and lead to the irreversible extinctions of the unsuccessful forms (Kanygin, 2001). Periodical pulsations of "cooling–warming" are what forces the biota to continuously adapt to the changing situation (Dobretsov, 2003). The transition from the cold climate of the Paleozoic to the warm climate of the Mesozoic was marked by the extinction of 78.1% of radiolarian genera and 81.1% of species at the Permian–Triassic boundary. The total extinction of the Paleozoic radiolarians was 95.5% of genera and 98.9% of species.

The transition from the warm Mesozoic climate to the cold Cenozoic climate was marked by a similarly significant extinction at the Cretaceous–Tertiary boundary of 90.7% genera and 97.0% radiolarian species. The total disappearance of the Mesozoic radiolarian fauna was accompanied by the extinction of 96.6% of genera and 99.4% of species, which is comparable with the data for the Paleozoic.

In total, in the Early Paleozoic (Cambrian–Silurian), 180 species of radiolarians with the average rate of speciation of 1.1 species/Myr appeared, while in the Late Paleozoic (Devonian–Permian), 487 species are known (these appeared with an average rate of 2.9 species/Myr). The Mesozoic shows the greatest number of species (3328) and a maximum average rate of speciation of 18.8 species/Myr. In the Cenozoic (without modern radiolarians), the total number of species sharply decreased to 922, while the average rate of speciation decreased to 12.8 species/Myr (Figs. 50; 51b, 51c).

The most important changes in the taxonomic diversity and extraordinary extinctions of radiolarians completely coincide with the Five Great Extinctions of the biota recognized by Alekseev (1989, 1998) and Alekseev *et al.* (2001): Serpukhovian/Bashkirian, Permian/Triassic, Triassic/Jurassic, Jurassic/Cretaceous, and Cretaceous/Tertiary. The Permian/Triassic Great Extinction changed the entire course of the evolution of the biota (Fig. 52).

On the other hand, the Botomian/Toyonian, Ordovician/Silurian, Frasnian/Famennian, Devonian/Carboniferous, and Cenomanian/Turonian Mass Extinctions were not marked in the history of radiolarians at the level of the mass extinctions in this group (Fig. 52).

At the same time, important events of the mass extinction of radiolarians at the Silurian/Devonian and Neogene/Quaternary boundaries are not recognized on the scale of mass extinctions of the entire biota (Fig. 52). However, at the Silurian/Devonian boundary 88.9% of the Early Paleozoic radiolarian species and 65.5% of the genera disappeared, whereas 78.3% of the Cenozoic radiolarian species became extinct at the Neogene/Quaternary boundary. The structural plan of the skeletons changed and the taxonomic composition of the radiolarian assemblages was renewed.

CHAPTER 5. ECOLOGY AND TAPHONOMY OF RADIOLARIANS

Many, if not all textbooks, special papers, and monographs refer to radiolarians as "exclusively marine unicellular solitary or colonial animals, living in water with oceanic salinity (32–38 PSU), and of planktonic mode of life" (Khabakov *et al.*, 1959; Kruglikova and Maksimova, 1973; Kling, 1978; Petrushevskaya, 1981a, 1986; Nazarov, 1988; Nazarov and Petrushevskaya, 1995; Anderson *et al.*, 2002; etc.). The prevailing opinion is that "Radiolarians are able to populate the whole water body of the oceans from the surface to the deepest layers… The vast majority of radiolarians live in the open sea and oceans. Only some representatives inhabit coastal waters and may be regarded as neritic" (Khabakov *et al.*, 1959, p. 412).

Geologists commonly believe that radiolarians are inhabitants of the open ocean and reliable indicators of deep facies suggesting bathyal and abyssal zones. For instance, radiolarians are used as a "reliable" indication of the presence of deep water facies in the Devonian of the Gornyi Altai: "The oceanic basin was quite deep, below the level of carbonate compensation (layers of limestones and other carbonates are absent from the section). Fossil remains are represented by planktonic organisms (conodonts, radiolarians, etc.)" (Gutak, 2002, p. 19). Based on similar conclusions, very important geological conclusions concerning paleodepths and the development of the oceanic crust are made.

In fact, the presence of radiolarians in sediments says very little about paleodepth. Modern oceans have rich associations of radiolarians, inhabiting basins 100–200 m deep. They only differ slightly from the associations of radiolarians living 100, 200, and 1000 km from the shoreline, where the basin is 10–20 times as deep.

The general pattern of biogeography and paleobiogeography of radiolarians is much more complex and involved than is generally believed. The data obtained in recent years show that, in contrast to the established views and hypotheses, radiolarians may not be restricted to the central zones of the seas and oceans, but also occur in brackish waters of estuaries (Boltovskoy *et al.*, 2003). Radiolarians may be abundant near the coast, especially in narrow shelf regions, while their preferred depth tends to be near the upper part of the water column (Boltovskoy *et al.*, 1993, 1996; Boltovskoy, 1998, 1999; Zasko, 2000, 2004; Zasko and Vedernikov, 2003; Bjørklund and Kruglikova, 2003; Afanasieva and Amon, 2004b). Approaches to the biogeography of radiolarians are very often oversimplified, when only the direct influence of physical-chemical parameters of the environment on their distribution is taken into account. Apart from the direct influence of abiotic factors of the environment, the distribution and abundance of radiolarians is very much affected by biotic factors, especially the state of the food resources and symbiosis with algae, competition with other groups of protists, reproduction patterns, type and abundance of predators feeding on radiolarians, etc.

Geologists, using data and results of radiolarian analysis in paleogeographic, paleoceanographic, paleotectonic, and other reconstructions, often make an involuntary error when they consider radiolarians to be an ordinary paleontological group, without making a distinction between them and foraminifers, conodonts, ammonoids, brachiopods, etc. However, the taphonomy and fossilization of radiolarian remains distinguish this group from many others. One of the major distinctive features is that radiolarians are not normally represented by a few specimens in biocenoses, thanato-

cenoses, and taphocenoses. Therefore, when the presence of radiolarians in sedimentary rocks is mentioned, it should be taken into account that a whole fossilized community was not represented by a few specimens of radiolarians preserved, as sometimes may be suggested from some poorly preserved specimens, but an infinitely large number of individuals constituting the population in their lifetime.

ECOLOGY OF RADIOLARIANS

Polycystine radiolarians are marine planktonic protists with a siliceous skeleton, typically pelagic organisms, very scarce or absent altogether in coastal waters, especially where salinity drops below normal open-ocean values (Kling, 1978; Anderson, 1983; Caron and Swanberg, 1990; Anderson *et al.*, 2002). Close to the coast they may occur in sizable numbers in locations where the continental shelf is very narrow and oceanic waters impinge on the shore (Beers and Stewart, 1969, 1971), or in very special environments, like some Norwegian fjords (Swanberg and Bjørklund, 1987, 1992), yet almost invariably at salinities above 30 PSU (but see below). Polycystines have been found neither in landlocked seas (Black and Caspian Seas), nor in marginal seas with low salinity, such as the White and Baltic seas (Kruglikova, 1995).

Based on the data on the distribution of modern radiolarians in the water and the surface sediments of the oceans, oceanic and neritic groups of radiolarian species are usually recognized (Petrushevskaya, 1966, 1981a, 1986; Kruglikova, 1966, 1989a, 1990; Kruglikova and Maksimova, 1973; McMillen, 1979; Palmer, 1986; Nishimura *et al.*, 1997). It is believed that the taxonomic diversity and bioproduction of oceanic radiolarians are higher than those of neritic radiolarian associations in the shelf waters and, especially, than those of coastal species.

However, so-called neritic associations are, in most cases, impoverished assemblages due to inadequate conditions. The number of specimens and species of radiolarians decreases in the direction to the coast. From this point of view, radiolarians are similar to foraminifers in that they do not have (or have only one or two) truly neritic species, like those that can be found in many other zooplanktonic groups (Boltovskoy, 1999).

The vertical and horizontal distribution of radiolarians in the body of water is determined by a set of biotic and abiotic factors.

Biotic Factors

The main biotic factors directly affecting the life of an organism and patterns of its distribution in the water are feeding of radiolarians and their symbiosis with algae.

Feeding. Seasonal fluctuations of radiolarian populations may be determined by seasonal changes in the number of organisms serving as the food basis for radiolarians. Anderson *et al.* (1989b) showed that the main food of discoidal radiolarians is bacteria (1–3 μm in size). Rarely do food vacuoles of radiolarians contain any larger organic material. In contrast, nassellarians, collected in the same place, preferred to feed on nannoplankton (5–10 μm), including cells of phytoplankton. These differences in the preferred food decrease the competition for food resources between different taxonomic groups of radiolarians in the same water mass.

There is a direct connection between the fluctuations of the seasonal concentration of cyanobacteria, which are the main food of the radiolarians *Spongaster tetras tetras*, and the concentrations of this species in the water. The optimal physical-chemical parameters in the waters of Barbados occur in early spring (March–April), at the beginning of summer (June–July), and at the end of summer (August). A peak of concentrations of cyanobacteria is recorded in July, and the highest density of radiolarian populations is also registered in July: on average 37.8 specimens per m^3. There is a distinct positive correlation between seasonal changes in the abundance of phytoplankton and changes in the abundance of radiolarians (Boltovskoy *et al.*, 1993).

In addition, it is necessary to emphasize that, despite the fact that many species possess symbionts, radiolarians are mainly heterotrophic organisms, and, what is more, active predators. They have several behavioral strategies in feeding. For instance, the observations of *Pseudocubus obeliscus* from the subfamily Plagiacanthinae catching its food (microflagellates 2–3 μm in size) showed that radiolarians have seven periods of hunting activity in one hour, while the intervals between these acts of hunting are on average nine minutes (Matsuoka, 2003). The main food of radiolarians includes bacteria, unicellular algae, ciliates, various growth stages of copepods, larvae, and other living or dead microscopic objects. Therefore, judging from the trophic relationships, it is clear that, when radiolarians have a peak in abundance above the pycnocline in the well-illuminated environment, their main food includes microalgae, ciliates, and bacteria. When the peak of the abundance of radiolarians is observed below the pycnocline in the poorly lit water, the main food includes animals and dead remains of algae (Zasko and Vedernikov, 2003; Zasko, 2004). The oligotrophic central zones of oceans (Fig. 53), which have an insufficient biomass and productivity of phytoplankton, are regions not suitable for plankton in general and radiolarians in particular. Only colonial radiolarians with symbionts are abundant is this oligotrophic environment (Caron and Swanberg, 1990).

Symbiosis with algae. Radiolarians normally have symbionts. The presence or absence of symbiotic unicellular Peridinea, Cryptomonadinae, and other microorganisms, which are dependent on daylight, is different in acantharians and polycystines. This influences the vertical distribution of these microorganisms in the

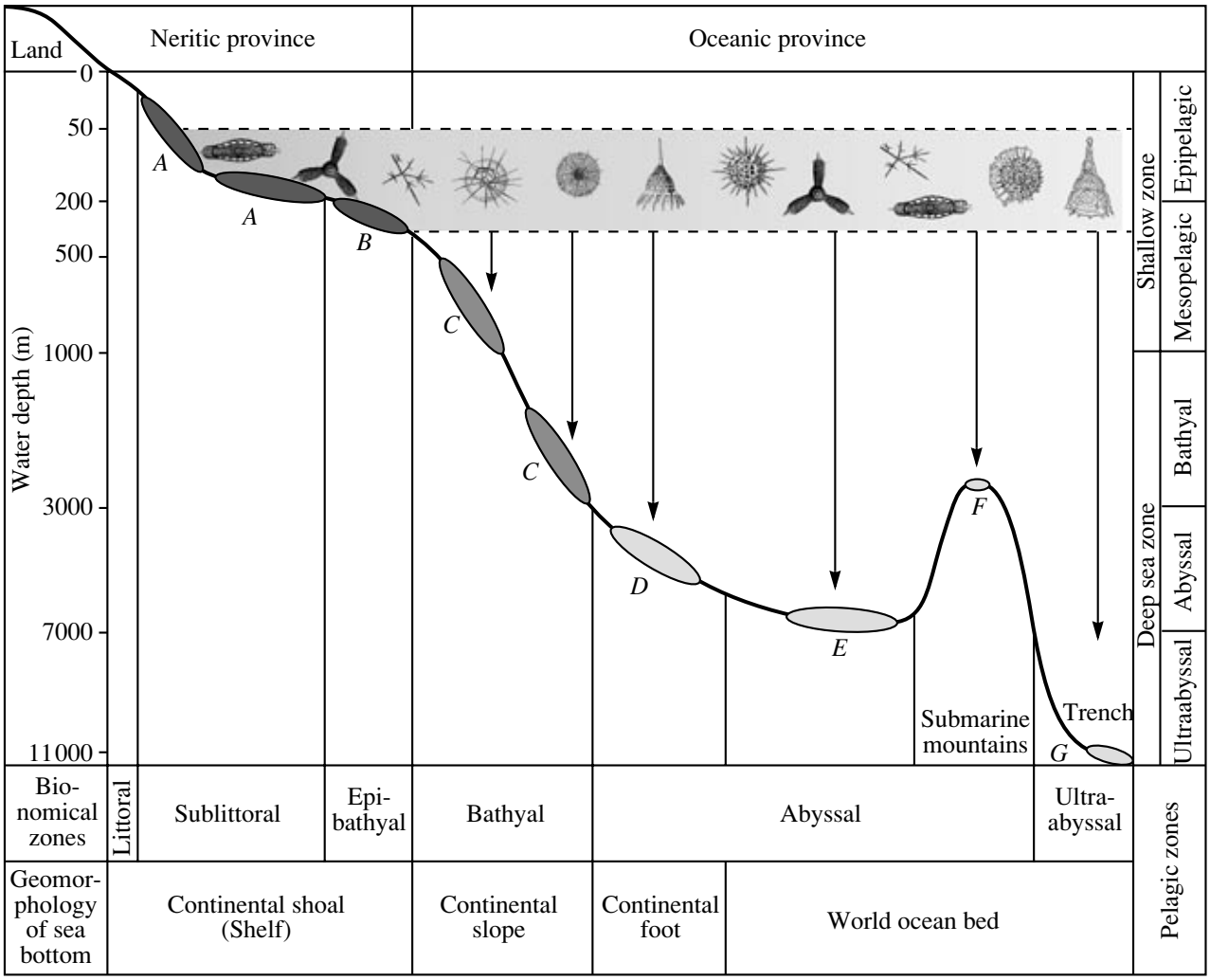

Fig. 53. Vertical zonation of the oceans and open seas and radiolarian taphocenosis (*A*–*G*); the interval of the water column with maximum bioproductivity of radiolarians is indicated by the color. No scale intended.

water and development of maxima of biomass at different depths. In many cases, radiolarians are in symbiotic relationships with the microalgae-dinoflagellate *Scrippsiella nutricula* (Gast and Caron, 2001). Symbionts play an important role in providing the host organism (a radiolarian) with nutrients in unfavorable conditions, e.g., in the oligotrophic oceanic water. Even the reproductive cycle of symbionts is calibrated to match the time of subdivision of the radiolarian cell (Swanberg, 1979; Petrushevskaya, 1986).

A comparison of the vertical distribution of chlorophyll and the biomass of radiolarians suggests that the maxima of the biomass of the collodarian colonies in the subsurface water and of acantharians, mainly living at the depths up to 50–75 m, are related to the higher light optimum of the photosynthesis of zooxanthellae (A), contained in the cell cytoplasm (Fig. 54) (Strelkov and Reshetnyak, 1971; Anderson and Matsuoka, 1992; Zasko, 2004).

Radiolarians of the superclass Phaeodaria, living at depths of over 100–200 m, do not contain zooxanthellae (Reshetnyak, 1966; Zasko, 2004).

Possibly, the main mass of radiolarians of the superclass Polycystina are better adapted to poor light because of the relatively low content of zooxanthellae compared to polycystine radiolarians of the class Collodaria and members of the phylum Acantharia (Zasko, 2004). But, on the other hand, modern studies showed that the maximum biomass of plankton, in particular, polycystine radiolarians is achieved at the depth of 75–100 m.

At this depth, zooplankton feeds at night on intensely producing phytoplankton. Many (if not most) zooplanktonic organisms migrate vertically, ascending during the night (for grazing) and descending in the daytime. One of the alleged reasons for such migrations is precisely the fact that zooplankton tends to avoid layers where the phytoplankton is metabolically active (that is, in the photic strata), because algae secrete substances that are toxic to animals in order to mitigate grazing.

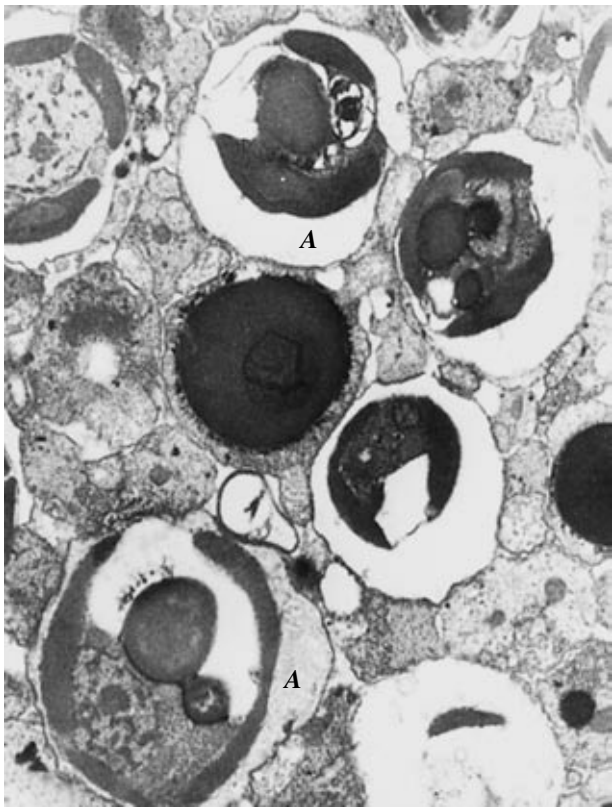

Fig. 54. Morphology and thin cytoplasmatic structure of *Dictyocoryne truncatum.* General appearance of microalgae (*A*) inside intracapsular vacuoles, ×7200; after Anderson and Matsuoka, 1992, text-figs. 1–4 (3).

Polycystine radiolarians reach the maximum abundance at the depth of 150–400 m. Vertical profiles of total radiolarian abundance in tropical and subtropical waters indicate that the bulk of their populations are usually located in the upper 50–100 m (Petrushevskaya, 1971; Renz, 1976; Kling, 1979; Dworetzky and Morley, 1987; Kling and Boltovskoy, 1995; Abelmann and Gowing, 1997). Quite often several discrete maxima are recorded, one at or near the surface, and a second one between 50 and 100 m (Petrushevskaya, 1971; Kling and Boltovskoy, 1995). In the Antarctic, however, peak abundances seem to be associated with the Warm Deep Water and occur deeper, at 200–400 m (Petrushevskaya, 1967; Boltovskoy and Alder, 1992; Abelmann and Gowing, 1997).

The study of the total biomass of radiolarians at various depths in the waters of the Sargasso Sea showed that the maximum biomass of radiolarians (2.6 mg/m^3) is at a depth of 150 m (Michaels *et al.*, 1990), which is a well lit photic zone.

There are interesting data on the symbiosis of microalgae with radiolarians and other sarcodines in the surface waters of the Sargasso Sea near Bermuda (Caron *et al.*, 1995). Twice a year, in different seasons, the tempo of the primary bioproductivity of the symbiotic algae and coefficients of the biomass of the symbionts in a cell of the host in various Acantharia, Radiolaria, Foraminifera were estimated. It was shown that Acantharia have the lowest coefficients of the biomass of symbionts, while solitary and colonial Radiolaria showed the highest coefficient. Algae of over 70 μm in size make the highest input in the total primary production of symbionts (8–67%).

It is noteworthy that different groups of pelagic sarcodines prefer different groups of symbionts. For instance, dinoflagellates symbiotic with radiolarians are considerably taxonomically different from dinoflagellates associated with benthic foraminifers, and even more so with planktonic foraminifers (Gast and Caron, 2001).

The reproduction of algae inside the host organism does not change seasonally, as was observed in the surrounding "wild" area, and this is probably one of the benefits that algae get from this symbiosis with radiolarians. On the other hand, radiolarians and other sarcodines may benefit from the symbiosis with algae because algae contribute considerably to the budget of carbon in the host organism (up to 80%) (Caron *et al.*, 1995). The algae mainly produce carbon (fixation of dissolved CO_2). The animals (and the algae) utilize these organic substances with carbon for their metabolism.

The symbiosis of radiolarians and microscopic algae may be related not only to the carbon budget of the radiolarians, but also to the use of algae as food. The study of living radiolarians *Didymocyrtis tetrathalamus tetrathalamus* caught near Barbados showed that the food vacuoles contain many diatoms, other algae, eubacteria, microflagellates, and, what is particularly important, the cytoplasm of microautotrophs, i.e., algae lacking tests (Anderson *et al.*, 1990a).

The laboratory study of the cytoplasmic structure of *Dictyocoryne truncatum* and microalgae inside the intracapsular vacuoles (Fig. 54) confirmed that radiolarians use symbionts as a reserve food source in unfavorable environments. Living radiolarians caught near Barbados 2 km west of the port of Holetown were kept in special tanks, in which the temperature, salinity, and light were changed (Anderson and Matsuoka, 1992).

In addition, in the opinion of Anderson *et al.* (1990a), radiolarians may use the organogenic opal of diatoms as a source of silica to form their own skeleton, especially in unfavorable environments with a silica deficiency. This significantly increases the radiolarians' ability to adapt and their resistance to unfavorable environments. Outside the photic zone, diatoms cannot exist because their photosynthesis requires light. Hence, the aphotic zone is not suitable for radiolarians with symbionts.

Takahashi (1991) suggested that radiolarians and diatoms compete for the source of natural SiO_2 dissolved in water. Therefore, in the Neogene Paleoantarctic ocean, some of the radiolarian communities are adapted to live in subsurface water layers using microalgae as symbionts and feeding on diatoms, while others moved to

deeper poorly lit water, where the role of diatoms as competitors is much lower (Lazarus, 2002).

In addition, according to Harper and Knoll (1975), the loss in weight of skeletons of radiolarians, observed in the Cenozoic, is a consequence of the increasing role of diatoms in the circulation of silica beginning from the end of the Mesozoic.

Abiotic Factors

Among the most important abiotic environmental factors affecting the geographic distribution, density of population, bioproductivity, adaptive potential, and, eventually, the distribution of radiolarians in facies, the following factors may be recognized:

(1) temperature and density of water;

(2) salinity;

(3) dynamics of water masses (currents, upwelling, uprising of the deep water);

(4) depth of the basin and distribution of radiolarians in the water column;

(5) light penetration;

(6) climatic zones;

(7) rifts, aulacogens and deep faults;

(8) influx of silica in the sea water;

(9) deposition of silica.

Four main hydrographic barriers restricting the distribution and affecting the population dynamics of radiolarians are usually considered (in diminishing order of importance): temperature, salinity, hydrodynamics, and depth (Chuvashov *et al.*, 1999). The light penetration and climatic zones have a particular influence on the distribution of radiolarians. In addition, radiolarians require natural SiO_2, which they extract directly from the sea water as ions of ortho-siliceous acid. And, eventually, the development of the zones of the increased bioproductivity of radiolarians is controlled by the tectonic factors (aulacogens and deep fault).

Temperature and density of water. Generally, the density of water is in inverse proportion to the temperature, although other factors also influence it. In oceanic conditions, there are some reasons why changes in temperature can engender changes in radiolarian assemblages. In many areas, changes in temperature are associated with changes in the local influence of different currents and water masses, each having its own characteristic radiolarian assemblage. Thus, when one is sampling a fixed near location, changes in temperature involve changes in the prevailing currents, which in turn bring different assemblages to the site sampled.

The change in temperatures differently affects the bioproductivity and species diversity of radiolarians.

Firstly, the cold water environment and the insufficient light penetration in particular, which occurs at great depths, cause a sharp decrease in the population number of tropical radiolarians. At the temperatures of about 15°C or below, the axopodia in thermophilic radiolarians contract, are aggregated together, and loose the ability to capture and transport food particles. Very few individuals are capable of reproduction by cell division at a temperature of 15°C and completely lose their reproductive function at a temperature 10°C (Anderson *et al.*, 1989a, 1989b, 1989c).

Secondly, changes in temperature (both increase and decrease) result in changes in the taxonomic composition of assemblages. Some groups of species disappear completely, while others become sharply reduced in numbers, a third group are resistant and indifferent, and a fourth sharply increase their numbers and productivity (Kruglikova, 1990; Matul, 1994a, 1994b). Radiolarian assemblages acquire cold water, warm water, and intermediate aspects corresponding to the Arctic–Boreal, Tropical, Equatorial, and Antarctic zones of ocean (Petrushevskaya, 1986; Kruglikova, 1990).

It is usually believed that the maximum density of radiolarian populations and the largest species diversity occur in warm waters of the equatorial and subequatorial zones of the ocean.

In the central part of the Pacific, a thermocline, i.e., a sharp change in the density and temperature of water (increase in density and decrease in temperature), is recorded at a depth of 70–140 m. At the same depth, the concentration and species diversity of radiolarians sharply decreases (Petrushevskaya, 1986). The pattern described may be somewhat distorted in the upwelling zones, e.g., in the waters of the Peruvian–Chilean intense upwelling, where accumulations of radiolarians are found above and below the thermocline (Kruglikova, 1990).

However, in some cases, a sharp change in temperature or a decrease in the mean annual temperature of the water does not always result in a decrease in number and productivity of radiolarians. For instance, in the Pacific in the basins of South Californian Current, the thermocline layer occurs at a depth of 80 m, but the decrease in diversity of radiolarians begins from a depth of 25 m (Kling and Boltovskoy, 1995).

In addition, seasonal fluctuations of temperature and environment should be taken into account. For instance, Takahashi (1991, 1994) studied the dynamics of the changes of the productivity of populations of modern radiolarians during one year in the basins of high and low latitudes (Gulf of Alaska, Bering Sea, Arabian Sea) and showed relationships between the changes in productivity and seasonal environmental changes (*Lithomelissa setosa* is a "spring" taxon in the Gulf of Alaska, etc.). Takahashi suggested that the seasonal fluctuations of productivity induce significant changes in the composition ofbiocenoses, reflected in the paleontological record, and must be taken into account for paleogeographic reconstruction of the geological past.

Direct evidence of seasonal fluctuations of temperature are quite rarely preserved in the fossil record, and they can only be assumed (Boltovskoy, 1994). Seasonal

differences in bioproductivity, sedimentation, feeding, etc. of plankton may form such a taphocenosis which would tend to correspond to one particular season when the bioproductivity is highest, while the effect of predation is the lowest. The effect of the seasonal shifts in the fossil material is more distinct in higher latitudes. For instance, in the Antarctic Zone, in the Weddell and Scotia seas, more than 80–90% of the total annual radiolarian productivity is restricted to a short period when the water is free of ice, which may be one or two months (Abelmann, 1992). It is shown that diatoms in the sediments of the fjords of British Columbia in Canada are poor indicators of planktonic floras, since because of the seasonal changes in bioproductivity they are almost completely eaten by the dominant zooplankton (Sancetta, 1989). However, in the tropics, seasonal changes in plankton are often too insignificant (Boltovskoy *et al.*, 1993; Boltovskoy, 1994). Comparing different groups of fossil plankton, autotrophic organisms will be more affected by seasonal changes than heterotrophs because of the differences in the life cycles. Coccolithophorids, diatoms, and silicoflagellates have much higher reproductive rates than foraminifers and radiolarians. Thus, changes in their bioproductivity in response to short-term seasonal ecological changes fluctuate widely. For instance, in the Subarctic Zone of the Pacific in the period between September 1982 and September 1983, the ratio between the maximum and minimum of polycystines was 1 : 6, while for silicoflagellates and diatoms (in the same samples at the same stations), this ratio was 1 : 15 and 1 : 41, respectively (Takahashi's data cited from Boltovskoy, 1994).

Fluctuations in the number of diatoms in the eastern equatorial Atlantic, calculated in the period of a complete year, have a considerable range of differences (over 100 times) between the highest and the lowest seasons in bioproductivity, while the maximum of the number of polycystines (at the same station) was only nine times higher than the minimum (Boltovskoy *et al.*, 1993).

All these factors suggest that, while phytoplankton is more sensitive to changes in the environment in the uppermost, subsurface layers of the ocean, the zooplankton association smoothens and levels the ecological differences in the entire water column. Thus, phytoplankton is constantly so rigidly controlled by the environment that it immediately responds to even the slightest changes (with large deviations from the mean annual value). These deviations are absent, or at least less clearly developed in zooplankton, for which the response to the change in the ecological situation in most cases is similar to the mean annual value. For instance, if the environment suddenly improves for a short time (one–two months), phytoplankton immediately responds to this change, and this response will eventually be reflected in the bottom sediments by a sharp change contrasting to the normal, statistically average situation in the water column. Because zooplankton is less sensitive to changes in the environment, its response to the change in the ecological situation will also be recorded in the bottom sediment, but it will be less marked (Boltovskoy *et al.*, 1993).

At the same time, there is evidence of the direct influence of temperature on biodiversity and productivity of radiolarians.

Nishimura *et al.* (1997) published well documented evidence of that the shallowest assemblages in the coastal zones of Antarctic are considerably impoverished compared to neritic assemblages. The analyses included Late Pleistocene radiolarians from the bottom sediments collected along the 60th parallel in the region of the South Orkney Islands, South Shetland Islands in basins of the Ross Sea, Dumont d'Urville Sea, etc. It was established that radiolarian associations in the shallowest coastal zone much, ten times, poorer than neritic associations. The coastal association is represented by only two species, while the neritic association is composed of more than 70 species. This phenomenon is explained by the fact that the coastal shallow-water zone was affected by the seasonal summer development of the ice shield.

A similar drop in the number and productivity of radiolarians occurred in the North Atlantic 17–12 thousand years ago and was related to very low temperatures because of the complete ice coverage of this region (Matul, 1994a). In this environment, only those radiolarian species could survive which were most resistant to the low temperatures and deficiency of phytoplankton associated with the low light penetration caused by the ice cover.

Matul (1994a, 1994b) published interesting data on that, in one of the regions of the North Atlantic in the interval of the Late Wurm Stadial, there are several levels of increase in absolute concentration of radiolarian skeletons in sediments, with the maximum concentrations at the level of *minimal* temperatures. This phenomenon is also explained by the position of the studied zone with the largest concentration of radiolarians in the Upper Wurm sediment near the zone affected by the Pra-Gulf Stream.

Salinity. Radiolarians inhabit the basins with normal oceanic or marine salinity 30–32–38–40 PSU and are rarely found when the salinity is below 30–32 PSU, being intolerant to the falls in salinity. At the same time, quiet coastal basins, such as reef lagoons, closed bays and fjords, and estuaries of large rivers are of special interest.

Radiolarian populations living in the large fjords of Norway (Sognefjord, Handangerfjord, region of Tromsø), are considerably different taxonomically and morphologically from populations inhabiting the same latitudes in the neritic region of the North Atlantic (Swanberg, Bjørklund, 1992; Bjørklund and Ciesielski, 1994; Kruglikova and Bjørklund, 1995; Cortese and Bjørklund, 1995). The total taxonomic diversity of radiolarians decreases in fjords. In assemblages from the sediments of fjords, Spumellaria quantitatively dominate over Nassellaria. Among the Nassellaria, Pla-

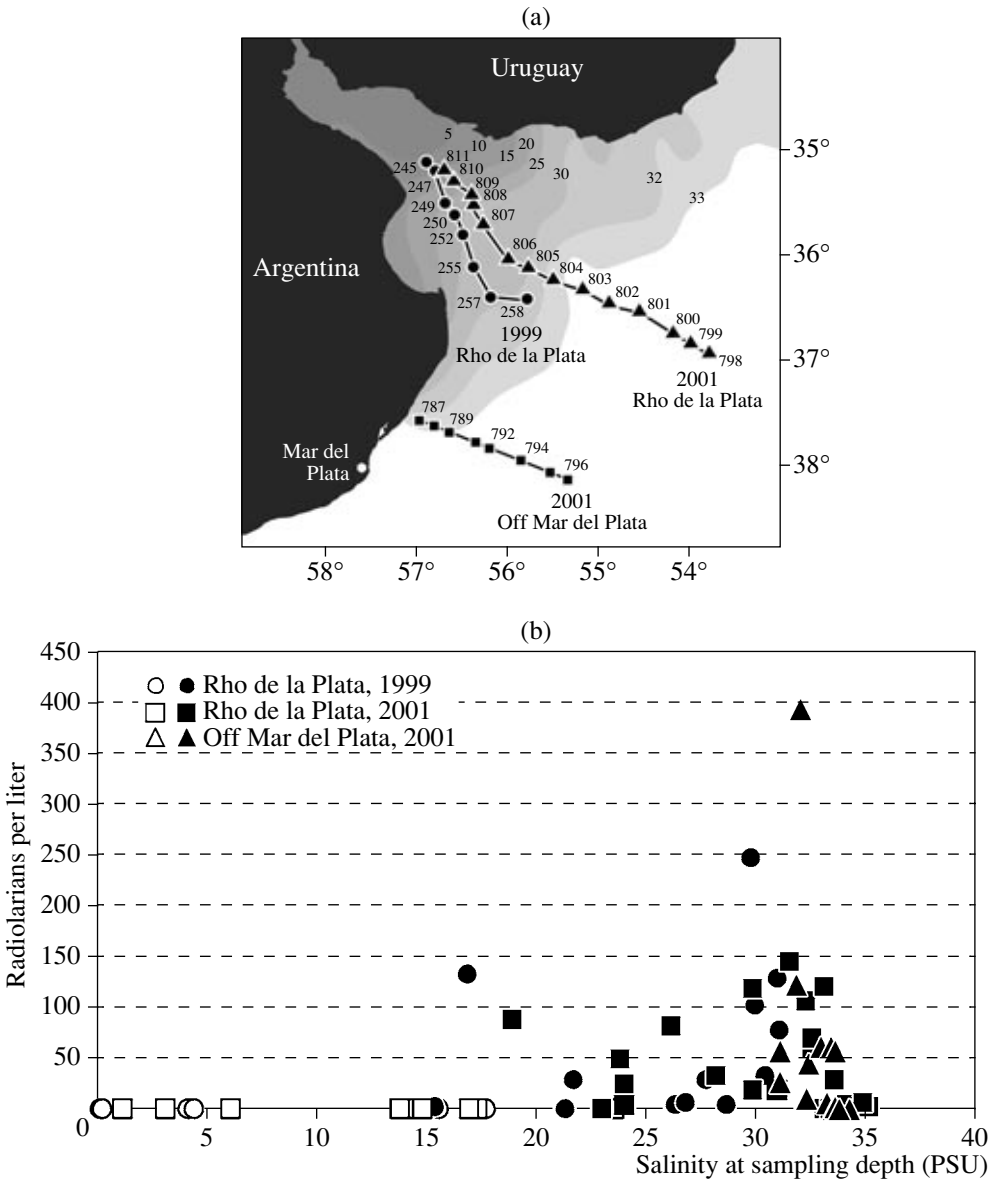

Fig. 55. Radiolarians and salinity in the estuaries of the Rio de la Plata and in the coastal basins of the southern Atlantic Region: (a) stations of the sampling of the surface and bottom probes in the profiles, 1999, 2001; (b) density of radiolarian populations (number of living cells per liter of water); empty symbols indicate zero number of radiolarians (absence); light gray and dark gray symbols designate the isohaline points (after Boltovskoy *et al.*, 2003).

giacanthidae and Eucyrtidiidae make up to 70–95%. Some radiolarian groups sharply decrease in number (e.g., species of the order Spyridinata), while the shells of some species of the family Actinommidae become very large. Possibly, among other environmental factors responsible for the inhabitancy by radiolarians of basins of fjords, one of the most important was the factor of the abundance of food in the water (Cortese and Bjørklund, 1995), resembling the situation in the upwelling zones, in particular, the upwelling near South Africa (Kruglikova and Bjørklund, 1995).

Interesting data were recently published by Boltovskoy *et al.* (2003) in the distribution of radiolarians in estuaries of the Rio de la Plata on the Atlantic coast of South America, one of the largest rivers on Earth (Fig. 55). The estuary of the Rio de la Plata is inhabited by the monotaxonic radiolarian assemblage, represented by a single nassellarian species, *Lophophaena rioplatensis.* The density of populations reaches fantastic figures, largest of presently known: 248 specimens per liter in the estuary and 394 specimens per liter in more open basin. For comparison, the average density of population of radiolarians in the open ocean is as follows: in South Atlantic, 1–2 specimens per liter (Boltovskoy, 1998); in North Atlantic, 0.075–0.17 specimens per liter (Boltovskoy, 1998), 0.075 specimens per

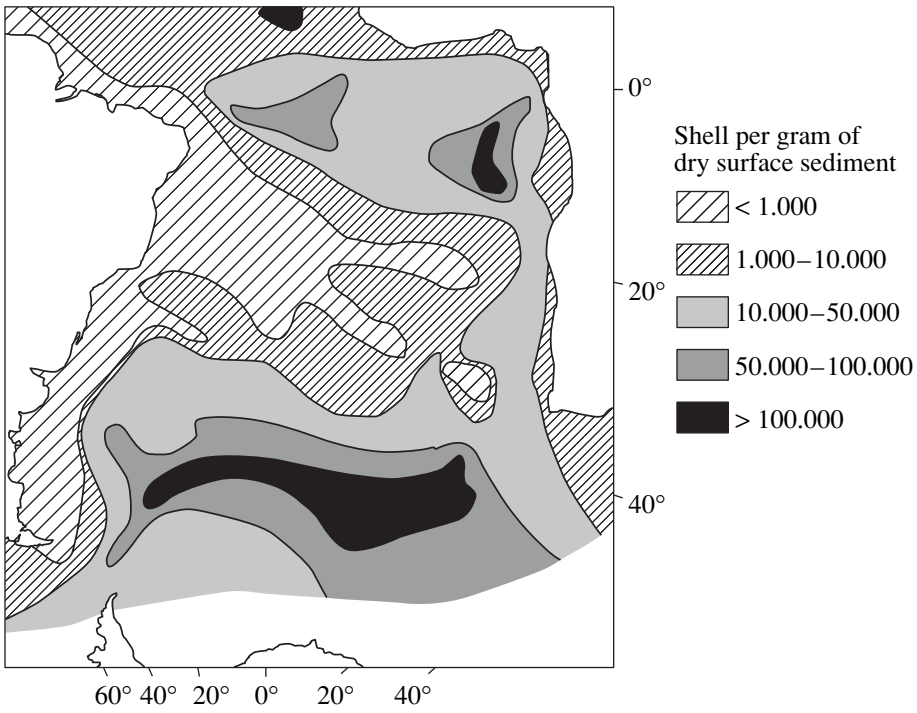

Fig. 56. Bioproductivity and density of radiolarian populations in the southern Atlantic Region (after Boltovskoy, 1999).

liter (nassellarians), or 0.170 specimens per liter (spumellarians) (Zasko, 2000).

The estuary of the Rio de la Plata is cut deep into the South American continent at the latitude of about 35–38° S for a distance of 320 km, being 230 km wide and forming a semiclosed interior system with reduced salinity.

The depth of the estuary ranges from 5 to 15 m, while the depth of the coastal zones of the ocean reaches 150–180 m. Radiolarians are found in the estuary up to a distance of 100 km from the coast. The maximum density of population in the ocean is recorded at a distance of 20 km from the coast. In the estuaries, radiolarians live at salinity of 17–30 PSU, and the density of population sharply decreases toward normal oceanic salinity (above 30.5–31 PSU). Hence, according to Boltovskoy *et al.* (2003), radiolarians in general should not be only connected with open sea environments. It is noteworthy that a similar pattern of the appearance of monospecific assemblages of nannoplankton and diatoms, accounted for by the catastrophic change in salinity, was observed in the Eastern Paratethys (Taman Peninsula of the Black Sea, western Ciscaucasia) in the Middle–Late Miocene (Golovina and Radionova, 2003).

The above data on Recent radiolarians suggest that, in some cases, when the coastline contained very large numbers of closed and semiclosed bays, fjords, and estuaries, sediments of the coastal and estuarial zones could have contained peculiar oryctocenoses of radiolarians.

Thus, the maximum radiolarian abundance often depends on the general trophic status of the area, rather than on temperature or (within certain limits) distance from the coast. Where primary production is higher there is more zooplankton in general and radiolarians in particular, and vice versa. While assemblages are chiefly qualitatively governed by temperature, they are quantitatively (density) governed by food.

Dynamics of water masses. The maximum productivity of radiolarians is usually considered to be found in the neritic and central zones of the ocean.

Radiolarians are thought to avoid shallow water zones with high water turbulence (tidal, wavy, stormy-wave, and other activities). Their population usually decreases sharply toward the coastline. Even in regions with an intense coastal upwelling "The maximum population number of radiolarians is found further out to sea from the zone of divergence or upwelling" (Kruglikova, 1990, p. 94).

Currents. Systems of currents, including coastal currents, significantly affect the distribution of radiolarians in different bionomic zones of the ocean (Fig. 53). Currents play a double role: on the one hand, they facilitate the influx of nutrients, mixing of water and aeration, and, on the other hand, transport radiolarian plankton for great distances, enabling the inhabitation of new zones of the basins (Amon, 2003).

In the southern South Atlantic, the maximum density of population is connected to the Subantarctic and Guinean currents (Fig. 56). The lowest concentrations

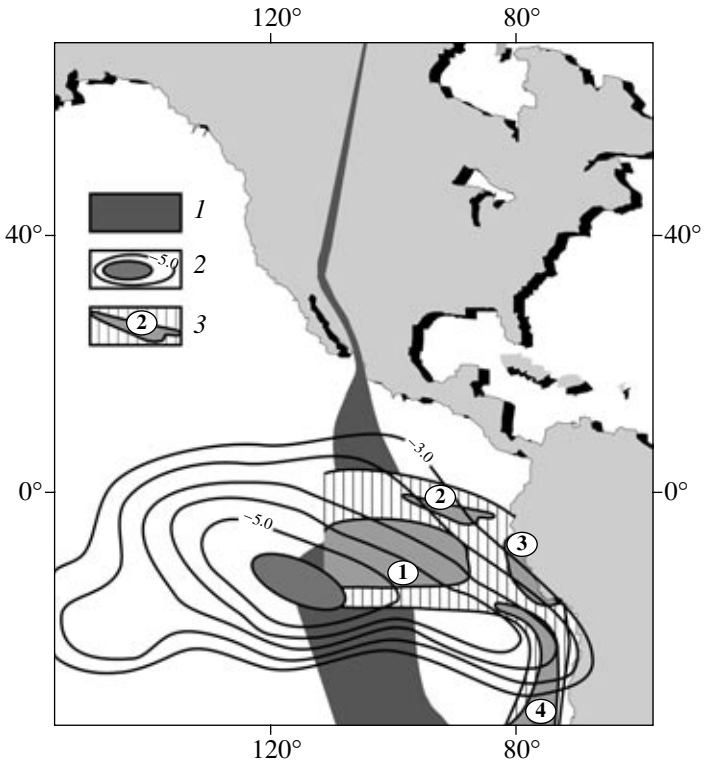

Fig. 57. Rift, ozone anomaly and radiolarians of the eastern Pacific: (*1*) elements of the eastern Pacific rift belt (after Syvorotkin, 1994); (*2*) center of the ozone anomaly above the East Pacific Uplift in January, 1998 (satellite data processed at the Central Aerogeological Laboratory, Dolporudnyi, Moscow Region; after Syvorotkin, 1998); (*3*) distribution of radiolarians in the subtropical and equatorial surface sediments of the eastern Pacific (after Molina-Cruz, 1977): (**1**) *Subtropical Assemblage*, related to the subtropical surface water mass and South Equatorial Current; (**2**) *Equatorial Undercurrent Assemblage*, related to a decrease in the trade winds and South Equatorial Current, the El Nino events; and (**3**) *Peru Current Assemblage* related to the coastal upwelling of Peru; and (**4**) *Chile Current Assemblage* related to the temperature of water in the northern part of the Chile Current.

of radiolarians were established in the regions of the Central circulation of the South Atlantic (Fig. 56) (Goll and Bjørklund, 1974).

In the profile between the Antarctic and the point with coordinates of approximately 30° S, 10° E (near Namibia), Abelmann and Gowing (1997) recorded the highest density of population at the depth of 100–300 m in the Antarctic waters, and at the depth of 0–150 m in Subantarctic water (up to 0.3 specimens per liter, but these values are underestimates). In the southwestern Atlantic (30–60° S, 55° W), surface waters (depth 5–15 m) contained radiolarians with a mean concentration of 0.5 specimens per liter, and a maximum concentration of up to three specimens per liter (Boltovskoy and Alder, 1992).

The development of the bottom assemblage of radiolarians (thanatocenosis) is strongly influenced by the lateral influx of dead organisms by currents and the dissolving of some dead organisms (including both soft organic and biomineral organelles of cells) during their deposition or transport by water convection (Kruglikova, 1981, 1984; Petrushevskaya, 1966, 1981a, 1986).

At the same time, the effect of lateral transport is sometimes overestimated (e.g., by Khudyaev (1931) who suggested that radiolarians were transported for great distances from the oceanic depths of the Paleoatlantic to the shallow water bays of the Valanginian Sea in the eastern margin of the Russian Platform).

Upwelling. In some cases, a steep continental slope enables the development of a coastal upwelling. Combined with feeding, the upwelling results in the outburst of the number of radiolarians and other planktonic fauna, as observed in modern Californian, Peruvian–Chilean (Fig. 57), Angola, and Somalia upwellings.

The highest density of population of polycystines in the South Atlantic is found in the zones of coastal upwelling near the African coast (Abelmann and Gowing, 1997) and in the system of equatorial currents (Boltovskoy *et al.*, 1996). Observations of foraminifers and radiolarians in the upwelling zone of the Somalia Basin in the last 160 000 years showed that the upwelling has a considerable effect on the quantity of organisms (Anderson *et al.*, 1990b; Venec-Peyre *et al.*, 1995, Vernaud-Grazzini and Caulet, 1995; Boltovskoy, 1998, 1999).

The role of upwelling in the biogeography of radiolarians is large, although the mechanism of the upwelling should not be always used to explain the

increased bioproductivity of radiolarians and other zoo- and phytoplankton.

For instance, Riegraf (1995), based on the high percentage of planktonic foraminifers, radiolarians, and spicules of sponges in the deposits of distal turbidites in a systems of grabens in the Campanian of Westphalia, concluded that an upwelling existed in this paleobasin. However, the actual paleodepths in the environment of distal turbidites were there approximately 200–600 m, hence, the existing of a true upwelling is doubtful.

New data suggest that the upwelling, as a hydrographic and hydrodynamic phenomenon, is not an obligatory condition for the appearance of zones of the sea with increased bioproductivity. For example, remarkable accumulations of phytoplankton biomass have been observed along coastal and open ocean fronts (Allanson *et al.*, 1981; Fukuchi and Tamura, 1982; Watanabe and Nakajima, 1982; Lutjeharms *et al.*, 1985; Taniguchi *et al.*, 1986; Brandini *et al.*, 2000) and in the vicinity of retreating pack-ice, due to the enhanced stability of the surface water layer from input of low salinity meltwater (Smith and Nelson, 1986), etc.

Handoh *et al.* (2003) reconstructed the evolution of the upwelling in South and North Atlantic based on five intervals (Recent, Early Eocene, Maastrichtian, Cenomanian, and Kimmeridgian) and concluded that the upwelling is not an obligatory independent condition for the accumulation organically enriched marine sediments. Most of the organically enriched sedimentary deposits formed in the above epochs, could only possibly be connected with the zones of upwelling.

Some periods of geological history show a maximum abundance of radiolarians in coastal basins of epicontinental basins, while more open sea regions contained fewer radiolarians.

In the Late Cretaceous Western Siberian Sea with depths up to several hundred meters, the maximum quantity and species diversity of radiolarians is observed in a zone of 200–300 km along the eastern slope of the Ural Mountains. In Transuralia, the number of radiolarian skeletons may be up to several tens of thousands (Kuznetsovskaya Formation) and more (radiolarites of the Zaikovskaya Formation) in a standard sample. Further to the east, in Western Siberia, i.e., at a considerable distance from the coastline, in the same intervals of the sections, the number of the specimens decreases several tens of times (Amon, 2000c, 2001).

The depth of the Carboniferous–Early Permian Ural Paleoocean did not exceed 1000 m. The highest numbers of radiolarians occur in the facies of thin flysch of the Ural Fore-Deep (100–150 km from the coastline), whereas the minimal numbers are recorded at the margin of the Russian Platform (200–250 km from the shore) (Chuvashov *et al.*, 1999; Amon, 1999; Afanasieva *et al.*, 2002). Note that the skeletons of radiolarians are present in the coarse flysch, i.e., the biotope of these microorganisms was very close to the coastline. In addition, radiolarians are found on the slope and even in the lagoon of the Early Permian reef Karachaganak in the northern Caspian Sea Region (Afanasieva *et al.*, 1986, 2002; Afanasieva, 1987; 2000a; Afanasieva and Zamilatskaya, 1993).

Radiolarians are especially abundant in the Upper Devonian Domanik Beds of the Timan–Pechora Region, where they formed extremely dense huge populations in the Frasnian. The biomass of these populations was so high that the organic material of dead radiolarians could be one of the sources of hydrocarbons for oil. The depth of Frasnian basins in this region was also not great (maximum 250 m), and they were a shallow western periphery of a developed Ural Paleoocean (Afanasieva, 2000a).

Upwelling is traditionally used to explain this phenomenon. However, the success of ancient radiolarians is attributable to different reasons, two of which were most important: (1) closeness of the shoreline and, hence, influx of nutrients from the land and (2) presence of permanent system of currents, precluding the development of stagnation.

In addition, the development of zones of increased bioproductivity is controlled by the tectonic factors: unique conditions develop above the zones of faults, which are a source of nutrients of endogenic origin (Syvorotkin, 1994, 1998; Afanasieva, 2000a).

Thus, in the Paleozoic and Mesozoic, the coastal areas of the seas and oceans were more favorable for living than the deeper central zones.

Uprising of the deep water. Apart from the coastal upwelling, the areas of the rising deep waters near the zones of oceanic convergence are also important. For instance, some workers suggest that about 75% of modern biogenic silica is accumulated in the deep water sediments of the Antarctic. The major planetary belt of modern siliceous sediments about 900–2000 km wide surrounds the Antarctic. The northern boundary of the belt coincides with the Antarctic convergence, whereas in the south, siliceous sediments are replaced by glacial-marine sediments. Over 75% of all oceanic silica is accumulated in this belt. Biogenic silica mainly represented by the skeletons of diatoms may constitute up to 70% of the total weight of sediments (Kennett, 1982). The rate of the deposition of silica in deep water regions to the south of Antarctic convergence is about 2×10^{-2} g/(cm · year). Strong winds blowing from the Antarctic and around it cause the rise of the water and move the surface water to the north. It is replaced by the uprising intermediate water, rich in nutrients, which favors the primary bioproductivity of phyto- and zooplankton, including radiolarians (Fig. 56).

In the equatorial regions, the divergence of the surface water, caused by the distributions of winds over the surface of the ocean near the geographic equator, results in the large uprising of water, causing the increase of biological productivity and increased accumulation of calcareous and siliceous sediments. There, radiolarians dominate in the siliceous sediments,

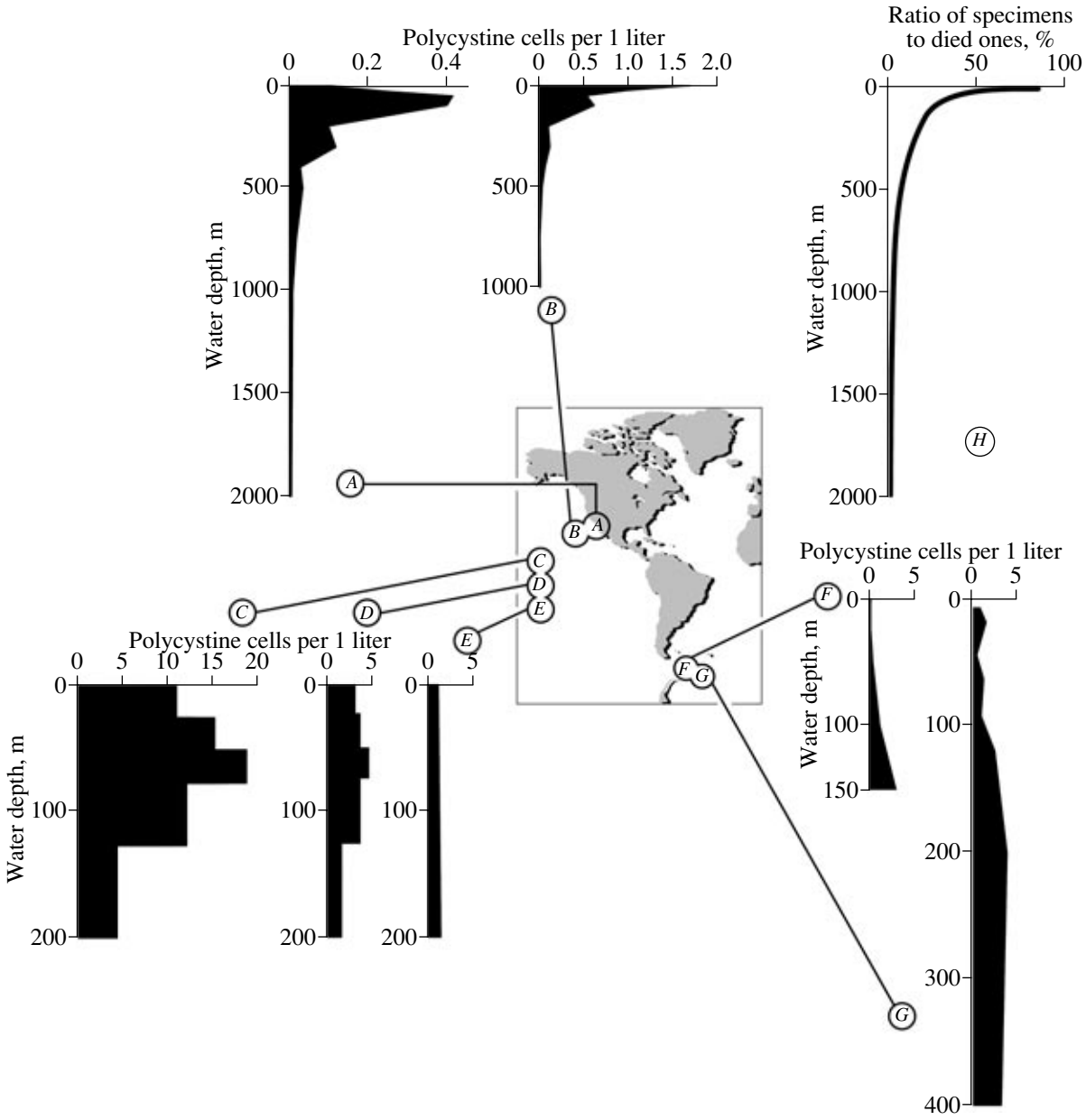

Fig. 58. Distribution of extant radiolarians (Polycystina) in the water column (after Boltovskoy, 1998): (*A*–*G*) quantitative vertical distribution of live polycystine radiolarians in different climatic zones in the water column (number of live individuals of polycystines per liter); (*H*) proportion of live individuals of polycystines to their skeletal remains, depending on depth, %.

although the sedimentation rate is much lower than in the higher southern latitudes (Kennett, 1982).

Depth of the basin and the distribution of radiolarians in the water column. Living radiolarians are found at all levels from the surface to the maximum depths of the oceans (Fig. 53), but they are most abundant in the horizon of 0–100, 0–150 m of the Tropical Realm, and in the horizon of 10–400 m of the Boreal Realm of the ocean (Petrushevskaya, 1986; Kruglikova, 1989b, 1990, 1993; Boltovskoy, 1998; Zasko, 2004).

The upper, well-illuminated layer of water (0–75 m) is mainly inhabited by acantharians. The phaeodarians occur from 100–200 m down to the deepest waters. The skeletons of Acantharia and most Phaeodaria are dissolved immediately after the death of the organisms, and very rarely they reach the sea bottom (Takahashi, 1981; Bernstein *et al.*, 1999).

Polycystina are most abundant in the interval of 50–400 m (Figs. 58*A*–58*G*) (Kling and Boltovskoy, 1995; Abelmann and Gowing, 1997; Boltovskoy, 1998, 1999). The siliceous skeletons of polycystine radiolarians are resistant to postmortem dissolution and are well-preserved in fossils. Hence, radiolarians are repre-

sented in the thanatocenoses, taphocenoses, and oryctocenoses mainly by polycystine radiolarians.

Often, the abundance of radiolarians is greatest in the uppermost surface water (Figs. 58*A*, 58*B*). However, sometimes, two peaks of abundance are seen in the vertical distribution of radiolarians: one near the surface, and the second in the interval between 50 and 100 m. In the Subantarctic water, a peak of abundance is shifted deeper, to the depths of 200–400 m (Boltovskoy, 1998).

Based on the vertical distribution of polycystine radiolarians in the Atlantic and Pacific oceans, four major groups were established (Petrushevskaya, 1986; Boltovskoy, 1998, 1999; Zasko, 2004):

(1) polycystines predominantly inhabiting the upper water layers 0–50 m above the pycnocline. However, they are often absent in this interval;

(2) polycystines mainly living in the water deeper than 50 m with a maximum abundance at 50–200 m depth;

(3) polycystines whose abundance is maximum below 200–300 m;

(4) a few polycystines, evenly distributed across the entire water column.

In addition, there is quite a number of records of radiolarians collected by planktonic nets in significantly deep waters (4000, 5000, 8000 m) (Khabakov *et al.*, 1959; Petrushevskaya, 1986). However, it was very rarely indicated whether these were *living* or *dead* radiolarians.

This information may lead to an erroneous conclusion that radiolarians inhabit the entire water column of the ocean, from the surface to the bottom, including very deep depressions. According to Boltovskoy *et al.* (1993), Kling and Boltovskoy (1995), Boltovskoy (1998), the number of living radiolarian cells sharply decreases at the depth over 500 m: 100% living cells in the upper layer of water, 50–60% at the depth of 100 m, 20–40% at the depth of 200 m, 10–20% at the depth of 500 m, 5% at the depth of 1000 m, while below the depth of 2000 m they are virtually absent (Fig. 58*H*).

The dominance of living radiolarians, according to Petrushevskaya (1966), Zasko (2000), and Abelmann and Goving (1997) is more than 90% at the depth of 100–200 m and not more than 70% in the interval of 300–500 m. However, it should be noted that estimates of the concentration of living radiolarians at the depth over 50–100 m are often too high, due to the fact that different methods to evaluate the living radiolarians are used by different workers (Boltovskoy *et al.*, 1993; Boltovskoy, 1998).

Complete vertical profiles of the abundance of radiolarians in tropical and subtropical areas show that a large proportion of their populations inhabit the upper 50–100 m of the water column (Kling, 1979; Kling and Boltovskoy, 1995; Abelmann and Gowing, 1997; Boltovskoy, 1998, 1999) (Fig. 58). Quite often, several discrete maxima are observed, with one on or near the surface, and the second, between 50 and 100 m (Petrushevskaya, 1966; Kling and Boltovskoy, 1995; Boltovskoy, 1998, 1999). In the Subantarctic, however, the maximum abundance is connected with warm deep waters, and it is fixed deep, at an interval of 200–400 m (Petrushevskaya, 1966; Abelmann and Gowing, 1997; Boltovskoy, 1998, 1999).

Many radiolarian species occupy discrete intervals in the water column. Kling and Boltovskoy (1995), based on a study of probes from planktonic catches in the upper 2000 m in the eastern subtropical Pacific established the following bathymetric groups, the distribution of which is restricted to certain water layers:

(1) the surface group with peaks of abundance only at the depth of 0, 25, or 50 m and bimodal species, distributed at the depth of 0 and 50 m, 0 and 100 m;

(2) the subsurface group with maximum abundance at 100 m of depth;

(3) the deepwater group with the maximum abundance at 200 and 300 m, and bimodal taxa, occurring at depths of 200 and 300 m;

(4) species that form peaks of abundance deeper than 300 m.

A similar depth zonation was also established by several other workers (Renz, 1976; Kling, 1979; Dworetzky and Morley, 1987). At the same time, a general scheme of the zonal distribution of radiolarians at certain depths may not be created based on the values of already known depths, because the distribution of radiolarian species is related to such water masses that move both vertically and laterally.

For instance, the same warm water association lives in the eastern subtropical Pacific in the coastal Californian waters and in a typical oceanic basin at the depth of 0–25 m. This association is moved to the oceanic region by the surface advection of the South Californian Circulation, but, at the same time, at half distance between these two basins (coastal and oceanic) the same depths are inhabited by noticeably different, colder water association connected with the cooler waters of the Californian Current (Kling and Boltovskoy, 1995). Many cold-water radiolarians, inhabiting the upper layers at higher latitudes, sink together with the host water masses and may be found at a greater depth at the middle and lower latitudes (Kling, 1978, 1979; Boltovskoy, 1988, 1999). *Siphocampe arachnea*, for instance, is a dominant component of the surface of the Pacific and Subarctic plankton. In the center of the northern North Pacific, this species reaches its maximum abundance at the depth of 100–300 m, while in the subtropical part of the eastern Pacific, it reaches it at the depth of 300–1000 m (Boltovskoy, 1994).

The distribution of radiolarians depthwise may be caused by different salinity at different water levels. Interesting data on the depthwise distribution of the extant and Pleistocene species *Cycladophora davisiana davisiana* are reported by Bjørklund and Ciesielski (1994).

It was shown that, in the Arctic and Greenland–Norwegian seas, radiolarians of this species are absent in subsurface waters and are most abundant in the layer of water 200–500 m below the surface of ice, which is explained by the seasonal melting of ice and, hence, by a decreased salinity in subsurface water layers. More so, these radiolarians use the bottom waters of the deepest fjords of Norway as a refuge and do not appear in the less saline upper layers.

Light penetration. The first data showing a close correlation between the illumination of different water layers and the distribution of radiolarians in the water column begin to appear. The facts published by Zasko in three studied regions in the epipelagial of the North Atlantic are very informative in this respect: (1) subarctic waters, (2) subtropical waters, and (3) waters of the intermediate zone between the subtropics and subarctic (Vinogradov *et al.*, 2003; Zasko and Vedernikov, 2003; Zasko, 2004). It was revealed that, in the upper layers of the water column (depth in the interval of 0–100–200 m), illumination and density stratification of the water are the most important abiotic factors affecting the vertical profiles of the radiolarian distribution, the first factor being more significant for radiolarians than the second.

In subtropical waters, the maximum biomass forms two peaks: above the pycnocline at illumination of more than 10% E_0 and below it, at illumination near 1% E_0. In the intermediate zone, the maximum mass of radiolarians was recorded near the lower boundary of the pycnocline, in the middle and upper layers of the euphotic zone.

The combined effect of salinity, temperature, and illumination was studied by Anderson *et al.* (1989a, 1989b, 1989c) in living radiolarians of the tropical *Spongaster tetras tetras* collected near Barbados and cultured in artificial laboratory media. Anderson *et al.* studied the effect of temperature, salinity, and illumination on the culture of this radiolarian species and showed the main patterns of influence of variations of the above factors on growth, increase in size of the skeletons, and on the primary production of organogenic opal. It was shown that the longest survival of radiolarian individuals in laboratory conditions and the optimal general growth and increase in the size of skeleton occurred at mean temperatures and high salinity (temperature 25.7°C, salinity 40 PSU). A decrease in temperature to 21°C and salinity to 30 PSU, or an increase in temperature to 33–36°C sharply (four–five times) decrease the rate of survival of radiolarians.

Climatic zones. Many papers report that the observations of the distribution of extant and Pleistocene radiolarians in the water and sediments of the ocean showed a clear climatic zonation in distribution of radiolarians (Petrushevskaya, 1986; Kruglikova, 1990; De Wever *et al.*, 1994, 2001). "The Arctic Boreal, Tropical, Equatorial, and Antarctic zones of the ocean are clearly distinguished by having sediments in which the abundance of radiolarians is different by several orders of magnitude" (Kruglikova, 1990, p. 93).

It is usually thought that each climatic zone has a particular generic and species composition of radiolarians. Three groups of taxa may be present among the genera and species of a climatic zone: *endemic* (taxa restricted to these particular water masses), *intermediate* (species occurring at the borders of the climatic zones), and *cosmopolitan* (species with global distribution) (Petrushevskaya, 1981a; Kruglikova, 1990).

Petrushevskaya (1981a, pp. 34–35) noted the zonal distribution of the species and emphasized that (1) tropical water is inhabited by the greatest number of nassellarian species; (2) considerable number of nassellarian species are characteristic of deep waters; (3) a group of species inhabits the transitional zones (amphiboreal, notal–boreal, bipolar); (4) only one species is endemic to the Arctic; and (5) there is a large group of species endemic to the Antarctic and Subantarctic. In another paper, Petrushevskaya (1986, pp. 76–85) distinguished between oceanic and neritic species. The oceanic species include (1) circumtropical (tropical or widely tropical, also equatorial and tropical–boreal, (2) species of moderate zones (bipolar, notal–boreal), (3) cosmopolitans (species restricted to the central zones of the ocean, absent from the shelf, live at large depths in the tropics, and even in the cold-water regions rarely approach the coast, and (4) Antarctic. Regarding neritic species, it was said that they are rarely found, and the composition of their assemblages is different from those of oceanic taxa.

According to Petrushevskaya, strict endemism in Recent radiolarians is difficult to recognize because of the lack of precise data on the geographical distribution of the radiolarian species, and the uncertain taxonomy of many groups. From this point of view, the zonation of the ocean on the basis of the endemism of radiolarian associations inhabiting its different regions is difficult. The only thing which is certain is that, in the direction from the tropics to the poles, diversity decreases, whereas in the tropics, representatives of all radiolarian genera and families are present (Petrushevskaya, 1981a, 1986). This decrease, however, is often punctuated by a peak in the subtropical transitional area, where many cold-water and warm-water taxa coexist, especially in the sediments (Boltovskoy, 1981a, 1982, 1986).

Radiolarian associations in the sediments of the Boreal Realm of the Pacific contain the endemics of the Arctic Boreal Realm (amphiboreal species and Pacific endemics), cosmopolitans, and tropical species entering the transitional and Boreal Realms during the climatic warmings. Cosmopolitan species are the basis of the cold-water association (in the number of specimens in the sediment) (Kruglikova, 1990, p. 95).

Supposedly, the development of cosmopolitanism requires a rare combination of adaptive features (such taxa should be eurythermal, euryhaline, eurybathic, i.e., should be capable of survival at large depths up to 1000 m and more (Kruglikova, 1990). For instance, *Siphocampe arachnea*, the species mentioned above with cosmopolitan features, usually lives in the subsurface

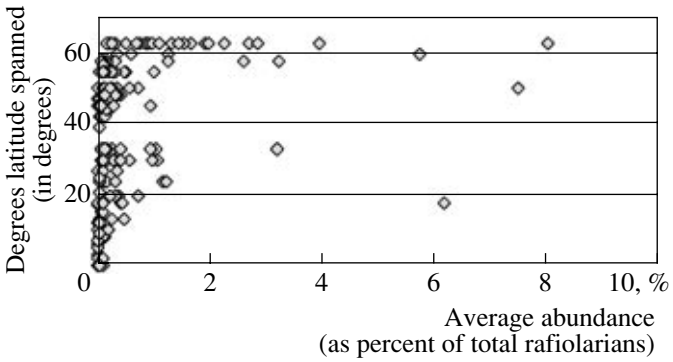

Fig. 59. The relationship between radiolarian abundance (average percentage contribution to overall radiolarian in each sample) and geographic distribution (latitudinal span, in degrees) as illustrated by a collection of 18 surface sediment samples (195 polycystine species) from the South Pacific (after Boltovskoy, 1987). (◌) each datapoint represents one species.

layer of water in the northern Pacific, while in the subtropics, it lives in deeper water layers (Boltovskoy, 1998).

However, this is not necessarily a cosmopolitan species, and neither is it eurythermic because in its distribution it is following a rather narrow temperature regime. Radiolarians, as a group, are nearly cosmopolitans, but not ecological cosmopolitans. Generally, the same species will be found anywhere in the World Ocean where ecological conditions are appropriate for its survival (these conditions may or may not be adequate), but most species will be restricted in their distribution by at least temperature.

The relative role of endemics of the Arctic Boreal Zone, bipolar species, and cosmopolitan species changes asynchronously with time, which is apparently related to the fact that different biogeographical groups of species live at different depths. The endemic and bipolar species live at the higher levels of surface water, whereas cosmopolitan species inhabit deeper levels. Rare cases when the quantitative maxima of these groups coincide in time, correspond to the cold sedimentary settings, because, in this case, the deeper waters inhabited by cosmopolitans are involved (Kruglikova, 1990, pp. 95–96).

The problem of endemism may be considered from a different point of view, that of the relationships between the oceanic and neritic species in different (coastal or central) basins of the ocean. For instance, the study of radiolarians from the sediments of the Sea of Okhotsk, Bering, Norwegian, and Philippine seas and from the coastal zones of the ocean showed that there are neritic (nearshore, marine) faunas of radiolarians that are certainly different from those of the latitudinal (central) zones of the ocean (Kruglikova, 1990). "Differences are primarily seen in that the abundance and diversity of radiolarian associations from the oceanic deposits are considerably higher than of the marine associations. Marine associations are characteristically sharply dominated by a few species, different in different zones of a given marine basin…. Radiolarians from the sediments of seas and bottom sediments of neritic regions of the oceans are distinguished by a number of morphological features, i.e., the presence of a large number of small-sized taxa (especially among nassellarians), small-sized porosity, noticeable presence of spines, and very pronounced variability of the skeleton" (Kruglikova, 1990, p. 96).

In the South Atlantic in the zone from the equator to the coast of the Antarctic, seven climatic zones are recognized (five warm-water and two cold-water).

The warm-water zones include the high bioproductivity equatorial zone, the low productivity equatorial zone, tropical/subtropical, central circulation, and the transitional zone. The cold-water zones include the Subantarctic and Antarctic zones (Boltovskoy, 1998).

An opinion exists according to which the climatic zonation does not put such a great pressure on the composition and features of radiolarian assemblages inhabiting different climatic regions. According to the data on the distribution of Recent radiolarians, a complete "certainty and dependence" of the assemblages on the climatic zones is not observed or is "very vague," because the species common for several climatic zones are often more numerous than the endemics (Petrushevskaya, 1986; Boltovskoy, 1998, 1999). A similar pattern was apparently present in the geological past. At least this is characteristic of Cretaceous and Paleogene radiolarians (Amon, 2000c). Indeed, large climatic regions based on the general appearance of the radiolarian associations may be recognized, but it should also be taken into account that the species inhabiting them much more commonly occur in several regions, rather than just in one (Boltovskoy, 1998, 1999).

Cosmopolitan species may have a high bioproductivity. The analysis of large quantities of primary data show a pattern of distribution of radiolarians in which the maximum of bioproductivity is closely associated with the extent of the species distribution (Fig. 59). In fact, there is a group of species, which, showing the features of cosmopolitanism, occur across the entire southern Pacific from the equator to the Antarctic, crossing all existing climatic belts (Boltovskoy, 1987). The abundance of members of this group is one of the highest, and such species have a strong biological potential. It is noteworthy that, based on the data on Recent radiolarians alone, without the geological time factor taken into account, the relationships between endemism and cosmopolitism are difficult to estimate (Petrushevskaya, 1986; Boltovskoy, 1987, 1998, 1999).

Petrushevskaya believed that only a few species among Recent radiolarians show a bimodal or bipolar distribution, and this phenomenon is generally rare (Petrushevskaya, 1986). At the same time, new data indicate that the bimodal and bipolar distribution of

radiolarians is quite common now and played a significant role in the geological past.

Stepanjants *et al.* (2004) concluded that there are at least 32 bipolar radiolarian species in the modern oceans. Lazarus (2002) reported that many post-Miocene species had a bipolar distribution in the Norwegian–Greenland and southern Atlantic basins. There is a striking similarity between the Early Paleogene assemblages from New Zealand described by Hollis (2002) and from the Russian Platform and Western Siberia described by Kozlova (1999). A distinct bipolar distribution of the species of the Late Cretaceous genus *Prunobrachium* was shown by Amon (2000c, 2003). Possible bipolarity of some Jurassic and Cretaceous species from the Boreal regions of Russia was suggested by Vishnevskaya (Bogdanov *et al.*, 1987; Basov and Vishnevskaya, 1991; Vishnevskaya, 2001). Aita and Bragin (1999) reported the similarity of the associations of Triassic radiolarians of Eastern Siberia (Omolon Massif) and New Zealand (Waipapa Terrane). A similarity in some species of the Late Devonian (Frasnian) radiolarians of the Timan–Pechora Basin in northern Russia and Canning Basin in western Australia was reported by Afanasieva and Aitchison (1999, 2000, 2001).

It is noteworthy that the bimodality is characteristic of thermophilic species and is restricted to the tropical zones of the ocean (Johnson and Nigrini, 1982), while the bipolarity is an ecological and geographical phenomenon, which embraced the entire World Ocean (Stepanjants *et al.*, 2004). The bipolarity of species is mainly determined by the temperature: species found in cold Arctic waters may be found at large depths in the tropics where the temperature is low.

Rifts, aulacogens, and deep faults. The zones of deep faults, rifts, and aulacogens are capable of producing an enormous effect on the increase in number and diversity of radiolarians. The aulacogens are stable in space and time slitlike degasification channels of the Earth. Within the Russian Platform, the Ural–Caspian Rift System is a region with a low concentration of ozone, which retains its status as a zone of intense degasification of the planet (Syvorotkin, 1994).

Mass accumulations of Paleozoic radiolarians in the Russian Platform are found in its modern eastern margins. If all known localities of Paleozoic radiolarians are placed on the map of aulacogens of the Russian Platform, a remarkable coincidence of the distribution of rich radiolarian assemblages with the aulacogen zones is seen (Fig. 60) (Klevtsova and Afanasieva, 1998; Klevtsova, 2000).

The Timan–Pechora Domanik Basin (Middle Frasnian, Late Devonian), with anomalous anoxic settings, existed above one of the most active regions of the ancient Fore-Timan aulacogens. This was responsible for the specific features of this basin, i.e., periodic enrichment with silica and outbursts of biological productivity of radiolarians (Afanasieva and Mikhailova, 1998; Afanasieva, 2000a).

Occasionally, a sudden boom of life on an incredible scale is observed in nature. For instance, in the Adriatic Sea, there are records of the phenomenon referred to as *mare sporco* by the Italians, which is a sudden massive production of diatoms (Vernadsky, 1926, 1983, 1987). A so-called *red tide*, which is a massive development of dinoflagellates (unicellullar algae), is observed near the Latin American coast of the Pacific (Erkhard and Sezhen, 1984; Syvorotkin, 1998). In the northwestern part of the Black Sea in a period of red blossoming, the biomass of diatoms in the subsurface water layer sharply increases (their concentration reaches 10 g per 1 m^3. These unicellular algae reproduce at such a high rate that the balance of silicon dissolved in the seawater has no time to restore. Accumulations of diatoms with impoverished silica content are formed. They cover the sea surface in a layer several meters thick (Borodkin, 1995; Volkov, 1995; Agarkov, 2000). Anoxic conditions unfavorable for the photosynthesis are formed, whereas the process of cell division is stopped. The volume of the extracellular organic matter that is cast out in this situation increases by 100%. Filamentous accumulations of organic matter enriched by the sulfur are formed. By aggregation of the filaments, the suspended organic flakes may reach 10 cm^2 in thickness (Alldredge and Gotschalk, 1990; Borodkin, 1995; Volkov, 1995), resulting in so-called *sea snow* (Agarkov, 2000). Accumulations of algae are deposited on the bottom as jellylike mass, which is quickly eaten or decomposed, thus restoring the distorted balance of the nature.

Apparently, the degasification and disintegration of the ozone layer took place in the Timan–Pechora Domanik Basin in the Late Devonian. This was apparently accompanied by *sea snow*, but instead of diatoms it was produced by the widespread acritarchians and tasmanites.

The presence of places with abnormal biological productivity in the ocean was, perhaps, related to the fact that these sites of maximum productivity were connected with zones of degasification of the Earth's interior, which are known to convey the vast amount of chemical compounds, including nitrogen, phosphorus, and other elements to the oceanic bottom and into the water (Syvorotkin, 1994, 1998; Walker, 1995; Kochemasov, 1997; Leyborne, 1998).

Modern territories of accumulation of radiolarian mud are connected with the zones of faults and ozone anomalies. The equatorial trail of high bioproductivity of radiolarians extending from South America toward the center of the Pacific is very characteristic in this respect. This trail is located in the area of the Eastern Pacific Rift Belt and ozone anomaly above the Eastern Pacific Uplift (Fig. 57). The position of the Equatorial Undercurrent Assemblage of radiolarians (Fig. 57) is connected with the South Equatorial Current and weak-

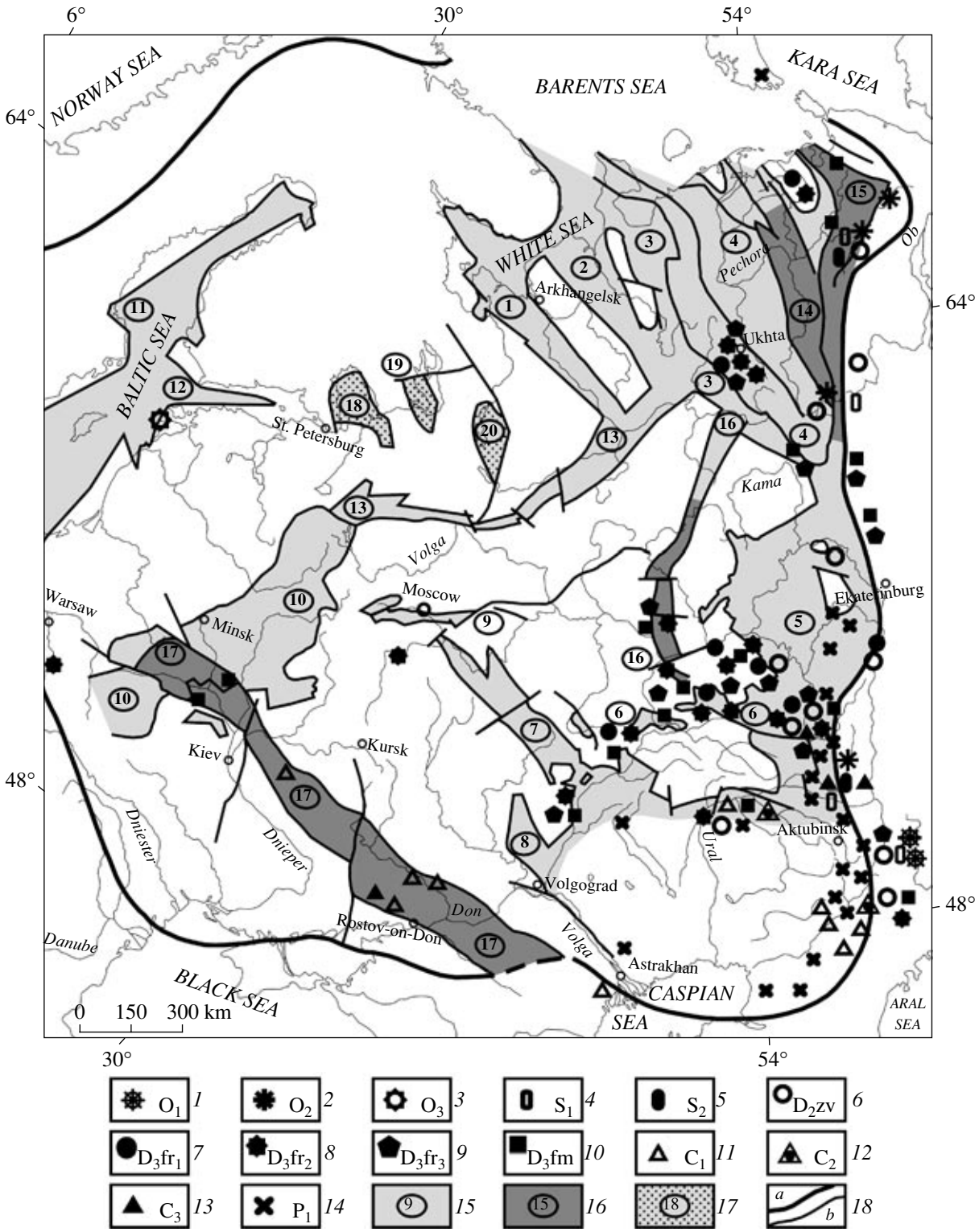

Fig. 60. Occurrences of Paleozoic radiolarians and aulacogens of the Russian Platform: (*1–14*) occurrences of Paleozoic radiolarians: (*1–3*) Ordovician: (*1*) Lower, (*2*) Middle, and (*3*) Upper; (*4*, *5*) Silurian: (*4*) Lower and (*5*) Upper; (*6*) Middle Devonian, Givetian; (*7–10*) Upper Devonian: (*7*) Lower Frasnian, (*8*) Middle Frasnian, (*9*) Upper Frasnian, and (*10*) Famennian; (*11–14*) Carboniferous: (*11*) Lower, (*12*) Middle, (*13*) Upper; and (*14*) Lower Permian; (*15*, *16*) aulacogens (**1–17**): (*15*) Baikalian (**1–13**) and Baikalian–Caledonian (**13**); (*16*) Baikalian–Hercynian (**14–17**) and Hercynian (**16**, **17**); (*17*) grabens (**18–20**): (**1**) Kandalaksha–Dvina, (**2**) Mezen, (**3**) Fore-Timan, (**4**) Timan–Izhem, (**5**) Kama–Ufa, (**6**) Sernovodsk-Abdulino, (**7**) Pachelma, (**8**) Don–Medveditsa, (**9**) Moscow, (**10**) Volyn'–Orsha, (**11**) Botnic–Baltic, (**12**) Finnish, (**13**) Central Russia, (**14**) Pechora–Kolva, (**15**) Varandei–Adz'vinck, (**16**) Vyatka–Kazan–Sergiev, (**17**) Pripyat'–Dnieper–Donets, (**18**) Onega, (**19**) Ladoga, (**20**) Vozhe–Lacha; (*18a*) border of the platform, (*18b*) borders of aulacogens (after Valeev, 1978; Klevtsova, 2000).

ening of trade winds is determined by the El Nino and controlled by the tectonics, i.e., the position above the Carnegie Ridge and Mendana Fault (Molina-Cruz, 1977; Syvorotkin, 1994, 1998).

Thus, the development of the zones of increased bioproductivity is controlled by the tectonics: unique conditions for life are created above the deep faults of the rift zones and aulacogens (sources of nutrients of endogenic nature).

Influx of silica in marine water. The supply of SiO_2 with the products of underwater volcanism and the flow of deep juvenile waters in the zones of active geological faults is an important source of silica. It is known that the content of silicon in the region of the uprising of the juvenile water may increase by an order of magnitude compared to normal values (20–40 times), while this siliceous water may spread for hundreds of kilometers. Moreover, the maximum content of silica (65–70%) in consolidated crust is found in the eastern margins of the platform, connected to the zones of aulacogens. One of the main factors influencing the mean amount of silica in the consolidated crust is the content of SiO_2 in the lower level of the crust (Egorkin, 2000). However, the only mechanism that can explain a constant influx of silica is the uprising of the deep highly siliceous water along faults (Maksimova, 1975; Klevtsova and Afanasieva, 1998; Klevtsova, 2000).

Another considerable source of silicon in seawater is its outflow from the continents by the rivers as products of chemical and physical weathering of the rocks. For instance, in regions of equatorial humid climate, during the weathering of the acid and basic magmatic rocks with high Si content of, this element becomes highly volatile. (*Vertical Accretion…*, 2002).

The scale of the evacuation of the dissolved Si is different in different climatic zones. The evacuation of Si in the moderate humid zone is 46% of the total dissolved material; in the tropical humid zone, it is 35–82%. Particularly high quantities of SiO_2 are driven by the rivers (4.26×10^{-4} g/l (*Vertical Accretion…*, 2002).

Elements dissolved in river waters, when transported from the continent, mix with and become part of the seawater. The large (or largest) proportion of the suspended and transported material flowing into the oceans is concentrated as sediments in the periphery of continents: in the marginal seas, on the shelf, in the upper part, and near the base of the continental slope. Apart from the transported material, up to 92% of the suspended material is deposited there, whereas only 7–8% reach the pelagic regions of the oceans (*Vertical Accretion…*, 2002). Thus, only the shelf and neritic settings of the marginal seas can provide radiolarians with maximum concentrations of dissolved natural SiO_2, compared to the central zones of the ocean. The central tropical zone of the oceans is an exception because, in the tropical humid regions, the outflow from the continents is the highest. According to the model of the marine cycle of biogenic silica, developed by marine geologists (Kennett, 1982), the main sources of silica are the following:

(1) river discharge (up to 4.27×10^{14} g/y);

(2) submarine volcanism. However, the amount of material formed as a result of the hydrothermal activity is apparently insignificant compared to the amount transported by the rivers and is approximately 20% only;

(3) submarine weathering;

(4) high temperature change of basalts;

(5) migration of silica up from the pore water sediments;

(6) dissolution of opaline shells before burial (the dissolution of the opaline skeletons on the bottom may also largely contribute to the balance of silica, but is difficult to distinguish from direct dissolution in the water);

(7) influx of silica as a result of the low temperature change of basalts, clastic siliceous rocks, and release from the porous water, circulating in deep water sediments, supplies more silica, than the annual river discharge.

Deposition of silica. The deposition of silica in the oceans includes the biogenic accumulation of silica, i.e., the sorption of the dissolved silica by organisms. The following main processes of the transformation of silica in the oceans may be recognized (Kennett, 1982):

(1) *Biogenic fixation by organisms.* It has been calculated that this process accounts for 40–75 times the discharge. The rate of transformation of silica in the ocean as a result of this process is considerably larger than the rate of the influx or removal.

(2) *Oxidative dissolution.* A rapid postmortem dissolution of fragile siliceous tests, which is caused by oxidation of the enclosing protoplasm. This process is very important, because before reaching the bottom approximately 95% of the silica is dissolved.

(3) *Dissolution without oxidation* affects opaline tests both in the water and on the bottom of the ocean.

Because biological processes play a dominant role in the marine cycle of silica, the oversaturation of water and, hence, chemogenic deposition of amorphous silica was apparently already unlikely beginning as early as the Cambrian, when many siliceous organisms appeared in the sediments, and virtually impossible from the Late Mesozoic, when diatoms became numerous in the sediments (Kennett, 1982; Kaleda, 1987; Fedonkin, 2003). In the modern ocean, only a small proportion (less than 4%) of silica contained in opaline skeletons reaches the sea bottom, whereas the remaining part of the silica returns to the water as a dissolved H_4SiO_4. Most radiolarians and diatoms dissolve in surface and subsurface waters at depths up to 1000 m, while the dissolution of calcareous microorganisms occurs mostly at the depth of more than 3.5 km (Fig. 61) (Berger, 1968a, 1968b; Kennett, 1987).

Those siliceous microorganisms which actually reach the bottom even as skeletons, carapaces, or fecal pellets undergo further dissolution before and after burial, because the bottom and mud waters are also

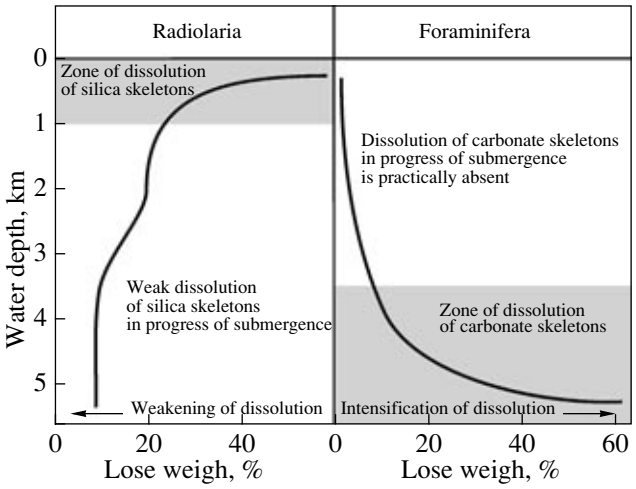

Fig. 61. Dependence of the dissolution of the radiolarian and foraminiferal skeletons on the environment obtained by experiments (after Berger, 1968a, 1968b; Kennett, 1982).

undersaturated by amorphous silica. The dissolution of dead radiolarians during their transport is caused by a combination of several environmental factors, of which pH and temperature of water are considered to be most important (Kruglikova, 1966, 1981, 1990).

Thermodynamic calculations for the central part of the equatorial zone of the Pacific show that 90–99% of biogenic opal produced in the surface water is dissolved before reaching the boundary separating the bottom from the sediment, while the additional dissolution occurs in the sedimentary strata, and silica comes into the bottom water. As a result, only about 2% of the opal originally produced by organisms is preserved in sedimentary sections (Kennett, 1982).

The most fragile siliceous skeletal elements are completely dissolved when they are transported through the water, whereas more stable forms with a thick wall are preserved longer during their descent or even on the oceanic bottom. Larger taxonomic groups can be recognized, in order of increasing resistance to dissolution: silicoflagellates, diatoms, fragile radiolarians, strong radiolarians, siliceous sponges (Mikkelsen, 1980; Pisias *et al.*, 1986). Because many assemblages are dissolved, the siliceous fauna preserved in bottom sediments is an impoverished relict of the original assemblages of the surface water (Kennett, 1982).

TAPHONOMY OF RADIOLARIANS

Modern radiolarian thanatocenoses and taphocenoces are formed in the bottom layer of sediment on the ocean and sea bottom (Fig. 53). Abundant fossilized skeletons of radiolarians in rocks often prompt geologists to draw the familiar conclusion that the paleobasin was an equivalent of modern oceans with abyssal depths. At the same time, research on fossil and extant radiolarians shows completely different patterns of habitats and subsequent transition into the sediment and the rocks.

The distribution of radiolarians in the sediment is a product of a combination of biotic and abiotic factors that distort the data on the composition of biocenoses, leading to loss of the primary information (Fig. 62) (Boltovskoy, 1987, 1994, 1997, 1998):

- various currents (surface, subsurface, bottom);
- vertical and lateral transport;
- upwelling;
- general and selective dissolution;
- integration of surface and bottom species in the sediment;
- different productivity of species;
- changes in the seasonal dynamics of the population size;
- predation on radiolarians and total and partial destruction of the shells;
- transportation and redeposition of the skeletons and their fragments;
- accumulation of organic matter in a form of sea snow.

Transportation of Radiolarians into the Bottom Sediment

Skeletal remains (lacking protoplasm) of polycystine radiolarians are not only found in the bottom sediment, but are present in all water layers. Depending on the depth, the radiolarian skeletons may represent 10–30% or even 90% of all living and dead Polycystina (Petrushevskaya, 1986; Kling and Boltovskoy, 1995).

This raises a justifiable question: Why are there so few radiolarian skeletons compared to living radiolarians? Can this indicate that the skeletons are largely postmortem decayed and dissolved, or the rate of descent of empty skeletons is considerably greater than the buoyancy of living radiolarians, and they simply fall on the bottom?

The speed with which empty skeletons and dead radiolarians with preserved cytoplasm are transported in seawater depends on many factors. The most important is the size of the radiolarian body. The smaller the optimal radius (r_{opt}) of a shape approximating the sphere, the slower it will descend to the bottom (Afanasieva and Timokhin, 1999).

The second reason is the density of the radiolarian body (ρ). The density of the opaline skeleton (ρ = 1.9–2.5 g/cm^3, on average, 2.2 g/cm^3) is larger than the density of the cytoplasm, which without counting lipid inclusions, is assumed to be equal to the density of seawater. The general density of the body of radiolarians is calculated based on the proportion between the volume of the cytoplasm and the opaline skeleton (Afanasieva, 2000a).

Finally, the third reason affecting the speed of the descent of radiolarian remains on the bottom of the

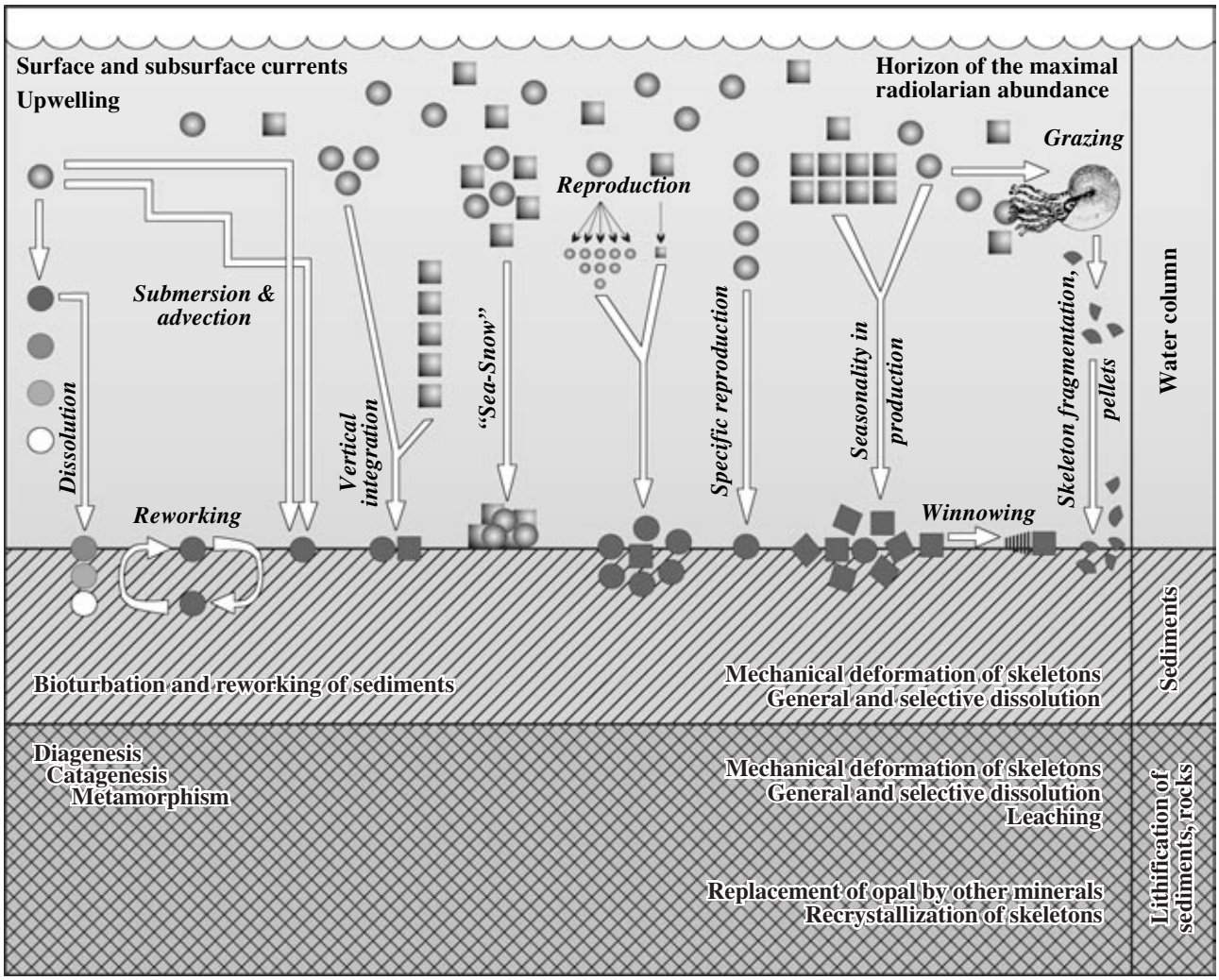

Fig. 62. Factors affecting radiolarian taphonomy (after Boltovskoy, 1997, 1998, modified).

basin is the density (ρ_0) and viscosity (η) of the sea water of normal salinity (35 PSU) at different temperatures: at 20°C, ρ_0 = 1.0232 g/cm^3, η = 1.084 mPa; at 5°C, ρ_0 = 1.0273 g/cm^3, η = 1.595 mPa.

In general, the rate of the descent of live and dead radiolarians of any shape is described by the modified Stokes' formula:

$$u = \Phi g r_{opt}^2 \frac{(\rho - \rho_0)}{\eta},$$

where g is the gravitational acceleration; Φ is shape dependent coefficient $\Phi = 0.222\varphi$; in this case, the shape factor φ equals the ratio between the surfaces of the spherical particle (S_{sph}) and real particle (S), which have the same volume ($\varphi = S_{sph}/S$).

Calculations show that the time required for postmortem descent of radiolarian cells in the seawater (Table 10) largely depends on the volume of the preserved cytoplasm of the cell. The more of organic matter remains, the slower the radiolarian remains will descend. At the same time, relatively large radiolarians (optimal radius of the cell is 100–200 μm), with a well-preserved cytoplasm (at $\rho - \rho_0 = 0.01$ g/cm^3), at most in three days will reach depths of 200 m.

These results are very important for oil geology, because they support the hypothesis developed by Afanasieva (Afanasieva and Mikhailova, 1998; Afanasieva, 2000a) that the potential oil host rocks are formed with the participation of remains of the organic matter of radiolarian cells in conditions of marginal basins with depth not exceeding 100–200 m.

The time of the descent of empty skeletons of radiolarians in the seawater considerably decreases, because the density of the opaline skeletons is almost twice the density of the seawater (Table 11). Our calculations agree and emend the results obtained by other workers, according to which the skeletons of radiolarians descend at speed of 14–416 m/day (Takahashi and Honjo, 1983) and even 1000 m/hour (Seravin, 1984).

Table 10. Time of the postmortem descent of radiolarian cells in the seawater

Conventional temperature of the seawater	Depth of the basin, m	Optimal radius of the radiolarian cells, μm		
		50	100	200
at $\rho - \rho_0 = 0.01$ g/cm^3				
20°C	50	11.57 days	2.89 days	17.27 hs
	100	23.15 days	5.79 days	1.44 days
	200	1.52 mths	11.57 days	2.88 days
5°C	500	4.88 mths	1.22 mths	9.24 days
	1000	9.76 mths	2.44 mths	18.49 days
	3000	2.44 yrs	7.32 mths	1.82 mths
	6000	4.88 yrs	1.22 yrs	3.65 mths
at $\rho - \rho_0 = 0.1$ g/cm^3				
20°C	50	1.16 days	6.94 hs	1.73 hs
	100	2.32 days	13.89 hs	3.45 hs
	200	4.63 days	1.16 days	6.91 hs
5°C	500	14.84 days	3.71 days	22.19 hs
	1000	29.68 days	7.42 days	1.85 days
	3000	2.93 mths	22.26 days	5.55 days
	6000	5.86 mths	1.46 mths	11.09 days
at $\rho - \rho_0 = 0.5$ g/cm^3				
20°C	50	5.56 hs	1.39 hs	20.73 mins
	100	11.11 hs	2.78 hs	41.46 mins
	200	22.22 hs	5.56 hs	1.38 hs
5°C	500	2.97 days	17.81 hs	4.45 hs
	1000	5.94 days	1.48 days	8.90 hs
	3000	17.81 days	4.45 days	1.11 days
	6000	1.17 mths	8.90 days	2.23 days

Table 11. Time of descent of radiolarian cells in the seawater

Conventional temperature of the seawater	Depth of the basin, m	Optimal radius of the radiolarian skeleton, μm		
		50	100	200
at $\rho - \rho_0 = 1$ g/cm^3				
20°C	50	2.78 hs	41.67 mins	10.36 mins
	100	5.56 hs	1.39 hs	20.73 mins
	200	11.11 hs	2.78 hs	41.46 mins
5°C	500	1.48 days	8.90 hs	2.22 hs
	1000	2.97 days	17.81 days	4.44 hs
	3000	8.90 days	2.23 days	13.31 hs
	6000	17.81 days	4.45 days	1.11 days

Radiolarian Thanatocenoses and Taphocenoses

Plankton and sediment are similar in that researchers tend to enhance the usefulness of their research by concluding that sedimentary samples are useful for understanding distribution patterns in the plankton rather than the opposite. However, a *quantitative* measure of this similarity, with comparisons of similarities between plankton samples and between sediment samples, is hardly ever offered. Boltovskoy suggested that the loss of primary information during the transition from the dead radiolarians in the sediment cannot be compensated for, while the difference between the biocenosis and thanatocenosis is *enormous*.

Swanberg and Bjørklund (1992) compared living radiolarian associations in planktonic catches and dead associations in bottom probes in the Norwegian fjords using multivariate mathematical analysis of their taxonomic compositions. The study has shown that planktonic catches and bottom probes differ considerably in composition: they vary in relation to season, depth, and place of location of fjords. While approximate paleogeographic reconstructions and assumptions concerning the radiolarian habitats are possible based on data from the bottom probes, the taxonomic composition of living associations and of proportions of species in it cannot be assumed with any degree of certainty. Welling and Pisias (1998) studied the distribution of tropical radiolarian species from the central western Pacific based on the bottom probes and concluded that the bottom probes do not precisely reflect the quantitative and qualitative composition of the plankton. Therefore, it is easy to make a mistake by increasing the range of tropical species, because in the intermediate water of subtropics, the species adapted to colder water are not deposited in the bottom sediment.

Bottom thanatocenoses and taphocenoses with radiolarians can be formed in all bionomic zones, including central oligotrophic regions of the oceans (Fig. 53). The maximum concentration of radiolarian thanatocenoses, not counting the fragments of skeletons, ranges from 3 to 30% (Berger, 1976; Petrushevskaya, 1981a, 1986; Kennett, 1982).

However, not all radiolarians, as mentioned above, can be transported from the biocenosis to the thanatocenosis, taphocenossis, or oryctocenosis. Petrushevskaya (1966, 1986) showed the pattern of the transition of polycystine radiolarians first in the sediment and then in the lithified beds:

(1) “In total in all horizons, empty skeletons are 10–30% of the total skeletons of Polycystina” (Petrushevskaya, 1986, p. 69).

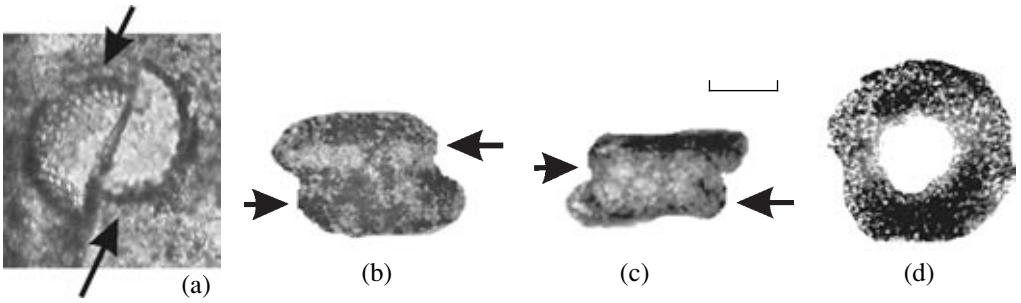

Fig. 63. Mechanical deformation of radiolarian skeletons in the rock: (a) fracture deformation, *Haplentactinia* sp., Ordovician, eastern slope of the Northern Ural Mountains; (b, c) sliding deformation, *Ommatodiscus* sp., Upper Cretaceous of Middle Transuralia; and (d) dissolution and removal of silica from the center of the skeleton, *Spongotrochus* sp., Middle Paleogene of southern Transuralia. Arrows indicate the vectors of physical forces applied to the specimen. Scale bar, 100 μm.

(2) "After diagenesis, few complete radiolarian skeletons remain, apparently, several tens times less than in the loose sediments" (Petrushevskaya, 1986, p. 73).

De Wever *et al.* (1994, 2001) calculated that not more than 30–50% from the total production of the radiolarian populations in the subsurface layer of the water column reaches the oceanic (sea) bottom.

Zasko (2004) studied extant polycystine radiolarians and showed a decrease in the quantity of dominant taxa by 15–55% in the sediment compared to the water.

According to Takahashi (1991), a residual content of empty radiolarian skeletons in the sediment does not exceed 1–10%.

The distortion of the data received from the plankton are observed even before the organisms reach the sea bottom. For instance, in the eastern tropical Atlantic (in the zone of 10° N–17° S), a considerable difference in both the taxonomic composition and the proportion of the constituent species are observed between the assemblage of radiolarians collected by the planktonic nets at the depth 0–300 m, and assemblages of radiolarians collected in traps at the depth 853 and 2195 m in the same stations, (Boltovskoy *et al.*, 1996). In some cases, populations inhabiting the meso- and bathypelagic depths can, in total, make a taphocenosis compared in density to the taphocenosis formed by the populations inhabiting the epipelagic depths 0–300 m (Kling and Boltovskoy, 1995).

Taking into account the taphonomy of radiolarians, the radiolarian populations from the biotopes occurring in the interval of depths 0–500 m play the most important role in the taphocenoses and oryctocenoses. The true depth of the basin in this region is of no significance, because the bottom of the sea under this water layer may have any type of geomorphology (from shelf to depression) (Fig. 53).

Therefore, based on the occurrence of fossil radiolarians, it would be unsafe to conclude that radiolarians are indicators of depth, and that paleobasins with sediments containing abundant radiolarians were exclusively deepwater (Paverd and Bjørklund, 1989). The main "radiolarian rain" comes from the water layer that does not exceed 500 m (Figs. 53, 62).

Further, the loose bottom sediments and, later, the rock at the stages of diagenesis, catagenesis, and metamorphism undergo processes causing further impoverishment of the initial radiolarian associations (Fig. 62): mechanical deformation of the skeletons, total and selective dissolution and leaching from the rock.

Mechanical deformations of radiolarian skeletons are frequent in the rock (Amon, 1990, 2000d; Vitukhin, 1990). Deformations of fracture (Fig. 63a), crush, slide (Figs. 63b, 63c), and twist of skeletons may be caused by the flow of the rock during tectonic dislocation. The processes of chemical leaching of the radiolarian skeletons from the rock are noticeable, for instance, in the Santon siliceous rocks and sandstones with siliceous cement from the Subpolar Trans-Urals and Fore-Urals (Amon, 2000c, 2000d) (Fig. 63d). The thermal metamorphism influences the fossilized radiolarian associations, impoverishing and distorting their compositions (Bustillo *et al.*, 1994).

The fact that at present we observe many cases of the abundance of radiolarian skeletons in various marine rocks indicates a high primary bioproductivity of radiolarians and excellent environment of burial of their skeletal remains. The combination of these conditions was able to overcome the subsequent negative influence of the factors precluding the formation and preservation of thanatocenoses, taphocenoses, and especially oryctocenoses.

Radiolarian Oryctocenoses

The organic world is very closely connected with the environment and habitats. As the Cambrian radiolarians changed from a benthic or near bottom dwelling mode of life to a planktonic mode of life (free floating or even transported in different water layers) and later perfected it over almost the entire Phanerozoic, their occurrences in certain biotopes and types of sediments also changed: from mainly shallow water siliceous and carbonate deposits in the Paleozoic to the rela-

tively deepwater carbonate–siliceous sediments in the Mesozoic and, then, deepwater mud of the modern oceans (Kennett, 1982; Afanasieva and Vishnevskaya, 1993b).

While the depth of accumulation of the Recent siliceous–carbonate mud is known (Kruglikova, 1981), assumed in the case of the Mesozoic sediments (Vishnevskaya, 1984), it is open to question in the case of Paleozoic sediments (Timofeev and Kholodov, 1984). Some workers believe these were oceanic depths (Monin, 1977; Mizens, 2002, 2003), whereas others prefer to assume that the sediments were accumulated in the shallow water environment (Khvorova, 1984; Timofeev and Kholodov, 1984; Afanasieva and Zamilatskaya, 1987, 1993; Afanasieva and Vishnevskaya, 1993b).

The hypothesis of the mainly shallow water epicontinental seas of the distant past of our planet was recently supported by new facts. Radiolarian analysis provides new data in the view of this hypothesis.

General ecological patterns of Recent radiolarians often do not coincide with the data of the geological past. In particular, the paleopopulations of radiolarians of the past geological epochs reached the maximum abundance in the nearshore zones of marine basins or those with little depth, which is not comparable with the bathyal or abyssal depths of the modern oceans.

Many factors of the occurrence of abundant radiolarian remains in sediments of paleobasins of various types (epiplatform, epicontinental, marginal) lead to a conclusion that the biotopes near the continents or at a short distance from the continent, rather than pelagic or central zones of the oceans were most favorable for radiolarians.

The richest and most diverse radiolarian oryctocenoses are formed: (1) in places with a system of currents, (2) in sublittoral areas near the continents, (3) under the influence of the upwelling, and (4) in the regions of increased bioproductivity above the deep faults are zones of rift systems.

This conclusion is supported by abundant radiolarian occurrences in the relatively deep outer shelf of the epicontinental Middle Frasnian Domanik Sea of the Timan–Pechora Basin; in relatively deepwater marginal sea near the south Ural land Uraltau in the Late Devonian; in the coastal basin in the Ural Foredeep in the Late Carboniferous–Early Permian, in the coastal western zone of the epicontinental Late Cretaceous West Siberian Sea, etc. The currents created favorable conditions for radiolarians in region of relatively deepwater depressions in the Late Devonian West Ural Sea, near the Carboniferous–Early Permian biostrome-reef Karachaganak Massif north of the Caspian Sea Region, in the region of the Late Carboniferous–Early Permian basin of the Ural Foredeep, in the nearshore areas of the Late Cretaceous West Siberian Sea.

Nutrients brought from the land dissolved in the river discharge are vital for radiolarians, but most of the suspended and carried material is accumulated as sediments on the periphery of the continents: in the marginal seas, on the shelf, in the upper part and near the bottom of the continental slope. Thus, only shelf and neritic settings of the marginal seas can provide radiolarians with the highest concentrations of the dissolved natural SiO_2 and other necessary matters compared to central zones of the oceans.

The proximity of the land favored the flourishing of radiolarians not only for the above reason, but, in some cases, the continental slope created conditions for the development of the coastal upwelling, which in turn led to the rapid increase in number of radiolarians.

The role of the upwelling in biogeography of radiolarians is very large, although the mechanism of upwelling should not be always used for explaining the increased bioproductivity of radiolarians. In the zones of deep faults and aulacogens, the abundance and diversity of radiolarians are hugely increased. Mass accumulations of radiolarians in the Paleozoic of the Russian Platform are found in its modern eastern margins with the zones of aulacogens and deep faults.

The activation of volcanism facilitating the change in the chemical composition of the water, on the one hand, facilitated the increase in the bioproductivity of radiolarians and, on the other hand, accumulation of the beds. In the periods of prolonged volcanic activity, thick members of siliceous rocks were formed, while the interrupted volcanism was accompanied by the deposition of the clayey–carbonate–siliceous series of sediments. Both types of rocks contain radiolarians, whereas the carbonate members separating those do not contain radiolarians or contain very few.

These facts pose a very important question: to what extent and with which limitations can we use the method of uniformism frequently used for the paleostructural and paleogeographic reconstructions in radiolarian analysis?

The geological past of radiolarians is much richer than their modern state. This is evident from the example of the environment of radiolarians in the basins with hydrosulfide contamination and their participation in the deposition of oil source rocks in the Domanik Age (Middle Frasnian) of the Late Devonian, the example of the distribution of radiolarians of the Carboniferous and Early Permian epochs in the basins of reefs (not present in modern seas), and the example of different conditions of the formation of radiolarian mud in the Paleozoic, Mesozoic, and Cenozoic, and in the modern oceans.

CHAPTER 6. INFORMATION TECHNOLOGY IN RADIOLARIAN STUDIES

The accumulation of large amounts of information on the systematics and distribution of highly diverse groups of microfauna leads to considerable difficulties in its use and, often, to redescription of already described species, which increases information noise. Radiolarians are no exception. Several information systems and databases were created in both Russia and

abroad to store and analyze various data in radiolarian studies.

Some of these are for solving specific tasks, others aim to resolve complex problems of informatization of studies, but are restricted by temporal or spatial limits. In recent years, universal databases on recent and fossil radiolarians are beginning to be developed.

A REVIEW OF EXISTING DATABASES AND INFORMATION SYSTEMS ON RADIOLARIANS

Riedel was the first to use computers in radiolarian studies. He headed the project for creating the BIBLIOTIX program, which included all English language literature on radiolarians.

The first information retrieval databases or systems for radiolarians were created in the Soviet Union by Chedija (1978). Later, a computerized updated version was proposed by Petrushevskaya and Menshutkin (1990). Later, Amon (1996, 1999a, 2000c, 2000d) improved Petrushevskaya's program using the database management system PARADOX and proposed his new version for the system of the Radiolaria of the Ural Mountains.

At the end of the 1980s, a group of French and Swedish specialists led by De Wever proposed the programs BIOSTRAT (to account for the distribution of radiolarians in beds), GENETAB (distribution of species across the geochronological levels), and GESPAL (for numerical taxonomic systematics of Triassic–Jurassic radiolarians).

The appearance of extensive material from deep ocean drilling required new databases operating with the large amount of data published in various sources. Among those are the programs on the Cenozoic of the world's oceans composed by Riedel's group (Riedel, 1989; Riedel *et al.*, 1994) and informational database on marine micropaleontology of all voyages of DSDP-ODP (*Deep Sea…*, 1990).

At the same time, computer input of data using digitizers, scanners, and video cameras, and storage of images of paleontological objects (IMAGIX, PALAEODMS-A, etc.) became widespread.

In recent years, universal databases on extant and extinct radiolarians were introduced. One of those is the database of the extant radiolarians (Benson, 2003), integrated micropaleontological database PALAEODMS. Based on several systematic collections of ocean drilling, a database continuously supplemented by the working group of IUBS Taxonomic Database was developed (Lazarus, 1997). The European group of radiolarian workers created a database on Jurassic–Cretaceous radiolarians of the Tethys (Baumgartner *et al.*, 1995, 2003), and RADWORLD for radiolarian workers worldwide (Caulet and Nigrini, 2003).

INFORMATION SYSTEM RADBASE

Agarkov proposed a multipurpose information system (IS) of radiolarians of the world RADBASE, which has been continuously updated (Agarkov, 1996, 1998, 1999, 2000, 2004).

This database is a complex geoinformation system, which contains constantly updating data on the fossil and recent microorganisms studied by this author, and extensive published data. The database is composed of several interconnected blocks, including micropaleontological and bibliographic databases, a database of the codes of geological space, and cartography. Each of these blocks is a separate information system, which can be used also for creating other databases (Fig. 64).

The micropaleontological block is universal and allows the storage of information on any groups of fauna and flora irrespective of their morphology, geochronological range, and variations of ecological settings. Presently, to access the morphological analysis of micropaleontological data it includes data on extant and fossil radiolarians, diatoms, silicoflagellates, ebriideans, actinomycids, coccolithophorides, and foraminifers.

In total, the micropaleontological block includes series of relational worksheets for each of the above groups of microorganisms connected by the systems of key fields. Because of the uniformity of the worksheets of storages of information and flexibility of data processing, the system allows the analysis for both each class, or section, and all taxa of higher rank together. The following worksheets are most important in the block described:

(1) Check-list of species
(2) Systematics of species
(3) Description of species
(4) Images of species
(5) Distribution of species
(6) Morphological feature of species
(7) Glossary of morphological characters of species
(8) Skeletal parameters of species
(9) Ecology of species
(10) Geochronological distribution of species
(11) Check-list of genera
(12) Descriptions of genera
(13) Systematics of generic taxa
(14) Check-list of suprageneric taxa
(15) Systematics of suprageneric taxa
(16) Descriptions of suprageneric taxa
(17) Worksheet of synthesis for the analysis of distribution.

The main check-list of species and subspecies taxa contains about 15000 synonyms of radiolarians of about 10000 valid species and subspecies.

The check-list of genera includes data on 1722 valid taxa and their synonyms (Appendix). For each of

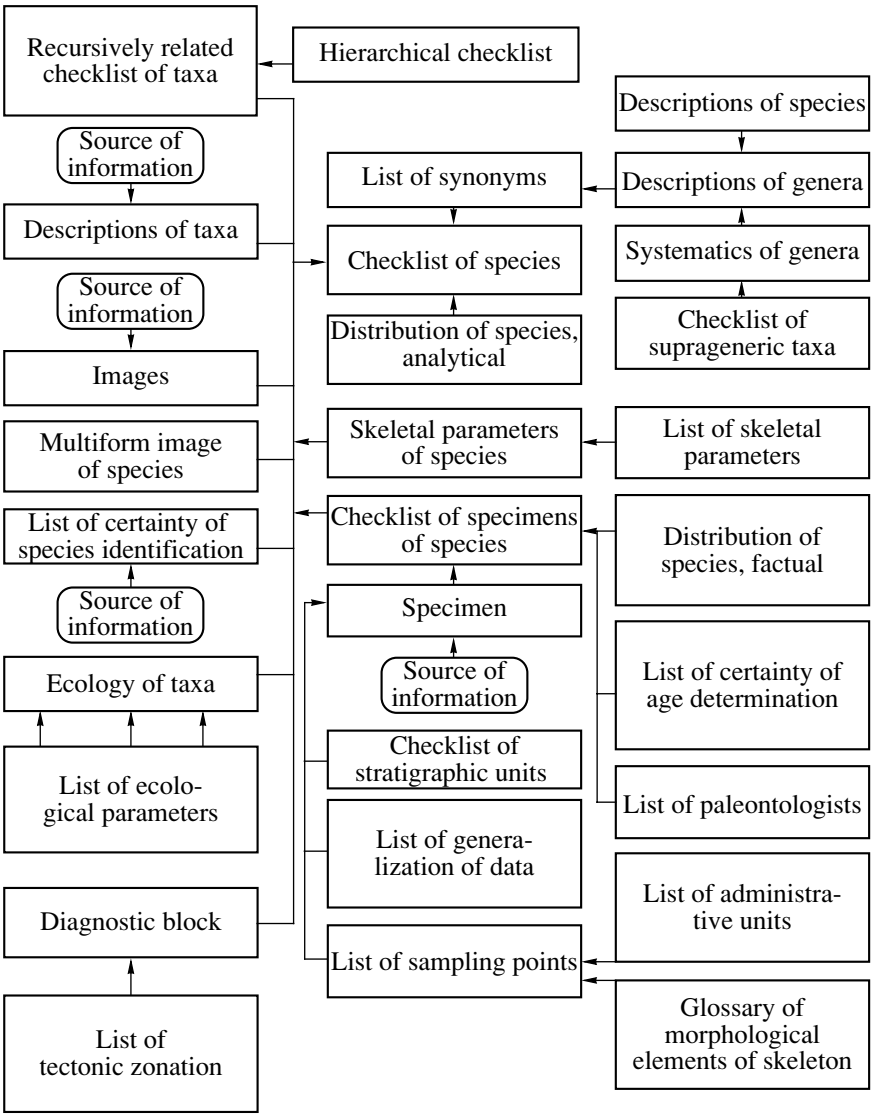

Fig. 64. A model of data provided by the radiolarian informational system used.

them, all available description in the original language and data on the geochronological range based on the ranges of the species of this genus are provided.

Apart from the existing synonymy encoding, the program allows alternative encoding of taxonomic synonyms and choice of variants of suprageneric systematics.

The above worksheets in accordance with the structure shown in Fig. 64 include over 40 various glossaries and check-lists determining the type of a record in the information system (species, basinonym, synonym, doubtful species, etc.), methods of quantities calculations, author who determined the taxon in a probe, type of presentation of the material in a publication (data on a sample, a group of samples, group of outcrops, or borings, general summary for a region), the level of certainty in identification of a specimen, precision and method of obtaining coordinates for the sample collection, weather, lithotypes of rocks and their description, and many other parameters, which are presented in a uniform style (Fig. 65).

The main form contains series of bookmarks reflecting a certain type of information of this name (record). Figure 65 shows a fragment from the list of names (Edit species information). When the cursor is pointing a certain name (species) from this list, the list includes the main attributes (name, author, code of the source of information, old name of the genus), while a complete name of the taxon appears at the top of the general part of the form, and the right part contains complete synonymy. A series of buttons above the list are highlighted menu items that allow quick entry of a new record, identification of synonyms, or to enter information on the taxonomy of the species and the possibility of generalized information on all synonyms of this name.

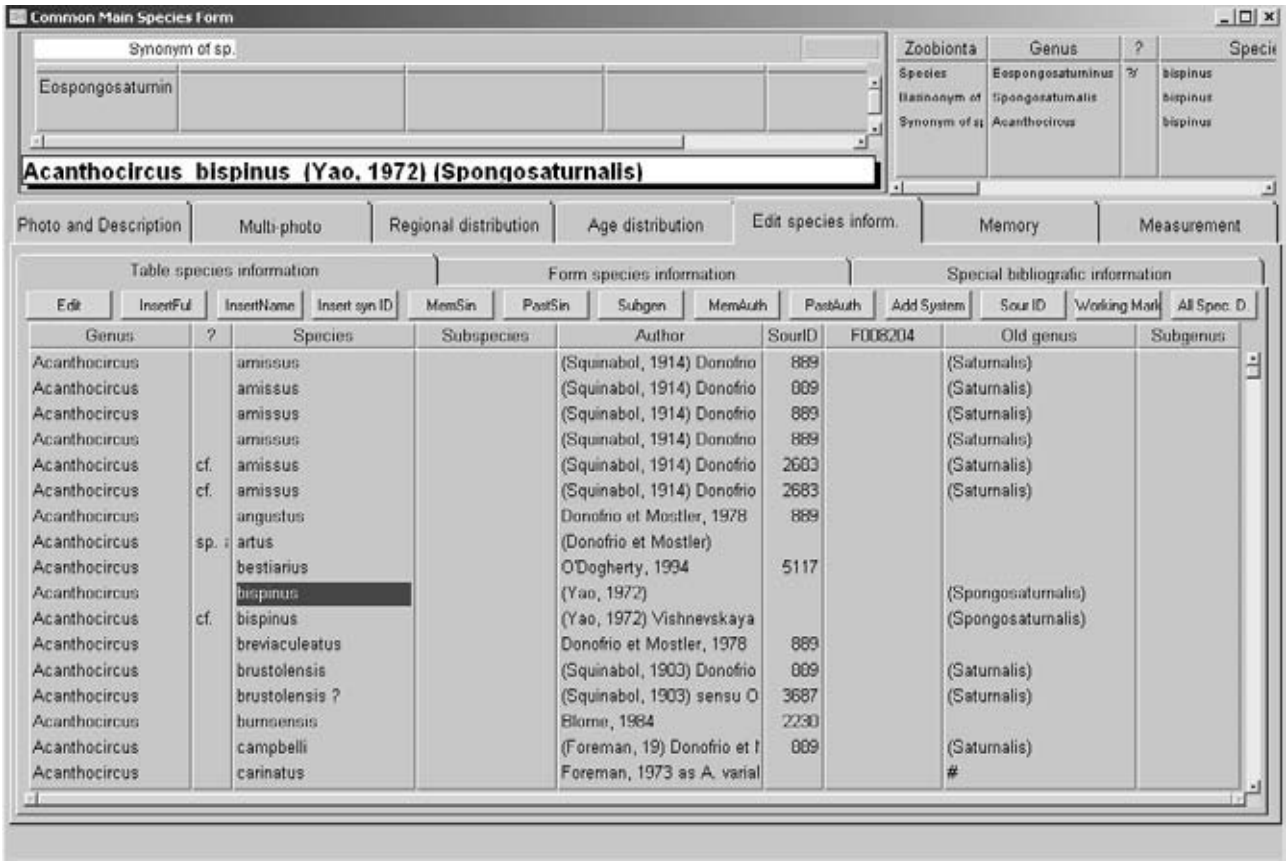

Fig. 65. Page "Editing of the list of species" in the main sheet of the radiolarian informational system.

The page "Photo and Description", the field "Name" gives the opportunity to screen all images and descriptions related to this name (scanned and reduced in a same format) that are related to this name (Fig. 66). The same field provides the information on the geochronological range of the species. The series of deeper fields "Name table" contains all lists of images with explanations and all descriptions with notification of the type of data (descriptions of the holotype, redescriptions, notes, etc.). When necessary these data, but for the entire species with a possibility of choice of the alternative synonymy, may be found in the field "Species".

To view several images of a synonym or species, there is a page "Multiphoto" (Fig. 67). Using it, it is possible to view eight images simultaneously or retune it to any amount of simultaneously viewed images depending on the hardware. This page, like the previous one, contains all images in a uniform format. Special fields of the worksheet of images contain the same images, which are shown in two standard scales depending on the quality of the original source, which allows small and large radiolarians to be viewed. This system of presentation of graphic information allows evaluation of morphological features of specimens and to visually estimate changes in their size, which is especially valuable in analyzing the geographical distribution and introducing the images onto the maps.

The block of spatial–age distribution allows storage of information on the taxa in any convenient system of identification of locations (administrative, tectonic, etc.), including geographical coordinates connecting the information system with electronic maps. The information is organized on principle taxon–sample, with all available information on the sample, including the certainty of species identification, age, and geographical location of the site provided. The age is given in various variants (stages, formations, zones) and does not restrict the user's opportunity to input an alternative dating based on other fossil groups, multiple alternative encoding, etc.). The stratigraphic dictionary includes over 1100 stratigraphic terms, while the block itself includes over 200000 records.

The bibliographic block in the micropaleontological analysis is generally used for data about the source of information, although it can work as an independent bibliographic information system, including over 9000 papers and representing the most complete Russian-language bibliography of radiolarians (over 4500 papers). Apart from the standard description of the source of information in the original language, this block contains a summary of the publication and,

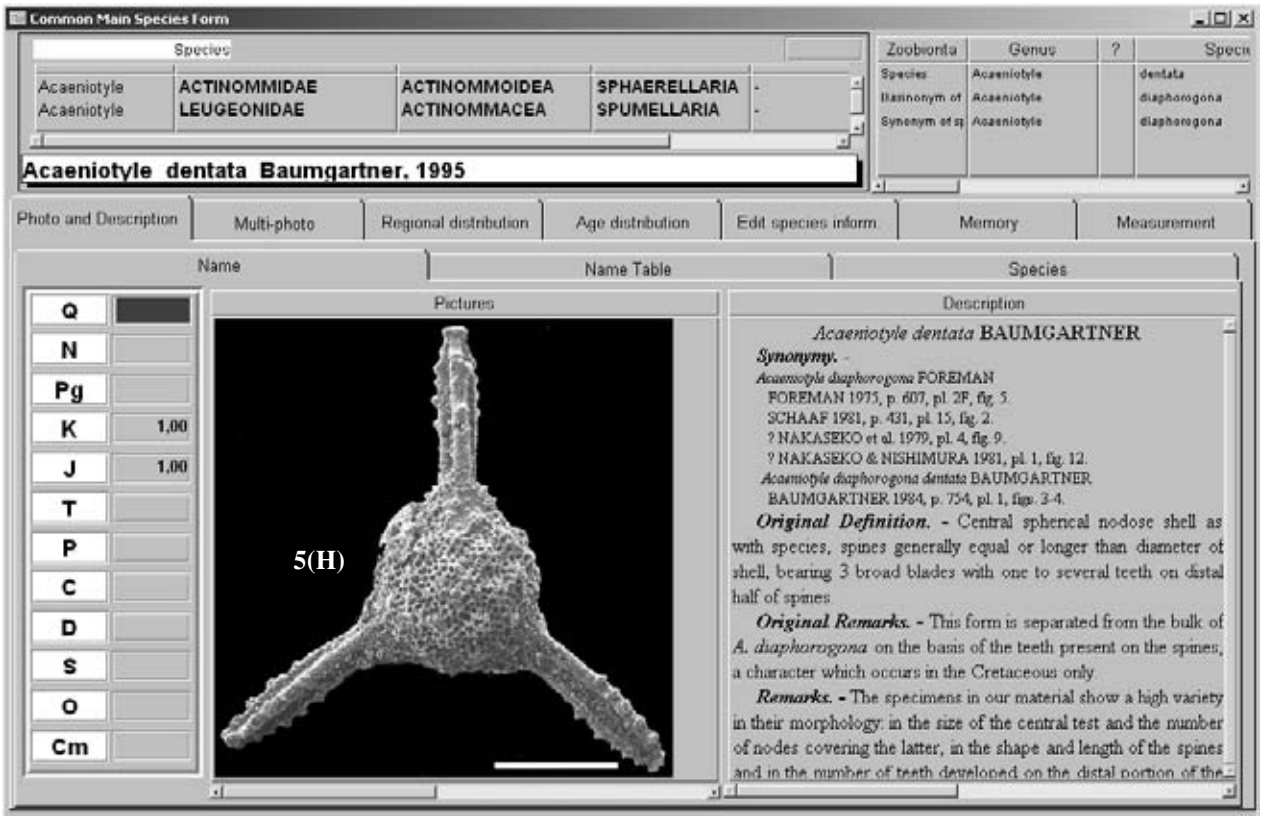

Fig. 66. Representation of comprehensive information of the species description, illustrations, synonymy, and taxonomy of a species.

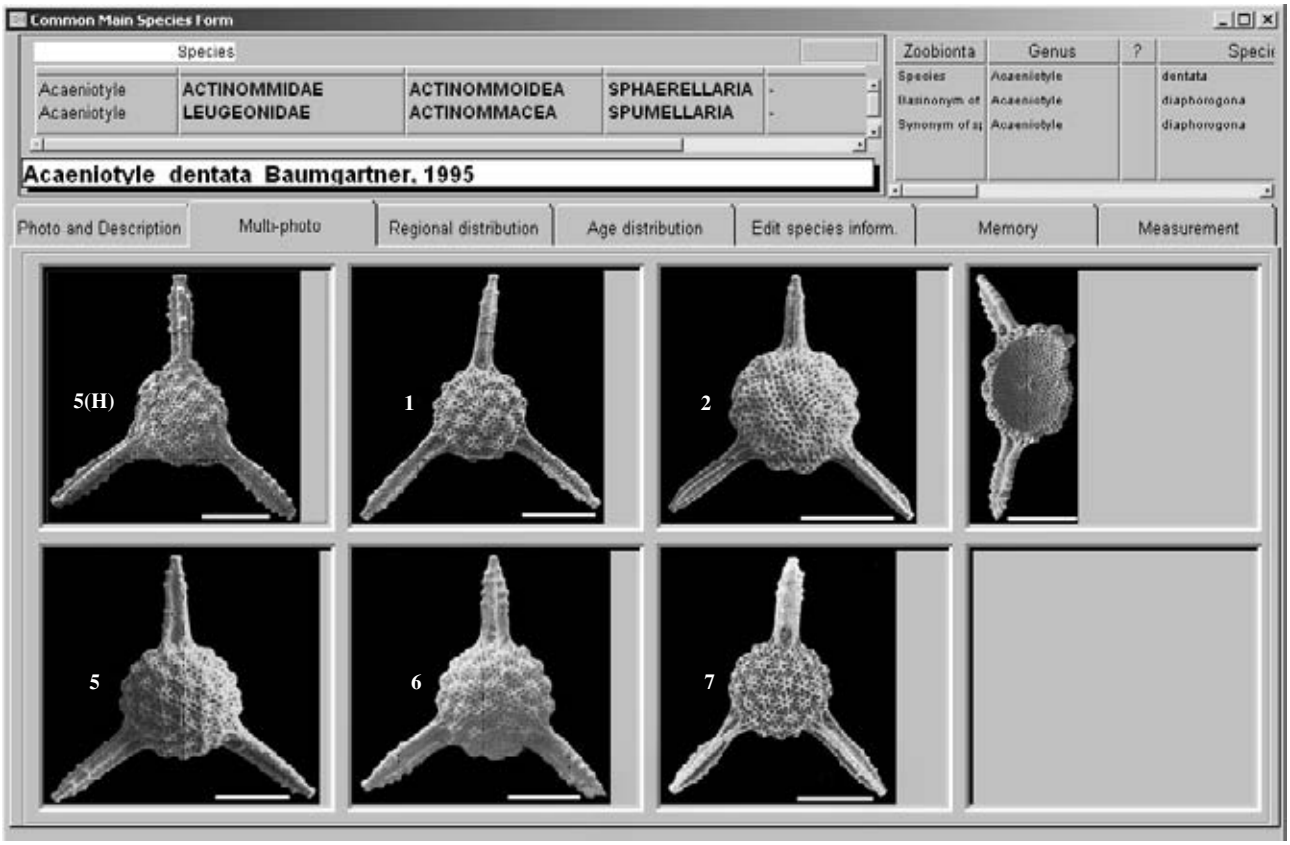

Fig. 67. Multiform representation of the illustrations of a species.

sometimes, the complete source with all available illustrations. The search system of this block allows publications and manuscripts to be found based on virtually any key (three-levelled indicator of the topic of the publication, author and year of publication, language, classes of organisms described, geological age, four-levelled indicator of the geographical scope of the paper, petrographic characterization of objects, etc.).

The use of the information system allows the construction of the maps of the geographical ranges of species, establishment of zones of divergence, determination of the geological age of samples based on the summary of their morphological features, analysis of the ecological conditions of the environment, estimation of the species diversity of the supraspecific taxa with a precision from erathem to subage, taking into account any additional conditions (morphological elements and parameters of skeletons, ecology, etc.) Calculation of rates of speciation and appearance of genera is based on the data of Afanasiev (1998, 2004) on the durations of the main geochronological subdivisions and uses the information from 4020 papers and 110 000 species/sample identifications, constantly updated from new publications.

APPENDIX. ALPHABETICAL INDEX OF RADIOLARIAN GENERA, THEIR DISTRIBUTION AND SYNONYMS FROM THE DATABASE RADBASE

Acaeniotyle Fereman, 1973, $J_1t–K_2km$

Acaeniotylopsis Kito et De Wever, 1994, $J_1t–J_3o$

Acaenispongus Kozur et Mostler, 1981, T_2l

Acanthobotrys Popofsky, 1913, nom. invalid. (sin.: *Botryocyrtis* Ehrenberg, 1860, sensu Petrushevskaya, 1965)

Acanthocircus Squinabol, 1903, emend. Donofrio et Mostler, 1978, $T_3c–K_2m$

Acanthocorallium Haeckel, 1887, nom. oblit.

Acanthocoronium Haeckel, 1887, emend. Petrushevskaya, 1981, $N–Q_4$

Acanthocorys Haeckel, 1882, $K–Q_4$

Acanthocorythium Haeckel, 1887, nom. oblit.

Acanthocyrtis Haeckel, 1881, Kz

Acanthodesmia Müller, 1856, $N_1?–Q_4$

Acantholonche Haeckel, 1881, Q_4

Acanthopyle Vinassa de Regny, 1898, $T_3c–J_3t$

Acanthosphaera Ehrenberg, 1858, $S_1–Q_4$

Acastea Yang, 1993, $J_2b–K_1al$

Acerahedrina Vinassa, 1900, sensu Riedel et Sanfilippo, 1970, nom. invalid. (sin.: *Lychnocanium* Ehrenberg, 1847)

Acerocanium Vinassa, 1900, sensu Riedel et Sanfilippo, 1970, nom. invalid. (sin.: *Lychnocanium* Ehrenberg, 1847)

Acidnomelos Foreman, 1968, K

Aciferopylorum Nazarov et Ormiston, 1987, $S_1–S_2$

Acotripus Haeckel, 1881, $J_3t–K_2s$

Acrobotrissa Haeckel, 1887, sensu Petrushevskaya, 1981, nom. invalid. (sin.: *Acrobotrys* Haeckel, 1881, sensu Petrushevskaya, 1965)

Acrobotrys Haeckel, 1881, sensu Petrushevskaya, 1965, $Pg–Q_4$

Acrocorona Haeckel, 1881, Q_4

Acrocubus Haeckel, 1881, nom. invalid. (sin.: *Eucoronis* Haeckel, 1881)

Acromelisa Haeckel, 1881, emend Petrushevskaya, 1981, Pg

Acropyramis Haeckel, 1881, $K?–Q_4?$

Acrosphaera Haeckel, 1881, $D–Q_4$

Acrospyris Haeckel, 1881, nom. invalid. (sin.: *Dendrospyris* Haeckel, 1881)

Actinomma Haeckel, 1860, emend. Nigrini, 1967, $D_3–Q_4$

Actinopyramis Haeckel, 1887, nom. oblit.

Actinosphaera Hollande et Enjument, 1960, Q_4

Actissa Haeckel, 1887, Q_4

Acutacapsula Tikhomirova, 1983, $J_3–K_1$

Adamas Afanasieva, 2000, D_3fm

Adelocyrtis Pantanelli, 1880, $Є–Q_4$

Aegospyris Haeckel, 1881, nom. invalid. (sin.: *Dendrospyris* Haeckel, 1881)

Afens Riedel et Sanfilippo, 1974, $K_2t–K_2km$

Alacorys Haeckel, 1881, $T–Q_4$

Alatipicapora Tekin, 1999, $T_3c–T_3n$

Albaillella Deflandre, 1952, $C_1t–P_2s$

Albatrossidium Sanfilippo et Riedel, 1992, $Pg_2y–Pg_2p$

Alievium Pessagno, 1972, $J_1t–K_2m$

Allocyrtium Afanasjeva, 1986, $C_1t–C_1v$

Amphiactura Haeckel, 1881, Q_4

Amphibracchium Haeckel, 1881, emend. Baumgartner, 1980, $D–Q_4$

Amphicarydiscus Lipman, 1972, $Pg_1d–N_1s$

Amphicraspedum Haeckel, 1881, $Pg_1t–Q_4$

Amphicyclia Haeckel, 1881, $Pg_2p–Q_4$

Amphimelissa Jörgensen, 1905, sensu Petrushevskaya, 1971, $N_2?–Q_4$

Amphimenium Haeckel, 1882, $Pg_2–Q_4$

Amphiplecta Haeckel, 1881, sensu Petrushevskaya, 1971, $N_1–Q_4$

Amphipternis Foreman, 1973, emend. Petrushevskaya, 1975, $K_1al–Pg_2l$

Amphipyle Haeckel, 1881, Q_4

Amphipylonium Haeckel, 1881, Q_4

Amphipylura Haeckel, 1887, Q_4

Amphipyndax Foreman, 1966, emend. Empson-Morin, 1981, 1982, $J_2b–Pg_1d$

Amphirhopalum Haeckel, 1882, nom. invalid. (sin.: *Amphirrhopalum* Haeckel, 1887)

Amphisphaera Haeckel, 1881, $T_2a–T_2?$

Amphispyris Haeckel, 1881, Q_4

Amphistylus Haeckel, 1882, $J_3t–Q_4$

Amphitholonium Haeckel, 1887, Q_4

Amphitholus Haeckel, 1887, Q_4

Amphymenium Haeckel, 1881, $D_3–Q_4$

Anachoreta O'Dogherty, 1994, $K_1al_3–K_2s_2$

Anakrusa Nazarov, 1977, $O_1a–O_2ll$

Androcyclas Jörgensen, 1905, $N–Q_4$

Andromeda Baumgartner, 1980, in Baumgartner *et al.*, 1980, J_3

Androspyris Haeckel, 1887, $N–Q_4$

Angulobracchia Baumgartner, 1980, $J_1t–K_1a_3$

Angulocircus Lahm, 1984, T

Anisicyrtis Kozur et Mostler, 1981, $T_2a–J$

Annikaella De Wever, 1988, $K_2s–K_2st$

Annulatospira Clark et Campbell, 1945, nom. invalid. (sin.: *Spongocyclia* Haeckel, 1862)

Annulopoulpus Kozur et Mostler, 1981, $T_3c–T_3n$

Annulosaturnalis Dosztaly, 1991, T_3c

Annulotriassocampe Kozur in Kozur et Mostler, 1994, $T_2l–T_3n$

Anomalacantha Benson, $N_1a–Q_4$

Antarctissa Petrushevskaya, 1967, $Pg_2p–Q_4$
Anthocorys Haeckel, 1881, J–N
Anthocyrtella Haeckel, 1887, sensu Petrushevskaya et Kozlova, 1972, T–Pg
Anthocyrtidium Haeckel, 1881, $Pg_2–Q_4$
Anthocyrtis Ehrenberg, 1847, $K–Q_4$
Anthocyrtissa Haeckel, 1887, sensu Petrushevskaya, 1981, nom. invalid. (sin.: *Anthocyrtidium* Haeckel, 1881)
Anthocyrtium Haeckel, 1887, $Pg_2–Q_4$
Anthocyrtoma Haeckel, 1887, sensu Riedel et Sanfilippo, 1970, $Pg–Q_4$
Anthocyrtonium Haeckel, 1887, sensu Petrushevskaya, 1981, Kz
Anthocyrtura Haeckel, 1887, sensu Petrushevskaya, 1981, N
Anthospyris Haeckel, 1881, Q_4
Apophysisphaera Won, 1997, $D_2–D_3f_2$
Arachnocalpis Haeckel, 1881, Q_4
Arachnocorallium Haeckel, 1887, sensu Petrushevskaya, 1971, $N–Q_4$
Arachnocorys Haeckel, 1860, $Pg–Q_4$
*Arachnopegm*a Haeckel, 1881, Q_4
Arachnopila Haeckel, 1887, Q_4
Arachnopilium Haeckel, 1881, nom. invalid. (sin.: *Clathrolychnus* Haeckel, 1881)
Arachnoplecta Dumitrica et Zugel, 2003, J_3t
Arachnosphaera Haeckel, 1862, Q_4
Arachnostylus Hollande et Enjument, 1960, Q_4
Arcanicapsa Takemura, 1986, J_3t
Archaeocenosphaera Pessagno et Yang, 1989, in Pessagno *et al.*, 1989, $T_3r–K_2t$
Archaeocenosphaera Obut et Iwata, 2000, $Є_1–Є_2$
Archaeodictyomitra Pessagno, 1976, $J_1t–Pg_3h$
Archaeohagiastrum Baumgartner, 1984, $J_1s–J_3o$
Archaeosemantis Dumitrica, 1978, $T_1o–T_3n$
Archaeospongoprunum Pessagno, 1973, $T_3c–K_2m–Pg_2$?
Archaeothamunulus Dumitrica, 1982, $T_2a–T_2l$
Archaeotritrabs Steiger, 1992, $K_1v–K_1br$
Archibursa Haeckel, 1881, Kz
Archicapsa Haeckel, 1881, $T_1i–Q_4$
Archicircus Haeckel, 1887, nom. invalid. (sin.: *Lithocircus* Müller, 1858, sensu Petrushevskaya, 1971)
Archicorys Haeckel, 1881, $K–Q_4$
Archidiscus Haeckel, 1887, C_1?$–Q_4$
Archinella Kozur et Mostler, 1981, $D_3fm–D_3fm$
Archipera Haeckel, 1881, nom. oblit., Q_4
Archiperidium Haeckel, 1887, sensu Petrushevskaya, 1981, $Q_1–Q_4$
Archiphaena Haeckel, 1881, Q_4
Archiphatna Haeckel, 1881, $Pg–Q_1$
Archiphormis Haeckel, 1881, Q_4
Archipilium Haeckel, 1881, Q_4
Archiscenium Haeckel, 1881, $Kz–Q_4$
Archistephus Haeckel, 1887, nom. oblit.
Archocyrtium Deflandre, 1972, S_2?$–C_1v$
Arcicubulus Dumitrica, 1980, T_2a
Ares De Wever, 1982, $J_1s–J_2bt$
Arrectoalatus Nazarov et Ormiston, 1985, $C_3g–P_1$
Artiscus Haeckel, 1881, $N_1a–Q_4$
Artobotrys Petrushevskaya, 1971, $K–Q_4$
Artocapsa Haeckel, 1881, $J_3t–Q_4$
Artocyrtis Haeckel, 1887, sensu Petrushevskaya, 1981, $Pg–Q_4$
Artopera Haeckel, 1881, $N–Q_4$
Artoperina Campbell, 1951, Pg
Artophaena Haeckel, 1881, Q_4
Artophormis Haeckel, 1881, $K_2–Q_4$
Artopilium Haeckel, 1881, nom. invalid. (sin.: *Trictenartus* Haeckel, 1882)
Artostrobium Haeckel, 1887, $K_1al–Q_4$
Artostrobus Haeckel, 1881, sensu Petrushevskaya, 1971, $J_3t–Q_4$
Asecta Popofsky, 1913, nom. invalid. (sin.: *Carpocanarium* Haeckel, 1887, sensu Petrushevskaya et Kozlova, 1972)
Astractura Haeckel, 1881, $K_1–Q_4$
Astrocapsa Haeckel, 1887, Q_4
Astrocentrus Kozur et Mostler, 1979, T_2l
Astrocyclia Haeckel, 1881, $K_1–Q_4$
Astroentactinia Nazarov, 1975, $D_2ef–P_1$
Astromma Ehrenberg, 1847, nom. invalid. (sin.: *Cypassis* Haeckel, 1887)
Astrophacus Haeckel, 1881, $Pg_2y–Q_4$
Astrophormis Haeckel, 1887, sensu Petrushevskaya, 1981, nom. invalid. (sin.: *Retraphormis* Haeckel, 1882)
Astrosestrum Haeckel, 1881, $Pg_1d–Q_4$
Astrosphaera Haeckel, 1887, Q_4
Atactodiscus Haeckel, 1882, J
Atichocapsa Campbell et Clark, 1944
Aulielina Nazarov, 1977, $O_2ll–S_2$
Aulophacus Pessagno, 1962, K_2
Aurisaturnalis Dumitrica-Jud, 1994, $K_1v_3–K_1a_1$
Austrisaturnalis Kozur et Mostler, 1972, T_3c
Axellipsis Haeckel, 1887, $C–Q_4$
Axocorys Haeckel, 1881, $Pg–Q_4$
Axodiscus Haeckel, 1887, Q_4
Axoprunum Haeckel, 1887, $Pg_1d–Q_4$

Bacus Wu Hao-Ruo, 1986, K_2s
Bagotella Tikhomirova, 1987, J
Bagotum Pessagno et Whalen, 1982, $J_1s–J_2c$
Baloghisphaera Kozur et Mostler, 1979, T_3c
Baratuna Kozur et Mostler, 1981, T_2a
Bathrocalpis Clark et Campbell, 1942, sensu Petrushevskaya, 1971, nom. invalid. (sin.: *Ceratocyrtis* Butschli, 1882)
Bathropyramis Haeckel, 1881, $J_2c–Q_4$
Baumgartneria Dumitrica, 1982, T_2l
Becomiforma, $N_1l–N_1t$
Becus Wu Hao-Ruo, 1986, $J_3t_3–K_2t_1$
Bekoma Riedel et Sanfilippo, 1971, $Pg_1t–Pg_2y$
Belonostaurus Haeckel, 1887, Q_4
Belonozoum Haeckel, 1887, Q_4
Belowea Won Moon-Zoo, 1983, C_1
Bernoullius Baumgartner, 1984, $T_3c–K_1br$
Betraccium Pessagno 1979, in Pessagno, Finch et Abbott, 1979, $T_3c–J_1s$
Beturiella Dumitrica, Kozur et Mostler, 1980, $T_2a–T_2l$
Bientactinosphaera Afanasieva, 2000, $S_1r–T_2l$
Bikinella Tikhomirova, 1986, nom. invalid. (sin.: *Spinotriassocampe* Kozur, 1984)
Bipedis De Wever, 1982, $T_3n–J_1t$
Birkenmajeria Widz et De Wever, 1993, $T_3r–K_2s$
Bisphaerocephalina Petrushevskaya, 1965, $K_2km–Q_4$
Bisphaerocephalus Popofsky, 1908, ?$–Q_4$
Bissylentactinia Nazarov, 1975, $Є_1a–D_3f_2$
Bistarkum Yen, 1987, $T_3r–K_1br$
Bivallupus Pessagno et MacLeod, 1987, $J_3t–J_3t$
Bogdanella Kolar-Jurkovsek, 1989, T_2l

Borgertella Dumitrica, 1973, Pg_1
Borisella Afanasieva, 2000, O?–D_3f–D_3fm
Botryocampe Ehrenberg, 1860, emend. Petrushevskaya, 1975, N_1?–Q_4
Botryocella Haeckel, 1881, sensu Petrushevskaya, 1975, Pg–Q_4
Botryocephalina Petrushevskaya, 1965, Q_4
Botryocylinder Petrushevskaya, 1975, K–Pg
Botryocyrtis Ehrenberg, 1860, sensu Petrushevskaya, 1965, N_1l–Q_4
Botryometra Petrushevskaya, 1975, K–Pg
Botryopera Haeckel, 1887, sensu Petrushevskaya, 1975, Pg–Q_4
Botryopyle Haeckel, 1881, emend. Petrushevskaya, 1965, Pg_2p–Q_4
Botryostrobus Haeckel, 1887, emend. Nigrini, 1977, Pg_2l–Q_4
Brachiospyris Haeckel, 1881, Pg_2–Q_4
Braginastrum Tekin, 1999, T_3c–T_3n
Braginella Sugiyama, 1997, T_3n–T_3r
Broctus Pessagno et Whalen, 1982, J_1s–J_2
Buccinosphaera Haeckel, 1887, Q_1k–Q_4
Bulbocyritum Kozur et Mosrler, 1981, emend. Tekin, 1999, T_2l–T_3n
Bullacapsula Tikhomirova, 1983, J_3–K_1
Buryella Foreman, 1973, Pg_1d–Q_4
Busuanga Yeh, 1990, T_2l
Byssulentactinia Nazarov, 1988, O_2ll

Cachecreekaria Dumitrica et Carter, 1999, K_2c
Callela Won Moon-Zoo, 1983, C_1
Callimitra Haeckel, 1881, Q_1?–Q_4
Calocapsa Haeckel, 1887, nom. oblit.
Calocyclas Ehrenberg, 1847, K–Q_4
Calocycletta Haeckel, 1887, sensu Riedel et Sanfilippo, 1970, Pg_2p–Q_2s
Calocycloma Haeckel, 1887, sensu Petrushevskaya, 1981, Pg_2y–Pg_2p
Calocyclura Haeckel, 1887, sensu Petrushevskaya, 1981, Pg_1t–Pg_2l
Calompterium Clark et Campbel, 1942, nom. oblit.
Calosphaera Campbell, 1951, nom. invalid. (sin.: *Thalassosphaera* Haeckel, 1887)
Calpophaena Haeckel, 1881, Q_4
Caltrop Carter, 1988 in Carter, Cameron et Smith, 1988, J_1t
Calyptocoryphe Foreman, 1968, K
Caminosphaera Haeckel, 1887, Q_4
Campanuilithus Nazarov et Rudenko, 1981, P_1s–P_1ar
Camptoalatus Nazarov et Rudenko, 1981, C_3g–P_1ar
Canarachnium Caulet, 1971
Cancellosphaera Afanasieva, 2000, D_3f_1–D_3f_2
Canesium Blome, 1984, T_3c
Caneta Pessagno, Blome et Hull, 1993, J_3–K_1br
Cannartidium Haeckel, 1887, Q_4
Cannartiscus Haeckel, 1887, Q_4
Cannartus Haeckel, 1881, emend. Riedel, 1971, N_1a–Q_4
Cannobotrys Haeckel, 1881, J_1–Q_4
Cannocapsa Haeckel, 1887, Q_4
Canoptum Pessagno in Pessagno *et al.*, 1979, T_2a–K_1v
Cantalum Pessagno in Pessagno, Finch et Abbott, 1979, T_3n–J_3t
Cantharospyris Haeckel, 1887, Pg_2?–Q_4
Canutus Pessagno et Whalen, 1982, T_3n–J_3o
Capnodoce De Wever, 1979, emend. Pessagno, 1979, emend. Blome, 1983, T_3c–T_3n
Capnuchosphaera De Wewer, 1979, T_2l–T_3n_2
Carinaheliosoma Kozur et Mostler, 1981, T_3c–T_3n
Carpocanarium Haeckel, 1887, sensu Petrushevskaya et Kozlova, 1972, nom. invalid. (sin.: *Tricolocapsa* Haeckel, 1881)
Carpocanistrum Haeckel, 1887, J_3t–Q_4
Carpocanium Ehrenberg, 1847, sensu Petrushevskaya et Kozlova, 1972, N_1–Q_4
Carpocanobium Haeckel, 1887, sensu Petrushevskaya, 1981, nom. invalid. (sin.: *Carpocanarium* Haeckel, 1887, sensu Petrushevskaya et Kozlova, 1972)
Carpocanopsis Riedel et Sanfilippo, 1971, Pg_3h–N_1s
Carpocryptocapsa Petrushevskaya, 1981, K–Pg
Carposphaera Haeckel, 1881, D–Q_4
Caryomma Haeckel, 1887, Q_4
Caryosphaera Haeckel, 1881, D–Q_4
Caryostylus Haeckel, 1881, Q_4
Caspiaza Afanasieva, 1986, emend. Afanasieva 1993, D_3fm–C_2b
Cassideus Pessagno, 1969, K_2s–N
Castrum Blome, 1984, T_2l–T_3n
Catenopyle Dumitrica, 1989, K_2m–Pg1d
Catoma Blome, 1983, T_3c–T_3n
Caucasicus Mamedov, 1984, Pg
Cavabracchia Kito et De Wever, 1992, J_2b–J_2bt
Cavaspongia Pessagno, 1973, K_1al$_2$–K_2km
Cavidiscus Pessagno, 1976, J_3–K_2t
Cecrops Pessagno, 1977, J_3t–K_1a
Cecryphalium Haeckel, 1881, C–Q_4
Cenellipsis Haeckel, 1882, $Є_1$t– Q_4
Cenocapsa Haeckel, 1887, Q_4
Cenodiscus Haeckel, 1887, S_1–Q_4
Cenolarcopyle Tan Sin Hok, 1931, K?
Cenolarcus Haeckel, 1887, Q_4
Cenosphaera Ehrenberg, 1854, $Є_3$–Q_4
Centracontarium Popofsky, 1912, Q_4
Centracontium Popofsky, 1912, Q_4
Centrobotrys Petrushevskaya, 1965, Pg_3r–Q_4
Centrocubus Haeckel, 1887, Q_4
Centrolonche Popofsky, 1912, Q_4
Cephalopyramis Haeckel, 1881, Pg
Cephalospyris Haeckel, 1881, Q_4
Cephaluspinus Martin, 1971, nom. invalid. (sin.: *Lophophaena* Ehrenberg, 1847, sensu Petrushevskaya, 1971)
Ceratarachnium Haeckel, 1881, sensu Petrushevskaya, 1981, nom. invalid. (sin.: *Cornutella* Ehrenberg, 1838, sensu Petrushevskaya, 1967)
Ceratobotrys Nishimura, 1990, Q_4
Ceratocyrtis Butschli, 1882, sensu Petrushevskaya, 1971, K_1b–Q_4
Ceratoikiscum Deflandre, 1953, O_2ll–P_2c
Ceratospyris Ehrenberg, 1847, sensu Nigrini, 1967, Pg_2y–Q_4
Cessipylorum Nazarov, 1986, O_2ll–S_1
Chaenicosphaera Haeckel, 1887, Q_4
Challengeron Haeckel, 1887, N_2z–Q_4
Chitonastrum Haeckel, 1881, N_1–Q_4
Choenicosphaera Haeckel, 1887, Q_4
Cinclopyramis Haeckel, 1881, K_2km–Q_4
Cinguloturris Dumitrica, 1982, J_2c–K_1v
Circodiscus Kozlova, 1972, Pg_1t–N_1s
Circospyris Haeckel, 1881, Q_4
Circotympanum Haeckel, 1887, Q_4
Circulaforma Cheng, 1986, D_3f_2–C_1
Citriduma De Wever, 1982, T_3n–J_1s

Cladarachnium Haeckel, 1881, Kz
Cladococcus Müller, 1856, Q_4
Cladoscenium Haeckel, 1881, N–Q_4
Cladospyris Ehrenberg, 1847, nom. invalid. (sin.: *Ceratocyrtis* Butschli, 1882)
Clathrobursa Haeckel, 1881, Pg_3–Q_4
Clathrocanium Ehrenberg, 1860, N_1s–Q_4
Clathrocorona Haeckel, 1881, Kz
Clathrocorys Haeckel, 1881, Pg_3r–Q_4
Clathrocyclas Haeckel, 1881, emend. Foreman, 1968, J_1–Q_4
Clathrocycloma Haeckel, 1881, sensu Petrushevskaya, 1981, Pg_1d–Q_4
Clathrocyrcus Haeckel, 1881, Q_4
Clathrolychnus Haeckel, 1881, Pg–N
Clathromitra Haeckel, 1881, sensu Petrushevskaya, 1971, Kz
Clathropyrgus Haeckel, 1881, K_2t–Kz
Clathrosphaera Haeckel, 1881, Q_4
Clathrospyris Haeckel, 1881, Pg_2y–Q_4
Clistophaena Haeckel, 1881, K_2–Q_4
Coccocyclia Haeckel, 1881, Q_4
Coccodiscus Haeckel, 1862, K_1–Q_4
Coccolarcus Haeckel, 1887, Q_4
Coccolarnacium Dumitrica, 1989, Pg_2
Collosphaera Müller, 1855, Q_2s–Q_4
Collozoum Haeckel, 1862, Q_4
Combusta Yeh, 1987, J_1
Conarachnium Haeckel, 1881, Q
Coniforma Pessagno, 1969, K_2km–K_2m_1
Conoactinomma Gorbunov, 1979, Pg_1t–Pg_2l
Conocaryomma Haeckel, 1887, sensu Petrushevskaya, 1981, K–Q_4
Conocaryomma Lipman, 1969, emend. Kozlova, 1999, Pg_2y–Pg_2p
Conosphaera Haeckel, 1881, T_1i–Q_4
Conostrobus Haeckel, 1887, sensu Petrushevskaya, 1981, ?–Q_4
Copicyntra Nazarov et Ormiston, 1985, C_3g–P_2s
Copicyntroides Nazarov et Ormiston, 1985, C_3–P_2
Copiellintra Nazarov et Ormiston, 1985, C_3–P_2
Cornucapsula Tikhomirova, 1983, J_3–K_1
Cornustrobus Haeckel, 1887, sensu Petrushevskaya, 1981, nom. invalid. (sin.: *Lithostrobus* Buetschli, 1882)
Cornutanna Haeckel, 1881 = *Cornutella* Ehrenberg, 1838, subjective syn.
Cornutella Ehrenberg, 1838, sensu Petrushevskaya, 1967, J_3o–Q_4
Cornutellium Haeckel, 1881, J–Q_4
Cornutosa Haeckel, 1881, sensu Petrushevskaya, 1981, nom. invalid. (sin.: *Cornutella* Ehrenberg, 1838, sensu Petrushevskaya, 1967)
Cornutovum Foreman, 1968, K_1
Cornutura Haeckel, 1881, nom. invalid. (sin.: *Cornutella* Ehrenberg, 1838, sensu Petrushevskaya, 1967)
Corocalyptra Haeckel, 1887, N_1l–Q_4
Coronidium Haeckel, 1881, Q_4
Coronosphaera Haeckel, 1887, Q_4
Cortina Haeckel, 1887, Kz–Q_4
Cortiniscus Haeckel, 1887, nom. oblit., Q_4
Corum Blome, 1984, T_2l–T_3n
Corythoecia Foreman, 1963, D_3fm–P_1a
Corythomelissa Campbell, 1951, sensu Petrushevskaya, 1975, Pg_3r–Pg_3h
Corythospyris Haeckel, 1881, emend. Goll, 1978, Pg_2l–Q_4
Coscinomma Haeckel, 1887, Q_4
Craterocyclas Haecker, 1908, nom. invalid. (sin.: *Lamprocyclas* Haeckel, 1881)
Cristallosphaera Popofsky, 1912, Q_4
Crolanium Pessagno, 1977, J_3t–K_2km
Cromyatractus Haeckel, 1887, Pg_2p–Q_4
Cromydruppocarpus Campbell et Clark, 1944, N_1
Cromyechinus Haeckel, 1881, K_1–Q_4
Cromyocarpus Haeckel, 1887, Pg_1d–Q_4
Cromyodrimus Haeckel, 1881, K_1al–Q_4
Cromyodruppa Haeckel, 1887, C–Q_4
Cromyomma Haeckel, 1881, S_1–Q_4
Cromyosphaera Haeckel, 1881, C–Q_4
Cromyostaurolonche Clark et Campbell, 1944, N_1
Cromyostaurus Haeckel, 1881, Q_4
Cromyostylus Haeckel, 1881, Q_4
Crubus Yeh, 1987, J_1t–J_2b
Crucella Pessagno, 1971, T_3c–Pg_2y
Crucidiscus Haeckel, 1887, S_1?–J_1–Q_4
Cryptamphorella Dumitrica, 1970, T_3c–K_2km_1
Cryptocapsa Haeckel, 1881, J_2b–Q_4
Cryptocarpium Sanfilippo et Riedel, 1992, Pg_1t–Pg_2p
Cryptocephalus Dumitrica, 1978, J
Cryptolarnacium Dumitrica, 1989, Pg_1–Pg_2
Cryptoprora Ehrenberg, 1860, Pg_2–Q_4
Cryptostephanidium Dumitrica, 1978, T_1o–T_3c
Cubaxonium Haeckel, 1887, C_1t–Q_4
Cuboctostylus Bragina, 1999, K_2s–K_2k
Cubosphaera Haeckel, 1887, Q_4
Cubotholonium Haeckel, 1887, Q_4
Cubotholus Haeckel, 1887, Q_4
Cuniculiformis De Wever, 1982, J_1s
Curvechidnina Won, 1990, Є
Cycladophora Ehrenberg, 1872, emend. Lombari et Lazarus, 1988, T_3c–N
Cyclampterium Haeckel, 1887, Pg_2l–N_2z
Cyclastrum Rüst, 1898, J_3t–K_1a_2
Cyclocarpus Li et Wang, 1991, D_3f_3
Cypassis Haeckel, 1887, N_1a–Q_4
Cyphanta Haeckel, 1887, D_1–Q_4
Cyphinidium Haeckel, 1887, Q_4
Cyphinus Haeckel, 1881, K–Q_4
Cyphocolpus Haeckel, 1887, Q_4
Cyphoniun Haeckel, 1887, K–Q_4
Cyrcotympanum Haeckel, 1887, Q_4
Cyrthentactinia Foreman, 1963, D_3fm
Cyrtisphaeractenium Deflandre, 1972, D_3fm–C_1v
Cyrtisphaeronemium Deflandre, 1972, D_3fm–C_1v
Cyrtocalpis Haeckel, 1860, D–Q_4
Cyrtocapsa Haeckel, 1881, J_2b–Q_4
Cyrtocapsella Haeckel, 1887, emend. Sanfilippo et Riedel, 1970, J_3t–Q_2s
Cyrtocapsoma Haeckel, 1887, sensu Petrushevskaya, 1981, nom. invalid. (sin.: *Cyrtocapsella* Haeckel, 1887, emend. Sanfilippo et Riedel, 1970)
Cyrtocorys Haeckel, 1887, nom. oblit.
Cyrtolagena Haeckel, 1879, emend. Petrushevskaya, 1971, K–Q_4
Cyrtolepis Rüst, 1885, nom. invalid. (sin.: *Cyrtocalpis* Haeckel, 1860)
Cyrtopera Haeckel, 1881, N_2z–Q_4
Cyrtophormis Haeckel, 1887, K_2k–Q_4
Cyrtophormiscus Haeckel, 1887, sensu Petrushevskaya, 1981, nom. invalid. (sin.: *Cyrtophormis* Haeckel, 1887)

Cyrtostephanus Popofsky, 1913, nom. invalid. (sin.: *Platybursa* Haeckel, 1881)

Cystidium Hertwig, 1879, Q_4

Cystophormis Haeckel, 1887, emend. Petrushevskaya, 1975, Pg_3–N_2

Dactyliodiscus Squinabol, 1903, K_1b_2–K_2s_2

Dactyliosphaera Squinabol, 1904, K_1a_2–K_2s

Deflandrastrum De Wever, 1983, T_3r–K

Deflandrecyrtium Kozur et Mostler, 1979, T_3c–T_3r

Deflandrella Loeblich et Tappan, 1961, T_2–Q_4

Deflandrella De Wever et Caridroit, 1984, P_2

Deflandrellium Cheng, 1986, D_3fm–C_1v

Deflantrica Wakamatsu, Sugiyama et Furutani, 1990, S–D

Dendrocyrcus Haeckel, 1881, Q_4

Dendrospyris Haeckel, 1881, emend. Goll, 1968, Pg_2y–Q_4

Desmartus Haeckel, 1887, Q_4

Desmocampe Haeckel, 1887, Q_4

Desmospyris Haeckel, 1881, Pg_2y–Q_4

Deviatus Li, 1986, J_3o–K_1al

Diacanthocapsa Squinabol, 1903, J_2b–Pg

Diartus Sanfilippo et Riedel, 1980, N_1s–Q_2s

Dibolachras Foreman, 1973, J_2bt–K_1a

Dicapnuchosphaera Tekin, 1999, T_3c–T_3n

Diceratigalea Takemura et Nakaseko, 1982, J

*Dicerosaturnali*s Dumitrica-Jud, J_3–K_2t

Dicolocapsa Haeckel, 1881, sensu Sanfilippo et Riedel, 1970, T_3c–N_1s

Distympanium Haeckel, 1887, C_1?–Q_4

Dicorys Popofsky, 1913, nom. invalid. (sin.: *Psilomelissa* Haeckel, 1881)

Dicranastrum Haeckel, 1881, Q_4

Dicroa Foreman, 1975, J_2b–K_2t_1

Dictyastrella Haeckel, 1887, nom. invalid. (sin.: *Dictyastrum* Ehrenberg, 1860)

Dictyastromma Haeckel, 1887, nom. invalid. (sin.: *Dictyastrum* Ehrenberg, 1860)

Dictyastrum Ehrenberg, 1860, C–Q_4

Dictyocephalus Ehrenberg, 1860, C?–J_3o–Q_4

Dictyoceras Haeckel, 1862, Pg_1t–Q_4

Dictyocircus Jörgensen, 1905, Q_4

Dictyocodoma Haeckel, 1887, sensu Petrushevskaya, 1981, Kz

Dictyocodon Haeckel, 1881, ?–Q_4

Dictyocoryne Ehrenberg, 1860, J_1h–Q_4

Dictyocryphalus Haeckel, 1887, sensu Loeblich et Tappan, 1961, nom. invalid. (sin.: *Lophophaena* Ehrenberg, 1847, sensu Petrushevskaya, 1971)

Dictyodedalus O'Dogherty, 1994, K_1al_2–K_2m

Dictyomitra Zittel, 1876, emend. Pessagno, 1976, D?–T_3c–N_1a

Dictyomitrella Haeckel, 1887, T_3c–J_3t

Dictyomitrissa Haeckel, 1887, sensu Petrushevskaya, 1981, nom. invalid. (sin.: *Dictyomitra* Zittel, 1876, emend. Pessagno, 1976)

Dictyophimium Haeckel, 1887, J–Q_4

Dictyophimus Ehrenberg, 1847, sensu Nigrini, 1967, J–Q_4

Dictyoplegma Haeckel, 1862, J

Dictyopodium Ehrenberg, 1847, Pg–Q_4

Dictyoprora Haeckel, 1881, sensu Nigrini, 1977, K?–Pg_3h

Dictyospyrella Haeckel, 1887, Pg_2y–Pg_2p

Dictyospyris Ehrenberg, 1847, Pg_2y–Q_4

Didactylum Baumgartner, 1980, J

Didymocyrtis Haeckel, 1860, Pg_3r–Q_4

Dimelissa Campbell, 1951, sensu Petrushevskaya, 1971, nom. invalid. (sin.: *Psilomelissa* Haeckel, 1881)

Diplactura Haeckel, 1881, J_1h–Q_4

Diplellipsis Popofsky, 1908, Q_4

Diplocyclas Haeckel, 1881, K–Q_4

Diploplegma Hinde, 1890, S_1–Pg_2l

Diplosphaera Haeckel, 1860, Q_4

Diplospongus Mast, 1910, Q_4

Diplostrobus Squinabol, 1903, K_2km

Dipocoronis Haeckel, 1881, Pg_2?–N_1

Dipodospyris Haeckel, 1881, Pg

Dipospyris Haeckel, 1881, N_1–Q_4

Dipylissa Dumitrica, 1988, Pg_1d

Discopyle Haeckel, 1887, Pg_1t–Q_4

Discospira Haeckel, 1862, J

Discozonium Haeckel, 1887, Q_4

Disolenia Ehrenberg, 1860, Q_4

Dispongia Popofsky, 1912, Q_4

Dispongotripus Squinabol, 1903, K_1al_2–K_2s

Distriactis Haeckel, 1887, D?–Pg–Q_4

Distylocapsa Squinabol, 1904, K_1al_2–K_2km

Ditrabs Baumgartner, 1980, J_3t–K_1br

Divatella Kozur et Mostler, 1981, T_3c–T_3c

Dizonites Haeckel, 1887, Q_4

Dizonium Haeckel, 1881, C?–K–Q_4

Doracantha Haeckel, 1881, Q_4

Dorcadospyris Haeckel, 1881, emend. Goll, 1969, Pg_2l–Q_4

Doryconchidium Vinassa de Regny, 1898, J_3t

Dorydictium Hinde, 1890, S_1–K_2k

Dorydiscus Carnavale, 1908, N_1

Dorydruppa Vinassa de Regny, 1900, N_1

Dorylonchidium Vinassa de Regny, 1898, J_3t–Pg_2

Doryphacus Carnavale, 1908, N_1

Doryplegma Hinde, 1890, S_1–T

Dorypyle Squinabol, 1904, K_1al_2–K_2s_3

Dorysphaera Hinde, 1890, S_1–N_1

Dreyerella Kozur et Mostler, 1979, Q_4

Dreyericyrtium Kozur et Mostler, 1979, nom. invalid. (sin.: *Anthocyrtella* Haeckel, 1887, sensu Petrushevskaya et Kozlova, 1972)

Dreyeropyle Kozur et Mostler, 1979, Q_4

Droltus Pessagno et Whalen, 1982, T_3r–J_3k

Drulanta Yeh, 1987, J_1p–J_2b

Druppalonche Hinde, 1899, D

Druppastylus Cayeux, 1897, K_2

Druppatractus Haeckel, 1887, C_1–Q_4

Druppatractylis Haeckel, 1887, Pg_2–N_1

Druppocarpus Haeckel, 1887, K_2–Q_4

Druppula Haeckel, 1887, S–Q_4

Drymosphaera Haeckel, 1881, Q_4

Drymyomma Jörgensen, 1905, Q_4

Dumetum Popofsky, 1908, ?–Q_4

Dumitricaella De Wever, 1982, J_1h–J_1s
Dumitricaia Pessagno, 1976, K_2t
Dumitricasphaera Kozur et Mostler, 1979, T_2l–T_3c
Duodecimentactinia Won Moon-Zoo, 1997, D_3f_1
Duplexia Won Moon-Zoo, 1983, D_3fm–P_1a
Dyostephus Haeckel, 1881, nom. oblit.
Dystympanum Haeckel, 1887, Q_4

Eastonerius Empson-Morin, 1981, K_2km
Echidnina Won, 1998, Є
Echinactura Haeckel, 1887, Q_4
Echinomma Haeckel, 1881, C–Q_4
Echinosphaera Hertwig, 1879, Q_4
Ectonocorys Foreman, 1968, J_1s–K
Elaphococcus Haeckel, 1881, Q_4
Elaphospyris Haeckel, 1881, N_1–Q_4
Elatomma Haeckel, 1887, Q_4
Ellipsidium Haeckel, 1887, D–Q_4
Ellipsostygma Hinde, 1899, D
Ellipsostylus Haeckel, 1887, C–Q_4
Ellipsoxiphus Dunikowski, 1882, D–Q_4
Elodium Carter, 1988, in Carter *et al.*, 1988, J_1t–J_2a
Emiluvia Foreman, 1973, emend. Pessagno, 1977, T_3–K_1br
Enneaphormis Haeckel, 1881, sensu Petrushevskaya, 1971, K–Q_4
Enneaplagia Haeckel, 1881, nom. oblit., Q_4
Enneaplegma Haeckel, 1881, Kz
Enneapleuris Haeckel, 1887, sensu Petrushevskaya, 1981, nom. invalid. (sin.: *Acropyramis* Haeckel, 1881)
Enoplocampe Sugiyama, 1997, T_3r
Entactinia Foreman, 1963, D_2–T_1o
Entactinosphaera Foreman, 1963, nom. delendum (nom. subst.: *Bientactinosphaera* Afanasieva, 2000)
Entapium Sanfilippo et Riedel, 1973, Pg_1t–N_1s
Eonapora Kozur et Mostler, 1979, T_2a–T_2l
Eospongosaturninus Kozur et Mostler, 1990, J_2b–J_3t
Eostichomitra Empson-Morin, 1981, K_2t–K_2m
Eostylodictya Ormiston et Lane, 1976, C_1
Eoxitus Kozur, 1985, J_2b–J_3
Eptingium Dumitrica, 1978, T_2a–T_3r
Eribotrys Foreman, 1968, K_1al_2–K_2m
Ethmosphaera Haeckel, 1862, J_1–Q_4
Etymalbaillella Li, 1995, O_2
Eucecryphalium Haeckel, 1887, Pg_2–Q_4
Eucecryphalus Haeckel, 1860, Pg_1d–Q_4
Euchitonia Ehrenberg, 1872, J_3–Q_4
Eucoronis Haeckel, 1881, Pg_2p–Q_4
Eucyrtidiellum Baumgartner, 1984, T_3c–K_2km
Eucyrtidium Ehrenberg, 1847, emend. Nigrini, 1967, T_3c–Q_4
Eucyrtis Haeckel, 1887, sensu Foreman, 1973, J_2c–K_2st
Euscenarium Haeckel, 1887, sensu Petrushevskaya, 1981, Q_1–Q_4
Euscenium Haeckel, 1887, N–Q_4
Eusyringium Haeckel, 1881, T_1i–Q_4
Eusyringoma Haeckel, 1887, nom. invalid. (sin.: *Eusyringium* Haeckel, 1882)
Eutympanium Haeckel, 1881, Q_4
Ewingella Pessagno, 1969, K_1al–K_2s
Excentroconcha Hollande et Enjument, 1960, Q_4
Excentropylomma Dumitrica, 1970, K_1al–K_2t
Excingula Kozlova, 1994, J_3k

Falcispongus Dumitrica, 1982, T_2l–T_3c
Falsocromyodrymus O'Dogherty, 1994, K_1al_2–K_2t
Fantus Yeh, 1987, J_1
Farcus Pessagno, Whalen et Yeh, 1986, J_1p_2– J_1t_1
Fenestracantha Bertolini, 1935, nom. invalid. (sin.: *Lychnocanium* Ehrenberg, 1847)
Ferresium Blome, 1984, emend Carter, 1993, T_3n–T_3r
Follicucullus Ormiston et Babcock, 1979, P_2u–T_1o
Fontinella Carter, 1993, T_3n–J_1h
Foremanella Muzavor, 1977, nom. invalid. (sin.: *Deviatus* Li, 1986)
Foremanellina Dumitrica, 1982, T_2a–T_2l
Foremanhelena De Wever et Caridroit, 1984, P_2
Foremaniella Deflandre, 1972, D_3?–C_1
Foremanina Empson-Morin, 1981, K_2km
Foremina Empson-Morin, 1981, K_2km
Fueloepicyrtis Kozur et Mostler, 1981, T_2a
Fukujius Furutani, 1990, S–D
Fungomacula Won, 1999, Є
Fusalfanus Furutani, 1990, S_1w–S_2
Futobari Furutani, 1990, S_1w–D

Gamospyris Haeckel, 1881, nom. invalid. (sin.: *Dorcadospyris* Haeckel, 1881)
Gedauia Won Moon-Zoo, 1983, C_1–P_2
Gigi De Wever, 1982, J_1s
Giraffospyris Haeckel, 1881, Pg_2y–Q_4
Globolaxtorum Carter, 1993, T_3n–T_3r
Glomeropyle Aita et Bragin, 1999, T_2a–T_2l
Godia Wu, 1986, K_1v_1–K_2s_3
Goestlingella Kozur et Mostler, 1979, T_2a–Pg?
Gomberellus Dumitrica, Kozur et Mostler, 1980, T_2a–T_2l
Gondwanaria Petrushevskaya, 1975, Pg_1d–Q_4?
Gongylothorax Foreman, 1968, emend. Dumitrica, 1970, J_2b–K_2m
Gonosphaera Jörgensen, 1905, Q_4
Goodbodium Furutani, 1990, S–D
Gorgansium Pessagno et Blome, 1980, T_3c–K_1b
Gorgospyris Haeckel, 1881, Pg_2?–Pg_3h–Q_4
Grandetortura Sashida et Tonishi, 1991, P_2u–P_2s
Grandicapsula Kazintsova, 1985, K_1al–K_2st
Grosmorneus Won, 1990, Є
Guangxitrisphaera Wang, 1993, C_1
Guexella Baumgartner, 1984, J_2bt–J_3o
Guttacapsa O'Dogherty, K_1br–K_2s_3

Haeckelella Chabakov, 1937, K_1v
Haeckelicyrtium Kozur et Mostler, 1979, T_3c–T_3r
Haeckeliella Hollande et Enjument, 1960, Q_4
Hagiastrella Haeckel, 1887, nom. invalid. (sin.: *Hagiastromma* Haeckel, 1887)
Hagiastromma Haeckel, 1887 Q_4
Hagiastrum Haeckel, 1881, emend. Baumgartner, 1980, P–Q_4
Halesium Pessagno, 1971 emend. Baumgartner, 1980, J_3t–K_2t
Halicalyptra Ehrenberg, 1847, C?–J_1h–Q_4
Halicapsa Haeckel, 1881, C_1?–J_3t–Q_4
Halidictyum Ichikawa, 1950, T
Haliodictya Hojnos, 1916, J_2b–J_3t
Haliodictyum Ichikawa, 1950, T
Haliomma Ehrenberg, 1838, S_1–Q_4
Haliphormatidium Campbell, 1951, Kz

Haliphormis Ehrenberg, 1847, Q_4
Haplentactinia Foreman, 1963, O_1a–P
Haplodiacanthus Nazarov et Rudenko, 1981, C_3–P_1
Haplopolus Li Hong-sheng, 1994, O_2
Haplosphaera Hollande et Enjument, 1960, Q_4
Haplotaeniatum Nazarov et Ormiston, 1987, S_1
Hegleria Nazarov et Ormiston, 1985, P_2u–P_2s
Helenofore Nazarov et Ormiston, 1983, S_1r–C_1
Heliaster Hollande et Enjument, 1960, Q_4
Heliocryptocapsa Dumitrica, 1970, K_2km
Heliodiscus Haeckel, 1862, sensu Nigrini, 1967, S_1–Q_4
Heliodrymus Haeckel, 1881, Q_4
Helioentactinia Nazarov, 1975, D_2–T_2l
Heliosaturnalis Kozur et Mostler, 1972, emend. De Wever, 1984, T_3c–J_1p
Heliosestarium Campbell et Clark, 1944, K_2?
Heliosestrum Haeckel, 1881, D?–N_1a–Q_4
Heliosoma Haeckel, 1881, S_1–Q_4
Heliosphaera Haeckel, 1862, D–Q_4
Heliostylus Haeckel, 1881, Pg_1t N_1s
Helminentactinia Li Hong-sheng, 1994, S_2
Helotholus Jörgensen, 1905, sensu Petrushevskaya, 1971, Pg_3h–N_2p
Hemicryptocapsa Tan Sin Hok, 1927, J_3o–K_2m
Heptacladus Dumitrica, Kozur et Mostler, 1980, T_2a–T_2l
Heptaplegma Haeckel, 1881, nom. invalid. (sin.: *Ennaeplegma* Haeckel, 1882)
Hergelia Nazarov et Ormiston, 1985, Pz
Heterosestrum Clark et Campbell, 1945, Pg_1t–Pg_2p
Hexacaryum Haeckel, 1881, Q_4
Hexacontarium Haeckel, 1887, Q_4
Hexacontium Haeckel, 1882, emend. Kozur et Mostler, 1979, T_2a–Q_4
Hexacorys Haeckel, 1887, nom. oblit.
Hexacromyum Haeckel, 1881, Q_4
Hexactura Haeckel, 1882, Q_4
Hexacyclia Totchilina, 1970, Pg_2p
Hexadendron Haeckel, 1881, Q_4
Hexadoras Haeckel, 1881, K_2?–Q_4
Hexadoridium Haeckel, 1881, K_2–Q_4
Hexadorium Campbell et Clark, 1944, J
Hexadrymium Haeckel, 1882, nom. invalid. (sin.: *Hexacontium* Haeckel, 1882)
Hexalastromma Haeckel, 1887, nom. invalid. (sin.: *Hexactura* Haeckel, 1882)
Hexalastrum Haeckel, 1881, nom. invalid. (sin.: *Hexactura* Haeckel, 1882)
Hexalatractus Haeckel, 1887, Q_4
Hexalodus Haecker, 1908, nom. invalid. (sin.: *Lamprocyclas* Haeckel, 1881)
Hexaloncharium Haeckel, 1887, Q_4
Hexalonche Haeckel, 1881, J_3o–Q_4
Hexalonchidium Haeckel, 1881, Q_4
Hexancistra Haeckel, 1881, Q_4
Hexaphormis Haeckel, 1881, sensu Petrushevskaya, 1981, nom. invalid. (sin.: *Lamprodiscus* Ehrenberg, 1860)
Hexaplagia Haeckel, 1881, nom. oblit., Q_4
Hexaplecta Haeckel, 1887, nom. oblit., Q_4
Hexaplegma Haeckel, 1881, nom. oblit.
Hexaporobrachia Kozur et Mostler, 1979, T_3c
Hexapyle Haeckel, 1881, Q_4
Hexapylomella Kozur et Mostler, 1979, T_3c
Hexapyramis Squinabol, 1903, T–K_2t
Hexasaturnalis Kozur et Mostler, 1983, J_1t–J_2bt
Hexaspongonium Haeckel, 1881, Q_4
Hexaspyridium Haeckel, 1887, sensu Petrushevskaya, 1981, Pg_2–N_1
Hexaspyris Haeckel, 1887, Pg_2l–Q_4
Hexastylarium Haeckel, 1887, Q_4
Hexastylidium Haeckel, 1881, Q_4
Hexastylurus Haeckel, 1881, J_2c–K_2s
Hexastylus Haeckel, 1881, T_3c–Q_4
Hexinastrum Haeckel, 1881, K_1a–Q_4
Higumastra Baumgartner, 1980, J_1t–K_1br
Hilarisirex Takemura et Nakaseko, 1982, emend. Pessagno *et al.*, 1986, J_2b–J_3k
Hindeosphaera Kozur et Mostler, 1979, T_2a–T_3c
Hinedorcus Dumitrica, Kozur et Mostler, 1980, T_2a–T_3c
Hiscocapsa O'Dogherty, 1994, K_1br–K_1al_2
Histiastrella Haeckel, 1887, nom. invalid. (sin.: *Histiastrum* Ehrenberg, 1847)
Histiastromma Haeckel, 1887, nom. invalid. (sin.: *Histiastrum* Ehrenberg, 1847)
Histiastrum Ehrenberg, 1847, J_3t–Q_4
Histigiastrum Levikina, 1986, nom. invalid. (sin.: *Histiastrum* Ehrenberg, 1847)
Holdsworthum Furutani, 1990, S–D
Holocryptocanium Dumitrica, 1970, K_1b–K_2km
Holocryptocapsa Tan Sin Hok, 1926, K_1v_3–K_2km
Holoeciscus Foreman, 1963, D_3fm–C_1t
Homeoarchicorys Empson-Morin, 1981, K_2km
Homeoparonaella Baumgartner, 1980, T_3c–K_2t
Hozmadia Dumitrica, Kozur et Mostler, 1980, T_1o–T_3c
Hsuum Pessagno, 1977, emend. Takemura, 1986, J_1t–K_2s
Huasha Cheng, 1986, D_3fm–C_1
Hungarosaturnalis Kozur et Mostler, 1983, emend. Mostler et Krainer, 1994, T_2l–T_3c
Hymenactura Haeckel, 1881, Q_4
Hymeniastrella Haeckel, 1887, nom. invalid. (sin.: *Euchitonia* Ehrenberg, 1860)
Hymeniastromma Haeckel, 1887, nom. invalid. (sin.: *Euchitonia* Ehrenberg, 1860)
Hymeniastrum Ehrenberg, 1847, K_1–Q_4

Icrioma De Wever, 1979, emend. Blome, 1983, emend. Tekin, 1999, T_3c–T_3r
Immersothorax Dumitrica, 1970, K_2km–Q_4
Inanibigutta Nazarov, 1984, O_1a–S
Inanigutta Nazarov et Ormiston, 1984, $Є_1at$–S
Inanihella Nazarov et Ormiston, 1984, O_1a–S_2
Intermediella Lahm, 1984, nom. invalid. (sin.: *Paurinella* Kozut et Mostler, 1981)
Intocapsa Tikhomirova, 1987, J
Ishigaum De Wever et Caridroit, 1984, P_2u–P_2s

Jacus De Wever, 1982, J_1h–K_1h
Japonisaturnalis Kozur et Mostler, 1972, T_3c–J_2b–Kz
Japonocampe Kozur, 1984, T_3c–T_3n
Justium Blome, 1983, T_3c–T_3n

Kafanella Tikhomirova, 1987, J_2
Kahlerosphaera Kozur et Mostler, 1979, T_3c–T_3r
Karnospongella Kozur et Mostler, 1981, T_2l–T_3n
Kashiwara Blome, 1992, P

Kassinia Chabakov, 1937 emend. Petrushevskaya, 1981, J_3o–J_3k
Katorella Kozur et Mostler, 1981, T_2a–T_2l
Katroma Pessagno et Poisson, 1979, emend. De Wever, 1982, T_3r–K_1h
Kozurastrum De Wever, 1984, T_3n–J_2
Kozuricyrtium Tekin, 1999, T_3c–T_3n
Kozurium Pessagno, 1977, sensu Petrushevskaya, 1981, Mz
Krempelinella Empson-Morin, 1981, K_2km
Kreutzstella Empson-Morin, 1981, K_2km
Kungalaria Dumitrica et Carter, 1999, T_3r
Kuppelella Empson-Morin, 1981, K_2km

Lachnosphaera Haeckel, 1881, Q_4
Laevileugeo Yang et Wang, 1990, nom. invalid. (sin.: *Leugeo* Yang et Wang, 1990)
Lampoxanthium Haeckel, 1887, Q_4
Lamprocyclas Haeckel, 1881, Pg_3h–Q_4
Lamprocycloma Haeckel, 1887, sensu Petrushevskaya, 1981, nom. invalid. (sin.: *Lamprocyclas* Haeckel, 1881)
Lamprocyrtis Kling, 1973, N_1s–Q
Lamprodiscus Ehrenberg, 1860, N–Q_4
Lampromitra Haeckel, 1881, Pg–Q_4
Lamprospyris Haeckel, 1881, Q_4
Lamprotripus Haeckel, 1881, sensu Petrushevskaya, 1971, N_1?–Q_4
Lampterium Haeckel, 1881, sensu Riedel et Sanfilippo, 1970, Pg_1d–Pg_2
Lamptidium Haeckel, 1887, sensu Petrushevskaya et Kozlova, 1972, nom. invalid. (sin.: *Lampterium* Haeckel, 1881, sensu Riedel et Sanfilippo, 1970)
Lamptonium Haeckel, 1887, sensu Foreman, 1973, Pg_1d–Pg_3r
Lanubus Pessagno et Yang, 1989, in Pessagno, Six et Yang, 1989, J_2b–J_3t
Lapidopiscum Deflandre, 1958, C_1
Laracospongus Haeckel, 1887, Q_4
Larcarium Haeckel, 1887, Q_4
Larcidium Haeckel, 1887, Pg_2?–Q_4
Larcopyle Dreyer, 1889, Q_4
Larcospira Haeckel, 1887, N_1s–Q_4
Larnacalpis Haeckel, 1887, Pg_1d–Q_4
Larnacantha Haeckel, 1887, Q_4
Larnacidium Haeckel, 1887, Q_4
Larnacilla Haeckel, 1887, Q_4
Larnacoma Haeckel, 1887, Q_4
Larnacopylomma Dumitrica, 1989, K_2c–Pg_2
Larnacospongus Haeckel, 1887, Q_4
Larnacostupa Haeckel, 1887, Q_4
Latentibifistula Nazarov et Ormiston, 1983, P_1s–P_2s
Latentidiota Nazarov et Ormiston, 1985, C_3g–P_1a
Latentifistula Nazarov et Ormiston, 1983, C_1–P_2
Latium Blome, 1984, T_3c–T_3n
Laxtorum Blome, 1984, emend. Carter, 1993, T_3n–J_2b
Leptosphaera Haeckel, 1887, Q_4
Leugeo Yang et Wang, J_2b–J_2c
Liassosaturnalis Kozur et Mostler, 1990, T_3c–J_1h
Lichnosphaera Haeckel, 1881, Q_4
Linaresia El Kadiri, 1992, J_1t–J_3t
Liosphaera Haeckel, 1881, S–Q_4
Lipmanella Loeblich et Tappan, 1961, Pg_3–Q_4
Lipmanium Pessagno, 1969, K_1al–K_2t
Lirella Ehrenberg, 1872, Q_4
Liriospyris Haeckel, 1881, Pg_2b–Q_4
Lithacanthus Popofsky, 1908, Q_4
Lithamphora Popofsky, 1908, sensu Petrushevskaya, 1971, K–Q_4
Lithapium Haeckel, 1887, sensu Riedel et Sanfilippo, 1970, S_1–Q_4
Litharachnidium Haeckel, 1887, sensu Petrushevskaya, 1981, nom. invalid. (sin.: *Litharachnium* Haeckel, 1860)
Litharachnium Haeckel, 1860, N?–Q_4
Lithatractus Haeckel, 1887, C–Q_4
Lithelius Haeckel, 1862, C_1?–Pg_1t–Q_4
Lithobotrys Ehrenberg, 1844, sensu Haeckel, 1887, J?–Pg–Q_4
Lithocampana Clark et Campbell, 1942, K–Q_4
Lithocampe Ehrenberg, 1838, emend. Haeckel, 1862, D?–T_1i–Q_4
Lithocampium Haeckel, 1881, J
Lithocarpium Stohr, 1880, emend. Petrushevskaya, 1975, Pg_1t–N_1s
Lithochytris Ehrenberg, 1847, J_1h–Q_4
Lithocircus Müller, 1858, sensu Petrushevskaya, 1971, K–Q_4
Lithocorcys Ichikawa, 1950, nom. oblit.
Lithocorythium Ehrenberg, 1847, nom. invalid. (sin.: *Lithostrobus* Buetschli, 1882)
Lithocubus Haeckel, 1881, K–Q_4
Lithocyclia Ehrenberg, 1847, D–Q_4
Lithomelissa Ehrenberg, 1847, sensu Petrushevskaya, 1971, T_3c– Q_4
Lithomespilus Haeckel, 1881, S–Q_4
Lithomitra Butschli, 1882, T_1i–Q_4
Lithomitrella Haeckel, 1887, sensu Petrushevskaya et Kozlova, 1979, K–Pg_1d
Lithomitrissa Haeckel, 1887, sensu Petrushevskaya, 1981, Pg_3–N_1
Lithopera Ehrenberg, 1847, sensu str. Petrushevskaya, 1981, N_1a–Q_4
Lithophyllium Müller, 1858, Q_4
Lithopilium Popfsky, 1913, nom. invalid. (sin.: *Pterocorys* Haeckel, 1881)
Lithornithium Ehrenberg, 1847, sensu Riedel et Sanfilippo, 1970, nom. invalid. (sin.: *Lychnocanium* Ehrenberg, 1847)
Lithostrobus Buetschli, 1882, C?–T_1i–Q
Lithotympanium Haeckel, 1881, emend. Petrushevskaya, 1981, N_1–Q_4
Livarella Kozur et Mostler, 1981, T_3n–T_3r
Lobactinocapsa Dumitrica, 1978, T_2l
Loffa Pessagno in Pessagno, Finch et Abbott, 1979, T_3c–T_3n
Lonchosphaera Popofsky, 1908, Q_4
Lophoconus Haeckel, 1887, Kz
Lophocorys Haeckel, 1881, J_1h–Q_4
Lophocyrtis Haeckel, 1887, Pg_1t–Q_4
Lophophaena Ehrenberg, 1847, sensu Petrushevskaya, 1971, J_1–Q_4
Lophophaenoma Haeckel, 1887 Petrushevskaya, 1981, nom. invalid. (sin.: *Arachnocorys* Haeckel, 1860)
Lophospyris Haeckel, 1881, T_3r–Q_4
Loupanus Carter, 1993, T_3r
Lupherium Pessagno et Whalen, 1987, J_1t–J_2b
Lychnocanella Haeckel, 1887, sensu Petrushevskaya, 1981, Pg_1t–Q_4
Lychnocanium Ehrenberg, 1847, K–Q_4
Lychnocanoma Ehrenberg, 1847, sensu Riedel et Sanfilippo, 1970, Pg_1t–N_2z
Lychnodictyum Haeckel, 1881, K–Q_4
Lychnosphaera Haeckel, 1881, Q_4

Magnentactinia Won Moon-Zoo, 1997, D_3f_1–D_3f_2
Magnisphaera Won Moon-Zoo, 1997, D_3f_1

Mallanites O'Dogherty, 1994, K_1al_2–K_2s_1
Maudia Carter, 1988 in Carter, Cameron et Smith, 1988, J_1t
Mazosphaera Ehrenberg, 1860, Q_4
Meschedea Won Moon-Zoo, 1983, C_1–P_2
Mesosaturnalis Kozur et Mostler, 1981, T_3n–K_2m
Mesovallupus Pessagno et MacLeod, 1987, J_3t
Meyenella Davis, 1950, nom. invalid. (sin.: *Pantanellium* Pessagno 1977, emend. Pessagno 1979, sensu Pessagno et Blom 1980)
Microcubus Haeckel, 1881, N–Q_4
Micromelissa Haeckel, 1881, K–Q_4
Microsciadiocapsa Pessagno, 1969, K_2t–K_2km
Middourium Kozlova, 1999, Pg_1d–Pg_2p
Milax Blome, 1984, J_2c–K_1h
Minocapsa Matsuoka, 1991, J_1
Mirifusus Pessagno, 1977, J_1t–K_1a
Miropyle Dumitrica, 1988, K_2
Mita Pessagno, 1977, J_2b–K_2m
Mitrocalpis Haeckel, 1881, Q_4
Monaxonium Popofsky, 1912, Q_4
Monobrachium Kozlova, 1999, Pg_1d–Pg_2y
Monocapnuchosphaera Tekin, 1999, T_3c–T_3n
Monosera Takemura et Nakaseko, 1986, J
Monostephus Haeckel, 1881, T–Q_4
Monostylus Cayeaux, 1897, nom. invalid. (sin.: *Dorysphaera* Hinde, 1890)
Monotrabs Baumgartner, 1984, J_2bt–J_3k
Monotubus Popofsky, 1913, Q_4
Monozonites Haeckel, 1887, Q_4
Monozonium Haeckel, 1887, Q_4
Moskovistella Afanasieva, 2000, D_2gv–D_3fm
Mostlericyrtium Tekin, 1999, T_3c–T_3n
Mostlerium Cheng, 1986, C_1t–C_1v
Muellericyrtium Kozur et Mostler, 1981, T_2a
Muelleritortis Kozur, 1988, T_2a–T_3c
Multastrum Vishnevskaya, 1990, K_2km
Multiarcusella Kozur et Mostler, 1979, T
Multientactinia Won Moon-Zoo, 1997, D_3f_1
Multimonilis Yeh, 1989, T_2l–T_3c
Multisphaera Nazarov et Afanasieva, 2000, in Afanasieva, 2000, P_1ar
Myelastrum Haeckel, 1881, K–Q_4
Myllocercion Foreman, 1968, K_2k–Pg_1d

Nabolella Petrushevskaya, 1981, nom. nud., T
Nakasekoellus Kozur, 1984, T_3c–T_3n
Napora Pessagno, 1977, T_3c–K_2t
Nassella Haeckel, 1887, Q_4
Natoba, J_1s–J_2a
Natraglia Pessagno, 1979, in Pessagno, Finch et Abbott, 1979, T_2l–T_3r
Nazaromistonella Furutani, 1990, S
Nazarovella Kozur et Mostler, 1979, P_2u–T_3c
Nazarovites Afanasieva, 2000, D_3f_1–D_3f_3
Neoalbaillella Tekemura et Nakaseko, 1981, P_2u–P_2s
Neobotrys Popofsky, 1913, nom. invalid. (sin.: *Acrobotrys* Haeckel, 1881, sensu Petrushevskaya, 1965)
Neoholoeciscus Ormiston et Lane, 1976, C_1
Neoparonaella Yang, 1993, J_3t
Neopylentonema Kozur, 1984, T_3c–T_3n
Neosciadiocapsa Pessagno, 1969, K_2k–Q_4
Neosemantis Popofsky, 1913, sensu Petrushevskaya, 1971, N_1–Q_4
Neotripocyclia Pessagno et Yang, 1989, in Pessagno, Six et Yang, 1989, nom. invalid. (sin.: *Suna* Wu, 1993)
Neovallupus Yang et Pessagno, in Pessagno *et al.*, 1989, J_3t
Nephrodictyum Haeckel, 1881, N–Q_4
Nephrospyris Haeckel, 1881, N_1s–Q_4
Nevanellus Kozur et Mostler, 1981, T_3c
Nodocapnuchosphaera Tekin, 1999, T_3c–T_3n
Nodoteraedra Steiger, 1992, nom. invalid. (sin.: *Pyramispongia* Pessagno, 1973)
Nofrema Dumitrica, Kozur et Mostler, 1980, T_2a–T_2l
Noritus Pessagno et Whalen, 1982, J_1p–J_2
Nothotripodiscinus Deflandre, 1972, nom. invalid. (sin.: *Archipilium* Haeckel, 1881)
Noviforemanella Pessagno, Blome et Hull, 1993, J_3o
Novixitus Pessagno, 1977, J_3t–K_2t
Novodiacanthocapsa Empson-Morin, 1981, K_1br–K_2m

Obeliscoites O'Dogherty, 1994, K_1h_2–K_2s_3
Obesacapsula Pessagno, 1977, J_2bt–K_2km
Octatormentum Nazarov et Ormiston, 1985, P_1–P_2
Octodendron Haeckel, 1887, J_3t–Q_4
Octopyle Haeckel, 1881, Q_4
Octopylura Haeckel, 1887, Q_4
Octosaturnalis Kozur et Mostler, 1990, T_3n
Octotympanum Haeckel, 1887, nom. oblit., Q_4
Odontosphaera Haeckel, 1887, S_1–Q_4
Oertlisphaera Kozur et Mostler, 1979, T_3c
Oertlispongus Dumitrica, Kozur et Mostler, 1980, T_2l–T_3c
Ommatartus Haeckel, 1881, emend. Riedel, 1971, N_1t–Q_4
Ommatocampe Ehrenberg, 1860, N_1a–Q_4
Ommatodiscinus Haeckel, 1887, nom. invalid. (sin.: *Ommatodiscus* Stohr, 1880)
Ommatodisculus Haeckel, 1887, nom. invalid. (sin.: *Ommatodiscus* Stohr, 1880)
Ommatodiscus Stohr, 1880, K_2m–Q_4
Ommatogramma Ehrenberg, 1860, Pg_1t–Q_4
Orbiculiforma Pessagno, 1973, T_2l–Pg_2b
Orbula Foreman, 1973, Pg_1t–N_1
Oriundogutta Nazarov et Ormiston, 1987, $Є_1at$–S_2
Ormistonella De Wever et Caridroit, 1984, P_2
Ormistonia Li Hong-sheng, 1994, S_2
Ornatisaturnalis Mostler et Krainer, 1994, T
Ornatoentactinia Afanasieva, 1999, D_2ef–D_3fm_3
Oroscena Haeckel, 1887, emend. Friend et Riedel, 1967, Q_4
Orthocornutanna Clark et Campbell, 1945, nom. invalid. (sin.: *Cornutella* Ehrenberg, 1838, sensu Petrushevskaya, 1967)
Otosphaera Haeckel, 1887, N_1a–Q_4
Ovulopyle Kozur et Mostler, 1979, Q_4
Ovum De Wever, 1982, J

Pachus Blome, 1984, T_3c–T_3n
Pachyoncus Pessagno et Blome, 1980, J_2b_2–J_3o
Palacantholithus Deflandre, 1973, D_3f_2–C_1v
Palaeacanthus Davis, 1950, T–J_1
Palaeoactinosphaera Noble, 1994, S_1w–S_2
Palaeodecaradium Goodbody, 1986, S_1
Palaeodiscus Afanasieva, 2000, D_2gv–D_3fm
Palaeoephippium Goodbody, 1986, O_2–S_2
Palaeoeuchitonia Kozur et Mostler, 1978, K_1
Palaeofripus Goodbody, 1986, S

Palaeopyramidatum Goodbody, 1986, S_1
Palaeorubus Ishiga, 1987, D_3f_3
Palaeosaturnalis Donofrio et Mostler, 1978, emend. De Wever, 1984, $T_3c–J_1s$
Palaeoscenidium Deflandre, 1953, $S_1r–C_1v$
Palaeospiculum Won, 1993, Є
Palaeotetrapyle Dumitrica, 1988, Pg_1d
Palaeothalomnus Deflandre, 1973, $D_3f–C_1$
Palaeotripus Goodbody, 1986, $O_2–D_3f_1$
Palaeoxyphostylus Won Moon-Zoo, 1983, C_1
Paleocenosphaera Nazarov, 1973 $Є_1$
Paleotripus Goodbody, 1986, S_1r
Paleoxiphosphaera Nazarov, 1973 $Є_1$
Palhindeolithus Deflandre, 1973, $S_2–T_2l$
Palinandromeda Pessagno, Blome et Hull, 1993, $J_1t–J_3t$
Panarium Haeckel, 1881, Q_4
Panartus Haeckel, 1887, $N_1a–Q_4$
Panicium Haeckel, 1887, Q_4
Pantanellium Pessagno 1977, emend. Pessagno 1979, sensu Pessagno et Blom 1980, $T_1o–K_1al_1$
Papiliocampe Tekin, 1999, $T_3c–T_3n$
Parabipedis Yeh et Cheng, 1996, T_3r
Paracanoptum Yeh, 1987, J_1h
Paracenodiscus Kraschenninikov, 1960, Pg_2y
Paracystidium Cachan et Cachon, 1969, Q_4
Paradictyum Haeckel, 1881, emend. Petrushevskaya, 1971, ?–Q_4
Parafollicucullus Holdsworth et Jones, 1980, P
Parahsuum Yao, 1982, $T_3–J_3t$
Paraplafkerium Kozur et Mostler, 1981, $T_2a–T_2l$
Parapodocapsa Steiger, 1992, $J_3t–K_1v$
Parapoulpus Kozur et Mostler, 1979, $T_3c–T_3n$
Pararcheoentactinia Won, 2001, Є
Pararchocyrtium Deflandre, 1972, C_1
Parares Takemura, 1986, J
Pararuesticyrtium Kozur et Mock, 1981, in Kozur et Mostler, 1981, $T_3c–T_3n$
Parasaturnalis (Japonisaturnalis) Kozur et Mostler, 1972, $T_3c–J_2b–K_2$
Parasepsagon Dumitrica, Kozur et Mostler, 1980, $T_2a–T_2l$
Parastephanus Haeckel, 1881, Q_4
Parastomatosphaera Kozur et Mostler, 1979, Q_4
Paratriassoastrum Kozur et Mostler, 1981, $T_3c–T_3r$
Paratympanum Haeckel, 1881, Q_4
Parechidnina Won M.–Z. et Iams, Є
Parentactinia Dumitrica, 1978, $T_1o–T_3c$
Parentactinosphaera Kozur et Mostler, 1979, T_3c
Paricrioma Tekin, 1999, $T_3n–T_3r$
Paroertlispongus Kozur et Mostler, 1981, T_2l
Paronaella Pessagno, 1971, emend. Baumgartner, 1980, $T_2l–K_2m$
Parvicingula Pessagno, 1977, $J_1t–K_2s$
Parvicuspis Pessagno, 1972, K_2km
Parvifavus Takemura, 1986, J
Parvifusus Takemura, 1986, J
Parvispingula Pessagno, 1977, nom. invalid. (sin.: *Stichocapsa* Haeckel, 1881, sensu Petrushevskaya et Kozlova, 1972)
Parvivacca Pessagno et Yang, $J_3o–K_1h$
Patagospyris Haeckel, 1881, $Pg_1t–Q_4$
Patellula Kozlova, 1972, in Petrushevskaya et Kozlova, 1972, emend. Empson-Morin, 1981, $K_1al–K_2km$
Patulibracchium Pessagno, 1971, $J_2c–K_2m$
Patyomma Haeckel, 1881, Q_4
Paurinella Kozut et Mostler, 1981, $T_2l–T_3c$
Pentactinocapsa Dumitrica, 1978, $T_2a–T_2l$
Pentactinocarpus Dumitrica, 1978, $T_2a–T_3r$
Pentactinorbis Dumitrica, 1978, $T_2a–T_2l$
Pentactinosphaera Nagata et Nishimura, 1983, $T_3–N_1l$
Pentactura Haeckel, 1881, $N_1a–Q_4$
Pentalastrella Haeckel, 1887, nom. invalid. (sin.: *Pentalastrum* Haeckel, 1881)
Pentalastromma Haeckel, 1887, nom. invalid. (sin.: *Pentalastrum* Haeckel, 1881)
Pentalastrum Haeckel, 1881, C?–Q_4
Pentalpagia Cachon et Cachon, 1969, Q_4
Pentaplegma Haeckel, 1881, nom. oblit.
Pentasphaera Squinabol, 1904, K_1br
Pentaspongodiscus Kozur et Mostler, 1979, emend. Dumitrica, Kozur et Mostler, 1980, $T_2l–J_1s$
Pentaspyris Haeckel, 1881, nom. invalid. (sin.: *Dendrospyris* Haeckel, 1881)
Pentatortis Kozur, 1988, T_2l
Pentinastrum Haeckel, 1881, Q_4
Pentophiastrum Haeckel, 1887, Q_4
Periarachnium Haeckel, 1881, Q_4
Perichlamydium Ehrenberg, 1847, $N_1a–Q_4$
Peridarium Haeckel, 1887, nom. oblit.
Peridium Haeckel, 1881, $N_1t–Q_4$
Peripanarium Haeckel, 1887, Q_4
Peripanartus Haeckel, 1887, $D_1–Q_4$
Peripanicium Haeckel, 1887, Q_4
Periphaena Ehrenberg, 1873, sensu Sanfilippo et Riedel, 1973, $Pg_1t–Q_4$
Periplecta Haeckel, 1881, Q_4
Peripyramis Haeckel, 1881, sensu Riedel, 1958, $Pg_2y–Q_4$
Perispongidium Haeckel, 1882, $T_3c–J$
Perispyridium Dumitrica, 1978, $J_1t–J_3t$
Perispyris Haeckel, 1881, $N_1–Q_4$
Perizona Haeckel, 1881, Q_4
Peromelissa Haeckel, 1881, sensu Petrushevskaya, 1971, K–Q_4
Perozona Zagorodnuk, 1970, $Pg_2y–Pg_2l$
Perseus Takemura et Nakaseko, 1983, J
Pessagnalus Dumitrica, 1982, K_2s
Pessagnobrachia Kozur et Mostler, 1978, $K_1br–K_2k$
Pessagnocyrtiun Kozur et Mostler, 1981, T_3c
Pessagnosaturnalis Kozur, 1979, nom. invalid. (sin.: *Pseudoheliodiscus* Kozur et Mostler, 1972, emend. Pessagno, 1979)
Petalospyrella Haeckel, 1887, sensu Petrushevskaya, 1981, $Pg_2y–N_1s$
Petalospyris Ehrenberg, 1847, $Pg_1t–Q_4$
Petasiforma Pessagno, 1969, $K_1al–K_2s$
Phacodiscinus Heackel, 1887, $Pg_2y–N_1m$
Phacodiscus Heackel, 1882, emend. Kozlova, 1999, $Pg_2y–Q_4$
Phacopyle Dreyer, 1889, Q_4
Phacostaurus Heackel, 1887, $Pg_2p–Q_4$
Phacostylus Heackel, 1882, $Pg_1t–Q_4$
Phacotriactis Sutton, 1896, Pg_2
Phaenocalpis Heackel, 1887, Q_4
Phaenoscenium Heackel, 1887, C_1?–Q_4
*Phalangite*s O'Dogherty, 1994, $K_1a_3–K_2t$
Pharyngosphaera Heackel, 1887, Q_4
Phaseliforma Pessagno, 1972, $K_1h–K_2m$
Phermostichoartus Campbell, 1951, emend. Nigrini, 1977, N–Q
Phizosphaera Haeckel, 1881, $N_2p–Q_2s$

Phlebarachnium Haeckel, 1881, sensu Petrushevskaya, 1981, N?–Q_4
Phormacantha Jörgensen, 1905, N–Q_4
Phormobotrys Haeckel, 1881, Kz–Q_4
Phormocampe Haeckel, 1887, J_3t–Q_4
Phormocyrtis Haeckel, 1887, T_1i–Q_4
Phormospyris Haeckel, 1881, emend. Goll, 1976, Q_4
Phormostichoartus Campbell, 1951, sensu Nigrini, 1977, N_1a–Q_4
Phorticium Haeckel, 1881, Pg_2p–Q_4
Phractacantha Haeckel, 1881, Q_4
Phractaspis Haeckel, 1881, Q_4
Phrenocodon Haeckel, 1887, Kz
Phyletripes Campbell, 1951, K–N_1
Physematium Meyen, 1834, Q_4
Picapora Kozur et Mostler, 1981, T_2a–T_3n
Pipetta Haeckel, 1887, Q_4
Pipettaria Haeckel, 1887, Q_4
Pipettella Haeckel, 1887, J_3t–Q_4
Pityomma Haeckel, 1881, Q_4
Plafkerium Pessagno, 1979, T_2a–T_3r
Plagiacantha Claparede, 1856, D?–Q_4
Plagiocarpa Haeckel, 1881, emend. Petrushevskaya, 1881, Q_4
Plagonidium Haeckel, 1881, nom. oblit., Q_4
Plagoniscus Haeckel, 1887, D?–Kz
Plagonium Haeckel, 1881, Q_4
Planispinocyrtis Kozur et Mostler, 1981, T_2a
Platybursa Haeckel, 1881, N–Q_4
Platycryphalus Haeckel, 1881 J_3t
Plectacantha Jörgensen, 1905, sensu Petrushevskaya, 1971, N–Q_4
Plectagonidium J. Cachon et M. Cachon, 1969, Q_4
Plectaniscus Haeckel, 1887, Kz–Q_4
Plectanium Haeckel, 1881, Q_4
Plectocoronis Haeckel, 1881, Q_4
Plectophora Haeckel, 1881, Q_4
Plectopyramis Haeckel, 1881, nom. invalid. (sin.: *Acropyramis* Haeckel, 1881)
Plectoscenium Nishimura, 1990, Q_4
Plegmatium Campbell, 1954, nom. oblit.
Plegmosphaera Haeckel, 1881, J_2c–Q_4
Plenoentactinia Won, 1997, D_3f_1
Pleuropodium Haeckel, 1881, sensu Petrushevskaya, 1971, nom. invalid. (sin.: *Pterocanium* Ehrenberg, 1847)
Pluristratoentactinia Nazarov, 1981 D_3fm–P_2
Pobum De Wever, 1984 J_1s–J_1p
Podobursa Wisniowski, 1889, emend. Foreman, 1973, T_3c–K_1al
Podocampe Haeckel, 1881, nom. oblit., J–Q_4
Podocapsa Rüst, 1885, sensu Foreman, 1973, J_2bt–K_2km
Podocoronis Haeckel, 1881, Q_4
Podocyrtecium Haeckel, 1887, sensu Petrushevskaja, 1981, Pg
Podocyrtis Ehrenberg, 1847, K–Q_4
Podocyrtonium Haeckel, 1887, sensu Petrushevskaja, 1981, K–Pg
Pogonias O'Dogherty, 1994, K_1al_2–K_2t_1
Poloctostylus Dumitrica, 1994, K_1–K_2
Polyalacorys Haeckel, 1887, Pg_2–Q_4
Polyentactinia Foreman, 1963, O_2ll–T_1o
Polyfistula Nazarov et Ormiston, 1984, P_1ar
Polynura Haeckel, 1887, Q_4
Polyplagia Haeckel, 1887, nom. oblit., Q_4
Polyplecta Haeckel, 1887, Q_4
Polypleuris Haeckel, 1887, sensu Petrushevskaya, 1971, N?–Q_4
Polysolenia Ehrenberg, 1872, emend. Nigrini, 1967, N_1s–Q_4
Polystichia Pantanelli, 1880, nom. invalid. (sin.: *Dictyomitra* Zittel, 1876, emend. Pessagno, 1976)
Polyzonium Haeckel, 1887, Q_4
Popofskyellum Deflandre, 1964, D_3fm–C_3g
Porocapsa Haeckel, 1887, Q_4
Porodiscus Haeckel, 1881, D?–T_3c–Q_4
Poulpus De Wever, 1979, in De Wever *et al.*, 1979, T_2l–J_2bt
Praeacanthocircus Kozur et Mostler, 1983, J_1s–J_1p
Praeamphibrachidium Kozur et Mostler, 1978, J
Praecatenopyle Dumitrica, 1989, J_3t
Praecitriduma Kozur, 1984, T_3n–T_3r
Praeconocaryomma Pessagno, 1976, J_1s–K_2km
Praeconosphaera Yang, 1993, J_3–K_1al
Praedruppatractylis Kozur et Mostler, 1979, T_3c
Praeflustrella Kozur et Mostler, 1978, S?–D–K_1
Praeheliostaurus Kozur et Mostler, 1972, T_2l
Praehexasaturnalis Kozur et Mostler, 1983, emend. Kozur et Mostler, 1990, T_3c–J_1s
Praemesosaturnalis Kozur et Mostler, 1981, T_3n–T_3r
Praeorbiculiformella Kozur et Mostler, 1978, T–J?
Praeparvicingula Pessagno, Blome et Hull, 1993, in Pessagno *et al.*, 1993, J_2b–J_3o
Praeprotunuma Tekin, 1999, T_3c–T_3n
Praerhopalastrum Kozur et Mostler, 1978, J_2–K_1
Praesaturnalis Li Hong-sheng, 1994, S_2
Praestylodictya Kozur et Mostler, 1978, J–K_1
Praestylosphaera Empson-Morin, 1981, K_2km
Praexiphospira Kozur et Mostler, 1978, J
Primaritripus Afanasieva, 2000, D_2gv–D_3fm
Prismatium Haeckel, 1862, C?–K–Q_4
Pristacantha Haeckel, 1887, Q_4
Procyrtis Li, 1995, O_2
Proparvicingula Carter, 1993, T_2l–T_3r
Protoalbaillella Cheng, 1986, D_3fm–C_1
Protoceratoikiscum Goto, Umeda et Ishiga, 1992, O_2
Protoentactinia Won, 1990, Є–O
Protoperispyridium Yeh, 1987, J_1t–J_2b
Protopsium Pessagno et Poisson, 1981, T_3c–J_3o
Protoscenium Jörgensen, 1905, N?–Q_4
Protosphaera Cayeux, 1897, K_2
Protostichocapsa Empson-Morin, 1982, K_1br–Pg_1d
Protovallupus Pessagno et MacLeod, 1987, J_3o–J_3t
Protoxiphotractus Pessagno, 1973, K_2s–K_2km
Protunuma Ichikawa et Yao, 1976 J_1t–K_1b
Protympanium Haeckel, 1881, Q_4
Proventocitum Nazarov et Ormiston, 1987, O_1a–O_2?
Provisocyntra Nazarov et Ormiston, 1987, D_3–C_2
Prunobrachium Pessagno, 1975, K_2st–K_2km
Prunocarpus Haeckel, 1887, Q_4
Prunopyle Dreyer, 1889, Pg_1t–Q_4
Prunulum Haeckel, 1887, D_3–Q_4
Pseudoacanthocircus Kozur et Mostler, 1990, T_3n–J_1s
Pseudoacanthosphaera O'Dogherty, 1994, J_3t–K_2m?
Pseudoalbaillella Holdsworth et–Jones, 1980, O_2–C_3g–P_2c
Pseudoaulophacus Pessagno, 1963, K_1b–K_2km
Pseudocrolanium Jud, 1994, K_1h–K_1br
Pseudocrucella Baumgartner, 1980, J_1s–K_2km
Pseudocubus Haeckel, 1887, sensu Petrushevskaya, 1971, Pg?–Q_4
Pseudodictyomitra Pessagno, 1977, J_2bt– K_2km
Pseudodictyophimus Petrushevskaya, 1971, Pg_2l–Q_4

Pseudoeucyrtis Pessagno, 1977, J_2bt–K_2t_1
Pseudogodia Tekin, 1999, T_2l–T_3c
Pseudohagiastrum Pessagno, 1979, in Pessagno *et al.*, 1979, T_3n–T_3r
Pseudoheliodiscus Kozur et Mostler, 1972, emend. Pessagno, 1979, T_3c–J_1t
Pseudopantanellium Yeh, 1987, J_1
Pseudopoulpus Takemura, 1986, J_2a–J_2b
Pseudoristola Yeh, 1987, J_1
Pseudorotasphaera Noble, 1994, S
Pseudosaturniforma Kozur et Mostler, 1979, T_3c–T_3n
Pseudospongoprunum Wakamatsu, Sugiyama et Furutani, 1990, P_2u–P_2s
Pseudostaurolonche Mamedov, 1969, Pg_2–Pg_2
Pseudostaurosphaera Krascheninnikov, 1960, Pg_2
Pseudostigmosphaera Kozur et Mostler, 1979, C_1
Pseudostylosphaera Kozur et Mostler, 1981, T_1o–T_3c
Pseudotheocampe Empson-Morin, 1981, K_2t–K_2m
Pseudotormentus De Wever et Caridroit, 1984, P_2
Psilomelissa Haeckel, 1881, K–Q_4
Psychospyris Riedel et Sanfilippo, 1971, Pg_3h–N_1l
Pteractis Ehrenberg, 1872, nom. invalid. (sin.: *Euchitonia* Ehrenberg, 1872)
Pterocampe Haeckel, 1887, N_1–Q_4
Pterocanidium Haeckel, 1887, sensu Petrushevskaya, 1981, nom. invalid. (sin.: *Pterocanium* Ehrenberg, 1847)
Pterocanium Ehrenberg, 1847, sensu Petrushevskaya, 1971, C?–Pg_2l–Q_4
Pterocodon Ehrenberg, 1847, Pg_1t–Q_4
Pterocorys Haeckel, 1881, K_2–Q_4
Pterocorythium Haeckel, 1887, sensu Petrushevskaya, 1981, Mz?–Kz
Pterocyrtidium Buetschli, 1882, sensu Petrushevskaya et Kozlova, 1972, Pg_2l–N_2p
Pteropilium Haeckel, 1881, Kz–Q_4
Pteroscenium Haeckel, 1887, Q_4
Pterospongus Dumitrica, 1982, T_2l
Pterosyringium Haeckel, 1887, sensu Petrushevskaya, 1981, nom. invalid. (sin.: *Eusyringium* Haeckel, 1881)
Pylentonema Deflandre, 1963, D_3fm–C_1v
Pylobotrys Haeckel, 1881, Kz–Q_4
Pylocapsa Haeckel, 1881, Q_4
Pylodiscus Haeckel, 1887, Q_4
Pylolena Haeckel, 1887, Q_4
Pylonium Haeckel, 1881, Q_4
Pylosphaera Ehrenberg, 1858, N_1a
Pylospira Haeckel, 1887, Q_4
Pylospyris Haeckel, 1881, Q_4
Pylostephanidium Dumitrica, 1978, T_2a–T_3n
Pylozonium Haeckel, 1887, Q_4
Pyramis Campbell, 1954, nom. invalid. (sin.: *Plectopyramis* Haeckel, 1882)
Pyramispongia Pessagno, 1973, K_1b–K_2km

Quadrapesus Cheng, 1986, D_3fm–C_2v
Quadricaulis Caridroit et De Wever, 1986, P_2
Quadrigastrum O'Dogherty, 1994, K_1al$_2$–K_2k_1
Quadrilonche Haeckel, 1887, Q_4
Quadriremis Nazarov et Ormiston, 1985, C_3–P_2
Quadrisaturnalis Yeh, 1989, T_3c–T_3n
Quarkus Pessagno, Blome et Hull, 1993, in Pessagno *et al.*, 1993, J_2c
Quarticella Takemura, 1986, J_2b
Quasipetatus Blome, 1984, T_3c–T_3n
Quinquecapsularia Pessagno, 1971, K_1br$_3$–K_2t
Quinqueremis Nazarov et Ormiston, 1983, C_3–P_1ar

Radiobisphaera Won, 1997, D_2ef–D_3fm
Ramuspiculum Won, 1990, Є
Raoultius De Wever, 1982, J
Raphidociclicus Nazarov et Rudenko, 1981, D_3–P_1ar
Rectotormentum Nazarov et Ormiston, 1985, P_1s–P_1ar
Relanus Pessagno et Whalen, 1982, T_3r–J_1h
Relindella Kozur et Mostler, 1980, in Dumitrica, Kozur et Mostler, 1980, T_2a–T_3c
Renzium Blome, 1983, T_3c–T_3n
Retentactinia Won, 1997, D_3f_1–D_3f_2
Reticulotubulus Takemura, 1986, J
Retisphaera Won, 1997, D_2–D_3fm
Rhabdolithis Ehrenberg, 1847, Pg_2y–N_1s
Rhaphidococcus Haeckel, 1862, J
Rhaphidozoum Haeckel, 1862, Q_4
Rhizoplegma Haeckel, 1881, C–Q_4
Rhizosphaera Haeckel, 1861, Pg_3h–Q_4
Rhodosphaera Haeckel, 1881, D–Q_4
Rhodospyris Haeckel, 1881, Pg_3r–Q_4
Rhopalastrum Ehrenberg, 1847, D–Q_4
Rhopalatractus Haeckel, 1881, Pg_3–Q_4
Rhopalocanium Ehrenberg, 1847, Pg_1t–Q_4
Rhopalodictyum Ehrenberg, 1860, D_3?–J_1h–Q_4
Rhopalosyringium Campbell et Clark, 1944, K_1a_1–K_2m
Riedelipyle Kozur et Mostler, 1979, Q_4
Riedelius De Wever, 1982, J_1s
Rikivatella Kozur et Mostler, 1981, T_2l
Risella Carter, 1993, T_3r
Ristola Pessagno et Whalen, 1982, J_2a–K_1br
Robotium Cheng, 1986, D_3fm–C_1v
Rolumbus Pessagno, Whalen et Yeh, 1986, J_1p–J_1t
Rotaforma Pessagno, 1970, K_1al$_2$–K_2s_3
Rotasphaera Noble, 1994, O_3–S
Ruestia Vinassa de Regny, 1898, nom. invalid. (sin.: *Stauracontium* Haeckel, 1882)
Ruesticyrtium Kozur et Mostler, 1979, T_3c
Russirad Afanasieva, 2000, D_3f_2–D_3fm
Ruzhencevispongus Kozur, 1980; emend. Nazarov et Ormiston, 1983, P_1s–P_2

Saccospyris Haeckel, 1908 emend Petrushevskaya, 1965, N_1s–Q_4
Saitoum Pessagno, 1977 emend. De Weaver, 1989, J_2b–K_1al$_2$?
Salpingocapsa Rüst, 1885, J
Sanflippoella Kozur et Mostler, 1979, T_3c–T_3n
Sarla Pessagno, 1979, T_2a–T_3r
Saturnalis Haeckel, 1881, C–Q_4
Saturniforma Pessagno, 1970, K_1al–K_2km
Saturninus Haeckel, 1887, Q_4
Saturnosphaera Tichomirova, 1975, T_3n
Saturnulus Haeckel, 1881, K_1–Q_4
Savaryella Jud, 1994, K_1b–K_2st
Schaafella Vishnevskaya, 1990, K_1al–K_2s
Schadelfusslerus Empson-Morin, 1981, K_2st–K_2km
Scharfenbergia Won Moon-Zoo, 1983, C_1
Schaumellus Empson-Morin, 1981, K_2km
Sciadiocapsa Squinabol, 1904, K_1v–K_2m

Scutispongus Kozur et Mostler, 1996, T_2l
Scyphiforma Pessagno, 1969, K_2k
Secuicollacta Nazarov et Ormiston, 1984, O_2–D_3
Semantidium Haeckel, 1887, Q_4
Semantis Haeckel, 1887, K–Q_4
Semantrum Haeckel, 1887, N_1–Q_4
Sematiscus Haeckel, 1887, Kz–Q_4
Semihsuum Pessagno, Blome et Hull, 1993, J_2c
Senelella Tekin, 1999, T_3n
Sepalospyris Haeckel, 1881, Q_4
Sepsagon Dumitrica, Kozur et Mostler, 1980, T_2a–T_3n
Sethamphora Haeckel, 1887, T–Q_4
Sethamphorus Burma, 1959, Kz
Sethocanium Nischimura, 1990, Q_4
Sethocapsa Haeckel, 1881, sensu Foreman, 1973, D–K_2m–Q_4?
Sethocephalus Haeckel, 1887, nom. oblit., K_2–Q_4
Sethochytris Haeckel, 1881, K–Q_4
Sethoconus Haeckel, 1881, K_2–Q_4
Sethocorys Haeckel, 1881, J_1–Q_4
Sethocyrtis Haeckel, 1887, C_1?–J_2bt–Q_4
Sethodiscus Haeckel, 1881, D?–J_1h–Q_4
Sethomelisa Haeckel, 1881, Q_4
Sethopera Haeckel, 1881, K–Q_4
Sethophaena Haeckel, 1881, Q_4
Sethophormis Haeckel, 1881, sensu Petrushevskaya, 1971, K_2–Q_4
Sethopilium Haeckel, 1881, sensu Petrushevskaya, 1981, Pg_2?–Q_4
Sethopyramis Haeckel, 1881, Pg_2y–Q_4
Sethornithium Haeckel, 1881, nom. oblit., Q_4
Sethosphaera Haeckel, 1881, Q_4
Sethostaurus Haeckel, 1881, S?–Q_4
Sethostylus Haeckel, 1881, Pg_1t–Q_4
Silicarmiger Dumitrica, Kozur et Mostler, 1980, T_2a–T_3n
Siphocampe Haeckel, 1881, sensu Nigrini, 1977, J–Q_4
Siphocampium Haeckel, 1881, sensu De Wever *et al.*, 1979, T_3c–K_1br
Siphocampula Haeckel, 1887, sensu Petrushevskaya, 1981, Kz
Siphonosphaera Müller, 1858, Q_4
Siphostichartus Nigrini, 1977, Pg_3r–N_2z
Solenosphaera Haeckel, 1887, N_1l–Q_4
Solenotryma Foreman, 1968, J_2bt–K_2km
Solicubulus Dumitrica, 1983, J_1h–J_3o
Somphoentactinia Nazarov, 1975, D_2ef–P_1
Sontonaella Yeh, 1987, nom. invalid. (sin.: *Paronaella* Pessagno, 1971)
Soreuma Haeckel, 1881, nom. oblit., Pg_2?–Q_4
Sorolarcus Haeckel, 1887, Q_4
Sphaerocapsa Haeckel, 1881, Q_4
Sphaerodiscus Won Moon-Zoo, 1983, C_1–P_2
Sphaeropyle Dreyer, 1889, T_1i
Sphaerospyris Haeckel, 1887, N_1–Q_4
Sphaerostylus Haeckel, 1881, T–Q_4
Sphaerozoum Meyen, 1834, S_1–Q_4
Spicularina Donofrio, 1991, T_3
Spinoellipsella Kozur et Mostler, 1990, J_1h
Spinopoulpus Kozur et Mock, 1981, in Kozur et Mostler, 1981, T_3c–T_3n
Spinosiocapsa Ozvoldova, 1975, nom. oblit.
Spinotriassocampe Kozur, 1984, T_2l–T_3c
Spirema Haeckel, 1887, K_1–Q_4
Spiremaria Kozlova, 1960, N_1
Spirocampe Haeckel, 1881, Kz
Spirocapsa Rüst, 1892, Mz
Spirocyrtis Haeckel, 1881, sensu Nigrini, 1967, K_2km–Q_4
Spirocyrtoma Haeckel, 1887, nom. invalid. (sin.: *Stichopodium* Haeckel, 1881)
Spiromultitunica Tochilina et Popova, 1985, Kz
Spironium Haeckel, 1887, C_1?–Q_4
Spiropyle Tochilina, 1985, Kz
Spirotunica Tochilina et Popova, 1985, N_1s
Spongaster Ehrenberg, 1860, J–Q_4
Spongastericulus Haeckel, 1887, nom. invalid. (sin.: *Spongasteriscus* Haeckel, 1882)
Spongasteriscus Haeckel, 1882, J_1h–Q_4
Spongatractus Haeckel, 1887, Pg_2y–Q_4
Spongechinus Haeckel, 1881, J_1–Q_4
Spongellipsis Haeckel, 1887, Q_4
Spongentactinella Nazarov, 1975, D_2ef–P
Spongentactinia Nazarov, 1975, S_1l–P_1ar
Spongiocanium Nishimura, 1990, Q_4
Spongioconcha Mast, 1910, Q_4
Spongiomma Haeckel, 1887, J_1–Q_4
Spongiopodium Nishimura, 1990, Pg_3–Q_4
Spongiostoma Carter, Cameron et Smith, 1988, J_1t
Spongoacanthus Squinabol, 1903, K_2km
Spongobrachium Haeckel, 1881, K–Q_4
Spongocapsula Pessagno, 1977, J_2bt–K_2s
Spongocoela Hinde, 1899, S–D_2
Spongocore Haeckel, 1887, K_1–Q_4
Spongocyclia Haeckel, 1862, K_1br–Pg_2y
Spongocyrtis Dunikowski, 1862, C_1?–J_1–Q_4
Spongodendron Hollande et Enjument, 1960, Q_4
Spongodictyon Haeckel, 1862, D–Q_4
Spongodiscus Ehrenberg, 1854, D–Q_4
Spongodruppa Haeckel, 1887, C1–Q_4
Spongodrymus Haeckel, 1881, Q_4
Spongolarcus Haeckel, 1887, Q_4
Spongolena Haeckel, 1887, nom. invalid. (sin.: *Amphibracchium* Haeckel, 1881, emend. Baumgartner, 1980)
Spongoliva Haeckel, 1887, N_1–Q_4
Spongolonche Haeckel, 1881, S_1w–Q_4
Spongolonchidium Chedia, 1959, D–Q_4
Spongomelissa Haeckel, 1887, Pg_2y–Pg_3h
Spongopallium Dumitrica, Kozur et Mostler, 1980, T_2a–T_2l
Spongophacus Haeckel, 1881, C_1–Q_4
Spongophortis Haeckel, 1881, Q_4
Spongopila Haeckel, 1881, C–Q_4
Spongoplegma Haeckel, 1881, S–Q_4
Spongoprunum Haeckel, 1887, C?–K_2st–Q_4
Spongopyle Dreyer, 1889, J_3t–K_2km
Spongopyramis Haeckel, 1887, Pg–Q_4
Spongosaturnalis Campbel et Clark, 1944, J_1t–K_2m
Spongosaturnaloides Kozur et Mostler, 1972, T_3c
Spongosaturninus Campbel et Clark, 1944, K_2
Spongoserrula Dumitrica, 1982, T_2l–T_3c
Spongosilicarmiger Kozur, 1984, T_2l–T_3c
Spongosphaera Ehrenberg, 1847, D_1–Q_4
Spongospira Stohr, 1880, nom. invalid. (sin.: *Spongocyclia* Haeckel, 1862)
Spongostaurus Haeckel, 1881, J_1t–Q_4
Spongostephanidium Dumitrica, 1978, T_2l–T_3c
Spongostichomitra O'Dogherty, 1994, K_1a_3–K_2s_3
Spongostylidium Haeckel, 1881, Q_4

Spongostylus Haeckel, 1881, T_2l–Q_4
Spongothamnus Haeckel, 1887, Q_4
Spongotractus Haeckel, 1887, S_1–Q_4
Spongotripus Haeckel, 1881, D–Q_4
Spongotrochus Haeckel, 1860, C_1–Q_4
Spongoxiphus Haeckel, 1887, N_1–Q_4
Spongurus Haeckel, 1862, D_3–Q_4
Spyridobotrys Haeckel, 1862
Squinabolella Kozur et Mostler, 1979, T_3c
Squinabolella Pessagno, 1969, T_2l–K_2km
Squinabollum Dumitrica, 1970, K_1v–K_2st
Stauracanthocircus Kozur et Mostler, 1983, J_1
Stauracontium Haeckel, 1881, emend. Kozur et Mostler, 1979, T_2a
Stauractura Haeckel, 1881, Q_4
Stauralastrum Haeckel, 1887, C–Q_4
Staurancistra Haeckel, 1881, Q_4
Stauroacanthocircus Kozur et Mostler, 1983, emend. Kozur et Mostler, 1990, T_3n–J_1h
Staurocaryum Haeckel, 1881, Q_4
Staurocromyum Haeckel, 1881, Q_4
Staurocyclia Haeckel, 1881, K_1br–Q_4
Staurodictya Haeckel, 1882, emend. Kozur et Mostler, 1978, J_3t–K_1–Q_4?
Staurodiscus Krascheninnikov, 1960, J_3t–Pg_2y
Staurodoras Haeckel, 1881, S_1–Q_4
Staurodruppa Hinde, 1899, D_2–D_3fm
Staurolonche Haeckel, 1881, emend. Pessagno, 1977, D–Q_4
Staurolonchidium Haeckel, 1887, D–Q_4
Stauromesosaturnalis Kozur et Mostler, 1990, J_1h–J_1p
Stauroplegma Hinde, 1890, S_1
Stauropylissa Dumitrica, 1989, T_2l_1
Staurosphaera Haeckel, 1881, S_1–Q_4
Staurosphaeretta Squinabol, 1904, K_1br–K_2st
Staurostylus Haeckel, 1881, D–Q_4
Staurotholonium Haeckel, 1887, Q_4
*Staurotholu*s Haeckel, 1887, Q_4
Stauroxiphos Haeckel, 1887, J_3t–Q_4
Steigerispongus Kozur et Mostler, 1996, T_2l
Stephanastrum Ehrenberg, 1847, J_1p–Q_4
Stephaniscus Haeckel, 1887, nom. oblit., Q_4
Stephanium Haeckel, 1887, Q_4
Stephanophaena Haeckel, 1887, nom. invalid. (sin.: *Archiphanta (Stephanophanta)* Haeckel, 1882)
Stephanospyris Haeckel, 1881, nom. invalid. (sin.: *Dorcadospyris* Haeckel, 1881)
Stichocampe Haeckel, 1881, Q_4
Stichocapsa Haeckel, 1881, sensu Petrushevskaya et Kozlova, 1972, D?–T_3r–Q_4
Stichocorys Haeckel, 1881, sensu Riedel et Sanfilippo, 1970, Pg_2p–Q_4
Stichocyrtis Haeckel, 1881, nom. oblit.
Stichomitra Cayeux, 1897, T_2a–Pg_1d
Stichopera Haeckel, 1881, C–Q_4
Stichoperina Haeckel, 1887, nom. oblit.
Stichophaena Haeckel, 1881, Q_4
Stichophaenidium Haeckel, 1887, nom. invalid. (sin.: *Stichophatna* Haeckel, 1881)
Stichophaenoma Haeckel, 1887, Kz
Stichophormis Haeckel, 1881, T–Q_4
Stichophormiscus Haeckel, 1887, sensu Petrushevskaya, 1981, nom. invalid. (sin.: *Cyrtolagena* Haeckel, 1879 emend. Petrushevskaya, 1971)
Stichophormium Haeckel, 1887, sensu Petrushevskaya, 1981, nom. invalid. (sin.: *Cyrtolagena* Haeckel, 1879 emend. Petrushevskaya, 1971)
Stichopilidium Haeckel, 1887, K–Pg
Stichopilium Haeckel, 1881, T_3c–Q_4
Stichopodium Haeckel, 1881, Pg_3–Q_4
Stichopterium Haeckel, 1881, nom. invalid. (sin.: *Pterocanium* Ehrenberg, 1847)
Stichopterygium Haeckel, 1881, nom. invalid. (sin.: *Artocyrtis* Haeckel, 1887, sensu Petrushevskaya, 1981)
Stigmospaera Haeckel, 1887, C–Q_4
Stigmospaerusa Hollande et Enjument, 1960, Q_4
Stigmostylus Hollande et Enjument, 1960, Q_4
Stomatodiscus Haeckel, 1887, Q_4
Stomatosphaera Dreyer, 1889, Q_4
Streblacantha Haeckel, 1887, Q_4
Streblonia Haeckel, 1887, Q_4
Streblopyle Haeckel, 1887, Q_4
Stychopylium Popofsky, Q
Styla Stechow, 1921, nom. invalid. (sin.: *Euchitonia* Ehrenberg, 1860)
Stylacontarium Popofsky, 1912, Q_4
Stylactis Ehrenberg, 1872, nom. invalid. (sin.: *Euchitonia* Ehrenberg, 1860)
Stylartus Haeckel, 1881, Q_4–Q_4
Stylatractus Haeckel, 1887, P–Q_4
Stylocapsa Principi, 1909, T_3c–J_3t
Stylochlamydium Haeckel, 1882, N_1a–Q_4
Stylochlamys Haeckel, 1887, nom. invalid. (sin.: *Stylochlamydium* Haeckel, 1882)
Stylochlamyum Haeckel, 1887, nom. invalid. (sin.: *Stylochlamydium* Haeckel, 1882)
Stylocromyum Haeckel, 1881, Q_4
Stylocryptocapsa Tan Sin Hok, 1926, K
Stylocyclia Ehrenberg, 1847, J_3t–Q_4
*Stylodicty*a Ehrenberg, 1847, emend. Kozlova, 1972, D_3–Q_4
Stylodiscus Haeckel, 1887, C_1–Q_4
Stylodruppa Kasinzova, 1979, K_2s–K_2km
Stylosphaera Ehrenberg, 1847, D–Q_4
Stylosphaerella Haeckel, 1887, Pg_1t–Pg_2p
Stylospongia Haeckel, 1862, K_1h–K_2km
Stylospongidium Haeckel, 1882, K
Stylostaurus Haeckel, 1881, N_1–Q_4
Stylotrochus Haeckel, 1862, C?–T_1i–Q_4
Stypolarcus Haeckel, 1887, K–Q_4
Styptosphaera Haeckel, 1881, S? K_2st–Q_4
Subechidnina Won, 1990, Є
Suna Wu, 1986 J_2c–K_1a
Supervallupus Yang et Pessagno, 1989, J_3t
Suttonium Schaaf, 1976, nom. oblit., Pg_1–Q_4
Syntagentactinia Nazarov, 1980, O_2ll–S_1
Syringium Principi, 1909, nom. invalid. (sin.: *Cyrtocapsella* Haeckel, 1887, emend. Sanfilippo et Riedel, 1970)
Syringocapsa Neviani, 1900, sensu Fereman, 1973, T_2l–K_1a

Takoum Takemura, 1986, T_2a–J
Tamnospyris Haeckel, 1881, nom. invalid. (sin.: *Archiphatna* Haeckel, 1881)
Tamonella Dumitrica, Kozur et Mostler, 1980, T_2a–T_2l

Tandarnia Dumitrica, 1982, T_2a–T_2l
Tapanella Hull, 1997 Tapanella, J_3k–J_3k
Tauridastrum Tekin, 1999, T_3n
Taurospyris Haeckel, 1881, nom. invalid. (sin.: *Dendrospyris* Haeckel, 1881)
Teichertus Hull, 1997, J_2b–J_3t
Tessarastrella Haeckel, 1887, nom. invalid. (sin.: *Histiastrum* Ehrenberg, 1847)
Tessarastromma Haeckel, 1887, nom. invalid. (sin.: *Histiastrum* Ehrenberg, 1847)
Tessarastrum Haeckel, 1887, nom. invalid. (sin.: *Histiastrum* Ehrenberg, 1847)
Tessarospyris Haeckel, 1881, Pg_2?–Q_4
Tetracanthellipsis Squinabol, 1903, K_2s–K_2t_1
Tetracanthus Popofsky, 1908, Q_4
Tetracapsa Haeckel, 1881, J_3o–J_3t
Tetracircinata Nazarov et Ormiston, 1984, P_1ar–P_2
Tetracorethra Haeckel, 1881, N–Q_4
Tetracoronis Haeckel, 1881, nom. invalid. (sin.: *Podocoronis* Haeckel, 1881)
Tetracubus Haeckel, 1887, sensu Petrushevskaya, 1981, Q_4
Tetraditryma Baumgartner, 1980, J_2a–K_1b
Tetraedrina Haeckel, 1881, nom. oblit.
Tetragregnon Ormiston et Lane, 1976, D_3f_2–P_2
Tetrahedrina Haeckel, 1887, nom. oblit., Q_4
Tetralacorys Haeckel, 1881, sensu Riedel et Sanfilippo, 1970, nom. invalid. (sin.: *Lampterium* Haeckel, 1881, sensu Riedel et Sanfilippo, 1970)
Tetrapetalon Hollande et Enjument, 1960, Q_4
Tetraplagia Haeckel, 1881, N_1t–Q_4
Tetraplecta Haeckel, 1881, Kz–Q_4
Tetraporobrachia Kozur et Mostler, 1979, T_3c–T_3r
Tetrapteroma Haeckel, 1881, nom. oblit.
Tetrapyle Muller, 1858, N_1m–Q_4
Tetrapylissa Haeckel, 1887, Q_4
Tetrapylonium Haeckel, 1881, C?–Q_4
Tetrarchiplagia Dumitrica, 1982, T_2l–J_3t
Tetraregnon Ormistone et Lane, 1976, P
Tetrarhabda Haeckel, 1881, nom. oblit.
Tetrarrhabda Haeckel, 1887, nom. oblit.
Tetrasphaera Popofsky, 1912, Q_4
Tetraspongodiscus Kozur et Mostler, 1979, T_2l–T_3c
Tetraspongonium Haeckel, 1882, Q_4
Tetraspyris Haeckel, 1881, Q_4
Tetratormentum Nazarov et Ormiston, 1985, C_1s–P_2
Tetratrabs Baumgartner, 1980, T_3c–K_1v
Tetrentactinia Foreman, 1963, S_1l–C_1
Thaisphaera Sashida et Igo, 1992, T_1o
Thalassicolla Huxley, 1851, Q_4
Thalassolampe Haeckel, 1862, Q_4
Thalassophysa Haeckel, 1881, Q_4
Thalassopila Haeckel, 1881, Q_4
Thalassoplancta Haeckel, 1862, Q_4
Thalassoplegma Hollande et Enjument, 1960, Q_4
Thalassosphaera Haeckel, 1862, Q_4
Thalassoxanthium Haeckel, 1881, Q_4
Thanarla Pessagno, 1977, J_2c–K_2km
Thecacapsula Tikhomirova, 1983, J_3–K_1
Thecoentactinia Nazarov, 1975, D_3f–P_1
Thecosphaera Haeckel, 1881, D–Q_4
Thecosphaerella Haeckel, 1887, Pg_1d–Q_4
Theocalyptra Haeckel, 1881, K?–Q_4
Theocampe Haeckel, 1887, emend Burma, 1959, emend. Empson-Morin, 1981, C?–T_3c–Q_4
Theocamptra Haeckel, 1887, sensu Petrushevskaya et Kozlova, 1972, Pg_3–N_1
Theocapsa Haeckel, 1882, J_1–Q_4
Theocapsilla Haeckel, 1887, sensu Petrushevskaya, 1981, nom. invalid. (sin.: *Theocorythium* Haeckel, 1887, sensu Petrushevskaya, 1981)
Theocapsomma Haeckel, 1887, emend. Foreman, 1977, J_2bt–K_2m
Theocapsura Haeckel, 1887, sensu Petrushevskaya, 1981, nom. invalid. (sin.: *Theocorythium* Haeckel, 1887, sensu Petrushevskaya, 1981)
Theoconus Haeckel, 1887, nom. invalid. (sin.: *Pterocorys* Haeckel, 1881)
Theocorbis Haeckel, 1887, sensu Petrushevskaya, 1981, nom. invalid. (sin.: *Lamprocyclas* Haeckel, 1881)
Theocoronium Haeckel, 1887, sensu Petrushevskaya, 1981, Pg–Q_4
Theocorys Haeckel, 1881, J_1h–Q_4
Theocorythium Haeckel, 1887, sensu Petrushevskaya, 1981, N_1m–Q_4
Theocotyle Riedel et Sanfilippo, 1970, K_2km–Pg_2p
Theocotylissa Foreman, 1973, Pg_2y–Q_4
Theocyrtis Haeckel, 1887, emend Sanfilippo et Riedel, 1992, T–Q_4
Theodiscus Haeckel, 1887, S_1–Q_4
Theopera Haeckel, 1881, Pg–Q_4
Theophaena Haeckel, 1881, Kz
Theophormis Haeckel, 1881, K–Q_4
Theopilium Haeckel, 1881, Q_4
Theopodium Haeckel, 1881, J–Q_4
Theosyringium Haeckel, 1881, P–Q_4
Therospyris Haeckel, 1881, nom. invalid. (sin.: *Dendrospyris* Haeckel, 1881)
Thetis De Wever, 1982, J_1s–J_2c
Tholartus Haeckel, 1887, Q_4
Tholocubus Haeckel, 1887, Q_4
Tholodes Haeckel, 1887, Q_4
Tholodiscus Kozlova, 1972, in Petrushevskaya et Kozlova, 1972, K_1al–K_2m
Tholoma Haeckel, 1887, Q_4
Tholonium Haeckel, 1887, Q_4
Tholospira Haeckel, 1887, N_1s–Q_4
Tholospyris Haeckel, 1881, Pg_1d–Q_4
Tholostaurus Haeckel, 1887, Q_4
Thurstonia Whalen et Carter, 1998, J_1s–J_2a
Thyrsocyrtis Ehrenberg, 1847, Pg_2y–Q_4
Tiarospyris Haeckel, 1881, Q_4
Tiborella Dumitrica, Kozur et Mostler, 1980, T_1o–T_3c
Tirodella Kozur et Mostler, 1981, T_3c
Tlecerina Furutani, 1983, T
Torculum O'Dogherty, 1994, K_1a_3–K_2s_3
Tormentum Nazarov et Ormiston, 1983, C_1v–P_2
Toxarium Haeckel, 1887, nom. invalid. (sin.: *Lithocircus* Müller, 1858, sensu Petrushevskaya, 1971)
Toxidium Haeckel, 1887, ?–Q_4
Transhsuum Takemura, 1986, J_1t–J_3t
Transylvanaria Dumitrica et Carter, 1999, J_2b–K_2k
Triacanthocircus Kozur et Mostler, 1990, J_1h
Triacornicyrtium Tekin, 1999, T_3n–T_3r
Triactinosphaera Dunikowski, 1882, nom. invalid. (sin.: *Rhopalodictyum* Ehrenberg, 1860)
Triactis Haeckel, 1881, J_2b–Q_4
Triactiscus Haeckel, 1881, D–Q_4

Triactofenestrella Nazarov et Ormiston, 1984, C_3g
Triactoma Rüst, 1885, J_1p–K_2k
Triadiscus Haeckel, 1887, Q_4
Triaenosphaera Deflandre, 1973, C_1
Trialatus Yeh, 1990, T_3c–T_3n
Triarcella Kozur et Mock, in Kozur et Mostler, 1981, T_3n
Triassistephanidium Dumitrica, 1978, T_2a–T_2l
Triassobipedis Kozur, 1984, T_2a–T_2l
Triassocampe Dumitrica, Kozur et Mostler, 1980, T_2a–T_3r
Triassocrucella Kozur, 1984, T_3c–T_3r
Triassocyrtium Kozur et Mostler, 1979, T_3c
Triassospongosphaera, Kozur et Mostler, 1981, T_2l–T_3c
Triastrum Cleve, 1901, nom. invalid. (sin.: *Rhopalodictyum* Ehrenberg, 1860)
Tribonospaera Haeckel, 1881, Q_4
Triborella Dumitrica, Kozur et Mostler, 1980, T_2–T_3
Tricapsula Wu Hao-Ruo, 1986, J_3K_2s
Triceraspyris Haeckel, 1881, Pg_2p–Q_4
Tricirconium Haeckel, 1887, nom. oblit.
Tricolocampe Haeckel, 1881, T_1i–Q_4
Tricolocampium Haeckel, 1887, sensu Petrushevskaya, 1981, K–Q_4
Tricolocamptra Haeckel, 1887, sensu Petrushevskaya, 1981, ?–Q_4
Tricolocapsa Haeckel, 1881, C–Q_4
Tricolocapsium Haeckel, 1887, nom. oblit.
Tricolospyris Haeckel, 1881, N_1–Q_4
Trictenartus Haeckel, 1881, Q_4
Tricyclidium Haeckel, 1881, N_1–Q_4
Tricyclonium Haeckel, 1887, nom. oblit.
Tridictyopus Haeckel, 1879, emend Petrushevskaya, 1981, ?–Q_4
Trigonactura Haeckel, 1881, J_3t–Q_4
Trigonastrum Haeckel, 1887, Q_4
Trigonocyclia Haeckel, 1881, D–Q_4
Trigonodiscus Neviani, 1900, J_3t
Trillus Pessagno et Blome, 1980, J_1s–J_3o
Trilobatum Popofsky, 1912, Q_4
Trilonche Hinde, 1899, D–K_2
Trimiduca Kozur et Mostler, 1979, T_3c
Trimulus O'Dogherty, 1994, K_1a$_1$–K_1al$_3$
Triodiscus Haeckel, 1887, Q_4
Triolena Haeckel, 1887, Q_4
Triopyle Haeckel, 1881, Q_4
Triospyrium Haeckel, 1887, sensu Petrushevskaya, 1981, Pg_1t–Q_4
Triostephus Haeckel, 1881, nom. oblit.
Tripedocassis Dumitrica, 1991, T_2a
Tripedocorbis Dumitrica, 1991, T_2a
Tripedurnula Dumitrica, 1991, T_2a
Tripilidium Haeckel, 1881, C_1–Q
Triplagia Haeckel, 1881, Kz
Triplanospongos Sashida et Tonishi, 1988, P_2u–P_2s
Triplecta Haeckel, 1881, nom. oblit., Q_4
Tripocalpis Haeckel, 1881, K_1br–Q_4
Tripocoronis Haeckel, 1881, nom. oblit.
Tripocubus Haeckel, 1887, sensu Petrushevskaya, 1981, nom. invalid. (sin.: *Dipocoronis* Haeckel, 1881)
Tripocyclia Haeckel, 1882, T_2a–K_1br
Tripocyrtis Haeckel, 1887, Pg_2?–Q_4
Tripodictya Haeckel, 1881, J_3t–Q_4
Tripodiscinus Haeckel, 1887, sensu Petrushevskaya et Kozlova, 1979, Pg_1d–Pg_2p
Tripodiscium Haeckel, 1881, J_3t–Q_4
Tripodisculus Haeckel, 1887, sensu Petrushevskaya, 1981, Kz–Q_4
Tripodiscus Haeckel, 1881, J
Tripodoconus Nishimura, 1990, Q_4
Tripodocorys Haeckel, 1881, sensu Foreman, 1968, J–Pg
Tripodonium Haeckel, 1881, nom. oblit., Q_4
Tripophaenoscenium Campbell et Clark, 1944, N_1
Triposphaera Hinde, 1890, S_1
Tripospyrantha Haeckel, 1887, nom. oblit.
Tripospyris Haeckel, 1881, Pg_2?–Q_4
Tripospyrissa Haeckel, 1887, nom. oblit.
Tripospyromma Haeckel, 1887, nom. oblit.
Triprionium Haeckel, 1881, J–Pg
Tripterocalpis Haeckel, 1881, Q_4
Trisphaera Vinassa de Regny, 1900, nom. invalid. (sin.: *Triposphaera* Hinde, 1890)
Trissocircus Haeckel, 1881, nom. invalid. (sin.: *Trissocyclus* Haeckel, 1881)
Trissocyclus Haeckel, 1881, D_3?–Pg_3h–Q_4
Trissopilium Haeckel, 1881, nom. oblit., Q_4
Tristephaniscus Haeckel, 1881, nom. oblit.
Tristephanium Haeckel, 1881, nom. oblit., Q_4
Tristylospyris Haeckel, 1887, nom. invalid. (sin.: *Tholospyris* Haeckel, 1881)
Tristylospyrium Haeckel, 1887, nom. oblit.
Trisulcus Popofsky, 1913, Pg_2?–Q_4
Trisyringium Vinassa, 1901, sensu Foreman 1973, K_1v$_3$–K_2s$_1$
Tritortis Kozur, 1988, T_2a–T_3c
Tritrabs Baumgartner, 1980, J_1t–K_2s
Triversus Takemura, 1986, J_2b–J_3
Trizonaris Haeckel, 1887, Q_4
Trizonium Haeckel, 1887, Q_4
Trochodiscus Haeckel, 1887, S_1–Q_4
Trypanosphaera Haeckel, 1887, Q_4
Tubilustrium O'Dogherty, 1994, K_1al$_2$–K_2s$_3$
Tugurium O'Dogherty, 1994, K_1al$_2$– K_1al$_3$
Turanta Pessagno et Blome, 1982, J_1t–J_3t
Turbocapsa O'Dogherty, 1994, K_1a–K_1al
Turbocapsula O'Dogherty, 1994, J_2bt–K_1a
Turriseiffelus Dumitrica et Zugel, 2003, J_3t
Tuscaritellum Deflandre, 1964, C_1
Tympaneides Carter, 1988, in Carter, Cameron et Smith, 1988, J_1t–J_2b
Tympanidium Haeckel, 1881, K–Q_4
Tympaniscus Haeckel, 1887, N_1?–Q_4
Tympanomma Haeckel, 1887, sensu Petrushevskaya, 1981, Pg_3–N_1

Udan Renz, 1976, Q_4
Ulcundia Nazarov, 1974, $\in_1$–O_3
Ultranapora Pessagno, 1977, J_1s–K_2t
Unuma Ichikawa et Yao, 1976, J_2a–J_3o
Urocyrtis Pantanelli, 1880, Q_4

Vallupus Pessagno et Blome, 1984, J_3t
Veghia Kozur et Mostler, 1981, T_3n
Veghicyclia Kozur et Mostler, 1972, T_3c–T_3n
Velicucullus Riedel et Campbell, 1952, Pg_3r–N_1l
Verticillata Popofsky, 1913, ?–Q_4
Vinassaspongus Kozur et Mostler, 1979, T_2l–T_3c
Vistularia Gorka, 1989, K_2km
Vitorfus Pessagno, 1977, K_1al$_2$–K_2m

Welirella Dumitrica, Kozur et Mostler, 1980, T_2a–T_3n
Weverella Kozur et Mostler, 1979, T_3c

Wildeus Empson-Morin, 1982, K_2km
Williriedellum Dumitrica, 1970, J_2b–K_1al
Wilvemia Pessagno, Blome et Hull, 1993, in Pessagno *et al.*, 1993, J_2c
Wonella Afanasieva, 2000, D_3f_1–D_3f_2
Wrangellium Pessagno et Whalen, 1982, J_1s–K_2s
Wuranella Kozur et Mostler, 1981, T_3c

X-astrum Neviani, 1900, J_3t
Xanthiosphaera Haeckel, 1881, Q_4
Xenorum Blome, 1984, T_3c–J_1h
Xipha Blome, 1984, nom. invalid. (sin.: *Nakasekoellus* Kozur, 1984)
Xiphacantha Haeckel, 1862, Q_4
Xiphatractus Haeckel, 1887, N_1a–Q_4
Xiphocabrium Deflandre, 1973, C_1
Xiphochistrella Deflandre, 1973, C_1
Xiphocladiella Deflandre, 1973, S_2?–C_1
Xiphodictya Haeckel, 1881, P–Q_4
Xiphoptera Haeckel, 1881, Q_4
Xiphosphaera Haeckel, 1881, D–Q_4
Xiphospira Haeckel, 1887, Pg_1t–N_1s
Xiphostaurus Vinassa de Regny, 1898, nom. invalid. (sin.: *Stauracontium* Haeckel, 1882)
Xiphostylus Haeckel, 1881, S_1–Q_4
Xiphotheca De Wever in De Wever, Sanfilippo, Riedel et Gruber, 1979, T_2l–T_3n
Xitus Pessagno, 1977, J_2b–Pg

Yamatoum Takemura, 1986, J_2a–J_2b
Yaosaturnalis Kozur et Mostler, 1983 J_2b
Yeharaia Nakaseko et Nishimura, 1979, T_2a–T_3n

Zadrappolus Furutani, 1990, S–D
Zaldacria Dumitrica, 1982, T_2a
Zamolxis Dumitrica, 1982, T_2a
Zartus Pessagno et Blome, 1980, J_1p–J_2b
Zhamoidellum Dumitrica, 1970, J_3–K_2km
Zhamojdasphaera Kozur et Mostler, 1979, T_2l–T_3c
Zifonidium Pessagno, 1977, K_2s
Zigocircus Butschli, 1882, N_1?–Q_4
Zigostephaniscus Haeckel, 1881, nom. oblit.
Zonarium Haeckel, 1887, Q_4
Zonidium Haeckel, 1887, Q_4
Zoniscus Haeckel, 1887, Q_4
Zonodiscus Haeckel, 1887, S?–Q_4
Zygacantha Müller, 1858, Q_4
Zygartus Haeckel, 1881, Q_4
Zygocampe Haeckel, 1887, Q_4
Zygocircus Butschli, 1882, emend. Petrushevskaya, 1971, K_1–Q_4
Zygospyris Haeckel, 1881, Q_4
Zygostaurus Haeckel, 1887, Q_4
Zygostephanium Haeckel, 1881, Q_4
Zygostephanus Haeckel, 1862, C?–K_1–Q_4

ACKNOWLEDGMENTS

We are grateful to A.Yu. Rozanov, A.I. Zhamoida, A.S. Alekseev, L.I. Kazintsova, and B.I. Chuvashov for valuable advice and discussions. We are indebted to the reviewers A.A. Shevyrev and L.A. Nevesskaja for their attentive and thorough review of the typescript and many valuable advice and remarks, and to G.S. Rautian, S.V. Nikolaeva, M.K. Emel'yanova, and Ya.M. Kuz'mina for their help in preparing the typescript for publication. We thank O.R. Anderson, P. De Wever, P. Dumitrica, S.N. Golubev, L.I. Kazintsova, H. Kozur, A. Matsuoka, K.A. Mikryukov, M.-Z. Won, and L.A. Zettler for their kind permission to reproduce their figures.

The study was supported by the Program of the Presidium of the Russian Academy of Sciences "Origin and Evolution of the Biosphere" and the Russian Foundation for Basic Research (project nos. 01-05-64450 and 04-05-64103).

REFERENCES

1. A. Abelmann, "Radiolarian Taxa from Southern Ocean Sediment Traps (Atlantic Sector)," Polar Biology **12**, 373–385 (1992).
2. A. Abelmann and M. M. Gowing, "Spatial Distribution of Living Polycystine Radiolarian Taxa—Baseline Study for Paleoenvironmental Reconstruction in the Southern Ocean (Atlantic Sector)," Mar. Micropaleontol., No. 30, 3–28 (1997).
3. S. L. Afanasiev, "Problems of Cyclicity: 2," in *Cycles in Nature and Human Society* (Stavropol Gos. Univ., Stavropol, 1998), Part 1, pp. 73–83 [in Russian].
4. S. L. Afanasiev, *Geology of the Western Caucasus* (Voentekhinizdat, Moscow, 2004) [in Russian].
5. M. S. Afanasieva, "Structural Elements of the Test Wall of the Buliminids (Foraminifera)," Paleontol. Zh., No. 4, 14–20 (1982).
6. M. S. Afanasieva, "Radiolarians of the Family Pylentonemidae," Paleontol. Zh., No. 3, 22–35 (1986).
7. M. S. Afanasieva, "Late Paleozoic Radiolarians from the Karachaganak Field and Their Facial Distribution," in *Stratigraphy and Paleontology of the Paleozoic of the Caspian Depression* (VNIGNI, Moscow, 1987), pp. 26–46 [in Russian].
8. M. S. Afanasieva, "Secondary Alterations of Radiolarian Skeletons," in *First International Conference on Radiolaria (EURORAD V), Marburg, Germany, July, 21–24, 1988: Paleontologic: Conference Book* (Marburg, 1988), p. 3.
9. M. S. Afanasieva, "Ultrastructure and Secondary Alterations of Radiolarian Tests," Paleontol. Zh., No. 1, 28–38 (1990a).
10. M. S. Afanasieva, "Experimental Evidence for Changes during Fossilization of Radiolarian Tests and Implications for a Model of Biomineralizations," Mar. Micropaleontol., No. 15, 233–248 (1990b).
11. M. S. Afanasieva, "New Data on Early Paleozoic Radiolarians of the Genus *Caspiaza*," Paleontol. Zh., No. 4, 115–118 (1993a).
12. M. S. Afanasieva, "The Possible Reasons of Appearing, Biomineralization and Fossilization of Radiolarian Siliceous Skeletons and the Paleobiogeographic Reconstruction for the Early Permian Time," in *Zonenshain Memorial Conference on Plate Tectonics, Moscow, Russia, November 17–20 1993* (Moscow, 1993b), p. 26.

13. M. S. Afanasieva, "The Phylogenesis of Radiolaria: the Dawn and Evolution of Skeletons," *7th Meeting of the International Association of Radiolarian Paleontologists, Osaka City University, Abstracts* (Osaka Univ., 1994), p. 1.
14. M. S. Afanasieva, "Biomineralization and Fossilization of Radiolarian Skeletons," in *2nd International Seminar on Mineralogy and Life: Biomineral Interactions* (Geoprint, Syktyvkar, 1996), p. 64.
15. M. S. Afanasieva, "Morphological Characters of Skeletons of Paleozoic Radiolarians and Their Taxonomic Significance," in *1st International Symposium on the Evolution of Life on the Earth* (NTL, Tomsk, 1997a), pp. 32–34.
16. M. S. Afanasieva, "Morphological Skeleton Features of Paleozoic Radiolarians and Their Taxonomical Significance," in *The First International Conference on the Application of Micropaleontology in Environmental Sciences: Abstracts* (Tel Aviv, 1997b), pp. 19–20.
17. M. S. Afanasieva, "New Variant of Systematics of Paleozoic Radiolarians," in *13th Geological Congress of the Komi Republic on Geology and Mineral Resources of Northeastern European Russia: New Results and New Prospects* (Inst. Geol. Komi Nauchn. Tsentr. Ural. Otd. Ross. Akad. Nauk, Syktyvkar, 1999), Vol. 2, pp. 253–256 [in Russian].
18. M. S. Afanasieva, *Atlas of Paleozoic Radiolaria from the Russian Platform* (Nauchnyi Mir, Moscow, 2000a) [in Russian].
19. M. S. Afanasieva, "New Radiolarians of the Orders Aculearia and Sphaerellaria from the Upper Devonian of the Timan–Pechora Province (Russia)," Paleontol. Zh., No. 4, 3–19 (2000b) [Paleontol. J. **34** (4), 359–376 (2000b)].
20. M. S. Afanasieva, "A New Classification of Paleozoic Radiolaria," Paleontol. Zh., No. 2, 14–29 (2002) [Paleontol. J. **36** (2), 131–145 (2002)].
21. M. S. Afanasieva and J. C. Aitchison, "Upper Devonian, Frasnian, Radiolarian Zones," in *13th International Conference of Marine Geology on Geology of Seas and Oceans* (Ross. Akad. Nauk, Moscow, 1999), Vol. 1, pp. 16–18.
22. M. S. Afanasieva and J. C. Aitchison, "Frasnian Radiolarian Zones of Upper Devonian," in *31st International Geological Congress, Brazil, Rio de Janeiro, 2000* (Rio de Janeiro, 2000), CDR.
23. M. S. Afanasieva and J. C. Aitchison, "Biostratigraphy of the Frasnian Stage by Radiolarian Evidence," Stratigr. Geol. Korrelyatsiya **9** (1), 13–21 (2001) [Stratigr. Geol. Correlation **9** (1), 11–19 (2001)].
24. M. S. Afanasieva and E. O. Amon, "A New Approach to the Problem of Radiolarian Classification: Spiny and Spongy Radiolarians," in *All-Russia Scientific Conference on Geology, Geochemistry, and Geophysics at the Boundary of the 20th and 21st Centuries* (RFFI, Moscow, 2002), Vol. 1, pp. 122–124 [in Russian].
25. M. S. Afanasieva and E. O. Amon, "Origin of Radiolaria Phylum and Radiolarian Evolution during Paleozoic," in *10th Meeting of the International Association of Radiolarian Paleontologists, Lausane, Switzerland, September 7–12, 2003* (Univ. Lausane, Lausane, 2003a), pp. 22–23.
26. M. S. Afanasieva and E. O. Amon, "A New Classification of Radiolaria," in *10th Meeting of the International Association of Radiolarian Paleontologists, Lausane, Switzerland, September 7–12, 2003* (Univ. Lausane, Lausane, 2003b), pp. 24–25.
27. M. S. Afanasieva and E. O. Amon, "A New Classification of the Radiolaria," Paleontol. Zh., No. 6, 72–86 (2003) [Paleontol. J. **37** (6), 630–645 (2003c)].
28. M. S. Afanasieva and E. O. Amon, "Synergetics of Spatial–Structural Interrelations in the Biomineralization of Radiolarian Skeletons," in *4th International Conference on Biniology, Symmetrology, and Synergetics in Natural Sciences* (TyumGNGU, Tyumen, 2004a), pp. 167–172.
29. M. S. Afanasieva and E. O. Amon, "On Some Biogeographic Features of Radiolarians," in *Yearbook-2003 of the Institute of Geology and Geochemistry of the Ural Division of the Russian Academy of Sciences* (Ural. Otd. Ross. Akad. Nauk, Yekaterinburg, 2004b), pp. 3–10 [in Russian].
30. M. S. Afanasieva and E. O. Amon, "To a Question on a Problem of Biomineralization and Formation of Radiolarian Test Skeletal Elements," in *The Fourth International Congress on Environmental Micropaleontology, Microbiology and Meiobenthology: Program and Extended Abstracts, Isparta, Turkey, 2004* (Isparta, 2004c), pp. 15–16.
31. M. S. Afanasieva, E. O. Amon, and B. I. Chuvashov, "Radiolarians in Carboniferous Stratigraphy and Paleobiogeography in Eastern Europe (Caspian Region and Southern Fore-Urals)," Litosfera, No. 4, 22–62 (2002).
32. M. S. Afanasieva, E. O. Amon, and V. S. Vishnevskaya, "Main Events in History of Classification of Radiolarians: 1. Origin and Development of Radiolariology in the 19th and Middle 20th Centuries (1806–1979)," Byull. Mosk. O–va Ispyt. Prir., Otd. Geol. **79** (1), 48–64 (2004a).
33. M. S. Afanasieva, E. O. Amon, and V. S. Vishnevskaya, "Main Events in History of Classification of Radiolarians: 2. Progress of Radiolariology at the End of the 20th and Beginning of 21st Centuries (1980–2003)," Byull. Mosk. O–va Ispyt. Prir., Otd. Geol. **79** (3), 26–52 (2004b).
34. M. S. Afanasieva and M. V. Mikhailova, "Radiolarians As One of Possible Sources of Oil Organic Matter," Geol. Nefti Gaza, No. 1, 12–21 (1998).
35. M. S. Afanasieva and I. M. Timokhin, "Radiolarians and Questions of Hydrodynamics: A New Insight into the Problem," in *Materials of Stratigraphy and Paleontology of the Ural Mountains* (Ural. Otd. Ross. Akad. Nauk, Yekaterinburg, 1999), Vol. 2, pp. 219–226 [in Russian].
36. M. S. Afanasieva and V. S. Vishnevskaya, "Possible Reasons for the Appearance of Siliceous Skeletons in Radiolarians," Dokl. Akad. Nauk **325** (3), 590–596 (1992).
37. M. S. Afanasieva and V. S. Vishnevskaya, "Radiolarians: Benthos and Plankton," Paleontol. Zh., No. 3, 3–13 (1993a).
38. M. S. Afanasieva and V. S. Vishnevskaya, "Radiolarian Fossils As Guides to History of Sedimentation of Cherty Carbonates," Litol. Polezn. Iskop., No. 5, 52–68 (1993b) [Lithol. Min. Res. **28** (5), 415–426 (1993b)].

39. M. S. Afanasieva and T. K. Zamilatskaya, "Paleobiogeography of the Artinskian Age of the Southern Ural Mountains and Northern Caspian Region Based on the Study of Radiolarians and Foraminifers," in *The Origin and Practical Use of Siliceous Rocks* (VNIGNI, Moscow, 1987), pp. 78–85 [in Russian].

40. M. S. Afanasieva and T. K. Zamilatskaya, "The Paleobiogeography of the North-East Pricaspian in Artinskian Time Based on Radiolaria and Foraminifera," Micropaleontology, No. 6 (Spec. Pub.: Radiolaria of Giant and Subgiant Fields in Asia), 61–66 (1993).

41. Yu. V. Agarkov, "Information System for Radiolarians," *10th Seminar on Radiolarians: Abstracts* (Inst. Litosf. Ross. Akad. Nauk, Moscow, 1996), p. 6.

42. Yu. V. Agarkov, "Information System on Radiolarians," in *6th Zonenshain Conference on Plate Tectonics, Moscow, February 17–20, 1998* (Inst. Oceanolog. Russ. Acad. Sci., Moscow, 1998), pp. 149–150.

43. Yu. V. Agarkov, "Information Systems—The Future of Paleontology," in *45th Session of the Paleontological Society: Paleontology in the System of Sciences: Abstracts* (S.-Peterb. Gos. Univ., St. Petersburg, 1999), pp. 3–4 [in Russian].

44. Yu. V. Agarkov, "New Data on Species Diversity of Mesozoic Radiolarians," in *Radiolariology on the Eve of Millennium: Achievements and Perspectives* (Moscow–St. Petersburg, 2000a), pp. 9–10 [in Russian].

45. Yu. V. Agarkov, "Radiolarians, Diatom Algae and Hydrocarbon Potential of Petroleogenetic Rocks," in *Radiolariology on the Eve of Millennium: Achievements and Perspectives* (Moscow–St. Petersburg, 2000b), pp. 10–11 [in Russian].

46. Yu. V. Agarkov, "Micropaleontological Informational System," in *4th International Congress on Environmental Micropaleontology, Microbiology and Meiobenthology: Program and Extended Abstracts, Isparta, Turkey, 2004* (Isparta, 2004), p. 19.

47. Y. Aita and N. Yu. Bragin, "Non-Tethyan Triassic Radiolaria from New Zealand and Northeastern Siberia," Geodiversitas **21** (4), 503–526 (1999).

48. J. C. Aitchison, "Albaillellaria from the New England Orogen, Eastern NSW, Australia," Mar. Micropaleontol., No. 21, 353–367 (1993).

49. J. C. Aitchison, "A Lower Ordovician (Arenig) Radiolarian Fauna from the Ballantrae Complex, Scotland," Scottish J. Geol. **34**, 73–81 (1998).

50. S. A. Aivazyan, I. S. Enyukov, and L. D. Meshalkin, *Applied Statistics: Study of Dependences* (Finansy Statistika, Moscow, 1985) [in Russian].

51. A. S. Alekseev, "Quantitative Analysis of Extinction at the Boundary of the Mesozoic and Cenozoic," Byull. Mosk. O–va Ispyt. Prir., Otd. Geol. **59** (2), 87–102 (1984).

52. A. S. Alekseev, "Global Biotic Crises and Mass Extinctions in the Phanerozoic History of the Earth," in *Biotic Events at the Basic Boundaries of the Phanerozoic* (Mosk. Gos. Univ., Moscow, 1989), pp. 22–47 [in Russian].

53. A. S. Alekseev, "Mass Extinctions in the Phanerozoic," Doctoral Dissertation in Geology and Mineralogy (Mosk. Gos. Univ., Moscow, 1998).

54. A. S. Alekseev, V. Yu. Dmitriev, and A. G. Ponomarenko, *Evolution of Taxonomic Diversity* (GEOS, Moscow, 2001) [in Russian].

55. B. Allanson, R. Hart, and J. Lutjeharms, "Observations on the Nutrients, Chlorophyll and Primary Production of the Southern Ocean South of Africa," S. Afr. J. Antarctic Res. **10** (11), 3–14 (1981).

56. A. L. Alldredge and C. C. Gotschalk, "The Relative Contribution of Marine Snow of Different Origin to Biological Processes in Coastal Waters," Continental Shelf Res. **10**, 41–58 (1990).

57. E. O. Amon, "On Mechanical Deformations and Damages of Radiolarian Skeletons in the Course of Lithogenesis," in *11th All-Union Micropaleontological Meeting: Fundamentals of Modern Micropaleontology: Taxonomic, Biocenologic, and Evolutionary Aspects* (Geol. Inst. Akad. Nauk SSSR, Moscow, 1990), pp. 13–14 [in Russian].

58. E. O. Amon, "On Some Problems of Formalized Knowledge in Radiolarian Analysis," in *Yearbook-1994: Information Collected Works: Stratigraphy, Paleontology* (Inst. Geol. Geokhim., Yekaterinburg, 1995), pp. 3–5 [in Russian].

59. E. O. Amon, "Logical-and-Semantic Analysis of the Category Space of Characters in Paleontology," in *Materials of Stratigraphy and Paleontology of the Ural Mountains* (Inst. Geol. Geokhim., Yekaterinburg, 1996), Vol. 1, pp. 180–193 [in Russian].

60. E. O. Amon, "To the Position of Radiolaria in System of Protozoa and Macrosystematics of Fossil Radiolarians," in *1st International Symposium on the Evolution of Life on the Earth* (NTL, Tomsk, 1997), pp. 31–32.

61. E. O. Amon, "Systematics of Sphaerellarians (Radiolaria) from the Paleozoic of the Ural Mountains," in *Materials of Stratigraphy and Paleontology of the Ural Mountains* (Ural. Otd. Ross. Akad. Nauk, Yekaterinburg, 1999), Vol. 2, pp. 187–196 [in Russian].

62. E. O. Amon, "Materials to the Revision of the Spiny Radiolarian Family Palaeoscenidiidae from the Paleozoic of the Ural Mountains," in *Materials of Stratigraphy and Paleontology of the Ural Mountains* (Ural. Otd. Ross. Akad. Nauk, Yekaterinburg, 2000a), Vol. 4, pp. 50–86 [in Russian].

63. E. O. Amon, "System of Higher Taxa of Stauraxonic Radiolarians from the Paleozoic," in *Yearbook-1999 of the Institute of Geology and Geochemistry of the Ural Division of the Russian Academy of Sciences* (Ural. Otd. Ross. Akad. Nauk, Yekaterinburg, 2000b), pp. 3–11 [in Russian].

64. E. O. Amon, "Upper Cretaceous Radiolarians from the Ural Mountains," in *Materials of Stratigraphy and Paleontology of the Ural Mountains* (Inst. Geol. Geokhim. Ural. Otd. Ross. Akad. Nauk, Yekaterinburg, 2000c), Vol. 5, pp. 1–209 [in Russian].

65. E. O. Amon, "Some Taphonomic Features of Radiolarians," in *Environment and Life in the Geological Past* (SO RAN NITS OIGGM, Novosibirsk, 2000d), p. 49 [in Russian].

66. E. O. Amon, "Morphotypes of Higher Radiolarian Taxa in Paleobiogeographic Reconstruction: Methodology and Technique of Computer Modeling," in *Radiolariology on the Eve of Millennium: Achievements and Per-*

spectives (Moscow–St. Petersburg, 2000e), pp. 12–13 [in Russian].

67. E. O. Amon, "Marine Water Areas of the Ural Region in the Middle and Late Cretaceous," Geol. Geofiz. **42** (3), 471–483 (2001).
68. E. O. Amon, "Certain Patterns of the Global Geographical Distribution of Late Cretaceous Radiolarians of the Genus *Prunobrachium*," Litosfera, No. 4, 78–83 (2003).
69. O. R. Anderson, "Radiolaria," in *Biochemistry and Physiology of Protozoa* (New York, 1980), Vol. 10, No. 3, pp. 1–42.
70. O. R. Anderson, "Radiolarian Fine Structure and Silica Deposition," in *Silicon and Siliceous Structures in Biological Systems* (Springer, New York–Heidelberg–Berlin, 1981), pp. 347–379.
71. O. R. Anderson, *Radiolaria* (New York, 1983).
72. O. R. Anderson, "Physiological Studies of Polycystine Radiolaria," in *Morphology, Ecology, and Evolution of Radiolarians* (Nauka, Leningrad, 1984), pp. 31–34 [in Russian].
73. O. R. Anderson, "Silicification in Radiolaria—Deposition and Ontogenetic Origin of Forms," in *Biomineralization in Lower Plants and Animals*, Ed. by B. S. C. Leadbeater and R. Riding (Clarendon Press, Oxford, 1986), Vol. Spec. (Systemat. Assoc. UK), pp. 375–391.
74. O. R. Anderson, P. Bennet, and M. Bryan, "Experimental and Observational Studies of Radiolarian Physiological Ecology: 1. Growth, Abundance, and Opal Productivity of the Spongiose Radiolarian *Spongaster tetras tetras*," Mar. Micropaleontol. **14** (4), 257–266 (1989a).
75. O. R. Anderson, P. Bennet, and M. Bryan, "Experimental and Observational Studies of Radiolarian Physiological Ecology: 2. Trophic Activity and Symbiont Primary Productivity of *Spongaster tetras tetras* with Comparative Data on Predatory Activity of Some Nassellaridae," Mar. Micropaleontol. **14** (4), 267–273 (1989b).
76. O. R. Anderson, P. Bennet, and M. Bryan, "Experimental and Observational Studies of Radiolarian Physiological Ecology: 3. Effects of Temperature, Salinity and Light Intensity on the Growth and Survival of *Spongaster tetras tetras* Maintained in Laboratory Culture," Mar. Micropaleontol. **14** (4), 275–282 (1989c).
77. O. R. Anderson, M. Bryan, and P. Bennet, "Experimental and Observational Studies of Radiolarian Physiological Ecology: 4. Factors Determining the Distribution and Survival of *Didymocyrtis tetrathalamus tetrathalamus* with Implication for Paleoecological Interpretation," Mar. Micropaleontol. **16** (1), 155–167 (1990a).
78. O. R. Anderson, B. K. Linsley, and J. V. Gardner, "Expression of Seasonal and ENSO Forcing in Climatic Variability at Lower than ENSO Frequencies: Evidences from Pleistocene Marine Varves of California," Paleogeogr. Paleoclimatol. Paleoecol. **78** (3–4), 287–300 (1990b).
79. O. R. Anderson and A. Matsuoka, "Endocytoplasmic Microalgae and Bacteroids within the Central Capsule of the Radiolarian *Dictyocoryne truncatum*," Symbiosis, No. 12, 237–247 (1992).
80. O. R. Anderson, N. Nigrini, D. Boltovskoy, *et al.*, "Class Polycystinea," in *An Illustrated Guide to the Protozoa*, Ed. by J. Lee (Soc. Protozoologists, Lawrence, 2002), pp. 994–1022.
81. R. W. Angell, "Calcification during Chamber Development in *Rosalina floridana*," J. Foram. Res. **9** (4), 341–353 (1979).
82. D. K. Arkhipenko, T. N. Grigor'eva, and T. N. Moroz, "Diffraction and Nondiffraction Methods of Studying of Bony–Mineral Tissue," in *2nd International Seminar on Mineralogy and Life: Biomineral Interactions* (Geoprint, Syktyvkar, 1996), pp. 28–29.
83. I. S. Barskov, "Biochemical and Microstructural Methods in Paleontology," in *Itogi Nauk. Tekhn., Ser. Stratigr. Paleontol.* **6** (Biochemical Methods in Paleontology and the Earliest Signs of Life on the Earth), pp. 5–59 (1975).
84. I. S. Barskov, "Biomineralization and Evolution," Paleontol. Zh., No. 4, 5–13 (1982).
85. I. S. Barskov, "Paleontological Aspects of Biomineralization," in *Reports of the 17th International Geological Congress, 1984, Section C.02. Paleontology* (Nauka, Moscow, 1984), Vol. 2, pp. 61–66 [in Russian].
86. I. S. Barskov, J. P. Guif, Y. Dauphin, and S. I. Kiyashko, "Comparative Studies of the Calcitic and Aragonitic Rostra of Some Coleoid Cephalopoda," in *2nd International Seminar on Mineralogy and Life: Biomineral Interactions* (Geoprint, Syktyvkar, 1996), pp. 89–90.
87. I. A. Basov and V. S. Vishnevskaya, *Stratigraphy of the Upper Mesozoic of the Pacific Ocean* (Nauka, Moscow, 1991) [in Russian].
88. P. O. Baumgartner, P. Dumitrica, I. I. Chiari, *et al.*, "A Proposition for the Revision of the Middle Jurassic to Lower Cretaceous Radiolarian Database (INTERRAD Jurassic–Cretaceous Working Group 1995)," in *10th Meeting of the International Association of Radiolarian Paleontologists, Lausane, Switzerland, September 7–12, 2003* (Univ. Lausane, Lausane, 2003), p. 33.
89. P. O. Baumgartner, O'Dogherty, S. Gprican, *et al.*, "Middle Jurassic to Lower Cretaceous Radiolarian of Tethys: Occurrences, Systematics, Biochronology," Mém. Geol. Lausanne, No. 23, 1–1143 (1995).
90. J. R. Beers and G. L. Stewart, "The Vertical Distribution of Microzooplankton and Some Ecological Observations," J. Cons. Int. Explor., No. 33, 30–44 (1969).
91. Y. R. Beers and G. L. Stewart, "Micro-Zoolplankters in the Plankton Communities of the Upper Waters of the Eastern Tropical Pacific," Deep-Sea Res. **18** (9), 62–74 (1971).
92. V. N. Beklemishev, *Fundamentals of Invertebrate Comparative Anatomy*, Vol. 1: *Promorphology* (Nauka, Moscow, 1964) [in Russian].
93. S. Bellemo, "The Compound and Intermediate Wall Structures in Cibicidinae (Foraminifera) with Remarks on the Radial and Granular Wall Structures," Bull. Geol. Inst. Univ., New Ser. **6**, 1–11 (1974).
94. N. V. Belov, *Sketches on the Structural Mineralogy* (Nauka, Moscow, 1976) [in Russian].
95. R.-N. Benson, "Gulf of California Radiolaria on the Web," in *10th Meeting of the International Association of Radiolarian Paleontologists, Lausane, Switzerland, September 7–12, 2003* (Univ. Lausane, Lausane, 2003), p. 36.

96. W. H. Berger, "Radiolarian Skeletons: Solution at Depths," Science **159** (3820), 1237–1239 (1968a).

97. W. H. Berger, "Planktonic Foraminifera: Selective Solution and Paleoclimatic Interpretation," Deep-Sea Res. **15**, 31–43 (1968b).

98. W. H. Berger, "Biogenous Deep-Sea Sediments: Production, Preservation and Interpretation," Chem. Oceanogr. **5**, 265–388 (1976).

99. R. Bernstein, S. A. Kling, and D. Boltovskoy, "Acantharia," in *South Atlantic Zooplankton*, Ed. by D. Boltovskoy (Backhuys Publ., Leiden, 1999), pp. 75–147.

100. A. G. Betekhtin, *Mineralogy* (Gosgeolizdat, Moscow, 1950) [in Russian].

101. K. R. Bjørklund and P. F. Ciesielski, "Ecology, Morphology, Stratigraphy, and Paleoceanographic Significance of *Cycladophora davisiana davisiana*: 1. Ecology and Morphology," Mar. Micropaleontol. **24** (1), 71–88 (1994).

102. K. R. Bjørklund and R. M. Goll, "Final Stages of Skeletogenesis and Early Stages of Disintegration for Modern Polycystine Radiolaria," Mar. Micropaleontol. **11** (1–3), 171–184 (1986).

103. K. R. Bjørklund and S. B. Kruglikova, "Polycystine Radiolarians in Surface Sediments in the Arctic Ocean Basins and Marginal Seas," Mar. Micropaleontol. **49**, 231–273 (2003).

104. N. A. Bogdanov, V. S. Vishnevskaya, P. K. Kepezhinskas, *et al.*, *Geology of the South of the Koryak Plateau* (Nauka, Moscow, 1987) [in Russian].

105. G. Bohrmann, A. Abelmann, R. Gersonde, *et al.*, "Pure Siliceous Ooze, a Diagenetic Environment for Early Chert Formation," Geology **22** (3), 207–210 (1994).

106. D. Boltovskoy, "Características biológicas del Atlántico Sudoccidental," in *Atlas del Zooplancton del Atlántico Sudoccidental y métodos de trabajo con el zooplancton marino*, Ed. by D. Boltovskoy (Public. Esp. Inst. Nac. Inv. Desarrollo Pesq., Mar del Plata, 1981a), pp. 239–251.

107. D. Boltovskoy, "Radiolaria," in *Atlas del Zooplancton del Atlántico Sudoccidental y métodos de trabajo con el zooplancton marino*, Ed. by D. Boltovskoy (Public. Esp. Inst. Nac. Inv. Desarrollo Pesq., Mar del Plata, 1981b), pp. 261–316.

108. D. Boltovskoy, "Variación latitudinal de la diversidad zooplanctonica en el Atlántico Sudoccidental," Physis Buenos Aires, Sec. A **41** (100), 1–6 (1982).

109. D. Boltovskoy, "Biogeography of the Southwestern Atlantic: Overview, Current Problems and Prospects," UNESCO Techn. Pap. Mar. Sci. **49** (Pelagic Biogeography, Ed. by A. C. Pierrot-Bults, S. van der Spoel, B. J. Zahuranec, and R. K. Johnson), 14–24 (1986).

110. D. Boltovskoy, "Sedimentary Record of Radiolarian Biogeography in the Equatorial to Antarctic Western Pacific Ocean," Micropaleontology **33** (3), 267–281 (1987).

111. D. Boltovskoy, "The Sedimentary Record of Pelagic Biogeography," Progr. Ocenogr. **34** (2–3), 135–160 (1994).

112. D. Boltovskoy, "Deformation of the Radiolarian Fossil Record: Plankton vs. Sediments Traps vs. Surface Sediment," in *INTERRAD VIII, Paris–Bierville, September 8–13, 1997* (Paris, 1997), p. 25.

113. D. Boltovskoy, "Classification and Distribution of South Atlantic Recent Polycystine Radiolaria," Paleontologica Electronica **1** (2), 1–116 (1998) (http://palaeo-electronica.org/1998_2/boltovskoy/issue2.htm).

114. D. Boltovskoy, "Radiolaria Polycystina," in *South Atlantic Zooplankton*, Ed. by D. Boltovskoy (Backhuys Publ., Leiden, 1999), pp. 149–212.

115. D. Boltovskoy and V. A. Alder, "Paleoecological Implications of Radiolarian Distribution and Standing Stocks versus Accumulation Rates in the Weddell Sea," Antarc. Res. Ser. Am. Geophys. Union **56** (The Antarctic Environment: A Perspective on Global Change, Ed. by J. P. Kennett and D. A. Warnke), 377–384 (1992).

116. D. Boltovskoy, V. A. Alder, and A. Abelmann, "Annual Flux of Radiolaria and Other Shelled Plankters in the Eastern Equatorial Atlantic at 853 m: Seasonal Variations and Polycystine Species-Specific Response," Deep-Sea Res. **40**, 1863–1895 (1993).

117. D. Boltovskoy and S. S. Jankilevich, "Radiolarian Distribution in East Equatorial Pacific Plankton," Oceanol. Acta **8**, 101–123 (1985).

118. D. Boltovskoy, M. Kogan, V. A. Alder, and H. Mianzan, "First Record of a Brackish Radiolarian (Polycystina): *Lophophaena rioplatensis* n. sp. in the Rio de la Plata Estuary," J. Plankt. Res. **25** (12), 1551–1559 (2003).

119. D. Boltovskoy, H. Oberhaensli, and G. Wefer, "Radiolarian Assemblages in the Eastern Tropical Atlantic: Patterns in the Plankton and in Sediment Trap Samples," J. Mar. Syst. **8** (1/2), 31–51 (1996).

120. S. O. Borodkin, "Ecological Features of the Chemical Structure of Marine Plankton," in *Chemistry of Seas and Oceans* (Nauka, Moscow, 1995), pp. 223–240 [in Russian].

121. N. Yu. Bragin, "Triassic Period As a Unique Stage of Radiolarian Evolution," in *Radiolariology on the Eve of Millennium: Achievements and Perspectives* (Moscow–St. Petersburg, 2000), pp. 23–24 [in Russian].

122. N. Yu. Bragin, "Triassic Radiolarians: Zonal Stratigraphy and Paleobiogeographic Zonation," Doctoral Dissertation in Geology and Mineralogy (Geol. Inst. Ross. Akad. Nauk, Moscow, 2002) [in Russian].

123. N. Yu. Bragin, V. S. Vishnevskaya, A. I. Zhamoida, and L. I. Kazintsova, *Mesozoic Radiolarians: Practical Handbook of Microfauna* (Vseross. Geol. Inst., St. Petersburg, 1999), Vol. 6 [in Russian].

124. L. G. Bragina, "Late Cretaceous Representatives of the Superorder Phaeodaria (Radiolaria)," Paleontol. Zh., No. 1, 10–12 (2003) [Paleontol. J. **37** (1), 8–10 (2003)].

125. F. Brandini, D. Boltovskoy, A. Piola, *et al.*, "Multiannual Trends in Fronts and Distribution of Nutrients and Chlorophyll in the Southwestern Atlantic (30–62° S)," Deep-Sea Res. **47** (6), 1015–1033 (2000).

126. K. Brandt, "Ueber die morphologische und physiologische des *Chlorophylles beii* Thierren," Mittheil. Zool. Stat. Neapel. **4**, 191–302 (1882).

127. K. Brandt, "Beiträge zur Kenntnis der Colliden," Arch. Protisten. **1** (1), 59–88 (1902).

128. K. Brandt, "Zur Systematik der koloniebildenden Radiolarien," Zool. Jahrb., Abt. Anat. Ontog. Tiere., No. Suppl. 8, 311–352 (1905).

129. M. A. Bustillo, A. Nishimura, V. Atana, and I. Hattori, "Paleocene Radiolarians from Xenoliths Hosted in Holocene Lavas of Lanzarote (Canary Islands)," Geobios **27** (2), 181–188 (1994).

130. J. Cachon and M. Cachon, "Recherches sur le metabolosme de la silice chez les Radiolaires: Absorption et excretion," C. R. Acad. Sci., D, No. 272, 1652–1654 (1971).

131. J. Cachon and M. Cachon, "Les modalités du depot de la silice chez Radiolaires," Arch. Protisten. **114**, 1–13 (1972).

132. J. Cachon and M. Cachon, "Le Systeme axopodail des Collodaires (Radiolaires Polycystines): 1. Les Exoaxopodiata," Arch. Protisten. **118**, 227–234 (1976a).

133. J. Cachon and M. Cachon, "Les axopodes de Radiolaires dans Ieur partie libre et ectoplasmique: structure et function," Arch. Protisten. **118**, 310–320 (1976b).

134. A. S. Campbell, "Radiolaria," in *Treatise on Invertebrate Paleontology: Protista*, Ed. by R. C. Moore (Univ. Kansas Press Geol. Soc. Am., Lawrence, 1954), Part D, pp. 11–163.

135. M. Caridroit, P. De Wever, and P. Dumitrica, "Un nouvel ordre, une nouvelle famille et un nouveau genre de Radiolaires du Paleozoique: Latentifistularia, Cauletellidae et Cauletella," C. R. Acad. Sci., Ser. 2, No. 329, 603–608 (1999).

136. D. A. Caron, A. F. Michaels, N. R. Swanberg, and F. A. Howse, "Primary Productivity by Symbiont-bearing Planktonic Sarcodines (Acantharia, Radiolaria, Foraminifera)," J. Plankt. Res. **17** (1), 103–129 (1995).

137. D. A. Caron and N. R. Swanberg, "The Ecology of Planktonic Sarcodines," Rev. Aquat. Sci. **3**, 147–180 (1990).

138. R. Casey, T. M. Partridge, and J. R. Sloan, "Radiolarian Life Spans, Mortality Rates, and Seasonality Gained from Recent Sediment and Plankton Samples," in *Proceedings of the 2nd Planktonic Conference*, Ed. by A. Farinacci (Edizioni Tecnoscienza, Roma, 1970), Vol. 1, pp. 159–165.

139. J. P. Caulet and C. Nigrini, "RADWORD and RADSEARCH: A Comprehensive Radiolarian Relational Database and Web Site," in *10th Meeting of the International Association of Radiolarian Paleontologists, Lausane, Switzerland, September 7–12, 2003* (Univ. Lausane, Lausane, 2003), p. 40.

140. T. Cavalier-Smith, "Kingdom Protozoa and Its 18 Phyla," Microbiol. Rev. **57**, 953–994 (1993).

141. D. M. Chedija, *Review of the Radiolarian Systematics* (Tadzh. Gos. Univ., Stalinabad, 1959) [in Russian].

142. D. M. Chedija, "Haeckel's Systematics and Evolutionary Development of Radiolarians," in *Paleontology of Tajikistan* (Tadzh. Gos. Univ., Dushanbe, 1964), pp. 86–134 [in Russian].

143. D. M. Chedija, "Proposed Principles of the Development of Systematics of Some Radiolarians of the Order Spumellaria," in *Ancient Radiolarians of Central Asia* (Dushanbe, 1978), Vol. 5, pp. 3–29 [in Russian].

144. N. M. Chumakov, "Periodicity of the Main Glacial Events and Their Correlation with the Endogenous Activity of the Earth," Dokl. Akad. Nauk **378** (5), 656–659 (2001) [Dokl. Russ. Acad. Sci. **378** (5), 616–619 (2001)].

145. N. M. Chumakov, "Patterns of Global Climatic Changes Based on Geological Data," Stratigr. Geol. Korrelyatsiya **12** (2), 7–32 (2004) [Stratigr. Geol. Correlation **12** (2), 112–137 (2004)].

146. B. I. Chuvashov, *The History of Development and Bionomic Characteristics of the Late Devonian Basin on the Western Slope of the Middle and Southern Ural Mountains* (Nauka, Moscow, 1968) [in Russian].

147. B. I. Chuvashov, "Permian Reefs of the Urals," Facies **8**, 191–212 (1983).

148. B. I. Chuvashov, E. O. Amon, J. N. Proust, and M. Caridroit, "Radiolarians in the Polyfacial Late Paleozoic Formations of the Ural Foredeep," Stratigr. Geol. Korrelyatsiya **7** (6), 41–55 (1999) [Stratigr. Geol. Correlation **7** (6), 566–580 (1999)].

149. B. I. Chuvashov and S. Crasquin-Soleau, "Palaegeopraphy and Palaeotectonic of the Jointing Area between the Eastern European Basin and the Tethys Basin during Late Carboniferous (Moscovian) and Early Permian (Asselian and Artinskian)," Mem. Mus. Nat. Hist. Nat. **182**, 203–238 (2000).

150. G. R. Clark II and R. A. Lutz, "Pyritization in the Shells of Living Bivalves," Geology **8**, 268–271 (1980).

151. J. O. Corliss, "What Are the Taxonomic and Evolutionary Relationship of the Protozoa and Protista?," Biosystems **14**, 445–459 (1981).

152. J. O. Corliss, "The Kingdom Protista and 45 Phylla," Biosystems **17**, 87–126 (1984).

153. J. O. Corliss, "An Interim Utilitarian ("User-Friendly") Hierarchical Classification and Characterization of the Protists," Acta Protozool. **33**, 1–51 (1994).

154. G. Cortese and K. R. Bjørklund, "Morphometric Study of the Radiolarian *Actinomma borealis* in the Sediments of the Norwegian-Iceland Seas in the Western Norwegian Fjords," in *5th Zonenshain Conference on Plate Tectonics: Abstracts* (Moscow, 1995), pp. 199–200.

155. P. De Wever, "Radiolaires du Trias et du Lias de la Tethys (Systématique, Stratigraphie)," Sciet. Geol. Nord **7**, 1–599 (1982).

156. P. De Wever, J. Azema, and E. Fourcade, "Radiolarians and Radiolarite: Primary Production, Diagenesis and Paleogeography," Bull. Centr. Rech. Explor.-Product. d'Elf-Aquitaine **18** (1), 315–379 (1994).

157. P. De Wever, P. Dumitrica, J. P. Caulet, *et al.*, *Radiolarians in the Sedimentary Record* (Gordon and Breach Sci. Publ., 2001).

158. P. De Wever and I. Origlia, "A Classification of Saturnalid-Types Forms Based on Symmetry," in *Morphology, Ecology, and Evolution of Radiolarians* (Nauka, Leningrad, 1984), pp. 103–113 [in Russian].

159. P. De Wever, A. Sanfilippo, W. R. Riedel, and B. Gruber, "Triassic Radiolarians from Greece, Sicily and Turkey," Micropaleontology **225** (1), 75–110 (1979).

160. *Deep Sea Drilling Project: Index and Reference Files: Paleontological Cumulative Index* (1990).

161. G. Deflandre, "Classe de Radiolaires," in *Traite de Paleontologie*, Ed. by J. Piveteau (Masson et Gie, Paris, 1952a), Vol. 1, pp. 303–313.

162. G. Deflandre, "*Albaillella* nov. gen., Radiolaire fossile du Carbonifere inferieur, type d'une lignee aberrante eteinte," C. R. Acad. Sci. **234** (8), 872–874 (1952b).

163. G. Deflandre, "Radiolaires fossiles," in *Traite de Zooligie*, Ed. by P. Grasse (Masson et Gie, Paris, 1953), Vol. 1, Part 2, pp. 389–436.

164. G. Deflandre, "*Lapidopiscum* nov. gen., type nouveau de Radiolaire vissen, famille des Lapidopiscidae fam. nov., de l'ordre des Albaillellidae Defl., 1953," C. R. Acad. Sci. **246** (15), 2278–2280 (1958).

165. G. Deflandre, "A propos du developpment des recherches sur les Radiolaires fossiles," Rev. Micropaleontol. **2** (4), 212–218 (1960).

166. G. Deflandre, "*Pylentonema*, nouveau genre de Radiolaire du viscen: Sphaerellaria on Nassellarie?," C. R. Acad. Sci. **257** (25), 3981–3984 (1963).

167. G. Deflandre, "Sur le sens du developpment, centrifuge ou centripete, des elements de la coque des Radiolaires Sphaerellaires," C. R. Acad. Sci. **259** (13), 2117–2119 (1964a).

168. G. Deflandre, "La famille des Popofskyellidae fam. nov. et le genre *Popofskyellum* Deflandre, radiolaires viseen de la Montagne noire," C. R. Acad. Sci. **259** (18), 3055–3058 (1964b).

169. G. Deflandre, "Le systeme trabeculaire interne chez les *Pylentonemides* et les *Popofskyellides*, Radiolaires de Paleozoique: Phylogenese de Nassellaires," C. R. Acad. Sci. **274** (26), 3535–3540 (1972).

170. G. Deflandre, "Sur quelques nouveaux types de Radiolaires Polycystines viseens, d'attribution systématique ambigue, certains evoquant a la fois des plectellaires et des spumellaires," C. R. Acad. Sci. **276**, 289–293 (1973).

171. G. Deflandre and M. Deflandre-Rigaud, "Donnees paleontologiques sur l'ontogenese de la coque des Radiolaires Sphaerellaires: Consequences taxinomiques," C. R. Acad. Sci. **246** (6), 968–970 (1958).

172. F. I. Demin, "The Study of Processes Gelation and Germformation by the Method of Optical (Rayleigh) Scattering," in *2nd International Seminar on Mineralogy and Life: Biomineral Interactions* (Geoprint, Syktyvkar, 1996), pp. 22–23.

173. G. A. Dmitriev and M. S. Potapova, "The Theory of Symmetry As a General Method for Investigation of Developmental Patterns of the Earth," in *Approaches to the Investigation of the Earth* (Nauka, Moscow, 1971), pp. 153–171 [in Russian].

174. N. L. Dobretsov, "Correlation of Biological and Geological Events in the History of the Earth and Probable Mechanisms of Biological Evolution," Paleontol. Zh., No. 6, 4–15 (2003) [Paleontol. J. **37** (6), 579–590 (2003)].

175. N. L. Dobretsov and N. M. Chumakov, *Global Periodicity in the Evolution of Lithosphere and Biosphere,* in *Global Changes in Natural Environment*, Ed. by N. L. Dobretsov and V. I. Kovalenko (Geo, Novosibirsk, 2001), pp. 11–27 [in Russian].

176. V. A. Dogel, "New Data on Radiolarian Phylogeny," Zool. Zh. **29** (6), 562–565 (1950).

177. V. A. Dogel, *General Protistology* (Sovetskaya Nauka, Moscow, 1951) [in Russian].

178. P. Dumitrica, "Triassic Palaeosceniidae and Entactiniidae from Vicentinian Alps (Italy) and Eastern Carpathians (Romania)," Dari de seama ale medinteler. Inst. Geol. Geofis. **64**, Part 3, 39–54 (1978).

179. P. Dumitrica, "Middle Triassic Spicular Radiolaria," Rev. Espan. Micropaleontol. **14**, 401–428 (1982).

180. P. Dumitrica, "Systematics of Sphaerellarian Radiolarians," in *Morphology, Ecology, and Evolution of Radiolarians* (Nauka, Leningrad, 1984), pp. 91–102 [in Russian].

181. P. Dumitrica, "Internal Morphology of the Saturnalidae (Radiolaria): Systematic and Phylogenetic Consequences," Rev. Micropaleontol. **28** (3), 181–196 (1985).

182. P. Dumitrica, "New Families and Subfamilies of Pyloniacea (Radiolaria)," Rev. Micropaleontol. **31** (3), 178–195 (1988).

183. P. Dumitrica, "Internal Skeletal Structures of the Superfamily Pyloniacea (Radiolaria), a Basis of a New Systematics," Rev. Esp. Micropaleontol. **21** (2), 207–264 (1989).

184. P. Dumitrica, "Systematic Framework of Jurassic and Cretaceous Radiolaria, Middle Jurassic to Lower Cretaceous Radiolaria of Tethys: Occurrences, Systematics, Biochronology," Mem. Geol. Lausanne, No. 23, 19–35 (1995).

185. P. Dumitrica, M. Caridroit, and P. De Wever, "Archaiospicularia, ordre nouveau de radiolaires: une nouvelle etape pour la classification des radiolaires du Paleozoique inferieur," C.R. Acad. Sci. Paris, Sci. Terre Planet., Earth Planet. Sci. **330**, 563–569 (2000).

186. P. Dumitrica and E. S. Carter, "Family Kungalariidae, n. fam., New Mesozoic Entactinarian Radiolaria with a Nassellarian-Type Initial Spicule," Micropaleontology **45**, 418–428 (1999).

187. P. Dumitrica and P. Zugel, "Lower Tithonian Mono- and Dicyrtid Nassellaria (Radiolaria) from the Solnhofen Area (Southern Germany)," Geodiversitas **25** (1), 5–72 (2003).

188. B. A. Dworetzky and J. J. Morley, "Vertical Distribution of Radiolaria in the Eastern Equatorial Atlantic: Analysis of a Multiple Series of Closely Spaced Plankton Tows," Mar. Micropaleontol., No. 12, 1–19 (1987).

189. A. V. Egorkin, "Silica Content in the Consolidated Crust in the Territory of Russia," Razved. Okhr. Nedr, No. 2, 15–17 (2000).

190. Ch. G. Ehrenberg, "Über die Bildung der Kreidefelsen und des Kreidemergels durch unsichtbare Organismen," in *Abh. Preuss. Berliner Akad. Wissensch.* (Berlin, 1838), pp. 59–147.

191. Ch. G. Ehrenberg, "Über eine halibiolithische, von Herrn R. Schomburgk entdeckte, vorherrschend aus microskopischen Polycystinen gebildete, Gebirgsmasse von Barbados," in *Monatsber. Kgl. Preuss. Akad. Wissensch.* (Berlin, 1847a), pp. 236–250.

192. Ch. G. Ehrenberg, "Beobachtungen über die microskopischen kieselschaligen Polycystinen als mächtige Gebirgsmasse von Barbados und über das Verhältnis der aus mehr als 300 neuen Arten bestehenden ganz eigentümlichen Formengruppe jener Felsmasse zu den lebenden Thieren und zur Kreidebildung," *Monat. Kgl. Preuss. Akad. Wissensch.* (Berlin, 1847b), pp. 40–60.

193. Ch. G. Ehrenberg, "Fortsetzung der mikrogeologischen Studien als Gesammt-Uebersicht der mirkoskopischen Paläontologie gleichartig analysirter Gebirgsarten der Erde, mit specieller Rücksicht auf den Polycystinen

Mergel von Barbados," in *Abh. Kgl. Preuss. Akad. Wissensch.* (Berlin, 1875), pp. 1–226.

194. P. Enriques, "Formazione e sviluppo dello scheltor siliceo nei radiolari," Boll. Soc. Ital. Biol. Sperimentale **6** (4), 350–356 (1931).
195. P. Enriques, "Saggio di una classificazione dei Radiolari," Arch. Zool. Torino **6**, 69–78 (1932).
196. Zh. P. Erkhard and Zh. Sezhen, *Plankton* (Gidrometeoizdat, Leningrad, 1984) [in Russian].
197. M. A. Fedonkin, "Reduction of Geochemical Basis of Life and Eucaryotization of the Biosphere: Causal Relationship," Paleontol. Zh., No. 6, 33–40 (2003) [Paleontol. J. **37** (96), 608–615 (2003)].
198. H. P. Foreman, "Upper Devonian Radiolaria from the Huron Member of the Ohio Shale," Micropaleontology **9** (3), 267–304 (1963).
199. F. Francois, "Deep-Sea Biogenic Silica: New Structural and Analytical Data from Infra-Red Analysis Geological Implications," Terra Nova **1** (3), 267–273 (1989).
200. J. Fricke, "Aerogels," Scientific American, No. 7, 50–56 (1988).
201. M. Fukuchi and S. Tamura, "Chlorophyll a Distribution in the Indian Sector of the Antarctic Ocean in 1978–1979," Antarctic Rec. **74**, 143–162 (1982).
202. R. V. Galiulin, "Ideal Crystals in the Spaces of Constant Curvature," Kristallografiya **39** (4), 581–585 (1994) [Crystallogr. Rep. **39** (4), 571–575 (1994)].
203. R. V. Galiulin, "Principal Difference between Organic and Inorganic Structures," in *2nd International Seminar on Mineralogy and Life: Biomineral Interactions* (Geoprint, Syktyvkar, 1996a), pp. 9–10.
204. R. V. Galiulin, "How the Life Saves the Universe from Mineralization," in *2nd International Seminar on Mineralogy and Life: Biomineral Interactions* (Geoprint, Syktyvkar, 1996b), pp. 103–104.
205. R. J. Gast and D. A. Caron, "Photosymbiotic Associations in Planktonic Foraminifera and Radiolaria," Hydrobiologia **461**, 1–7 (2001).
206. *Geochemistry of Silica*, Ed. by N. M. Strakhov (Nauka, Moscow, 1966) [in Russian].
207. R. M. Goll and K. R. Bjørklund, "Radiolaria in Surface Sediments of the South Atlantic," Micropaleontology **20**, 38–75 (1974).
208. L. A. Golovina and E. P. Radionova, "Monospecific Assemblages of Nannoplankton and Diatoms in the Middle–Upper Miocene of the Eastern Paratethys," in *Modern Questions of Geology* (Nauchnyi Mir, Moscow, 2003), pp. 322–323 [in Russian].
209. S. N. Golubev, *Real Crystals from Coccolithophorid Skeletons* (Nauka, Moscow, 1981) [in Russian].
210. S. N. Golubev, "Crystallophysic Mechanisms of Skeletal Remains Fossilization," Izv. Akad. Nauk SSSR, Ser. Geol., No. 3, 91–97 (1984).
211. S. N. Golubev, "Mineral Crystals inside Organisms and Their Role in the Origin of Life," Zh. Obshch. Biol. **48** (6), 784–806 (1987).
212. E. L. Grossman, P. Bruckschen, Mii Horng-sheng, *et al.*, "Carboniferous Paleoclimate and Global Change: Isotopic Evidence from the Russian Platform," in *Carboniferous Stratigraphy and Paleogeography in Eurasia* (Inst. Geol. Geophys. Ural Br. Russ. Acad. Sci., Yekaterinburg, 2002), pp. 61–71.
213. Ya. M. Gutak, "Evolution of Devonian Basins of Sedimentation in the Mountain Altai," in *International Symposium on the Geology of the Devonian System* (Geoprint, Syktyvkar, 2002), pp. 18–20.
214. E. Haeckel, *Die Radiolarien (Rhizopoda radiata): Eine Monograph* (Berlin, 1862).
215. E. Haeckel, "Über die Phäodarien, eine neue Gruppe Kieselschaliger mariner Rhizopoden," in *Sitzungsber. Jen. Ges. Med. U. Naturwissensch.* (1879), pp. 151–157.
216. E. Haeckel, "Prodromus Systematis Radiolarium: Entwurf eines Padiolariaen-System auf Grund von Studien der Challengen-Radiolarien," Jen. Z. Naturwissensch. **15** (3), 418–472 (1882).
217. E. Haeckel, "Report on the Radiolaria Collected by H.M.S. "Challenger" during the Years 1873–1876," Rept. Sci. Result Voy. "Challenger". Zool. Edinburg. **18** (Part 1–2), 1–1803 (1887).
218. V. Haecker, *Tiefsee-Radiolarien: Ergeb. Dt. Tiefsee-Exped. Dampfer "Valdivia" 1898–1899* (Jena, 1908), Vol. 14.
219. P. Hallock, "Fluctuations in the Trophic Resource Continuum: A Factor in Global Diversity Cycles?," Paleoceanography, No. 2, 457–471 (1987).
220. I. C. Handoh, G. R. Bigg, and E. J. W. Jones, "Evolution of Upwelling in the Atlantic Ocean Basin," Palaeogeogr., Palaeoclimatol., Palaeoecol. **202** (1), 31–58 (2003).
221. H. J. Hansen, "Electron-Microscopical Studies of the Ultrastructures of Some Perforate Calcite Radiate and Granulate Foraminifera," Kongel. Dan. Vid. Selsk. Biol. Skr. **7** (2), 3–16 (1970).
222. H. E. Harper and A. H. Knoll, "Silica, Diatoms and Cenozoic Radiolarian Evolution," Geology **3** (4), 175–177 (1975).
223. R. Hertwig, *Zur Histologie der Radiolarien. Untersuchungen über den Bau und die Entwicklung der Sphaerozoiden und Thalassicolliden* (Leipzig, 1876).
224. R. Herwig, *Der Organismus Der Radiolarien* (Jena, 1879).
225. G. J. Hinde and H. Fox, "On a Well-Marked Horizon of Radiolarian Rocks in the Lower Culm Measures of Devon, Cornwall and West Soomerset," Quart. J. Geol. Soc. London **51**, 609–667 (1895).
226. B. K. Holdsworth, "The Relationship between the Genus *Albaillella* Deflandre and Ceratoikscid Radiolaria," Micropaleontology **15** (2), 230–236 (1969).
227. B. K. Holdsworth, "The Radiolaria of the Baltalimani Formation, Lower Carboniferous, Istanbul," *Paleozoic of Istanbul*, Ed. by Q. Kaya (Ege Univ. Fen. Fakult. Kitaplar, 1973), Ser. i, No. 40, pp. 117–134.
228. B. K. Holdsworth, D. L. Jones, and C. Allison, "Upper Devonian Radiolarians Separated from Chert of the Ford Lake Shale, Alaska," J. Res. US Geol. Surv. **6** (6), 775–788 (1978).
229. A. Hollande, J. Cachon, and M. Cachon, "La signification de la membrane capsulaire des Radiolaires et ses rapports avec le plasmalemme et les membranes du reticulum endoplasmatique: Affinites entre, Radi-

olaires, heliozoaires et Peridiniens," Protistologica **6** (3), 311–318 (1970).

230. A. Hollande and M. Enjumet, "Contribution a l'etude biologique des Sphaerocollides (Radiolaires Collodares et Radiolaires Polycyttares) et de leures parasites: 1. Thalassicollidae, Physematiddae, Thalassophysidae," Ann. Sci. Nat. Zool. Biol. Animal. **15** (1), 99–183 (1953).
231. A. Hollande and M. Enjumet, "Cytologie, evolution et systématique des Sphaeroides (Radiolaires)," Arch. Mus. Nat. Hist. Paris, Ser. 7 **7**, 1–134 (1960).
232. A. Hollande and R. Martoja, "Identification du cristalloide des isospores de radiolaires a un cristal de celestite ($SrSO_4$): Determination de la constitution du cristalloide par voie cytochimique et a l'aide de la microsonde electronique et du microanalyseur par emission ionique secondaire," Protistologica **10** (6), 603–609 (1974).
233. C. J. Hollis, "Biostratigraphy and Paleoceanographic Significance of Paleocene Radiolarians from Offshore Eastern New Zealand," Mar. Micropaleontol., No. 46, 265–316 (2002).
234. Mii Horng-sheng, E. L. Grossman, and T. E. Yancey, "Carboniferous Isotope Stratigraphies of North America: Implications for Carboniferous Paleoceanography and Mississippian Glaciation," GSA Bull. **111** (7), 960–973 (1999).
235. Mii Horng-sheng, E. L. Grossman, T. E. Yancey, *et al.*, "Isotopic Records of Brachiopod Shells from the Russian Platform—Evidence for the Onset of Mid-Carboniferous Glaciation," Chem. Geol. **175**, 133–147 (2001).
236. D. C. Hurd and K. Takahashi, "On the Estimation of Minimum Mechanical Loss during an *in situ* Biogenic Silica Dissolution Experiment," Mar. Micropaleontol., No. 6, 169–182 (1981).
237. H. Ishiga, T. Kito, and N. Imoto, "Late Permian Radiolarian Assemblage in the Tamba District and Adjacent Area, Southwest Japan," Earth Sci. J. Assoc. Geol. Coll. Jap. **36** (1), 10–22 (1982).
238. K. Iwata, N. V. Sennikov, M. M. Buslov, *et al.*, "Late Cambrian–Early Ordovician Age of the Bazalt–Siliceous–Terrigenous Zasur'ya Formation (Northwestern Area of the Mountain Altai)," Geol. Geofiz. **8** (9), 1427–1444 (1997).
239. D. A. Johnson and C. Nigrini, "Radiolarian Biogeography in Surface Sediments of the Western Indian Ocean," Mar. Micropaleontol., No. 5, 111–152 (1982).
240. E. Jörgensen, "The Protist Plankton and Diatoms in Bottom Samples: Radiolaria," Bergen Mus. Skr. **7**, 114–151 (1905).
241. G. A. Kaleda, "Evolution of Siliceous Sedimentation on the Continental Block," in *The Origin and Practical Use of Siliceous Rocks* (Nauka, Moscow, 1987), pp. 43–59 [in Russian].
242. A. V. Kanygin, "The Ordovician Phenomenon of Explosive Differentiation of the Organic World of the Earth: Causes and Evolutionary Consequences for the Biosphere," Geol. Geofiz. **42** (4), 631–667 (2001).
243. J. P. Kennett, *Marine Geology* (Prentice-Hall, New Jork, 1982).
244. A. V. Khabakov, A. A. Strelkov, and R. Kh. Lipman, "Subclass Radiolaria or Radiolarians," in *Fundamentals of Paleontology: General Part, Protists* (Akad. Nauk SSSR, Moscow, 1959), pp. 369–482 [in Russian].
245. V. E. Khain, *The Basic Problems of Modern Geology* (Nauchnyi Mir, Moscow, 2003) [in Russian].
246. I. V. Khvorova, "Carbonate Accumulation," Tr. Geol. Inst. Akad. Nauk SSSR **369**, 82–102 (1984).
247. I. E. Khudyaev, "On the Radiolaria in Phosphorites of the Sysol'skii District," Tr. Glav. Geol.-Razved. Upravl., No. 46, 1–48 (1931).
248. V. S. Kireev, *Course of Physical Chemistry* (Khimich. Lit., Moscow, 1951) [in Russian].
249. A. A. Klevtsova, "Aulacogens of the Russian Platform—Centers of Formation of Hydrocarbons," Razved. Okhr. Nedr, No. 4, 10–15 (2000).
250. A. A. Klevtsova and M. S. Afanasieva, "Rifting, Radiolarians and Oil-and-Gas Potential of Russian Platform," in *6th Zonenshain Conference on Plate Tectonics, February 17–20, 1998: Programme and Abstracts* (Inst. Oceanolog. Russ. Acad. Sci.-GEOMAR, Moscow, 1998), pp. 161–162.
251. S. A. Kling, "Radiolaria," in *Introduction to Marine Micropaleontology*, Ed. by B. U. Haq and A. Boersma (Elsevier, New York, 1978), pp. 203–244.
252. S. A. Kling, "Vertical Distribution of Polycystine Radiolarians in the Central North Pacific," Mar. Micropaleontol., No. 4, 295–318 (1979).
253. S. A. Kling and D. Boltovskoy, "Radiolarian Vertical Distribution Patterns across the Southern California Current," Deep-Sea Res. **42** (2), 191–231 (1995).
254. G. G. Kochemasov, "El Nintideo and Sector Tectonics of the Earth," in *Regularities and Symmetry in the Structure of the Earth* (ROST, Moscow, 1997), pp. 133–141 [in Russian].
255. G. E. Kozlova, *Radiolarians from the Paleogene of the Boreal Region of Russia: Practical Handbook of the Microfauna of Russia* (Vsesoyuzn. Nauchno-Issled. Geol. Razved. Inst., St. Petersburg, 1999), Vol. 9 [in Russian].
256. G. E. Kozlova and A. N. Gorbovets, *Radiolarians of the Upper Cretaceous and Upper Eocene Beds of the West Siberian Lowland* (Nauka, Leningrad, 1966) [in Russian].
257. H. Kozur and H. Mostler, "Beitrage zur Erforschung der mesozoishen Radiolarien: Teil. I. Revision der Oberfamilie Coccodiscacea Haeckel 1862 emend. und Beschreibung ihrer triassischen Vertreuter," Geol. Paläontol. Mitt. Innsbruck **2** (8/9), 1–60 (1972).
258. H. Kozur and H. Mostler, "Entractinaria subordo nov., a New Radiolarian Suborder," Geol. Paläontol. Mitt. Innsbruck. Sonderbd **11** (12), 399–414 (1982).
259. H. Kozur and H. Mostler, "Review of the Systematics of Triassic Radiolarians," in *Morphology, Ecology, and Evolution of Radiolarians* (Nauka, Leningrad, 1984), pp. 114–123 [in Russian].
260. H. Kozur and H. Mostler, "Saturnaliacea Deflandre and Some Other Stratigraphically Important Radiolaria from the Hettangian of Lenggries/Isar (Bavaria, Northern Calcareous Alps)," Geol. Paläontol. Mitt. Innsbruck **17**, 179–248 (1990).
261. H. Kozur, H. Mostler, and J. E. Repetski, "Well-Preserved Tremadocian Primitive Radiolarian from the

Win-Fall Formation of the Antelope Range, Eureka Country, Nevada, USA," Geol. Paläontol. Mitt. Innsbruck. Sonderbd. **21**, 245–271 (1996).

262. S. B. Kruglikova, "Quantitative Distribution of Radiolarians in the Upper Layer of Bottom Deposits of the Northern Part of the Pacific Ocean," in *Geochemistry of Silica* (Nauka, Moscow, 1966), pp. 246–261 [in Russian].
263. S. B. Kruglikova, "Some Features of Ecology and Distribution of Recent and Cenozoic Radiolarians," in *Systematics, Evolution, and Stratigraphic Significance of Radiolarians* (Nauka, Moscow, 1981), pp. 118–139 [in Russian].
264. S. B. Kruglikova, "Paleoecological Reconstructions Based on Radiolarian Studies," in *Morphology, Ecology, and Evolution of Radiolarians* (Nauka, Leningrad, 1984), pp. 41–53 [in Russian].
265. S. B. Kruglikova, "Certain Aspects of Radiolarian Data As Evidence of the Paleoenvironment," Palaeogeogr. Palaeoclimat. Palaeoecol. **69**, 303–320 (1989a).
266. S. B. Kruglikova, "Arctic Ocean Radiolarians," in *The Arctic Seas: Climatology, Oceanography, Geology and Biology*, Ed. by Y. Herman (Van Nostrand Reinhold Pub., New York, 1989b), pp. 461–479.
267. S. B. Kruglikova, "Radiolarians As Indicators of Certain Factors of the Paleoenvironment," in *Radiolarians in Biostratigraphy: Collected Works* (Ural. Otd. Akad. Nauk SSSR, Sverdlovsk, 1990), pp. 92–106 [in Russian].
268. S. B. Kruglikova, "Observation on the Distribution of Polycystine Radiolaria in Marine Sediments (Mainly at High Taxonomic Levels)," Micropaleontology, No. 6 (Spec. Pub.: Radiolaria of Giant and Subgiant Fields in Asia), 17–21 (1993).
269. S. B. Kruglikova, "The Structure of Associations of Polycystine Radiolarians at the Species and Superspecies Levels and Paleoenvironment," in *Recent and Extinct Microplankton of the World Ocean* (Nauka, Moscow, 1995), pp. 76–89 [in Russian].
270. S. B. Kruglikova, "Higher Radiolarian Taxa As Indicators of Environmental Conditions," in *Radiolariology on the Eve of Millennium: Achievements and Perspectives* (Moscow–St. Petersburg, 2000), pp. 36–37 [in Russian].
271. S. B. Kruglikova, "Composition (Structure) of the Specific and Supraspecific Assemblages of Polycystina and Environment," in *10th Meeting of the International Association of Radiolarian Paleontologists, Lausane, Switzerland, September 7–12, 2003* (Univ. Lausane, Lausane, 2003), pp. 75–76.
272. S. B. Kruglikova and K. R. Bjørklund, "Comparative Study of Quantitative Distribution of Radiolaria High Rank Taxa in the Surface Layer of the Norwegian Sea and Norwegian Fjords," in *5th Zonenshain Conference on Plate Tectonics: Abstracts* (Moscow, 1995), pp. 201–202.
273. S. B. Kruglikova and S. V. Maksimova, "Radiolarians," in *Atlas of Rock-Building Organisms (Calciferous and Silicon)* (Nauka, Moscow, 1973), pp. 94–97 [in Russian].
274. M. V. Krylov, A. A. Dobrovol'skii, I. V. Issi, *et al.*, "New Ideas about the System of Unicellular Animals," in *Principles of Reconstruction of the Macrosystem of Unicellular Animals* (Zool. Inst. Akad. Nauk SSSR, Leningrad, 1980), pp. 122–132 [in Russian].
275. G. V. Kukolev, *Chemistry of Silicon and Physical Chemistry of Silicates* (Vyssh. Shkola, Moscow, 1966) [in Russian].
276. O. G. Kusakin and A. A. Drozdov, *Phylema of the Organic World* (Nauka, St. Petersburg, 1994), Part 1 [in Russian].
277. L. S. Kuz'menkov, "The Growth of Structures with the Preservation of Proportions: The Theory of A.A. Vlasov," in *The Processes of Actual Formation of Crystals* (Nauka, Moscow, 1977), p. 227 [in Russian].
278. D. B. Lazarus, "Paleontological Databases, EURORAD-I Lille, 1978 to INTERRAD-VIII, 1997," in *8th Meeting of the International Association of Radiolarian Paleontologists* (Paris–Bierville, 1997), p. 85.
279. D. B. Lazarus, "Environmental Control of Diversity, Evolutionary Rates and Taxa Longevities in Antarctic Neogene Radiolaria," Palaeontologia Electronica **5** (1), 1–32 (2002).
280. N. D. Levine, J. P. Corliss, E. F. G. Cox, *et al.*, "A Newly Revised Classification of the Protozoa," J. Protozool. **27**, 37–58 (1980).
281. B. A. Leyborne, "Can El Nino Be Controlled by Tectonic Vortex Structures and Explained with Surge Tectonics?," in *New Concepts in Global Tectonics* (1998), pp. 5–6.
282. R. Kh. Lipman, "The Major Approaches to the Development of the Radiolarian Systematics and the System of the Order Spumellaria (Sphaeroidea, Prunoidea, Discoidea)," in *Systematics and Stratigraphic Significance of Radiolarians* (Vsesoyuzn. Geol. Inst., Leningrad, 1974), pp. 35–40 [in Russian].
283. R. Kh. Lipman, *Guide to the Study of Extinct Radiolarians* (Nedra, Leningrad, 1979) [in Russian].
284. N. V. Logvinenko and L. V. Orlova, *Formation and Changes of Sedimentary Rocks in the Continent and Ocean* (Nedra, Leningrad, 1987) [in Russian].
285. H. Lowenstam, "Minerals Formed by Organisms," Science **221** (4487), 1126–1131 (1981).
286. H. Lowenstam, "Processes and Products of Biomineralization and the Evolution of Biomineralization," in *Reports of the 17th International Geological Congress, 1984, Section C.02. Paleontology* (Nauka, Moscow, 1984), Vol. 2, pp. 51–56 [in Russian].
287. J. R. E. Lutjeharms, N. Walters, and B. Allanson, "Oceanic Frontal Systems and Biological Enhancement," in *Antarctic Nutrient Cycles and Food Webs*, Ed. by W. R. Siegfried, P. R. Condy, and R. M. Laws (Springer, Berlin, 1985), pp. 11–21.
288. S. V. Maksimova, "Rock-Forming Role of Silicious Organisms and Volcanism," Izv. Vyssh. Shkol., Ser. Geol. Razved., No. 5, 22–27 (1975).
289. L. Margulis, "The Classification and Evolution of Prokaryotes and Eukaryotes," Handb. Genet. **1** (4), 1–41 (1974).
290. A. Matsuoka, "Skeletal Growth of a Spongiose Radiolarian *Dictyocoryne truncatum* in Laboratory Culture," Mar. Micropaleontol., No. 19, 287–298 (1992).

291. A. Matsuoka, "Feeding Behavior and Strategy of the Radiolarian *Pseudocubus obeliscus* Haeckel," in *10th Meeting of the International Association of Radiolarian Paleontologists, Lausane, Switzerland, September 7–12, 2003* (Univ. Lausane, Lausane, 2003), p. 87.

292. A. Matsuoka and O. R. Anderson, "Experimental and Observational Studies of Radiolarian Physiological Ecology: Temperature and Salinity Tolerance of *Dictyocoryne truncatum*," Mar. Micropaleontol., No. 19, 299–313 (1992).

293. A. G. Matul, "On Late Quaternary Paleoceanology of the Northern Atlantic Region Based on Radiolariological Analysis," Okeanologiya **34** (4), 607–613 (1994a).

294. A. G. Matul, "On the Problem of Paleoceanological Evolution of the Area of the Reykjaness Mountains (Northern Atlantic) during the Last Deglaciation Based on the Data of Radiolarian Studies," Okeanologiya **34** (6), 881–889 (1994b).

295. K. J. McMillen, "Radiolarian Ratios and the Pleistocene–Holocene Boundary," Trans. Gulf Coast Ass. Geol. Soc. **29**, 298–301 (1979).

296. Yu. P. Melnik, A. A. Drozdovskaya, and K. A. Vorob'eva, "New Experimental and Calculated Data on Conditions of Sedimentation of Precambrian Iron–Siliceous Deposits," Geol. Zh. **33** (2), 12–23 (1973).

297. F. Meyen, "Beiträge zur Zoologie, Gesammelt auf einer Reise um die Erde: Familie Physeamtium, Sphaerozoum Thiere Gattung Sphaerozoum," Nova Acta Acad. Leopoldin.-Carolin. **16** (Suppl. 1), 163–164 (1834a).

298. F. Meyen, "Über das Leuchten des Meeres und Beschreibeng einiger Polypen und anderer niederer Thiere," Verh. Kaiserl. Leopoldin.-Carolin. Akad. Naturwissensch. **16** (Suppl. 1), 125–216 (1834b).

299. A. F. Michaels, D. A. Caron, N. R. Swanberg, *et al.*, "Planktonic Sarcodines (Acantharia, Radiolaria, Foraminifera) in Surface Waters near Bermuda: Abundance, Biomass, and Vertical Flux," J. Plankton Res. **17** (1), 131–163 (1990).

300. N. Mikkelsen, "Experimental Dissolution of Pliocene Diatoms," Nova Hedwigia **33**, 893–911 (1980).

301. K. A. Mikryukov, "Analysis of the System and Phylogeny of the Heliozoa," Doctoral Dissertation in Biology (Mosk. Gos. Univ., Moscow, 2000a) [in Russian].

302. K. A. Mikryukov, "The Modern State of the Sarcodine System," in *Radiolariology on the Eve of Millennium: Achievements and Perspectives* (Moscow–St. Petersburg, 2000b), pp. 46–47 [in Russian].

303. K. A. Mikryukov, "Heliozoans As an Important Component of Microbenthos," in *Radiolariology on the Eve of Millennium: Achievements and Perspectives* (Moscow–St. Petersburg, 2000c), pp. 47–49 [in Russian].

304. G. A. Mizens, *Sedimentation Basins and Geodynamic Conditions in the Late Devonian–Early Permian of the Southern Ural Mountains* (Inst. Geol. Geokhim., Yekaterinburg, 2002) [in Russian].

305. G. A. Mizens, "Fluctuations of the Level of the World Ocean and Sedimentation in the Devonian Deep-Water Basins of the Southern Ural Mountains," Litosfera, No. 4, 43–64 (2003).

306. A. Molina-Cruz, "Radiolarian Assemblages and Their Relationship to the Oceanography of the Subtropical Southeastern Pacific," Mar. Micropaleontol., No. 4, 315–352 (1977).

307. A. S. Monin, *History of the Earth* (Nauka, Leningrad, 1977) [in Russian].

308. T. C. Moore, "Radiolaria: Change in Skeletal Weight and Resistance to Solution," Geol. Soc. Am. Bull. **80** (10), 2103–2107 (1969).

309. D. D. Mordukhai-Boltovskoy, "Geometry of Radiolarians," Uch. Zap. Rostov. Univ., No. 8, 1–91 (1936).

310. G. Mutvei, "Ultrastructural Study of Molluskan Nacre," in *Reports of the 17th International Geological Congress, 1984, Section C.02. Paleontology* (Nauka, Moscow, 1984), Vol. 2, pp. 56–61 [in Russian].

311. J. Müller, "Über Sphaerozoum und Thalassicolla," in *Monatsber. Kgl. Preuss. Akad. Wissensch.* (Berlin, 1855a), pp. 229–253.

312. J. Müller, "Über die im Hafen von Messina beobachteten Polycystinen," in *Monatsber. Kgl. Preuss. Akad. Wissensch.* (Berlin, 1855b), pp. 671–674.

313. J. Müller, "Über die Thalassicollen, Polycystinen und Acanthometren des Mittelmeeres," in *Monatsber. Kgl. Preuss. Akad. Wissensch.* (Berlin, 1857), pp. 474–503.

314. J. Müller, *Über die Thalassicollen Polycystinen und Acanthometren des Mittelmeeres* (Abh. Kgl. Preuss. Akad. Wissensch., Berlin, 1858).

315. B. B. Nazarov, "Radiolarians from the Lowermost Horizons of the Batenev Mountain Ridge," in *Problems of Paleontology and Biostratigraphy of the Lower Cambrian of Siberia and the Far East* (Nauka, Novosibirsk, 1973), pp. 5–13 [in Russian].

316. B. B. Nazarov, "On the Systematics of Paleozoic Sphaeroideans," Tr. Vsesoyuzn. Geol. Inst., Nov. Ser. **226** (Systematics and Stratigraphic Significance of Radiolarians), 35–40 (1974a).

317. B. B. Nazarov, "Albaillellidae and Paleoscenidiidae from the Upper Devonian Beds of the Southern Ural Mountains," Tr. Vsesoyuzn. Geol. Inst., Nov. Ser. **226** (Systematics and Stratigraphic Significance of Radiolarians), 41–47 (1974b).

318. B. B. Nazarov, "Problematic Siliceous Formations from the Lower Paleozoic of Kazakhstan," in *Biostratigraphy and Paleoecology of the Lower Cambrian of Europe and Northern Asia* (Nauka, Moscow, 1974c), pp. 110–112 [in Russian].

319. B. B. Nazarov, "Radiolarians from the Lower and Middle Paleozoic of Kazakhstan: Research Methods, Systematics, and Stratigraphic Significance," Tr. Geol. Inst. Akad. Nauk SSSR **275**, 1–202 (1975).

320. B. B. Nazarov, "Evolution of Radiolarians in the Paleozoic and Questions of Their Systematics," in *Systematics, Evolution, and Stratigraphic Significance of Radiolarians* (Nauka, Moscow, 1981), pp. 22–37 [in Russian].

321. B. B. Nazarov, "Radiolarians of the Paleozoic," Doctoral Dissertation in Geology and Mineralogy (Geol. Inst. Akad. Nauk SSSR, Moscow, 1984).

322. B. B. Nazarov, *Paleozoic Radiolarians: Practical Handbook of the Microfauna of the USSR* (Nedra, Leningrad, 1988), Vol. 2 [in Russian].

323. B. B. Nazarov and A. R. Ormiston, "A New Superfamily of Stauraxon Polycystine Radiolaria from the Late Paleozoic of the Soviet Union and North America," Senckenberg. Lethaea **64** (2/4), 363–379 (1983).

324. B. B. Nazarov and A. R. Ormiston, "Tentative System of Paleozoic Radiolaria," in *Morphology, Ecology, and Evolution of Radiolarians* (Nauka, Leningrad, 1984), pp. 64–87 [in Russian].

325. B. B. Nazarov and A. R. Ormiston, "Evolution of Radiolaria in the Paleozoic and Its Correlation with the Development of Other Marine Fossil Groups," Senckenberg. Lethaea **66** (3/5), 203–215 (1985).

326. B. B. Nazarov and A. R. Ormiston, "Trends in the Development of Paleozoic Radiolaria," Mar. Micropaleontol., No. 11, 3–32 (1986).

327. B. B. Nazarov and A. R. Ormiston, "New Biostratigraphically Important Paleozoic Radiolaria of Eurasia and North America," Micropaleontology **6** (Spec. Pub.: Radiolaria of Giant and Subgiant Fields in Asia), 22–60 (1993).

328. B. B. Nazarov and M. G. Petrushevskaya, "Class Radiolaria (Radiolarians)," in *Manual on Micropaleontology* (Mosk. Gos. Univ., Moscow, 1995), pp. 111–158 [in Russian].

329. B. B. Nazarov and V. S. Rudenko, "Some Bilateral Radiolarians of the Late Paleozoic of the Southern Ural Mountains," Vopr. Mikropaleontol., No. 24, 129–139 (1981).

330. K. N. Negadaev-Nikonov, Yu. N. Pecherskii, I. A. Vanchurov, and S. V. Mein, *Mathematics and Computer in Paleontology* (Shtiintsa, Chisinau, 1983) [in Russian].

331. A. Nishimura, K. Nakaseko, and Y. Okuda, "A New Coastal Water Radiolarian Assemblage Recovered from Sediment Samples from the Antarctic Ocean," Mar. Micropaleontol., No. 30, 29–44 (1997).

332. P. J. Noble, "Silurian Radiolarian Zonation for the Caballos Novaculite, Marathon Uplift, West Texas," Bull. Am. Paleontol., No. 106, 1–55 (1994).

333. O. T. Obut and K. Iwata, "Lower Cambrian Radiolaria from the Gorny Altai (Southern West Siberia)," Nov. Paleontol. Stratigr., No. 2–3, 33–38 (2000).

334. A. R. Ormiston and L. C. Babcock, "*Follicucullus*, New Radiolarian Genus from Guadelupian (Permian) Lamar Limestone of the Deflandre Basin," J. Paleontol. **53** (2), 328–334 (1979).

335. A. R. Ormiston and H. R. Lane, "A Unique Radiolarian Fauna from the Sycamore Limestone (Mississippian) and Its Biostratigraphic Significance," Palaeontographica, Abh. A **154**, 154–180 (1976).

336. *Paleontology and Paleoecology: Dictionary–Reference Book*, Ed. by V. P. Makridin and I. S. Barskov (Nedra, Moscow, 1995) [in Russian].

337. A. A. Palmer, "Cenozoic Radiolarians As Indicators of Neritic versus Oceanic Conditions in Continental-Margin Deposits: US Mid-Atlantic Coastal Plain," Palaios **1**, 122–132 (1986).

338. P. J. Paverd van de, "Recent Polycystine Radiolaria from the Snellius-II Expedition," PhD Theses (Free Univ., Amsterdam, 1995).

339. P. J. Paverd van de and K. R. Bjørklund, "Frequency Distribution of Polycystine Radiolarians in Surface Sediments of the Banda Sea, Eastern Indonesia," Netherl. J. Sea Res. **24** (4), 511–512 (1989).

340. E. A. Pessagno, "Upper Cretaceous Spumellariinae from the Great Valley Sequence, California Coast Ranges," Bull. Am. Paleontol. **63** (276), 45–100 (1973).

341. E. A. Pessagno, "Upper Jurassic Radiolaria and Radiolarian Biostratigraphy of the Great Valley Sequence," Micropaleontology, No. 2 (Spec. Pub.), 1–95 (1976).

342. E. A. Pessagno, "Radiolaria Zonation and Stratigraphy of the Upper Cretaceous Portion of the California Coast Ranges," Micropaleontology **23** (1), 56–113 (1977).

343. M. G. Petrushevskaya, "Significance of the Growth of Radiolarian Skeletons for Their Systematics," Zool. Zh. **41** (3), 331–341 (1962).

344. M. G. Petrushevskaya, "Radiolaria in the Plankton and Bottom Sediments," in *Geochemistry of Silica* (Nauka, Moscow, 1966), pp. 219–245 [in Russian].

345. M. G. Petrushevskaya, "The Radiolarians Nassellaria in Plankton of the World Ocean: Exploration of the Fauna of the Seas," in *Radiolarians of the Ocean* (Nauka, Leningrad, 1971), pp. 5–294 [in Russian].

346. M. G. Petrushevskaya, "On the Origin of Radiolaria," Zool. Zh. **56** (10), 1448–1458 (1977).

347. M. G. Petrushevskaya, "A New Variant of the Polycystina Systems," in *Extinct and Extant Radiolarians* (Leningrad, 1979), pp. 101–118 [in Russian].

348. M. G. Petrushevskaya, *Radiolarians of the Order Nassellaria of the World Ocean* (Nauka, Leningrad, 1981a) [in Russian].

349. M. G. Petrushevskaya, "Sarcodines of the Superclass Actinopoda Calkins, 1909: System and Phylogeny," in *Systematics, Evolution, and Stratigraphic Significance of Radiolarians* (Nauka, Moscow, 1981b), pp. 10–17 [in Russian].

350. M. G. Petrushevskaya, "On the Classification of Polycystine Radiolarians," in *Morphology, Ecology, and Evolution of Radiolarians* (Nauka, Leningrad, 1984), pp. 124–148 [in Russian].

351. M. G. Petrushevskaya, *Radiolarian Analysis* (Nauka, Leningrad, 1986) [in Russian].

352. M. G. Petrushevskaya and V. V. Menshutkin, "Information Content Necessary and Sufficient for the Systematics of Radiolarians," in *Radiolarians in Biostratigraphy: Collected Works* (Ural. Otd. Akad. Nauk SSSR, Sverdlovsk, 1990), pp. 107–118 [in Russian].

353. N. G. Pisias, D. W. Murray, and A. K. Roelofs, "Radiolarian and Silicoflagellate Response to Oceanographic Changes Associated with the 1983 El Nino," Nature **320**, 259–262 (1986).

354. V. M. Podobina and S. A. Rodygin, *Historical Geology* (NTL, Tomsk, 2000) [in Russian].

355. A. Popofsky, "Die Radiolarien der Antarktis," in *Deutsche Südpolar-Expedition 1901–1903* (Berlin, 1908), Vol. 10 (Zoologie, Vol. 3), pp. 185–305.

356. A. Popofsky, "Die Sphaerellarien des Warmwassergebietes," in *Deutsche Südpolar-Expedition 1901–1903* (Berlin, 1912), Vol. 13 (Zoologie, Vol. 5), pp. 75–159.

357. A. Popofsky, "Die Nassellarien des Warmwassergebietes," in *Deutsche Südpolar-Expedition 1901–1903* (Berlin, 1913), Vol. 14, pp. 217–416.

358. K. G. Popov and N. A. Tikhonov, "Features of Gelation Process in the Vicinity of the Critical Point of the Reaction Yield," in *2nd International Seminar on Mineralogy and Life: Biomineral Interactions* (Geoprint, Syktyvkar, 1996), pp. 12–14.

359. B. V. Poyarkov, *Development and Distribution of Devonian Foraminifers* (Nauka, Moscow, 1979) [in Russian].

360. *Protista: Handbook on Zoology* (Nauka, St. Petersburg, 2000), Part 1 [in Russian].

361. V. I. Rakin, "Self-Organization of Crystal-Forming Gel System," in *2nd International Seminar on Mineralogy and Life: Biomineral Interactions* (Geoprint, Syktyvkar, 1996), pp. 11–12 [in Russian].

362. G. W. Renz, "The Distribution and Ecology of Radiolaria in the Central Pacific: Plankton and Surface Sediments," Bull. Scr. Inst. Oceanogr. **22**, 1–267 (1976).

363. V. V. Reshetnyak, *Deep-water Radiolarians Phaeodaria from the Northwestern Part of the Pacific Ocean: Fauna of the USSR: Radiolarians* (Nauka, Moscow–Leningrad, 1966) [in Russian].

364. W. R. Riedel, "Radiolaria in Antarctic Sediments," Rep. B.A.N.Z. Antarctic Res. Exped., Ser. B **6**, 17–255 (1958).

365. W. R. Riedel, "Class Actinopoda, Protozoa," in *The Fossil Record* (London, 1967), pp. 291–298.

366. W. R. Riedel, "Systematic Classification of Polycystine Radiolaria," *The Micropaleontology of Oceans* (Cambridge, 1971), pp. 649–660.

367. W. R. Riedel, "IDENTIFY; a Prolog Program to Help Identify Fossils," Computers Geosc. **15** (5), 809–823 (1989).

368. W. R. Riedel, L. E. Tway, and A. Sanfilippo, "Rad. Notes: Software to Assist Non-Expert to Identify Radiolarians," *Computer Software* (1994).

369. W. Riegraf, "Radiolarien, Datomeen, Cephalopoden und Stratigraphie im pelagischen Campanium Westphalens (Oberkreide, NW-Deutchalnd)," Neues Jahrb. Geol. Paläontol. Abh. **197** (2), 129–200 (1995).

370. D. A. Rodionov, *Statistical Solutions in Geology* (Nedra, Moscow, 1981) [in Russian].

371. A. Yu. Rozanov, *What Happened 600 Million Years Back?* (Nedra, Moscow, 1986) [in Russian].

372. A. Yu. Rozanov, "Evolution of Biosphere and Skeletization," in *Sedimentary Sphere of the Earth in Space and Time* (Nauka, Moscow, 1989), pp. 18–27 [in Russian].

373. A. Yu. Rozanov, "Extinct Bacteria, Sedimentogenesis and Early Stages of Biosphere Evolution," Paleontol. Zh., No. 6, 41–49 (2003) [Paleontol. J. **37** (6), 616–624 (2003)].

374. C. Samtleben, P. Schafer, H. Andruleit, *et al.*, "Plankton in the Norwegian Greenland Sea: From Living Communities to Sediment Assemblages—An Actualistic Approach," Geol. Rundsch. **84** (1), 108–136 (1995).

375. C. Sancetta, "Processes Contolling the Accumulation of Diatoms in Sediments: A Model Derived from British Columbian Fjords," Paleoceanography, No. 4, 235–251 (1989).

376. K. Sashida, "Lower Triassic Radiolaria from the Kanto Mountains, Central Japan: Part. 1. Palaeoscenidiidae," Trans. Proc. Palaeontol. Soc. Japan. New Ser., No. 131, 168–177 (1983).

377. A. Schaaf, "Introduction a la morpholgie evolutive: une application a la classe des Radiolaires (Evolutionary Morphology Applied to Radiolaria)," Neues Jahrb. Geol. Paläontol. Abh. **161** (2), 209–253 (1981).

378. W. Schewiakoff, *Acantharia: Fauna e flora del golgo di Napoli, Monogr.* (Roma, 1926), Vol. 27.

379. Yu. N. Senkovsky, *Lithogenesis of the Siliceous Strata of the Southwestern USSR* (Naukova Dumka, Kiev, 1977) [in Russian].

380. J. J. Sepkoski, "Patterns of Phanerozoic Extinction: A Perspective from Global Data Bases," in *Global Events and Events Stratigraphy in the Phanerozoic: Results of International Interdisciplinary Cooperation in IGCP Project 216 on the Global Biological Events in Earth History*, Ed. by O. H. Walliser (Springer, Berlin–Heidelberg, 1996), pp. 35–52.

381. L. N. Seravin, *Protists… What Are They?* (Nauka, Leningrad, 1984) [in Russian].

382. I. I. Shafranovsky, *Symmetry in Nature* (Nedra, Leningrad, 1968) [in Russian].

383. V. V. Shilov, "Stratigraphy of the Upper Cenozoic Beds of the Clarion–Klipperton Structural Zone," *Candidate's Dissertation in Geology and Mineralogy* (Vseross. Nauchno-Issled. Inst. Okeangeol., St. Petersburg, 2004).

384. S. S. Shul'man and V. V. Reshetnyak, "Whether or not the Superclass Actinopoda Actually Exists in the Protist System," in *Principles of the Development of Macrosystem of Unicellular Animals* (Zool. Inst. Akad. Nauk SSSR, Leningrad, 1980), pp. 23–41 [in Russian].

385. W. O. Smith and D. M. Nelson, "Importance of Ice-Edge Phytoplankton Production in the Southern Ocean," Bio. Sci. **36**, 251–257 (1986).

386. B. S. Sokolov, "Organic World of the Earth on the Path to the Phanerozoic Differentiation," Vestn. Akad. Nauk SSSR, No. 1, 126–143 (1976).

387. B. S. Sokolov, "Stages of Development of the Precambrian Biosphere in the Light of the Paleozoic Data," in *Correlation of the Cambrian* (Nauka, Moscow, 1977), Vol. 1, pp. 269–278 [in Russian].

388. S. D. Stepanjants, S. B. Kruglikova, K. R. Bjørklund, and G. Cortese, "The Bipolar Distribution of Marine Organisms with Emphasis on Radiolaria and Cnidarians: A New Stage of Research," in *General Questions of Biogeography: In Memories of the Academician O.G. Kusakina*, Ed. by A.I. Kafanov (Dal'nauka, Vladivostok, 2004), pp. 124–178 [in Russian].

389. N. M. Strakhov, *Fundamentals of Historical Geology* (GIGL, Moscow, 1948), Vols. 1, 2 [in Russian].

390. A. A. Strelkov and V. V. Reshetnyak, "Colonial Spumellarian Radiolaria of the World Ocean: Exploration of the Fauna of the Seas," in *Radiolarians of the Ocean* (Nauka, Leningrad, 1971), pp. 295–373 [in Russian].

391. N. R. Swanberg, "The Ecology of Colonial Radiolarians," Doctoral Dissertation (Woods Holl Oceanogr. Inst.–Massachusetts Inst. Technol., Woods Hole, 1979).

392. N. R. Swanberg and O. R. Anderson, "The Nutrition of Radiolarians: Trophic Activity of Some Solitary Spumellaria," Limnol. Oceanogr. **30** (3), 646–652 (1985).

393. N. R. Swanberg and K. Bjørklund, "Radiolaria in the Plankton of the Some Fjords in Western and Northern Norway: The Distributions of Species," Sarsia, No. 72, 231–244 (1987).

394. N. R. Swanberg and K. Bjørklund, "The Radiolarian Fauna of Western Norwegian Fjords: A Multivariate Comparison of the Sediment and Plankton Assemblages," Micropaleontology **38** (1), 57–74 (1992).

395. N. R. Swanberg and G. R. Harbison, "Distribution, Ecology of a New Species of *Collozoum* in the Tropical Atlantic," Deep-Sea Res. Part A **27** (9A), 715–732 (1980).

396. V. L. Syvorotkin, *Ozone Layer, Earth Degassing, Rift Formation, and Global Catastrophe* (Geoinformmark, Moscow, 1994) [in Russian].

397. V. L. Syvorotkin, *Ecological Aspects of Earth Degassing* (Geoinformmark, Moscow, 1998) [in Russian].

398. K. Takahashi, "Vertical Flux, Ecology and Dissolution of Radiolaria in Tropical Oceans: Implications for the Silica Cycle," PhD Dissertation (Oceanogr. Inst. Massachusetts Inst. Technol, Woods Hole, 1981).

399. K. Takahashi, "Radiolaria: Sinking Population, Standing Stock, and Production Rate," Mar. Micropaleontol., No. 8, 171–181 (1983).

400. K. Takahashi, "Radiolaria: Flux, Ecology, and Taxonomy in the Pacific and Atlantic," in *Ocean Biocoenosis Ser.*, Ed. by S. Honjo (Woods Hole Oceanogr. Inst., Massachusetts, 1991), pp. 1–303.

401. K. Takahashi, "Environmental Proxy and Radiolarian Fluxes: A Review," in *INTERRAD VII, Osaka: 7th Meeting of the International Association of Radiolarian Paleontologists: Abstracts* (Osaka, 1994), p. 115.

402. K. Takahashi and S. Honjo, "Sinking Speed, Residence Time and Dissolution of Radiolaria," Geol. Soc. Am. Proc. **13** (17), 1–564 (1981).

403. K. Takahashi and S. Honjo, "Radiolarian Skeletons: Size, Weight, Sinking Speed and Residence Time in Tropical Pelagic Ocean," Deep-Sea Res. **30** (5), 543–568 (1983).

404. A. Takemura and K. Nakaseko, "A New Permian Radiolarian Genus *Neoalbaillella* from the Tamba Belt, Southwest Japan," Trans. Proc. Palaeontol. Soc. Jap. N. Ser., No. 124, 208–214 (1981).

405. Ir Tan Sin Hok, *Over de samenstelling en het ontstaan van Krijt-en mergelgesteenten van de Molukken, Jaarbock van het Mijnwezen in Nederlandschen Oost-Indie* (Verhandel, 1926), Vol. 55, Part 3.

406. A. Taniguchi, E. Hamada, M. Okazaki, and Y. Naito, "Distribution of Phytoplankton Continuously Recorded in the JARE-25 Cruise (1984/85) to Syowa Station, Antarctica (SIBEX I)," Mem. Nat. Inst. Polar Res., No. 44 (Spec. Iss.), 3–14 (1986).

407. P. P. Timofeev and V. N. Kholodov, "Evolution of Sedimentation Basins in the History of the Earth," Izv. Akad. Nauk SSSR, Ser. Geol., No. 7, 10–34 (1984).

408. S. V. Tochilina, *On the Problems of the Systematics of Nassellaria (Radiolaria). Biochemical Peculiarities: Evolution* (Far East Branch RAS, Vladivostok, 1996).

409. S. V. Tochilina, *Problems of the Nassellarian Systematics: Biochemical Features of Evolution* (Dal'nevost. Otd. Ross. Akad. Nauk, Vladivostok, 1997) [in Russian].

410. W. D'Archy Thompson, *On Growth and Form* (Cambridge Univ. Press, Cambridge, 1942).

411. M. Umeda, "Early to Middle Devonian Ceratoikiscidae (Radiolaria) from the Yokokurayama Group in the Kurosegawa Terrane, Southwest Japan," Paleontol. Res. Paleontol. Soc. Jap. **2** (2), 96–107 (1998).

412. R. N. Valeev, *Aulacogens from the East European Platform* (Nedra, Moscow, 1978) [in Russian].

413. I. A. Vanchurov, "On the Solution of Classification Paleontological Tasks by Mathematical Methods," Tr. Vseross. Nauchno-Issled. Geol. Neft. Inst., No. 135 (Mathematical Methods and Computers in Geology), 34–48 (1973).

414. I. A. Vanchurov, "Mathematical Method for Comparing Paleontological Objects," Paleontol. Zh., No. 2, 141–148 (1975).

415. I. A. Vanchurov, "Mathematical Models in Paleontology," Doctoral Dissertation in Geology and Mineralogy (Mosk. Gos. Univ., Moscow, 1979).

416. I. A. Vanchurov, "Mathematical Modeling in Paleontology," Paleontol. Zh., No. 2, 3–12 (2000) [Paleontol. J. **34** (2), 118–127 (2000)].

417. N. B. Vassoevich, "The Role of Living Matter in the Natural History of Petroleum in the Light of Ideas of the Academician V.I. Vernadsky," Geol. Nefti Gaza, No. 3, 49–52 (1963).

418. N. B. Vassoevich, *Selected Works: Geochemistry of Organic Matter and the Origin of Petroleum* (Nauka, Moscow, 1986) [in Russian].

419. N. B. Vassoevich, *Selected Works: Lithology and Oil-and-Gas Content* (Nauka, Moscow, 1990) [in Russian].

420. N. B. Vassoevich and G. A. Amosov, "Geological and Geochemical Proof of the Formation of Petroleum at the Expense of Living Matter," in *Genesis of Petroleum and Gas* (Nedra, Moscow, 1967), pp. 5–22 [in Russian].

421. M. T. Venec-Peyre, J.-P. Caulet, and C. Vernaud-Grazzini, "Paleohydrogeographic Changes in the Somali Basin (50 N Upwelling and Equatorial Areas) during the Last 160 Kyr, Based on Correspondence Analysis of Foraminiferal and Radiolarian Assemblages," Paleoceanography **10** (3), 437–491 (1995).

422. V. I. Vernadsky, *Biosphere* (Nauch. Khim.-Tekhn., Leningrad, 1926) [in Russian].

423. V. I. Vernadsky, *Geochemistry Sketches* (Nauka, Moscow, 1983) [in Russian].

424. V. I. Vernadsky, *Chemical Structure of the Earth's Biosphere and Its Environment* (Nauka, Moscow, 1987), Issue 2 [in Russian].

425. C. Vernaud-Grazzini and J.-P. Caulet, "Late Quaternary Evolution of Fertility Indicators and Moonsoon in the

Somalian Basin, Northwest Indian Ocean," Bull. Soc. Geol. Fr., Ser. 8 **166** (3), 259–270 (1995).

426. *Vertical Accretion of the Earth's Crust: Factors and Mechanisms*, Ed. by M. G. Leonov (Nauka, Moscow, 2002) [in Russian].
427. C. A. Villee, *Biology* (Saunders Comp., Philadelphia–London, 1967).
428. G. M. Vinogradov, A. L. Vereshchaka, E. I. Musaeva, and V. Yu. D'yakonov, "Vertical Distribution of Zooplankton above the Pork'yupain Abyssal Plain (Northeastern Atlantic) in the Summer Season of 2002," Okeanologiya **43** (4), 543–554 (2003) [Oceanology **43** (4), 534–545 (2003)].
429. D. I. Vitukhin, "Distribution of Radiolarians in Cenozoic Beds of the Far East of the USSR (Sakhalin, Kamchatka Regions)," in *The Use of Radiolarians in Stratigraphy and Paleobiology* (Ufa, 1990), pp. 22–24 [in Russian].
430. V. S. Vishnevskaya, *Radiolarites As Analogues of Recent Radiolarian Silts* (Nauka, Moscow, 1984) [in Russian].
431. V. S. Vishnevskaya, "New Data on the Evolution of the Class Radiolaria," Paleontol. Zh., No. 4, 3–14 (1993).
432. V. S. Vishnevskaya, "Radiolarian High Taxa Distribution in the Mesozoic of the Tethyan and Boreal Realms," in *Radiolariology on the Eve of Millennium: Achievements and Perspectives* (Moscow–St. Petersburg, 2000), pp. 28–29 [in Russian].
433. V. S. Vishnevskaya, *Jurassic to Cretaceous Radiolarian Biostratigraphy of Russia* (GEOS, Moscow, 2001) [in Russian].
434. Yu. L. Voitekhovsky, "Biomineral Homologies: Fullerenes, Radiolarians, and Volvoxes," in *Biniology, Connections with Other Paradigms of Natural Sciences: Interuniversity Collected Works* (Tyumen. Gos. Neft. Gaz. Univ., Tyumen, 2002), pp. 112–118.
435. Yu. L. Voitekhovsky, "Examples of Biomineral Homology: 1. Fullerenes and Radiolarians," in *4th International Conference on Biniology, Symmetrology, and Synergetics in Natural Sciences* (TyumGNGU, Tyumen, 2004a), pp. 59–62.
436. Yu. L. Voitekhovsky, "Examples of Biomineral Homology: 2. Volvoxes and Viruses," in *4th International Conference on Biniology, Symmetrology, and Synergetics in Natural Sciences* (TyumGNGU, Tyumen, 2004b), pp. 62–65.
437. I. I. Volkov, "Hydrogen Sulfide and Reduced Sulfur Compound in the Black Sea: Comparative Analysis," in *Chemistry of Seas and Oceans* (Nauka, Moscow, 1995), pp. 266–289 [in Russian].
438. D. A. Walker, "More Evidence Indicates Link between El Ninos and Seismicity," EOS Trans. AGU **76** (4), 33–36 (1995).
439. K. Watanabe and Y. Nakajima, "Vertical Distribution of Chlorophyll along 45° E in the Southern Ocean, 1981," Mem. Nat. Inst. Polar Res., No. 23 (Spec. Iss.), 73–86 (1982).
440. L. A. Welling and N. G. Pisias, "How Do Radiolarian Sediment Assemblages Represent Surface Ocean Ecology in the Central Equatorial Pacific?," Paleoceanography, No. 13, 131–149 (1998).
441. R. D. White, "Cambrian Radiolaria from Utah," J. Paleontol. **60** (3), 778–780 (1986).
442. M.-Z. Won, "Radiolarien aus dem Unter-Karbon des Rheinischen Schiefergebirges (Deutschaland)," Palaeontograph., Abt. A **182** (4–6), 116–175 (1983).
443. M.-Z. Won and W. J. Iams, "Late Cambrian Radiolarian Faunas and Biostratigraphy of the Cow Head Group, Western Newfoundland," J. Paleontol. **76** (1), 1–33 (2002).
444. M.-Z. Won and R. Below, "Cambrian Radiolaria from the Georgian Basin, Queensland, Australia," Micropaleontology **45** (4), 325–363 (1999).
445. A. Yao and K. Kuwahara, "Permian and Triassic Radiolarian Assemblages from the Yangzi Platform," in *Biotic and Geological Development of the Paleo-Tethys in China* (Peking Univ. Press, Peking, 1999a), pp. 1–16.
446. A. Yao and K. Kuwahara, "Paleozoic and Mesozoic Radiolarians from the Changning-Menglian Terrane, Western Yunna, China," in *Biotic and Geological Development of the Paleo-Tethys in China* (Peking Univ. Press, Peking, 1999b), pp. 17–42.
447. A. Yao and K. Kuwahara, "Permian and Triassic Radiolarians from the Southern Guizhou Province, China," J. Geosci. Osaka City Univ. **43** (1), 1–19 (2000).
448. T. Yuasa, O. Takahashi, and S. Mayama, "Molecular Phylogeny of the Solitary Shell-bearing Polycystinea," *10th Meeting of the International Association of Radiolarian Paleontologists, Lausane, Switzerland, September 7–12, 2003* (Univ. Lausane, Lausane, 2003), p. 118.
449. N. P. Yushkin, "Biomineral Interactions: From Biomineralogy to Vitamineralogy," in *2nd International Seminar on Mineralogy and Life: Biomineral Interactions* (Geoprint, Syktyvkar, 1996), p. 7 [in Russian].
450. D. N. Zasko, "Horizontal and Vertical Distribution of Living Radiolarians along a Transect (14° N–52° N) of the North Atlantic," in *Radiolariology on the Eve of Millennium: Achievements and Perspectives* (Moscow–St. Petersburg, 2000), pp. 29–30 [in Russian].
451. D. N. Zasko, "Deep-sea Radiolarians of the Northern Atlantic Region," Candidate's Dissertation in Geology and Mineralogy (Inst. Oceanol. Ross. Akad. Nauk, Moscow, 2004) [in Russian].
452. D. N. Zasko and V. I. Vedernikov, "Vertical Distribution of Radiolarians, Chlorophyll, and Zooplankton in Epipelagic Area of the Northern Atlantic," in *Modern Questions of Geology* (Nauchnyi Mir, Moscow, 2003), pp. 326–331 [in Russian].
453. G. A. Zavarzin, "Establishment of the System of Biogeochemical Cycles," Paleontol. Zh., No. 6, 16–24 (2003) [Paleontol. J. **37** (6), 591–599 (2003)].
454. A. I. Zhamoida, "Review of Studies of Extinct Radiolarians (1950–1966)," in *Scientific Results, Ser. Geology: Stratigraphy and Paleontology* (VINITI, Moscow, 1967), pp. 109–134 [in Russian].
455. A. I. Zhamoida, *Biostratigraphy of Mesozoic Siliceous Strata in the Eastern USSR* (Nedra, Leningrad, 1972) [in Russian].
456. A. I. Zhamoida, "Some Problems of Radiolarian Studies: Stepwise Developmental Pattern, Zonal Stratigraphy, Nomenclature of the Subclass," in *Systematics, Evolution, and Stratigraphic Significance of Radiolarians* (Nauka, Moscow, 1981), pp. 5–9 [in Russian].

457. A. I. Zhamoida and G. E. Kozlova, "Relationships of Suborders and Families in the Order Spumellaria (Radiolarians)," in *Novelties in the Systematics of the Microfauna* (Nedra, Leningrad, 1971), pp. 76–82 [in Russian].

458. M. A. Zharkov and N. M. Chumakov, "Humid and Arid States of the Warm Biosphere," Geol. Geofiz. **42** (4), 668–677 (2001).

459. A. L. Zettler, O. R. Anderson, and D. A. Caron, "Insights on the Diversity within a 'Species' of *Thalassicolla* (Spumellarida) Based on 16S-Like Ribosomal RNA Gene Sequencing," J. Euk. Microbiol. **45**, 488–501 (1998).

460. A. L. Zettler, O. R. Anderson, and D. A. Caron, "Towards a Molecular Phylogeny of Colonial Spumellarian Radiolaria," Mar. Micropaleontol., No. 36, 67–79 (1999).

461. L. A. Zettler, M. L. Sogin, and D. A. Caron, "Phylogenetic Relationships between the Acantharea and the Polycystinea: A Molecular Perspective on Haeckel's Radiolaria," Proc. Natl. Acad. Sci. USA **94**, 11411–11426 (1997).

ALPHABETICAL INDEX OF LATIN NAMES

Dr. Marina S. Afanasieva

Research interests: Radiolarian morphology, taxonomy, phylogeny, classification, evolution, habitat, taphonomy, paleoecology; biostratigraphy of the Paleozoic. She has published about 180 scientific works.

Dr. Edward O. Amon

Research interests: regional geology, paleogeography and stratigraphy of the Urals (Paleozoic, Cretaceous, Paleogene); Radiolarian morphology, taxonomy, classification, phylogeny, evolution; mathematics in geology; philosophical and methodological problems of science. He has published around 190 scientific works.

Dr. Yurii V. Agarkov

Research interests: lithology of silicite, paleontology of siliceous organisms, geoinformation technologies. Since 1993 he develops the multipurpose informational system of radiolarians of the world, know as RADBASE. He has published around 90 scientific works.

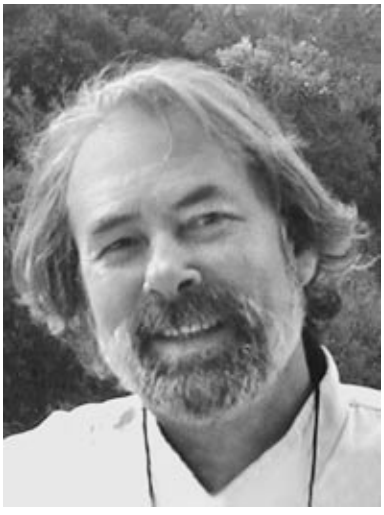

Dr. Demetrio Boltovskoy

Research interests: Recent and Pleistocene Radiolaria and other marine microzooplankton; ecology and paleoecology, distribution, taxonomy. He has published over 100 scientific papers and has edited 2 books on marine zooplankton.